An investigation into the potential of peptide mass fingerprinting for the study of Australian faunal assemblages

Dissertation

(kumulativ)

Zur Erlangung des akademischen Grades doctor philosophiae

(Dr. phil)

vorgelegt dem Rat der Philosophischen Fakultät

der Friedrich-Schiller-Universität Jena

von Carli Antoinette Elisabeth Peters

geboren am 20 März 1996 in Venlo, die Niederlande

Jena

2022

Gutachter/Gutachterin:

1. Prof. Dr. Nicole Boivin
2. Prof. Dr. Clemens Pasda

Tag der Verteidigung*:* 17 May 2023

Table of Contents

1. Introduction

The advent of novel biomolecular techniques to study the archaeological record has opened up an extensive range of key research questions and avenues that were previously unattainable. Some of the most striking recent developments in biomolecular archaeology have come in the field of palaeoproteomics, the study of ancient proteins. Here, Zooarchaeology by Mass Spectrometry (ZooMS) is becoming increasingly widespread in terms of the frequency and diversity of its applications. ZooMS is a minimally destructive, high-throughput approach that can be used to taxonomically identify fragmented faunal remains on the basis of their collagen fingerprint (Buckley et al., 2009). ZooMS has already demonstrated its ability to help address a wide range of research questions and topics, including those pertaining to 1) the reconstruction of past ecosystems and shifts in biodiversity (e.g. Rodrigues et al., 2018, Buckley and Herman, 2019, Rodrigues et al., 2019), 2) assessing the impact of climate change and anthropogenic activities, 3) tracking the introduction of non-native species (Prendergast et al., 2017, Harvey et al., 2019a) and domesticates (e.g. Taylor et al., 2018, Le Meillour et al., 2020, Taylor et al., 2020, Coutu et al., 2021, Culley et al., 2021, Janzen et al., 2021), 4) identifying human remains within fragmented assemblages (Welker et al., 2015a, Brown et al., 2016, Brown et al., 2022), and 5) provenancing tools and objects derived from bone and antler (e.g. Desmond et al., 2018, Bradfield et al., 2019, Jensen et al., 2020a, Martisius et al., 2020, Talamo et al., 2021).

The majority of ZooMS studies to date have, until recently, focused on Eurasian medium- to large-sized mammals. However, in recent years, peptide markers have been developed for additional taxonomic groups such as micromammals (Buckley et al., 2016, Prendergast et al., 2017, Buckley and Herman, 2019, Harvey et al., 2019a, Buckley et al., 2020), fish (Richter et al., 2011, Harvey et al., 2018, Richter et al., 2020), birds (Eda et al., 2020, Codlin et al., 2022), amphibians (Buckley and Cheylan, 2020), and reptiles (Harvey et al., 2019b). Furthermore, the focus of ZooMS studies has moved beyond Eurasia, and the last five years have seen the first ZooMS studies focused on African (e.g. Desmond et al., 2018, Bradfield et al., 2019, Le Meillour et al., 2020, Culley et al., 2021, Janzen et al., 2021), as well as North and South American contexts (e.g. Harvey et al., 2019a, McGrath et al., 2019, Rick et al., 2019, Mychajliw et al., 2020, Runge et al., 2021). Critically, this has included regions in which poor preservation had often previously been assumed, leading to assumptions that biomolecular approaches would face significant hurdles. Nonetheless, these studies have demonstrated the utility of ZooMS even in these challenging contexts.

Another region in which biomolecular preservation is assumed to be poor is Australia, a country that remains remarkably unexplored in the context of palaeoproteomics despite the unique nature of its palaeontological record and ongoing debates relating to human-animal interactions in the country. So far, only a single study has explored the potential of ZooMS to identify Australian marsupial remains (Buckley et al., 2017), which resulted in the characterization of incomplete marker profiles for a handful of marsupials. Larger-scale applications of ZooMS in Australia have the potential to open up an entirely new set of research directions utilizing the analysis of its faunal assemblages. Furthermore, Australia is an interesting target for future ZooMS studies because of its broad range of unique and endemic fauna that has evolved independently for 35 million years (Black et al., 2012). These animals are highly diverse, play key ecological roles (Woinarski et al., 2015), and were important subsistence resources in the past (Dortch and Wright, 2010, Cosgrove and Garvey, 2017).

Extinctions, extirpations and faunal turnovers in Australia, with potential linkages to humans and/or climate change have occurred on multiple occasions in the past and are still a major topic to this day. In the last 200 years Australia's faunal suite has suffered an incredible rate of extinction, with over 10% of all endemic terrestrial species now extinct, and another 21% threatened with extinction (Woinarski et al., 2015). Looking at the trajectories of faunal populations in deep time can provide us with the crucial information necessary to better understand the processes underlying, and the consequences of, present-day biodiversity loss resulting from overexploitation, habitat fragmentation and the overall modification

of the landscape (Butchart et al., 2010, Dirzo et al., 2014, Boivin et al., 2016). The inclusion of a long-term perspective, acquired through the analysis of fossil remains from palaeontological and archaeological sites, is crucial for the development of fitting conservation strategies to address current climatic and environmental challenges (Willis and Birks, 2006, Scharf, 2014, Barnosky et al., 2017); a field of study often referred to as conservation palaeobiology (Dietl and Flessa, 2011, Dietl et al., 2015, Barnosky et al., 2017).

However, one of the main challenges for the study of past fauna in Australia is the generally high fragmentation rate of faunal remains in archaeological and palaeontological assemblages. Australia has relatively high temperatures and low levels of precipitation that do not favor the preservation of fossil material (Langley et al., 2011, Manne and Veth, 2015). Marsupial carnivores, such as quolls and Tasmanian Devils, further fragment bones through frequent scavenging (Marshall and Cosgrove, 1990, Kos, 2003, Miscamble and Manne, 2016). This often results in bone assemblages with a significant number of highly fragmented, morphologically unidentifiable bone fragments. This complicates the study of faunal remains from Australian sites.

ZooMS has the potential to address these issues and improve the taxonomic identifications of fragmented bones in Australian contexts. As with other regions of the world, the large-scale application of ZooMS has the potential to reconstruct faunal turnovers in the past, address spatial and temporal questions concerning past extinctions and extirpations, provenance bone tools and objects, and track the introduction of domesticates and other non-native species. Nevertheless, before ZooMS can truly be incorporated as a staple method in Australian zooarchaeology and palaentology, more in-depth studies are needed that focus on the characterization of collagen peptide markers for a larger number of Australian animals. In the absence of these peptide markers, any ZooMS study aiming to analyze Australian fauna will be primarily restricted to introduced domesticated animal taxa, for which comprehensive marker sets exist. Furthermore, although there have been several studies investigating collagen preservation in temperate deposits (e.g. Nielsen-Marsh and Hedges, 2000, Colleary et al., 2021, Matthiesen et al., 2021), relatively little is still known about the preservation of collagen in Australian archaeological and palaeontological contexts. Structural studies investigating the preservation of collagen in a range of climatic conditions and depositional environments across time and space are thus required to get more insight into the preservation potential of collagen in Australia. Once these challenges have been addressed, the true potential of ZooMS in Australian contexts can be unlocked.

The research that was conducted for this thesis represents the first large-scale application of ZooMS in Australian contexts, with the aim of addressing the main limitations and challenges to the method's first application that have been highlighted. The first manuscript (Manuscript A), which represents and important building block for further work, characterizes collagen peptide markers for a large number of modern Australian marsupials, and subsequently uses these new peptide markers to identify fragmented faunal remains from a colonial-era pearl shell fishery at Bandicoot Bay, Barrow Island, Western Australia. The development of these peptide markers significantly amplifies the potential of ZooMS to study faunal remains from Australian archaeological and palaeontological contexts. Manuscript B draws on samples from multiple archaeological and palaeontological contexts across Australia to further explore the patterns and mechanisms of collagen preservation in Australia with the aim of acquiring a better understanding of when ZooMS can be successfully implemented to study archaeofaunal and fossil material from Australian contexts. This paper represents a second critical building block to help develop the potential of ZooMS applications in Australia. In Manuscript C, ZooMS is then applied in a case study to identify fragmented fossil material from a Late Pleistocene deposit at the site of Devil's Lair, southwest Australia. These results are compared to the zooarchaeological assemblage and bulk bone DNA metabarcoding data to obtain a holistic overview of faunal patterns at the site through time. Finally, Manuscript D introduces the concept of conservation palaeoproteomics and explores how ZooMS and shotgun palaeoproteomics have the potential to inform conservation and restoration strategies. Together, these manuscripts highlight the potential of ZooMS to further explore, understand, and amplify the

zooarchaeological and palaeontological records of Australia. The location of all the sites studied as part of the research conducted for this thesis are outlined in Figure 1.1.

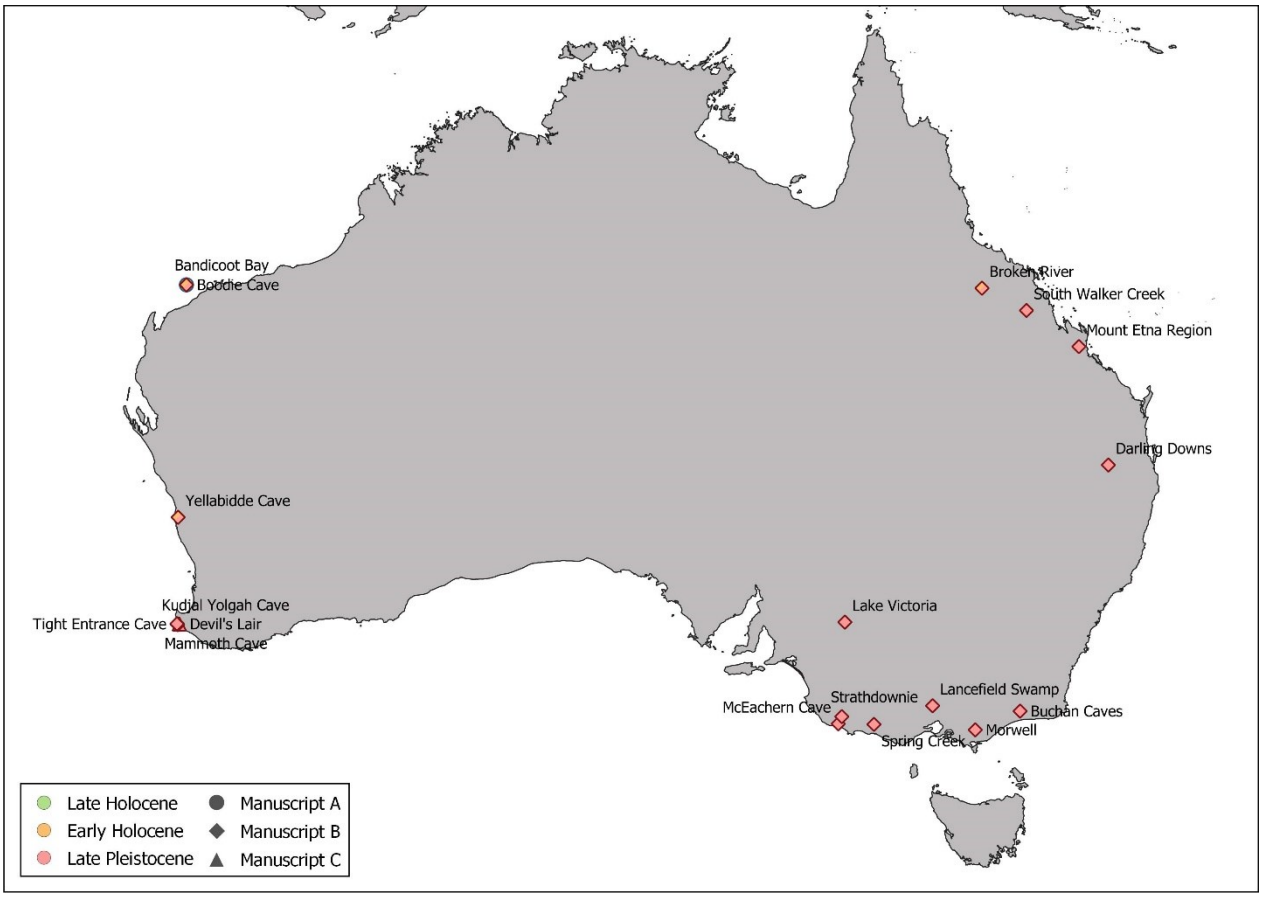

Figure 1.1: The location of the sites studied as part of the research conducted for this thesis.

2. Major faunal turnovers in Australia during the last 100,000 years

During the last 100 thousand years (*kilo annum*, ka), there have been a number of significant faunal turnovers in Australia that have dramatically affected faunal diversity across the continent. One of the most notable changes that occurred is the extinction of more than 60 land mammal species during this period. These extinctions can be grouped into three main temporal periods: 1) the extinction of megafaunal marsupials during the Late Pleistocene, 2) the extinction of large marsupial carnivores on mainland Australia during the Holocene, and 3) recent extinctions of small- and large-sized terrestrial animals following European settlement of Australia 200 years ago. This chapter will define these three major faunal turnovers discussed in the archaeological and palaeontological literature to identify the potential areas of research that would be most suitable to target using palaeoproteomic approaches.

2.1. Late Pleistocene megafauna extinctions

During the Late Quaternary, around two-thirds of all megafaunal species (>100 genera, >175 species) on Earth went extinct (Barnosky, 2008), an event that is sometimes referred to as the start of the Earth's sixth mass extinction event (Davis et al., 2018). The intensity of Late Quaternary extinctions differed between, and within, continents (Figure 2.1). Proportionally, Sahul (the joint landmass of Pleistocene Australia and New Guinea) was most affected by this extinction period; at least 55 species, accounting for 20 genera of mammalian megafauna, 4 genera of megafaunal birds, and 3 genera of megafaunal reptiles, went extinct during the late Quaternary period starting ca. 400 ka. This includes all taxa with a weight of over 100 kg (Brook and Johnson, 2006, Wroe et al., 2013), and three families went extinct completely: Diprotodontidae, Palorchestidae, and Thylacoleonidae (Koch and Barnosky, 2006). Twenty-two megafaunal species persisted until the end of the Late Pleistocene, until they eventually went extinct around 50 ka (Wroe et al., 2013).

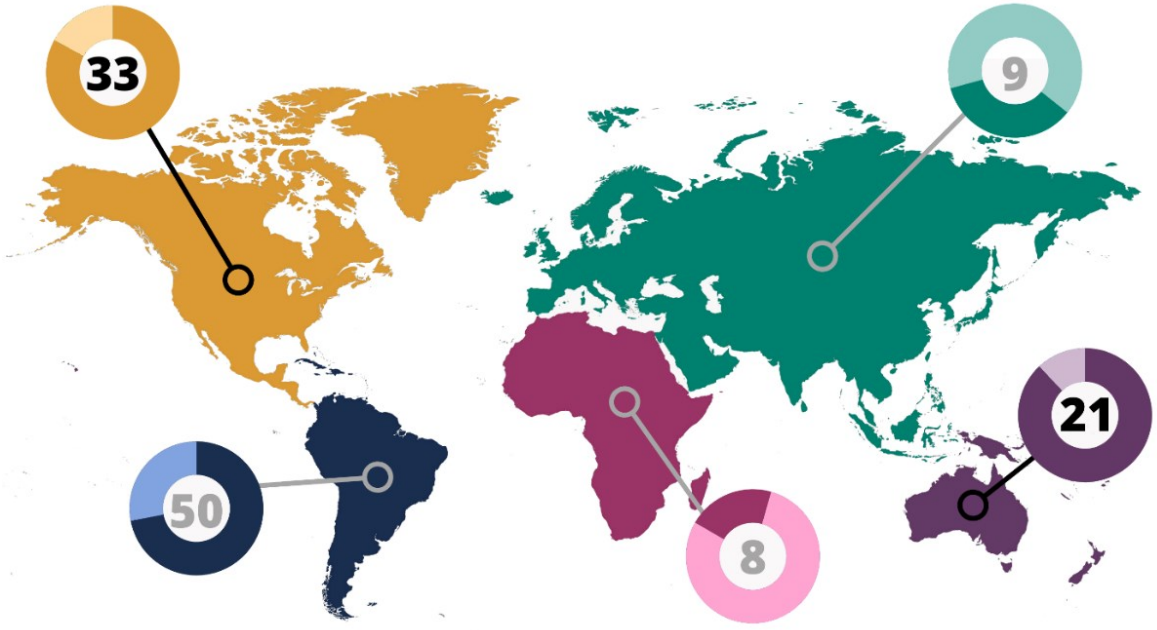

Figure 2.1: Overview of the number of megafauna species that went extinct globally during the Late Pleistocene extinction event. The number of species that went extinct are shown in a circle diagram showing the percentage of species of the total large mammal community that went extinct on the given continent. Numbers taken from Koch and Barnosky (2006).

What is megafauna?

The term megafauna is often used to refer to animals with a body mass of at least 44 kg (Martin and Klein, 1984, Surovell, 2008). However, this is an arbitrary threshold (Johnson et al., 2021), and is not representative of the worldwide biological and ecological diversity of large vertebrates during the Quaternary (Price et al., 2018). Alternatively, megafauna have also been defined as extinct species considerably larger than their extant counterparts (Price et al., 2018, Johnson et al., 2021). Overall, this definition fits better for the Australian continent, since smaller-bodied species also went extinct (Wroe et al., 2013). For example, *Megalibgwilia ramsayi*, an extinct relative of the extant echidna, weighing around 15 kg, also went extinct during the Pleistocene (Price et al., 2018). Therefore, this second definition of megafauna will be followed for the remainder of this thesis.

Megafauna were generally more susceptible to extinction than smaller species in the same ecosystems (Cardillo et al., 2005). This size-bias has also been observed for Late Quaternary extinctions globally and continues to be a trend in extinction rates to this day (Smith et al., 2019). Studies focused on extant large animals have shown that this high extinction risk is most likely the result of their long life-histories. Large animals generally have long generation times and low reproduction rates, making them more vulnerable to over-exploitation by new predators, or rapid environmental changes (Cardillo et al., 2005, Brook and Johnson, 2006).

2.1.1. Human arrival and extinction chronology

The exact timing of megafauna extinctions and human arrival to Sahul is one of the major unresolved questions that is fueling the megafauna extinction debate in Australia. There is much controversy about the precise chronology of megafauna extinction and human arrival to Sahul, which give rise to multiple different scenarios of human-megafauna overlap or the lack thereof (see e.g. Gillespie et al., 2006, Field et al., 2013, Johnson et al., 2016). The current knowledge about the timing of these two events is addressed in this section.

Human arrival

During the Late Pleistocene, Sahul was separated from the Sunda Shelf (the combined landmass of Southeast Asia during periods of low sea level) by the Wallacea Strait (Pettitt, 2013). This means that, in order to reach Sahul, humans needed to cross a sea barrier. It is currently hypothesized that humans first arrived to Sahul via the northern coast after which they spread across the entire continent. The spread of humans throughout Sahul is theorized to have taken place fairly rapidly following coastlines, major waterways and inland lake systems (Bird et al., 2016). The exact timing of the first human arrival on Sahul remains hotly contested, however. Currently, the oldest archaeological site known from Australia, although not undisputed, is Madjedbebe in northern Australia. Madjedbebe has been dated with single grain optically stimulated luminescence (OSL) to ca. 65 ka (Clarkson et al., 2017).

Evidence for more widespread occupation starts to occur from ca. 50 ka onwards, for example, at sites such as Nawarla Gabarnmang, northern Australia (David et al., 2019), Devil's Lair, southwestern Australia (Turney et al., 2001), Warratyi Rock Shelter, South Australia (Hamm et al., 2016), and Boodie Cave (Veth et al., 2017) and Minjiwarra in northwestern Australia (Veth et al., 2019). Tasmania was the last region of Australia to be colonized by humans, with the earliest sites, Warreen Cave and Parmerpar Meethaner shelter, dating to around ca. 35-40 ka (Cosgrove et al., 2010). There is a general consensus that humans were present in Sahul by ca. 45-50 ka (Bird et al., 2013, Johnson et al., 2021). While this could roughly coincide with megafaunal extinctions in Sahul, more chronometric and palaeoecological investigation is needed on a regional and taxon-specific basis. Regardless, there appears to be a potential period of human-megafauna overlap in Sahul, which is also evidenced by the presence of rock art interpreted as depicting extinct megafaunal species, such as *Genyornis newtoni* (Gunn et al., 2011, Cobden et al., 2017) and *Thylacoleo* (Akerman and Willing, 2009).

Extinction chronology

Evidence of megafauna surviving on Sahul until roughly 50 ka currently only exists for 22 taxa, almost half of which were solely inhabiting present-day New Guinea. For mainland Australia, there were 16 megafauna species that persisted until the final wave of extinction ca. 50 ka (Wroe et al., 2013). The majority of taxa went extinct well before this period in what is suggested to have been a step-wise extinction event already in motion well before human arrival to Australia (Price et al., 2011, Tyler Faith and O'Connell, 2011, Wroe et al., 2013) (Figure 2.2). Further confounding our understanding of the timing of megafauna extinctions is the paucity of spatial data and limited knowledge about the biogeography of many megafaunal species. For example, *Diprotodon optatum*, the best-represented megafauna species in the fossil record of Australia is only represented by less than 20 reliably dated deposits (Price et al., 2021).

The main issue in establishing reliable extinction chronologies for Australian megafauna is thus the lack of reliably dated megafaunal remains across time and space (Webb, 2013, Price et al., 2021). As a result, extinction chronologies are often based on presence/absence data of a single taxon (Lima-Ribeiro and Diniz-Filho, 2014), whilst detailed extinction chronologies are not available for the majority of species (Price et al., 2018, Saltré et al., 2019, Johnson et al., 2021, Price et al., 2021). Similarly, reports of human-megafauna overlap are also often based on the presence of only a single megafauna taxon, which further fuels the debate about a possible period of human-megafauna overlap.

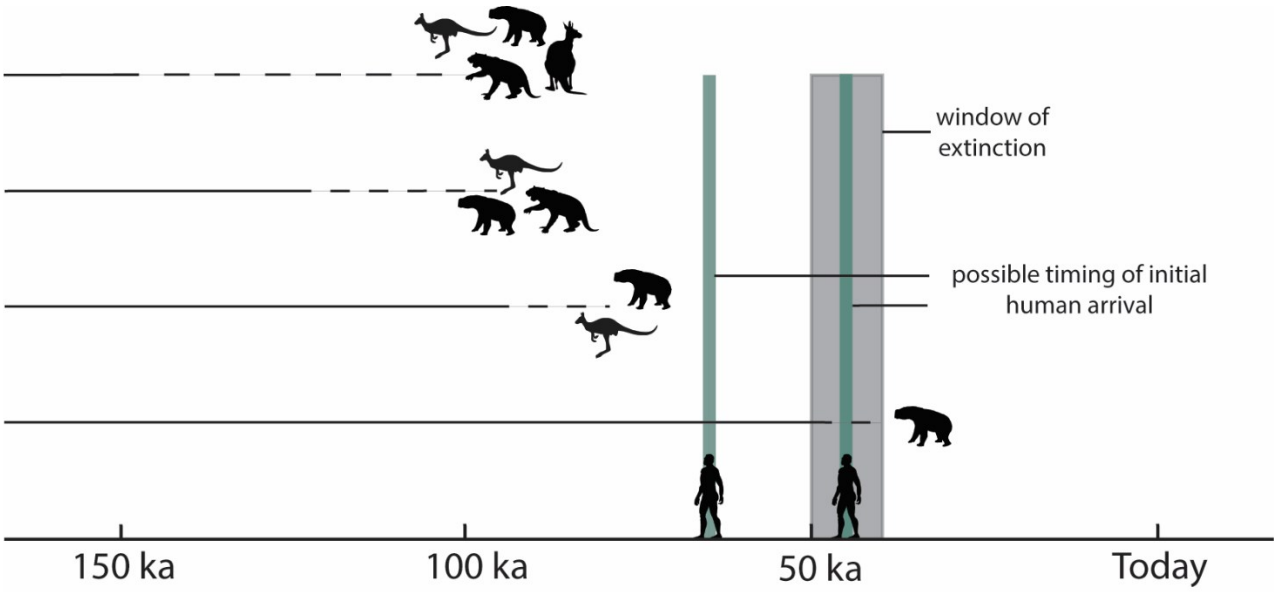

Figure 2.2: Schematic overview of the extinction of megafauna in Australia in relation to human arrival to the continent (data from Wroe et al., 2013, Clarkson et al., 2017).

2.1.2. Causes of extinction - Competing hypotheses

There is also, as in other regions of the world, an extended debate surrounding the cause of the late Quaternary megafaunal extinctions in Australia. Several hypotheses have been put forward to explain the extinction event for Sahul specifically: 1) humans were directly responsible through direct predation of megafauna (e.g. Brook and Johnson, 2006, Turney et al., 2008, Johnson et al., 2016, Miller et al., 2016, Van der Kaars et al., 2017); 2) humans were indirectly responsible through habitat alteration using novel fire regimes (e.g. Bowman and Prior, 2004); 3) climate change (e.g. Trueman et al., 2005, Wroe et al., 2013, Tyler Faith et al., 2017, Hocknull et al., 2020); and 4) a synergy between human impacts and climate change (Miller et al., 2005, Saltré et al., 2016). An extensive review surrounding these hypotheses is outside of the scope of this chapter (see Johnson et al., 2021) for a recent, in-depth review

on this topic). The major hypotheses and main supporting arguments are briefly discussed below, however.

Overkill hypothesis

The overkill hypothesis states that Sahul's megafauna went extinct rapidly following human colonization of Sahul as a result of massive overhunting. Overhunting of megafauna by humans is hypothesized to have resulted in population crashes for many now-extinct megafauna species (Flannery, 1990, Brook and Johnson, 2006). The key argument supporting the overkill hypothesis is the apparent widespread extinctions that immediately followed initial human colonization in many regions of the world (Martin, 1967). Megafauna in these regions were thought to be naïve to human hunters and thus easy to kill, since they evolved in the absence of people (Flannery, 1994). These arguments were further strengthened by the seemingly short period of human-megafauna overlap in Australia, which is sometimes argued to be the result of rapid human impacts (Wroe et al., 2013). The most compelling line of evidence for direct human exploitation of megafauna comes from the presence of burnt *Genyornis* eggshell fragments dating to ca. 50 ka, which has been interpreted as evidence for the human harvesting and subsequent cooking of the eggs (Miller et al., 2016). The taxonomic origin of these eggshell fragments was long contested, until recent palaeoproteomic analysis was able to attribute them to *Genyornis newtoni*, an extinct giant flightless bird (Demarchi et al., 2022b).

Nonetheless, beyond this, a direct archaeological association between human occupation and extinct megafauna is mostly absent from the Australian fossil record. Mass hunting events have not been recorded in the Australian archaeological record and obvious big game weapons are also absent at the time of the extinction period (Saltré et al., 2016). Other evidence of human predation or consumption of megafauna, such as cut marks, is rare (Davidson, 2013, Wroe et al., 2013), and no unequivocal kill-sites have been recorded in the archaeological record (Wroe and Field, 2006, Field et al., 2008). The sparse evidence that does exist for human-megafauna interaction, at Cuddie Springs (Field et al., 2001) and Devil's Lair for example, is often contested. At Cuddie Springs, the stratigraphic integrity and chronology of the deposits are questioned. Site disturbance and sediment mixing are alternatively proposed to explain the co-occurrence of megafauna fossils with archaeological material at the site (Roberts et al., 2001, Gillespie et al., 2006). At Devil's Lair, megafauna bones were recovered from the lowermost stratigraphic units, but the distinct taphonomic appearance of these bones differs from the other faunal material recovered from the cave, indicating that the megafauna bones were most likely washed in, and are not in their primary deposition (Dortch, 1979). Furthermore, the potential early scenarios of human occupation of Sahul at ca. 65 ka (Clarkson et al., 2017), although still debated, would significantly increase the window of human-megafauna overlap, and thus enhances the possibility of human hunting to have contributed to the demise of megafauna on Sahul.

Indirect human impact

A further set of hypotheses argues that humans had more diffuse impacts on megafaunal populations in the form of more prolonged periods of exploitation and habitat modification (e.g. Miller et al., 2005, Bird et al., 2013). It is well-known that the arrival of humans in novel ecosystems can lead to species extinction, extirpation and population decline resulting from ecosystem change, habitat loss, fragmentation, and degradation, and shifts in land use caused by anthropogenic activities (Dirzo et al., 2014, Boivin et al., 2016). The most commonly mentioned process of ecosystem transformation by early humans in Australia is increased fire frequency through the introduction of novel fire regimes, such as fire-stick farming (Bowman and Prior, 2004, Miller et al., 2005). Increased fire frequency could lead to the reduction of forest cover (David et al., 2021) and an increase in shrubs and grasses (Bird et al., 2013). Such vegetation changes would positively impact grazers, while having a negative impact on the distribution of browsing animals (Webb, 2013), which would have included many now-extinct megafaunal species. Humans are thus argued to be indirectly responsible for the extinctions via

prolonged periods of exploitation, and human-induced habitat loss and vegetation change, ultimately leading to bottom-up trophic cascades (Llewelyn et al., 2022).

However, charcoal records show little evidence of changes in fire frequency during the Late Pleistocene. Even if changes would have been recorded, these could also be explained by climatic changes (Johnson et al., 2021). Furthermore, there is often no direct association between changes in charcoal frequency, human arrival, and megafaunal remains (Johnson et al., 2021). Cuddie Springs is currently the only site at which charcoal records have been directly associated to megafaunal remains, but no changes in fire frequency were recorded, and evidence of human-megafauna overlap at the site is also contested (Field et al., 2008). Furthermore, some megafaunal species that went extinct are unlikely to have been significantly affected by changes in fire frequency (Johnson et al., 2021). Finally, while sites such as Madjedbebe may hint at a prolonged period of human-megafauna overlap in at least some parts of Australia, these longer chronologies still remain somewhat debated, something that would undermine the possibility of long-term, diffuse human impacts to have significantly contributed to megafauna extinctions in Sahul.

Climate change

The third hypothesis claims that climatic and environmental change played a significant role in the extinction of Australian megafauna (e.g. Trueman et al., 2005, Wroe et al., 2013, Tyler Faith et al., 2017, Hocknull et al., 2020). The Late Quaternary period in Australia can be characterized as a long period of deteriorating environmental conditions starting ca. 450 ka and ending with the Last Glacial Maximum (LGM) ca. 20 ka (Yokoyama et al., 2000, Wroe et al., 2013). This long-term trend resulted in a steady increase in aridity on Sahul during the last 300 ka (Wroe and Field, 2006, Murphy et al., 2012). The interval from 100-60 ka was particularly characterized by a sharp increase in aridity (Black et al., 2012) resulting in an increase in woody herbaceous shrubs (Van der Kaars et al., 2017), and a decrease in the availability of C_4 vegetation reliant on warm, wet conditions (DeSantis et al., 2017), as well as a decrease in the availability of drinking water (Johnson, 2006). These changes likely had a negative effect on many megafaunal species, and would fit well with a suggested step-wise extinction event. Aridification and vegetation change may have led to resource competition between species, significantly impacting already vulnerable animals (DeSantis et al., 2017) and catalyzing trophic cascades (Llewelyn et al., 2022).

These climatic and environmental changes have also been used to explain extinctions on a regional scale. In eastern Australia, for example, megafauna extinctions have been shown to coincide with deteriorating hydroclimate conditions (Hocknull et al., 2020). However, environmental deterioration alone might not be able to explain the extinctions across all of Sahul's highly varied environmental contexts. The effect of climatic changes that occurred during the Pleistocene is different between ecosystems and also had different levels of impact on the fauna within them (Black et al., 2012). In some regions, such as the highlands of New Guinea, precipitation levels remained relatively stable, or in some cases even increased (Johnson, 2006, Barrows et al., 2020). Furthermore, there is no compelling evidence that climatic changes during the window of extinction were more severe than previous climatic fluctuations in the Pleistocene which these animals had successfully endured (Gillespie, 2008), and some taxa, short-faced kangaroos for example, were well-adapted to the arid conditions under which they evolved (Prideaux, 2004). This highlights the need for taxon-specific approaches which consider the specific dietary and environmental preferences of taxa (Price et al., 2018).

2.2. Moving beyond megafauna – Extinctions during the Holocene

The extinction of Australia's largest animals was followed by a major vegetation change characterized by a loss of forest cover and increase in sclerophyll vegetation in many regions. This is one of the direct results of the loss of large herbivores from the landscape and a changing fire regime (Johnson, 2009,

Rule et al., 2012). The loss of megafauna on the continent also led to a loss of ecosystem function. Megafauna are keystone species and play many pivotal roles in the maintenance of ecosystems (Galetti et al., 2018). The removal of megafauna from the landscape can thus have major effects on trophic structure (Malhi et al., 2016), biogeochemical cycling, nutrient recycling (Doughty et al., 2013, Doughty et al., 2016), and microbe, parasite (Doughty et al., 2020) and seed dispersal (Johnson, 2009, Spengler et al., 2021). At the same time, the period following megafauna extinctions is marked by the unambiguous presence of humans across much of the continent. The end of the Pleistocene also witnessed an increase in sea levels, temperature and precipitation. Sahul was once again submerged and geographic barriers between Papua New Guinea, mainland Australia, and Tasmania resurrected (Bellwood and Hiscock, 2013).

The faunal diversity of mainland Australia remained stable throughout most of the Holocene. However, a major shift occurred during the mid-late Holocene (ca. 3200 years BP) when the thylacine (*Thylacinus cynocephalus*) and Tasmanian devil (*Sarcophilus harrisii),* Australia's largest marsupial carnivores to have survived the Late Pleistocene extinction event, as well as the Tasmanian native hen (*Gallinula mortieri*), were extirpated from mainland Australia. These animals were widespread across mainland Australia during the Pleistocene, but after the mid-late Holocene only persisted on the island of Tasmania (Letnic et al., 2014, White et al., 2018b). Many other endemic species also underwent significant population decline and range reductions at this time (Johnson, 2006). While these extinctions and range declines are often considered to have a common cause (White et al., 2018b), there is much debate about the exact drivers behind the decline of endemic species during the Holocene. A number of hypotheses have been put forward to explain the extinctions: a) the introduction of the dingo (Wroe et al., 2007, Letnic et al., 2012), b) human intensification (Lourandos, 1997, Johnson and Wroe, 2003), c) climatic and vegetation changes (Brown, 2006), or d) a combination of these factors (Brüniche–Olsen et al., 2018).

2.2.1. The introduction of the dingo

The range reduction and extirpation of endemic species shortly followed the arrival of the dingo on mainland Australia (Woinarski et al., 2015). The earliest evidence for the presence of dingo (*Canis lupus* dingo) in Australia dates to ca. 3300-3000 years ago (Balme et al., 2018). Dingoes are often assumed to have been brought in from Southeast Asia as a commensal animal for companionship, protection, and hunting (Balme and O'Connor, 2016). Following their introduction, dingoes quickly became widespread across mainland Australia, although they never became established on Tasmania (Johnson, 2006).

The exact role of the dingo in the extirpation of the thylacine, Tasmanian devil, and Tasmanian native hen is contested. One key argument highlighting the role of dingo, is the survival of these species on Tasmania, where the dingo was absent. Some scholars argue that dingoes played a direct role in these extirpations (Baird, 1991) via competition for prey (Wroe et al., 2007) or direct predation (Letnic et al., 2012). Dingoes, Tasmanian devils, and thylacines occupy similar ecological niches. However, dingoes are cooperative hunters, are more opportunistic feeders with a more diverse diet, have a larger body-size, and have higher reproductive rates. Because of these competitive advantages, dingoes could have outcompeted endemic predators (Brüniche–Olsen et al., 2018). Dingoes may also have indirectly contributed to the extirpations through the introduction of novel diseases (Brüniche–Olsen et al., 2018). Even though dingoes directly competed with endemic predators for food resources, multispecies modelling has shown that their contribution to the extirpation of endemic species on mainland Australia was not necessarily substantial, and that they are unlikely to have been the sole drivers of the extirpations (Prowse et al., 2014).

2.2.2. Human intensification

Other scholars instead argue that an intensification of human activities was the main factor behind the extirpation of these two marsupial carnivores and decline of other endemic species (Johnson and Wroe, 2003). Human population density started to increase on mainland Australia during the Holocene. In this period, a wide variety of novel, advanced stone tool technologies were introduced, as well as wood, bone and shell tools. Furthermore, a more sedentary lifestyle was adopted and exploitation strategies became more diverse (Johnson and Brook, 2011, Bellwood and Hiscock, 2013). There was an increased level of social complexity and trade, evidenced by pigment use and the presence of rock art depictions, and an increased number of personal ornaments recovered from the archaeological record (Langley et al., 2011, Langley et al., 2019). These materials were exchanged in long-distance trade networks with distances of up to 300 km (Balme and Morse, 2006). During the Holocene there was also a shift in resource exploitation to include a wider range of resources, such as the exploitation of marine resources (Johnson and Wroe, 2003, Dortch, 2004). Zooarchaeological assemblages from Holocene rock shelters also show an increase in the exploitation of small mammals by Aboriginal communities, while exploitation of large-sized mammals decreased (Dortch, 2004, Dortch and Wright, 2010). Although this would have decreased pressured on large herbivores (e.g. kangaroos), it could have increased competition over food resources with medium-sized carnivores, such as the thylacine and Tasmanian devil.

Human population density on mainland Australia markedly increased during the Late Pleistocene and Early Holocene. It has been proposed that this increase of population density, combined with the adoption of new hunting technologies, led to increased hunting pressure that could have resulted in significantly reduced population sizes of many endemic species (Lourandos, 1997, Johnson and Wroe, 2003), including the carnivore species now extirpated from mainland Australia. In comparison, human population sizes in Tasmania remained low during the Holocene and clear technological changes were also absent (Lourandos, 1997, Johnson and Wroe, 2003); a key argument to explain why these species persisted on Tasmania. In addition to the recovery of advanced tool technologies from archaeological deposits, further (indirect) evidence for hunting comes from rock art depictions of people hunting prey, which has been interpreted as thylacine hunting scenes (Johnson and Wroe, 2003). Furthermore, a necklace made of Tasmanian devil incisors has been recovered from a burial site, indicating that humans may have hunted Tasmanian devils for ceremonial purposes (Johnson and Wroe, 2003).

Human intensification is also associated with a change in fire regime during the Holocene, with an overall increase in fire frequency on the landscape. Indigenous people used small-scale fire-stick burning to manage vegetation cover, increase vegetation growth, fertility, and productivity of the landscape, and to facilitate hunting (Gott, 2005, Hallam, 2014). This could result in a vegetation mosaic of woody vegetation contrasted by relatively open savannah-like grasslands (Mariani et al., 2022). Alternatively, in some regions, it has also been proposed that the increase in fire frequency was the result of the loss of megafauna during the Late Pleistocene, which led to an increase of fire fuel on the landscape (Rule et al., 2012).

2.2.3. Climate change

Finally, climate change has also been proposed as a possible driver of these Holocene extirpations. The mid-Holocene was a period of relative climate stability, with overall high rainfall and high temperatures. However, the period from 5-3 ka BP was marked by an increase in the intensity of ENSO (El Niño Southern Oscillation), leading to climate instability, increased aridity, and vegetation changes (Petherick et al., 2013, Reeves et al., 2013).

Ancient DNA studies have shown that there was a population bottleneck in both Tasmanian devil (Brüniche-Olsen et al., 2014, Brüniche–Olsen et al., 2018) and thylacine populations (Menzies et al., 2012, White et al., 2018a) in mainland Australia and Tasmania in the period over which the last mainland

populations of these species went extinct. Brüniche–Olsen et al. (2018) argue that climate change related to increased ENSO activity is the only common factor between these two species, populations, and regions. They hypothesize that the mainland extirpations were multi-causal, since mainland populations were affected by the introduction of the dingo, human intensification, and the effects of climate change, while the Tasmanian population was only impacted by the effects of climate change (Brüniche–Olsen et al., 2018). A recent modelling study also rejects climate change as the sole driver in the Holocene extinction of the Tasmanian devil on mainland Australia (Morris et al., 2022).

2.3. Species introductions – Extinctions following European colonization

A final extinction wave in Australia started shortly after European colonization of the Australian continent. From the onset of 1788, many Australian animals experienced significant range reductions. A number of species, such as the Western Barred bandicoot (*Perameles bougainville*), the Rufous hare-wallaby (*Lagorchestes hirsutus*), and the burrowing bettong (*Bettongia lessueur*), amongst others, now exclusively inhabit small islands off the Australian coast as final surviving relic populations. In addition, over 50 animal species went extinct in the last 200 years following European colonization. These extinctions included 28 land mammals endemic to Australia, including small rodents (e.g. the Darling Downs hopping mouse, *Notomys mordax)*, bandicoots (e.g. the desert bandicoot, *Perameles eremiana*), macropods (e.g. the Toolache wallaby, *Macropus greyi*, the central hare-wallaby, *Lagorchestes asomatus*, and the crescent nail-tail wallaby, *Onynchogalea lunata*), and perhaps most notoriously, the extinction of the final thylacine populations on Tasmania (Webb, 2013, Woinarski et al., 2015, Woinarski et al., 2019, Sheppard and Glanznig, 2021).

Many, but not all, of these now-extinct species were widespread and abundant prior to European colonization and inhabited a wide range of habitats (Woinarski et al., 2015). A number of possible drivers have been implicated in the Late Holocene extinctions. None of these extinctions can clearly be attributed to a single cause, and there are likely differences in causes for different species that went extinct. It is clear, however, that these extinctions are ultimately the result of human interference. While there is still debate about the details underlying modern extinctions in Australia, there is overall consensus that the introduction of non-native species, the marginalization of Indigenous land management practices, such as fire-stick burning, and the introduction of new European ideas of land use, were the main drivers of these extinctions (Webb, 2013, Woinarski et al., 2015).

2.3.1. Introduction of non-native species

It has been proposed that the introduction of non-native species, such as cats, foxes, rabbits, and rats had a deleterious effect on Australia's endemic fauna. The timing of the introduction and subsequent spread of cats and foxes on mainland Australia coincides broadly with endemic species declines observed in Australia in the 1800s and 1900s (Woinarski et al., 2015), and these two introduced predators have clearly played a significant role in the decline of Australia's endemic fauna. The majority of the species that went extinct in the last 200 years were relatively small in size, and were foragers that spent most of their time on the ground, therefore making them ideal prey for these two introduced predators (Woinarski et al., 2015). Historical records have also shown that the introduction of these predators in novel ecosystems, often leads to a rapid decline in endemic fauna (Burbidge and Manly, 2002, Hanna and Cardillo, 2014). Interestingly, the geographical range of cats and foxes in Australia is almost a perfect match to the geographical range of many now-extinct animals (Johnson, 2006) and, up until this day, predation by cats and foxes is one of the most important drivers of extinction risk for Australian fauna (Woinarski et al., 2015), posing a great problem for programs aiming to reintroduce locally extirpated species (Johnson, 2006).

The introduction of other non-native animals, such as mice, rats, and rabbits, negatively impacted endemic populations by competition for resources. For example, the European rabbit (*Oryctolagus cuniculus*) was introduced to Australia by early settlers in 1788. Rabbits quickly became established in

settlements across the country, until their population size increased significantly and they quickly spread all over the continent in the 19th century (Alves et al., 2022). Rabbits are now one of the most widespread pest animals in Australia and they represent one of the largest recorded biological invasions in recent history (Fenner, 2010, Alves et al., 2022). Next to competition for resources, the introduction of non-native species may have also had indirect effects on endemic animal populations. For example, the introduction of novel diseases and parasites through cats and foxes has been suggested to have played a role in the major decline in quoll populations (Peacock and Abbott, 2014). There have also been instances of the bubonic plague, being spread by infected rats, infecting and killing endemic species (Peacock and Abbott, 2014).

2.3.2. Pastoralism

The arrival of Europeans also brought the introduction of livestock animals, mostly cattle and sheep, for farming. The introduction of domestic animals was associated with land clearing practices and changes in land use, which also had detrimental effects on endemic species. The large-scale grazing pressure that came with the introduction of livestock animals has been argued to have led to overall soil and habitat degradation, loss of vegetation cover, range reduction, and competition with endemic species over resources (Letnic, 2007, Woinarski et al., 2015). Extensive grazing also resulted in a shift in vegetation. Plant species that are often consumed by livestock species decreased in abundance, while plant species unaffected by the new grazers increased in abundance (Hacker and McDonald, 2021). The direct effects of large-scale grazing and trampling are most evident in close proximity to watering points (rivers, lakes and artificial water stations), where livestock animals cluster together (Letnic, 2007).

Much of the fertile land in Australia is now in use for pastoralism, which has also resulted in habitat loss and fragmentation for endemic species. This is primarily the result of anthropogenic barriers that are part of farming infrastructure, such as watering points and fences. These barriers prevent endemic species from passing through, and thus break their habitat up into smaller areas (Letnic, 2007, Hacker and McDonald, 2021). Further detrimental to endemic animals are attempts to control populations of pest species. For example, the usage of poison baits to control the size of rabbit populations also killed a large number of endemic animals (Letnic, 2007).

2.3.3. Marginalization of indigenous land management practices

European colonization of Australia was also followed by a marginalization of Indigenous land management practices, with the potential for significant vegetation shifts as a result. As discussed in section 2.2.2, Indigenous people managed landscapes by small-scale fire-stick burning. The marginalization of these management practices led to a rapid shift from open savannah-like grasslands to more forested, covered areas with an increased contribution of shrubby, sub-canopy vegetation (Fletcher et al., 2021, Mariani et al., 2022). This negatively impacted biodiversity (Schuster et al., 2019), particularly impacting fauna well-adapted to open forests such as tree kangaroos (Roberts et al., 2021). The increase of available biofuel on the continent also led to a shift in fire regime across the continent increasing the frequency and intensity of wildfires (Fletcher et al., 2021, Mariani et al., 2022).

2.3.4. Direct human impacts

Direct human impacts have, of course, been proposed as another important factor leading to the extinction, extirpation and range reductions of endemic species over the past 200 years. Humans directly impacted endemic species by controlling populations of introduced pest animals through trapping, shooting, and poisoning, as well as hunting endemic animals for food and fur trade (Peacock and Abbott, 2014). Perhaps the best-known species that went extinct in the last 200 years is the thylacine (*Thylacinus cynocephalus*), the largest marsupial carnivore upon European colonization of Australia. At the time of

European colonization, the thylacine solely inhabited Tasmania, as it was previously extirpated from mainland Australia during the mid-Holocene (Woinarski et al., 2015). As opposed to many of the other species that went extinct, or experienced significant range reduction following European colonization, the thylacine was actively hunted to protect sheep pastoralism, leading to its extinction in 1936 (Menzies et al., 2012).

2.4. The potential of palaeoproteomics

This temporal review identifies the current gaps in knowledge and identifies key regions in which palaeoproteomics can contribute to address questions about faunal turnovers in Australia in the past. First, ZooMS has the potential to address questions about extinctions and extirpations in the past (from Pleistocene extinctions up to recent extinctions and extirpations) by increasing the number of identified specimens for a given species. The availability of an increased number of specimens through the identification of fragmented remains can help address spatial questions, while simultaneously informing us about the biogeography of these animals in the past. For example, many Late Pleistocene megafauna species have only been identified at a small number of sites, which significantly limits our understanding of their palaeobiogeography (Price et al., 2018, Swift et al., 2019).

Furthermore, coupled with exact dating techniques such as radiocarbon and U-series dating, questions concerning extinction chronology can be tackled. This would be particularly useful in the absence of clear extinction chronologies, as is the case for the Late Pleistocene extinctions. Similarly, ZooMS coupled with stable isotope analysis has the potential to identify fragmented specimens for subsequent isotope analysis which can aid our understanding of megafauna ecology and dietary habits. For example, *Palorchestes azael*, the marsupial tapir, is thought to have been a highly specialized browser based on their limb bone morphology and dental microwear analysis (DeSantis et al., 2017, Richards et al., 2019). Stable isotope analysis could help shed more light on the diet of these now extinct animals. By addressing these three major knowledge gaps, ZooMS can indirectly be used to address questions about the factors contributing to extinctions and extirpations in the past.

ZooMS can also help address questions concerning shifts in faunal diversity through time. One of the major challenges associated with studying faunal assemblages in Australia is the high fragmentation rates of osseous material. In Manuscript C, a combined approach utilizing both ZooMS and zooarchaeology is used to get a more holistic understanding of shifts in faunal diversity in the past through the combined study of fragmented and unfragmented remains from the same assemblage. Similarly ZooMS can aid our understanding of past subsistence strategies. In Manuscript A, new insights into the subsistence strategies of Aboriginal labourers at a colonial pearling station on Barrow Island, Western Australia, are presented. This revealed that the labourers at the site exploited green sea turtle in addition to local terrestrial resources. Both these studies highlight the potential of ZooMS as a tool to complement Australian zooarchaeological investigations. Finally, studies aiming to track the introduction of non-native species, the introduction of the dingo in the Late Holocene or more recent introductions, for example, can benefit greatly from the inclusion of ZooMS. While it is roughly known when non-native species were introduced to Australia, their spread across the country is often less well documented.

With an increasing number of palaeoproteomic studies focused on faunal diversity in the past, the potential of such studies to be of importance for present-day conservation and restoration strategies also increases. In Manuscript D, all existing palaeoproteomics studies that to some extent can be used to inform conservation efforts today are pulled together. This data is synthesized to identify what the key research areas in conservation are that palaeoproteomics has the most potential to address.

3. Methods used for this thesis

The study of ancient proteins preserved in the archaeological record originated in the 1950s when the presence of amino acids in fossils was first identified (Abelson, 1954). Initially, the presence of amino acids in fossils was used to determine their relative age through amino acid racemization (Hare and Abelsen, 1968, Schroeder and Bada, 1976). In the decades that followed, the identification of proteins in fossil material was first achieved through the detection of antibody-based immunoassays (Loy and Wood, 1989, Newman and Julig, 1989, Kooyman et al., 2001) and efforts to directly sequence proteins followed shortly after with the introduction of Edman sequencing, although these methods turned out not to be suitable for the study of ancient proteins due to issues with degradation, diagenesis, and contamination (Cappellini et al., 2014).

The major revolution in the study of ancient proteins came with the invention and adoption of soft ionization mass spectrometry-based approaches, first applied to ancient protein studies in 2000 by Ostrom et al. (2000). The introduction of mass spectrometry to the study of ancient proteins for the first time allowed the characterization of ancient proteins by the identification of peptides in a sample following enzymatic digestion. This development was the gateway to later advances in the field of palaeoproteomics, such as the development of peptide mass fingerprinting and shotgun palaeoproteomics.

3.1. Collagen structure and genetic diversity

Collagen is a structural protein that is one of the most abundant proteins in vertebrates (Shoulders and Raines, 2009, Ricard-Blum, 2011). There are just under 30 different collagen proteins that, in total, make up 25-35% of the entire mammal protein content. Collagen type I (COL1) is the most abundant collagen protein, accounting for ca. 80% of the entire bone proteome (Buckley, 2018, Henriksen and Karsdal, 2019), and it is the most abundant protein in bone, skin, tendons, ligaments, fish scales, antler, horn cores, and dentine.

COL1 is a fibrillar triple helical molecule that provides structural support to connective tissues. It is organized into a triple helix structure of three polypeptide chains, typically referred to as alpha-chains (COL1α chains). These COL1α chains bundle together to form collagen microfibrils which, in turn, bundle together to form collagen fibres (Shoulders and Raines, 2009). The primary structure of the COL1α chains is characterized by a repeating motif of three amino acids: G-X-Y. In this repeating sequence, every third amino acid is a glycine (Gly). This is the smallest amino acid that exists naturally, and it is the only one small enough to fit into the centre of the triple helix. Amino acids X and Y are often proline (Pro) and hydroxyproline (Hyp). These amino acids have the ability to form hydrogen bonds, which stabilize the triple helix structure (Shoulders and Raines, 2009, Ricard-Blum, 2011, Richter et al., 2022). The recurring G-X-Y pattern induces the helical structure of the COL1α chains that makes COL1 particularly robust (Buckley, 2018). For most vertebrate animals, COL1 is made up of three COL1α chains, two of which are identical and called alpha-1 chains (COL1α1), and one distinct alpha-2 chain (COL1α2) (Henriksen and Karsdal, 2019), while in fish COL1 has three unique alpha chains, COL1α1, COL1α2 and COL1α3 (Buckley, 2018).

COL1 is a highly conserved protein that has many important functions in bone development and remodeling (Richter et al., 2022). Because of the key function COL1 plays in bone formation, it is functionally constrained. There are restrictions as to which mutations can occur in the peptide sequence of COL1. For example, amino acids with large side groups prevent the formation of the triple helix structure, and therefore generally do not occur in COL1 (Richter et al., 2022). Similarly, mutations of the Gly residue in the centre of the triple helical structure of COL1 are particularly deleterious, and can result in *osteogenesis imperfecta*, for example (Shoulders and Raines, 2009). Because of these

restrictions, COL1 exhibits a slow rate of evolutionary change and accumulation of sequence mutations compared to other genes (Stover and Verrelli, 2010). Overall, the more evolutionary diverged species are, the larger the number of differences between their collagen sequences.

3.2. Zooarchaeology by Mass Spectrometry (ZooMS)

Zooarchaeology by Mass Spectrometry (ZooMS) is a method of peptide mass fingerprinting focused on bone collagen that was developed in 2009 by Buckley et al. (2009) as a screening method to taxonomically identify highly fragmented, morphologically unidentifiable bone fragments. ZooMS is a high-throughput approach that relies upon differences in the COL1 protein sequence between taxonomic groups to identify faunal remains. ZooMS is faster and cheaper than ancient DNA (aDNA)-based approaches (Buckley et al., 2009, Buckley et al., 2014, Welker et al., 2015b, Richter et al., 2020) such as DNA metabarcoding (Murray et al., 2013, Antonosyan et al., 2019, Seersholm et al., 2020, Seersholm et al., 2021), and the amount of starting material and the amount of collagen needed for successful extractions is lower than with radiocarbon dating or stable isotope analysis (Wang et al., 2021). The high-throughput and cheap costs of ZooMS makes the method better applicable to larger scale assemblages than many other biomolecular approaches. The major downside of ZooMS is that, because of the slow evolutionary rate of COL1, it has less taxonomic resolution compared to shotgun proteomic or aDNA-based approaches.

The last couple of years has seen an explosive increase in the application of ZooMS to identify faunal remains from archaeological sites (Brown et al., 2021a). This has resulted in an improved ability to reconstruct shifts in biodiversity over time (Rodrigues et al., 2018, Garrison et al., 2019, Harvey et al., 2019a), track the spread of domesticates (Taylor et al., 2018, Prendergast et al., 2019, Le Meillour et al., 2020, Culley et al., 2021, Taylor et al., 2021), identify ancient hominin remains (Brown et al., 2016, Welker et al., 2016, Brown et al., 2022), and provenance bone tools and objects (Desmond et al., 2018, Bradfield et al., 2019, Martisius et al., 2020). For example, the application of ZooMS has increased our understanding of the geographical distribution of the gray whale in the past, showing this species was widespread in the past including in the North Atlantic (Garrison et al., 2019) and Western Mediterranean (Rodrigues et al., 2018); much more widely spread than previously understood. ZooMS has also been used to track the introduction of domesticated caprines to the islands offshore of eastern Africa, revealing that goats were introduced to these islands one or two centuries before sheep. Simultaneously it was shown these animals were more widely spread than previously understood (Culley et al., 2021, Janzen et al., 2021). Besides the taxonomic identification of osseous materials, ZooMS can also be used to identify other collagenous materials encountered in the archaeological record, such as antler (Von Holstein et al., 2014, Ashby et al., 2015), ivory (Coutu et al., 2016, Coutu and Damgaard, 2019), leather (Brandt et al., 2014, Ebsen et al., 2019, Brandt et al., 2020), and animal skin parchment (Fiddyment et al., 2015, Teasdale et al., 2017, Ruffini-Ronzani et al., 2021).

3.2.1. Collagen extraction

There are multiple methodological approaches for extracting collagen for peptide mass fingerprinting (see Figure 2.1 for a general overview of the ZooMS workflow). Most widely used is a destructive approach, in which the first step is to demineralize a small bone sample of 10-20 mg using an acid (most commonly hydrochloric acid (HCl)) to free the collagen from the mineral matrix of the bone. Then, either the acid-insoluble (Buckley et al., 2009, Welker et al., 2015b) or the acid-soluble (Van der Sluis et al., 2014) collagen is extracted. The acid-insoluble protocol utilizes the bone shadow that is left after demineralization. The remaining acid supernatant is removed, after which the sample is washed to remove any remaining acid and other soil-derived humic acids that interfere with mass spectrometry. Then, the sample is heated to gelatinize the peptides in the sample, leaving the peptides in their primary structure to facilitate enzymatic digestion. The acid-soluble protocol instead utilizes the remaining acid

supernatant, from which the peptides are collected using ultrafiltration. Following these pre-treatment steps, the peptides in the sample are enzymatically digested (commonly using the protease trypsin). Trypsin is an enzyme commonly found in the small intestine and is part of the digestive system. It cuts the C-terminal collagen peptides after the amino acids arginine (R) and lysine (K), resulting in a range of collagen peptides with different masses. In the final step of the extraction, the peptides are purified and concentrated using C18 ZipTips, before being analyzed with a mass spectrometer. For a more detailed description of the extraction methods used for this thesis see the methods sections of Manuscripts A, B, and C.

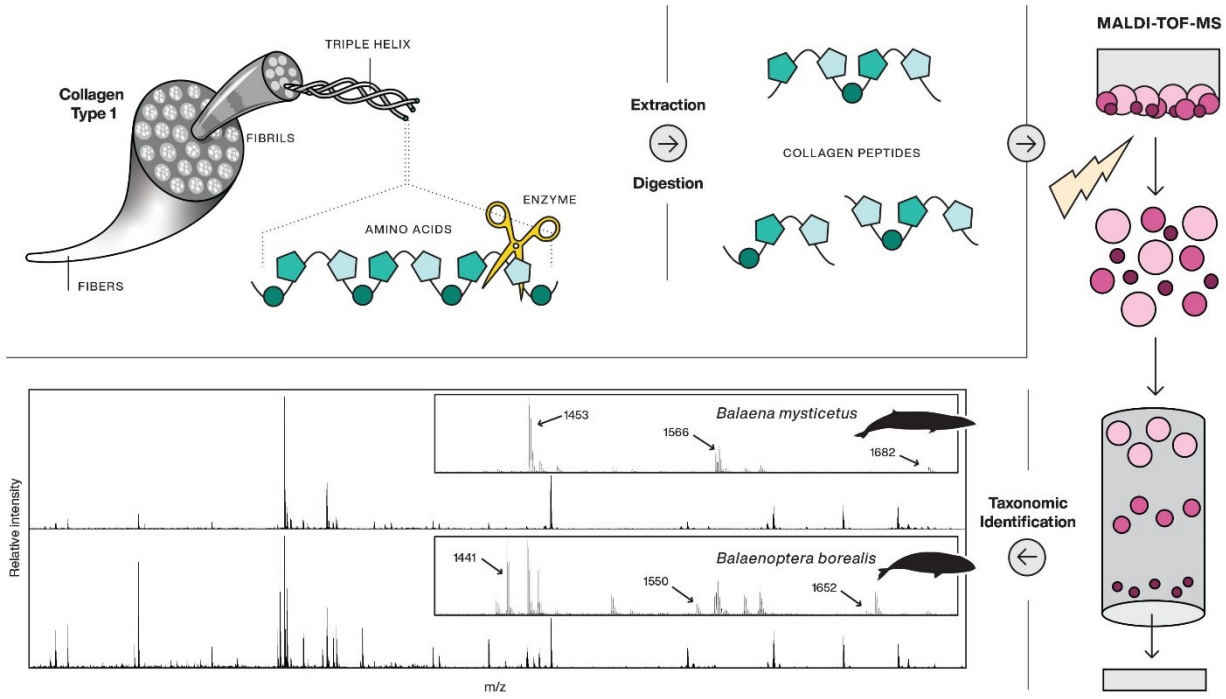

Figure 3.1: Overview of the ZooMS workflow. Image from (Manuscript D, Peters et al., 2022).

Minimally or non-destructive approaches to the extraction of collagen for peptide mass fingerprinting have also been developed, and are most often applied to the analysis of highly valuable bone tools and objects (McGrath et al., 2019, Jensen et al., 2020a, Martisius et al., 2020) and parchment (Fiddyment et al., 2015, Teasdale et al., 2017, Ruffini-Ronzani et al., 2021). First developed, was a protocol utilizing an ammonium bicarbonate (AmBic) buffer as an alternative to HCl to avoid demineralization of the bone (Van Doorn et al., 2011). Collagen proteins can also be extracted via eraser sampling, an approach that was first developed to extract collagen proteins from parchment (Fiddyment et al., 2015). The friction that is created by rubbing a PVC eraser against the material that is sampled generates triboelectric charge that captures the protein molecules from the surface (McGrath et al., 2019). Similarly, the friction between plastic sample bags and the bones in them also generates triboelectric charge, leading to the development of a non-destructive approach that analyzes collagen proteins from empty plastic sample bags that previously contained bone specimens of interest (McGrath et al., 2019). Although originally eraser sampling was thought to be a non-destructive technique, recently it has been shown that the rubbing of a PVC eraser on bone results in micro-striations on the bone surface that could impact the results of later use-wear analysis of the bone (Sinet-Mathiot et al., 2021). Overall, non-destructive approaches are best-suited to bones with good collagen preservation, while the acid-based approaches are better suited for the analysis of bones with lower levels of collagen preservation (Sinet-Mathiot et al., 2021, Wang et al., 2021).

3.2.2. MALDI-ToF-MS and taxonomic identification

The extracted collagen is analyzed using a Matrix-Assisted Laser Desorption/Ionisation Time of Flight mass spectrometer (MALDI-ToF-MS) (Figure 2.1) to obtain peptide mass fingerprints. The samples are first spotted onto a stainless-steel target plate and co-crystalized with an energy-absorbent matrix. The stainless-steel target plate is then inserted into the MALDI-ToF-MS. Each sample spot is hit with a laser beam to vaporize and ionize the peptides. The ionized peptides are then accelerated into the machine with electromagnets and they are separated based on the time it takes for them to hit the detector at the other end of the flight tube; their time of flight. Heavier peptides take longer to travel through the flight tube than lighter peptides. This is reflected in the resulting mass spectrum in which time is converted to mass-to-charge (*m/z*) ratios. For a more detailed description of the extraction methods and MALDI-ToF-MS machine settings used for this thesis see the methods sections of Manuscripts A, B, and C.

The *m/z* ratios observed in the MALDI-ToF-MS are compared against a reference database of known taxa. Comparison of the sample with established peptide markers allows for the taxonomic identification of the sampled bone fragments. Medium- to large sized-mammals are best represented in the existing reference database (out of 400 taxa for which peptide markers currently exist, 184 are represented by medium- to large-sized mammals) although in recent years peptide markers have been developed for additional taxonomic groups such as micromammals (Buckley et al., 2016, Prendergast et al., 2017, Buckley and Herman, 2019, Harvey et al., 2019a, Buckley et al., 2020), fish (Richter et al., 2011, Harvey et al., 2018, Richter et al., 2020), birds (Eda et al., 2020, Codlin et al., 2022), amphibians (Buckley and Cheylan, 2020), and reptiles (Harvey et al., 2019b). Notably, marsupials are still mostly absent from this database limiting the potential of ZooMS studies in Australia to date. Manuscript A seeks to address this gap by providing new ZooMS peptide markers for a large number of Australian marsupials to allow ZooMS studies in Australia with research questions other than the presence/absence of domesticated animals.

Because ZooMS is based on sequence differences of COL1 between species, the degree of taxonomic specificity that can be reached with ZooMS is dependent on the phylogenetic distance between taxa (Hendy, 2021). In most cases, it is possible to differentiate between families and genera, while differentiating between species can be more challenging. ZooMS is, for example, not able to separate between a number of bovid species (Janzen et al., 2021), or between the North Atlantic right whale (*Eubaleana glacialis*) and bowhead whale (*Balaena mysticetus*) (Buckley et al., 2014), as these species are too closely related. Similarly, it is not possible to differentiate between domesticates and their wild progenitors using ZooMS (Buckley et al., 2010).

Originally, eight peptide markers (labelled A-G) were selected to make taxonomic identifications using ZooMS (Buckley et al., 2009). Over the years, many more taxon-specific peptide markers have been reported with a range of different reported names. Recently, a standardized nomenclature system has been introduced for the reliable and consistent naming of peptide markers across taxonomic groups (Brown et al., 2021a). According to this new nomenclature system, ZooMS peptide markers are labelled according to the collagen gene on which the peptide is located and their position in the gene (Brown et al., 2021a).

3.3. Shotgun palaeoproteomics and *de novo* sequencing

In contrast to peptide mass fingerprinting, which targets the most frequently occurring peptides in a sample, shotgun proteomics allows for the analysis of the complete proteome; the entire set of proteins represented in a single tissue, organism, or genome. A proteome can consist of hundreds to thousands of proteins and depends on the tissue of origin that is being examined (Hendy et al., 2018c). With shotgun proteomics, all peptides present in a sample are analyzed using Liquid Chromatography tandem Mass Spectrometry (LC-MS/MS), which greatly increases the acquired resolution. A wide range of materials is suitable for shotgun palaeoproteomic studies including, but not limited to, bone (Buckley et

al., 2011, Cappellini et al., 2012, Welker et al., 2015b), dentine and enamel (Cappellini et al., 2019, Welker et al., 2019, Welker et al., 2020), dental calculus (Warinner et al., 2014a, Hendy et al., 2018b, Wilkin et al., 2021), textiles (Li et al., 2015, Gong et al., 2016, Solazzo, 2019), and ceramic residues (Solazzo et al., 2008, Hendy et al., 2018a, Shevchenko et al., 2018).

The identification of peptides with MS/MS is achieved in two fragmentation steps. In the first fragmentation step, the *m/z* values of the peptides in the sample (the parent ions) are determined in the first mass analyzer. The peptides that occur most frequently are automatically selected and further fragmented (the daughter ions). The *m/z* of these daughter ions is measured in a second mass analyzer, the second fragmentation step. The peptide sequence of the parent ion can then be inferred through the reconstruction of the mass shifts that occur in the daughter ions (Hendy, 2021). The resulting amino acid sequences are then matched to a known protein reference, which is generally derived from the annotation of a known genome sequences database, to identify the peptides present in the sample, which protein they originate from, and their taxonomic origins.

The higher resolution that can be obtained with shotgun palaeoproteomics means that the method can reliably be used to detect the range of proteins in complex mixtures, increasing the amount of information that can be derived from a single sample. Shotgun palaeoproteomics can thus be used to address a wider range of archaeological questions. For example, shotgun palaeoproteomics has been employed to reconstruct past diets (Geber et al., 2019, Maixner et al., 2021, Scott et al., 2021), investigate health and disease in the past (Warinner et al., 2014b, Barbieri et al., 2017, Jersie-Christensen et al., 2018, Fotakis et al., 2020), sex skeletal remains (Stewart et al., 2017, Lugli et al., 2019, Parker et al., 2019), and detect post-translational modifications at specific locations in the peptide sequence (Van Doorn et al., 2012, Ramsøe et al., 2020). Shotgun palaeoproteomics can also be used to reconstruct protein sequences of extinct species. These reconstructed sequences can subsequently be used to reconstruct phylogenetic relationships, which is particularly beneficial in the absence of aDNA (Rybczynski et al., 2013, Welker et al., 2015a, Welker et al., 2017, Buckley et al., 2019, Cappellini et al., 2019, Welker et al., 2019, Buckley et al., 2020, Welker et al., 2020). However, sample preparation, extraction, and data analysis of shotgun palaeoproteomics studies are much costlier and more time-consuming than it is with ZooMS, which is reflected in the number of samples that can be analyzed.

3.3.1. *De novo*/error tolerant sequencing

Due to its higher resolution, shotgun palaeoproteomics can also be used to obtain peptide sequences that are not represented in the available reference databases. This is achieved through *de novo* or error tolerant sequencing; an approach that is especially valuable in the absence of aDNA survival and when no suitable protein database is available. Instead, a reference database of phylogenetically closely-related species is utilized. With *de novo* or error tolerant sequencing, novel peptide sequences are directly inferred from the MS/MS data from the product ion spectra by calculating the mass difference between its daughter ions. This ultimately allows for the identification of single amino acid polymorphisms (SAPs) compared to the reference sequences in the used database.

For the scope of this thesis, shotgun palaeoproteomics has been used specifically for error tolerant sequencing to reconstruct peptide sequences of extant and extinct Australian species for which genomic information and collagen peptide sequences were not yet available. Extracted collagen peptides for ZooMS were further analyzed with LC-MS/MS to obtain novel peptide sequences with error tolerant sequencing. This data was subsequently used to develop and confirm ZooMS peptide markers for the targeted species. For a more detailed description of the MS/MS machine settings and error tolerant sequencing methods used for this thesis see the methods section of Manuscript A.

3.4. Protein preservation

Ancient proteins are generally better preserved in archaeological contexts than ancient DNA (aDNA). Proteins preserve for longer periods of time than aDNA (Rybczynski et al., 2013), and are more resistant to degradation in harsh environments, such as hot, humid, and tropical contexts (Buckley et al., 2009, Demarchi et al., 2016). As of yet, the oldest collagen peptides that have been identified in the palaeoanthropological record were extracted from a High Arctic camel dating back to 3.4 million years ago (Rybczynski et al., 2013), while the oldest surviving peptide sequence identified in a palaeoanthropological context belongs to an ostrich eggshell fragment from Laetoli, Tanzania, dating back to 3.8 million years ago (Demarchi et al., 2016). In Australia, the oldest peptide sequences recovered originate from *Genyornis* eggshell and date to ca. 50 kyr ago (Demarchi et al., 2022b). However, although peptides have successfully been recovered from eggshell dating to the Late Pleistocene, proteins bind differently to eggshell than to bone (Demarchi et al., 2016). Manuscript B aims to provide more insight into the preservation potential of collagen in bone in Australia through the analysis of osseous material from a variety of assemblages across time and space, and to identify the limits of ZooMS in Australian contexts.

The preservation of collagen in archaeological contexts is highly variable between sites because the rate in which collagen degrades over time varies between archaeological contexts due to a variety of different factors (Collins et al., 2002, Sponheimer et al., 2019). The rate of protein degradation depends on the chemical and environmental characteristics of the burial context. Proteins in substrates such as bone, dental calculus and eggshell are generally better preserved than proteins in other substrates, and closed systems are better suited for the preservation of proteins than open systems (Demarchi et al., 2016). In bone, collagen is preserved in the mineral matrix of the bone, which protects it against degradation (Kendall et al., 2018).

Environmental variables also have a significant impact on the molecular degradation of proteins (Hendy et al., 2018c). First and foremost, the time that has passed since the material has entered the archaeological record significantly impacts the survival of biomolecules. The longer time since burial, the more degraded the biomolecules in the sample will be (Collins et al., 2002). Mean annual temperature, and fluctuations therein, are another important variable that affects protein preservation. Under cooler conditions, proteins generally experience lower rates of chemical reactions, while in warmer conditions chemical degradation occurs at a faster pace (Demarchi et al., 2016). Similarly, protein loss will be accelerated by exposure to fire or cooking activities (Roberts et al., 2002, Faillace et al., 2020). The pH of the burial environment also has an effect on the preservation of bone proteins. Fossil material, and the proteins therein, often does not survive in the archaeological record at low (acidic) pH levels, while protein degradation occurs at a higher pace in high (alkaline) pH levels (Wilson et al., 2012). Similarly, the consumption of bone by scavenging animals also exposes the bone to highly acidic environments in the intestinal tract, resulting in collagen degradation through acid hydrolysis (Collins et al., 2002). Other characteristics of the burial environment, such as soil hydrology (Kendall et al., 2018) and burial depth (Smith et al., 2003), or the presence of specific chemical elements, such as metal ions (Schroeter and Cleland, 2016), or phosphatisation of the soil (Brown et al., 2021b), also affect the preservation of collagen in archaeological bone. Finally, the nature and extent of microbial attack on bone, shortly after skeletal material enters the fossil or archaeological record, also affects the preservation of biomolecules, including proteins, in bone (Collins et al., 2002, Hedges, 2002, Jans et al., 2004). Bacteria and fungi found in soil and intestinal tracts produce specific enzymes, collagenases, that are capable of rapidly degrading collagen (Child, 1995, White and Booth, 2014).

Together, all of these chemical and environmental variables impact the speed with which proteins degrade over time. Diagenetic changes generally lower the concentration of proteins in a sample, change the amino acid sequences of these proteins, and increase the likelihood that a sample is contaminated with exogenous proteins (Hendy et al., 2018c). It is therefore important to explore the patterns of protein degradation and diagenesis in local and regional contexts. In Manuscript B, collagen preservation at Australian sites is compared across a series of local depositional and climatic conditions in order to gain

more insights into the patterns and mechanisms of collagen preservation in the generally harsh environments of Australia.

3.4.1. Thermal age estimates

The relationship between temperature and protein degradation means that the expected level of protein degradation can be estimated based on the age of the material and local temperature averages, a metric generally referred to as thermal age. This metric can be used to compare the likelihood of biomolecular preservation in fossils between archaeological and palaeontological sites. Thermal age was originally defined as *'the time taken to produce a given degree of DNA degradation when the temperature is held at a constant 10°C.'* ((Smith et al., 2003), 204). All sites are treated as having experienced the same constant temperature, which allows for the comparison of preservation potential between sites (Smith et al., 2003, Demarchi et al., 2016). Thermal age was originally developed to estimate the degree of DNA preservation (Smith et al., 2003). The degree of collagen preservation at a site can be calculated in a similar way. The main difference in the resulting thermal age values of these two molecules stems from a slight difference in activation energy, the minimum amount of energy needed for the chemical reaction to occur, between collagen denaturation (172 kJ mol^{-1} (Buckley et al., 2008)) and DNA depurination (127 kJ mol^{-1} (Lindahl and Nyberg, 1972)).

Using this approach, thermal ages have to be calculated for each site in order to account for site-specific climate conditions. The two main factors that influence thermal age are mean annual temperature and the fluctuations of temperature around this mean (Smith et al., 2003). These metrics change over time, meaning that both modern climate data and palaeoclimate reconstructions are needed to calculate thermal age. Generally speaking, thermal ages from sites from cooler climates will be younger than the chronological age of these sites, reflecting the slow speed with which the chemical reaction occurs. Sites from warmer climates, on the other hand, will have a thermal age older than their chronological age, since the chemical reaction will occur at a quicker pace (Demarchi et al., 2016). In Manuscript B, thermal age estimates were calculated in order to acquire a theoretical limit of collagen preservation for the sites included in the study. For a more detailed description of the methods used to calculate thermal age estimates for the sites studied in this thesis see the methods section of Manuscript B.

3.4.2. Fourier transform infrared spectroscopy (FTIR)

The past decade has seen the development of a number of pre-screening techniques to rapidly assess the molecular preservation of fossil material and identify well-preserved fossils suitable for palaeoproteomic or palaeogenetic analyses. One of the most widely used pre-screening methods in recent years is Attenuated Total Reflectance Fourier Transform Infrared Spectroscopy (ATR-FTIR) (Lebon et al., 2016, Pothier Bouchard et al., 2019, Sponheimer et al., 2019, Kontopoulos et al., 2020, Cienkosz-Stepańczak et al., 2021, Pal Chowdhury et al., 2021, Presslee et al., 2021). FTIR is a minimally destructive technique with the ability to rapidly assess the preservation state of osseous material. The nature and structure of organic (including collagen) and inorganic content can be inferred from FTIR measurements. The presence of organic content in bone is most commonly assessed by the amide-to-phosphate (Am/P) ratio (Trueman et al., 2004, Lebon et al., 2016, Kontopoulos et al., 2020, Presslee et al., 2021). The presence of the Amide I (~1650 cm^{-1}) and Amide II (~1550 cm^{-1}) absorption peaks, specifically, indicates the presence of proteins and peptides in a sample (Gourion-Arsiquaud et al., 2008, Kontopoulos et al., 2020). The presence of inorganic content can be assessed by the measurement of the infrared splitting factor (IRSF), and the carbonate-to-phosphate ratio (C/P) (Beasley et al., 2014, Presslee et al., 2021). In Manuscript B, FTIR values were measured to evaluate collagen preservation of fossil material from Late Pleistocene deposits in Australia. For a more detailed description of the FTIR machine settings and methods used for this thesis see the methods section of Manuscript B.

3.4.3. Deamidation

The final method that can be used to assess collagen preservation is deamidation. Deamidation is the post-translational modification of glutamine and asparagine to glutamic acid and aspartic acid, respectively, by the loss of an amide functional group (Figure 3.2). This chemical reaction results in a mass shift of +0.98402 Da (Van Doorn et al., 2012, Wilson et al., 2012). The deamidation of glutamine and asparagine occurs at different rates. Asparagine deamidation occurs fairly rapidly, and has therefore mostly been used to study modern materials. Glutamine deamidation, on the other hand, occurs at a significantly slower rate, and is therefore the more informative when studying archaeological remains (Van Doorn et al., 2012, Wilson et al., 2012).

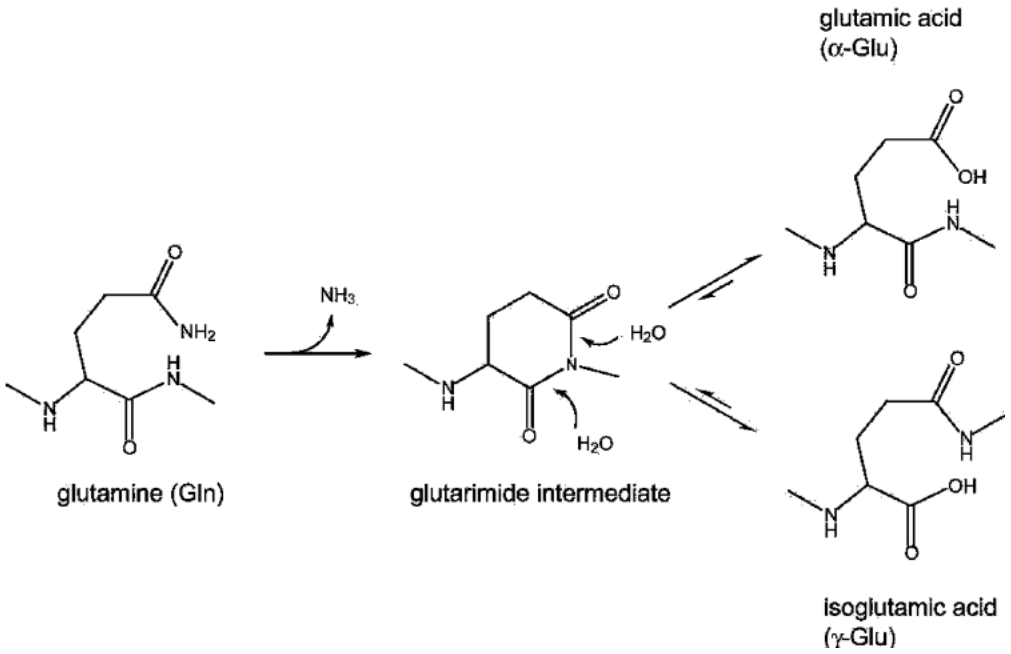

Figure 3.2: Graphical schematic of the degradation of glutamine into glutamic acid. Figure from (Li et al., 2010).

The +0.98402 Da mass shift that occurs when a peptide is deamidated can be detected by mass spectrometry, both via MALDI-ToF-MS and LC-MS/MS approaches (Van Doorn et al., 2012, Wilson et al., 2012, Ramsøe et al., 2020). Levels of glutamine deamidation can be directly calculated from MALDI spectra resulting from ZooMS analysis, and they do not require any additional sample processing (Van Doorn et al., 2012). In MALDI spectra, deamidation leads to a shift in the isotope distribution of the affected peptide. This shifted isotope distribution can be used to calculate deamidation levels in a peptide (Wilson et al., 2012).

In general, older, more damaged samples have higher levels of deamidation than younger, better preserved samples. Therefore, deamidation has been proposed as a method to distinguish between ancient proteins and modern contaminants, and has also been suggested as a useful method to evaluate the relative age of ancient proteins (Van Doorn et al., 2012, Wilson et al., 2012, Mackie et al., 2017). However, more recently, it has been shown that deamidation rates cannot be used reliably as a relative measure of time, because they are significantly affected by site-specific burial conditions, including temperature and pH (Wilson et al., 2012, Pal Chowdhury et al., 2019, Brown et al., 2021b), as well as the chosen extraction method (Simpson et al., 2016, Procopio and Buckley, 2017). Instead, deamidation is now thought to be more useful as an overall measure of collagen preservation (Schroeter and Cleland, 2016, Ramsøe et al., 2020, Brown et al., 2021b). In Manuscript B, deamidation rates were calculated to assess collagen preservation across Late Pleistocene deposits in Australia and assess whether this method is a reliable measure of collagen preservation. For a more detailed description of the methods used to calculate deamidation rates in this thesis see the methods section of Manuscript B.

4. Aims and objectives

The main objective of the research presented in this thesis is to explore the potential of ZooMS in Australian contexts. The first two papers of this thesis address the two major challenges that currently restrict ZooMS applications in Australia: the absence of a reference database and the limited understanding of collagen preservation in the Australian archaeological and palaeontological record. ZooMS peptide markers are developed for a large number of medium- to large-sized Australian marsupials and monotremes to facilitate larger-scale ZooMS applications on Australian faunal assemblages (Manuscript A). Meanwhile, the patterns and mechanisms underlying collagen preservation in Australian assemblages are explored to identify possible challenges associated with the practical implementation of ZooMS to study Australian fauna on a wider scale (Manuscript B).

In the third and fourth paper, the potential of ZooMS to study Australian assemblages is further explored. The novel peptide markers developed in Manuscript A are applied to identify faunal remains from archaeological contexts to get a better understanding about biodiversity in the past. These results are combined with existing zooarchaeological records to illuminate the potential of a combined approach to study Australian faunal assemblages (Manuscript C). Finally, this thesis further explores how palaeoproteomics can be used to inform conservation and restoration strategies in the future (Manuscript D).

Drawing on the background outlined in Chapters 2 and 3, the specific research questions that this thesis aims to address are:

- What is the potential of ZooMS to study the Australian faunal record?
    - What are the main areas of research in Australian zooarchaeology and palaeontology that ZooMS can help address? (Manuscripts A and C)
    - What is the taxonomic resolution that can be reached with ZooMS for the identification of Australian marsupials? (Manuscript A)
    - What is the spatial and temporal limit of ZooMS applications in Australia? (Manuscript B and C)
    - How can ZooMS and zooarchaeology best be combined to reach maximum potential for the study of past faunal assemblages? (Manuscript C)
- What are the challenges, pitfalls, and limitations associated with the application of ZooMS to study Australian faunal assemblages?
    - To what extent is collagen preservation at Australian archaeological and palaeontological sites amenable to ZooMS studies? (Manuscript B)
    - How do the local depositional environment and climatic conditions influence collagen preservation? (Manuscript B)
- In what way can ZooMS and shotgun palaeoproteomics be used to inform conservation, restoration, and rewilding strategies? (Manuscript D)

5. Overview of manuscripts and author contributions

5.1. Manuscript A

"Species identification of Australian marsupials using collagen fingerprinting"

C. Peters, K.K. Richter, T. Manne, J. Dortch, A. Paterson, K. Travouillon, J. Louys, G.J. Price, M. Petraglia, A. Crowther, and N. Boivin

Published in *Royal Society Open Science*, 27 October 2021

In Manuscript A, collagen peptide markers are characterized for a significant number of extant and recently extinct marsupial and monotreme species to significantly amplify the potential of ZooMS in Australian contexts. The utility of these new peptide markers for ZooMS analyses of Australian faunal assemblages is demonstrated by using them to taxonomically identify fragmented bones from a nineteenth-century colonial pearlshell fishery at Bandicoot Bay, Barrow Island, in Western Australia. The site was selected to enable evaluation of the utility of ZooMS in the continent's arid zone, where organic preservation conditions are often challenging, and because a thorough zooarchaeological study of the site's fauna had already been completed, enabling a comparison of osteology and ZooMS results.

Author contributions: C. Peters, K.K. Richter, T. Manne, J. Dortch, J. Louys, G.J. Price, M. Petraglia, A. Crowther, and N. Boivin conceived and designed the study. C. Peters performed ZooMS analysis and prepared samples for LC-MS/MS analysis; C. Peters and K.K. Richter analyzed ZooMS and LC-MS/MS data; T. Manne, A. Paterson, K. Travouillon, J. Louys, and G.J. Price provided samples. C. Peters and N. Boivin wrote the paper, with critical input from all authors

In total, C. Peters contributed 80% to the project, including sampling, extraction of collagen for ZooMS, analysis of MALDI data, the majority of the analysis of LC-MS/MS data, and manuscript construction.

5.2. Manuscript B

"Systematic survey of collagen preservation in Australia reveals unexpected tropical survival at >50,000 years"

C. Peters, Y. Wang, J. Dortch, S. Hocknull, R. Lawrence, J. Louys, T. Manne, C. Monks, G.J. Price, G.E. Röβner, H. Ryan, M. Siversson, T. Ziegler, N. Boivin and M.J. Collins

In preparation for publication

In Manuscript B, collagen preservation in Australian archaeological and palaeontological deposits is systematically examined utilizing a multi-method approach. For seventeen localities, thermal age estimates are calculated to chemically predict the survival of collagen at these sites. Collagen preservation of individual bones is predicted through visual taphonomic assessments and FTIR analysis, and ZooMS success rates and collagen deamidation rates are used as a proxy of true collagen preservation. The results of these analyses are brought together to get a better understanding of collagen preservation in Australian deposits across time and space, as well as to get a deeper understanding of

the environmental and depositional conditions that impact collagen survival and the mechanisms involved therein.

Author contributions: C. Peters, N. Boivin, and M.J. Collins conceived and designed the study; J. Dortch, S. Hocknull, R. Lawrence, J. Louys, T. Manne, C. Monks, G.J. Price, G.E. Röβner, H. Ryan, M. Siversson, and T. Ziegler provided samples; C. Peters and M.J. Collins calculated thermal age estimates; C. Peters performed FTIR and ZooMS analyses, analyzed FTIR and ZooMS data, and calculated deamidation rates; Y. Wang performed statistical analysis; C. Peters wrote the draft of the paper that is included in this thesis, with input from M.J. Collins, Y. Wang, J. Louys and G.J. Price.

In total, C. Peters contributed 85% to the project, including sampling, data collection for thermal age calculations, visual taphonomic assessments, FTIR analysis, extraction of collagen for ZooMS, analysis of MALDI data, calculation of deamidation rates, and manuscript construction.

5.3. Manuscript C

"ZooMS and zooarchaeology, a match made in heaven? Integrating ZooMS into existing faunal records at Devil's Lair, SW Australia"

C. Peters, N. Amano, A. Ghassemifar, H. Ryan, M. Siversson, W. Webb, J. Dortch, and N. Boivin

In preparation for publication

In Manuscript C, the novel ZooMS markers that were established in Manuscript A are used in this study to identify fragmented faunal remains from Devil's Lair, the oldest known human occupation site in southwestern Australia. ZooMS results are then compared to existing zooarchaeological records and bulk bone DNA metabarcoding data from the site to explore the broader question of how to best incorporate ZooMS in existing zooarchaeological record. The results from these analyses are pulled together to get a more holistic understanding of faunal diversity at Devil's Lair in the past. This manuscript explores in more depth what we learn from different methods, what their strengths and weaknesses are, and most importantly, how to combine them for maximal effect.

Author contributions: C. Peters, N. Amano, W. Webb, J. Dortch, and N. Boivin conceived and designed the study; H. Ryan, M. Siversson, and W. Webb provided access to material; C. Peters and A. Ghassemifar undertook sampling; C. Peters performed ZooMS analysis, and analyzed ZooMS data; C. Peters wrote the draft of the paper that is included in this thesis, with input from N. Amano and J. Dortch.

In total, C. Peters contributed 90% to the project, including sampling, extraction of collagen for ZooMS, analysis of MALDI data, data collection for comparison, and manuscript construction.

5.4. Manuscript D

"Leveraging palaeoproteomics to address conservation and restoration agendas"

C. Peters, K.K. Richter, J.-C. Svenning, and N. Boivin

In Manuscript D, we review the potential of palaeoproteomics to inform conservation, restoration and rewilding strategies. We demonstrate the scope for conservation palaeoproteomics by showing how the study of ancient protein can provide information that contributes to: 1) assessing past species richness; 2) establishing ecological baselines; 3) detecting shifts in species abundance and geographic range; 4) disentangling human-environment interactions; 5) tracking the introduction of non-native species; 6) identifying illicitly traded material; and 7) prioritizing species for conservation. We provide examples from the literature of ways that palaeoproteomics has, or is beginning to, address these kinds of aims, by improving taxonomic identifications as well as our understanding of phylogenetic relationships.

Author contributions: C. Peters and N. Boivin conceived and designed the study. C. Peters compiled and reviewed the literature. C. Peters and N. Boivin wrote the manuscript with input from K.K. Richter, and J.-C. Svenning.

In total, C. Peters contributed 75% to the project, including data collection, synthesis and manuscript construction.

-

6. Manuscript A

Species identification of Australian marsupials using collagen fingerprinting

Carli Peters[1,*], Kristine K. Richter[2], Tiina Manne[3], Joe Dortch[4], Alistair Paterson[4], Kenny Travouillon[5], Julien Louys[6], Gilbert J. Price[7], Michael Petraglia[1,3,6,8], Alison Crowther[1,3], Nicole Boivin[1,3,8,9,*]

1. Department of Archaeology, Max Planck Institute for the Science of Human History, Jena, Germany
2. Department of Anthropology, Harvard University, Cambridge, MA, USA
3. School of Social Science, The University of Queensland, Brisbane, Qld 4071, Australia
4. School of Social Sciences, University of Western Australia, Perth, WA 6009, Australia
5. Western Australian Museum, Collections and Research, 49 Kew Street, Welshpool, WA 6106, Australia
6. Australian Research Centre for Human Evolution, Griffith University, Nathan, Qld 4111, Australia
7. School of Earth and Environmental Sciences, The University of Queensland, Brisbane, Qld 4072, Australia
8. Department of Anthropology, National Museum of Natural History, Smithsonian Institution, Washington DC, USA
9. Department of Anthropology and Archaeology, University of Calgary, Calgary, Canada

*Corresponding authors: Carli Peters and Nicole Boivin

ROYAL SOCIETY OPEN SCIENCE

royalsocietypublishing.org/journal/rsos

Research

Cite this article: Peters C *et al*. 2021 Species identification of Australian marsupials using collagen fingerprinting. *R. Soc. Open Sci.* **8**: 211229.
https://doi.org/10.1098/rsos.211229

Received: 4 August 2021
Accepted: 30 September 2021

Subject Category:
Organismal and evolutionary biology

Subject Areas:
palaeontology/molecular biology

Keywords:
ZooMS, zooarchaeology, palaeontology, archaeology, Australia

Authors for correspondence:
Carli Peters
e-mail: peters@shh.mpg.de
Nicole Boivin
e-mail: boivin@shh.mpg.de

†Present address: Department of Archaeology, Max Planck Institute for the Science of Human History, Kahlaische Strasse 10, 07745 Jena, Germany.

Electronic supplementary material is available online at https://doi.org/10.6084/m9.figshare.c.5665537.

THE ROYAL SOCIETY PUBLISHING

Species identification of Australian marsupials using collagen fingerprinting

Carli Peters[1,†], Kristine K. Richter[2], Tiina Manne[3], Joe Dortch[4], Alistair Paterson[4], Kenny Travouillon[5], Julien Louys[6], Gilbert J. Price[7], Michael Petraglia[1,3,6,8], Alison Crowther[1,3] and Nicole Boivin[1,3,8,9,†]

[1]Department of Archaeology, Max Planck Institute for the Science of Human History, Jena, Germany
[2]Department of Anthropology, Harvard University, Cambridge, MA, USA
[3]School of Social Science, The University of Queensland, Brisbane, Qld 4071, Australia
[4]School of Social Sciences, University of Western Australia, Perth, WA 6009, Australia
[5]Western Australian Museum, Collections and Research, 49 Kew Street, Welshpool, WA 6106, Australia
[6]Australian Research Centre for Human Evolution, Griffith University, Nathan, Qld 4111, Australia
[7]School of Earth and Environmental Sciences, The University of Queensland, Brisbane, Qld 4072, Australia
[8]Department of Anthropology, National Museum of Natural History, Smithsonian Institution, Washington, DC, USA
[9]Department of Anthropology and Archaeology, University of Calgary, Calgary, Canada

CP, 0000-0001-7942-6108; KT, 0000-0003-1734-4742; JL, 0000-0001-7539-0689; GJP, 0000-0001-8406-4594

The study of faunal remains from archaeological sites is often complicated by the presence of large numbers of highly fragmented, morphologically unidentifiable bones. In Australia, this is the combined result of harsh preservation conditions and frequent scavenging by marsupial carnivores. The collagen fingerprinting method known as zooarchaeology by mass spectrometry (ZooMS) offers a means to address these challenges and improve identification rates of fragmented bones. Here, we present novel ZooMS peptide markers for 24 extant marsupial and monotreme species that allow for genus-level distinctions between these species. We demonstrate the utility of these new peptide markers by using them to taxonomically identify bone fragments from a nineteenth-century colonial-era pearlshell fishery at Bandicoot Bay, Barrow Island. The suite of peptide biomarkers presented in this study, which focus on a range of ecologically and culturally important species, have the potential to significantly amplify the zooarchaeological and paleontological record of Australia.

1. Introduction

Australia is home to an extremely rich and unique fauna [1], with more than 85% of its terrestrial mammal species classed as endemic [2]. It is the only region globally, other than Papua New Guinea, where marsupials, placentals and monotremes coexist [3]. The unique nature of Australian terrestrial fauna is the outcome of an evolutionary trajectory strongly shaped by the isolation of the Australian continent from Antarctica *ca* 40 Myr ago [3,4]. Among the best-recognized of Australia's fauna are its marsupials, including macropods such as kangaroos and wallabies (members of the suborder Macropodiformes, generally characterized by their long powerful hind legs and feet), as well as other taxa such as koalas and wombats. Australian marsupials inhabit a broad range of ecosystems spanning the continent's arid inland zones, alpine regions, temperate and tropical rainforest, and coastal wetlands [5], and play key ecological roles in many of the ecosystems they inhabit [2]. In the past, marsupials were an important subsistence resource for Aboriginal communities [6–8], while their bones were also used as raw materials for the creation of tools and other artefacts [9–11]. Research on past Australian terrestrial faunas, and particularly marsupials, can provide insight into early human activity on the Australian continent, enable reconstruction of palaeoenvironmental conditions and shifts in biodiversity over time, and help assess the impact of past climate change.

Archaeologists, palaeontologists and other researchers have uncovered an assortment of faunal remains in Australia, dating from the late Pleistocene to the historical period [12–19]. However, the continent's often harsh environmental conditions [20–22], together with other factors like scavenging by marsupial carnivores [23–25], frequently result in a large number of highly fragmented, morphologically unidentifiable bone fragments in archaeological and palaeontological assemblages. Together with a scarceness of reference materials and a tendency toward osteological similarities between species [18,26–28], these factors complicate the study of faunal remains from Australian sites. Zooarchaeology by mass spectrometry (ZooMS) has provided a means to improve taxonomic identifications of fragmented osteological material at sites around the world [29–33] and offers exciting potential to address these challenges in Australian contexts.

ZooMS is a high-throughput, proteomics-based approach that uses differences in the collagen type I (COL1) protein sequence between taxonomic groups to identify faunal remains [34]. COL1 is the most abundant protein in bone, skin, antler and dentine, and these substrates can thus be successfully targeted using ZooMS. In archaeology, ZooMS is increasingly used to identify morphologically unidentifiable bone fragments [29,35], resulting in an improved ability to reconstruct palaeoenvironmental conditions and shifts in biodiversity over time, help assess the impacts of climate change and anthropogenic activities [30,36,37], track the spread of domesticates [32,38–41], identify ancient hominin remains [29,42] and provenance bone tools [31,43,44]. ZooMS is faster and cheaper than ancient DNA (aDNA)-based approaches [34,45,46] and requires less collagen than radiocarbon or stable isotope analyses [47]. While aDNA is often minimally applicable in hot, humid or tropical contexts [48,49], or when studying older assemblages, proteins can preserve over long time periods [50–52] and are more resistant to harsh environments [34].

The prospects for the application of peptide mass fingerprinting on the Australian continent have only been minimally explored. Buckley *et al*. [53] are so far alone in exploring the potential of ZooMS to taxonomically identify Australian marsupials. Although peptide mass fingerprints have been characterized for only eight extant species and the extinct short-faced kangaroo, *Simosthenurus occidentalis*, preliminary findings suggest that ZooMS is an effective method for taxonomically identifying marsupial remains [53]. Here, we build on this research by characterizing collagen peptide markers for a significantly expanded number of extant and recently extinct marsupial and monotreme species to significantly amplify the potential of ZooMS in Australian contexts. We demonstrate the utility of these new markers for ZooMS analyses of Australian faunal assemblages by using them to taxonomically identify fragmented bones from a nineteenth-century colonial pearlshell fishery at Bandicoot Bay, Barrow Island, in Western Australia. The site was selected to enable evaluation of the utility of ZooMS in the continent's arid zone, where organic preservation conditions are often challenging, and because a thorough zooarchaeological study of the site's fauna had already been completed [15,54], enabling a comparison of osteology and ZooMS results.

2. Material and methods

2.1. Materials

2.1.1. Modern reference specimens

Modern bone samples were collected from the Mammalogy collections of Museums Victoria and the Western Australian Museum, the Zooarchaeology Laboratory of the University of Queensland and the

ARCHE Laboratories at Griffith University. Peptide mass fingerprints and collagen sequences were obtained for the short-beaked echidna (*Tachyglossus aculeatus*) and 23 marsupial species: Tasmanian devil (*Sarcophilus harrisii*), thylacine (*Thylacinus cynocephalus*), koala (*Phascolarctos cinereus*), common wombat (*Vombatus ursinus*), hairy-nosed wombat (*Lasiorhinus* sp.), spectacled hare wallaby (*Lagorchestes conspicillatus*), banded hare wallaby (*Lagostrophus fasciatus*), eastern grey kangaroo (*Macropus giganteus*), western grey kangaroo (*Macropus fuliginosus*), red kangaroo (*Osphranter rufus*), common wallaroo (*Osphranter robustus*), Bennett's wallaby (*Notamacropus rufogriseus*), tammar wallaby (*Notamacropus eugenii*), agile wallaby (*Notamacropus agilis*), western brush wallaby (*Notamacropus irma*), Parma wallaby (*Notamacropus parma*), swamp wallaby (*Wallabia bicolor*), northern brown bandicoot (*Isoodon macrourus*), long-nosed bandicoot (*Perameles nasuta*), common brushtail possum (*Trichosurus vulpecula*), ringtail possum (*Pseudocheirus peregrinus*), brush-tailed phascogale (*Phascogale tapoatafa*) and sugar glider (*Petaurus breviceps*). The museum accession numbers for all sampled specimens are listed in electronic supplementary material, table SI.

2.1.2. Archaeological specimens

Archaeological specimens were sampled from a late nineteenth-century (1880s/1890s) pearlshell fishery settlement (D24-001) at Bandicoot Bay, Barrow Island, located *ca* 60 km off the northwest coast of Western Australia [15]. The site was surveyed and excavated in 2013 and 2014 as part of the Barrow Island Archaeology Project [15,54–56].

The faunal assemblage consists of 2922 bone fragments, 810 (27.7%) of which were previously identified to the taxonomic class as a part of the zooarchaeological analysis of the site [54]. This rate of morphological identification reflects the harsh taphonomic conditions at the site, which sits on an exposed floodplain subject to summer temperatures approaching 50°C. Bone fragmentation is also considerable at the site; 66% of the identified remains are between 7 and 28 mm in length, and there is a peak in remains between 13 and 16 mm. Although there is evidence of fresh fragmentation, the uniformity of small specimen fragments, along with limited evidence of trampling, is argued by Dooley *et al*. [54] to be the result of weathering at an open-air site.

Zooarchaeological investigations at the Bandicoot Bay site revealed a broad historical exploitation of local resources evidenced by the presence in the assemblage of the golden bandicoot (*I. auratus barrowensis*), brushtail possum (*T. vulpecula*), spectacled hare wallaby (*L. conspicillatus*) and the common wallaroo (*O. robustus isabellinus*). Chelonioidae (sea turtle), microfauna, bird, fish, crab and shark specimens were also identified [54]. Domesticated animals appear to be absent from the bone assemblage [15,54]. For the present study, 134 morphologically unidentifiable bone fragments from the Bandicoot Bay assemblage were sampled for ZooMS analysis.

2.2. Collagen extraction

Collagen was extracted from the modern and archaeological bone samples alongside extraction blank controls. For modern specimens, an acid-insoluble approach was used, in which collagen was extracted based upon previously published methods [34,46]. Bone chips of approximately 30 mg were demineralized in 500 µl of 0.6 M hydrochloric acid (HCl) for 48 h. The supernatant was removed, after which the samples were washed three times in 200 µl of 50 mM ammonium bicarbonate (AmBic). Then, the samples were heated at 65°C in 100 µl of 50 mM AmBic. The resulting supernatant was digested with 1 µl of 0.4 µl μg^{-1} trypsin solution (Pierce™ Trypsin Protease, Thermo Scientific) for 18 h at 37°C. Subsequent to enzymatic digestion, peptides were purified and concentrated using C18 ZipTips (Pierce™ C18 Tips, Thermo Scientific).

For archaeological specimens, we employed an acid-soluble approach based on Van der Sluis *et al*. [57]. Bone chips of approximately 30 mg were demineralized in 500 µl of 0.6 M HCl for one week, after which the supernatant was transferred to a 30 kDa ultrafilter (Sartorius, Vivaspin®) and centrifuged until completely passed through the filter. Five hundred microlitres AmBic was then added to the ultrafilter and the samples were centrifuged a second time. The filtrates were resuspended in 100 µl of AmBic followed by digestion and peptide purification as described above. Samples with sufficient collagen preservation for ZooMS were reanalysed with the previously described acid-insoluble approach to get higher quality spectra. The exact protocols are described in detail in Wang *et al*. [47] and are publicly available on protocols.io [58,59].

2.3. Matrix-assisted laser desorption/ionization–tandem time of flight mass spectrometry

Modern reference samples were spotted in triplicate onto an MTP AnchorChip 384-target plate, together with matrix solution (10 mg of α-cyano-4-hydroxycinnamic acid in 7 ml of 85% acetonitrile (ACN)/0.1% trifluoracetic acid (TFA)). Archaeological samples were mixed with matrix solution (α-cyano-4-hydroxycinnamic acid of 10 mg ml^{-1} in 50% ACN/0.1% TFA) and spotted onto an MTP Groundsteel 384-target plate. All samples were analysed using an Autoflex Speed LRF matrix-assisted laser desorption/ionization–tandem time of flight mass spectrometer (MALDI-TOF-MS, Bruker Daltonics) with a smartbeam-II laser. A SNAP averaging algorithm was used to obtain monoisotopic masses (C: 4.9384, N: 1.3577, O: 1.4773, S: 0.0417, H: 7.7583).

2.4. Liquid chromatography with tandem mass spectrometry

For every modern reference species, one sample with a good MALDI spectrum was selected for further analysis using liquid chromatography with tandem mass spectrometry (LC-MS/MS). Twenty microlitres of the final collagen extract was dried down and sent for LC-MS/MS analysis at the Functional Genomics Center Zurich. LC-MS/MS was conducted using a Q-Exactive HF mass spectrometer (Thermo Scientific) coupled with an ACQUITY UPLC M-Class system (Waters AG). Solvent composition at the two channels was 0.1% formic acid for channel A and 0.1% formic acid, 99.9% ACN for channel B. Column temperature was 50°C. For each sample, 4 µl of peptides was loaded on a commercial MZ Symmetry C18 Trap Column (100 Å, 5 µm, 180 µm × 20 mm, Waters) followed by nanoEase MZ C18 HSS T3 Column (100 Å, 1.8 µm, 75 µm × 250 mm, Waters). The peptides were eluted at a flow rate of 300 nl min^{-1} by a gradient from 5 to 40% B in 120 min and 98% B in 5 min. The column was cleaned after each run with 98% solvent B for 5 min and holding 98% B for 8 min prior to re-establishing loading condition. The mass spectrometers were operated in data-dependent mode performing higher energy collision dissociation (HCD) fragmentation on the 12 most intense signals per cycle. Full-scan MS spectra (300–1500 m/z) were acquired at a resolution of 120 000 at 200 m/z after accumulation to a target value (AGC) of 3 000 000, while HCD spectra were acquired at a resolution of 30 000 using a normalized collision energy of 28 (maximum injection time: 50 ms; AGC: 10 000 ions). Unassigned singly charged ions and ions were excluded. Precursor masses previously selected for MS/MS measurement were excluded from further selection for 30 s, and the exclusion window was set at 10 ppm. The samples were acquired using internal lock mass calibration on m/z 371.1012 and 445.1200.

2.5. Identification and confirmation of biomarkers

The identification and confirmation of peptide biomarkers were performed following the methodology described in Richter *et al*. [60]. MALDI spectra were visually inspected with FlexAnalysis v. 3.4 (Bruker Daltonics) and compared to a list of published peptide markers for Australian marsupials [53]. When published peptide markers were not available, candidate peptide biomarkers were identified.

Candidate peptide biomarkers were confirmed with LC-MS/MS data analysed in a multi-stage approach using Byonic v. 3.2.0 (Protein Metrics Inc. [61]). First, the product ion spectra were searched against a reference database including the amino acid sequences of COL1A1 and COL1A2 of *P. cinereus* (XP_020853290.1; XP_020855640.1), *V. ursinus* (A0A4X2KF99; A0A4X2M815), *S. harrisii* (G3WK23; G3VSR0) and *Macropus* sp. [62] and common contaminants [63], with the following parameter settings: cleavage sites fully specific C-term R and K; 3 missed cleavages allowed; mass changes: 6 common, 0 rare; common: oxidation on K, M, and P, deamidation on N and Q; no sequence variations allowed; wildcard search disabled. Masses of published and candidate peptide markers were checked to identify the corresponding amino acid sequence (protein FDR 2%, peptide PEP2D score lower than 0.01).

Next, species without confirmed sequence data for all candidate markers were reanalysed using an error-tolerant search strategy to identify novel sequence variants. The following parameter settings were used: cleavage sites fully specific C-term R and K; 2 missed cleavages allowed; mass changes: 3 common, 1 rare; common: oxidation on K, M and P, deamidation on N and Q; rare: all sequence variants allowed; wildcard search disabled. The locations of the peptide markers on the collagen gene were checked and all possible sequence variants and their corresponding masses were recorded (protein FDR 2%, peptide PEP2D score lower than 0.01).

Other proteins in the samples were identified by searching the MS/MS spectral data against the proteomes of *V. ursinus* (UP000314987) and *S. harrisii* (UP000007648) and all sequence data available

in Swissprot, using the following parameter settings: cleavage sites fully specific C-term R and K; 3 missed cleavages allowed; mass changes: 2 common, 1 rare; common: oxidation on K, M and P, deamidation on N and Q; rare: pyro-Glu on N-term E and Q, ammonia-loss on N-term C; no sequence variations allowed; wildcard search disabled; protein FDR 2%. The results were checked for identified bone proteins, other than COL1A1 and COL1A2, and common contaminants.

The results of the first three searches were used to create a new database consisting of (i) the COL1A1 and COL1A2 sequences of the original reference database, (ii) all sequence variants found in the error-tolerant search, (iii) all proteins identified in the whole proteome validation and (iv) common contaminants. The MS/MS data were then analysed with Byonic using this database and the same parameter settings as the first non-error-tolerant search. The protein FDR was set to 2%. Only peptides recurring at least three times, and with a PEP2D score lower than 0.01, were considered confirmed. This resulted in a list of confirmed peptide markers and corresponding peptide sequences.

3. Results

All modern reference samples yielded high-quality MALDI and MS/MS spectral data that could be used to characterize collagen peptide markers. Collagen was identified as the main protein component in all samples, and no common contaminants were identified in high quantities (see electronic supplementary material, table II). The ZooMS markers for the studied species are presented in table 1 with the corresponding peptide sequences presented in table 2. Overall, collagen peptide markers generally allow for genus-level distinctions of Australian marsupials, with some limitations within the group of macropods.

3.1. Novel ZooMS peptide markers

In addition to the set of peptide markers that is regularly reported for ZooMS studies, we report two additional peptide markers that can be used to distinguish between marsupial taxa. Peptide marker COL1A2 10–42 is represented by *m*/*z* 2975 for the majority of the studied reference species. However, this mass value also represents COL1A2 757–789 (G′) in *P. cinereus*, *Lasiorhinus* sp. and *V. ursinus*. Caution is thus needed when interpreting a peak at *m*/*z* 2975. It is only possible to confidently assign this peak to either COL1A2 757–789 (G′) or COL1A2 10–42 when another mass peak corresponding to a different COL1A2 757–789 (G′) or COL1A2 10–42 peptide marker has also been identified.

Furthermore, a second novel peptide marker has been identified, peptide marker COL1A2 889–906. This marker is located at the same position in the COL1A2 sequence as the recently reported additional marker to differentiate between bovid taxa [33]. It is thus possible that this novel peptide marker is informative not only for bovids and marsupials, but also for other taxonomic groups.

3.2. Marsupial versus monotreme ZooMS markers

Peptide marker COL1A1 508–519 (P1) is often characterized as highly conserved with a peak at *m*/*z* 1105 for most terrestrial mammals [65] and at *m*/*z* 1079 for cetaceans [45]. For marsupials, this marker is present at *m*/*z* 1162, and for *T. aculeatus* at *m*/*z* 1120. This difference is particularly interesting as it offers the opportunity to distinguish Australian marsupials and monotremes from other mammalian species on the basis of a single peptide marker. It should be noted, however, that this peptide marker has also been identified at *m*/*z* 1162 for many species of birds and reptiles [30], and the reported peptide sequence is identical to the one found in marsupials.

Other peptide markers that have the ability to distinguish between monotremes and marsupials are COL1A2 502–519 (C) and COL1A2 454–483 (E). Both of these markers have been reported at identical mass values in all marsupial species studies (*m*/*z* 1598 and *m*/*z* 2335, respectively). However, in *T. aculeatus*, these peptide markers were reported at different mass values (*m*/*z* 1607 and *m*/*z* 2848, respectively). The large offset between the *m*/*z* values of peptide marker COL1A2 454–483 (E) for monotremes and marsupials is the result of an amino acid change after a tryptic cut site. In monotremes, the peptide contains a proline following a lysine, resulting in a missed cleavage. The peptide thus contains an additional four amino acids in comparison to the corresponding marsupial marker. This highlights a potential issue with the recently introduced nomenclature system for ZooMS [64], which relies on the location of peptides in the collagen sequence. The change in the location of

Table 1. ZooMS markers for Australian marsupial species and the monotreme *T. aculeatus*. Naming of peptide markers follows Brown *et al.* [64]. Masses in italics are not visible in MALDI spectra but are present in LC-MS/MS data. Masses in bold can be used to differentiate monotremes from marsupials.

	peptide markers													
	COL1A1 508–519	COL1A2 978–990		COL1A2 484–498	COL1A2 502–519	COL1A2 292–309	COL1A2 793–816	COL1A2 454–483	COL1A1 586–618		COL1A2 757–789		COL1A2	COL1A2
	P1	A	A′	B	C	P2	D	E	F	F′	G	G′	10–42[a]	889–906
Tachyglossus aculeatus	**1120**	**1182**	**1198**	1453	**1607**	x	**2121**	**2848**	**2873**	**2889**	***2999***	**3015**	**3009**	**1606**
Phascogale tapoatafa	1162	x	x	1453	1598	**1725**	**2163**	*2335*	2897	2913	**2929**	***2945***	2975	1652
Sarcophilus harrisii	1162	**1159**	**1175**	1453	1598	**1725**	**2177**	*2335*	**2869**	**2885**	**2929**	***2945***	2975	1652
Thylacinus cynocephalus	1162	**1159**	**1175**	1453	*1598*	x	**2121**	*2335*	**2869**	**2885**	**2929**	***2945***	2975	*1652*
Lagorchestes conspicillatus	1162	1150	1166	1453	1598	x	2145	*2335*	2897	2913	2943	*2959*	2975	1652
Lagostrophus fasciatus	1162	1150	1166	1453	1598	*1680*	2145	*2335*	**2881**	**2897**	2943	*2959*	2975	1652
Macropus fuliginosus	1162	1150	1166	1453	1598	*1680*	2145	*2335*	2897	2913	2943	*2959*	**2989**	1652
Macropus giganteus	1162	1150	1166	1453	1598	*1680*	2145	*2335*	2897	2913	2943	*2959*	**2989**	1652
Osphranter robustus	1162	1150	1166	1453	1598	*1680*	2145	*2335*	2897	2913	2943	*2959*	2975	1652
Osphranter rufus	1162	*1150*	1166	1453	1598	*1680*	2145	*2335*	2897	*2913*	2943	*2959*	2975	1652
Notamacropus agilis	1162	1150	1166	1453	1598	*1680*	2145	*2335*	2897	2913	2943	*2959*	2975	1652
Notamacropus eugenii	1162	*1150*	1166	1453	1598	*1680*	2145	*2335*	2897	2913	2943	*2959*	2975	**1624**
Notamacropus irma	1162	*1150*	*1166*	**1427**	1598	*1680*	2145	*2335*	2897	2913	2943	*2959*	2975	1652
Notamacropus parma	1162	*1150*	1166	1453	1598	*1680*	2145	*2335*	2897	2913	2943	*2959*	2975	1652
Notamacropus rufogriseus	1162	*1150*	1166	1453	1598	*1680*	2145	*2335*	2897	2913	2943	*2959*	2975	1652
Wallabia bicolor	1162	*1150*	1166	1453	1598	*1680*	2145	*2335*	2897	2913	2943	*2959*	2975	**1624**
Petaurus breviceps	1162	***1159***	***1175***	**1411**	1598	***1650***	2145	*2335*	2897	2913	**2971**	***2987***	*2975*	**1624**
Trichosurus vulpecula	1162	**1137**	***1153***	1453	1598	x	2145	*2335*	2897	2913	**2945**	***2961***	2975	**1624**

(*Continued.*)

Table 1. (*Continued.*)

	peptide markers												
	COL1A1 508–519	COL1A2 978–990		COL1A2 484–498	COL1A2 502–519	COL1A2 292–309	COL1A2 793–816	COL1A2 454–483	COL1A1 586–618		COL1A2 757–789		COL1A2	COL1A2
	P1	A	A′	B	C	P2	D	E	F	F′	G	G′	10–42[a]	889–906
Phascolarctos cinereus	1162	**1159**	**1175**	**1397**	1598	**1692**	2145	*2335*	**2869**	***2885***	**2959**	**2975**	2975	**1624**
Pseudocheirus peregrinus	1162	***1137***	***1153***	**1439**	1598	***1650***	**2161**	*2335*	2897	2913	**2929**	***2945***	2975	**1624**
Lasiorhinus sp.	1162	x	x	**1397**	1598	**1692**	2145	*2335*	**2869**	***2885***	**2959**	***2975***	2975	**1624**
Vombatus ursinus	1162	**1159**	**1175**	**1439**	1598	***1650***	**2119**	*2335*	2897	2913	**2959**	***2975***	**2991**	**1624**
Isoodon macrourus	1162	1150	1166	1453	1598	x	**2177**	*2335*	2897	2913	**2957**	***2973***	2975	**1624**
Perameles nasuta	1162	***1159***	***1175***	1453	1598	x	**2177**	*2335*	**2869**	**2885**	**2957**	***2973***	2975	**1624**

[a]Additional marsupial peptide marker first proposed by Buckley *et al*. [53] with tryptic name 2T3.

Table 2. Peptide sequences corresponding to ZooMS markers presented in table 1. Naming of peptide markers follows Brown *et al*. [64]. Masses in parentheses represent the mass of the peptide with an additional oxidation. Differences between sequences are in bold and underlined.

marker		sequence	mass
COL1A1 508–519	P1	GVQGP**A**GPQGPR	1120
		GVQGP**P**GPQGPR	1162
COL1A2 978–990	A	**P**G**N**A**G**A**V**GPAG**L**R	1137 (1153)
		PG**Q**A**G**A**V**GPAG**L**R	1150 (1166)
		PG**H**A**G**A**V**GPAG**L**R	1159 (1175)
		SG**Q**P**G**T**V**GPAG**V**R	1182 (1198)
COL1A2 484–498	B	G**V**A**G**EFG**L**P**G**PAGPR	1397
		G**P**A**G**EFG**L**P**G**PAGPR	1411
		G**S**P**G**EFG**L**P**G**PAGPR	1427
		G**V**P**G**EFG**L**P**G**PAGPR	1439
		G**L**P**G**EFG**L**P**G**PAGPR	1453
COL1A2 502–519	C	GPPGESGA**V**GPTG**S**IG**S**R	1598
		GPPGESGA**A**GPTG**P**LG**N**R	1607
COL1A2 292–309	P2	GPNGEPGSTGP**S**GPPGLR	1650
		GPNGEPGSTGP**T**GPPGLR	1680
		GPNGEPGSTGP**P**GPPGLR	1692
		GPNGEPGSTGP**M**GPPGLR	1725
COL1A2 793–816	D	GLPGVSG**SL**GEPGPLGI**A**GP**A**GAR	2119
		GLPGVSG**SV**GEPGPLGI**A**GP**A**GAR	2121
		GLPGVSG**GL**GEPGPLGL**S**GP**S**GAR	2121
		GLPGVSG**AL**GEPGPLGI**A**GP**P**GAR	2145
		GLPGVSG**SL**GEPGPLGI**A**GP**P**GAR	2161
		GLPGVSG**SV**GEPGPLGI**S**GP**P**GAR	2163
		GLPGVSG**SL**GEPGPLGI**S**GP**P**GAR	2177
COL1A2 454–483	E	GEQGPAGPPGFQGLPGPSGPAGE**G**GK	2335
		GEQGPAGPPGFQGLPGPSGPAGE**V**GKPGER	2848
COL1A1 586–618	F	GLTGPIGPPGPAG**PS**GDKGESGPSGP**A**GPTGAR	2869 (2885)
		GLTGPIGPPGPAG**TS**GDKGESGPSGP**A**GPTGAR	2873 (2889)
		GLTGPIGPPGPAG**PA**GDKGESGPSGP**V**GPTGAR	2881 (2897)
		GLTGPIGPPGPAG**PS**GDKGESGPSGP**V**GPTGAR	2897 (2913)
COL1A2 757–789	G	GP**P**GE**A**GA**S**GPPGSSGPQGL**L**GAPGILGLPGSR	2929 (2945)
		GP**P**GE**A**GA**T**GPPGSSGPQGL**L**GAPGILGLPGSR	2943 (2959)
		GP**E**GE**A**GA**S**GPPGSSGPQGL**L**GAPGILGLPGSR	2945 (2961)
		GP**P**GE**S**GA**V**GPPGSSGPQGL**L**GAPGILGLPGSR	2957 (2973)
		GP**P**GE**S**GA**T**GPPGSSGPQGL**L**GAPGILGLPGSR	2959 (2975)
		GP**P**GE**S**GA**L**GPPGSSGPQGL**L**GAPGILGLPGSR	2971 (2987)
		GP**P**GE**A**GA**T**GPPGSSGPQGL**W**GAPGILGLPGSR	2999 (3015)
COL1A2 10–42		GPPGA**S**GPPGAQGFQGPAGEPGE**P**GQTGPAG**A**R	2975
		GPPGA**T**GPPGAQGFQGPAGEPGE**P**GQTGPAG**A**R	2989
		GPPGA**S**GPPGAQGFQGPAGEPGE**P**GQTGPAG**S**R	2991
		GPPGA**S**GPPGAQGFQGPAGEPGE**D**GQTGPAG**A**R	3009
COL1A2 889–906		GEPGP**V**GSVGPVGP**T**GAR	1606
		GEPGP**A**GSVGPVGP**F**GAR	1624
		GEPGP**V**GSVGPVGP**F**GAR	1652

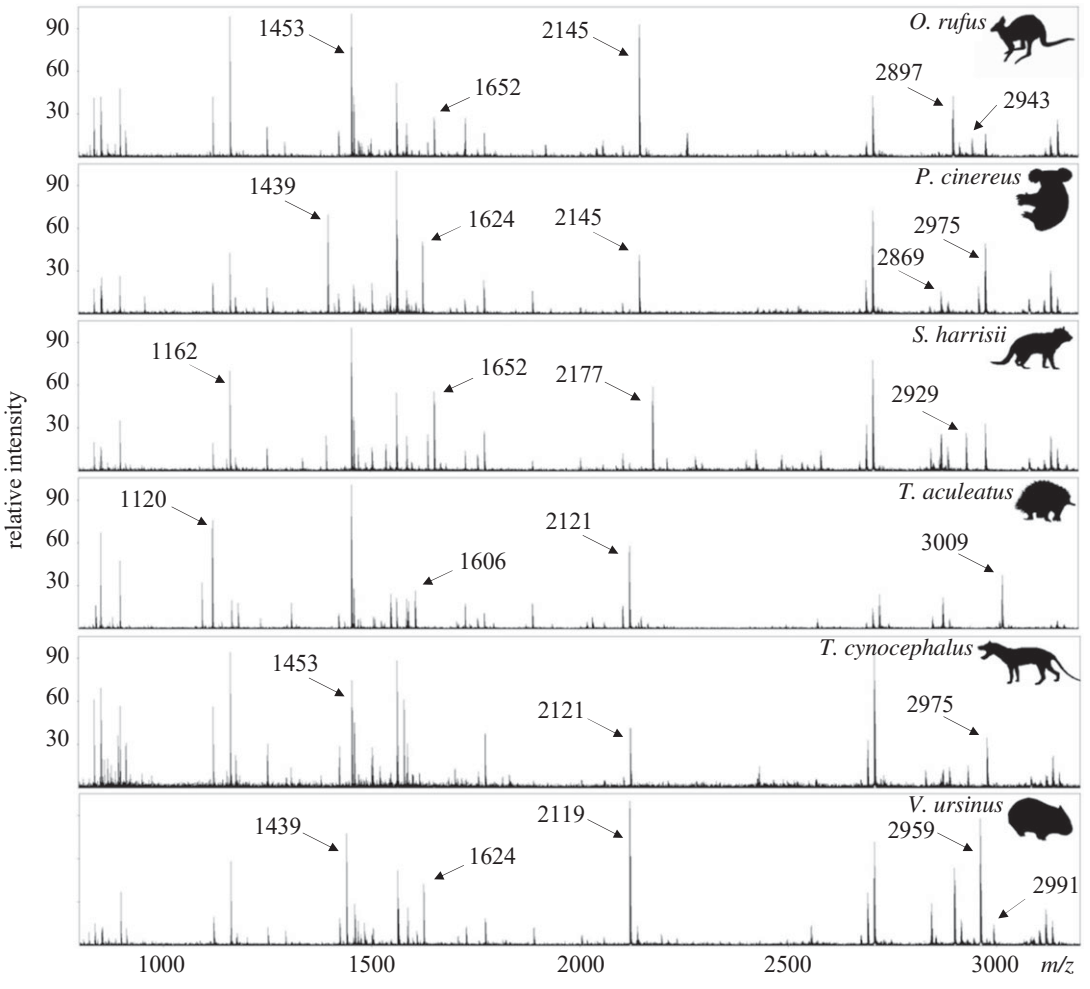

Figure 1. Examples of peptide mass fingerprints for *O. rufus*, *P. cinereus*, *S. harrisii*, *T. aculeatus*, *T. cynocephalus* and *V. ursinus*.

the tryptic cut site, as shown above, also results in a change of the starting location of the next peptide in the collagen sequence.

Next to the differences at COL1A1 508–519 (P1), COL1A2 502–519 (C) and COL1A2 454–483 (E), the monotreme *T. aculeatus* also differs from the studied marsupials in the majority of the other peptide markers. The observed differences between *T. aculeatus* and the other species studied are most likely the result of the unique evolutionary trajectory of *T. aculeatus* [4], which is the only monotreme species included in this study. However, caution should be taken when extrapolating these results to Ornithorhynchidae, the other monotreme family, as it is possible that these peptide markers may differ between taxa.

3.3. Marsupial ZooMS markers

Peptide markers that show a high level of variation between marsupial taxa are COL1A2 978–990 (A), COL1A2 484–498 (B), COL1A2 292–309 (P2), COL1A2 793–816 (D), COL1A1 586–618 (F/F′), COL1A2 757–789 (G/G′), COL1A2 10–42 and COL1A2 889–906. With the exception of *I. macrourus*, peptide marker COL1A2 978–990 (A) has the ability to distinguish macropods from other marsupials. A combination of the other peptide markers can be used to differentiate between other marsupial species (table 1 and figure 1).

Peptide marker COL1A2 (P2) shows a high level of variation between marsupial species. However, for most species, this marker was not visible in the MALDI spectra and was only identified in the MS/MS spectral data in low quantities. Therefore, this marker has only been reported for species where the peptide sequence could be confirmed in the final Byonic search. Peptide marker COL1A2 793–816 (D) also has the ability to differentiate between marsupial species. It must be noted, however, that the peaks at *m*/*z* 2161 and *m*/*z* 2177 are not mutually exclusive. For these peptide sequences,

Table 3. Peptide marker differences between macropods. Peptide markers in bold represent those that can be used to distinguish between taxa.

	COL1A2 484–498	COL1A1 586–618	COL1A2 10–42	COL1A2 889–906
L. conspicillatus	1453	2897/2913	2975	1652
L. fasciatus	1453	**2881/2897**	2975	1652
Macropus sp.	1453	2897/2913	**2989**	1652
Osphranter sp.	1453	2897/2913	2975	1652
Notamacropus sp.[a]	1453	2897/2913	2975	1652
N. irma	**1427**	2897/2913	2975	1652
N. eugenii	1453	2897/2913	2975	**1624**
W. bicolor	1453	2897/2913	2975	**1624**

[a]All species of the genus except for *N. irma and N. eugenii.*

peptides with both two and three oxidations of proline are identified in the MS/MS data. A peak at *m*/*z* 2177 could, in theory, also match to the peptide sequence reported for *m*/*z* 2161, and vice versa. Furthermore, the peptide sequence for *V. ursinus* is visible in the MS/MS data with both two and three oxidations. For most species, the variant with three oxidations is most visible in the MALDI spectra, but for *V. ursinus*, the variant with two oxidations was most visible. We therefore reported this marker at *m*/*z* 2119, corresponding to the variant with two oxidations.

Peptide marker COL1A2 757–789 (G/G′) is highly diverse between marsupial species and thus holds the potential to be used to uniquely identify taxonomic groups. However, some of the masses are identical for different peptide sequences. The peak at *m*/*z* 2945 can represent both COL1A2 757–789 (G′) for *P. tapoatafa*, *S. harrisii*, *T. cynocephalys* and *P. peregrinus*, as well as COL1A2 757–789 (G) for *T. vulpecula*. Similarly, *m*/*z* 2959 can represent COL1A2 757–789 (G′) for macropods as well as COL1A2 757–789 (G) for *P. cinereus*, *Lasiorhinus* sp. and *V. ursinus*. These *m*/*z* values can thus only be reliably used to make taxonomic identifications when found in combination with their corresponding G or G′ masses.

3.4. Using ZooMS to identify macropods

The ZooMS spectra of all studied macropods (*L. conspicillatus*, *L. fasciatus*, *M. giganteus*, *M. fuliginosus*, *O. rufus*, *O. robustus*, *N. rufogriseus*, *N. eugenii*, *N. agilis*, *N. irma*, *N. parma* and *W. bicolor*) are largely similar, with the majority of the studied species characterized by identical peptide markers. However, it is possible to identify some species based on differences in their peptide markers (table 3). Peptide marker COL1A2 484–498 (B) at *m*/*z* 1427 (sequence: GSPGEFGKOGPAGPR) can be used to identify *N. irma*. This peptide marker is located at *m*/*z* 1453 (sequence: GLPGEFGLPGPAGPR) in other macropods (figure 2). *N. eugenii* and *W. bicolor* can be distinguished from other macropods on the basis of peptide marker COL1A2 292–309 (P2), with the former two at *m*/*z* 1625, compared to *m*/*z* 1652 in other macropods. Furthermore, a difference at peptide marker COL1A1 586–618 (F/F′) has been observed between *L. fasciatus* (*m*/*z* 2881/2897) and other macropods (*m*/*z* 2897/2913). However, because of the partial overlap between these *m*/*z* values, it is only possible to confidently assign this peptide marker when both peaks are visible in the MALDI spectra. Finally, *m*/*z* 2989, attributed to COL1A2 10–42, can be used to separate *Macropus* (*M. giganteus* and *M. fuliginosus*) from other macropods in which this peptide marker corresponds to *m*/*z* 2975.

LC-MS/MS analysis provides a further opportunity to differentiate between macropod species with identical ZooMS peptide markers. Differences have been observed between the amino acid sequence of peptide COL1A2 671–700 for *L. conspicillatus* (sequence GENG**A**VGPTGPVGAAGP**S**GPNGPPGPVGGR) and all other macropod species (sequence GENG**V**VGPTGPVGAAGP**A**GPNGPPGPVGGR). However, the corresponding *m*/*z* peaks were not detectable in the MALDI spectra. *L. conspicillatus* is thus only identifiable on the basis of peptide sequence data obtained through LC-MS/MS analysis.

3.5. Collagen fingerprinting of archaeological specimens

Of the 134 archaeological samples analysed from Bandicoot Bay, 43 samples (32%) had sufficient collagen preservation to make taxonomic identifications using ZooMS (table 4). Macropods ($n = 36$) make up the

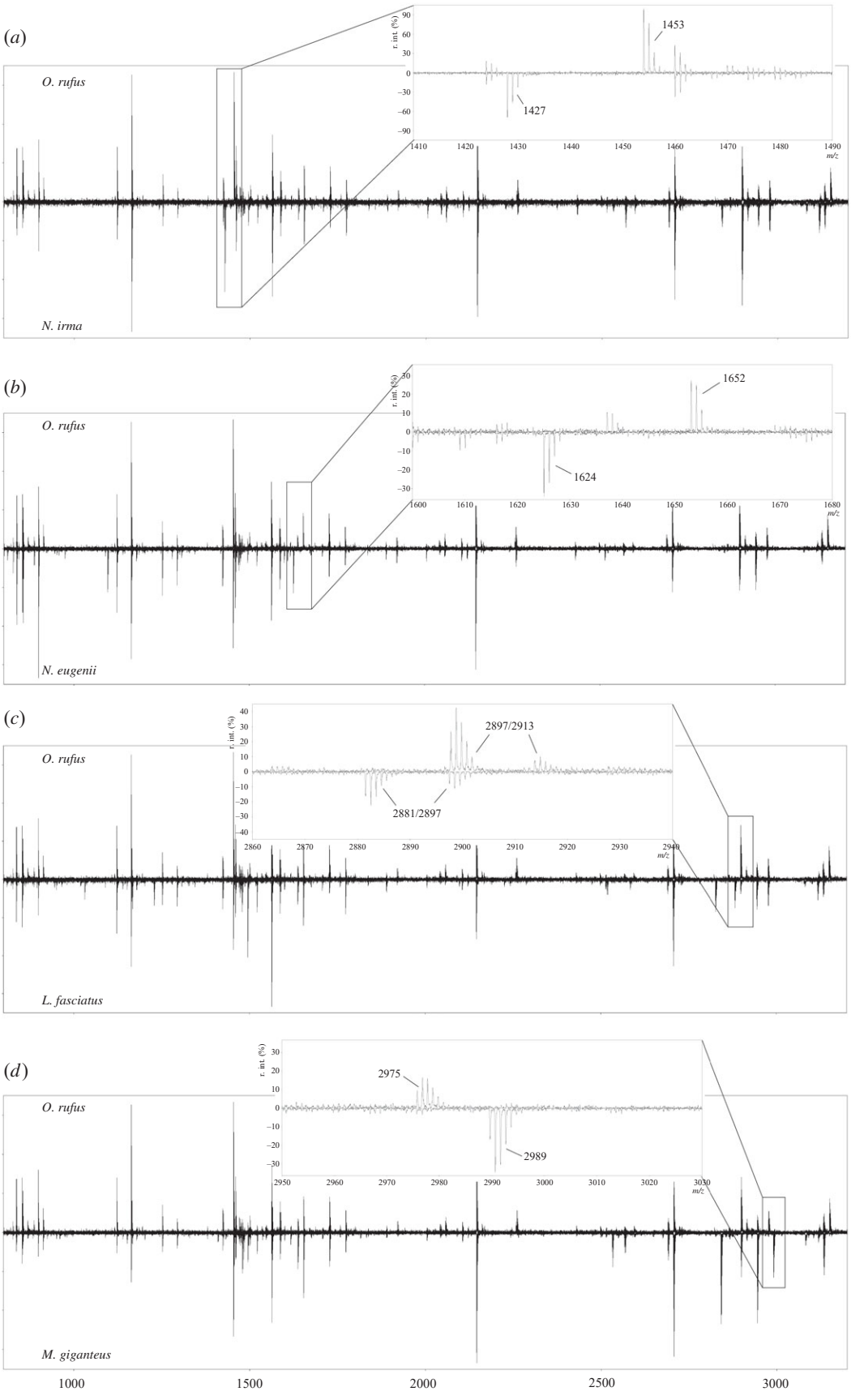

Figure 2. Example of differences in peptide mass fingerprints between macropods: (*a*) the difference at COL1A2 484–498 (B) between *O. rufus* and *N. irma*; (*b*) the difference at COL1A2 292–309 (P2) between *O. rufus* and *W. bicolor*; (*c*) the difference at COL1A1 586–618 (F/F′) between *O. rufus* and *L. fasciatus*; (*d*) the difference at COL1A2 10–42 between *O. rufus* and *M. giganteus*.

Table 4. ZooMS identifications of analysed archaeological specimens. Morphological ID refers to taxa identified in the Bandicoot Bay zooarchaeological assemblage [15,54]. Samples that failed or were unidentifiable with ZooMS reference data were excluded ($n = 85$).

ZooMS ID	ZooMS NISP	morphological ID
Isoodon sp.	3	*Isoodon auratus barrowensis*
Trichosurus vulpecula	1	*Trichosurus vulpecula*
Macropodidae	36	*Lagorchestes conspicillatus*
		Osphranter robustus isabellinus
Bovidae/Cervidae	1	
Chelonia mydas	2	Chelonioidea
total	43	

bulk of the analysed bone fragments. We can exclude *L. fasciatus*, *M. giganteus*, *M. fuliginosus*, *N. irma*, *N. eugenii* and *W. bicolor* as the origin of these samples on the basis of peptide markers COL1A2 484–498 (B), COL1A1 586–618 (F), COL1A2 10–42 and COL1A2 889–906, which leaves *L. conspicillatus*, *O. robustus*, *O. rufus*, *N. agilis*, *N. parma* and *N. rufogriseus* as possible origins for these bone fragments. It is most likely that the identified macropods represent the two species already identified in the zooarchaeological assemblage, *L. conspicillatus* (spectacled hare wallaby) and *O. robustus isabellinus* (common wallaroo). Three specimens are assigned to *Isoodon* sp.; on the basis of the zooarchaeological identifications of *I. auratus barrowensis* (golden bandicoot), the ZooMS identified specimens most likely represent this species. The collection of a reference sample of *I. auratus barrowensis* would be advantageous in this case. However, this was outside of the scope of the current study, for which this case study served solely as a test of the developed peptide markers. One specimen has been identified as *T. vulpecula* (brushtail possum).

Using previously published peptide markers [66], two specimens were identified as *Chelonia mydas* (green sea turtle). While the presence of sea turtles at Bandicoot Bay was known from zooarchaeological investigations [15,54], the exact species was unknown. In addition, one Bandicoot Bay specimen was identified as Bovidae/Cervidae, fauna that are not present in the wild on Barrow Island. The specimen is most likely a bovid, as only limited introduced cervid populations have been established in Australia, and none in north-western Australia. Possible bovid species that this specimen could represent are sheep and goat, which are known to have been present during the colonial period as livestock, or perhaps cattle, but only if it was brought in as processed, barrelled meat. Since domesticated species were not identified at the site through standard zooarchaeological methods [54], this specimen represents the first reported domesticated animal at Bandicoot Bay and provides evidence for food provisioning.

In addition to the 43 samples that were taxonomically identifiable using ZooMS, six specimens had spectra that were not attributable to any known taxa. Based on the lack of the characteristic COL1A1 508–519 (P1) marker, these specimens are tentatively identified as fish or bird specimens. Furthermore, seven samples only showed a peak at peptide marker COL1A1 508–519 (P1) at m/z 1162, but lacked other peptide markers to make taxonomic identifications. Overall, despite analysing only 4.6% of the total faunal fragments, two previously unidentified taxa (*C. mydas*, and a probable bovid) were identified using ZooMS, increasing the total number of identified taxa at the site from four to six.

4. Discussion

The novel set of reference peptide markers developed for this study allow for genus-level identifications of Australian marsupials using ZooMS, with some limitations only with regards to macropods. Collagen fingerprinting of fragmented bones from Bandicoot Bay, Barrow Island has shown the utility of these peptide markers, and we were able to successfully identify bone fragments that were not able to be morphologically identified, highlighting the potential of ZooMS in Australian contexts even in extremely harsh environments. The large-scale application of ZooMS, combined with zooarchaeology, has tremendous potential to contribute to the study of biodiversity trends, past subsistence strategies and material culture at Australian sites.

4.1. ZooMS insights at Bandicoot Bay

Despite the poor preservation of the faunal material at Bandicoot Bay, ZooMS was successfully employed to identify a range of marsupials, all of which were previously reported based on standard zooarchaeological techniques. This is an important finding, highlighting the potential of ZooMS in Australia even under harsh taphonomic conditions. The zooarchaeological record at the site was also further expanded with the identification of two green turtle specimens, as well as the first reported domesticated species from the site. While not identified at the site using morphological techniques, the presence of domesticated bovid makes sense in light of the kinds of foods imported to pearling stations, such as salted beef, pork, mutton and other barrelled meats [67–69]. The identification of new species in the Bandicoot Bay assemblage through ZooMS highlights the added value of collagen fingerprinting, especially when applied alongside more standard zooarchaeological investigations using osteological methods. Only a small number of archaeological specimens from Bandicoot Bay were analysed using ZooMS; a much larger study would likely yield further identifications not made on the basis of standard zooarchaeological techniques.

The identification of *C. mydas* (green sea turtle) provides valuable insight into seasonal site use at Bandicoot Bay. Six of the world's seven turtle species visit Barrow Island, with three of these species (*C. mydas*, *Natator depressus* (flatback sea turtle), *Eretmochelys imbricata* (hawksbill sea turtle)) found annually nesting along Barrow Island's sandy beaches [70]. Although *C. mydas* has been observed feeding along the west coast of Barrow Island throughout the year, its population numbers peak between November and March during the nesting season [71]. Nesting primarily takes place along the east coast of Barrow Island and in the sheltered beaches within Little Bandicoot Bay [71], adjacent to the Bandicoot Bay archaeological site. Turtles may have been targeted in open water but the proximity of the archaeological site to a known *C. mydas* nesting location, along with ZooMS identifications of *C. mydas*, suggests the site was occupied during the summer pearling season. This timing supports Dooley *et al*.'s [54] suggestion that the site may represent mid-season provisioning of a pearling lugger and reveals how Aboriginal labourers targeted turtle, which is a highly valued food. This further adds to the story of survival for indentured Aboriginal divers on Barrow Island.

4.2. Comparison to published markers

The results from this study broadly align with the incomplete marker profiles published previously for Australian marsupials [53]. Particularly interesting is peptide marker COL1A1 586–618 (F/F′), which differs between *L. fasciatus* at *m*/*z* 2881/2897 and other macropods at *m*/*z* 2897/2913. Incomplete published marker profiles for *S. occidentalis*, the extinct short-faced kangaroo, also presented the peaks for COL1A1 586–618 (F/F′) at *m*/*z* 2881/2897 [53], resembling *L. fasciatus*. Both morphological [72–74] and genetic studies [75–78] have proposed *L. fasciatus* as the closest living relative of the extinct sthenurine kangaroos, and the collagen peptide sequences identified here agree with this proposed close phylogenetic relationship.

There are five instances in which our data do not match the incomplete marker profiles published by Buckley *et al*. [53]. In two cases, the differences stem from increasing the number of reference samples and therefore providing increased taxonomic resolution. Our analysis of collagen sequence data and LC-MS/MS data confirm that there are differences in peptide marker COL1A2 10–42 between *Macropus* and *Osphranter*, contradicting previous uniform reporting of this peptide marker for these genera [53]. We also analysed MALDI spectra and LC-MS/MS data from an additional species in the genus *Isoodon* and found that it is possible to distinguish between both on the basis of peptide markers COL1A2 793–816 (D) and COL1A1 586–618 (F/F′).

In three other cases, our markers directly disagreed with previously published markers. We found different *m*/*z* values for peptide marker COL1A2 10–42 for *P. peregrinus* reported at *m*/*z* 2987 by Buckley *et al*., and for peptide markers COL1A2 793–816 (D), COL1A2 757–789 (G/G′) and COL1A2 10–42 for *V. ursinus*, reported at *m*/*z* 2161, 2929, and 2959, respectively [53]. Our analysis of collagen sequence data and LC-MS/MS data confirmed the peptide markers we proposed on the basis of the MALDI-TOF-MS spectral data and aligns with genetic data available for *V. ursinus*. In the case of *P. peregrinus*, our proposed peptide marker aligns with the other species reported in this study, and no other species have peptide marker COL1A2 10–42 at *m*/*z* 2987. We therefore argue that the peptide markers presented in this study, that differ from the ones reported previously, are correct. Since neither the MALDI spectra nor the raw MS/MS data were openly available for the previous study, we are unable to re-evaluate the previously published markers. We thus stress the importance of

confirming peptide biomarkers using collagen sequence data obtained through LC-MS/MS analysis, and where possible genetic data, as well as making MALDI spectra and raw MS/MS data openly available.

4.3. Challenges and future prospects

One of the main challenges for the identification of marsupials using ZooMS is that some species are only distinguishable on the basis of a single peptide marker. This often requires high-quality spectral data, in which the high mass peaks are clearly defined. However, collagen preservation has proven to be problematic in Australian faunal assemblages [20,21], and our own results support this finding. Collagen preservation in the Bandicoot Bay assemblage was variable; in some specimens, collagen was reasonably well preserved and spectra were suitable to make taxonomic identifications, while poorer preservation in other specimens meant that resolution of spectra was not sufficient for ZooMS identifications. These issues surrounding collagen preservation can be expected to increase considerably when older assemblages are analysed. The recent development of pre-screening techniques, such as Fourier transform infrared spectroscopy, that can be used to assess the molecular preservation of fossil material [79–82] could offer a partial solution to this challenge. These methods allow for the rapid identification of well-preserved specimens that are suitable for proteomic analysis.

As with other ZooMS markers that have been developed, the markers presented here do not show a straightforward relationship between phylogenetic distance and sequence variation. COL1 is functionally constrained and therefore exhibits a slow rate of evolutionary change and accumulation of sequence mutations. Accordingly, only a small percentage of the COL1 sequence produces usable ZooMS markers, with the result that divergence time alone is not a sufficient predictor of the ability to discriminate taxa using ZooMS. Within marsupials, genus-level identifications are possible within some families. The genera *Phascogale* and *Sarcophilus* (diverged 13–21.2 Ma [83]) from the family Dasyuridae can be distinguished, for example, as can the genera *Isoodon* and *Perameles* (diverged 12.1–4.8 Ma [83]) from the family Peramelidae. In the Macropodidae family, the genus *Lagostraphus* can be distinguished from the rest of the genera in the family (diverged 25.7–11.9 Ma [75]). However, for *Macropus*, *Notamacropus*, *Osphranter* and *Wallabia* (common ancestor 13.7–8 Ma [75]), divergence time does not line up with the number of variations in the COL1 sequence. For example, within *Notamacropus*, *N. eugenii* and *N. agilis* (diverged less than 2 Ma [75]) can be distinguished, while *N. eugenii* and *W. bicolor*, which are more distantly related, have identical ZooMS marker profiles.

Although it is not possible to uniquely identify every marsupial species using ZooMS alone, peptide mass fingerprinting combined with biogeographical and zooarchaeological data does provide the opportunity to significantly increase the accuracy of taxonomic identifications. For example, while eastern and western grey kangaroos (*M. giganteus* and *M. fuliginosus*, respectively) share an identical set of ZooMS peptide markers, the eastern species is today found in the eastern states of Australia, while the western species occurs in the southern and western parts of Australia [84]. However, the potential for recent local extinctions as well as range shifts should not be overlooked [19,85–87]. Eastern and western kangaroo ranges overlap in south-central Australia, and a recent aDNA study has demonstrated that, historically, both species were found on Kangaroo Island, whereas it was previously thought that only the western variety had roamed there [88]. Nonetheless, species biogeography can in some cases still help support the attribution of more specific taxonomic identifications, if used cautiously and bearing the clear caveats in mind.

The development of ZooMS peptide markers for Australian marsupials is significant for zooarchaeological endeavours on the continent. Marsupial taxa form a significant component of Australian zooarchaeological and palaeontological assemblages, yet due to the challenges of discriminating between related taxa, they are currently rarely identified beyond the very broad family level [18,28,87]. This significantly limits the interpretive power of zooarchaeological and palaeontological studies on the continent [28]. The current set of peptide markers holds promise for enhancing research into marsupial biodiversity change in Australia, as well as palaeoenvironmental change and human behaviour.

To further expand the capabilities of ZooMS in Australian contexts, it will be necessary to develop peptide markers for other Australian taxa, such as other extant monotremes. The highly fragmented nature of bone assemblages at Australian sites due to poor preservation conditions, carnivore activity and extensive carcass processing by humans necessitated by the limited food resources available in arid environments [89] will likely make ZooMS an important tool in the repertoire available to Australian zooarchaeologists and palaeontologists moving forward. ZooMS will also be useful when morphological similarities make it challenging to differentiate between genera. Macropods, for

example, can be represented by multiple extant genera in a single region [7,90]. These are challenging to distinguish with morphological approaches unless dental remains are present and even then, heavy toothwear may confound identifications [28,91]. This inherently limits the identification of faunal material through morphological approaches, leaving a significant proportion of postcranial bones from Australian archaeological sites unidentified beyond family level. By offering the ability to undertake higher level taxonomic attributions of a broader range of faunal remains, ZooMS can help to significantly enhance Australian faunal datasets.

Future extension of Australian ZooMS markers to include small mammal species will be particularly useful. ZooMS has the potential to address a critical deficit in examining biodiversity trends in native rodents, bandicoots and dasyurids on the continent. These are often overlooked in both archaeological and palaeontological sites due to difficulties in identification. Nevertheless, they are critical environmental indicators [92,93] and were an important food source for some Australian indigenous groups [94–96]. Improved identification rates of these species in early contact sites is also important for tracking the spread of non-native species in Australia, information that is also critical for modern conservation efforts [97]. Furthermore, the possibility of identifying extinct megafauna species using collagen fingerprints holds significant potential to aid the study of megafauna extinctions on the continent. One of the main issues for understanding these extinctions in Australia is the significant knowledge gaps that exist for many species. Data on species biochronology and palaeobiogeography are mostly patchy, with many species only having been reported at a handful of sites [18,98,99]. ZooMS offers a significant opportunity to address these issues by improving identification rates of fragmented bones.

The peptide biomarkers developed for this study hold tremendous potential for the increasing application of ZooMS in Australia, where the method has so far been minimally applied relative to European contexts. Future years will see the important set of reference markers published here added to and enhanced, offering significant potential for addressing new research questions and themes, and enhancing the ability of researchers to examine topics of current interest in Australian archaeology and palaeontology.

Ethics. The handling, sampling and analysis of modern and archaeological specimens were conducted in accordance with CITES regulations. No live animals were included in the study.

Data accessibility. MALDI-TOF-MS spectra for modern references (https://doi.org/10.5281/zenodo.5040049) [100] and archaeological specimens (https://doi.org/10.5281/zenodo.5040055) [101] have been uploaded to Zenodo and are publicly available. MS/MS data files are available at PXD027107 and were uploaded through MassIVE (MSV000087755, https://doi.org/10.25356/C5TC2H) [102]. The URL link to the dataset is ftp://massive.ucsd.edu/MSV000087755/.

Authors' contributions. C.P., K.K.R., T.M., J.D., J.L., G.J.P., M.P., A.C. and N.B. conceived and designed the study; C.P. performed ZooMS analysis and prepared samples for LC-MS/MS analysis; C.P. and K.K.R. analysed ZooMS and LC-MS/MS data; T.M., A.P., K.T., J.L. and G.J.P. provided samples; C.P. and N.B. wrote the paper, with critical input from all authors. All authors reviewed and approved the manuscript.

Competing interests. We declare we have no competing interests.

Funding. This research was supported by the Max Planck Society, and the Australian Research Council (grant no. DP130100802, awarded to T.M. and A.P.; grant no. DE150101597, awarded to T.M.; and grant no. FT150100168, awarded to A.P.).

Acknowledgements. We are grateful to the Mammalogy collection of the Western Australian Museum, and Kylea Clarke from the Mammalogy collection of Museums Victoria for granting us access to their collections. We would also like to thank Sandra Hebestreit for the technical assistance with ZooMS extractions. Finally, we would like to thank the two anonymous reviewers for their comments and suggestions, which helped improve the paper.

References

1. Holt BG *et al.* 2013 An update of Wallace's zoogeographic regions of the world. *Science* **339**, 74–78. (doi:10.1126/science.1228282)
2. Woinarski JCZ, Burbidge AA, Harrison PL. 2015 Ongoing unraveling of a continental fauna: decline and extinction of Australian mammals since European settlement. *Proc. Natl Acad. Sci. USA* **112**, 4531–4540. (doi:10.1073/pnas.1417301112)
3. Black KH, Archer M, Hand SJ, Godthelp H. 2012 The rise of Australian marsupials: a synopsis of biostratigraphic, phylogenetic, palaeoecological and palaeobiogeographic understanding. In *Earth and life* (ed. JA Talent), pp. 983–1078. Dordrecht, The Netherlands: Springer.
4. Bininda-Emonds ORP *et al.* 2007 The delayed rise of present-day mammals. *Nature* **446**, 507–512. (doi:10.1038/nature05634)
5. Laurance WF *et al.* 2011 The 10 Australian ecosystems most vulnerable to tipping points. *Biol. Conserv.* **144**, 1472–1480. (doi:10.1016/j.biocon.2011.01.016)
6. Dortch J, Wright H. 2010 Identifying palaeo-environments and changes in Aboriginal subsistence from dual-patterned faunal assemblages, south-western Australia. *J. Archaeol. Sci.* **37**, 1053–1064. (doi:10.1016/j.jas.2009.12.006)

7. Balme J, O'Connor S, Maloney T, Vannieuwenhuyse D, Aplin K, Dilkes-Hall IE. 2019 Long-term occupation on the edge of the desert: Riwi Cave in the southern Kimberley, Western Australia. *Archaeol. Oceania* **54**, 35–52. (doi:10.1002/arco.5166)
8. Cosgrove R, Garvey J. 2017 Behavioural inferences from late Pleistocene Aboriginal Australia: seasonality, butchery and nutrition in southwest Tasmania. In *The Oxford handbook of zooarchaeology* (eds U Albarella, M Rizzetto, H Russ, K Vickers, S Viner-Daniels). Oxford, UK: Oxford University Press.
9. Allen H, Langley MC, Taçon PSC. 2016 Bone projectile points in prehistoric Australia: evidence from archaeologically recovered implements, ethnography and rock art. In *Osseous projectile weaponry* (ed. M Langley), pp. 209–218. Dordrecht, The Netherlands: Springer.
10. Langley M, O'Connor S, Aplin K. 2016 A >46 000-year-old kangaroo bone implement from Carpenter's Gap 1 (Kimberley, northwest Australia). *Quat. Sci. Rev.* **154**, 199–213. (doi:10.1016/j.quascirev.2016.11.006)
11. Langley M, Clarkson C, Ulm S. 2019 Symbolic expression in Pleistocene Sahul, Sunda and Wallacea. *Quat. Sci. Rev.* **221**, 105883. (doi:10.1016/j.quascirev.2019.105883)
12. Clarkson C *et al.* 2015 The archaeology, chronology and stratigraphy of Madjedbebe (Malakunaja II): a site in northern Australia with early occupation. *J. Hum. Evol.* **83**, 46–64. (doi:10.1016/j.jhevol.2015.03.014)
13. Jankowski NR, Gully GA, Jacobs Z, Roberts RG, Prideaux GJ. 2016 A late Quaternary vertebrate deposit in Kudjal Yolgah Cave, south-western Australia: refining regional late Pleistocene extinctions. *J. Quat. Sci.* **31**, 538–550. (doi:10.1002/jqs.2877)
14. Ditchfield K, Manne T, Hook F, Ward I, Veth P. 2018 Coastal occupation before the 'Big Swamp': results from excavations at John Wayne Country Rockshelter on Barrow Island. *Archaeol. Oceania* **53**, 163–178. (doi:10.1002/arco.5164)
15. Byrne C, Dooley T, Manne T, Paterson A, Dotte-Sarout E. 2020 Island survival: the anthracological and archaeofaunal evidence for colonial-era events on Barrow Island, north-west Australia. *Archaeol. Oceania* **55**, 15–32. (doi:10.1002/arco.5202)
16. Monks C, Dortch J, Jacobsen G, Baynes A. 2016 Pleistocene occupation of Yellabidde Cave in the northern Swan Coastal Plain, southwestern Australia. *Aust. Archaeol.* **82**, 275–279. (doi:10.1080/03122417.2016.124416)
17. Veth P *et al.* 2017 Early human occupation of a maritime desert, Barrow Island, north-west Australia. *Quat. Sci. Rev.* **168**, 19–29. (doi:10.1016/j.quascirev.2017.05.002)
18. Hocknull SA *et al.* 2020 Extinction of eastern Sahul megafauna coincides with sustained environmental deterioration. *Nat. Commun.* **11**, 2250. (doi:10.1038/s41467-020-15785-w)
19. Price GJ, Louys J, Smith GK, Cramb J. 2019 Shifting faunal baselines through the Quaternary revealed by cave fossils of eastern Australia. *PeerJ* **6**, e6099. (doi:10.7717/peerj.6099)
20. Langley M, Clarkson C, Ulm S. 2011 From small holes to grand narratives: the impact of taphonomy and sample size on the modernity debate in Australia and New Guinea. *J. Hum. Evol.* **61**, 197–208. (doi:10.1016/j.jhevol.2011.03.002)
21. Manne T, Veth P. 2015 Late Pleistocene and early Holocene exploitation of estuarine communities in northwestern Australia. *Quat. Int.* **385**, 112–123. (doi:10.1016/j.quaint.2014.12.049)
22. Aplin K, Manne T, Attenbrow V. 2016 Using a 3-stage burning categorization to assess post-depositional degradation of archaeofaunal assemblages: some observations based on multiple prehistoric sites in Australasia. *J. Archaeol. Sci. Rep.* **7**, 700–714. (doi:10.1016/j.jasrep.2015.11.029)
23. Miscamble T, Manne T. 2016 A taphonomic signature for quolls in the Australian archaeological record. *J. Archaeol. Sci. Rep.* **7**, 689–699. (doi:10.1016/j.jasrep.2016.01.011)
24. Marshall B, Cosgrove R. 1990 Tasmanian Devil (*Sarcophilus harrisii*) scat-bone: signature criteria and archaeological implications. *Archaeol. Oceania* **25**, 102–113. (doi:10.1002/j.1834-4453.1990.tb00240.x)
25. Kos AM. 2003 Characterisation of post-depositional taphonomic processes in the accumulation of mammals in a pitfall cave deposit from southeastern Australia. *J. Archaeol. Sci.* **30**, 781–796. (doi:10.1016/S0305-4403(02)00252-2)
26. Murray D, Haile J, Dortch J, White NE, Haouchar D, Bellgard MI, Allcock RJ, Prideaux GJ, Bunce M. 2013 Scrapheap challenge: a novel bulk-bone metabarcoding method to investigate ancient DNA in faunal assemblages. *Sci. Rep.* **3**, 3371. (doi:10.1038/srep03371)
27. Grealy A, Macken A, Allentoft ME, Rawlence NJ, Reed E, Bunce M. 2016 An assessment of ancient DNA preservation in Holocene-Pleistocene fossil bone excavated from the world heritage Naracoorte Caves, South Australia. *J. Quat. Sci.* **31**, 33–45. (doi:10.1002/jqs.2830)
28. Mein E, Manne T. 2021 Identifying marsupials from Australian archaeological sites: current methodological challenges and opportunities in zooarchaeological practice. *Archaeol. Oceania* **56**, 133–141. (doi:10.1002/arco.5234)
29. Brown S *et al.* 2016 Identification of a new hominin bone from Denisova Cave, Siberia using collagen fingerprinting and mitochondrial DNA analysis. *Sci. Rep.* **6**, 23559. (doi:10.1038/srep23559)
30. Harvey VL, Egerton VM, Chamberlain AT, Manning PL, Sellers WI, Buckley M. 2019 Interpreting the historical terrestrial vertebrate biodiversity of Cayman Brac (Greater Antilles, Caribbean) through collagen fingerprinting. *Holocene* **29**, 531–542. (doi:10.1177/0959683618824793)
31. Martisius NL *et al.* 2020 Non-destructive ZooMS identification reveals strategic bone tool raw material selection by Neandertals. *Sci. Rep.* **10**, 7746. (doi:10.1038/s41598-020-64358-w)
32. Culley C, Janzen A, Brown S, Prendergast ME, Shipton C, Ndiema E, Petraglia MD, Boivin NL, Crowther A. 2021 Iron Age hunting and herding in coastal eastern Africa: ZooMS identifications of domesticates and wild bovids at Panga ya Saidi, Kenya. *J. Archaeol. Sci.* **130**, 105368. (doi:10.1016/j.jas.2021.105368)
33. Janzen A *et al.* 2021 Distinguishing African bovids using zooarchaeology by mass spectrometry (ZooMS): new peptide markers and assessments of Iron Age economies in Zambia. *PLoS ONE* **16**, e0251061. (doi:10.1371/journal.pone.0251061)
34. Buckley M, Collins M, Thomas-Oates J, Wilson JC. 2009 Species identification by analysis of bone collagen using matrix-assisted laser desorption/ionisation time-of-flight mass spectrometry. *Rapid Commun. Mass Spectrom.* **23**, 3843–3854. (doi:10.1002/rcm.4316)
35. Sinet-Mathiot V, Smith GM, Romandini M, Wilcke A, Peresani M, Hublin JJ, Welker F. 2019 Combining ZooMS and zooarchaeology to study late Pleistocene hominin behaviour at Fumane (Italy). *Sci. Rep.* **9**, 12350. (doi:10.1038/s41598-019-48706-z)
36. Rodrigues ASL, Charpentier A, Bernal-Casasola D, Gardeisen A, Nores C, Millán JAP, McGrath K, Speller C. 2018 Forgotten Mediterranean calving grounds of grey and North Atlantic right whales: evidence from Roman archaeological records. *Proc. R. Soc. B* **285**, 20180961. (doi:10.1098/rspb.2018.0961)
37. Garrison EG, Morgan GS, McGrath K, Speller C, Cherkinsky A. 2019 Recent dating of extinct Atlantic gray whale fossils (*Eschrichtius robustus*), Georgia Bight and Florida, western Atlantic Ocean. *PeerJ* **7**, e6381. (doi:10.7717/peerj.6381)
38. Prendergast ME, Janzen A, Buckley M, Grillo KM. 2019 Sorting the sheep from the goats in the Pastoral Neolithic: morphological and biomolecular approaches at Luxmanda, Tanzania. *Archaeol. Anthropol. Sci.* **11**, 3047–3062. (doi:10.1007/s12520-018-0737-0)
39. Le Meillour L *et al.* 2020 Palaeoproteomics gives new insight into early southern African pastoralism. *Sci. Rep.* **10**, 14427. (doi:10.1038/s41598-020-71374-3)
40. Taylor WTT *et al.* 2021 Evidence for the early dispersal of domestic sheep into Central Asia. *Nat. Hum. Behav.* **5**, 1169–1179. (doi:10.1038/s41562-021-01083-y)
41. Coutu AN, Taurozzi AJ, Mackie M, Jensen TZT, Collins MJ, Sealy J. 2021 Palaeoproteomics confirm earliest domesticated sheep in southern Africa ca. 2000 BP. *Sci. Rep.* **11**, 6631. (doi:10.1038/s41598-021-85756-8)
42. Welker F *et al.* 2016 Palaeoproteomic evidence identifies archaic hominins associated with the Châtelperronian at the Grotte du Renne. *Proc. Natl Acad. Sci. USA* **113**, 11 162–11 167. (doi:10.1073/pnas.1605834113)
43. Desmond A, Barton N, Bouzouggar A, Douka K, Fernandez P, Humphrey L, Morales J, Turner E, Buckley M. 2018 ZooMS identification of bone tools from the north African Later Stone Age. *J. Archaeol. Sci.* **98**, 149–157. (doi:10.1016/j.jas.2018.08.012)
44. Bradfield J, Forssman T, Spindler L, Antonites AR. 2019 Identifying the animal species used to manufacture bone arrowheads in South Africa.

Archaeol. Anthropol. Sci. **11**, 2419–2434. (doi:10.1007/s12520-018-0688-5)

45. Buckley M, Fraser S, Herman J, Melton ND, Mulville J, Pálsdóttir AH. 2014 Species identification of archaeological marine mammals using collagen fingerprinting. *J. Archaeol. Sci.* **41**, 631–641. (doi:10.1016/j.jas.2013.08.021)
46. Welker F, Soressi M, Rendu W, Hublin JJ, Collins M. 2015 Using ZooMS to identify fragmentary bone from the Late Middle/Early Upper Palaeolithic sequence of Les Cottés, France. *J. Archaeol. Sci.* **54**, 279–286. (doi:10.1016/j.jas.2014.12.010)
47. Wang N *et al.* 2021 Testing the efficacy and comparability of ZooMS protocols on archaeological bone. *J. Proteomics* **233**, 104078. (doi:10.1016.j.jprot.2020.104078)
48. Kehlmeier C *et al.* 2017 Tropical ancient DNA reveals relationships of the extinct Bahamian giant tortoise *Chenoloidis alburyorum*. *Proc. R. Soc. B* **284**, 20162235. (doi:10.1098/rspb.2016.2235)
49. Hofreiter M, Paijmans JLA, Goodchild H, Speller C, Barlow A, Fortes GG, Thomas JA, Ludwig A, Collins M. 2014 The future of ancient DNA: technical advances and conceptual shifts. *Bioessays* **37**, 284–293. (doi:10.1002/bies.201400160)
50. Demarchi B *et al.* 2016 Protein sequences bound to mineral surfaces persist into deep time. *eLife* **5**, e17092. (doi:10.7554/eLife.17092)
51. Cappellini E *et al.* 2019 Early Pleistocene enamel proteome from Dmanisi resolves *Stephanorhinus* phylogeny. *Nature* **574**, 103–107. (doi:10.1038/s41586-019-1555-y)
52. Buckley M, Collins MJ. 2011 Collagen survival and its use for species identification in Holocene-lower Pleistocene bone fragments from British archaeological and paleontological sites. *Antiqua* **1**, e1. (doi:10.4081/antiqua.2011.e1)
53. Buckley M, Cosgrove R, Garvey J, Prideaux GJ. 2017 Identifying remains of extinct kangaroos in late Pleistocene deposits using collagen fingerprinting. *J. Quat. Sci.* **32**, 653–660. (doi:10.1002/jqs.2964)
54. Dooley T, Manne T, Paterson A. 2020 Power in food on the maritime frontier: a zooarchaeology of enslaved pearl divers on Barrow Island, Western Australia. *Int. J. Hist. Archaeol.* **25**, 544–576. (doi:10.1007/s10761-020-00575-3)
55. Paterson A. 2017 Unearthing Barrow Island's past: the historical archaeology of colonial-era exploitation, northwest Australia. *Int. J. Hist. Archaeol.* **21**, 346–368. (doi:10.1007/s10761-017-0411-8)
56. Paterson A, Veth P. 2020 The point of pearling: colonial pearl fisheries and the historical translocation of Aboriginal and Asian workers in Australia's northwest. *J. Anthropol. Archaeol.* **57**, 101143. (doi:10.1016/j.jaa.2020.101143)
57. Van der Sluis LG, Hollund HI, Buckley M, De Louw PGB, Rijsdijk KF, Kars H. 2014 Combining histology, stable isotope analysis and ZooMS collagen fingerprinting to investigate the taphonomic history and dietary behaviour of extinct giant tortoises from the Mare aux Songes deposit on Mauritius. *Palaeogeogr. Palaeoclimatol. Palaeoecol.* **416**, 80–91. (doi:10.1016/j.palaeo.2014.06.003)
58. Brown S, Hebestreit S, Wang N, Boivin NL, Douka K, Richter KK. 2020 Zooarchaeology by mass spectrometry (ZooMS) for bone material: acid insoluble protocol. *protocols.io*. (doi:10.17504/protocols.io.bf43jqyn)
59. Brown S, Hebestreit S, Wang N, Boivin NL, Douka K, Richter KK. 2020 Zooarchaeology by mass spectrometry (ZooMS) for bone material: acid soluble protocol. *protocols.io*. (doi:10.17504/protocols.io.bf5bjq2n)
60. Richter KK *et al.* 2020 What's the catch? Archaeological application of rapid collagen-based species identification. *J. Archaeol. Sci.* **116**, 105116. (doi:10.1016/j.jas.2020.105116)
61. Bern M, Kil YJ, Becker C. 2012 Byonic: advanced peptide and protein identification software. *Curr. Protoc. Bioinformatics* **40**, 13.20.11–13.20.14. (doi:10.1002/0471250953.bi1320s40)
62. Buckley M, Harvey VL, Chamberlain AT. 2017 Species identification and decay assessment of late Pleistocene fragmentary vertebrate remains from Pin Hole Cave (Creswell Crags, UK) using collagen fingerprinting. *Boreas* **46**, 402–411. (doi:10.1111/bor.12225)
63. Keller BO, Sui J, Young AB, Whittal RM. 2008 Interferences and contaminants encountered in modern mass spectrometry. *Anal. Chim. Acta* **627**, 71–81. (doi:10.1016/j.aca.2008.04.043)
64. Brown S, Douka K, Collins MJ, Richter KK. 2021 On the standardization of ZooMS nomenclature. *J. Proteomics* **235**, 104041. (doi:10.1016/j.jprot.2020.104041)
65. Buckley M, Cheylan M. 2020 Collagen fingerprinting for the species identification of archaeological amphibian remains. *Boreas* **49**, 709–717. (doi:10.1111/bor.12443)
66. Harvey VL, LeFebvre MJ, deFrance SD, Toftgaard C, Drosou K, Kitchener AC, Buckley M. 2019 Preserved collagen reveals species identity in archaeological marine turtle bones from Caribbean and Florida sites. *R. Soc. Open Sci.* **6**, 191137. (doi:10.1098/rsos.191137)
67. Guiry EJ, Staniforth M, Nehlich O, Grimes V, Smith C, Harpley B, Noël S, Richards MP. 2015 Tracing historical animal husbandry, meat trade, and food provisioning: a multi-isotopic approach to the analysis of shipwreck faunal remains from the William Salthouse, Port Phillip, Australia. *J. Archaeol. Sci. Rep.* **1**, 21–28. (doi:10.1016/j.jasrep.2014.10.001)
68. Gibbs M. 2005 Archaeology of subsistence on the maritime frontier: faunal analysis of the Cheyne Beach whaling station 1845–1877. *Australas. Hist. Archaeol.* **23**, 115–122.
69. English AJ. 1990 Salted meats from the wreck of the 'William Salthouse': archaeological analysis of nineteenth century butchery patterns. *Aust. J. Hist. Archaeol.* **8**, 63–69.
70. Department of Parks and Wildlife. 2015 *Barrow group reserves: management plan 82*. Kensington, WA: State Government of Western Australia.
71. Pendoley KL. 2005 Sea turtles and the environmental management of industrial activities in north west Western Australia. PhD thesis, Murdoch University, Perth, Australia.
72. Prideaux GJ. 2004 *Systematics and evolution of the sthenurine kangaroos*. Berkeley, CA: University of California Press.
73. Flannery TF. 1983 Revision in the subfamily Sthenurinae (Marsupialia: Macropodoidea) and the relationships of species of *Troposodon* and *Lagostrophus*. *Aust. Mammal.* **6**, 15–28.
74. Flannery TF. 1989 Phylogeny of the Macropodoidea: a study in convergence. In *Kangaroos, wallabies and rat-kangaroos* (eds G Grigg, P Jarman, I Hume), pp. 1–46. Chipping Norton, UK: Surrey Beaty & Sons.
75. Meredith RW, Westerman M, Springer MS. 2008 A phylogeny and timescale for the living genera of kangaroos and kin (Macropodiformes: Marsupialia) based on nuclear DNA sequences. *Aust. J. Zool.* **56**, 395–410. (doi:10.1071/Z008044)
76. Phillips MJ, Haouchar D, Pratt RC, Gibb GC, Bunce M. 2013 Inferring kangaroo phylogeny from incongruent nuclear and mitochondrial genes. *PLoS ONE* **8**, e57745. (doi:10.1371/journal.pone.0057745)
77. Cascini M, Mitchell KJ, Cooper A, Phillips MJ. 2019 Reconstructing the evolution of giant extinct kangaroos: comparing the utility of DNA, morphology, and total evidence. *Syst. Biol.* **68**, 520–537. (doi:10.1093/sysbio/syy080)
78. Llamas B *et al.* 2014 Late Pleistocene Australian marsupial DNA clarifies the affinities of extinct megafaunal kangaroos and wallabies. *Mol. Biol. Evol.* **32**, 574–584. (doi:10.1093/molbev/msu338)
79. Pothier Bouchard G, Mentzer SM, Riel-Salvatore J, Hodgkins J, Miller CE, Negrino F, Wogelius RA, Buckley M. 2019 Portable FTIR for on-site screening of archaeological bone intended for ZooMS collagen fingerprint analysis. *J. Archaeol. Sci. Rep.* **26**, 101862. (doi:10.1016/j.jasrep.2019.05.027)
80. Kontopoulos I *et al.* 2020 Screening archaeological bone for palaeogenetic and palaeoproteomic studies. *PLoS ONE* **15**, e0235146. (doi:10.1371/journal.one.0235146)
81. Sponheimer M, Ryder CM, Fewlass H, Smith EK, Pestle WJ, Talamo S. 2019 Saving old bones: a non-destructive method for bone collagen prescreening. *Sci. Rep.* **9**, 13928. (doi:10.1038/s41598-019-50443-2)
82. Chowdhury MP *et al.* 2021 Machine learning ATR-FTIR spectroscopy data for the screening of collagen for ZooMS analysis and mtDNA in archaeological bone. *J. Archaeol. Sci.* **126**, 105311. (doi:10.1016/j.jas.2020.105311)
83. Kumar S, Stecher G, Suleski M, Hedges SB. 2017 TimeTree: a resource for timelines, timetrees, and divergence times. *Mol. Biol. Evol.* **34**, 1812–1819. (doi:10.1093/molbev/msx116)
84. Kirsch JAW, Poole WE. 1972 Taxonomy and distribution of the grey kangaroos, *Macropus giganteus* Shaw and *Macropus fuliginosus* (Desmarest), and their subspecies (Marsupialia: Macropodidae). *Aust. J. Zool.* **20**, 315–339. (doi:10.1071/Z09720315)
85. Helgen KM, Flannery TF. 2003 Taxonomy and historical distribution of the wallaby genus *Lagostrophus*. *Aust. J. Zool.* **51**, 199–212. (doi:10.1071/Z002078)
86. Munro NT, McIntyre S, Macdonald B, Cunningham SA, Gordon IJ, Cunningham RB,

Manning AD. 2019 Returning a lost process by reintroducing a locally extinct digging marsupial. *PeerJ* **7**, e6622. (doi:10.7717/peerj.6622)

87. Price GJ, Cramb J, Louys J, Travouillon KJ, Pease EM, Feng YX, Zhao JX, Irvin D. 2020 Late Quaternary fossil vertebrates of the Broken River karst area, northern Queensland, Australia. *Rec. Austral. Mus.* **72**, 193–206. (doi:10.3853/j.2201-4349.72.2020.1723)
88. Seersholm FV, Grealy A, McDowell MC, Cole TL, Arnold LJ, Prideaux GJ, Bunce M. 2021 Ancient DNA from bulk bone reveals past genetic diversity of vertebrate fauna on Kangaroo Island, Australia. *Quat. Sci. Rev.* **262**, 106962. (doi:10.1016/j.quascirev.2021.106962)
89. Gould RA. 1996 Faunal reduction at Puntutjarpa rockshelter, Warburton Ranges, Western Australia. *Archaeol. Oceania* **31**, 72–86. (doi:10.1002/j.1834-4453.1996.tb00350.x)
90. Southwell CJ, Cairns SC, Pople AR, Delaney R. 1999 Gradient analysis of macropod distribution in open forest and woodland of eastern Australia. *Aust. Ecol.* **24**, 132–143. (doi:10.1046/j.1442-9993.1999.241954.x)
91. Fillios M, Blake N. 2015 *Animal bones in Australian archaeology*. Sydney, Australia: Sydney University Press.
92. Wayne AF, Wilson BA, Woinarski JCZ. 2017 Falling apart? Insights and lessons from three recent studies documenting rapid and severe decline in terrestrial mammal assemblages of northern, south-eastern and south-western Australia. *Wildl. Res.* **44**, 114–126. (doi:10.1071/WR16178)
93. Moro D. 1991 The distribution of small mammal species in relation to heath vegetation near Cape Otway, Victoria. *Wildl. Res.* **18**, 605–617. (doi:10.1071/WR9910605)
94. Fiedler LA. 1990 Rodents as a food source. In *Proc. 14th Vertebrate Pest Conf., Sacramento, CA, USA, 6–8 March 1990* (eds LR Davis, RE Marsh). Davis, CA: University of California.
95. Bradley J, Holmes M, Marrngawi DN, Karrakayn AI, Miller J, Wuwarlu N, Ida N. 2006 *Yumbulyumbulmantha ki-awarawu=All kinds of things from country: yanyuwa ethnobiological classification*. Brisbane, Australia: University of Queensland.
96. Burbidge AA, Johnson KA, Fuller PJ, Southgate RI. 1988 Aboriginal knowledge of the mammals of the central deserts of Australia. *Wildl. Res.* **15**, 9–39. (doi:10.1071/WR9880009)
97. Algar D, Angus GJ. 2008 Feasibility study for the eradication of feral cats from Faure Island, Shark Bay, Western Australia. *Rec. Western Austral. Mus.* **75**, 71. (doi:10.18195/ISSN.0313-122X.75.2008.071-075)
98. Price GJ, Louys J, Tyler Faith J, Lorenzen ED, Westaway MC. 2018 Big data little help in megafauna mysteries. *Nature* **558**, 23–25. (doi:10.1038/d41586-018-05330-7)
99. Johnson CN, Dortch J, Worthy TH. 2021 Interactions with megafauna. In *The Oxford handbook of the archaeology of indigenous Australia and New Guinea* (eds IJ McNiven, B David). Oxford, UK: Oxford University Press.
100. Peters C, Richter KK. 2021 MALDI-TOF-MS spectra of modern Australian marsupials for ZooMS (Zooarchaeology by Mass Spectrometry) (Version 1) [Data set]. *Zenodo*. (doi:10.5281/zenodo.5040049)
101. Peters C, Richter KK. 2021 MALDI-TOF-MS spectra of archaeological bone fragments from Bandicoot Bay, Barrow Island (Australia) for ZooMS (Zooarchaeology by Mass Spectrometry) (Version 1) [Data set]. *Zenodo*. (doi:10.5281/zenodo.5040055)
102. Peters C, Richter KK. 2021 Bone collagen from Australian marsupials for ZooMS peptide markers [Data set]. *MassIVE*. (doi:10.25345/C5TC2H)

Supplementary Information

Species identification of Australian marsupials using collagen fingerprinting

Carli Peters[1,*], Kristine K. Richter[2], Tiina Manne[3], Joe Dortch[4], Alistair Paterson[4], Kenny Travouillon[5], Julien Louys[6], Gilbert J. Price[7], Michael Petraglia[1,3,6,8], Alison Crowther[1,3], Nicole Boivin[1,3,8,9,*]

1. Department of Archaeology, Max Planck Institute for the Science of Human History, Jena, Germany
2. Department of Anthropology, Harvard University, Cambridge, MA, USA
3. School of Social Science, The University of Queensland, Brisbane, Qld 4071, Australia
4. School of Social Sciences, University of Western Australia, Perth, WA 6009, Australia
5. Western Australian Museum, Collections and Research, 49 Kew Street, Welshpool, WA 6106, Australia
6. Australian Research Centre for Human Evolution, Griffith University, Nathan, Qld 4111, Australia
7. School of Earth and Environmental Sciences, The University of Queensland, Brisbane, Qld 4072, Australia
8. Department of Anthropology, National Museum of Natural History, Smithsonian Institution, Washington DC, USA
9. Department of Anthropology and Archaeology, University of Calgary, Calgary, Canada

*Corresponding authors: Carli Peters and Nicole Boivin

Supplementary Tables

Supplementary Table 1: Sample numbers, storage locations, and accession numbers of sampled specimens.

Supplementary Table 2: Collagen coverage (in%) of MS/MS spectral data matched to sequence data in reference database. The species in the reference data with the closest match to the sample is indicated in brackets.

Other Supplementary Materials for this Manuscript

MALDI-ToF-MS data for modern reference specimens: Zenodo [doi.org/10.5281/zenodo.5040049]

MALDI-ToF-MS data for archaeological specimens: Zenodo [doi.org/10.5281/zenodo.5040055]

MS/MS data for modern reference specimens: ProteomExchange via MassIVE [doi.org/10.25345/C5TC2H]

Table S1: Sample numbers, storage locations and accession numbers of sampled specimens.

Sample number	Species	Storage location	Accession number
DA-UQU0220-001	*Isoodon macrourus*	University of Queensland	82-25
DA-UQU0220-002	*Isoodon macrourus*	University of Queensland	248
DA-UQU0220-003	*Phascogale tapoatafa*	University of Queensland	73
DA-UQU0220-004	*Parameles nasuta*	University of Queensland	62-27
DA-UQU0220-005	*Parameles nasuta*	University of Queensland	26
DA-UQU0220-006	*Trichosurus vulpecula*	University of Queensland	390
DA-UQU0220-007	*Petaurus breviceps*	University of Queensland	111
DA-UQU0220-008	*Pseudocheirus peregrinus*	University of Queensland	84-31
DA-UQU0220-009	*Pseudocherus peregrinus*	University of Queensland	19
DA-UQU0220-010	*Pseudocheirus peregrinus*	University of Queensland	84-29
DA-UQU0220-011	*Pseudocheirus peregrinus*	University of Queensland	30
DA-UQU0220-012	*Trichosurus vulpecula*	University of Queensland	102
DA-UQU0220-013	*Phascolarctos cinereus*	University of Queensland	287
DA-UQU0220-014	*Phascolarctos cinereus*	University of Queensland	64/65
DA-UQU0220-015	*Tachyglossus aculeatus*	University of Queensland	21
DA-UQU0220-016	*Tachyglossus aculeatus*	University of Queensland	286/288
DA-UQU0220-017	*Tachyglossus aculeatus*	University of Queensland	91-22
DA-UQU0220-018	*Notamacropus rufogriseus*	University of Queensland	198
DA-UQU0220-019	*Notamacropus eugenii*	University of Queensland	192
DA-UQU0220-020	*Macropus robustus*	University of Queensland	268
DA-UQU0220-021	*Wallabia bicolor*	University of Queensland	161
DA-UQU0220-022	*Macropus rufus*	University of Queensland	196
DA-UQU0220-023	*Macropus rufus*	University of Queensland	197
DA-UQU0220-024	*Isoodon macrourus*	University of Queensland	1
DA-UQU0220-025	*Lagorchestes conspicillatus*	University of Queensland	264/265/266
DA-UQU0220-026	*Pseudocheirus peregrinus*	University of Queensland	247
DA-UQU0220-027	*Lasiorhinus* sp.	University of Queensland	42
DA-UQU0220-028	*Wallabia bicolor*	University of Queensland	98
DA-UQU0220-029	*Macropus robustus*	University of Queensland	199
DA-UQU0220-030	*Lagorchestes conspicillatus*	University of Queensland	No accession number available
DA-UQU0220-031	*Vombatus ursinus*	University of Queensland	No accession number available
DA-UQU0220-032	*Macropus fuliginosus*	University of Queensland	No accession number available
DA-GRU0220-001	*Vombatus ursinus*	Griffith University	No accession number available
DA-MEL0220-001	*Lagostrophus fasciatus*	Melbourne Museum	C.6460
DA-MEL0220-002	*Lagostrophus fasciatus*	Melbourne Museum	C.06459.1
DA-MEL0220-003	*Macropus giganteus*	Melbourne Museum	C.2620
DA-MEL0220-004	*Macropus giganteus*	Melbourne Museum	C.26619
DA-MEL0220-005	*Notamacropus eugenii*	Melbourne Museum	C.17615
DA-MEL0220-006	*Notamacropus eugenii*	Melbourne Museum	C.17529
DA-MEL0220-007	*Notamacropus eugenii*	Melbourne Museum	C.17531
DA-MEL0220-008	*Notamacropus eugenii*	Melbourne Museum	C.6452.1
DA-MEL0220-009	*Phascolarctos cinereus*	Melbourne Museum	C.6729
DA-MEL0220-010	*Phascolarctos cinereus*	Melbourne Museum	C.2412
DA-MEL0220-011	*Notamacropus rufogriseus*	Melbourne Museum	C.5991.1
DA-MEL0220-012	*Notamacropus rufogriseus*	Melbourne Museum	C.5990.1
DA-MEL0220-013	*Notamacropus rufogriseus*	Melbourne Museum	C.31681
DA-MEL0220-014	*Macropus rufus*	Melbourne Museum	C.18572

DA-MEL0220-015	*Macropus rufus*	Melbourne Museum	C.30597.2
DA-MEL0220-016	*Macropus fuliginosus*	Melbourne Museum	C.23508
DA-MEL0220-017	*Macropus fuliginosus*	Melbourne Museum	C.23508
DA-MEL0220-018	*Vombatus ursinus*	Melbourne Museum	C.31660
DA-MEL0220-019	*Vombatus ursinus*	Melbourne Museum	C.6660
DA-MEL0220-020	*Wallabia bicolor*	Melbourne Museum	C.23514
DA-MEL0220-022	*Tachyglossus aculeatus*	Melbourne Museum	C.2562
DA-MEL0220-023	*Thylacinus cynocephalus*	Melbourne Museum	C.33021
DA-MEL0220-024	*Sarcophilus harrisii*	Melbourne Museum	C.6250
DA-WAM0220-001	*Phascolarctos cinereus*	Western Australian Museum	M6081
DA-WAM0220-002	*Phascolarctos cinereus*	Western Australian Museum	M7642
DA-WAM0220-003	*Vombatus ursinus*	Western Australian Museum	M55232
DA-WAM0220-004	*Vombatus ursinus*	Western Australian Museum	M11241
DA-WAM0220-005	*Lagostrophus fasciatus*	Western Australian Museum	M6303
DA-WAM0220-006	*Lagostrophus fasciatus*	Western Australian Museum	M3636
DA-WAM0220-007	*Macropus fuliginosus*	Western Australian Museum	M7019
DA-WAM0220-008	*Macropus fuliginosus*	Western Australian Museum	M12218
DA-WAM0220-009	*Macropus giganteus*	Western Australian Museum	M24650
DA-WAM0220-010	*Macropus giganteus*	Western Australian Museum	M16203
DA-WAM0220-011	*Notamacropus agilis*	Western Australian Museum	M11620
DA-WAM0220-012	*Notamacropus agilis*	Western Australian Museum	M14325
DA-WAM0220-013	*Notamacropus agilis*	Western Australian Museum	M4619
DA-WAM0220-014	*Notamacropus eugenii*	Western Australian Museum	M24482
DA-WAM0220-015	*Notamacropus eugenii*	Western Australian Museum	M3889
DA-WAM0220-016	*Notamacropus irma*	Western Australian Museum	M52388
DA-WAM0220-017	*Notamacropus irma*	Western Australian Museum	M40556
DA-WAM0220-018	*Notamacropus irma*	Western Australian Museum	M19871
DA-WAM0220-019	*Notamacropus parma*	Western Australian Museum	M23219
DA-WAM0220-020	*Notamacropus parma*	Western Australian Museum	M19065
DA-WAM0220-021	*Notamacropus parma*	Western Australian Museum	M11016
DA-WAM0220-022	*Notamacropus rufogriseus*	Western Australian Museum	M24661

Table S2: Collagen coverage (in %) of MS/MS spectral data matched to sequence data in reference database. The species in the reference data with the closest match to the sample is indicated in brackets.

Sample number	Species	COL1A1 coverage (%)	COL1A2 coverage (%)
DA-MEL0220-024	*Sarcophilus harrisii*	68.1 (*Sarcophilus harrisii*)	72.8 (*Sarcophilus harrisii*)
DA-UQU0220-027	*Lasiorhinus* sp.	92.1 (*Phascolarctos cinereus*)	93.2 (*Phascolarctos cinereus*)
DA-UQU0220-009	*Pseudocheirus peregrinus*	92.3 (*Phascolarctos cinereus*)	67.1 (*Phascolarctos cinereus*)
DA-MEL0220-023	*Thylacinus cynocephalus*	69.1 (*Sarcophilus harrisii*)	60.3 (*Sarcophilus harrisii*)
DA-WAM0220-019	*Notamacropus parma*	86.5 (*Vombatus ursinus*)	82.4 (*Macropus* sp.)
DA-UQU0220-012	*Trichosurus vulpecula*	96.6 (*Phascolarctos cinereus*)	78.8 (*Phascolarctos cinereus*)
DA-MEL0220-022	*Tachyglossus aculeatus*	81.2 (*Phascolarctos cinereus*)	38.5 (*Sarcophilus harrisii*) 41.3 (*Vombatus ursinus*)
DA-MEL0220-018	*Vombatus ursinus*	97.3 (*Vombatus ursinus*)	93.8 (*Vombatus ursinus*)
DA-UQU0220-032	*Macropus fuliginosus*	88.6 (*Vombatus ursinus*)	83.1 (*Macropus* sp.)
DA-UQU0220-030	*Lagorchestes conspicillatus*	87.6 (*Phascolarctos cinereus*)	81.7 (*Macropus* sp.)
DA-WAM0220-002	*Phascolarctos cinereus*	93.7 (*Phascolarctos cinereus*)	92.2 (*Phascolarctos cinereus*)
DA-UQU0220-021	*Wallabia bicolor*	95.6 (*Vombatus ursinus*)	82.4 (*Macropus* sp.)
DA-WAM0220-016	*Notamacropus irma*	88.6 (*Vombatus ursinus*)	86.8 (*Macropus* sp.)
DA-UQU0220-029	*Macropus robustus*	83.9 (*Phascolarctos cinereus*)	79.0 (*Macropus* sp.)
DA-MEL0220-002	*Lagostrophus fasciatus*	79.8 (*Phascolarctos cinereus*)	70.0 (*Macropus* sp.)
DA-MEL0220-003	*Macropus giganteus*	78.1 (*Vombatus ursinus*)	78.0 (*Macropus* sp.)
DA-MEL0220-005	*Notamacropus eugenii*	80.9 (*Phascolarctos cinereus*)	80.4 (*Macropus* sp.)
DA-UQU0220-018	*Notamacropus rufogriseus*	95.3 (*Vombatus ursinus*)	92.1 (*Macropus* sp.)
DA-UQU0220-022	*Macropus rufus*	92.3 (*Phascolarctos cinereus*)	91.0 (*Macropus* sp.)
DA-UQU0220-003	*Phascolage tapoatafa*	70.3 (*Sarcophilus harrisii*)	70.1 (*Sarcophilus harrisii*)
DA-UQU0220-001	*Isoodon macrourus*	67.7 (*Sarcophilus harrisii*) 32.9 (*Vombatus ursinus*)	58.9 (*Macropus* sp.) 44.3 (*Sarcophilus harrisii*)
DA-UQU0220-007	*Petaurus breviceps*	94.1 (*Phascolarctos cinereus*)	77.8 (*Phascolarctos cinereus*)
DA-UQU0220-005	*Parameles nasuta*	64.3 (*Sarcophilus harrisii*)	64.6 (*Phascolarctos cinereus*)
DA-WAM0220-011	*Notamacropus agilis*	85.8 (*Vombatus ursinus*)	80.3 (*Macropus* sp.)

7. Manuscript B

Systematic survey of collagen preservation in Australia reveals unexpected tropical survival at >50,000 years

Carli Peters[1,*], Yiming Wang[1], Joe Dortch[2], Scott Hocknull[3,4], Rochelle Lawrence[3], Tiina Manne[5], Carly Monks[2], Gertrud E. Röβner[6,7], Helen Ryan[8], Mikael Siversson[8], Tim Ziegler[9], Julien Louys[10], Gilbert J. Price[11], Nicole Boivin[1,5,12,13], Matthew J. Collins[14,15,*]

1. Department of Archaeology, Max Planck Institute for Geoanthropology, Jena, Germany
2. School of Social Sciences, University of Western Australia, Perth, WA 6009, Australia
3. Geosciences, Queensland Museum, Hendra, Qld 4011, Australia
4. School of Biosciences, Faculty of Science, University of Melbourne, Melbourne Vic 3010, Australia
5. School of Social Science, The University of Queensland, Brisbane, Qld 4071, Australia
6. Staatliche Naturwissenschaftliche Sammlungen Bayerns – Bayerische Staatssammlung für Paläontologie und Geologie, Munich, Germany
7. Department für Geo- und Umweltwissenschaften, Ludwig-Maximilians-Universität München, Munich, Germany
8. Western Australian Museum, Collections and Research, 49 Kew Street, Welshpool, WA 6106, Australia
9. Museums Victoria, Melbourne, Vic 3001, Australia
10. Australian Research Centre for Human Evolution, Griffith University, Nathan, Qld 4111, Australia
11. School of Earth and Environmental Sciences, The University of Queensland, Brisbane, Qld 4072, Australia
12. Department of Anthropology, National Museum of Natural History, Smithsonian Institution, Washington DC, USA
13. Department of Anthropology and Archaeology, University of Calgary, Calgary, Canada
14. Department of Archaeology, Cambridge University, Cambridge, United Kingdom
15. Section for Evolutionary Genomics, Globe Institute, University of Copenhagen, Copenhagen, Denmark

*Corresponding authors: Carli Peters and Matthew J. Collins

Key words: Palaeoproteomics; Bone diagenesis; FTIR; ZooMS; Deamidation

Abstract

Ancient protein studies have demonstrated their utility for looking at a wide range of evolutionary and historical questions, from the evolution and dispersal of hominin species, to the reconstruction of past ecosystems and shifts in biodiversity, and the emergence of dairying. The majority of palaeoproteomics studies to date have been restricted to high latitudes with relatively temperate environments. However, a better understanding of protein preservation at lower latitudes is critical for disentangling the mechanisms involved in the deep-time survival of ancient proteins. In this study, we show that protein preservation in Australia exceeds chemical predictions of collagen survival in bone. Collagen preservation in the Australian fossil record was systematically examined using a combination of thermal age estimates, Fourier Transform Infrared Spectroscopy (FTIR), Zooarchaeology by Mass Spectrometry (ZooMS), and protein deamidation calculations. Our results reveal the unexpected tropical survival of

collagen in bones of over 50 thousand years (ka) old, which significantly pushes back the limit of collage preservation in tropical contexts. We further explore potential causes for this unexpected result to identify the underlying mechanisms leading to this exceptional preservation. This study serves as a starting point for the analysis of ancient proteins in other tropical contexts, and at deeper timescales.

Introduction

The analysis of ancient proteins and ancient DNA (aDNA) has rapidly been adopted in archaeological science as important tools to study the archaeological record. Much early research focused on the high Arctic[1,2] where cold conditions slowed rates of chemical and biological decay of these biomolecules. Over time, research has moved into lower latitudes[3,4], and further back in time[5,6], but research in the tropics, except at high elevation, remains limited.

Proteins have a higher preservation potential than aDNA in harsh environments[4,7,8], and thus have potential to survive over longer timescales. Unlike proteins in tooth enamel or shell, protein in bone is not entrapped within a mineral but is rather an intimately mineralized composite, connected to and influenced by the burial environment. Low pH will dissolve the bioapatite and expose the bone to degradation, whereas in neutral and higher pH, bioapatite is more stable and the extent of protein degradation will depend upon the chemical and environmental conditions of the burial context, including pH and site hydrology[7,9-11]. The preservation of proteins in the archaeological record can thus vary significantly between sites[7,10,12]. To date, the oldest collagen peptides identified in the palaeontological record were extracted from high Arctic material dating back to 3.4 million years (Ma) ago[2]. The oldest surviving peptide sequences originate from eggshell and were recovered from the early hominin site of Laetoli, Tanzania[7]. The predicted surviving peptide matched the sequence independently recovered from samples dating to 3.8 Ma in Africa and 6.5-9 Ma in China[5]. The entropic effect of the binding of this peptide to the mineral component of the eggshell dropped the local system energy by the equivalent of 30°C, thus offering the first insight into mechanisms of survival. The persistence of the same peptide on two continents and 3-million years apart highlights the power of mineral binding to slow protein decay.

In *closed* systems, in which pH and water availability are constrained, biomolecular decay is fairly predictable. It is this predictable decay (assuming a known thermal history) which enables amino acid racemization to work so successfully[13,14]. However, it now seems that predictions of the survival of aDNA and proteins can in certain cases underestimate direct evidence of sequence recovery. Attempts to predict survival[15,16] and degradation[17] in *open* systems, such as bone, is even more challenging due to variations in water availability, pH, cations and anions, and small organic molecules which may be involved in cross-reactions, even in cases where there is no evidence of microbial activity. It is therefore possible to observe enhanced preservation in arid environments[18], or accelerated decay as a result of alkaline conditions (e.g. bat guano in caves). In the case of bone apatite, the mineral does not dissolve at alkaline pH, while both DNA and proteins undergo accelerated hydrolysis[19]. However, cases in which biomolecular preservation exceeds chemical predictions are far more interesting[6]. The predictive upper limit of collagen survival in bone[9] was thought to be robust, as evidenced by the prediction of the successful recovery of collagen for radiocarbon dating[11]. Here, we show that this is not the case.

So far, studies examining the molecular degradation of collagen in archaeological and fossil material have mostly been restricted to the relatively temperate environments of Eurasia[20-22] and North America[23], although some studies have started to explore collagen preservation in warmer and wetter environments that are less amenable to the long-term preservation of biomolecules[23]. Australia is an ideal place to explore collagen preservation in challenging environments more closely. The environmental conditions in Australia are highly variable ranging from extremely warm and wet conditions in the northern tropical regions, to more temperate conditions in the south. These highly variable environments significantly affect the preservation potential of ancient biomolecules across the country. However, the survival of biomolecules in the Australian archaeological and palaeontological record has yet to be quantitatively assessed, and for most regions biomolecular studies are lacking altogether.

In this study, we try to bridge this gap by systematically examining the survival of collagen in the Australian fossil record by a) establishing thermal age estimates to chemically predict the survival of collagen, b) examining collagen preservation of individual bones by visual taphonomic assessments and FTIR analyses, and c) using ZooMS success rates and collagen deamidation rates as a proxy for true collagen preservation. The results of these analyses are then compared to each other as well as between sites, and they are also set out against local environmental conditions that potentially affect collagen survival. We show that ancient proteins can be extracted from osseous material from tropical Australian contexts dating back to the Late Pleistocene, contrary to chemical predictions of collagen preservation. The results of this study can be used to guide future studies and help assess whether the analysis of fossil material from archaeological and palaeontological sites has sufficient potential to result in successful proteomic analysis. Furthermore, this study strengthens our understanding of collagen preservation in harsh environments over long timescales.

Results

Thermal age estimates

Thermal age estimates were calculated for each locality using both a shallow and deep model (Table S2). For the majority of the localities, thermal age estimates are >200ka (even when using the more optimistic deep model with a lower degree of thermal fluctuations). For some sites, thermal ages even exceed 1 Ma in both models (Robert Broom Cave and Tripot Cave), as well as Lake Victoria, South Walker Creek, and all sites in the Darling Downs and Rockhampton localities when considering only the shallow model. It is thus also these sites where little to no collagen preservation is expected. On the other hand, there are also some sites with thermal age estimates of the deep model <200 ka: Beehive, Devil's Lair, Kudjal Yolgah Cave, Lake Victoria, Lancefield Swamp, Mammoth Cave, Tight Entrance Cave, and Yellabidde Cave. These sites are expected to have better collagen preservation compared to the other sites included in this study.

ZooMS and deamidation

In total, 166 samples had sufficient collagen preservation for taxonomic identification using ZooMS (Dataset S5). A high variability was observed in ZooMS success rates between localities (Figure 1, Table S3). On the one hand, there are a number of localities with extremely poor collagen preservation, and where no samples were successfully analysed (Boodie Cave, Darling Downs, Lake Victoria, Morwell, South Walker Creek, and Strathdownie). On the other hand, relatively good collagen preservation has been observed at other sites (Broken River, Devil's Lair, and Kudjal Yolgah Cave). Millennium Cave and Devil's Lair had the highest overall success rates at 100% and 85%, respectively.

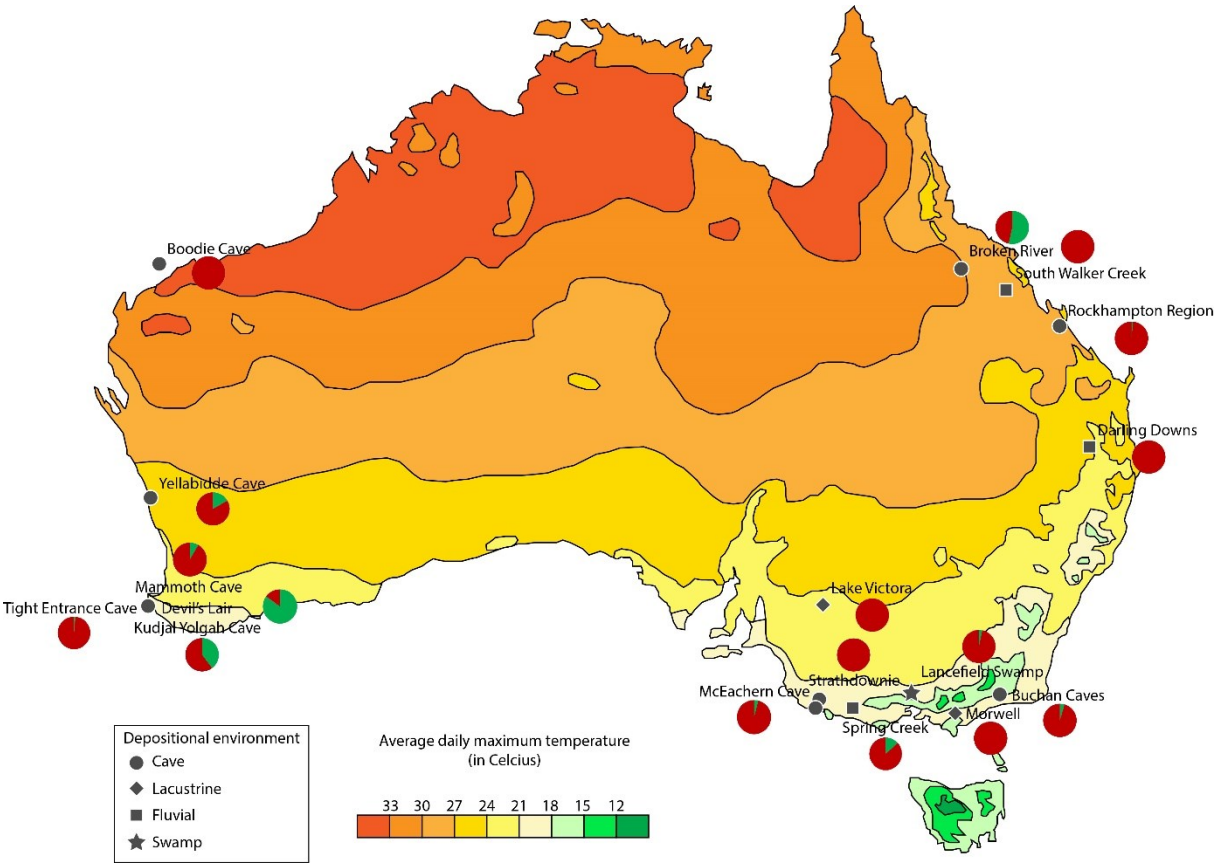

Figure 1: ZooMS success rates for each locality; green: samples with sufficient collagen preservation to make a taxonomic identification with ZooMS, red: samples with insufficient collagen preservation to make a taxonomic identification with ZooMS. Temperature data from Australian Government, Bureau of Meteorology.

Deamidation rates were calculated for the 166 samples that were successfully analysed with ZooMS. The resulting deamidation rates range between 0.16 and 0.99. Average deamidation rates fluctuate between 0.17 and 0.95 (Table S3), indicating high variability in collagen preservation between sites. The locality with the lowest overall deamidation rate, and thus the highest level of deamidation, is Spring Creek, while the locality with the highest average deamidation rate, and thus the lowest level of deamidation, is McEachern Cave.

Method comparison

No correlation has been observed between thermal age estimates and ZooMS success rates. Both localities with relatively young thermal age estimates and sites with old thermal age estimates forecasting a complete absence of collagen, yielded enough collagen for relatively high ZooMS success rates (>35%) (Figure 2). Similarly, localities with ZooMS success rates of <10% had thermal age estimates ranging from 52.3 to 6923.5 ka.

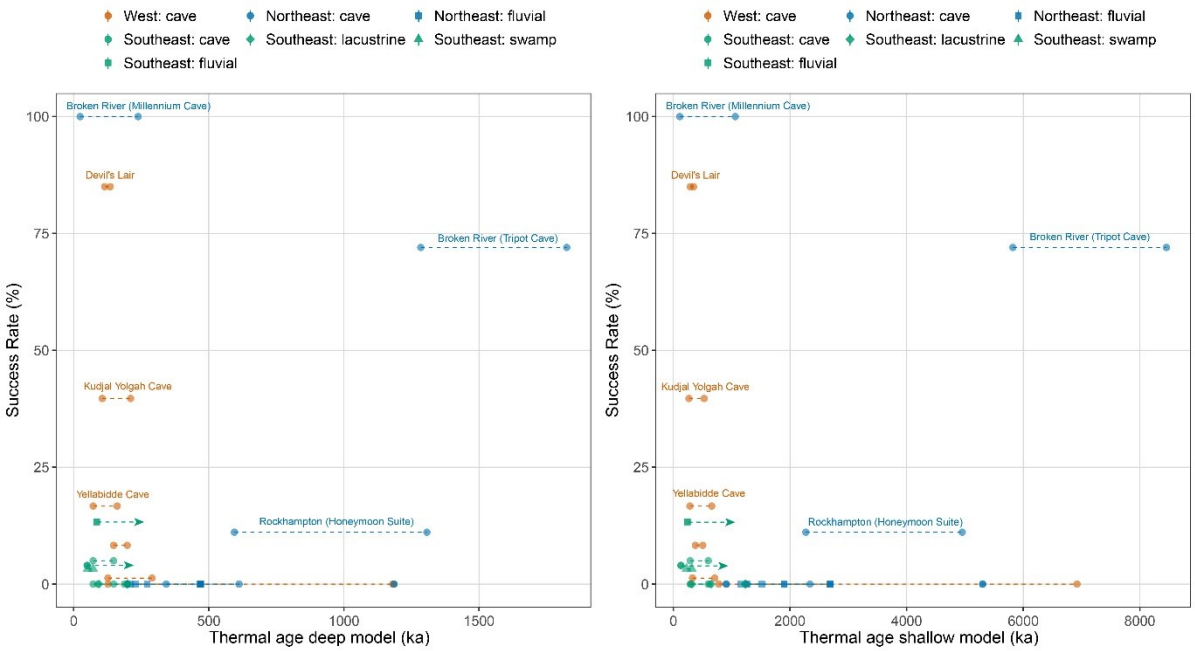

Figure 2: Comparison between thermal age estimates (for both the deep and shallow models) and ZooMS success rates.

Likewise, no correlation has been observed between ZooMS success rates and bone weathering stages (Figure S2). For bone weathering stages 3 and 4, the number of samples without sufficient collagen preservation to make taxonomic identifications with ZooMS is notably higher than those successfully analysed with ZooMS. For weathering stage 2, the number of samples successfully analysed with ZooMS is slightly higher than those unsuccessfully analysed. However, the sample size for this group is too small to make any reliable conclusions. Our results indicate that bone weathering stages are not a good indicator to predict ZooMS success rates. This roughly follows the results of previous studies, in which the macroscopic appearance of bones was shown not to be a reliable indicator of collagen preservation for biomolecular analysis[25].

On the other hand, a significant difference ($p<0.01$) has been observed between FTIR (Am1/P and Am2/P) values of samples with sufficient collagen preservation to make taxonomic identifications with ZooMS, and samples unsuccessfully analysed with ZooMS (Figure 3). In previous studies, cut-off points from Am/1P of >0.02[25] and >0.04[26] have been suggested to eliminate samples without sufficient collagen preservation for subsequent ZooMS analysis. However, for our sample set, these proposed cut-off points would also eliminate a large number of samples that later turned out to have sufficient collagen preservation for ZooMS. Instead, a cut-off point for Am1/P of >0.05 would agree better with our dataset, even though this would still result in the loss of 20.6% of the successful samples. Average deamidation rates also show a correlation with ZooMS success rates (Figure 4), but deamidation rates of individual samples show no sign of correlation with FTIR (Am1/P and Am2/P) values (Figure S3).

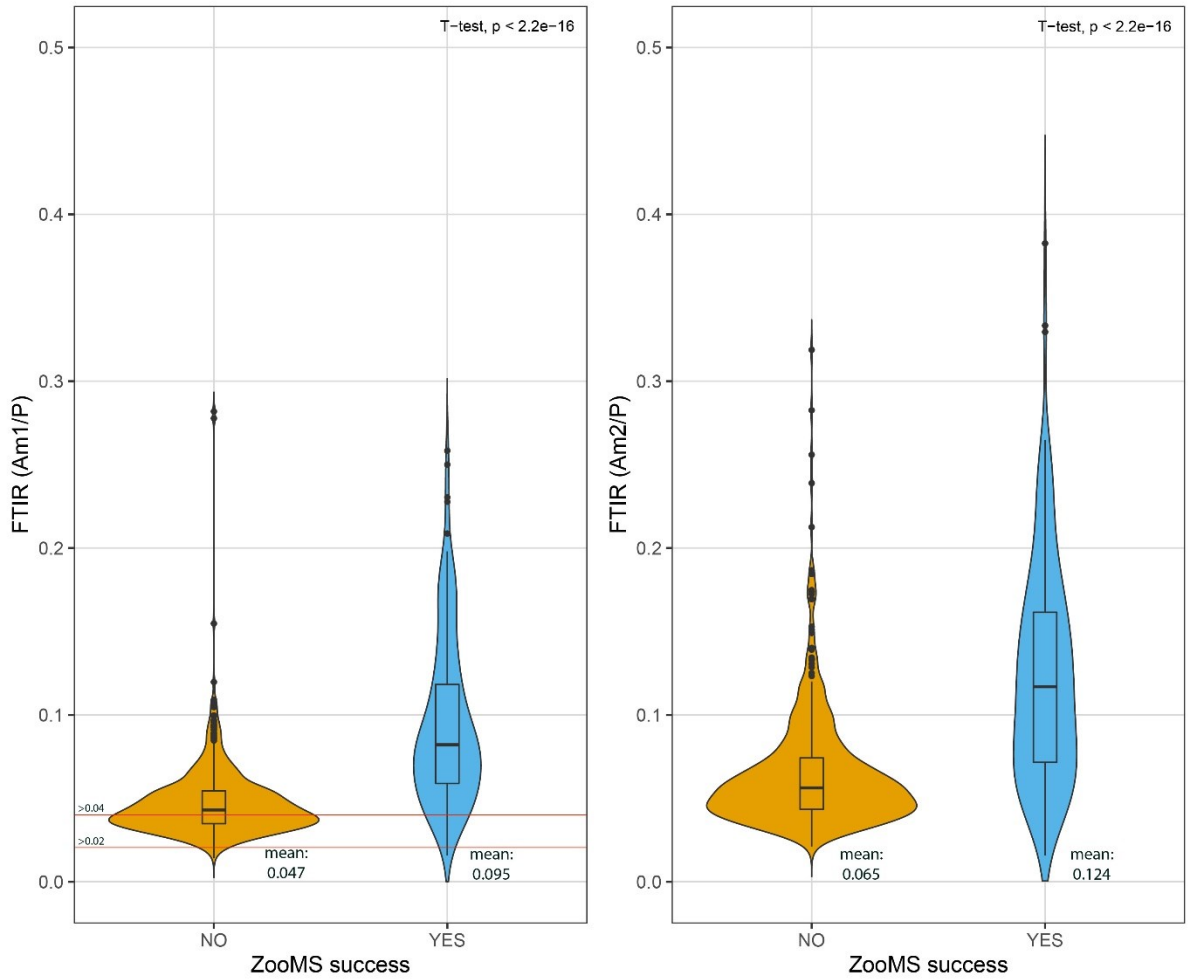

Figure 3: Violin plot showing the distribution of Am1/P and Am2/P values for samples with (n = 162) and without (n = 486) successful ZooMS results. Mean values are indicated. The results of the t-test, indicating that these two distributions differ significantly, are shown in the top right. Horizontal red lines indicate previously proposed cut-off points for Am1/P at >0.02[25] and >0.04[26].

Collagen preservation and environmental conditions

The localities that were part of the study were grouped into three regions (northeast, southeast, and west) to get a better understanding of regional differences in the preservation potential of collagen. This revealed that localities in southeast Australia have the lowest ZooMS success rates, indicating low levels of collagen preservation (Figure 4a). On the other hand, ZooMS analysis of sites in west and northeast Australia were more successful, indicating higher levels of collagen preservation in these areas.

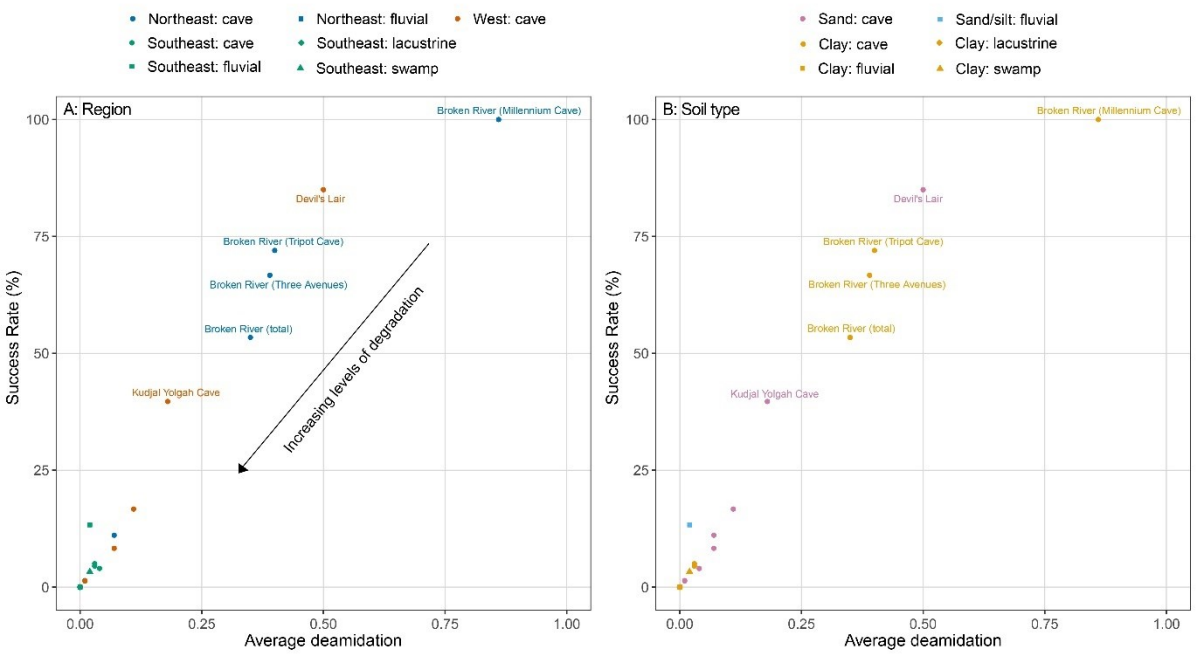

Figure 4: ZooMS success rates and average deamidation rates for each depositional environment by (a) region, and (b) soil type.

There is no correlation between different soil types and the overall ZooMS success rates at a locality (Figure 4b). The depositional environment, on the other hand, does appear to play an important role in the preservation of collagen and thus ZooMS success rates. Caves have the highest overall ZooMS success rates in all regions of Australia, independent from their respective soil types (Figure 4). It is however important to note that the majority of cave sites included in this study were limestone caves (Dataset S1), which may have also influenced the preservation potential of collagen in these caves. The better preservation of collagen in cave settings is further highlighted by a heat map outlining ZooMS success rates against the depositional environments of the localities (Figure 5).

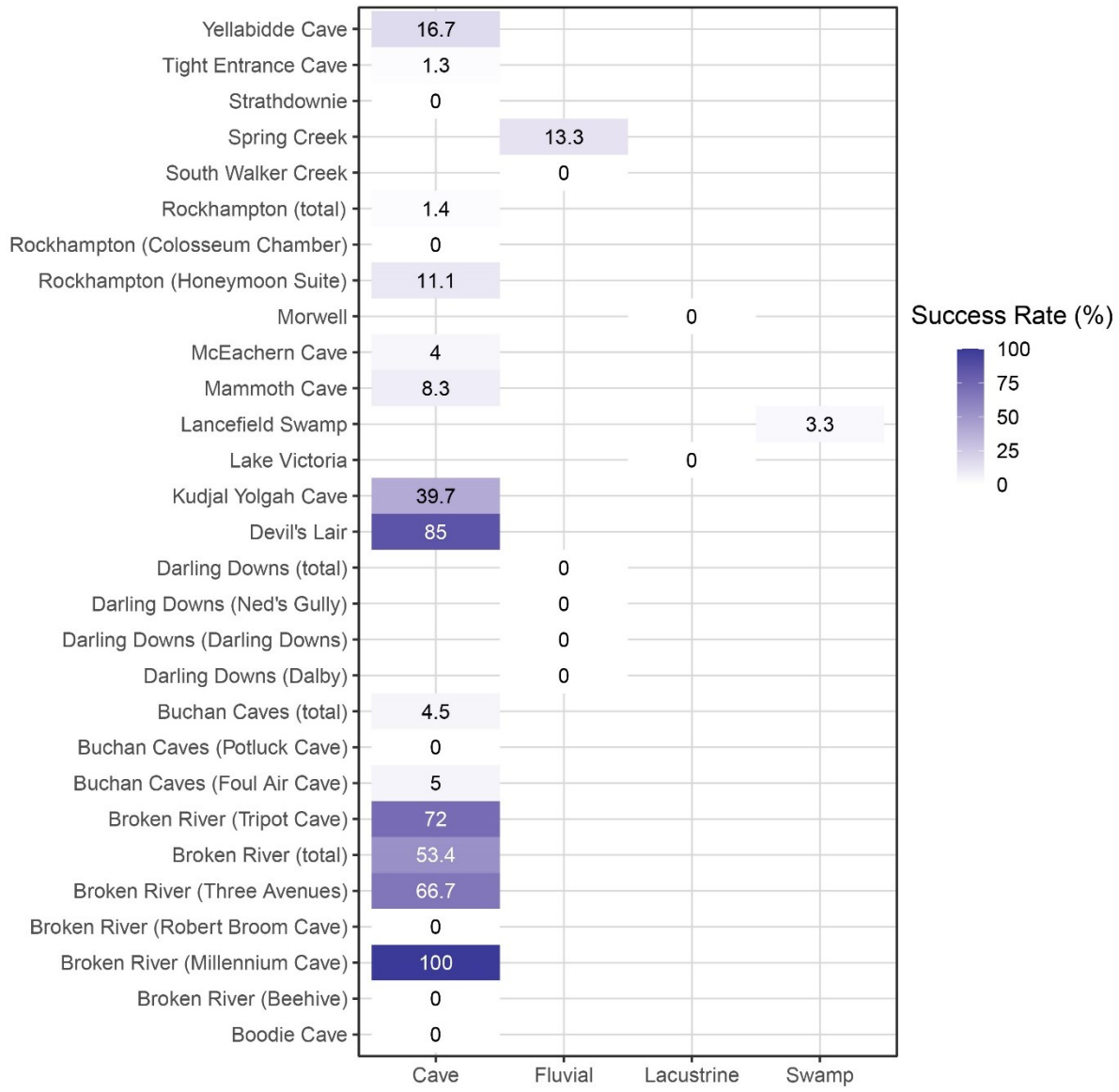

Figure 5: Heat map indicating the ZooMS success rates of each site set out against their depositional environments.

Another heat map was constructed to further assess the relationship between collagen preservation, mean annual temperature, and annual levels of precipitation (Figure 6). This heat map and associated dendrogram indicate that collagen preservation is more closely related to mean annual temperature and fluctuations therein, than to levels of annual precipitation.

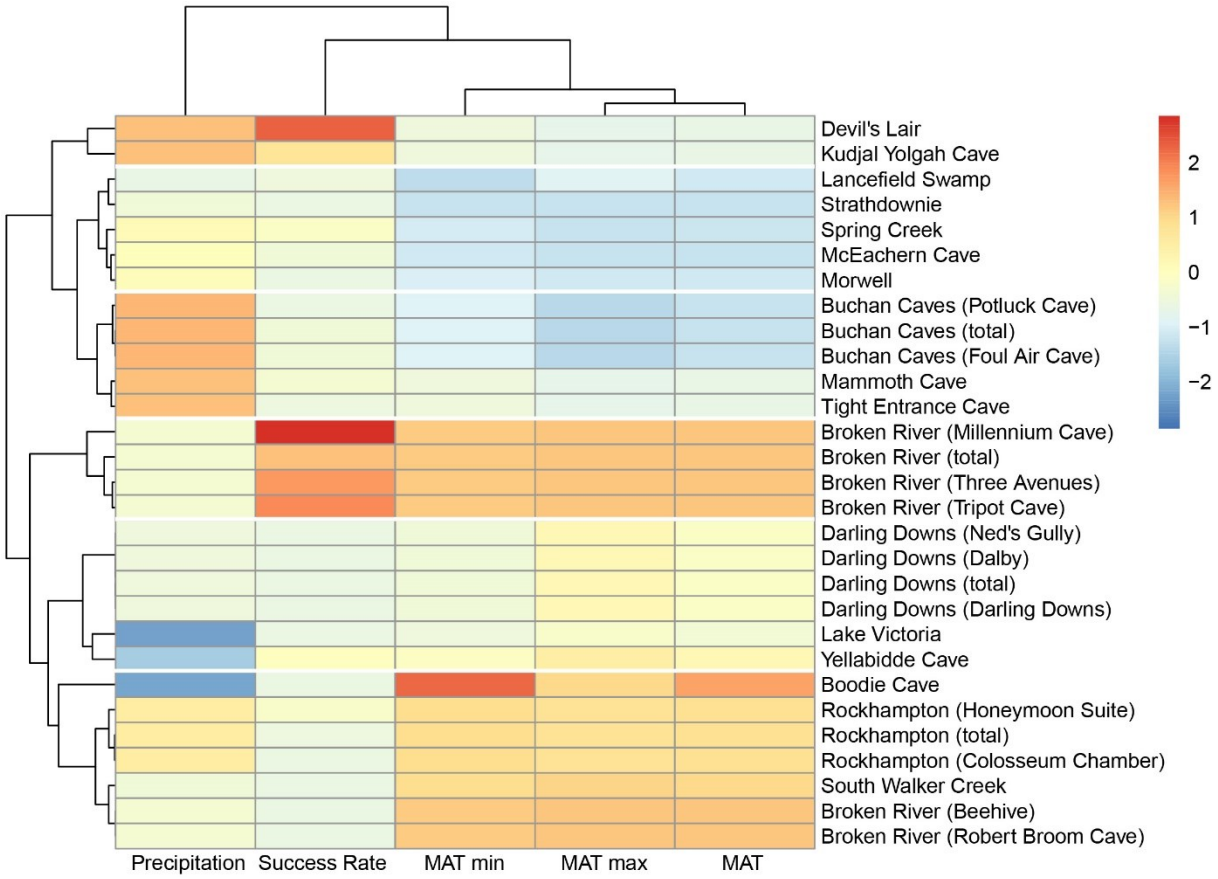

Figure 6: Heat map showing the relationship between ZooMS success rates, mean annual temperature (MAT), and annual precipitation. Dendrogram shows which variables are more closely related, and which sites have more similar climatic conditions.

Discussion

Collagen preservation at Tripot Cave

The results of this study show that collagen is exceptionally well preserved at Tripot Cave, a Late Pleistocene site situated in a limestone cave in the Broken River Karst area. This exceptional preservation goes fully against chemical predictions of collagen preservation for a site of this age in this geographic location. In the following discussion, we consider what underlying causes could have resulted in such an unexpected and exceptional finding.

Contamination?

In the past, fossil material has often been conserved using animal glues, which largely consist of collagen. Animal glue was not used during the excavation and preservation of the bones included in our analysis. Furthermore, the presence of animal glue, which is typically made from horse, cattle, rabbit, or fish[27], could have been identified in the ZooMS identifications. This is not the case. The conservation of the bones with animal glue could thus not have been the origin of the collagen extracted from the material.

Errors in dating?

If the bones are much younger than what is currently assumed, the good preservation of collagen in them would be in line with chemical predictions of collagen preservation at the site, and would thus be expected. However, multiple U-series dates were taken from flowstones at the top and bottom of the stratigraphic sequence, as well as from intermediate flowstones situated within the sequence (pers. comm. G. Price). The dating of Tripot Cave is thus very robust, and does not provide an explanation for the exceptional collagen preservation observed at the site.

Possible explanation: polymer-in-a-box

Collagen melts by shrinkage and expansion of the fibrils. If the radial expansion is constrained, this will result in the overall stabilization of the collagen fibril, the so-called polymer-in-a-box model[28]. A strong association of collagen with the bone mineral phase thus prevents collagen in bone from melting, since the mineral is holding it together. Once the mineral starts to degrade, collagen follows soon after[29]. The persistent and efficient introduction of minerals, preventing the collapse of the mineral phase of the bone, could thus explain the exceptional preservation of collagen at Tripot Cave. To further investigate this possibility, C/P ratios were calculated from the FTIR spectra (Figure S4). This shows that sites with high ZooMS success rates had relatively high C/P values, indicating a high concentration of carbonates in the bones. Interestingly, a similar correlation has been observed between the C/P ratio and DNA preservation[30]. However, when looking at C/P values of individual specimens from Tripot Cave, there does not appear to be a correlation between collagen preservation and C/P ratios (Figure S5). Tripot Cave is humid, not particularly warm for Northwest Australia, and there are not a lot of speleothems in the cave. In the absence of large amounts of calcium carbonate moving through the cave system, it is most likely that another mineral present is responsible for the remineralization process. For example, in leather tanning, chromium(III) has been shown to be able to form a matrix that is tightly bound to collagen, increasing the hydrothermal stability of the collagen[29]. However, detailed information about the geochemistry of Tripot Cave is currently unavailable, rendering it impossible to disentangle which minerals are moving through the cave system leading to the exceptional preservation of collagen at the site.

Methodological considerations

The absence of a correlation between thermal age estimates and ZooMS success rates, combined with high ZooMS success rates at sites with high thermal age estimates, indicates that collagen preserves over longer time-scales than would be expected based on chemical predictions of collagen survival. There are a large number of possible explanations for the absence of this correlation, including: i) uncertainties in the model used to predict temperature fluctuations throughout the year; ii) uncertainties in the used palaeoclimate model; iii) uncertainties attributed to burial depths; and iv) uncertainties in age estimates for the localities that were included in the study. Moreover, other micro-environmental factors that impact collagen preservation are not included in thermal age calculations, which instead rely solely on age and temperature. However, such micro-environmental factors significantly impact collagen preservation and thus influence the accuracy of thermal age estimates (see also[31]).

Average deamidation rates do correspond to ZooMS success rates, although they do not correlate with the absolute and thermal ages of the sites. This implies that deamidation rates can be useful to assess levels of collagen preservation at a given site. The results of this study thus support earlier claims that glutamine deamidation cannot be used reliably as a relative measure of time, but should rather be used as a measure of collagen preservation[31-34]. Furthermore, deamidation rates do not correlate with the recorded Am1/P values. In addition to the FTIR parameters recorded in this study, for future studies it would also be interesting to measure the splitting factor to get further insight into bone crystallinity[30,35,36] and its possible relationships with collagen deamidation rates.

Further interesting to note is that collagen denaturation has a high temperature sensitivity compared to DNA depurination[37]. This also means that at high temperatures, the difference in speed between collagen and DNA degradation becomes smaller; up to the point where collagen may even degrade quicker than DNA at extremely high temperatures. For Australian contexts, especially those with high temperature extremes, this is particularly interesting and could accommodate future studies comparing the preservation of both collagen and aDNA in these contexts.

Future prospects

This study has shown that it is possible to successfully extract collagen from Australian fossil material of >50 ka old from apparently less than ideal preservation conditions, pushing back the limit of collagen preservation in these contexts. This also raises further questions about the potential preservation of

biomolecules in other environments that were previously deemed unfavorable to the preservation of ancient proteins, such as the tropics, of preservation at deeper timescales.

The preservation of collagen in the archaeological and palaeontological record of Australia does not seem to follow one given pattern, but instead appears to be dependent on site-specific burial environments, including microclimate and environmental conditions (e.g. soil type, pH, and site hydrology) in addition to more recognized factors such as age, temperature and humidity. One important outcome of this study is that collagen preservation in Australia was best in limestone caves, regardless of the age of the deposits. Limestone caves typically have slightly alkaline burial environments, which are more favorable to the long-term preservation of collagen in bone than more acidic environments[38-40]. The limited movement of water, and oversaturation of groundwater with calcium phosphate in limestone caves could further increase the potential for collagen preservation in these environments[38]. Deep caves also serve as a buffer against extreme temperature fluctuations, instead keeping a relatively stable temperature which further facilitates the preservation of collagen and other biomolecules[10].

There are many micro-environmental factors that contribute to the degradation of biomolecules in the archaeological record. However, as with aDNA[6,41], the exact impacts of these micro-environmental factors on protein degradation are still unclear. However, some insights have been acquired. For example, soil phophatisation[32] and the presence of metal ions[31] have been shown to negatively affect collagen preservation. In order to make a good assessment of expected collagen preservation, it is thus crucial that data of site-specific burial conditions is available for the deposits from which the material derives. The color of fossil material can also provide crucial information about the site-specific burial environment. For example, the adsorption of manganese and iron oxides from anoxic soils leads to brown or black staining on archaeological bones[11,42].

Aside from micro-environmental factors that have possibly impacted collagen preservation, it is also critical to consider the taphonomic history of fossil material and the effect it may have had on the preservation of biomolecules within the material. Exposure of osseous material to extremely high temperature through cooking or exposure to fire has been shown to negatively affect collagen preservation[43,44], for example. Similarly, when bones have passed through the digestive tract, the highly acidic environment they were exposed to also degrades collagen in bone[10]. Such processes can leave taphonomic marks on osseous material[42], that can provide valuable information regarding the potential for collagen preservation in the specimens.

There are a myriad of additional geo- and biochemical methods that could be used in the future to better understand the mechanisms involved in the long-term preservation of collagen at sites which exceed chemical expectations, such as Tripot Cave. X-ray diffraction (XRD) and X-ray fluorescence (XRF) can be used to identify any possible anomalies in the structural and elemental composition of the bones[45]. Scanning electron microscopy (SEM) can also give more insight into bone mineralization and microstructure[46]. Similarly, transmission electron microscopy (TEM) or atomic force microscopy (AFM) can be used to visualize the structural properties of individual collagen fibrils[47,48]. The preservation quality of ancient proteins can be further investigated through amino acid profiling and amino acid racemization, which can give insight into the level of protein degradation[49], while shotgun proteomics can provide a deeper, proteome-wide understand of the full suite of proteins preserved[50].

While fossil material can offer valuable information about the past, the finality of the fossil record should also be considered prior to destructive sampling[51,52]. Thermal age calculations, FTIR measurements, and other pre-screening techniques offer valuable information about the expected degradation state of fossil material, and the likelihood of successful biomolecular analysis. Approaches that allow for the rapid identification of suitable specimens for biomolecular analysis will likely only gain importance as biomolecular archaeology moves towards a more sustainable approach in the future. However, as shown in this study, these pre-screening techniques are not always fully accurate; we thus highlight the importance of small-scale pilot studies on a small number of fragmented bones to test preservation prior to destructively sampling large numbers of highly valuable fossil material. Furthermore, this study

highlights the importance of publishing negative results. While often overlooked, negative results can provide critical information about the degradation of ancient biomolecules in the archaeological and palaeontological record. Such data is crucial to get a better understanding of the spatial and temporal range of collagen preservation, and the role of microenvironment variability therein.

Material

Seventeen localities ranging from north-eastern to south-western Australia, dating from the Late Pleistocene to recent were included in this study (Table S1). The localities represent a wide range of depositional environments and environmental conditions. The depositional environment for each locality was categorized as either *cave, fluvial, lacustrine*, or *swamp*, and for each locality data was collected about the age of the fossils, burial environment, soil type, and pH (Dataset S1). In total, 765 bone fragments were included in this study (Dataset S2).

Methods

Thermal age estimates

Past and present climate data was used to calculate thermal age estimates for collagen for each locality. Present-day mean annual temperature (MAT), mean monthly temperature, and mean annual precipitation data was collected from local weather stations in the vicinity of the localities (Dataset S3). Palaeoclimate estimates were extracted from a statistically-derived high-resolution dataset of global terrestrial climate, bioclimate and vegetation of the last 120 kyr[53]. MAT (BIO01), maximum annual temperature (BIO05), minimum annual temperature (BIO06), annual temperature range (BIO07), annual precipitation (BIO12), and altitude data was extracted from the dataset with R v. 4.0.1. with R Studio v. 1.2.1717[54] using the Pastclim package v. 0.9.0[55,56]. For each locality, these variables were collected in a time-series of 1000-year intervals up to a maximum of 100 kyr (Dataset S4). Modern weather station data was compared to palaeoclimate estimates to verify the accuracy of the palaeoclimatic reconstruction. This comparison shows that the predicted temperatures based on the palaeoclimate reconstructions are in line with what would be expected based on modern local temperature conditions (Figure S1).

Present-day altitudes of the localities have been estimated from (https://www.advancedconverter.com/map-tools/find-altitude-by-coordinates) and were used to correct for altitude differences between the localities, nearby weather stations, and the raster tiles of the palaeoclimate dataset. To account for differences in burial depth between localities, two models were used to calculate thermal age estimates for each locality; a shallow model, and a deep model[57]. For the shallow model, it was assumed that temperature fluctuates throughout the year, while for the deep model temperature was assumed to remain stable all-year-round.

Taphonomic assessment

All bone fragments included in the analysis were subjected to visual taphonomic assessment prior to sampling for destructive analysis. All bones were photographed, and the colour and weight class of each fragment were documented. Bone weathering stages were also recorded for each fragment following the weathering stages outlined by Behrensmeyer[58].

Fourier Transform Infrared Spectroscopy (FTIR)

FTIR analysis was carried out using a handheld FTIR (4300 Handheld, Agilent Technologies) with an attenuated total reflectance (ATR) diamond. One to two mg of bone powder from each sample was used for FTIR analysis and pressed against the ATR diamond to measure absorbance spectra with a spectral range of 2000-650 cm^{-1}, a resolution of 4 cm^{-1}, and 32 sample scans. Background measurements were taken between every sample. Resulting absorbance spectra were analysed using the MicroLab PC software package v. 5.2.1748.0 (Agilent Technologies). The height of the phosphate υ_3 (~1035/1010 cm^{-1}), carbonate (~1415 cm^{-1}), Amide I (~1650 cm^{-1}), and Amide II (~1550 cm^{-1}) absorption peaks were recorded. These were used to calculate the Amide I to phosphate ratio (Am1/P), the Amide II to phosphate (Am2/P) ratio, and the carbonate to phosphate (C/P) ratio.

Zooarchaeology by Mass Spectrometry (ZooMS)

Collagen was extracted from fossil bone samples alongside extraction blanks following an acid-soluble approach adapted from previously published methods[8,59]. Fifty to seventy mg of bone powder was demineralized in 400µl of 0.6M hydrochloric acid (HCl) for 5 days. The samples were heated for 30 min at 65ºC, after which the supernatant was transferred to a 10 kDa ultrafilter (Microcon, Merck Millipore®) and centrifuged until completely passed through the filter. The samples were washed two times by adding 300µl of 50mM ammonium bicarbonate (AmBic) to the ultrafilter and centrifuging until completely passed through the filter. The fraction that did not pass through the filter was resuspended in 100µl of 50mM AmBic and digested on the filter with 1µl of 0.4µg/µl trypsin solution (Pierce™ Trypsin Protease, Thermo Scientific) for 18h at 37ºC. Subsequent to enzymatic digestion, the samples were centrifuged a final time until completely passed through the filter. Peptides were purified and concentrated using C18 ZipTips (Pierce™ C18 Tips, Thermo Scientific).

Samples were spotted in duplicate onto an MTP Groundsteel 384-target plate, together with matrix solution (α-cyano-4-hydroxycinnamic acid of 10mg/ml in 50% acetonitrile (ACN)/0.1% trifluoroacetic acid (TFA)). Samples were analysed using an Autoflex Speed LRF matrix-assisted laser desorption/ionization time of flight mass spectrometer (MALDI-TOF-MS, Bruker Daltonics) with a smartbeam-II laser. A SNAP averaging algorithm was used to obtain monoisotopic masses (C: 4.9384, N: 1.3577, O: 1.4773, S: 0.00417, H: 7.7583). Resulting MALDI spectra were visually inspected using FlexAnalysis v. 3.4 (Bruker Daltonics) and compared to a reference database consisting of published peptide markers for marsupials[60,61].

Deamidation

Levels of glutamine deamidation were calculated from MALDI spectral data in R v. 4.0.1. with R Studio v. 1.2.1717[54] using the Q2E package[62]. This resulted in a quality score (%Gln) between 0-1 for all spectra, in which a quality score of 0 represents a fully deamidated peptide, and a quality score of 1 represents a peptide that shows no sign of deamidation[62]. Deamidation rates were only calculated for samples that could be taxonomically identified to family-level or higher using ZooMS. Samples with insufficient collagen preservation for taxonomic identification were given a deamidation score of 0 for statistical analysis, representing the absence of measurable collagen in the sample.

Statistics

All statistical analyses were performed in R v. 4.0.1. with R Studio v. 1.2.1717[54]. To test whether FTIR values (Am1/P and Am2/P) can predict the success of ZooMS extractions, violin plots were used to show whether the FTIR value distributions for samples that were successfully and unsuccessfully analysed with ZooMS differed. Student t-tests were performed to assess whether there were significant differences in FTIR values between failed and successful ZooMS samples. Unless otherwise stated, statistical significance was assessed at $p<0.01$. A cut-off point was determined by calculating the third quantile of the failed samples. Clustered heatmaps were rendered to visualize variations in meteorological conditions between sites and reveal hierarchical clusters – a two-way display of a data-matrix in which the colour of a cell is proportional to its position along a colour gradient. Because the variables in the matrix are highly divergent, each variable column was normalized for the cluster algorithms. The dendrogram on the heatmap computes the distance between each pair of rows and columns, and orders them by similarity. The length of the branches on the heatmap represents the Euclidean distance, or dissimilarity, between clusters. All figures were made using the "ggplot2" package[63].

Acknowledgements

We are grateful to Andrea Manica for sharing a beta version of the Pastclim R package with us, and to Simon Hickinbotham and Julie Wilson for assistance in using the Q2E R package. We would also like to thank Sandra Hebestreit for technical assistance with ZooMS extractions, and Erin Scott for technical assistance with FTIR measurements. We are also grateful to Kristine Korzow Richter for helpful discussions about the paper. This research was supported by the Max Planck Society.

References

1 Miller, W. *et al.* Sequencing the nuclear genome of the extinct woolly mammoth. *Nature* **456**, 387-390, doi:10.1038/nature07446 (2008).

2 Rybczynski, N. *et al.* Mid-Pliocene warm-period deposits in the High Arctic yield insight into camel evolution. *Nat. Commun.* **4**, 1-9, doi:10.1038/ncomms2516 (2013).

3 Chen, F. *et al.* A late Middle Pleistocene Denisovan mandible from the Tibetan Plateau. *Nature* **569**, 409-412, doi:10.1038/s41586-019-1139-x (2019).

4 Cappellini, E. *et al.* Early Pleistocene enamel proteome from Dmanisi resolves *Stephanorhinus* phylogeny. *Nature* **574**, 103-107, doi:10.1038/s41586-019-1555-y (2019).

5 Demarchi, B. *et al.* Survival of mineral-bound peptides into the Miocene. *bioRxiv*, 2022.2008.2019.502663, doi:10.1101/2022.08.19.502663 (2022).

6 Slon, V. *et al.* Extended longevity of DNA preservation in Levantine Paleolithic sediments, Sefunim Cave, Israel. *Sci. Rep.* **12**, 14528, doi:10.1038/s41598-022-17399-2 (2022).

7 Demarchi, B. *et al.* Protein sequences bound to mineral surfaces persist into deep time. *eLife* **5**, e17092, doi:10.7554/eLife.17092 (2016).

8 Buckley, M., Collins, M., Thomas-Oates, J. & Wilson, J. C. Species identification by analysis of bone collagen using matrix-assisted laser desorption/ionisation time-of-flight mass spectrometry. *Rapid Commun. Mass Spectrom.* **23**, 3843-3854, doi:10.1002/rcm.4316 (2009).

9 Smith, C. I., Chamberlain, A. T., Riley, M. S., Stringer, C. & Collins, M. J. The thermal history of human fossils and the likelihood of successful DNA amplification. *J. Hum. Evol.* **45**, 203-217, doi:10.1016/S0047-2484(03)00106-4 (2003).

10 Collins, M. *et al.* The survival of organic matter in bone: a review. *Archaeometry* **44**, 383-394, doi:10.1111/1475-4754.t01-1-00071 (2002).

11 Kendall, C., Eriksen, A. M. H., Kontopoulos, I., Collins, M. J. & Turner-Walker, G. Diagenesis of archaeological bone and tooth. *Palaeogeogr. Palaeoclimatol. Palaeoecol.* **491**, 21-37, doi:10.1016/j.palaeo.2017.11.041 (2018).

12 Sponheimer, M. *et al.* Saving Old Bones: a non-destructive method for bone collagen prescreening. *Sci. Rep.* **9**, 13928, doi:10.1038/s41598-019-50443-2 (2019).

13 Dickinson, M. R., Lister, A. M. & Penkman, K. E. H. A new method for enamel amino acid racemization dating: A closed system approach. *Quat. Geochronol.* **50**, 29-46, doi:10.1016/j.quageo.2018.11.005 (2019).

14 Tesakov, A. S. *et al.* Aminostratigraphical test of the East European Mammal Zonation for the late Neogene and Quaternary. *Quat. Sci. Rev.* **245**, 106434, doi:10.1016/j.quascirev.2020.106434 (2020).

15 Allentoft, M. E. *et al.* The half-life of DNA in bone: Measuring decay kinetics in 158 dated fossils. *Proc. Royal Soc. B* **279**, 4724-4733, doi:10.1098/rspb.2012.1745 (2012).

16 Kistler, L., Ware, R., Smith, O., Collins, M. & Allaby, R. G. A new model for ancient DNA decay based on paleogenomic meta-analysis. *Nucleic Acids Res.* **45**, 6310-6320, doi:10.1093/nar/gkx361 (2017).

17 Van Doorn, N. L., Wilson, J. C., Hollund, H. I., Soressi, M. & Collins, M. Site-specific deamidation of glutamine: A new marker of bone collagen deterioration. *Rapid Commun. Mass Spectrom.* **26**, 2319-2327, doi:10.1002/rcm.6351 (2012).

18 Shevchenko, A. *et al.* Proteomics identifies the composition and manufacturing recipe of the 2500-year old sourdough bread from Subeixi cemetery in China. *J. Proteomics* **105**, 363-371, doi:10.1016/j.jprot.2013.11.016 (2014).

19 Collins, M. J., Riley, M. S., Child, A. M. & Turner-Walker, G. A basic mathematical simulation of the chemical degradation of ancient collagen. *J. Archaeol. Sci.* **22**, 175-183, doi:10.1006/jasc.1995.0019 (1995).

20 Matthiesen, H., Høier Eriksen, A. M., Hollesen, J. & Collins, M. Bone degradation at five Arctic archaeological sites: Quantifying the importance of burial environment and bone characteristics. *J. Archaeol. Sci.* **125**, 105296, doi:10.1016/j.jas.2020.105296 (2021).

21 Eriksen, A. M. H. *et al.* Rapid loss of endogenous DNA in pig bone buried in five different environments. *Archaeometry* **62**, 827-846, doi:10.1111/arcm.12553 (2020).

22 Nielsen-Marsh, C. M. & Hedges, R. E. M. Patterns of diagenesis in bone I: The effects of site environments. *J. Archaeol. Sci.* **27**, 1139-1150, doi:10.1006/jasc.1999.0537 (2000).

23 Colleary, C., Lamadrid, H. M., O'Reilly, S. S., Dolocan, A. & Nesbitt, S. J. Molecular preservation in mammoth bone and variation based on burial environment. *Sci. Rep.* **11**, 2662, doi:10.1038/s41598-021-81849-6 (2021).
24 Pestle, W. J. & Colvard, M. Bone collagen preservation in the tropics: A case study from ancient Puerto Rico. *J. Archaeol. Sci.* **39**, 2079-2090, doi:10.1016/j.jas.2012.03.008 (2012).
25 Kontopoulos, I. *et al.* Screening archaeological bone for palaeogenetic and palaeoproteomic studies. *PLoS ONE* **15**, e0235146, doi:10.1371/journal.pone.0235146 (2020).
26 Pothier Bouchard, G. *et al.* Portable FTIR for on-site screening of archaeological bone intended for ZooMS collagen fingerprint analysis. *J. Archaeol. Sci. Rep.* **26**, 101862, doi:10.1016/j.jasrep.2019.05.027 (2019).
27 Dallongeville, S. *et al.* Identification of animal glue species in artworks using proteomics: Application to a 18th century gilt sample. *Anal. Chem.* **83**, 9431-9437, doi:10.1021/ac201978j (2011).
28 Miles, C. A. & Ghelashvili, M. Polymer-in-a-box mechanism for the thermal stabilization of collagen molecules in fibers. *Biophys. J.* **76**, 3243-3252, doi:10.1016/S0006-3495(99)77476-X (1999).
29 Covington, A. D., Song, L., Suparno, O., Collins, M. J. & Koon, H. E. C. Link-Lock: The mechanism of stabilising collagen by chemical reactions. *J. Soc. Leather Technol. Chem.* **92**, 1-7 (2006).
30 Tamara, L., Irena, Z. P., Ivan, J. & Matija, Č. ATR-FTIR spectroscopy as a pre-screening technique for the PMI assessment and DNA preservation in human skeletal remains – A review. *Quat. Int.* doi:10.1016/j.quaint.2022.09.004 (2022).
31 Schroeter, E. R. & Cleland, T. P. Glutamine deamidation: An indicator of antiquity, or preservational quality? *Rapid Commun. Mass Spectrom.* **30**, 251-255, doi:10.1002/rcm.7445 (2016).
32 Brown, S. *et al.* Examining collagen preservation through glutamine deamidation at Denisova Cave. *J. Archaeol. Sci.* **133**, 105454, doi:10.1016/j.jas.2021.105454 (2021).
33 Ramsøe, A. *et al.* DeamiDATE 1.0: Site-specific deamidation as a tool to assess authenticity of members of ancient proteomes. *J. Archaeol. Sci.* **115**, 105080, doi:10.1016/j.jas.2020.105080 (2020).
34 Pal Chowdhury, M. *et al.* Collagen deamidation in archaeological bone as an assessment for relative decay rates. *Archaeometry* **61**, 1382-1398, doi:10.1111/arcm.12492 (2019).
35 Weiner, S. & Bar-Yosef, O. States of preservation of bones from prehistoric sites in the Near East: A survey. *J. Archaeol. Sci.* **17**, 187-196, doi:10.1016/0305-4403(90)90058-D (1990).
36 Surovell, T. A. & Stiner, M. C. Standardizing infra-red measures of bone mineral crystallinity: An experimental approach. *J. Archaeol. Sci.* **28**, 633-642, doi:10.1006/jasc.2000.0633 (2001).
37 Smith, C. I., Nielsen-Marsh, C. M., Jans, M. M. E. & Collins, M. J. Bone diagenesis in the European Holocene I: Patterns and mechanisms. *J. Archaeol. Sci.* **34**, 1485-1493, doi:10.1016/j.jas.2006.11.006 (2007).
38 Martínez Cortizas, A. & López-Costas, O. Linking structural and compositional changes in archaeological human bone collagen: an FTIR-ATR approach. *Sci. Rep.* **10**, 17888, doi:10.1038/s41598-020-74993-y (2020).
39 López-Costas, O., Lantes-Suárez, Ó. & Martínez Cortizas, A. Chemical compositional changes in archaeological human bones due to diagenesis: Type of bone vs soil environment. *J. Archaeol. Sci.* **67**, 43-51, doi:10.1016/j.jas.2016.02.001 (2016).
40 Kaal, J., López-Costas, O. & Martínez Cortizas, A. Diagenetic effects on pyrolysis fingerprints of extracted collagen in archaeological human bones from NW Spain, as determined by pyrolysis-GC-MS. *J. Archaeol. Sci.* **65**, 1-10, doi:10.1016/j.jas.2015.11.001 (2016).
41 Raffone, C. *et al.* Intrinsic and extrinsic factors that may influence DNA preservation in skeletal remains: A review. *Forensic Sci. Int.* **325**, 110859, doi:10.1016/j.forsciint.2021.110859 (2021).
42 Fernández-Jalvo, Y. & Andrews, P. *Atlas of taphonomic identifications. 1001+ images of fossil and recent mammal bone modification*, (Springer Science+Business Media, Dordrecht, 2016).
43 Roberts, S. J., Smith, C. I., Millard, A. & Collins, M. J. The taphonomy of cooked bone: Characterizing boiling and its physico–chemical effects. *Archaeometry* **44**, 485-494, doi:10.1111/1475-4754.t01-1-00080 (2002).

44 Faillace, K. E., Foody, M. G. B. & Madgwick, R. Exploring the potential of TEM analysis for understanding cooking at prehistoric feasting sites. *Sci. Rep.* **10**, 13635, doi:10.1038/s41598-020-70628-4 (2020).
45 Piga, G. *et al.* An X-ray Diffraction (XRD) and X-ray Fluorescence (XRF) investigation in human and animal fossil bones from Holocene to Middle Triassic. *J. Archaeol. Sci.* **36**, 1857-1868, doi:10.1016/j.jas.2009.04.013 (2009).
46 Shah, F. A., Ruscsák, K. & Palmquist, A. 50 years of scanning electron microscopy of bone - A comprehensive overview of the important discoveries made and insights gained into bone material properties in health, disease, and taphonomy. *Bone Res.* **7**, 15, doi:10.1038/s41413-019-0053-z (2019).
47 Reiche, I. *et al.* A multi-analytical study of bone diagenesis: The Neolithic site of Bercy (Paris, France). *Meas. Sci. Technol.* **14**, 1608-1619, doi:10.1088/0957-0233/14/9/312 (2003).
48 Chen, X. *et al.* Mechanical heterogeneity in the bone microenvironment as characterized by atomic force microscopy. *Biophys. J.* **119**, 502-513, doi:10.1016/j.bpj.2020.06.026 (2020).
49 McCoy, V. E. *et al.* Ancient amino acids from fossil feathers in amber. *Scientific Reports* **9**, 6420, doi:10.1038/s41598-019-42938-9 (2019).
50 Cappellini, E. *et al.* Proteomic Analysis of a Pleistocene mammoth femur reveals more than one hundred ancient bone proteins. *J. Proteome Res.* **11**, 917-926, doi:10.1021/pr200721u (2012).
51 Pálsdóttir, A. H., Bläuer, A., Rannamäe, E., Boessenkool, S. & Hallsson, J. H. Not a limitless resource: Ethics and guidelines for destructive sampling of archaeofaunal remains. *R. Soc. Open Sci.* **6**, 191059, doi:10.1098/rsos.191059 (2019).
52 Austin, R. M., Sholts, S. B., Williams, L., Kistler, L. & Hofman, C. A. To curate the molecular past, museums need a carefully considered set of best practices. *PNAS* **116**, 1471-1474, doi:10.1073/pnas.1822038116 (2019).
53 Beyer, R. M., Krapp, M. & Manica, A. High-resolution terrestrial climate, bioclimate and vegetation for the last 120,000 years. *Sci. Data* **7**, 236, doi:10.1038/s41597-020-0552-1 (2020).
54 R Core Team. *R: A language and environment for statistical computing*, (R Foundation for statistical computing, Vienna, 2021).
55 pastclim: This package provides helper functions to interact with timeseries of worldwide climate reconstructions (2022).
56 Leonardi, M., Hallett, E. Y., Beyer, R., Krapp, M. & Manica, A. pastclim: An R package to easily access and use paleoclimatic reconstructions. *bioRxiv*, 2022.2005.2018.492456, doi:10.1101/2022.05.18.492456 (2022).
57 Gilbert, M. T. P. *et al.* Whole-genome shotgun sequencing of mitochondria from ancient hair shafts. *Science* **317**, 1927-1930, doi:10.1126/science.1146971 (2007).
58 Behrensmeyer, A. K. Taphonomic and ecologic information from bone weathering. *Paleobiology* **4**, 150-162, doi:10.1017/S0094837300005820 (1978).
59 Van der Sluis, L. G. *et al.* Combining histology, stable isotope analysis and ZooMS collagen fingerprinting to investigate the taphonomic history and dietary behaviour of extinct giant tortoises from the Mare aux Songes deposit on Mauritius. *Palaeogeogr. Palaeoclimatol. Palaeoecol.* **416**, 80-91, doi:10.1016/j.palaeo.2014.06.003 (2014).
60 Peters, C. *et al.* Species identification of Australian marsupials using collagen fingerprinting. *R. Soc. Open Sci.* **8**, 211229, doi:10.1098/rsos.211229 (2021).
61 Buckley, M., Cosgrove, R., Garvey, J. & Prideaux, G. J. Identifying remains of extinct kangaroos in Late Pleistocene deposits using collagen fingerprinting. *J. Quat. Sci.* **32**, 653-660, doi:10.1002/jqs.2964 (2017).
62 Wilson, J. C., Van Doorn, N. L. & Collins, M. Assessing the Extent of Bone Degradation Using Glutamine Deamidation in Collagen. *Anal. Chem.* **84**, 9041-9048, doi:10.1021/ac301333t (2012).
63 Wickham, H. *ggplot2. Elegant Graphics for Data Analysis*, (Springer-Verlag, New York, 2016).

Supplementary Information

Systematic survey of collagen preservation in Australia reveals unexpected tropical survival at >50,000 years

Carli Peters[1,*], Yiming Wang[1], Joe Dortch[2], Scott Hocknull[3,4], Rochelle Lawrence[3], Tiina Manne[5], Carly Monks[2], Gertrud E. Röβner[6,7], Helen Ryan[8], Mikael Siversson[8], Tim Ziegler[9], Julien Louys[10], Gilbert J. Price[11], Nicole Boivin[1,5,12,13], Matthew J. Collins[14,15,*]

1. Department of Archaeology, Max Planck Institute for Geoanthropology, Jena, Germany
2. School of Social Sciences, University of Western Australia, Perth, WA 6009, Australia
3. Geosciences, Queensland Museum, Hendra, Qld 4011, Australia
4. School of Biosciences, Faculty of Science, University of Melbourne, Melbourne Vic 3010, Australia
5. School of Social Science, The University of Queensland, Brisbane, Qld 4071, Australia
6. Staatliche Naturwissenschaftliche Sammlungen Bayerns – Bayerische Staatssammlung für Paläontologie und Geologie, Munich, Germany
7. Department für Geo- und Umweltwissenschaften, Ludwig-Maximilians-Universität München, Munich, Germany
8. Western Australian Museum, Collections and Research, 49 Kew Street, Welshpool, WA 6106, Australia
9. Museums Victoria, Melbourne, Vic 3001, Australia
10. Australian Research Centre for Human Evolution, Griffith University, Nathan, Qld 4111, Australia
11. School of Earth and Environmental Sciences, The University of Queensland, Brisbane, Qld 4072, Australia
12. Department of Anthropology, National Museum of Natural History, Smithsonian Institution, Washington DC, USA
13. Department of Anthropology and Archaeology, University of Calgary, Calgary, Canada
14. Department of Archaeology, Cambridge University, Cambridge, United Kingdom
15. Section for Evolutionary Genomics, Globe Institute, University of Copenhagen, Copenhagen, Denmark

*Corresponding authors: Carli Peters and Matthew J. Collins

Supplementary Text

Supplementary Text 1: Extended methods

Supplementary Figures

Supplementary Figure 1: The predicted mean annual temperature (MAT) following palaeoclimate reconstructions set out against modern weather station data. Modern weather station data was corrected for altitude differences using the standard lapse rate.

Supplementary Figure 2: Grouped bar chart comparing ZooMS success rates with bone weathering stages.

Supplementary Figure 3: Correlation between FTIR values (Am1/P and Am2/P) and deamidation rates (%Gln) of samples that were successfully analysed with ZooMS.

Supplementary Figure 4: Box-and-whiskers plot of C/P values per site.

Supplementary Figure 5: Box-and-whiskers plot of C/P values of samples from Tripot Cave.

Supplementary Tables

Supplementary Table 1: Overview of the localities included in the study, their age in thousand years (ka), depositional environment, mean annual temperature (MAT), mean annual precipitation, and sample size.

Supplementary Table 2: Results of thermal age calculations. Thermal age estimates are relative to equal years of exposure at 10°C. The theoretical limit of collagen preservation (<1% collagen left) is based on a half-life of 180 ka at 10°C.

Supplementary Table 3: ZooMS success rates and average deamidation rates for each locality.

Other Supplementary Materials for this Manuscript

Supplementary Dataset 1: Overview of depositional environments of each locality.

Supplementary Dataset 2: Sample numbers, storage locations, and registration number of sampled materials.

Supplementary Dataset 3: Modern weather station data.

Supplementary Dataset 4: Palaeoclimate data.

Supplementary Dataset 5: Overview of bone weathering stages, FTIR results, ZooMS results, and deamidation estimates for individual samples.

Supplementary Text 1: Extended methods

Thermal age estimates.
Thermal age is a metric that can be used to predict the survival of biomolecules in fossil material. Thermal age was originally defined as 'the time taken to produce a given degree of DNA degradation when the temperature is held at a constant 10°C.' (p.204;[1]). All sites are treated as having experienced the same constant temperature of 10°C, which allows for the comparison of preservation potential between sites[1,2]. Even though thermal age was originally developed to estimate the degree of DNA preservation[1], a similar calculation can be used to estimate the degree of collagen preservation at a given site. The main difference between the two calculations is the difference in activation energy between collagen denaturation (172 kJ mol-1[3]) and DNA depurination (127 kJ mol-1[4]), reflecting the higher temperature sensitivity of collagen denaturation. Furthermore, collagen denaturation is more affected by slight changes in the surrounding mineral fraction[5]. The predicted survival of collagen as a function of burial temperature appears to define the limit of radiocarbon collagen dates from the ADS OxCal database (Fig.7,[6]).

Fourier Transform Infrared Spectroscopy (FTIR).
FTIR is increasingly used in archaeology and forensic studies to characterize bone diagenesis prior to palaeoproteomics and palaeogenetic analyses[7-14]. FTIR is a minimally destructive technique that can be used to rapidly assess the preservation state of osseous remains. Both the presence of organic and inorganic content can be inferred from FTIR measurement[12-15]. The presence of organic content in bone is most commonly assessed by the amide-to-phosphate (Am/P) ratio, and the intensity of the amide I peak has been linked to the presence of proteins and peptides specifically[7,11,16]. The Am/P ratio can thus be used to assess protein preservation in archaeological bone, and several cut-off points have been suggested that indicate the presence of sufficient collagen for successful palaeoproteomics analysis[9,11].

Zooarchaeology by Mass Spectrometry (ZooMS) and deamidation.
The state of collagen preservation was assessed from ZooMS results in two ways. First, by calculating the percentage of ZooMS successfully analysed specimens for each site. Successful ZooMS spectra were defined as spectra that allowed for a higher resolution taxonomic identification that morphological identification of the same specimen. In practice, this refers to spectra allowing taxonomic identifications of family-level or higher.

The state of collagen preservation was further assessed by calculating glutamine deamidation levels of peptide COL1α1 508-519 from MALDI spectral data. Deamidation is the post-translational modification of glutamine and asparagine to glutamic acid and aspartic acid, respectively, by the loss of an amide functional group. This results in a +0.98402 Da mass shift[17,18]. Commonly, peptide COL1α1 508-519 is used to measure glutamine deamidation levels from MALDI spectra, since this peptide is conserved across many mammal species at *m/z* 1105.6 (sequence GVQGPPGPAGPR), only contains a single glutamine that can deamidate, and is commonly well-represented across spectra[17,18]. For marsupials, however, this peptide has a *m/z* of 1162.6 (sequence GVQGPPGPQGPR[19]), and contains two glutamines that can deamidate. This peptide is well-represented across marsupial spectra, and it was thus used to calculate deamidation rates.

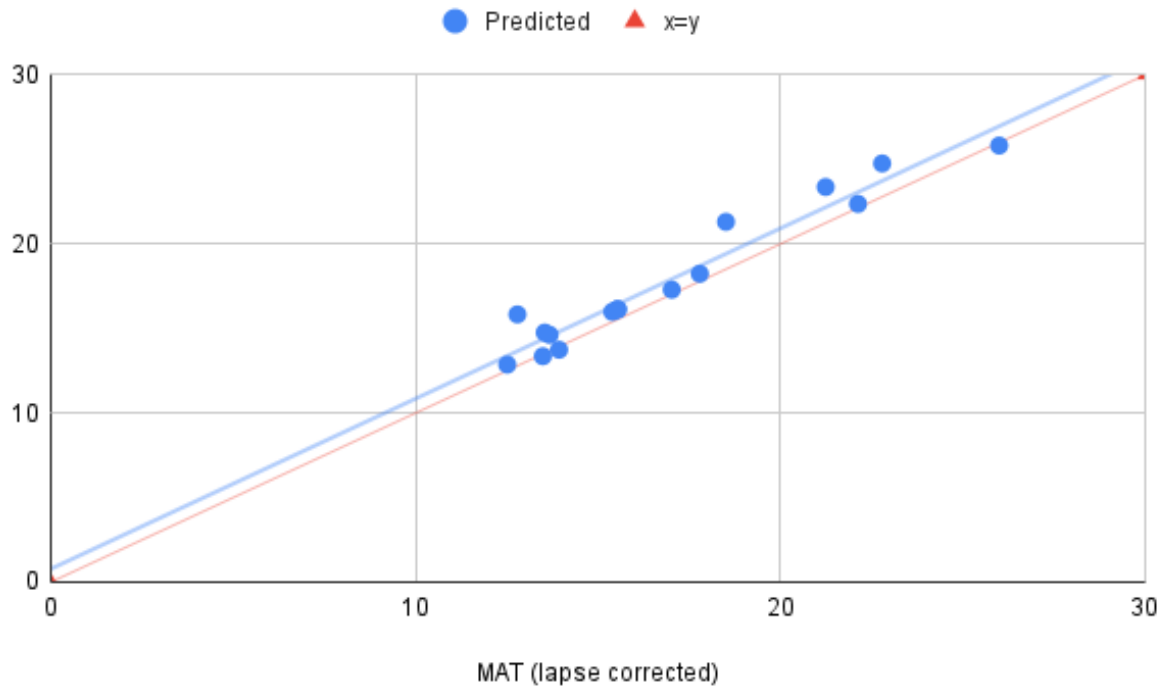

Fig. S1. The predicted mean annual temperature (MAT) following palaeoclimate reconstructions set out against modern weather station data. Modern weather station data was corrected for altitude differences using the standard lapse rate.

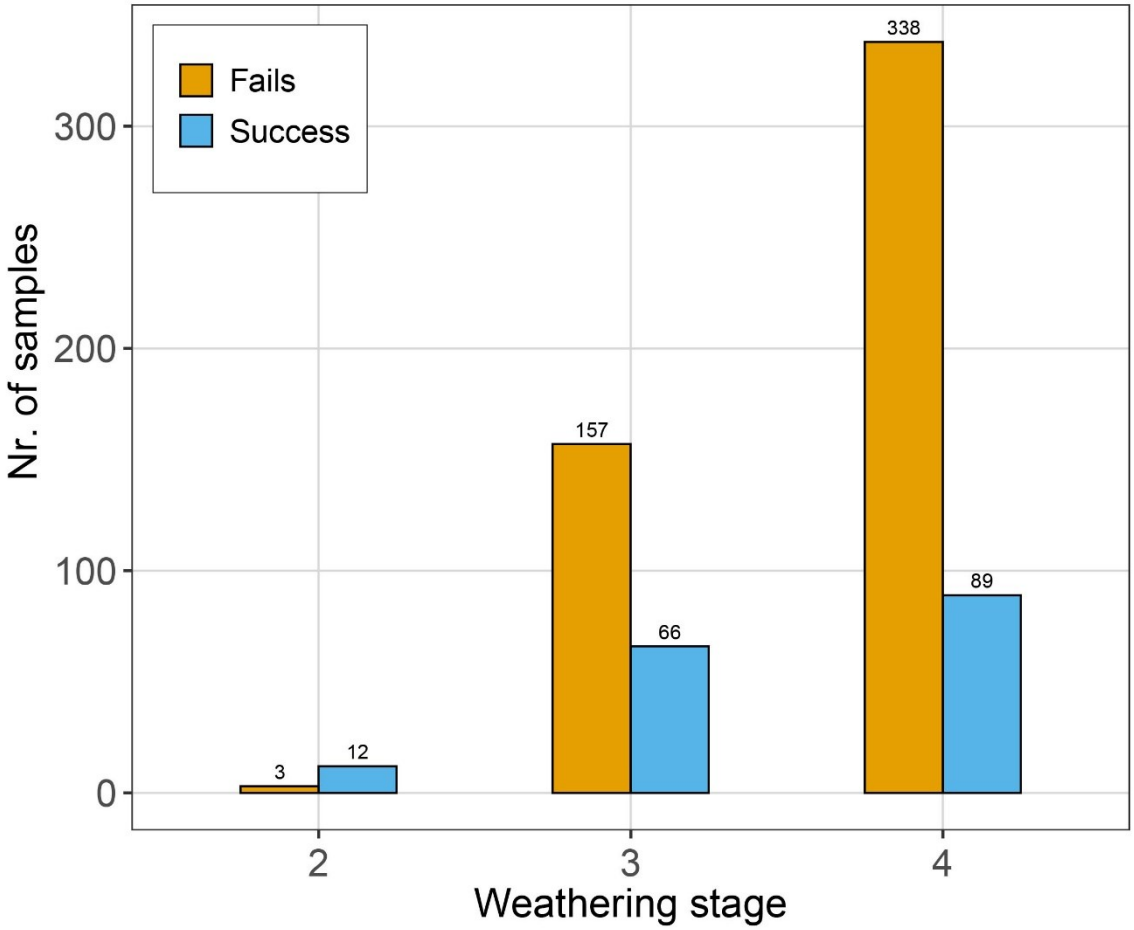

Fig. S2. Grouped bar chart comparing ZooMS success rates with bone weathering stages.

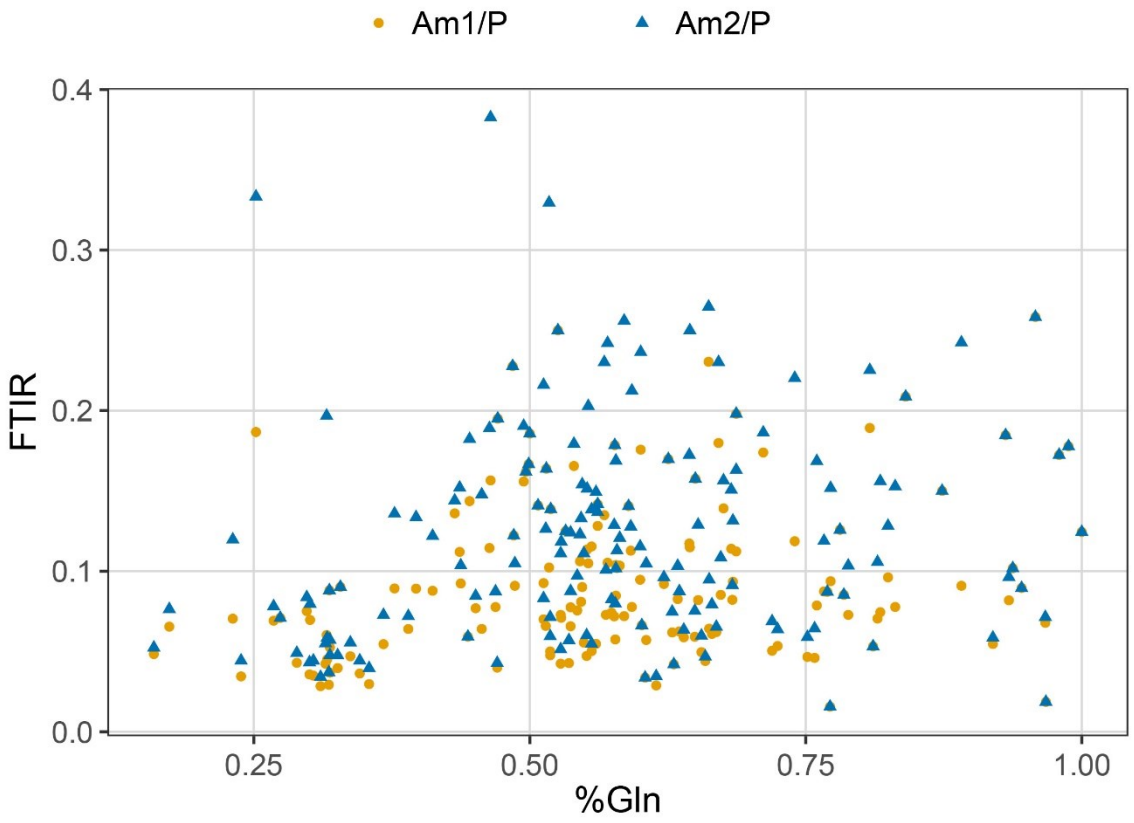

Fig. S3. Correlation between FTIR values (Am1/P and Am2/P) and deamidation rates (%Gln) of samples that were successfully analysed with ZooMS.

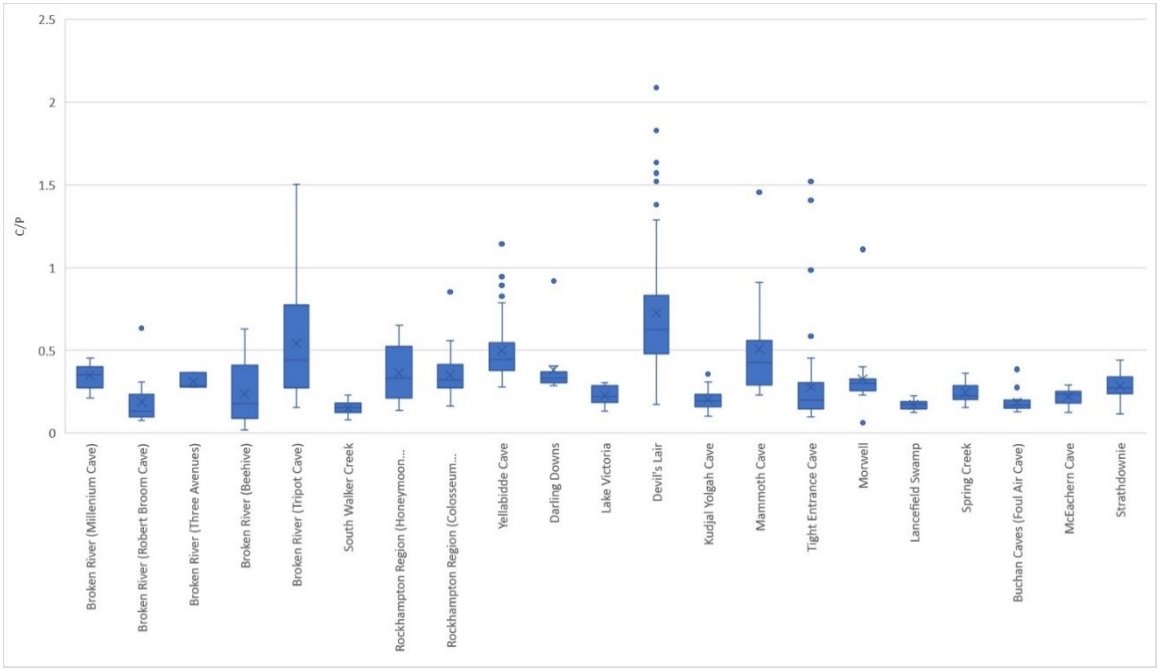

Fig. S4. Box-and-whiskers plot of C/P values per site.

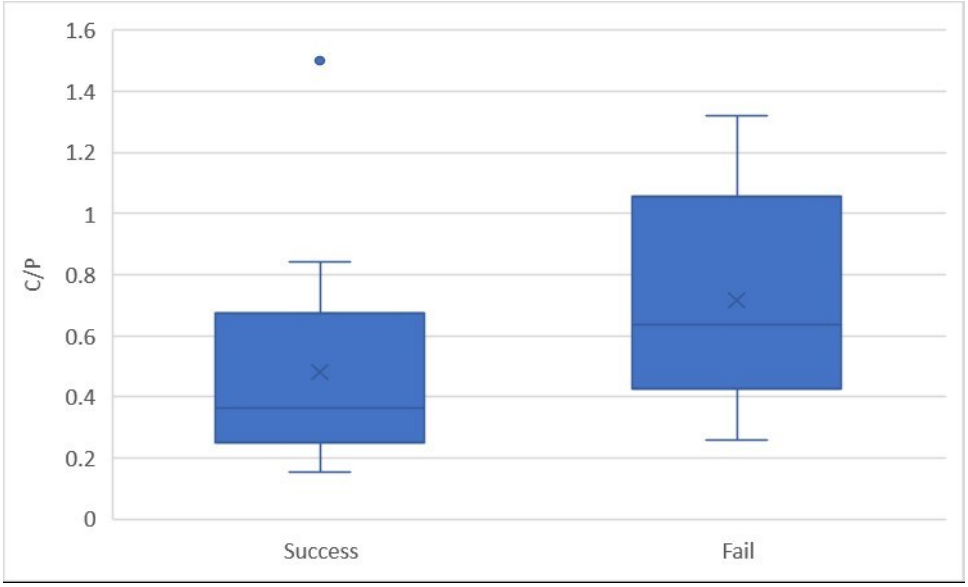

Fig. S5. Box-and-whiskers plot of C/P values of samples from Tripot Cave.

Table S1. Overview of the localities included in the study, their age in thousand years (ka), depositional environment, mean annual temperature (MAT), mean annual precipitation, and sample size.

Locality	Age (in ka)	Depositional environment	MAT (°C)	Precipitation (mm/year)[2]	Sample size[2]	Ref.
Boodie Cave	2.5-43.5	Cave	25.9	269.3	41	[20]
Broken River[1]		Cave	24.1	641.7	58	
Beehive	8.5				5	[21]
Millennium Cave	recent				11	Price pers. comm.
Robert Broom Cave	70				14	Price et al. unpublished
Three Avenues	recent				3	
Tripot Cave	ca. 350-75				25	Price et al. unpublished
Buchan Caves[1]		Cave	13.7	981.1	22	
Foul Air Cave	Late Pleistocene				20	
Potluck Caves	Late Pleistocene				2	
Darling Downs[1]		Fluvial	18.3	610.9	23	
Dalby	Late Pleistocene				1	
Darling Downs	112-107				21	[22]
Ned's Gully	60-46				1	[23,24]
Devil's Lair	51.1-43.4	Cave	16.1	951.7	100	[25]
Kudjal Yolgah Cave	80-41	Cave	16.1	951.7	78	[26]
Lake Victoria	52	Lacustrine	17.3	259.2	10	[23]
Lancefield Swamp	59.4-44.1	Swamp	14	577.7	30	[27]
Mammoth Cave	74-55	Cave	16.1	951.7	12	[23]
McEachern Cave	>25.6	Cave	13.6	713.3	25	[28]
Morwell	Late Pleistocene	Lacustrine	14.2	723.3	20	[29]
Rockhampton region*		Cave	22.7	815.1	140	
Honeymoon Suite	Late Pleistocene				18	
Colosseum Chamber	51.4-25.3				122	[30]
South Walker Creek (SW9)	40.1	Fluvial	23.2	614.2	41	[31]
Spring Creek	>53.5	Fluvial	13.8	732.1	15	[32]
Strathdownie	Late Pleistocene	Cave	13.5	616.8	15	
Tight Entrance Cave	137-48	Cave	16.1	951.7	75	[33]
Yellabidde Cave	9-25.5	Cave	19.8	375.6	60	[34]

[1]These localities represent site clusters: **Broken River** (Millennium Cave, Beehive, Robert Broom Cave, Three Avenues, Tripot Cave), **Buchan Caves** (Foul Air Cave, Potluck Caves), **Darling Downs** (Darling Downs, Dalby, Ned's Gully), **Rockhampton region** (Colosseum Chamber, Honeymoon Suite).

[2] MAT and precipitation data was collected from local weather stations (http://www.bom.gov.au/climate/data/, accessed on 23 Nov. 2021).

Table S2. Results of thermal age calculations. Thermal age estimates are relative to equal years of exposure at 10°C. The theoretical limit of collagen preservation (<1% collagen left) is based on a half-life of 180 ka at 10°C.

Locality	**Age (in ka)**	**Thermal age estimates (in ka)**		**Theoretical limit of collagen preservation (in ka)**	
		Deep model	*Shallow model*	*Deep model*	*Shallow model*
Boodie Cave	2.5-43.5	127.3-1180.9	780.7-6923.5	44.4	3.9
Broken River				70.9	11.3
Beehive	8.5	199.7	907.7		
Millennium Cave	recent[3]	23.9-238.8	111.1-1062.6		
Robert Broom Cave	70	1185.6	5304.3		
Three Avenues	recent[3]	23.9-238.8	111.1-1062.6		
Tripot Cave	75-350[1]	1284.5->1824.6	5822.7->8455.9		
Buchan Caves				>100	>100
Foul Air Cave[2]	Late Pleistocene	72.1-148	289.4-599.3		
Potluck Caves[2]	Late Pleistocene	72.1-148	289.4-599.3		
Darling Downs				>100	47.8
Dalby[2]	Late Pleistocene	228.4-468.4	1270.3-2688.7		
Darling Downs	107-112[1]	>468.4	>2688.7		
Ned's Gully	46-60	211.2-272.4	1155.9-1519.3		
Devil's Lair	43.4-51.1	114.7-135.3	291.5-347.1	>100	>100
Kudjal Yolgah Cave	41-80	105.9-210.8	268.2-528.3	>100	>100
Lake Victoria	52	197.6	1236.4	>100	50.9
Lancefield Swamp	44.1-59.4	52.3-71.7	228.4-315.3	>100	>100
Mammoth Cave	55-74	148.3-198.3	378.2-504.9	>100	>100
McEachern Cave	>25.6	>49.9	>131.3	>100	>100
Morwell[2]	Late Pleistocene	93.8-201	317.4-651.5	>100	>100
Rockhampton Region				93.6	23.7
Honeymoon Suite[2]	Late Pleistocene	595-1307.1	2272.3-4954.5		
Colosseum Chamber	25.3-51.4	342.7-612.1	1253.5-2342.9		
South Walker Creek	40.1	470.6	1902.9	97.4	21.9
Spring Creek	>53.5	>85.6	>242.8	>100	>100
Strathdownie[2]	Late Pleistocene	89.6-187.9	299.9-627.2	>100	>100
Tight Entrance Cave	48-137[1]	127.7-290.3	328.6-710.3	>100	>100
Yellabidde Cave	9-25.5	72.3-161.2	284.9-658.6	>100	49.2

[1]Thermal age estimates were calculated for 100 ka, which represents the upper limit of the palaeoclimate model data that has been extracted for the calculations.
[2]For localities without sufficient age information, thermal ages were calculated for 50-100 ka, since these are all localities from which megafauna remains have been recovered.
[3]Thermal ages calculated for 1-10 ka.

Table S3. ZooMS success rates and average deamidation rates for each locality.

Locality	Sample size	ZooMS success rate	Average deamidation rate[1]
Boodie Cave	41	0%	- (0)
Broken River	58	53.4%	0.66 (0.35)
Beehive	5	0%	- (0)
Millennium Cave	11	100%	0.86
Robert Broom Cave	14	0%	- (0)
Three Avenues	3	66.7%	0.58 (0.39)
Tripot Cave	25	72%	0.55 (0.4)
Buchan Caves	22	4.5%	0.6 (0.03)
Foul Air Cave	20	5%	0.6 (0.03)
Potluck Caves	2	0%	- (0)
Darling Downs	23	0%	- (0)
Dalby	1	0%	- (0)
Darling Downs	21	0%	- (0)
Ned's Gully	1	0%	- (0)
Devil's Lair	100	85%	0.58 (0.5)
Kudjal Yolgah Cave	78	39.7%	0.44 (0.18)
Lake Victoria	10	0%	- (0)
Lancefield Swamp	30	3.3%	0.67 (0.02)
Mammoth Cave	12	8.3%	0.89 (0.07)
McEachern Cave	25	4%	0.95 (0.04)
Morwell	20	0%	- (0)
Rockhampton Region	140	1.4%	0.64 (0.01)
Colosseum Chamber	122	0%	- (0)
Honeymoon Suite	18	11.1%	0.64 (0.07)
South Walker Creek	41	0%	- (0)
Spring Creek	15	13.3%	0.17 (0.02)
Strathdownie	15	0%	- (0)
Tight Entrance Cave	75	1.3%	0.61 (0.01)
Yellabidde Cave	60	16.7%	0.65 (0.11)

[1]The average deamidation rate in brackets represents the average deamidation rates including failed samples given a deamidation score of 0.

Dataset S1. Overview of depositional environments of each locality.

Dataset S2. Sample numbers, storage locations, and registration number of sampled materials.

Dataset S3. Modern weather station data.

Dataset S4. Palaeoclimate data.

Dataset S5. Overview of bone weathering stages, FTIR results, ZooMS results, and deamidation estimates for individual samples.

SI References

1 Smith, C. I., Chamberlain, A. T., Riley, M. S., Stringer, C. & Collins, M. J. The thermal history of human fossils and the likelihood of successful DNA amplification. *J. Hum. Evol.* **45**, 203-217, doi:10.1016/S0047-2484(03)00106-4 (2003).

2 Demarchi, B. *et al.* Protein sequences bound to mineral surfaces persist into deep time. *eLife* **5**, e17092, doi:10.7554/eLife.17092 (2016).

3 Buckley, M. *et al.* Comment on "Protein sequences from Mastodon and Tyrannosaurus rex revealed by mass spectrometry". *Science* **319**, 33, doi:10.1126/science.1147046 (2008).

4 Lindahl, T. & Nyberg, B. Rate of depurination of native deoxyribonucleic acid. *Biochemistry* **11**, 3610-3618, doi:10.1021/bi00769a018 (1972).

5 Smith, C. I., Nielsen-Marsh, C. M., Jans, M. M. E. & Collins, M. J. Bone diagenesis in the European Holocene I: patterns and mechanisms. *J. Archaeol. Sci.* **34**, 1485-1493, doi:10.1016/j.jas.2006.11.006 (2007).

6 Kendall, C., Eriksen, A. M. H., Kontopoulos, I., Collins, M. J. & Turner-Walker, G. Diagenesis of archaeological bone and tooth. *Palaeogeogr. Palaeoclimatol. Palaeoecol.* **491**, 21-37, doi:10.1016/j.palaeo.2017.11.041 (2018).

7 Lebon, M., Reiche, I., Gallet, X., Bellot-Gurlet, L. & Zazzo, A. Rapid quantification of bone collagen content by ATR-FTIR spectroscopy. *Radiocarbon* **58**, 131-145, doi:10.1017/RDC.2015.11 (2016).

8 Pal Chowdhury, M. *et al.* Machine learning ATR-FTIR spectroscopy data for the screening of collagen for ZooMS analysis and mtDNA in archaeological bone. *J. Archaeol. Sci.* **126**, 105311, doi:10.1016/j.jas.2020.105311 (2021).

9 Pothier Bouchard, G. *et al.* Portable FTIR for on-site screening of archaeological bone intended for ZooMS collagen fingerprint analysis. *J. Archaeol. Sci. Rep.* **26**, 101862, doi:10.1016/j.jasrep.2019.05.027 (2019).

10 Sponheimer, M. *et al.* Saving Old Bones: A non-destructive method for bone collagen prescreening. *Sci. Rep.* **9**, 13928, doi:10.1038/s41598-019-50443-2 (2019).

11 Kontopoulos, I. *et al.* Screening archaeological bone for palaeogenetic and palaeoproteomic studies. *PLoS ONE* **15**, e0235146, doi:10.1371/journal.pone.0235146 (2020).

12 Presslee, S. *et al.* Assessment of different screening methods for selecting palaeontological bone samples for peptide sequencing. *J. Proteomics* **230**, 103986, doi:10.1016/j.jprot.2020.103986 (2021).

13 Cienkosz-Stepańczak, B., Szostek, K. & Lisowska-Gaczorek, A. Optimizing FTIR method for characterizing diagenetic alteration of skeletal material. *J. Archaeol. Sci. Rep.* **38**, 103059, doi:10.1016/j.jasrep.2021.103059 (2021).

14 Tamara, L., Irena, Z. P., Ivan, J. & Matija, Č. ATR-FTIR spectroscopy as a pre-screening technique for the PMI assessment and DNA preservation in human skeletal remains – A review. *Quat. Int.*, doi:10.1016/j.quaint.2022.09.004 (2022).

15 Beasley, M. M., Bartelink, E. J., Taylor, L. & Miller, R. M. Comparison of transmission FTIR, ATR, and DRIFT spectra: Implications for assessment of bone bioapatite diagenesis. *J. Archaeol. Sci.* **46**, 16-22, doi:10.1016/j.jas.2014.03.008 (2014).

16 Trueman, C. N. G., Behrensmeyer, A. K., Tuross, N. & Weiner, S. Mineralogical and compositional changes in bones exposed on soil surfaces in Amboseli National Park, Kenya: Diagenetic mechanisms and the role of sediment pore fluids. *J. Archaeol. Sci.* **31**, 721-739, doi:10.1016/j.jas.2003.11.003 (2004).

17 Van Doorn, N. L., Wilson, J. C., Hollund, H. I., Soressi, M. & Collins, M. Site-specific deamidation of glutamine: A new marker of bone collagen deterioration. *Rapid Commun. Mass Spectrom.* **26**, 2319-2327, doi:10.1002/rcm.6351 (2012).
18 Wilson, J. C., Van Doorn, N. L. & Collins, M. Assessing the extent of bone degradation using glutamine deamidation in collagen. *Anal. Chem.* **84**, 9041-9048, doi:10.1021/ac301333t (2012).
19 Peters, C. *et al.* Species identification of Australian marsupials using collagen fingerprinting. *R. Soc. Open Sci.* **8**, 211229, doi:10.1098/rsos.211229 (2021).
20 Veth, P. *et al.* Early human occupation of a maritime desert, Barrow Island, North-West Australia. *Quat. Sci. Rev.* **168**, 19-29, doi:10.1016/j.quascirev.2017.05.002 (2017).
21 Price, G. J. *et al.* Late Quaternary fossil vertebrates of the Broken River karst area, Northern Queensland, Australia. *Rec. Aust. Mus.* **72**, 193-206, doi:10.3853/j.2201-4349.72.2020.1723 (2020).
22 Price, G. J. *et al.* Dating megafaunal extinction on the Pleistocene Darling Downs, Eastern Australia: the promise and pitfalls of dating as a test of extinction hypotheses. *Quat. Sci. Rev.* **30**, 899-914, doi:10.1016/j.quascirev.2011.01.011 (2011).
23 Roberts, R. G. *et al.* New ages for the last Australian megafauna: Continent-wide extinction about 46,000 years ago. *Science* **292**, 1888-1892, doi:10.1126/science.1060264 (2001).
24 Price, G. J. *et al.* New ages of the world's largest-ever marsupial: *Diprotodon optatum* from Pleistocene Australia. *Quat. Int.* **603**, 64-73, doi:10.1016/j.quaint.2021.06.013 (2021).
25 Turney, C. S. M. *et al.* Early human occupation at Devil's Lair, Southwestern Australia 50,000 years ago. *Quat. Res.* **55**, 3-13, doi:10.1006/qres.2000.2195 (2001).
26 Jankowski, N. R., Gully, G. A., Jacobs, Z., Roberts, R. G. & Prideaux, G. J. A Late Quaternary vertebrate deposit in Kudjal Yolgah Cave, South-Western Australia: refining regional Late Pleistocene extinctions. *J. Quat. Sci.* **31**, 538-550, doi:10.1002/jqs.2877 (2016).
27 Dortch, J. *et al.* The timing and cause of megafauna mass deaths at Lancefield Swamp, South-Eastern Australia. *Quat. Sci. Rev.* **145**, 161-182, doi:10.1016/j.quascirev.2016.05.042 (2016).
28 Hope, J. H. & Wilkinson, H. E. *Warendja wakefieldi*, a new genus of wombat (Marsupialia, Vombatidae) from Pleistocene sediments in McEacherns Cave, Western Victoria. *Mem. Mus. Vic.* **43**, 109-120 (1982).
29 Flannery, T. F. *Macropus munjabus*, a new kangaroo (Marsupialia: Macropodidae) of uncertain age from Victoria, Australia. *Aust. Mammal.* **3**, 35-51 (1980).
30 Price, G. J. *et al.* Temporal overlap of humans and giant lizards (Varanidae; Squamata) in Pleistocene Australia. *Quat. Sci. Rev.* **125**, 98-105, doi:10.1016/j.quascirev.2015.08.013 (2015).
31 Hocknull, S. A. *et al.* Extinction of eastern Sahul megafauna coincides with sustained environmental deterioration. *Nat. Commun.* **11**, 2250, doi:10.1038/s41467-020-15785-w (2020).
32 Gillespie, R., Wood, R., Fallon, S., Stafford Jr, T. W. & Southon, J. New 14C dates for Spring Creek and Mowbray Swamp megafauna: XAD-2 processing. *Archaeol. Oceania* **50**, 43-48, doi:10.1002/arco.5045 (2015).
33 Ayliffe, L. K. *et al.* Age constraints on Pleistocene megafauna at Tight Entrance Cave in Southwestern Australia. *Quat. Sci. Rev.* **27**, 1784-1788, doi:10.1016/j.quascirev.2008.07.008 (2008).
34 Monks, C., Dortch, J., Jacobsen, G. & Baynes, A. Pleistocene occupation of Yellabidde Cave in the northern Swan Coastal Plain, Southwestern Australia. *Aust. Archaeol.* **82**, 275-279, doi:10.1080/03122417.2016.1244216 (2016).

Dataset S1: Overview of depositional environments of each locality.

Locality	Age	Dating Method	DepositionalEnvironment	SoilType	pH	Notes	REFS
Boodie Cave	2.5-43.5 ka[1]	Bayesian modelling of AMS and OSL data	Limestone cave	Sand[1]	8.5[2]		(1) Veth et al. 2017; (2) Ward et al. 2017; (3) Skippington et al. 2018
Broken River							
Beehive	8.5 ka	U-series	Limestone cave	Haematite-rich clay matrix-supported breccias	Alkaline	Bones prepared with acetic acid	Price et al. 2020
Millennium Cave	recent		Limestone cave	Haematite-rich clay matrix-supported breccias	Alkaline		Price et al. 2020
Robert Broom Cave	70 ka[1]	U-series	Limestone cave	Haematite-rich clay matrix-supported breccias[2]	Alkaline	Bones prepared with acetic acid	(1) Price unpublished; (2) Price et al. 2020
Three Avenues	recent		Limestone cave	Haematite-rich clay matrix-supported breccias	Alkaline		Price et al. 2020
Tripot Cave	75-350 ka[1]	U-series	Limestone cave	Haematite-rich clay matrix-supported breccias[2]	Alkaline		(1) Price unpublished; (2) Price et al. 2020
Buchan Caves	275 ka	U-Th of calcite flowstone		Clay	Neutral	Soft terra rossa	Shean 2017
Foul Air Cave			Limestone cave		Alkaline		
Potluck Caves			Limestone cave		Alkaline		
Darling Downs							
Dalby			Fluvial	Clay, silt, sand from erosion of underlying basalts and sandstones	Alkaline		Price 2008
Darling Downs	112-107 ka[1]	OSL	Fluvial	Clay, silt, sand from erosion of underlying basalts and sandstones[2]	Alkaline		(1) Price et al. 2011; (2) Price 2008
Ned's Gully	60-46 ka[1,2]	U-series & OSL	Fluvial	Clay[2]	Alkaline		(1) Roberts et al. 2001; (2) Price et al. 2021
Devil's Lair	43.3-51.1 ka[1]	OSL	Limestone cave	Sand[2]	Alkaline		(1) Turney et al. 2001; (2) Balme et al. 1978
Kudjal Yolgah Cave	80-41 ka	OSL	Limestone cave	Sand	Alkaline		Jankowski et al. 2016
Lake Victoria	52 ka	OSL	Lacustrine				Roberts et al. 2001
Lancefield Swamp	59.4-44.1 ka	OSL	Swamp	Clay			Dortch et al. 2016
Mammoth Cave	74-55 ka[1]	OSL	Limestone cave	Sand[2]	Alkaline		(1) Roberts et al. 2001; (2) Glauert 1910
McEachern Cave	>25.6 ka (max.	AMS	Limestone cave	Sand	Alkaline		Hope and Wilkinson 1982
Morwell			Lacustrine				
Rockhampton Region							
Honeymoon Suite	>6.3 ka - this c	U/Th	Limestone cave	Sand	Alkaline		Hocknull et al. 2007
Colosseum Chamber	51.4-25.3 ka	U/Th and AMS	Limestone cave	Sand	Alkaline		Price et al. 2015
South Walker Creek	50.1 ka	OSL and ESR	Fluvial	Clay		Iron-oxide precipitation	Hocknull et al. 2020
Spring Creek	>53.5 ka[2]	AMS	Fluvial	Silty and sandy gravels[1]			(1) Porch and Kershaw 2010; (2) Gillespie et al. 2014
Strathdownie			Limestone cave		Alkaline		
Tight Entrance Cave	137-48 ka	OSL, ESR and U/Th	Limestone cave	Sand	Alkaline		Ayliffe et al. 2008
Yellabidde Cave	25.5-9 ka	AMS	Limestone cave	Sand	Alkaline		Monks et al. 2016

References

Ayliffe, L.K., Prideaux, G.J., Bird, M.I., Grün, R., Roberts, R.G., Gully, G.A., Jones, R., Fifield, L.K., & Creswell, R.G. (2008). Age constraints on Pleistocene megafauna at Tight Entrance Cave in southwestern Australia. *Quaternary Science Reviews 27*, 1784-1788.

Balme, J., Merrilees, D. & Porter, J.K. (1978). Late Quaternary mammal remains, spanning about 30 000 years, from excavations in Devil's Lair, Western Australia. *Journal of the Royal Society of Western Australia 61*, 33-65.

Dortch, J., Cupper M., Grün, R., Harpley, B., Lee, K., & Field, J. (2016). The timing and cause of megafauna mass deaths at Lancefield Swamp, southeastern Australia. *Quaternary Science Reviews 145*, 161-182.

Gillespie, R., Wood, R., Fallon, S., Stafford Jr, T.W. & Southon, J. (2015). New 14C dates for Spring Creek and Mowbray Swamp megafauna: XAD-2 processing. *Archaeology in Oceania 50*, 43-48.

Glauert, L. (1910). The Mammoth Cave. *Records of the Western Australian Museum 1*, 11-36.

Hocknull, S.A., Zhao, J., Feng, Y. & Webb, G.E. (2007). Responses of Quaternary rainforest vertebrates to climate change in Australia. *Earth and Planetary Science Letters 264*, 317-331.

Hocknull, S.A., Lewis, R., Arnold, L.J., Pietsch, T., Joannes-Boyau, R., Price, G.J., Moss, P., Wood, R., Dosseto, A., Louys, J., et al. (2020). Extinction of eastern Sahul megafauna coincides with sustained environmental deterioration. *Nature Communications 11*, 2250.

Hope, J.H. & Wilkinson, H.E. (1982). *Warendja wakefieldi*, a new genus of wombat (Marsupialia, Vombatidae) from Pleistocene sediments in McEacherns Cave, Western Victoria. *Memoirs of the National Museum Victoria 43*, 109-120.

Jankowski, N.R., Gully, G.A., Jacobs, Z., Roberts, R.G. & Prideaux, G.J. (2016). A late Quaternary vertebrate deposit in Kudjal Yolgah Cave, south-western Australia: refining regional late Pleistocene extinctions. *Journal of Quaternary Science 31*, 538-550.

Monks, C., Dortch, J., Jacobsen, G. & Baynes, A. (2016). Pleistocene occupation of Yellabidde Cave in the northern Swan Coastal Plain, southwestern Australia. *Australian Archaeology 82*, 275-279.

Porch, N. & Kershaw, A.P. (2010). Comparative AMS 14C dating of plant macrofossils, beetles and pollen preparations from two late Pleistocene sites in southeastern Australia, in Haberle, S.G., Stevenson, J. & Prebble, M (eds). *Altered ecologies: Fire, climate and human influence on terrestrial landscapes*. Terra Australis 32. ANU Press.

Price, G.J. (2008). Taxonomy and palaeobiology of the largest-ever marsupial, Diprotodon Owen, 1838 (Diprotodontidae, Marsupialia). *Zoological Journal of the Linnean Society 153*, 369-397.

Price, G.J., Webb, G.E., Zhao, J., Feng, Y., Murray, A.S., Cooke, B.N., Hocknull, S.A. & Sobbe, I.H. (2011). Dating megafaunal extinction on the Pleistocene Darling Downs, eastern Australia: the promise and pitfalls of dating as a test of extinction hypotheses. *Quaternary Science Reviews 30*, 899-914.

Price, G.J., Louys, J., Cramb, J., Feng, Y., Zhao, J., Hocknull, S.A., Webb, G.E., Nguyen, A.D. & Joannes-Boyau, R. (2015). Temporal overlap of humans and giant lizards (Caranidae; Squamata) in Pleistocene Australia. *Quaternary Science Reviews 125*, 98-105.

Price, G.J., Cramb, J., Louys, K., Travouillon, K.J., Pease, E.M., Feng, Y., Zhao, J. & Irvin, D. (2020). Late Quaternary fossil vertebrates of the Broken River Karst Area, Northern Queensland, Australia. *Records of the Australian Museum 72*, 193-206.

Price, G.J., Fitzsimmons, K.E., Nguyen, A.D., Zhao, J., Feng, Y., Sobbe, I.H., Godthelp, H, Archer, M., & Hand, S.J. (2021). New ages of the world's largest ever marsupial: Diprotodon optatum from Pleistocene Australia. *Quaternary International 603*, 64-73.

Roberts, R.G., Flannery, T.F., Ayliffe, L.K., Yoshida, H., Olley, J.M., Prideaux, G.J., Laslett, G.M., Baynes, A., Smith, M.A., Jones, R., et al. (2001). New ages for the last Australian megafauna: Continent-wide extinction about 46,000 years ago. *Science 292*, 1888-1892.

Shean, D.A. (2017) Geochronology, taxonomy, and morphology of select fossils of the Buchan Caves, southeastern Australia. *Monash University* (unpublished thesis).

Skippington, J., Manne, T. Veth, P. (2018). Macropods and measurables: A critical review of contemporary isotopic approaches to palaeo-environmental reconstructions in Australian zooarchaeology. *Journal of Archaeological Science: Reports 17*, 144-154.

Turney, C.S.M., Bird, M.I., Fifield, L.K., Roberts, R.G., Smith, M., Dortch, C.E., Grün, R., Lawson, E., Ayliffe, L.K., Miller, G.H., et al. (2001). Early human occupation at Devil's Lair, Southwestern Australia 50,000 years ago. *Quaternary Research 55*, 3-13.

Veth, P., Ward, I., Manne, T., Ulm, S., Ditchfield, K., Dortch, J., Hook, F., Petchey, F., Hoog, A., Questiaux, D., et al. (2017). Early human occupation of a maritime desert, Barrow Island, North-West Australia. *Quaternary Science Reviews 168*, 19-29.

Ward, I., Veth, P., Prossor, L., Denham, T., Ditchfield, K., Manne, T., Kendrick, P., Byrne, C., Hook, F. Troitzsch, U. (2017). 50,000 years of archaeological site stratigraphy and micromorphology in Boodie Cave, Barrow Island, Western Australia. *Journal of Archaeological Science: Reports 15*, 344-369.

Dataset S2: Sample numbers, storage locations, and registration numbers of sampled materials.

Locality	Sample number	Storage location	Registration number (storage)
Boodie Cave	CP999	University of Queensland	A107-28
Boodie Cave	CP1000	University of Queensland	A107-21
Boodie Cave	CP1001	University of Queensland	A107-26
Boodie Cave	CP1002	University of Queensland	A107-05
Boodie Cave	CP1003	University of Queensland	G100-10
Boodie Cave	CP1004	University of Queensland	G100-07
Boodie Cave	CP1005	University of Queensland	G100-05
Boodie Cave	CP1006	University of Queensland	G100-06
Boodie Cave	CP1007	University of Queensland	A103-27
Boodie Cave	CP1008	University of Queensland	A103-17
Boodie Cave	CP1009	University of Queensland	A103-11
Boodie Cave	CP1010	University of Queensland	A103-26
Boodie Cave	CP1011	University of Queensland	A103-19
Boodie Cave	CP1012	University of Queensland	A103-13
Boodie Cave	CP1013	University of Queensland	A103-24
Boodie Cave	CP1014	University of Queensland	A102-04
Boodie Cave	CP1015	University of Queensland	A102-05
Boodie Cave	CP1016	University of Queensland	E101-11
Boodie Cave	CP1017	University of Queensland	E101-03
Boodie Cave	CP1018	University of Queensland	E101-12
Boodie Cave	CP1019	University of Queensland	E101-06
Boodie Cave	CP1020	University of Queensland	E101-07
Boodie Cave	CP1021	University of Queensland	A102-01
Boodie Cave	CP1022	University of Queensland	A102-03
Boodie Cave	CP1023	University of Queensland	A102-06
Boodie Cave	CP1024	University of Queensland	A102-07
Boodie Cave	CP1025	University of Queensland	A102-09
Boodie Cave	CP1026	University of Queensland	A102-10
Boodie Cave	CP1027	University of Queensland	A102-11
Boodie Cave	CP1028	University of Queensland	A102-12
Boodie Cave	CP1029	University of Queensland	A103-01
Boodie Cave	CP1030	University of Queensland	A103-02
Boodie Cave	CP1031	University of Queensland	A103-03
Boodie Cave	CP1032	University of Queensland	A103-04
Boodie Cave	CP1033	University of Queensland	A103-05
Boodie Cave	CP1034	University of Queensland	A103-06
Boodie Cave	CP1035	University of Queensland	A103-08
Boodie Cave	CP1036	University of Queensland	A103-09
Boodie Cave	CP1037	University of Queensland	A103-10
Boodie Cave	CP1038	University of Queensland	A103-12
Boodie Cave	CP1039	University of Queensland	A103-14
Broken River (Tripot Cave)	CP154	University of Queensland	NA
Broken River (Tripot Cave)	CP155	University of Queensland	NA
Broken River (Tripot Cave)	CP156	University of Queensland	NA
Broken River (Tripot Cave)	CP157	University of Queensland	NA
Broken River (Tripot Cave)	CP158	University of Queensland	NA
Broken River (Tripot Cave)	CP159	University of Queensland	NA

Broken River (Tripot Cave)	CP160	University of Queensland	NA
Broken River (Tripot Cave)	CP161	University of Queensland	NA
Broken River (Tripot Cave)	CP162	University of Queensland	NA
Broken River (Tripot Cave)	CP163	University of Queensland	NA
Broken River (Tripot Cave)	CP164	University of Queensland	NA
Broken River (Tripot Cave)	CP165	University of Queensland	NA
Broken River (Tripot Cave)	CP166	University of Queensland	NA
Broken River (Tripot Cave)	CP167	University of Queensland	NA
Broken River (Tripot Cave)	CP168	University of Queensland	NA
Broken River (Millenium Cave)	CP1118	University of Queensland	MPMIL01
Broken River (Millenium Cave)	CP1119	University of Queensland	MPMIL02
Broken River (Millenium Cave)	CP1120	University of Queensland	MPMIL03
Broken River (Millenium Cave)	CP1121	University of Queensland	MPMIL04
Broken River (Millenium Cave)	CP1122	University of Queensland	MPMIL05
Broken River (Millenium Cave)	CP1123	University of Queensland	MPMIL06
Broken River (Millenium Cave)	CP1124	University of Queensland	MPMIL07
Broken River (Robert Broom Cave)	CP1125	University of Queensland	MPMC01
Broken River (Robert Broom Cave)	CP1126	University of Queensland	MPMC02
Broken River (Robert Broom Cave)	CP1127	University of Queensland	MPMC03
Broken River (Robert Broom Cave)	CP1128	University of Queensland	MPMC04
Broken River (Robert Broom Cave)	CP1129	University of Queensland	MPFJ01
Broken River (Robert Broom Cave)	CP1130	University of Queensland	MPFJ02
Broken River (Robert Broom Cave)	CP1131	University of Queensland	MPFJ03
Broken River (Robert Broom Cave)	CP1132	University of Queensland	MPFJ04
Broken River (Robert Broom Cave)	CP1133	University of Queensland	MPFJ05
Broken River (Robert Broom Cave)	CP1134	University of Queensland	MPFJ06
Broken River (Robert Broom Cave)	CP1135	University of Queensland	MPFJ07
Broken River (Robert Broom Cave)	CP1136	University of Queensland	MPFJ08
Broken River (Robert Broom Cave)	CP1137	University of Queensland	MPFJ09
Broken River (Robert Broom Cave)	CP1138	University of Queensland	MPFJ10
Broken River (Three Avenues)	CP1139	University of Queensland	MPTA01
Broken River (Three Avenues)	CP1140	University of Queensland	MPTA02
Broken River (Three Avenues)	CP1141	University of Queensland	MPTA03
Broken River (Tripot Cave)	CP1142	University of Queensland	MPLW01/QML1091S
Broken River (Beehive)	CP1154	University of Queensland	MPBH01
Broken River (Beehive)	CP1155	University of Queensland	MPBH02
Broken River (Beehive)	CP1156	University of Queensland	MPBH03
Broken River (Beehive)	CP1157	University of Queensland	MPBH04
Broken River (Beehive)	CP1158	University of Queensland	MPBH05
Broken River (Tripot Cave)	CP1236	University of Queensland	MPLWS01
Broken River (Tripot Cave)	CP1237	University of Queensland	MPLWS02
Broken River (Tripot Cave)	CP1238	University of Queensland	MPLWS03
Broken River (Tripot Cave)	CP1239	University of Queensland	MPU2T01
Broken River (Tripot Cave)	CP1240	University of Queensland	MPU2T02
Broken River (Tripot Cave)	CP1241	University of Queensland	MPU2T03
Broken River (Tripot Cave)	CP1242	University of Queensland	MPU2T04
Broken River (Tripot Cave)	CP1243	University of Queensland	MPU2T05
Broken River (Tripot Cave)	CP1244	University of Queensland	MPU2T06
Broken River (Millenium Cave)	CP1245	University of Queensland	MPMIL11
Broken River (Millenium Cave)	CP1246	University of Queensland	MPMIL12

Broken River (Millenium Cave)	CP1247	University of Queensland	MPMIL13
Broken River (Millenium Cave)	CP1249	University of Queensland	MPMIL15
Buchan Caves (Foul Air Cave)	CP242	Museums Victoria	Reg. No. P. 162074
Buchan Caves (Foul Air Cave)	CP243	Museums Victoria	Reg. No. P. 162074
Buchan Caves (Foul Air Cave)	CP244	Museums Victoria	Reg. No. P. 162072
Buchan Caves (Foul Air Cave)	CP245	Museums Victoria	Reg. No. P. 162072
Buchan Caves (Foul Air Cave)	CP246	Museums Victoria	Reg. No. P. 162072
Buchan Caves (Foul Air Cave)	CP247	Museums Victoria	Reg. No. P. 162072
Buchan Caves (Foul Air Cave)	CP248	Museums Victoria	Reg. No. P. 162072
Buchan Caves (Foul Air Cave)	CP249	Museums Victoria	Reg. No. P. 162072
Buchan Caves (Foul Air Cave)	CP250	Museums Victoria	Reg. No. P. 162072
Buchan Caves (Pot Luck Cave)	CP298	Museums Victoria	Reg. No. P. 21956
Buchan Caves (Pot Luck Cave)	CP311	Museums Victoria	Reg. No. P. 22506
Buchan Caves (Foul Air Cave)	CP333	Museums Victoria	Reg. No. P. 162071
Buchan Caves (Foul Air Cave)	CP334	Museums Victoria	Reg. No. P. 162071
Buchan Caves (Foul Air Cave)	CP335	Museums Victoria	Reg. No. P. 162071
Buchan Caves (Foul Air Cave)	CP336	Museums Victoria	Reg. No. P. 162071
Buchan Caves (Foul Air Cave)	CP337	Museums Victoria	Reg. No. P. 162071
Buchan Caves (Foul Air Cave)	CP338	Museums Victoria	Reg. No. P. 162071
Buchan Caves (Foul Air Cave)	CP339	Museums Victoria	Reg. No. P. 162071
Buchan Caves (Foul Air Cave)	CP340	Museums Victoria	Reg. No. P. 162071
Buchan Caves (Foul Air Cave)	CP341	Museums Victoria	Reg. No. P. 162071
Buchan Caves (Foul Air Cave)	CP376	Museums Victoria	Reg. No. P. 162071
Buchan Caves (Foul Air Cave)	CP377	Museums Victoria	Reg. No. P. 162071
Darling Downs	CP001	University of Queensland	NA
Darling Downs	CP002	University of Queensland	NA
Darling Downs	CP003	University of Queensland	NA
Darling Downs	CP004	University of Queensland	NA
Darling Downs	CP005	University of Queensland	NA
Darling Downs	CP006	University of Queensland	NA
Darling Downs	CP007	University of Queensland	NA
Darling Downs	CP080	University of Queensland	NA
Darling Downs	CP081	University of Queensland	NA
Darling Downs	CP082	University of Queensland	NA
Darling Downs	CP083	University of Queensland	NA
Darling Downs	CP084	University of Queensland	NA
Darling Downs	CP085	University of Queensland	NA
Darling Downs	CP086	University of Queensland	NA
Darling Downs	CP087	University of Queensland	NA
Darling Downs	CP088	University of Queensland	NA
Darling Downs	CP089	University of Queensland	NA
Darling Downs	CP090	University of Queensland	NA
Darling Downs	CP091	University of Queensland	NA
Darling Downs (Dalby)	CP179	University of Queensland	NA
Darling Downs (Ned's Gully)	CP180	University of Queensland	NA
Darling Downs	CP1259	Bavarian State Collection for Palaeontology and Geology	13.527
Darling Downs	CP1264	Bavarian State Collection for Palaeontology and Geology	13.539
Devil's Lair	CP767	Western Australian Museum	Reg. No. 76.8.765
Devil's Lair	CP768	Western Australian Museum	Reg. No. 76.8.765
Devil's Lair	CP769	Western Australian Museum	Reg. No. 76.8.765

Devil's Lair	CP770	Western Australian Museum	Reg. No. 76.8.765
Devil's Lair	CP771	Western Australian Museum	Reg. No. 77.6.511
Devil's Lair	CP772	Western Australian Museum	Reg. No. 77.6.511
Devil's Lair	CP773	Western Australian Museum	Reg. No. 77.6.511
Devil's Lair	CP774	Western Australian Museum	Reg. No. 77.6.511
Devil's Lair	CP775	Western Australian Museum	Reg. No. 77.6.511
Devil's Lair	CP776	Western Australian Museum	Reg. No. 77.6.511
Devil's Lair	CP777	Western Australian Museum	Reg. No. 73.9.979
Devil's Lair	CP778	Western Australian Museum	Reg. No. 73.9.979
Devil's Lair	CP779	Western Australian Museum	Reg. No. 73.9.979
Devil's Lair	CP780	Western Australian Museum	Reg. No. 73.9.979
Devil's Lair	CP781	Western Australian Museum	Reg. No. 73.9.979
Devil's Lair	CP782	Western Australian Museum	Reg. No. 73.9.979
Devil's Lair	CP783	Western Australian Museum	Reg. No. 77.4.875
Devil's Lair	CP784	Western Australian Museum	Reg. No. 77.4.875
Devil's Lair	CP785	Western Australian Museum	Reg. No. 77.4.875
Devil's Lair	CP786	Western Australian Museum	Reg. No. 77.4.875
Devil's Lair	CP787	Western Australian Museum	Reg. No. 77.4.875
Devil's Lair	CP788	Western Australian Museum	Reg. No. 76.7.410
Devil's Lair	CP789	Western Australian Museum	Reg. No. 76.7.410
Devil's Lair	CP790	Western Australian Museum	Reg. No. 76.7.410
Devil's Lair	CP791	Western Australian Museum	Reg. No. 76.7.410
Devil's Lair	CP792	Western Australian Museum	Reg. No. 76.7.410
Devil's Lair	CP793	Western Australian Museum	Reg No. 76.6.626
Devil's Lair	CP794	Western Australian Museum	Reg No. 76.6.626
Devil's Lair	CP795	Western Australian Museum	Reg No. 76.6.626
Devil's Lair	CP796	Western Australian Museum	Reg No. 76.6.626
Devil's Lair	CP797	Western Australian Museum	Reg. No. 76.7.993-5
Devil's Lair	CP798	Western Australian Museum	Reg. No. 76.7.993-5
Devil's Lair	CP799	Western Australian Museum	Reg. No. 76.7.993-5
Devil's Lair	CP800	Western Australian Museum	Reg. No. 76.7.993-5
Devil's Lair	CP801	Western Australian Museum	Reg. No. 76.7.993-5
Devil's Lair	CP802	Western Australian Museum	Reg. No. 76.6.442-3
Devil's Lair	CP803	Western Australian Museum	Reg. No. 76.6.442-3
Devil's Lair	CP804	Western Australian Museum	Reg. No. 76.6.442-3
Devil's Lair	CP805	Western Australian Museum	Reg. No. 76.6.442-3
Devil's Lair	CP806	Western Australian Museum	Reg. No. 76.6.442-3
Devil's Lair	CP807	Western Australian Museum	Reg. No. 77.4.822-4
Devil's Lair	CP808	Western Australian Museum	Reg. No. 77.4.822-4
Devil's Lair	CP809	Western Australian Museum	Reg. No. 77.4.822-4
Devil's Lair	CP810	Western Australian Museum	Reg. No. 77.4.822-4
Devil's Lair	CP811	Western Australian Museum	Reg. No. 77.4.822-4
Devil's Lair	CP812	Western Australian Museum	Reg. No. 76.9.242
Devil's Lair	CP813	Western Australian Museum	Reg. No. 76.9.242
Devil's Lair	CP814	Western Australian Museum	Reg. No. 76.9.242
Devil's Lair	CP815	Western Australian Museum	Reg. No. 76.9.242
Devil's Lair	CP816	Western Australian Museum	Reg. No. 76.9.242
Devil's Lair	CP817	Western Australian Museum	Reg. No. 76.8.580
Devil's Lair	CP818	Western Australian Museum	Reg. No. 76.8.580
Devil's Lair	CP819	Western Australian Museum	Reg. No. 76.8.580

Devil's Lair	CP820	Western Australian Museum	Reg. No. 76.8.580
Devil's Lair	CP821	Western Australian Museum	Reg. No. 76.8.580
Devil's Lair	CP822	Western Australian Museum	Reg. No. 77.4.755
Devil's Lair	CP823	Western Australian Museum	Reg. No. 77.4.755
Devil's Lair	CP824	Western Australian Museum	Reg. No. 77.4.755
Devil's Lair	CP825	Western Australian Museum	Reg. No. 77.4.755
Devil's Lair	CP826	Western Australian Museum	Reg. No. 77.4.755
Devil's Lair	CP827	Western Australian Museum	Reg. No. 76.6.350
Devil's Lair	CP828	Western Australian Museum	Reg. No. 76.6.350
Devil's Lair	CP829	Western Australian Museum	Reg. No. 76.6.350
Devil's Lair	CP830	Western Australian Museum	Reg. No. 76.6.350
Devil's Lair	CP831	Western Australian Museum	Reg. No. 76.6.350
Devil's Lair	CP832	Western Australian Museum	Reg. No. 76.7.136
Devil's Lair	CP833	Western Australian Museum	Reg. No. 76.7.136
Devil's Lair	CP834	Western Australian Museum	Reg. No. 76.7.136
Devil's Lair	CP835	Western Australian Museum	Reg. No. 76.7.136
Devil's Lair	CP836	Western Australian Museum	Reg. No. 76.7.136
Devil's Lair	CP837	Western Australian Museum	Reg. No. 76.6.863-4
Devil's Lair	CP838	Western Australian Museum	Reg. No. 76.6.863-4
Devil's Lair	CP839	Western Australian Museum	Reg. No. 76.6.863-4
Devil's Lair	CP840	Western Australian Museum	Reg. No. 76.6.863-4
Devil's Lair	CP841	Western Australian Museum	Reg. No. 76.6.863-4
Devil's Lair	CP842	Western Australian Museum	Reg. No. 76.6.572
Devil's Lair	CP843	Western Australian Museum	Reg. No. 76.6.572
Devil's Lair	CP844	Western Australian Museum	Reg. No. 76.6.572
Devil's Lair	CP845	Western Australian Museum	Reg. No. 76.6.572
Devil's Lair	CP846	Western Australian Museum	Reg. No. 76.6.572
Devil's Lair	CP847	Western Australian Museum	Reg. No. 77.4.806
Devil's Lair	CP848	Western Australian Museum	Reg. No. 77.4.806
Devil's Lair	CP849	Western Australian Museum	Reg. No. 77.4.806
Devil's Lair	CP850	Western Australian Museum	Reg. No. 77.4.806
Devil's Lair	CP851	Western Australian Museum	Reg. No. 77.4.806
Devil's Lair	CP852	Western Australian Museum	Reg. No. 76.9.113-4
Devil's Lair	CP853	Western Australian Museum	Reg. No. 76.9.113-4
Devil's Lair	CP854	Western Australian Museum	Reg. No. 76.9.113-4
Devil's Lair	CP855	Western Australian Museum	Reg. No. 76.9.113-4
Devil's Lair	CP856	Western Australian Museum	Reg. No. 76.9.113-4
Devil's Lair	CP857	Western Australian Museum	Reg. No. 77.4.862
Devil's Lair	CP858	Western Australian Museum	Reg. No. 77.4.862
Devil's Lair	CP859	Western Australian Museum	Reg. No. 77.4.862
Devil's Lair	CP860	Western Australian Museum	Reg. No. 77.4.862
Devil's Lair	CP861	Western Australian Museum	Reg. No. 77.4.862
Devil's Lair	CP862	Western Australian Museum	Reg. No. 76.8.220
Devil's Lair	CP863	Western Australian Museum	Reg. No. 76.8.220
Devil's Lair	CP864	Western Australian Museum	Reg. No. 76.8.220
Devil's Lair	CP865	Western Australian Museum	Reg. No. 76.8.220
Devil's Lair	CP866	Western Australian Museum	Reg. No. 76.8.220
Kudjal Yolgah Cave	CP413	Western Australian Museum	NA
Kudjal Yolgah Cave	CP414	Western Australian Museum	NA
Kudjal Yolgah Cave	CP415	Western Australian Museum	NA

Kudjal Yolgah Cave	CP416	Western Australian Museum	NA
Kudjal Yolgah Cave	CP417	Western Australian Museum	NA
Kudjal Yolgah Cave	CP418	Western Australian Museum	NA
Kudjal Yolgah Cave	CP419	Western Australian Museum	NA
Kudjal Yolgah Cave	CP420	Western Australian Museum	NA
Kudjal Yolgah Cave	CP421	Western Australian Museum	NA
Kudjal Yolgah Cave	CP422	Western Australian Museum	NA
Kudjal Yolgah Cave	CP423	Western Australian Museum	NA
Kudjal Yolgah Cave	CP424	Western Australian Museum	NA
Kudjal Yolgah Cave	CP425	Western Australian Museum	NA
Kudjal Yolgah Cave	CP426	Western Australian Museum	NA
Kudjal Yolgah Cave	CP427	Western Australian Museum	NA
Kudjal Yolgah Cave	CP428	Western Australian Museum	NA
Kudjal Yolgah Cave	CP429	Western Australian Museum	NA
Kudjal Yolgah Cave	CP430	Western Australian Museum	NA
Kudjal Yolgah Cave	CP431	Western Australian Museum	NA
Kudjal Yolgah Cave	CP432	Western Australian Museum	NA
Kudjal Yolgah Cave	CP433	Western Australian Museum	NA
Kudjal Yolgah Cave	CP434	Western Australian Museum	NA
Kudjal Yolgah Cave	CP435	Western Australian Museum	NA
Kudjal Yolgah Cave	CP436	Western Australian Museum	NA
Kudjal Yolgah Cave	CP437	Western Australian Museum	NA
Kudjal Yolgah Cave	CP438	Western Australian Museum	NA
Kudjal Yolgah Cave	CP439	Western Australian Museum	NA
Kudjal Yolgah Cave	CP440	Western Australian Museum	NA
Kudjal Yolgah Cave	CP441	Western Australian Museum	NA
Kudjal Yolgah Cave	CP442	Western Australian Museum	NA
Kudjal Yolgah Cave	CP443	Western Australian Museum	NA
Kudjal Yolgah Cave	CP444	Western Australian Museum	NA
Kudjal Yolgah Cave	CP445	Western Australian Museum	NA
Kudjal Yolgah Cave	CP446	Western Australian Museum	NA
Kudjal Yolgah Cave	CP447	Western Australian Museum	NA
Kudjal Yolgah Cave	CP448	Western Australian Museum	NA
Kudjal Yolgah Cave	CP449	Western Australian Museum	NA
Kudjal Yolgah Cave	CP450	Western Australian Museum	NA
Kudjal Yolgah Cave	CP451	Western Australian Museum	NA
Kudjal Yolgah Cave	CP452	Western Australian Museum	NA
Kudjal Yolgah Cave	CP453	Western Australian Museum	NA
Kudjal Yolgah Cave	CP454	Western Australian Museum	NA
Kudjal Yolgah Cave	CP455	Western Australian Museum	NA
Kudjal Yolgah Cave	CP456	Western Australian Museum	NA
Kudjal Yolgah Cave	CP457	Western Australian Museum	NA
Kudjal Yolgah Cave	CP458	Western Australian Museum	NA
Kudjal Yolgah Cave	CP459	Western Australian Museum	NA
Kudjal Yolgah Cave	CP460	Western Australian Museum	NA
Kudjal Yolgah Cave	CP461	Western Australian Museum	NA
Kudjal Yolgah Cave	CP462	Western Australian Museum	NA
Kudjal Yolgah Cave	CP463	Western Australian Museum	NA
Kudjal Yolgah Cave	CP464	Western Australian Museum	NA
Kudjal Yolgah Cave	CP465	Western Australian Museum	NA

Kudjal Yolgah Cave	CP466	Western Australian Museum	NA
Kudjal Yolgah Cave	CP467	Western Australian Museum	NA
Kudjal Yolgah Cave	CP468	Western Australian Museum	NA
Kudjal Yolgah Cave	CP469	Western Australian Museum	NA
Kudjal Yolgah Cave	CP470	Western Australian Museum	NA
Kudjal Yolgah Cave	CP471	Western Australian Museum	NA
Kudjal Yolgah Cave	CP472	Western Australian Museum	NA
Kudjal Yolgah Cave	CP473	Western Australian Museum	NA
Kudjal Yolgah Cave	CP474	Western Australian Museum	NA
Kudjal Yolgah Cave	CP475	Western Australian Museum	NA
Kudjal Yolgah Cave	CP476	Western Australian Museum	NA
Kudjal Yolgah Cave	CP477	Western Australian Museum	NA
Kudjal Yolgah Cave	CP478	Western Australian Museum	NA
Kudjal Yolgah Cave	CP479	Western Australian Museum	NA
Kudjal Yolgah Cave	CP480	Western Australian Museum	NA
Kudjal Yolgah Cave	CP481	Western Australian Museum	NA
Kudjal Yolgah Cave	CP482	Western Australian Museum	NA
Kudjal Yolgah Cave	CP483	Western Australian Museum	NA
Kudjal Yolgah Cave	CP484	Western Australian Museum	NA
Kudjal Yolgah Cave	CP485	Western Australian Museum	NA
Kudjal Yolgah Cave	CP486	Western Australian Museum	NA
Kudjal Yolgah Cave	CP487	Western Australian Museum	NA
Kudjal Yolgah Cave	CP488	Western Australian Museum	NA
Kudjal Yolgah Cave	CP1257	Western Australian Museum	Reg. No. 09.3.15
Kudjal Yolgah Cave	CP1258	Western Australian Museum	Reg. No. 09.3.16
Lake Victoria	CP284	Museums Victoria	Reg. No. P. 249839
Lake Victoria	CP285	Museums Victoria	Reg. No. P. 249839
Lake Victoria	CP286	Museums Victoria	Reg. No. P. 249839
Lake Victoria	CP287	Museums Victoria	Reg. No. P. 249839
Lake Victoria	CP288	Museums Victoria	Reg. No. P. 249839
Lake Victoria	CP289	Museums Victoria	Reg. No. P. 249839
Lake Victoria	CP290	Museums Victoria	Reg. No. P. 249839
Lake Victoria	CP291	Museums Victoria	Reg. No. P. 249839
Lake Victoria	CP292	Museums Victoria	Reg. No. P. 249839
Lake Victoria	CP293	Museums Victoria	Reg. No. P. 249839
Lancefield Swamp	CP251	Museums Victoria	NA
Lancefield Swamp	CP252	Museums Victoria	NA
Lancefield Swamp	CP253	Museums Victoria	NA
Lancefield Swamp	CP254	Museums Victoria	NA
Lancefield Swamp	CP255	Museums Victoria	NA
Lancefield Swamp	CP256	Museums Victoria	NA
Lancefield Swamp	CP257	Museums Victoria	NA
Lancefield Swamp	CP258	Museums Victoria	NA
Lancefield Swamp	CP259	Museums Victoria	NA
Lancefield Swamp	CP260	Museums Victoria	NA
Lancefield Swamp	CP261	Museums Victoria	NA
Lancefield Swamp	CP262	Museums Victoria	NA
Lancefield Swamp	CP263	Museums Victoria	NA
Lancefield Swamp	CP264	Museums Victoria	NA
Lancefield Swamp	CP265	Museums Victoria	NA

Lancefield Swamp	CP266	Museums Victoria	NA
Lancefield Swamp	CP267	Museums Victoria	NA
Lancefield Swamp	CP268	Museums Victoria	NA
Lancefield Swamp	CP269	Museums Victoria	NA
Lancefield Swamp	CP270	Museums Victoria	NA
Lancefield Swamp	CP271	Museums Victoria	NA
Lancefield Swamp	CP272	Museums Victoria	NA
Lancefield Swamp	CP273	Museums Victoria	NA
Lancefield Swamp	CP274	Museums Victoria	NA
Lancefield Swamp	CP275	Museums Victoria	NA
Lancefield Swamp	CP305	Museums Victoria	Reg. No. P. 252912; specimen A/A038
Lancefield Swamp	CP306	Museums Victoria	Reg. No. P. 252912; specimen A/A-30
Lancefield Swamp	CP307	Museums Victoria	Reg. No. P. 252912; specimen A/A-14
Lancefield Swamp	CP308	Museums Victoria	NA
Lancefield Swamp	CP309	Museums Victoria	NA
Mammoth Cave	CP403	Western Australian Museum	Reg. No. 70.9.4
Mammoth Cave	CP404	Western Australian Museum	NA
Mammoth Cave	CP405	Western Australian Museum	Reg. No. 64.11.58
Mammoth Cave	CP406	Western Australian Museum	Reg. No. 69.3.966
Mammoth Cave	CP407	Western Australian Museum	Reg. No. 69.3.383
Mammoth Cave	CP408	Western Australian Museum	Reg. No. Geol. Surv. 10087
Mammoth Cave	CP409	Western Australian Museum	Reg. No. 63.2.165
Mammoth Cave	CP410	Western Australian Museum	Reg. No. 62.4.7
Mammoth Cave	CP411	Western Australian Museum	Reg. No. 62.2.103
Mammoth Cave	CP412	Western Australian Museum	Reg. No. 63.2.163
Mammoth Cave	CP1255	Western Australian Museum	Reg. No. 63.2.145
Mammoth Cave	CP1256	Western Australian Museum	Reg. No. 63.2.161
McEachern Cave	CP217	Museums Victoria	NA
McEachern Cave	CP218	Museums Victoria	NA
McEachern Cave	CP219	Museums Victoria	NA
McEachern Cave	CP220	Museums Victoria	NA
McEachern Cave	CP221	Museums Victoria	NA
McEachern Cave	CP222	Museums Victoria	NA
McEachern Cave	CP223	Museums Victoria	NA
McEachern Cave	CP224	Museums Victoria	NA
McEachern Cave	CP225	Museums Victoria	NA
McEachern Cave	CP226	Museums Victoria	NA
McEachern Cave	CP310	Museums Victoria	Reg. No. P. 254351
McEachern Cave	CP312	Museums Victoria	NA
McEachern Cave	CP361	Museums Victoria	NA
McEachern Cave	CP362	Museums Victoria	NA
McEachern Cave	CP363	Museums Victoria	NA
McEachern Cave	CP364	Museums Victoria	NA
McEachern Cave	CP365	Museums Victoria	NA
McEachern Cave	CP366	Museums Victoria	NA
McEachern Cave	CP367	Museums Victoria	NA
McEachern Cave	CP368	Museums Victoria	NA
McEachern Cave	CP369	Museums Victoria	NA
McEachern Cave	CP370	Museums Victoria	NA
McEachern Cave	CP371	Museums Victoria	Reg. No. P. 229337

McEachern Cave	CP372	Museums Victoria	Reg. No. P. 229651
McEachern Cave	CP373	Museums Victoria	Reg. No. P. 212973
Morwell	CP187	Museums Victoria	Reg. No. P. 39128
Morwell	CP188	Museums Victoria	Reg. No. P. 39128
Morwell	CP189	Museums Victoria	Reg. No. P. 39128
Morwell	CP190	Museums Victoria	Reg. No P. 39118
Morwell	CP191	Museums Victoria	Reg. No P. 39118
Morwell	CP192	Museums Victoria	Reg. No P. 39118
Morwell	CP193	Museums Victoria	Reg. No P. 159917
Morwell	CP194	Museums Victoria	Reg. No P. 159917
Morwell	CP195	Museums Victoria	Reg. No P. 159917
Morwell	CP196	Museums Victoria	Reg. No P. 159917
Morwell	CP197	Museums Victoria	Reg. No P. 159917
Morwell	CP354	Museums Victoria	Reg. No. P. 39113
Morwell	CP355	Museums Victoria	Reg. No. P. 39113
Morwell	CP356	Museums Victoria	Reg. No. P. 39113
Morwell	CP357	Museums Victoria	Reg. No. P. 39113
Morwell	CP358	Museums Victoria	Reg. No. P. 39113
Morwell	CP359	Museums Victoria	Reg. No. P. 39113
Morwell	CP360	Museums Victoria	Reg. No. P. 39113
Morwell	CP374	Museums Victoria	Reg. No. P. 39113
Morwell	CP375	Museums Victoria	Reg. No. P. 39113
Rockhampton Region (Colosseum	CP008	University of Queensland	NA
Rockhampton Region (Colosseum	CP009	University of Queensland	NA
Rockhampton Region (Colosseum	CP010	University of Queensland	NA
Rockhampton Region (Colosseum	CP011	University of Queensland	NA
Rockhampton Region (Colosseum	CP012	University of Queensland	NA
Rockhampton Region (Colosseum	CP013	University of Queensland	NA
Rockhampton Region (Colosseum	CP014	University of Queensland	NA
Rockhampton Region (Colosseum	CP015	University of Queensland	NA
Rockhampton Region (Colosseum	CP016	University of Queensland	NA
Rockhampton Region (Colosseum	CP017	University of Queensland	NA
Rockhampton Region (Colosseum	CP018	University of Queensland	NA
Rockhampton Region (Colosseum	CP019	University of Queensland	NA
Rockhampton Region (Colosseum	CP020	University of Queensland	NA
Rockhampton Region (Colosseum	CP021	University of Queensland	NA
Rockhampton Region (Colosseum	CP022	University of Queensland	NA
Rockhampton Region (Colosseum	CP023	University of Queensland	NA
Rockhampton Region (Colosseum	CP024	University of Queensland	NA
Rockhampton Region (Colosseum	CP025	University of Queensland	NA
Rockhampton Region (Colosseum	CP026	University of Queensland	NA
Rockhampton Region (Colosseum	CP027	University of Queensland	NA
Rockhampton Region (Colosseum	CP028	University of Queensland	NA
Rockhampton Region (Colosseum	CP029	University of Queensland	NA
Rockhampton Region (Colosseum	CP030	University of Queensland	NA
Rockhampton Region (Colosseum	CP031	University of Queensland	NA
Rockhampton Region (Colosseum	CP032	University of Queensland	NA
Rockhampton Region (Colosseum	CP033	University of Queensland	NA
Rockhampton Region (Colosseum	CP034	University of Queensland	NA
Rockhampton Region (Colosseum	CP035	University of Queensland	NA

Rockhampton Region (Colosseum	CP036	University of Queensland	NA
Rockhampton Region (Colosseum	CP037	University of Queensland	NA
Rockhampton Region (Colosseum	CP038	University of Queensland	NA
Rockhampton Region (Colosseum	CP039	University of Queensland	NA
Rockhampton Region (Colosseum	CP040	University of Queensland	NA
Rockhampton Region (Colosseum	CP041	University of Queensland	NA
Rockhampton Region (Colosseum	CP042	University of Queensland	NA
Rockhampton Region (Colosseum	CP043	University of Queensland	NA
Rockhampton Region (Colosseum	CP044	University of Queensland	NA
Rockhampton Region (Colosseum	CP045	University of Queensland	NA
Rockhampton Region (Colosseum	CP046	University of Queensland	NA
Rockhampton Region (Colosseum	CP094	University of Queensland	NA
Rockhampton Region (Colosseum	CP095	University of Queensland	NA
Rockhampton Region (Colosseum	CP096	University of Queensland	NA
Rockhampton Region (Colosseum	CP097	University of Queensland	NA
Rockhampton Region (Colosseum	CP098	University of Queensland	NA
Rockhampton Region (Colosseum	CP099	University of Queensland	NA
Rockhampton Region (Colosseum	CP100	University of Queensland	NA
Rockhampton Region (Colosseum	CP101	University of Queensland	NA
Rockhampton Region (Colosseum	CP102	University of Queensland	NA
Rockhampton Region (Colosseum	CP103	University of Queensland	NA
Rockhampton Region (Colosseum	CP104	University of Queensland	NA
Rockhampton Region (Colosseum	CP105	University of Queensland	NA
Rockhampton Region (Colosseum	CP106	University of Queensland	NA
Rockhampton Region (Colosseum	CP107	University of Queensland	NA
Rockhampton Region (Colosseum	CP108	University of Queensland	NA
Rockhampton Region (Colosseum	CP109	University of Queensland	NA
Rockhampton Region (Colosseum	CP110	University of Queensland	NA
Rockhampton Region (Colosseum	CP111	University of Queensland	NA
Rockhampton Region (Colosseum	CP112	University of Queensland	NA
Rockhampton Region (Colosseum	CP113	University of Queensland	NA
Rockhampton Region (Colosseum	CP114	University of Queensland	NA
Rockhampton Region (Colosseum	CP115	University of Queensland	NA
Rockhampton Region (Colosseum	CP116	University of Queensland	NA
Rockhampton Region (Colosseum	CP117	University of Queensland	NA
Rockhampton Region (Colosseum	CP118	University of Queensland	NA
Rockhampton Region (Colosseum	CP119	University of Queensland	NA
Rockhampton Region (Colosseum	CP120	University of Queensland	NA
Rockhampton Region (Colosseum	CP121	University of Queensland	NA
Rockhampton Region (Colosseum	CP122	University of Queensland	NA
Rockhampton Region (Colosseum	CP123	University of Queensland	NA
Rockhampton Region (Colosseum	CP124	University of Queensland	NA
Rockhampton Region (Colosseum	CP125	University of Queensland	NA
Rockhampton Region (Colosseum	CP126	University of Queensland	NA
Rockhampton Region (Colosseum	CP127	University of Queensland	NA
Rockhampton Region (Colosseum	CP128	University of Queensland	NA
Rockhampton Region (Colosseum	CP129	University of Queensland	NA
Rockhampton Region (Colosseum	CP130	University of Queensland	NA
Rockhampton Region (Colosseum	CP131	University of Queensland	NA
Rockhampton Region (Colosseum	CP132	University of Queensland	NA

Rockhampton Region (Colosseum	CP133	University of Queensland	NA
Rockhampton Region (Colosseum	CP134	University of Queensland	NA
Rockhampton Region (Colosseum	CP135	University of Queensland	NA
Rockhampton Region (Colosseum	CP136	University of Queensland	NA
Rockhampton Region (Colosseum	CP137	University of Queensland	NA
Rockhampton Region (Colosseum	CP138	University of Queensland	NA
Rockhampton Region (Colosseum	CP139	University of Queensland	NA
Rockhampton Region (Colosseum	CP140	University of Queensland	NA
Rockhampton Region (Colosseum	CP141	University of Queensland	NA
Rockhampton Region (Colosseum	CP142	University of Queensland	NA
Rockhampton Region (Colosseum	CP143	University of Queensland	NA
Rockhampton Region (Colosseum	CP144	University of Queensland	NA
Rockhampton Region (Colosseum	CP145	University of Queensland	NA
Rockhampton Region (Colosseum	CP146	University of Queensland	NA
Rockhampton Region (Colosseum	CP147	University of Queensland	NA
Rockhampton Region (Colosseum	CP148	University of Queensland	NA
Rockhampton Region (Colosseum	CP149	University of Queensland	NA
Rockhampton Region (Colosseum	CP150	University of Queensland	NA
Rockhampton Region (Colosseum	CP151	University of Queensland	NA
Rockhampton Region (Colosseum	CP152	University of Queensland	NA
Rockhampton Region (Colosseum	CP153	University of Queensland	NA
Rockhampton Region (Honeymooı	CP749	Queensland Museum	QML1457
Rockhampton Region (Honeymooı	CP750	Queensland Museum	QML1457
Rockhampton Region (Honeymooı	CP751	Queensland Museum	QML1457
Rockhampton Region (Honeymooı	CP752	Queensland Museum	QML1457
Rockhampton Region (Honeymooı	CP753	Queensland Museum	QML1457
Rockhampton Region (Honeymooı	CP754	Queensland Museum	QML1457
Rockhampton Region (Honeymooı	CP755	Queensland Museum	QML1457
Rockhampton Region (Honeymooı	CP756	Queensland Museum	QML1457
Rockhampton Region (Honeymooı	CP757	Queensland Museum	QML1457
Rockhampton Region (Honeymooı	CP758	Queensland Museum	QML1457
Rockhampton Region (Honeymooı	CP759	Queensland Museum	QML1457
Rockhampton Region (Honeymooı	CP760	Queensland Museum	QML1457
Rockhampton Region (Honeymooı	CP761	Queensland Museum	QML1457
Rockhampton Region (Honeymooı	CP762	Queensland Museum	QML1457
Rockhampton Region (Honeymooı	CP763	Queensland Museum	QML1457
Rockhampton Region (Honeymooı	CP764	Queensland Museum	QML1457
Rockhampton Region (Honeymooı	CP765	Queensland Museum	QML1457
Rockhampton Region (Honeymooı	CP766	Queensland Museum	QML1457
Rockhampton Region (Colosseum	CP1143	University of Queensland	MPCC11201/QML1456
Rockhampton Region (Colosseum	CP1144	University of Queensland	MPCC11202/QML1456
Rockhampton Region (Colosseum	CP1145	University of Queensland	MPCC11203/QML1456
Rockhampton Region (Colosseum	CP1146	University of Queensland	MPCC12701/QML1456
Rockhampton Region (Colosseum	CP1147	University of Queensland	MPCC12702/QML1456
Rockhampton Region (Colosseum	CP1148	University of Queensland	MPCC12703/QML1456
Rockhampton Region (Colosseum	CP1219	University of Queensland	MPCC5055A01
Rockhampton Region (Colosseum	CP1220	University of Queensland	MPCC5055A02
Rockhampton Region (Colosseum	CP1221	University of Queensland	MPCC5055A03
Rockhampton Region (Colosseum	CP1222	University of Queensland	MPCC5055A04
Rockhampton Region (Colosseum	CP1223	University of Queensland	MPCC5055A05

Rockhampton Region (Colosseum	CP1224	University of Queensland	MPCC5055A06
Rockhampton Region (Colosseum	CP1225	University of Queensland	MPCC5055A07
Rockhampton Region (Colosseum	CP1226	University of Queensland	MPCC5055A08
Rockhampton Region (Colosseum	CP1227	University of Queensland	MPCC510A01
Rockhampton Region (Colosseum	CP1228	University of Queensland	MPCC510A02
Rockhampton Region (Colosseum	CP1229	University of Queensland	MPCC510A03
Rockhampton Region (Colosseum	CP1230	University of Queensland	MPCC510A04
Rockhampton Region (Colosseum	CP1231	University of Queensland	MPCC510A05
Rockhampton Region (Colosseum	CP1232	University of Queensland	MPCC510A06
Rockhampton Region (Colosseum	CP1233	University of Queensland	MPCC510A07
Rockhampton Region (Colosseum	CP1234	University of Queensland	MPCC510A08
Rockhampton Region (Colosseum	CP1235	University of Queensland	MPCC510A09
South Walker Creek (SW9)	CP579	Queensland Museum	QML1470
South Walker Creek (SW9)	CP580	Queensland Museum	QML1470
South Walker Creek (SW9)	CP581	Queensland Museum	QML1470
South Walker Creek (SW9)	CP582	Queensland Museum	QML1470
South Walker Creek (SW9)	CP583	Queensland Museum	QML1470
South Walker Creek (SW9)	CP584	Queensland Museum	QML1470
South Walker Creek (SW9)	CP585	Queensland Museum	QML1470
South Walker Creek (SW9)	CP586	Queensland Museum	QML1470
South Walker Creek (SW9)	CP587	Queensland Museum	QML1470
South Walker Creek (SW9)	CP588	Queensland Museum	QML1470
South Walker Creek (SW9)	CP589	Queensland Museum	QML1470
South Walker Creek (SW9)	CP590	Queensland Museum	QML1470
South Walker Creek (SW9)	CP591	Queensland Museum	QML1470
South Walker Creek (SW9)	CP592	Queensland Museum	QML1470
South Walker Creek (SW9)	CP593	Queensland Museum	QML1470
South Walker Creek (SW9)	CP594	Queensland Museum	QML1470
South Walker Creek (SW9)	CP595	Queensland Museum	QML1470
South Walker Creek (SW9)	CP596	Queensland Museum	QML1470
South Walker Creek (SW9)	CP597	Queensland Museum	QML1470
South Walker Creek (SW9)	CP598	Queensland Museum	QML1470
South Walker Creek (SW9)	CP599	Queensland Museum	QML1470
South Walker Creek (SW9)	CP600	Queensland Museum	QML1470
South Walker Creek (SW9)	CP601	Queensland Museum	QML1470
South Walker Creek (SW9)	CP602	Queensland Museum	QML1470
South Walker Creek (SW9)	CP603	Queensland Museum	QML1470
South Walker Creek (SW9)	CP604	Queensland Museum	QML1470
South Walker Creek (SW9)	CP605	Queensland Museum	QML1470
South Walker Creek (SW9)	CP606	Queensland Museum	QML1470
South Walker Creek (SW9)	CP607	Queensland Museum	QML1470
South Walker Creek (SW9)	CP608	Queensland Museum	QML1470
South Walker Creek (SW9)	CP609	Queensland Museum	QML1470
South Walker Creek (SW9)	CP610	Queensland Museum	QML1470
South Walker Creek (SW9)	CP611	Queensland Museum	QML1470
South Walker Creek (SW9)	CP612	Queensland Museum	QML1470
South Walker Creek (SW9)	CP613	Queensland Museum	QML1470
South Walker Creek (SW9)	CP614	Queensland Museum	QML1470
South Walker Creek (SW9)	CP615	Queensland Museum	QML1470
South Walker Creek (SW9)	CP616	Queensland Museum	QML1470

South Walker Creek (SW9)	CP617	Queensland Museum	QML1470
South Walker Creek (SW9)	CP618	Queensland Museum	QML1470
South Walker Creek (SW9)	CP619	Queensland Museum	QML1470
Spring Creek	CP276	Museums Victoria	Reg. No. P. 172976
Spring Creek	CP277	Museums Victoria	Reg. No. P. 172976
Spring Creek	CP278	Museums Victoria	Reg. No. P. 172976
Spring Creek	CP279	Museums Victoria	Reg. No. P. 172976
Spring Creek	CP280	Museums Victoria	Reg. No. P. 172976
Spring Creek	CP281	Museums Victoria	Reg. No. P. 172976
Spring Creek	CP282	Museums Victoria	Reg. No. P. 172976
Spring Creek	CP283	Museums Victoria	Reg. No. P. 172976
Spring Creek	CP343	Museums Victoria	Reg. No. P. 172976
Spring Creek	CP344	Museums Victoria	Reg. No. P. 172976
Spring Creek	CP345	Museums Victoria	Reg. No. P. 172976
Spring Creek	CP346	Museums Victoria	Reg. No. P. 172976
Spring Creek	CP347	Museums Victoria	Reg. No. P. 172976
Spring Creek	CP348	Museums Victoria	Reg. No. P. 172976
Spring Creek	CP349	Museums Victoria	Reg. No. P. 172976
Strathdownie	CP227	Museums Victoria	Reg. No. P. 173127
Strathdownie	CP228	Museums Victoria	Reg. No. P. 173127
Strathdownie	CP229	Museums Victoria	Reg. No. P. 173127
Strathdownie	CP230	Museums Victoria	Reg. No. P. 173127
Strathdownie	CP231	Museums Victoria	Reg. No. P. 173127
Strathdownie	CP232	Museums Victoria	Reg. No. P. 173127
Strathdownie	CP233	Museums Victoria	Reg. No. P. 173127
Strathdownie	CP234	Museums Victoria	Reg. No. P. 173127
Strathdownie	CP235	Museums Victoria	Reg. No. P. 173127
Strathdownie	CP236	Museums Victoria	Reg. No. P. 173127
Strathdownie	CP237	Museums Victoria	Reg. No. P. 173127
Strathdownie	CP238	Museums Victoria	Reg. No. P. 173127
Strathdownie	CP239	Museums Victoria	Reg. No. P. 173127
Strathdownie	CP240	Museums Victoria	Reg. No. P. 173127
Strathdownie	CP241	Museums Victoria	Reg. No. P. 173127
Tight Entrance Cave	CP489	Western Australian Museum	NA
Tight Entrance Cave	CP490	Western Australian Museum	NA
Tight Entrance Cave	CP491	Western Australian Museum	NA
Tight Entrance Cave	CP492	Western Australian Museum	NA
Tight Entrance Cave	CP493	Western Australian Museum	NA
Tight Entrance Cave	CP494	Western Australian Museum	NA
Tight Entrance Cave	CP495	Western Australian Museum	NA
Tight Entrance Cave	CP496	Western Australian Museum	NA
Tight Entrance Cave	CP497	Western Australian Museum	NA
Tight Entrance Cave	CP498	Western Australian Museum	NA
Tight Entrance Cave	CP499	Western Australian Museum	NA
Tight Entrance Cave	CP500	Western Australian Museum	NA
Tight Entrance Cave	CP501	Western Australian Museum	NA
Tight Entrance Cave	CP502	Western Australian Museum	NA
Tight Entrance Cave	CP503	Western Australian Museum	NA
Tight Entrance Cave	CP504	Western Australian Museum	NA
Tight Entrance Cave	CP505	Western Australian Museum	NA

Tight Entrance Cave	CP506	Western Australian Museum	NA
Tight Entrance Cave	CP507	Western Australian Museum	NA
Tight Entrance Cave	CP508	Western Australian Museum	NA
Tight Entrance Cave	CP509	Western Australian Museum	NA
Tight Entrance Cave	CP510	Western Australian Museum	NA
Tight Entrance Cave	CP511	Western Australian Museum	NA
Tight Entrance Cave	CP512	Western Australian Museum	NA
Tight Entrance Cave	CP513	Western Australian Museum	NA
Tight Entrance Cave	CP514	Western Australian Museum	NA
Tight Entrance Cave	CP515	Western Australian Museum	NA
Tight Entrance Cave	CP516	Western Australian Museum	NA
Tight Entrance Cave	CP517	Western Australian Museum	NA
Tight Entrance Cave	CP518	Western Australian Museum	NA
Tight Entrance Cave	CP519	Western Australian Museum	NA
Tight Entrance Cave	CP520	Western Australian Museum	NA
Tight Entrance Cave	CP521	Western Australian Museum	NA
Tight Entrance Cave	CP522	Western Australian Museum	NA
Tight Entrance Cave	CP523	Western Australian Museum	NA
Tight Entrance Cave	CP524	Western Australian Museum	NA
Tight Entrance Cave	CP525	Western Australian Museum	NA
Tight Entrance Cave	CP526	Western Australian Museum	NA
Tight Entrance Cave	CP527	Western Australian Museum	NA
Tight Entrance Cave	CP528	Western Australian Museum	NA
Tight Entrance Cave	CP529	Western Australian Museum	NA
Tight Entrance Cave	CP530	Western Australian Museum	NA
Tight Entrance Cave	CP531	Western Australian Museum	NA
Tight Entrance Cave	CP532	Western Australian Museum	NA
Tight Entrance Cave	CP533	Western Australian Museum	NA
Tight Entrance Cave	CP534	Western Australian Museum	NA
Tight Entrance Cave	CP535	Western Australian Museum	NA
Tight Entrance Cave	CP536	Western Australian Museum	NA
Tight Entrance Cave	CP537	Western Australian Museum	NA
Tight Entrance Cave	CP538	Western Australian Museum	NA
Tight Entrance Cave	CP539	Western Australian Museum	NA
Tight Entrance Cave	CP540	Western Australian Museum	NA
Tight Entrance Cave	CP541	Western Australian Museum	NA
Tight Entrance Cave	CP542	Western Australian Museum	NA
Tight Entrance Cave	CP543	Western Australian Museum	NA
Tight Entrance Cave	CP544	Western Australian Museum	NA
Tight Entrance Cave	CP545	Western Australian Museum	NA
Tight Entrance Cave	CP546	Western Australian Museum	NA
Tight Entrance Cave	CP547	Western Australian Museum	NA
Tight Entrance Cave	CP548	Western Australian Museum	NA
Tight Entrance Cave	CP549	Western Australian Museum	NA
Tight Entrance Cave	CP550	Western Australian Museum	NA
Tight Entrance Cave	CP551	Western Australian Museum	NA
Tight Entrance Cave	CP552	Western Australian Museum	NA
Tight Entrance Cave	CP553	Western Australian Museum	NA
Tight Entrance Cave	CP554	Western Australian Museum	NA
Tight Entrance Cave	CP555	Western Australian Museum	NA

Tight Entrance Cave	CP556	Western Australian Museum	NA
Tight Entrance Cave	CP557	Western Australian Museum	NA
Tight Entrance Cave	CP558	Western Australian Museum	NA
Tight Entrance Cave	CP559	Western Australian Museum	NA
Tight Entrance Cave	CP560	Western Australian Museum	NA
Tight Entrance Cave	CP561	Western Australian Museum	NA
Tight Entrance Cave	CP562	Western Australian Museum	NA
Tight Entrance Cave	CP563	Western Australian Museum	NA
Yellabidde Cave	CP1159	University of Western Australia	YC.1.35
Yellabidde Cave	CP1160	University of Western Australia	YC.1.35
Yellabidde Cave	CP1161	University of Western Australia	YC.1.35
Yellabidde Cave	CP1162	University of Western Australia	YC.1.35
Yellabidde Cave	CP1163	University of Western Australia	YC.1.35
Yellabidde Cave	CP1164	University of Western Australia	YC.1.35
Yellabidde Cave	CP1165	University of Western Australia	YC.1.35
Yellabidde Cave	CP1166	University of Western Australia	YC.1.35
Yellabidde Cave	CP1167	University of Western Australia	YC.1.35
Yellabidde Cave	CP1168	University of Western Australia	YC.1.35
Yellabidde Cave	CP1169	University of Western Australia	YC.1.36
Yellabidde Cave	CP1170	University of Western Australia	YC.1.36
Yellabidde Cave	CP1171	University of Western Australia	YC.1.36
Yellabidde Cave	CP1172	University of Western Australia	YC.1.36
Yellabidde Cave	CP1173	University of Western Australia	YC.1.36
Yellabidde Cave	CP1174	University of Western Australia	YC.1.36
Yellabidde Cave	CP1175	University of Western Australia	YC.1.36
Yellabidde Cave	CP1176	University of Western Australia	YC.1.36
Yellabidde Cave	CP1177	University of Western Australia	YC.1.36
Yellabidde Cave	CP1178	University of Western Australia	YC.1.36
Yellabidde Cave	CP1179	University of Western Australia	YC.1.50
Yellabidde Cave	CP1180	University of Western Australia	YC.1.50
Yellabidde Cave	CP1181	University of Western Australia	YC.1.50
Yellabidde Cave	CP1182	University of Western Australia	YC.1.50
Yellabidde Cave	CP1183	University of Western Australia	YC.1.50
Yellabidde Cave	CP1184	University of Western Australia	YC.1.50
Yellabidde Cave	CP1185	University of Western Australia	YC.1.50
Yellabidde Cave	CP1186	University of Western Australia	YC.1.50
Yellabidde Cave	CP1187	University of Western Australia	YC.1.50
Yellabidde Cave	CP1188	University of Western Australia	YC.1.50
Yellabidde Cave	CP1189	University of Western Australia	YC.1.51
Yellabidde Cave	CP1190	University of Western Australia	YC.1.51
Yellabidde Cave	CP1191	University of Western Australia	YC.1.51
Yellabidde Cave	CP1192	University of Western Australia	YC.1.51
Yellabidde Cave	CP1193	University of Western Australia	YC.1.51
Yellabidde Cave	CP1194	University of Western Australia	YC.1.51
Yellabidde Cave	CP1195	University of Western Australia	YC.1.51
Yellabidde Cave	CP1196	University of Western Australia	YC.1.51
Yellabidde Cave	CP1197	University of Western Australia	YC.1.51
Yellabidde Cave	CP1198	University of Western Australia	YC.1.51
Yellabidde Cave	CP1199	University of Western Australia	YC.1.54
Yellabidde Cave	CP1200	University of Western Australia	YC.1.54

Yellabidde Cave	CP1201	University of Western Australia	YC.1.54
Yellabidde Cave	CP1202	University of Western Australia	YC.1.54
Yellabidde Cave	CP1203	University of Western Australia	YC.1.54
Yellabidde Cave	CP1204	University of Western Australia	YC.1.54
Yellabidde Cave	CP1205	University of Western Australia	YC.1.54
Yellabidde Cave	CP1206	University of Western Australia	YC.1.54
Yellabidde Cave	CP1207	University of Western Australia	YC.1.54
Yellabidde Cave	CP1208	University of Western Australia	YC.1.54
Yellabidde Cave	CP1209	University of Western Australia	YC.1.57
Yellabidde Cave	CP1210	University of Western Australia	YC.1.57
Yellabidde Cave	CP1211	University of Western Australia	YC.1.57
Yellabidde Cave	CP1212	University of Western Australia	YC.1.57
Yellabidde Cave	CP1213	University of Western Australia	YC.1.57
Yellabidde Cave	CP1214	University of Western Australia	YC.1.57
Yellabidde Cave	CP1215	University of Western Australia	YC.1.57
Yellabidde Cave	CP1216	University of Western Australia	YC.1.57
Yellabidde Cave	CP1217	University of Western Australia	YC.1.57
Yellabidde Cave	CP1218	University of Western Australia	YC.1.57

Dataset S3: Modern weather station data.

Locality	Weather station	Mean T JAN	Mean T FEB	Mean T MAR	Mean T APR	Mean T MAY	Mean T JUN	Mean T JUL	Mean T AUG	Mean T SEP	Mean T OCT	Mean T NOV	Mean T DEC	MAT	MAT max	MAT min	Precipitation (mm)
Boodie Cave	005094 - Barrow Island Airport	29.7	29.9	30.1	28.1	24.4	21.6	20.8	21.5	23.4	25.6	26.8	28.5	25.9	29.4	22.3	269.3
Broken River	034084 - Charters Towers Airport	28.1	27.7	26.5	24.3	21.3	18.9	18.4	19.7	22.8	25.6	27.4	28.4	24.1	30.5	17.7	641.7
Buchan Caves	084143 - Combienbar AWS	19.7	18.9	16.9	13.9	11.1	8.9	8.2	9	11.2	13.4	15.7	17.4	13.7	18.3	9	981.1
Darling Downs	041359 - Oakey Aero	24.5	24	22.3	18.9	15	11.7	10.9	12.1	15.7	19.1	21.8	23.6	18.3	25.6	11	610.9
Devils Lair	009576 - Witchcliffe	20.3	20.8	19.5	16.9	14.7	13.2	12.4	12.5	13.1	14.5	16.9	18.7	16.1	21.4	10.8	951.7
Kudjal Yolgah Cave	009576 - Witchcliffe	20.3	20.8	19.5	16.9	14.7	13.2	12.4	12.5	13.1	14.5	16.9	18.7	16.1	21.4	10.8	951.7
Lake Victoria	047016 - Lake Victoria Storage	24.5	24.1	21.3	17.1	12.5	10.7	10.4	11.6	14.4	17.3	20.4	22.9	17.3	23.8	10.8	259.2
Lancefield Swamp	088051 - Redesdale	21.5	21.1	18.2	14.1	10.6	8.4	7.6	8.4	10.3	12.9	16.4	18.7	14	20.6	7.4	577.7
Mammoth Cave	009576 - Witchcliffe	20.3	20.8	19.5	16.9	14.7	13.2	12.4	12.5	13.1	14.5	16.9	18.7	16.1	21.4	10.8	951.7
McEachern Cave	026021 - Mount Gambier Aero	18.4	18.6	16.9	14.2	11.8	9.9	9.2	9.9	11.1	12.7	14.6	16.6	13.6	19	8.2	713.3
Morwell	085283 - Willow Grove	19.8	19.7	17.5	14.9	11.8	9.4	9	9.6	11.3	13.5	15.7	17.9	14.2	19.6	8.7	723.3
Rockhampton Region	039083 - Rockhampton Aero	27	26.7	25.8	23.4	20.2	17.4	16.5	17.9	20.7	23.5	25.5	26.8	22.7	28.5	16.8	815.1
South Walker Creek	034038 - Moranbah Water Treatment Plant	27.9	27.5	26.2	23.6	20.4	17.5	16.8	18.3	21.7	25	26.3	27.6	23.2	29.7	16.7	614.2
Spring Creek	090186 - Warrnambool Airport	18.2	18.5	17.1	14.5	12	9.9	9.5	10.1	11.4	12.7	14.9	15.9	13.8	19	8.5	732.1
Strathdownie	090173 - Hamilton Airport	19	19.1	17.3	14.1	11.1	9	8.3	9.1	10.6	12.3	14.7	16.9	13.5	19.2	7.7	616.8
Tight Entrance Cave	009576 - Witchcliffe	20.3	20.8	19.5	16.9	14.7	13.2	12.4	12.5	13.1	14.5	16.9	18.7	16.1	21.4	10.8	951.7
Yellabidde Cave	008025 - Carnamah	27.3	27.4	25.1	14.5	16.8	14	12.7	13.3	15.2	18.3	21.9	24.9	19.8	27	12.6	375.6

Dataset S4: Palaeoclimate data. Data extracted from Beyer et al. 2020.

Locality	Time BP	BIO01: MAT	BIO05: Maximum Annual Temperature	BIO06: Minimum Annual Temperature	BIO07: Annual Temperature Range	BIO12: Annual precipitation	Altitude
Boodie_Cave	1000	-	-	-	-	-	-
Boodie_Cave	2000	-	-	-	-	-	-
Boodie_Cave	3000	-	-	-	-	-	-
Boodie_Cave	4000	-	-	-	-	-	-
Boodie_Cave	5000	-	-	-	-	-	-
Boodie_Cave	6000	-	-	-	-	-	-
Boodie_Cave	7000	26.03356	39.65175	10.34757	29.30418	168.5779	12.785714
Boodie_Cave	8000	25.99494	39.36577	10.25229	29.11349	168.5775	12.433579
Boodie_Cave	9000	25.36762	37.49091	11.81315	25.67776	435.0232	11.110919
Boodie_Cave	10000	26.0271	38.90742	10.80941	28.09801	140.3654	6.745588
Boodie_Cave	11000	24.91858	35.73191	12.557342	23.17456	548.21759	-9.195652
Boodie_Cave	12000	24.42055	36.10975	10.647848	25.4619	195.96562	-14.591241
Boodie_Cave	13000	24.22775	36.12091	10.725141	25.39577	100.63329	-19.89172
Boodie_Cave	14000	24.11111	35.94833	10.698826	25.2495	106.12249	-24.286755
Boodie_Cave	15000	23.41869	35.5505	9.934195	25.6163	77.70192	-33.959084
Boodie_Cave	16000	21.66566	35.36169	5.506976	29.85471	101.73658	-37.40226
Boodie_Cave	17000	20.88541	34.60963	4.278712	30.33092	158.53036	-38.074944
Boodie_Cave	18000	20.74256	35.04964	4.160111	30.88953	128.87595	-38.319954
Boodie_Cave	19000	20.67982	35.34886	3.614376	31.73448	140.40048	-38.494995
Boodie_Cave	20000	20.18629	35.04655	2.921249	32.1253	182.07407	-38.319954
Boodie_Cave	21000	20.82209	36.14826	3.452604	32.69566	102.70244	-38.495
Boodie_Cave	22000	20.83875	36.41116	3.03952	33.37164	122.16216	-38.58445
Boodie_Cave	23000	20.78168	36.06627	3.595803	32.47047	127.22476	-38.58445
Boodie_Cave	24000	20.78168	36.06627	3.595803	32.47047	127.22476	-38.58445
Boodie_Cave	25000	20.84714	35.97842	3.829974	32.14844	133.1774	-38.58445
Boodie_Cave	26000	20.84714	35.97842	3.829974	32.14844	133.1774	-38.58445
Boodie_Cave	27000	21.47865	36.39321	5.341297	31.05191	97.24251	-38.23661
Boodie_Cave	28000	21.47865	36.39321	5.341297	31.05191	97.24251	-38.23661
Boodie_Cave	29000	22.55084	35.04006	8.372956	26.66711	220.85315	-37.61599
Boodie_Cave	30000	22.55084	35.04006	8.372956	26.66711	220.85315	-37.61599
Boodie_Cave	31000	22.81816	34.9887	9.011596	25.9771	125.8385	-37.26614
Boodie_Cave	32000	22.81816	34.9887	9.011596	25.9771	125.8385	-37.26614
Boodie_Cave	33000	22.70212	34.78115	9.097126	25.68403	228.0596	-36.93736
Boodie_Cave	34000	22.70212	34.78115	9.097126	25.68403	228.0596	-36.93736
Boodie_Cave	35000	22.79488	35.0023	9.149628	25.85267	127.392	-37.33371
Boodie_Cave	36000	22.79488	35.0023	9.149628	25.85267	127.392	-37.33371
Boodie_Cave	37000	22.90529	35.32556	9.050602	26.27496	175.4942	-36.36248
Boodie_Cave	38000	22.90529	35.32556	9.050602	26.27496	175.4942	-36.36248
Boodie_Cave	39000	22.40808	35.30071	8.122894	27.17782	194.083	-32.1868
Boodie_Cave	40000	22.40808	35.30071	8.122894	27.17782	194.083	-32.1868
Boodie_Cave	41000	22.59913	35.52946	8.328531	27.20093	203.92484	-23.53767
Boodie_Cave	42000	22.59913	35.52946	8.328531	27.20093	203.92484	-23.53767
Boodie_Cave	43000	23.03463	36.06805	8.764081	27.30397	97.08257	-22.48416
Boodie_Cave	44000	23.03463	36.06805	8.764081	27.30397	97.08257	-22.48416
Boodie_Cave	45000	22.89123	36.19099	8.394621	27.79637	116.11765	-21.57911
Boodie_Cave	46000	22.89123	36.19099	8.394621	27.79637	116.11765	-21.57911
Boodie_Cave	47000	22.53879	35.83458	7.951085	27.88349	180.06729	-22.48416
Boodie_Cave	48000	22.53879	35.83458	7.951085	27.88349	180.06729	-22.48416
Boodie_Cave	49000	23.45212	36.5409	9.249385	27.29151	147.04375	-20.32019
Boodie_Cave	50000	23.45212	36.5409	9.249385	27.29151	147.04375	-20.32019
Boodie_Cave	51000	23.19663	36.28936	8.864182	27.42517	132.67497	-21.05435
Boodie_Cave	52000	23.19663	36.28936	8.864182	27.42517	132.67497	-21.05435
Boodie_Cave	53000	23.34038	35.97221	9.408285	26.56393	80.47662	-21.95579
Boodie_Cave	54000	23.34038	35.97221	9.408285	26.56393	80.47662	-21.95579
Boodie_Cave	55000	23.64043	35.90848	9.722664	26.18582	100.26381	-28.05676
Boodie_Cave	56000	23.64043	35.90848	9.722664	26.18582	100.26381	-28.05676
Boodie_Cave	57000	23.8916	35.95463	10.234269	25.72036	148.08122	-30.90166
Boodie_Cave	58000	23.8916	35.95463	10.234269	25.72036	148.08122	-30.90166
Boodie_Cave	59000	23.28597	35.38051	9.84411	25.5364	136.46643	-27.02345
Boodie_Cave	60000	23.28597	35.38051	9.84411	25.5364	136.46643	-27.02345
Boodie_Cave	61000	22.80983	34.91694	9.079072	25.83787	240.044	-29.00265
Boodie_Cave	62000	22.80983	34.91694	9.079072	25.83787	240.044	-29.00265
Boodie_Cave	63000	22.56772	34.77363	8.654179	26.11945	198.4374	-27.02345
Boodie_Cave	64000	22.56772	34.77363	8.654179	26.11945	198.4374	-27.02345
Boodie_Cave	65000	22.0731	34.95768	7.884518	27.07316	204.4836	-30.38452
Boodie_Cave	66000	22.0731	34.95768	7.884518	27.07316	204.4836	-30.38452
Boodie_Cave	67000	22.33172	35.5855	7.97687	27.60863	155.4487	-21.05435
Boodie_Cave	68000	22.33172	35.5855	7.97687	27.60863	155.4487	-21.05435
Boodie_Cave	69000	23.1129	36.5901	8.61232	27.97778	117.8	-19.12804
Boodie_Cave	70000	23.1129	36.5901	8.61232	27.97778	117.8	-19.12804
Boodie_Cave	71000	23.72411	37.27359	9.518218	27.75537	102.75139	-12.114173
Boodie_Cave	72000	23.72411	37.27359	9.518218	27.75537	102.75139	-12.114173
Boodie_Cave	73000	24.22081	37.4381	9.879467	27.55863	118.83023	-7.826087
Boodie_Cave	74000	24.22081	37.4381	9.879467	27.55863	118.83023	-7.826087
Boodie_Cave	75000	23.87797	36.72873	10.005229	26.7235	76.60033	-5.020618
Boodie_Cave	76000	23.87797	36.72873	10.005229	26.7235	76.60033	-5.020618
Boodie_Cave	77000	23.87888	36.35351	9.990909	26.3626	129.28773	-5.464646
Boodie_Cave	78000	23.87888	36.35351	9.990909	26.3626	129.28773	-5.464646
Boodie_Cave	79000	24.2145	36.50299	10.664717	25.83827	161.02658	-7.534722
Boodie_Cave	80000	24.2145	36.50299	10.664717	25.83827	161.02658	-7.534722
Boodie_Cave	81000	24.29661	35.80823	11.130488	24.67774	218.9592	-6.895487
Boodie_Cave	82000	24.29661	35.80823	11.130488	24.67774	218.9592	-6.895487
Boodie_Cave	83000	24.67761	35.94676	11.577818	24.36894	186.5245	-5.464646
Boodie_Cave	84000	24.67761	35.94676	11.577818	24.36894	186.5245	-5.464646
Boodie_Cave	85000	24.32378	36.13504	11.320221	24.81482	225.4628	-7.826087
Boodie_Cave	86000	24.32378	36.13504	11.320221	24.81482	225.4628	-7.826087
Boodie_Cave	87000	23.58437	35.97298	10.051606	25.92138	289.7591	-11.253036
Boodie_Cave	88000	23.58437	35.97298	10.051606	25.92138	289.7591	-11.253036
Boodie_Cave	89000	23.60203	36.72277	9.589653	27.13311	220.282	-9.978858
Boodie_Cave	90000	23.60203	36.72277	9.589653	27.13311	220.282	-9.978858
Boodie_Cave	91000	23.88059	37.43569	9.527948	27.90774	117.20474	-10.461538
Boodie_Cave	92000	23.88059	37.43569	9.527948	27.90774	117.20474	-10.461538
Boodie_Cave	93000	23.99652	38.00508	9.278575	28.72651	80.86942	-11.253036
Boodie_Cave	94000	23.99652	38.00508	9.278575	28.72651	80.86942	-11.253036
Boodie_Cave	95000	24.05426	37.74701	9.311631	28.43538	105.79961	-4.522428
Boodie_Cave	96000	24.05426	37.74701	9.311631	28.43538	105.79961	-4.522428
Boodie_Cave	97000	25.04602	40.63756	7.993552	32.64401	80.95354	8.428349
Boodie_Cave	98000	25.04602	40.63756	7.993552	32.64401	80.95354	8.428349
Boodie_Cave	99000	25.16134	39.59377	8.889224	30.70454	145.71503	8.895404
Boodie_Cave	100000	25.16134	39.59377	8.889224	30.70454	145.71503	8.895404
Broken_River	1000	22.61543	34.11104	8.609074	25.50196	655.5471	214.8522

Broken_River	2000	22.46731	33.86148	8.298133	25.56335	603.6297	214.8522
Broken_River	3000	22.63766	33.91941	8.586405	25.333	484.8519	214.8522
Broken_River	4000	22.28535	33.69468	8.343449	25.35123	555.5273	214.8522
Broken_River	5000	22.67685	33.87017	8.72287	25.1473	452.5659	214.8522
Broken_River	6000	22.63665	34.18416	8.177632	26.00653	418.759	214.8522
Broken_River	7000	22.26039	33.2695	8.152937	25.11656	587.5533	214.8522
Broken_River	8000	22.55356	33.4227	9.076996	24.3457	557.896	214.8522
Broken_River	9000	23.00216	33.87529	9.49353	24.38176	482.6599	214.8522
Broken_River	10000	22.84211	33.17352	9.803629	23.36989	510.9126	214.8522
Broken_River	11000	23.60305	33.51496	10.647896	22.86707	487.8562	214.8522
Broken_River	12000	22.56643	32.83359	9.6611	23.17249	471.1723	214.8522
Broken_River	13000	22.43181	32.75433	8.917262	23.83707	435.1897	214.8522
Broken_River	14000	22.02589	32.40057	8.802616	23.59795	480.1342	214.8522
Broken_River	15000	21.30888	31.80392	7.843793	23.96012	399.8444	214.8522
Broken_River	16000	20.3868	31.10923	7.071871	24.03736	451.93	214.8522
Broken_River	17000	20.04893	30.78977	6.865646	23.92412	563.549	214.8522
Broken_River	18000	20.01145	31.37952	5.833228	25.54629	474.9528	214.8522
Broken_River	19000	19.63463	31.1484	5.417211	25.73119	523.8936	214.8522
Broken_River	20000	19.73201	31.28636	5.203579	26.08278	488.8103	214.8522
Broken_River	21000	19.52669	31.14231	4.803259	26.33905	466.2732	214.8522
Broken_River	22000	19.30316	31.0087	4.140648	26.86805	408.3335	214.8522
Broken_River	23000	19.66608	31.18286	4.778439	26.40442	527.6344	214.8522
Broken_River	24000	19.66608	31.18286	4.778439	26.40442	527.6344	214.8522
Broken_River	25000	19.38716	30.68383	5.366133	25.3177	579.1543	214.8522
Broken_River	26000	19.38716	30.68383	5.366133	25.3177	579.1543	214.8522
Broken_River	27000	20.43829	31.38292	5.940032	25.44288	482.8443	214.8522
Broken_River	28000	20.43829	31.38292	5.940032	25.44288	482.8443	214.8522
Broken_River	29000	20.62996	31.09053	7.299732	23.7908	601.8524	214.8522
Broken_River	30000	20.62996	31.09053	7.299732	23.7908	601.8524	214.8522
Broken_River	31000	20.91341	31.11814	7.766819	23.35132	564.8372	214.8522
Broken_River	32000	20.91341	31.11814	7.766819	23.35132	564.8372	214.8522
Broken_River	33000	20.67244	30.80333	8.010067	22.79326	593.1356	214.8522
Broken_River	34000	20.67244	30.80333	8.010067	22.79326	593.1356	214.8522
Broken_River	35000	20.84289	31.14783	8.024282	23.12355	503.9583	214.8522
Broken_River	36000	20.84289	31.14783	8.024282	23.12355	503.9583	214.8522
Broken_River	37000	20.66328	31.17461	7.657531	23.51708	576.2306	214.8522
Broken_River	38000	20.66328	31.17461	7.657531	23.51708	576.2306	214.8522
Broken_River	39000	20.49196	31.42783	6.994426	24.4334	629.9759	214.8522
Broken_River	40000	20.49196	31.42783	6.994426	24.4334	629.9759	214.8522
Broken_River	41000	20.58741	31.71349	6.363024	25.35047	554.9025	214.8522
Broken_River	42000	20.58741	31.71349	6.363024	25.35047	554.9025	214.8522
Broken_River	43000	20.68975	32.08884	6.209116	25.87972	564.4003	214.8522
Broken_River	44000	20.68975	32.08884	6.209116	25.87972	564.4003	214.8522
Broken_River	45000	20.93707	32.64348	6.022205	26.62127	511.9332	214.8522
Broken_River	46000	20.93707	32.64348	6.022205	26.62127	511.9332	214.8522
Broken_River	47000	20.35736	32.11086	5.161541	26.94932	599.9639	214.8522
Broken_River	48000	20.35736	32.11086	5.161541	26.94932	599.9639	214.8522
Broken_River	49000	21.34802	33.18929	5.776116	27.41317	398.135	214.8522
Broken_River	50000	21.34802	33.18929	5.776116	27.41317	398.135	214.8522
Broken_River	51000	21.29781	32.63051	5.832239	26.79827	483.1879	214.8522
Broken_River	52000	21.29781	32.63051	5.832239	26.79827	483.1879	214.8522
Broken_River	53000	21.06843	32.24251	6.292974	25.94953	523.2664	214.8522
Broken_River	54000	21.06843	32.24251	6.292974	25.94953	523.2664	214.8522
Broken_River	55000	21.47915	32.46283	7.177727	25.2851	487.1229	214.8522
Broken_River	56000	21.47915	32.46283	7.177727	25.2851	487.1229	214.8522
Broken_River	57000	22.02208	32.71341	8.015625	24.69778	404.5931	214.8522
Broken_River	58000	22.02208	32.71341	8.015625	24.69778	404.5931	214.8522
Broken_River	59000	21.27131	31.44552	7.908628	23.53689	480.2048	214.8522
Broken_River	60000	21.27131	31.44552	7.908628	23.53689	480.2048	214.8522
Broken_River	61000	20.73859	30.68029	8.039831	22.64046	562.8325	214.8522
Broken_River	62000	20.73859	30.68029	8.039831	22.64046	562.8325	214.8522
Broken_River	63000	20.64086	30.6311	8.869968	21.76114	646.131	214.8522
Broken_River	64000	20.64086	30.6311	8.869968	21.76114	646.131	214.8522
Broken_River	65000	20.39263	30.88928	7.646175	23.24311	630.8243	214.8522
Broken_River	66000	20.39263	30.88928	7.646175	23.24311	630.8243	214.8522
Broken_River	67000	20.92079	32.119	7.247514	24.87149	552.6642	214.8522
Broken_River	68000	20.92079	32.119	7.247514	24.87149	552.6642	214.8522
Broken_River	69000	21.08974	32.62432	6.666195	25.95812	556.345	214.8522
Broken_River	70000	21.08974	32.62432	6.666195	25.95812	556.345	214.8522
Broken_River	71000	21.47228	33.37434	6.314491	27.05984	561.5854	214.8522
Broken_River	72000	21.47228	33.37434	6.314491	27.05984	561.5854	214.8522
Broken_River	73000	22.07189	33.8286	7.341317	26.48729	551.9904	214.8522
Broken_River	74000	22.07189	33.8286	7.341317	26.48729	551.9904	214.8522
Broken_River	75000	21.92726	33.57378	6.873829	26.69995	410.1532	214.8522
Broken_River	76000	21.92726	33.57378	6.873829	26.69995	410.1532	214.8522
Broken_River	77000	21.83475	33.18054	6.91117	26.26937	463.834	214.8522
Broken_River	78000	21.83475	33.18054	6.91117	26.26937	463.834	214.8522
Broken_River	79000	22.48458	33.08097	8.763247	24.31772	406.0643	214.8522
Broken_River	80000	22.48458	33.08097	8.763247	24.31772	406.0643	214.8522
Broken_River	81000	22.47503	32.60316	9.371923	23.23124	428.5397	214.8522
Broken_River	82000	22.47503	32.60316	9.371923	23.23124	428.5397	214.8522
Broken_River	83000	22.91293	32.51037	11.118919	21.39145	477.1394	214.8522
Broken_River	84000	22.91293	32.51037	11.118919	21.39145	477.1394	214.8522
Broken_River	85000	22.43271	32.24038	10.486662	21.75372	522.823	214.8522
Broken_River	86000	22.43271	32.24038	10.486662	21.75372	522.823	214.8522
Broken_River	87000	21.60843	32.47571	9.36783	23.10788	668.2661	214.8522
Broken_River	88000	21.60843	32.47571	9.36783	23.10788	668.2661	214.8522
Broken_River	89000	21.63447	33.05301	7.397251	25.65576	592.7227	214.8522
Broken_River	90000	21.63447	33.05301	7.397251	25.65576	592.7227	214.8522
Broken_River	91000	21.94842	34.31073	6.190265	28.12046	602.6992	214.8522
Broken_River	92000	21.94842	34.31073	6.190265	28.12046	602.6992	214.8522
Broken_River	93000	21.78465	34.3336	5.697743	28.63586	632.5761	214.8522
Broken_River	94000	21.78465	34.3336	5.697743	28.63586	632.5761	214.8522
Broken_River	95000	22.12685	34.8942	5.493894	29.4003	525.7316	214.8522
Broken_River	96000	22.12685	34.8942	5.493894	29.4003	525.7316	214.8522
Broken_River	97000	22.14168	34.50126	5.865613	28.63565	450.7001	214.8522
Broken_River	98000	22.14168	34.50126	5.865613	28.63565	450.7001	214.8522
Broken_River	99000	22.69836	34.90107	7.087836	27.81324	428.5491	214.8522
Broken_River	100000	22.69836	34.90107	7.087836	27.81324	428.5491	214.8522
Buchan_Caves	1000	13.84546	25.79135	3.577759	22.21359	695.6868	149.525
Buchan_Caves	2000	14.00658	25.79613	4.028981	21.76715	732.7528	148.7852
Buchan_Caves	3000	14.09801	25.90646	4.208186	21.69827	764.0891	147.5554
Buchan_Caves	4000	13.83379	25.55077	4.159642	21.39113	797.792	145.605
Buchan_Caves	5000	13.81244	25.45483	3.916404	21.53843	759.3666	143.4404
Buchan_Caves	6000	13.83729	24.90458	3.796591	21.10799	772.5565	142.0197

Buchan_Caves	7000	13.94204	24.70068	4.034249	20.66643	750.942	135.8226
Buchan_Caves	8000	13.86124	24.5544	3.971041	20.58336	739.041	132.34
Buchan_Caves	9000	13.81664	24.13549	4.100368	20.03512	818.0167	127.7185
Buchan_Caves	10000	13.76923	24.77537	4.072064	20.70331	811.1196	111.8193
Buchan_Caves	11000	14.02818	24.29191	4.3960152	19.8959	860.7686	96.97757
Buchan_Caves	12000	12.97264	23.22086	3.3942711	19.82659	827.6979	89.83762
Buchan_Caves	13000	12.84032	23.284	3.1424637	20.14153	780.6624	88.70667
Buchan_Caves	14000	13.16153	24.10724	3.4361701	20.67107	845.9477	88.70667
Buchan_Caves	15000	12.19694	24.12088	2.0007825	22.1201	727.39	88.70667
Buchan_Caves	16000	11.53624	23.41692	1.2727872	22.14413	693.7263	88.70667
Buchan_Caves	17000	11.91276	24.20865	1.3708547	22.8378	668.0168	88.70667
Buchan_Caves	18000	11.76524	24.36349	0.9439523	23.41953	638.2201	88.70667
Buchan_Caves	19000	12.09214	24.89071	1.2764633	23.61425	729.1581	88.70667
Buchan_Caves	20000	11.66198	24.38835	0.6536117	23.73474	692.3623	88.70667
Buchan_Caves	21000	11.63994	24.10221	0.5702091	23.53201	676.4043	88.70667
Buchan_Caves	22000	10.92042	23.33994	-0.2299625	23.5699	564.0518	88.70667
Buchan_Caves	23000	11.63211	24.34879	0.7618462	23.58694	650.585	88.70667
Buchan_Caves	24000	11.63211	24.34879	0.7618462	23.58694	650.585	88.70667
Buchan_Caves	25000	11.87442	24.0142	1.2404974	22.7737	745.0068	88.70667
Buchan_Caves	26000	11.87442	24.0142	1.2404974	22.7737	745.0068	88.70667
Buchan_Caves	27000	12.04013	23.62074	1.546628	22.07411	759.0164	88.70667
Buchan_Caves	28000	12.04013	23.62074	1.546628	22.07411	759.0164	88.70667
Buchan_Caves	29000	12.11797	23.02679	1.8317069	21.19508	769.7214	88.70667
Buchan_Caves	30000	12.11797	23.02679	1.8317069	21.19508	769.7214	88.70667
Buchan_Caves	31000	12.66222	23.60148	2.390316	21.21117	812.9778	88.70667
Buchan_Caves	32000	12.66222	23.60148	2.390316	21.21117	812.9778	88.70667
Buchan_Caves	33000	12.4072	23.48022	2.348387	21.13184	792.829	88.70667
Buchan_Caves	34000	12.4072	23.48022	2.348387	21.13184	792.829	88.70667
Buchan_Caves	35000	12.45401	23.84837	2.364785	21.48358	769.0347	88.70667
Buchan_Caves	36000	12.45401	23.84837	2.364785	21.48358	769.0347	88.70667
Buchan_Caves	37000	12.61064	24.30726	2.623906	21.68335	793.2891	88.70667
Buchan_Caves	38000	12.61064	24.30726	2.623906	21.68335	793.2891	88.70667
Buchan_Caves	39000	12.87894	24.91904	2.189255	22.72979	760.3243	88.70667
Buchan_Caves	40000	12.87894	24.91904	2.189255	22.72979	760.3243	88.70667
Buchan_Caves	41000	12.62081	24.9409	2.003791	22.93711	748.0394	88.70667
Buchan_Caves	42000	12.62081	24.9409	2.003791	22.93711	748.0394	88.70667
Buchan_Caves	43000	12.87664	25.04285	2.020445	23.0224	801.0763	88.70667
Buchan_Caves	44000	12.87664	25.04285	2.020445	23.0224	801.0763	88.70667
Buchan_Caves	45000	12.93351	25.10462	2.075072	23.02954	766.5126	88.70667
Buchan_Caves	46000	12.93351	25.10462	2.075072	23.02954	766.5126	88.70667
Buchan_Caves	47000	12.73853	25.04956	1.658349	23.39122	744.301	88.70667
Buchan_Caves	48000	12.73853	25.04956	1.658349	23.39122	744.301	88.70667
Buchan_Caves	49000	12.90332	25.18694	1.981682	23.20525	782.4431	88.70667
Buchan_Caves	50000	12.90332	25.18694	1.981682	23.20525	782.4431	88.70667
Buchan_Caves	51000	13.2353	25.41756	2.336689	23.08088	798.7635	88.70667
Buchan_Caves	52000	13.2353	25.41756	2.336689	23.08088	798.7635	88.70667
Buchan_Caves	53000	12.75789	24.54632	2.461669	22.08466	854.525	88.70667
Buchan_Caves	54000	12.75789	24.54632	2.461669	22.08466	854.525	88.70667
Buchan_Caves	55000	12.69435	24.02766	2.295757	21.7319	781.5821	88.70667
Buchan_Caves	56000	12.69435	24.02766	2.295757	21.7319	781.5821	88.70667
Buchan_Caves	57000	13.11026	24.38636	2.810538	21.57582	824.2477	88.70667
Buchan_Caves	58000	13.11026	24.38636	2.810538	21.57582	824.2477	88.70667
Buchan_Caves	59000	12.74721	23.70025	2.719387	20.98087	834.3083	88.70667
Buchan_Caves	60000	12.74721	23.70025	2.719387	20.98087	834.3083	88.70667
Buchan_Caves	61000	12.39626	23.65541	2.430559	21.22485	759.3516	88.70667
Buchan_Caves	62000	12.39626	23.65541	2.430559	21.22485	759.3516	88.70667
Buchan_Caves	63000	12.30369	23.72943	2.135856	21.59357	759.8268	88.70667
Buchan_Caves	64000	12.30369	23.72943	2.135856	21.59357	759.8268	88.70667
Buchan_Caves	65000	12.33363	24.31651	2.012487	22.30402	763.3448	88.70667
Buchan_Caves	66000	12.33363	24.31651	2.012487	22.30402	763.3448	88.70667
Buchan_Caves	67000	12.48357	24.6221	1.862798	22.7593	769.0266	88.70667
Buchan_Caves	68000	12.48357	24.6221	1.862798	22.7593	769.0266	88.70667
Buchan_Caves	69000	12.52803	24.60505	2.190756	22.4143	756.6627	88.87542
Buchan_Caves	70000	12.52803	24.60505	2.190756	22.4143	756.6627	88.87542
Buchan_Caves	71000	13.4828	26.12562	2.794227	23.33139	840.5474	91.84886
Buchan_Caves	72000	13.4828	26.12562	2.794227	23.33139	840.5474	91.84886
Buchan_Caves	73000	13.42585	25.57977	2.866686	22.71309	851.1458	99.19208
Buchan_Caves	74000	13.42585	25.57977	2.866686	22.71309	851.1458	99.19208
Buchan_Caves	75000	13.0443	24.92438	2.450597	22.47378	860.0974	107.79002
Buchan_Caves	76000	13.0443	24.92438	2.450597	22.47378	860.0974	107.79002
Buchan_Caves	77000	12.88804	24.12455	2.667631	21.45692	882.1861	106.59264
Buchan_Caves	78000	12.88804	24.12455	2.667631	21.45692	882.1861	106.59264
Buchan_Caves	79000	13.08168	23.9973	2.960496	21.0368	810.7466	100.31235
Buchan_Caves	80000	13.08168	23.9973	2.960496	21.0368	810.7466	100.31235
Buchan_Caves	81000	12.96708	23.28126	3.175223	20.10603	829.8001	101.93382
Buchan_Caves	82000	12.96708	23.28126	3.175223	20.10603	829.8001	101.93382
Buchan_Caves	83000	13.5376	23.72457	4.070329	19.65424	848.0887	106.59264
Buchan_Caves	84000	13.5376	23.72457	4.070329	19.65424	848.0887	106.59264
Buchan_Caves	85000	13.13332	24.12423	3.264165	20.86007	845.902	99.19208
Buchan_Caves	86000	13.13332	24.12423	3.264165	20.86007	845.902	99.19208
Buchan_Caves	87000	13.0196	24.67885	2.945335	21.73351	770.5458	93.39195
Buchan_Caves	88000	13.0196	24.67885	2.945335	21.73351	770.5458	93.39195
Buchan_Caves	89000	13.18217	25.53718	2.649929	22.88725	806.1783	94.94302
Buchan_Caves	90000	13.18217	25.53718	2.649929	22.88725	806.1783	94.94302
Buchan_Caves	91000	13.57242	26.54489	2.677152	23.86774	832.4725	94.32291
Buchan_Caves	92000	13.57242	26.54489	2.677152	23.86774	832.4725	94.32291
Buchan_Caves	93000	13.44063	26.63325	2.573426	24.05983	746.9989	93.39195
Buchan_Caves	94000	13.44063	26.63325	2.573426	24.05983	746.9989	93.39195
Buchan_Caves	95000	13.18378	26.19168	2.181768	24.00991	736.1281	109.34974
Buchan_Caves	96000	13.18378	26.19168	2.181768	24.00991	736.1281	109.34974
Buchan_Caves	97000	13.06995	25.41294	2.36822	23.04472	771.4175	116.55738
Buchan_Caves	98000	13.06995	25.41294	2.36822	23.04472	771.4175	116.55738
Buchan_Caves	99000	13.26746	24.93966	2.822113	22.11755	785.2258	119.57262
Buchan_Caves	100000	13.26746	24.93966	2.822113	22.11755	785.2258	119.57262
Darling_Downs	1000	17.40052	30.48773	2.964122	27.52361	670.3624	476.0844
Darling_Downs	2000	17.3252	30.32515	2.897891	27.42726	579.4185	476.0844
Darling_Downs	3000	17.24416	29.98555	2.713302	27.27225	562.3771	476.0844
Darling_Downs	4000	16.97635	29.82774	2.582269	27.24547	524.2584	476.0844
Darling_Downs	5000	17.41702	29.82752	3.262505	26.56501	485.0202	476.0844
Darling_Downs	6000	17.16761	29.73859	3.280872	26.45772	521.076	476.0844
Darling_Downs	7000	16.76218	29.05828	2.897411	26.16087	673.9272	476.0844
Darling_Downs	8000	16.93562	28.8433	3.24566	25.59764	611.4831	476.0844
Darling_Downs	9000	17.35849	29.55577	3.944211	25.61156	529.4206	476.0844
Darling_Downs	10000	17.13105	28.53464	3.744756	24.78988	494.0184	476.0844
Darling_Downs	11000	17.20772	28.73674	4.28202391	24.45472	569.4163	476.0844

Darling_Downs	12000	16.54781	28.36543	3.25835395	25.10708	542.1331	476.0844
Darling_Downs	13000	16.36333	28.60419	2.66995001	25.93424	542.7856	476.0844
Darling_Downs	14000	16.07407	28.18728	2.64327168	25.54401	628.6998	476.0844
Darling_Downs	15000	15.31871	28.15417	1.25600207	26.89816	575.6709	476.0844
Darling_Downs	16000	14.73124	27.22922	0.65432143	26.57489	578.3586	476.0844
Darling_Downs	17000	14.65512	26.72428	1.04205847	25.68222	561.5953	476.0844
Darling_Downs	18000	14.4384	27.25819	-0.07499907	27.33319	562.9844	476.0844
Darling_Downs	19000	14.0911	26.84076	-0.35527274	27.19603	548.1617	476.0844
Darling_Downs	20000	14.24483	27.04144	-0.4047763	27.44622	534.1907	476.0844
Darling_Downs	21000	14.25506	26.81338	-0.1036986	26.91708	493.0746	476.0844
Darling_Downs	22000	14.11918	27.03722	-0.5492575	27.58648	392.7409	476.0844
Darling_Downs	23000	14.17073	26.76988	-0.3554399	27.12532	623.7667	476.0844
Darling_Downs	24000	14.17073	26.76988	-0.3554399	27.12532	623.7667	476.0844
Darling_Downs	25000	14.03463	26.07962	0.2745129	25.80511	698.0828	476.0844
Darling_Downs	26000	14.03463	26.07962	0.2745129	25.80511	698.0828	476.0844
Darling_Downs	27000	14.7087	26.4364	0.6405715	25.79583	615.2624	476.0844
Darling_Downs	28000	14.7087	26.4364	0.6405715	25.79583	615.2624	476.0844
Darling_Downs	29000	14.88558	25.91766	1.7297984	24.18786	671.7834	476.0844
Darling_Downs	30000	14.88558	25.91766	1.7297984	24.18786	671.7834	476.0844
Darling_Downs	31000	14.94227	26.0716	1.904516	24.16709	707.7189	476.0844
Darling_Downs	32000	14.94227	26.0716	1.904516	24.16709	707.7189	476.0844
Darling_Downs	33000	14.94775	26.16204	1.867348	24.2947	669.7477	476.0844
Darling_Downs	34000	14.94775	26.16204	1.867348	24.2947	669.7477	476.0844
Darling_Downs	35000	15.07149	26.7355	1.926496	24.809	618.4598	476.0844
Darling_Downs	36000	15.07149	26.7355	1.926496	24.809	618.4598	476.0844
Darling_Downs	37000	15.04557	27.40097	1.495681	25.90529	660.9352	476.0844
Darling_Downs	38000	15.04557	27.40097	1.495681	25.90529	660.9352	476.0844
Darling_Downs	39000	15.0717	27.08759	1.318762	25.76882	675.4152	476.0844
Darling_Downs	40000	15.0717	27.08759	1.318762	25.76882	675.4152	476.0844
Darling_Downs	41000	15.06412	27.26845	0.8149502	26.4535	588.5603	476.0844
Darling_Downs	42000	15.06412	27.26845	0.8149502	26.4535	588.5603	476.0844
Darling_Downs	43000	15.3375	28.298	0.8786763	27.41932	566.9736	476.0844
Darling_Downs	44000	15.3375	28.298	0.8786763	27.41932	566.9736	476.0844
Darling_Downs	45000	15.26476	28.09343	0.7230294	27.3704	555.8552	476.0844
Darling_Downs	46000	15.26476	28.09343	0.7230294	27.3704	555.8552	476.0844
Darling_Downs	47000	15.14419	27.9799	0.47004	27.50986	655.2041	476.0844
Darling_Downs	48000	15.14419	27.9799	0.47004	27.50986	655.2041	476.0844
Darling_Downs	49000	15.52381	28.90646	0.1741492	28.73231	468.0984	476.0844
Darling_Downs	50000	15.52381	28.90646	0.1741492	28.73231	468.0984	476.0844
Darling_Downs	51000	15.44684	27.826	0.6815829	27.14442	560.1264	476.0844
Darling_Downs	52000	15.44684	27.826	0.6815829	27.14442	560.1264	476.0844
Darling_Downs	53000	15.27044	27.77172	1.0507798	26.72094	626.8383	476.0844
Darling_Downs	54000	15.27044	27.77172	1.0507798	26.72094	626.8383	476.0844
Darling_Downs	55000	15.45895	27.91834	0.9682008	26.95014	581.3197	476.0844
Darling_Downs	56000	15.45895	27.91834	0.9682008	26.95014	581.3197	476.0844
Darling_Downs	57000	15.72392	27.7472	1.5815519	26.16565	532.481	476.0844
Darling_Downs	58000	15.72392	27.7472	1.5815519	26.16565	532.481	476.0844
Darling_Downs	59000	15.29698	26.82874	1.8361216	24.99261	603.513	476.0844
Darling_Downs	60000	15.29698	26.82874	1.8361216	24.99261	603.513	476.0844
Darling_Downs	61000	15.02015	26.20901	1.991748	24.21726	677.9974	476.0844
Darling_Downs	62000	15.02015	26.20901	1.991748	24.21726	677.9974	476.0844
Darling_Downs	63000	15.05921	26.15813	2.242372	23.91575	745.7487	476.0844
Darling_Downs	64000	15.05921	26.15813	2.242372	23.91575	745.7487	476.0844
Darling_Downs	65000	14.83648	26.52362	1.662188	24.86144	682.8265	476.0844
Darling_Downs	66000	14.83648	26.52362	1.662188	24.86144	682.8265	476.0844
Darling_Downs	67000	15.16411	27.31765	1.520557	25.79709	587.524	476.0844
Darling_Downs	68000	15.16411	27.31765	1.520557	25.79709	587.524	476.0844
Darling_Downs	69000	15.42682	28.4841	1.237065	27.24703	543.6326	476.0844
Darling_Downs	70000	15.42682	28.4841	1.237065	27.24703	543.6326	476.0844
Darling_Downs	71000	15.78416	29.31771	1.0128556	28.30486	595.8893	476.0844
Darling_Downs	72000	15.78416	29.31771	1.0128556	28.30486	595.8893	476.0844
Darling_Downs	73000	16.12666	29.27495	1.4322177	27.84273	499.396	476.0844
Darling_Downs	74000	16.12666	29.27495	1.4322177	27.84273	499.396	476.0844
Darling_Downs	75000	15.62938	28.40537	0.9667637	27.4386	523.3067	476.0844
Darling_Downs	76000	15.62938	28.40537	0.9667637	27.4386	523.3067	476.0844
Darling_Downs	77000	15.74424	28.03341	1.2598654	26.77354	480.9555	476.0844
Darling_Downs	78000	15.74424	28.03341	1.2598654	26.77354	480.9555	476.0844
Darling_Downs	79000	15.95567	27.77785	1.8889287	25.88892	545.0224	476.0844
Darling_Downs	80000	15.95567	27.77785	1.8889287	25.88892	545.0224	476.0844
Darling_Downs	81000	16.14558	27.36993	2.793823	24.57611	549.6044	476.0844
Darling_Downs	82000	16.14558	27.36993	2.793823	24.57611	549.6044	476.0844
Darling_Downs	83000	16.73333	28.10084	4.216975	23.88387	583.7488	476.0844
Darling_Downs	84000	16.73333	28.10084	4.216975	23.88387	583.7488	476.0844
Darling_Downs	85000	16.04418	27.83052	2.895159	24.93536	595.2322	476.0844
Darling_Downs	86000	16.04418	27.83052	2.895159	24.93536	595.2322	476.0844
Darling_Downs	87000	15.94413	28.16845	2.791527	25.37692	585.3653	476.0844
Darling_Downs	88000	15.94413	28.16845	2.791527	25.37692	585.3653	476.0844
Darling_Downs	89000	15.74409	29.08815	1.057294	28.03086	469.0418	476.0844
Darling_Downs	90000	15.74409	29.08815	1.057294	28.03086	469.0418	476.0844
Darling_Downs	91000	16.30934	30.50383	0.8168809	29.68695	520.004	476.0844
Darling_Downs	92000	16.30934	30.50383	0.8168809	29.68695	520.004	476.0844
Darling_Downs	93000	16.09243	30.28883	0.7080544	29.58078	490.7548	476.0844
Darling_Downs	94000	16.09243	30.28883	0.7080544	29.58078	490.7548	476.0844
Darling_Downs	95000	16.49087	30.92184	0.5217057	30.40014	517.0103	476.0844
Darling_Downs	96000	16.49087	30.92184	0.5217057	30.40014	517.0103	476.0844
Darling_Downs	97000	15.92134	29.44919	0.4474289	29.00176	526.2707	476.0844
Darling_Downs	98000	15.92134	29.44919	0.4474289	29.00176	526.2707	476.0844
Darling_Downs	99000	16.56546	29.77538	1.4796369	28.29574	471.7188	476.0844
Darling_Downs	100000	16.56546	29.77538	1.4796369	28.29574	471.7188	476.0844
Devils_Lair	1000	15.65348	24.63853	8.659369	15.97916	1064.222	57.5757
Devils_Lair	2000	15.75634	24.6187	8.777328	15.84137	1108.338	56.95478
Devils_Lair	3000	15.70492	24.38464	8.907191	15.47744	1130.548	56.41308
Devils_Lair	4000	15.56582	24.05301	8.867358	15.18565	1141.138	56.13699
Devils_Lair	5000	15.5681	23.98129	8.980975	15.00031	1130.494	56.04103
Devils_Lair	6000	15.60578	24.14386	8.891938	15.25192	1145.354	55.75
Devils_Lair	7000	15.97051	24.47577	9.323369	15.1524	1148.571	54.45258
Devils_Lair	8000	15.80044	24.17812	9.235932	14.94218	1106.94	53.65189
Devils_Lair	9000	15.51369	23.81608	9.139382	14.6767	1116.531	51.2575
Devils_Lair	10000	15.46621	23.74612	9.067594	14.67853	1064.719	46.30499
Devils_Lair	11000	15.59734	23.87964	9.097976	14.78166	1100.4368	39.52273
Devils_Lair	12000	15.01161	23.43469	8.579977	14.85471	1080.9426	28.8314
Devils_Lair	13000	14.75694	23.29108	8.295524	14.99556	1076.5558	26.6086
Devils_Lair	14000	14.72459	23.24693	8.179913	15.06701	1074.8472	25.96517
Devils_Lair	15000	14.24139	22.82243	7.70208	15.12035	1076.7528	25.72646
Devils_Lair	16000	13.09779	22.84186	5.980461	16.8614	985.7774	25.20312

Devils_Lair	17000	12.62714	24.32124	4.42841	19.89283	895.6552	24.77642
Devils_Lair	18000	12.50812	24.42835	4.321391	20.10696	898.0898	24.77642
Devils_Lair	19000	12.62606	24.62997	4.277765	20.3522	902.7986	24.77642
Devils_Lair	20000	12.40785	24.42624	4.051768	20.37447	904.0475	24.77642
Devils_Lair	21000	12.54167	24.46865	3.734348	20.7343	875.6848	24.77642
Devils_Lair	22000	12.1779	23.93848	3.481334	20.45715	848.8455	24.61111
Devils_Lair	23000	12.32087	24.02088	3.936624	20.08425	897.7261	24.61111
Devils_Lair	24000	12.32087	24.02088	3.936624	20.08425	897.7261	24.61111
Devils_Lair	25000	12.47892	24.23127	4.037971	20.1933	884.2087	24.77642
Devils_Lair	26000	12.47892	24.23127	4.037971	20.1933	884.2087	24.77642
Devils_Lair	27000	12.78323	23.66027	4.793723	18.86655	920.1155	24.77642
Devils_Lair	28000	12.78323	23.66027	4.793723	18.86655	920.1155	24.77642
Devils_Lair	29000	13.19083	23.94425	5.438779	18.50547	931.2445	25.06132
Devils_Lair	30000	13.19083	23.94425	5.438779	18.50547	931.2445	25.06132
Devils_Lair	31000	13.57178	24.21385	5.76635	18.4475	940.1076	25.34078
Devils_Lair	32000	13.57178	24.21385	5.76635	18.4475	940.1076	25.34078
Devils_Lair	33000	13.45711	23.40599	6.070285	17.3357	949.5594	25.47427
Devils_Lair	34000	13.45711	23.40599	6.070285	17.3357	949.5594	25.47427
Devils_Lair	35000	13.76456	23.65914	6.468184	17.19095	997.8962	25.34078
Devils_Lair	36000	13.76456	23.65914	6.468184	17.19095	997.8962	25.34078
Devils_Lair	37000	13.86513	23.46653	6.786896	16.67964	1041.8899	25.47427
Devils_Lair	38000	13.86513	23.46653	6.786896	16.67964	1041.8899	25.47427
Devils_Lair	39000	13.48474	24.86034	5.266641	19.5937	933.6008	25.72646
Devils_Lair	40000	13.48474	24.86034	5.266641	19.5937	933.6008	25.72646
Devils_Lair	41000	13.51492	24.72781	5.598298	19.12951	998.8045	26.07874
Devils_Lair	42000	13.51492	24.72781	5.598298	19.12951	998.8045	26.07874
Devils_Lair	43000	14.19298	24.13736	6.801324	17.33604	1107.9573	26.19144
Devils_Lair	44000	14.19298	24.13736	6.801324	17.33604	1107.9573	26.19144
Devils_Lair	45000	14.00626	24.64497	6.305242	18.33973	1078.009	26.19144
Devils_Lair	46000	14.00626	24.64497	6.305242	18.33973	1078.009	26.19144
Devils_Lair	47000	13.84667	25.16858	5.692578	19.476	1021.5567	26.19144
Devils_Lair	48000	13.84667	25.16858	5.692578	19.476	1021.5567	26.19144
Devils_Lair	49000	14.68823	23.81492	7.709465	16.10545	1132.239	26.2965
Devils_Lair	50000	14.68823	23.81492	7.709465	16.10545	1132.239	26.2965
Devils_Lair	51000	14.31456	24.49894	6.736322	17.76261	1089.729	26.19144
Devils_Lair	52000	14.31456	24.49894	6.736322	17.76261	1089.729	26.19144
Devils_Lair	53000	14.52832	23.86983	7.467487	16.40234	1123.522	26.19144
Devils_Lair	54000	14.52832	23.86983	7.467487	16.40234	1123.522	26.19144
Devils_Lair	55000	14.69434	23.43745	7.899209	15.53824	1101.495	25.84848
Devils_Lair	56000	14.69434	23.43745	7.899209	15.53824	1101.495	25.84848
Devils_Lair	57000	14.82946	23.39647	8.267693	15.12878	1084.866	25.84848
Devils_Lair	58000	14.82946	23.39647	8.267693	15.12878	1084.866	25.84848
Devils_Lair	59000	14.32823	23.29991	7.553968	15.74594	1055.926	25.96517
Devils_Lair	60000	14.32823	23.29991	7.553968	15.74594	1055.926	25.96517
Devils_Lair	61000	13.45189	24.13161	5.752106	18.3795	932.424	25.84848
Devils_Lair	62000	13.45189	24.13161	5.752106	18.3795	932.424	25.84848
Devils_Lair	63000	13.18086	23.888	5.487252	18.40075	920.4357	25.96517
Devils_Lair	64000	13.18086	23.888	5.487252	18.40075	920.4357	25.96517
Devils_Lair	65000	12.83017	24.45842	4.750762	19.70766	893.0936	25.84848
Devils_Lair	66000	12.83017	24.45842	4.750762	19.70766	893.0936	25.84848
Devils_Lair	67000	13.04524	24.53791	4.948052	19.58986	930.5558	26.19144
Devils_Lair	68000	13.04524	24.53791	4.948052	19.58986	930.5558	26.19144
Devils_Lair	69000	14.07939	24.18978	6.507333	17.68244	1047.0292	26.6086
Devils_Lair	70000	14.07939	24.18978	6.507333	17.68244	1047.0292	26.6086
Devils_Lair	71000	14.91359	24.12391	8.01097	16.11294	1157.918	33.49136
Devils_Lair	72000	14.91359	24.12391	8.01097	16.11294	1157.918	33.49136
Devils_Lair	73000	14.96962	23.95574	8.015412	15.94033	1139.54	41.88414
Devils_Lair	74000	14.96962	23.95574	8.015412	15.94033	1139.54	41.88414
Devils_Lair	75000	14.87418	23.37486	8.151423	15.22344	1148.28	44.96978
Devils_Lair	76000	14.87418	23.37486	8.151423	15.22344	1148.28	44.96978
Devils_Lair	77000	14.89677	23.37708	8.398487	14.9786	1118.628	44.66046
Devils_Lair	78000	14.89677	23.37708	8.398487	14.9786	1118.628	44.66046
Devils_Lair	79000	15.31511	23.33389	8.935754	14.39814	1086.164	42.19529
Devils_Lair	80000	15.31511	23.33389	8.935754	14.39814	1086.164	42.19529
Devils_Lair	81000	15.25891	23.37262	8.978312	14.39431	1053.496	42.60863
Devils_Lair	82000	15.25891	23.37262	8.978312	14.39431	1053.496	42.60863
Devils_Lair	83000	15.21348	23.43463	8.972734	14.4619	1077.45	44.66046
Devils_Lair	84000	15.21348	23.43463	8.972734	14.4619	1077.45	44.66046
Devils_Lair	85000	15.34074	23.81984	8.877457	14.94238	1072.676	41.88414
Devils_Lair	86000	15.34074	23.81984	8.877457	14.94238	1072.676	41.88414
Devils_Lair	87000	14.60155	24.51504	7.298839	17.21621	1024.292	34.53942
Devils_Lair	88000	14.60155	24.51504	7.298839	17.21621	1024.292	34.53942
Devils_Lair	89000	15.02899	24.42314	8.110478	16.31266	1131.487	36.83742
Devils_Lair	90000	15.02899	24.42314	8.110478	16.31266	1131.487	36.83742
Devils_Lair	91000	15.20909	24.87585	7.950784	16.92506	1154.33	35.5863
Devils_Lair	92000	15.20909	24.87585	7.950784	16.92506	1154.33	35.5863
Devils_Lair	93000	15.23665	24.96447	7.976819	16.98765	1180.171	34.53942
Devils_Lair	94000	15.23665	24.96447	7.976819	16.98765	1180.171	34.53942
Devils_Lair	95000	15.30713	24.87605	8.11492	16.76113	1187.608	45.38061
Devils_Lair	96000	15.30713	24.87605	8.11492	16.76113	1187.608	45.38061
Devils_Lair	97000	15.34107	24.51176	8.311613	16.20014	1209.637	48.02406
Devils_Lair	98000	15.34107	24.51176	8.311613	16.20014	1209.637	48.02406
Devils_Lair	99000	15.5101	24.21314	8.787323	15.42582	1128.883	48.83562
Devils_Lair	100000	15.5101	24.21314	8.787323	15.42582	1128.883	48.83562
Kudjal_Yolgah_Cave	1000	15.65348	24.63853	8.659369	15.97916	1064.222	57.5757
Kudjal_Yolgah_Cave	2000	15.75634	24.6187	8.777328	15.84137	1108.338	56.95478
Kudjal_Yolgah_Cave	3000	15.70492	24.38464	8.907191	15.47744	1130.548	56.41308
Kudjal_Yolgah_Cave	4000	15.56582	24.05301	8.867358	15.18565	1141.138	56.13699
Kudjal_Yolgah_Cave	5000	15.5681	23.98129	8.980975	15.00031	1130.494	56.04103
Kudjal_Yolgah_Cave	6000	15.60578	24.14386	8.891938	15.25192	1145.354	55.75
Kudjal_Yolgah_Cave	7000	15.97051	24.47577	9.323369	15.1524	1148.571	54.45258
Kudjal_Yolgah_Cave	8000	15.80044	24.17812	9.235932	14.94218	1106.94	53.65189
Kudjal_Yolgah_Cave	9000	15.51369	23.81608	9.139382	14.6767	1116.531	51.2575
Kudjal_Yolgah_Cave	10000	15.46621	23.74612	9.067594	14.67853	1064.719	46.30499
Kudjal_Yolgah_Cave	11000	15.59734	23.87964	9.097976	14.78166	1100.4368	39.52273
Kudjal_Yolgah_Cave	12000	15.01161	23.43469	8.579977	14.85471	1080.9426	28.8314
Kudjal_Yolgah_Cave	13000	14.75694	23.29108	8.295524	14.99556	1076.5558	26.6086
Kudjal_Yolgah_Cave	14000	14.72459	23.24693	8.179913	15.06701	1074.8472	25.96517
Kudjal_Yolgah_Cave	15000	14.24139	22.82243	7.70208	15.12035	1076.7528	25.72646
Kudjal_Yolgah_Cave	16000	13.09779	22.84186	5.980461	16.8614	985.7774	25.20312
Kudjal_Yolgah_Cave	17000	12.62714	24.32124	4.42841	19.89283	895.6552	24.77642
Kudjal_Yolgah_Cave	18000	12.50812	24.42835	4.321391	20.10696	898.0898	24.77642
Kudjal_Yolgah_Cave	19000	12.62606	24.62997	4.277765	20.3522	902.7986	24.77642
Kudjal_Yolgah_Cave	20000	12.40785	24.42624	4.051768	20.37447	904.0475	24.77642
Kudjal_Yolgah_Cave	21000	12.54167	24.46865	3.734348	20.7343	875.6848	24.77642

Kudjal_Yolgah_Cave	22000	12.1779	23.93848	3.481334	20.45715	848.8455	24.61111
Kudjal_Yolgah_Cave	23000	12.32087	24.02088	3.936624	20.08425	897.7261	24.61111
Kudjal_Yolgah_Cave	24000	12.32087	24.02088	3.936624	20.08425	897.7261	24.61111
Kudjal_Yolgah_Cave	25000	12.47892	24.23127	4.037971	20.1933	884.2087	24.77642
Kudjal_Yolgah_Cave	26000	12.47892	24.23127	4.037971	20.1933	884.2087	24.77642
Kudjal_Yolgah_Cave	27000	12.78323	23.66027	4.793723	18.86655	920.1155	24.77642
Kudjal_Yolgah_Cave	28000	12.78323	23.66027	4.793723	18.86655	920.1155	24.77642
Kudjal_Yolgah_Cave	29000	13.19083	23.94425	5.438779	18.50547	931.2445	25.06132
Kudjal_Yolgah_Cave	30000	13.19083	23.94425	5.438779	18.50547	931.2445	25.06132
Kudjal_Yolgah_Cave	31000	13.57178	24.21385	5.76635	18.4475	940.1076	25.34078
Kudjal_Yolgah_Cave	32000	13.57178	24.21385	5.76635	18.4475	940.1076	25.34078
Kudjal_Yolgah_Cave	33000	13.45711	23.40599	6.070285	17.3357	949.5594	25.47427
Kudjal_Yolgah_Cave	34000	13.45711	23.40599	6.070285	17.3357	949.5594	25.47427
Kudjal_Yolgah_Cave	35000	13.76456	23.65914	6.468184	17.19095	997.8962	25.34078
Kudjal_Yolgah_Cave	36000	13.76456	23.65914	6.468184	17.19095	997.8962	25.34078
Kudjal_Yolgah_Cave	37000	13.86513	23.46653	6.786896	16.67964	1041.8899	25.47427
Kudjal_Yolgah_Cave	38000	13.86513	23.46653	6.786896	16.67964	1041.8899	25.47427
Kudjal_Yolgah_Cave	39000	13.48474	24.86034	5.266641	19.5937	933.6008	25.72646
Kudjal_Yolgah_Cave	40000	13.48474	24.86034	5.266641	19.5937	933.6008	25.72646
Kudjal_Yolgah_Cave	41000	13.51492	24.72781	5.598298	19.12951	998.8045	26.07874
Kudjal_Yolgah_Cave	42000	13.51492	24.72781	5.598298	19.12951	998.8045	26.07874
Kudjal_Yolgah_Cave	43000	14.19298	24.13736	6.801324	17.33604	1107.9573	26.19144
Kudjal_Yolgah_Cave	44000	14.19298	24.13736	6.801324	17.33604	1107.9573	26.19144
Kudjal_Yolgah_Cave	45000	14.00626	24.64497	6.305242	18.33973	1078.009	26.19144
Kudjal_Yolgah_Cave	46000	14.00626	24.64497	6.305242	18.33973	1078.009	26.19144
Kudjal_Yolgah_Cave	47000	13.84667	25.16858	5.692578	19.476	1021.5567	26.19144
Kudjal_Yolgah_Cave	48000	13.84667	25.16858	5.692578	19.476	1021.5567	26.19144
Kudjal_Yolgah_Cave	49000	14.68823	23.81492	7.709465	16.10545	1132.239	26.2965
Kudjal_Yolgah_Cave	50000	14.68823	23.81492	7.709465	16.10545	1132.239	26.2965
Kudjal_Yolgah_Cave	51000	14.31456	24.49894	6.736322	17.76261	1089.729	26.19144
Kudjal_Yolgah_Cave	52000	14.31456	24.49894	6.736322	17.76261	1089.729	26.19144
Kudjal_Yolgah_Cave	53000	14.52832	23.86983	7.467487	16.40234	1123.522	26.19144
Kudjal_Yolgah_Cave	54000	14.52832	23.86983	7.467487	16.40234	1123.522	26.19144
Kudjal_Yolgah_Cave	55000	14.69434	23.43745	7.899209	15.53824	1101.495	25.84848
Kudjal_Yolgah_Cave	56000	14.69434	23.43745	7.899209	15.53824	1101.495	25.84848
Kudjal_Yolgah_Cave	57000	14.82946	23.39647	8.267693	15.12878	1084.866	25.84848
Kudjal_Yolgah_Cave	58000	14.82946	23.39647	8.267693	15.12878	1084.866	25.84848
Kudjal_Yolgah_Cave	59000	14.32823	23.29991	7.553968	15.74594	1055.926	25.96517
Kudjal_Yolgah_Cave	60000	14.32823	23.29991	7.553968	15.74594	1055.926	25.96517
Kudjal_Yolgah_Cave	61000	13.45189	24.13161	5.752106	18.3795	932.424	25.84848
Kudjal_Yolgah_Cave	62000	13.45189	24.13161	5.752106	18.3795	932.424	25.84848
Kudjal_Yolgah_Cave	63000	13.18086	23.888	5.487252	18.40075	920.4357	25.96517
Kudjal_Yolgah_Cave	64000	13.18086	23.888	5.487252	18.40075	920.4357	25.96517
Kudjal_Yolgah_Cave	65000	12.83017	24.45842	4.750762	19.70766	893.0936	25.84848
Kudjal_Yolgah_Cave	66000	12.83017	24.45842	4.750762	19.70766	893.0936	25.84848
Kudjal_Yolgah_Cave	67000	13.04524	24.53791	4.948052	19.58986	930.5558	26.19144
Kudjal_Yolgah_Cave	68000	13.04524	24.53791	4.948052	19.58986	930.5558	26.19144
Kudjal_Yolgah_Cave	69000	14.07939	24.18978	6.507333	17.68244	1047.0292	26.6086
Kudjal_Yolgah_Cave	70000	14.07939	24.18978	6.507333	17.68244	1047.0292	26.6086
Kudjal_Yolgah_Cave	71000	14.91359	24.12391	8.01097	16.11294	1157.918	33.49136
Kudjal_Yolgah_Cave	72000	14.91359	24.12391	8.01097	16.11294	1157.918	33.49136
Kudjal_Yolgah_Cave	73000	14.96962	23.95574	8.015412	15.94033	1139.54	41.88414
Kudjal_Yolgah_Cave	74000	14.96962	23.95574	8.015412	15.94033	1139.54	41.88414
Kudjal_Yolgah_Cave	75000	14.87418	23.37486	8.151423	15.22344	1148.28	44.96978
Kudjal_Yolgah_Cave	76000	14.87418	23.37486	8.151423	15.22344	1148.28	44.96978
Kudjal_Yolgah_Cave	77000	14.89677	23.37708	8.398487	14.9786	1118.628	44.66046
Kudjal_Yolgah_Cave	78000	14.89677	23.37708	8.398487	14.9786	1118.628	44.66046
Kudjal_Yolgah_Cave	79000	15.31511	23.33389	8.935754	14.39814	1086.164	42.19529
Kudjal_Yolgah_Cave	80000	15.31511	23.33389	8.935754	14.39814	1086.164	42.19529
Kudjal_Yolgah_Cave	81000	15.25891	23.37262	8.978312	14.39431	1053.496	42.60863
Kudjal_Yolgah_Cave	82000	15.25891	23.37262	8.978312	14.39431	1053.496	42.60863
Kudjal_Yolgah_Cave	83000	15.21348	23.43463	8.972734	14.4619	1077.45	44.66046
Kudjal_Yolgah_Cave	84000	15.21348	23.43463	8.972734	14.4619	1077.45	44.66046
Kudjal_Yolgah_Cave	85000	15.34074	23.81984	8.877457	14.94238	1072.676	41.88414
Kudjal_Yolgah_Cave	86000	15.34074	23.81984	8.877457	14.94238	1072.676	41.88414
Kudjal_Yolgah_Cave	87000	14.60155	24.51504	7.298839	17.21621	1024.292	34.53942
Kudjal_Yolgah_Cave	88000	14.60155	24.51504	7.298839	17.21621	1024.292	34.53942
Kudjal_Yolgah_Cave	89000	15.02899	24.42314	8.110478	16.31266	1131.487	36.83742
Kudjal_Yolgah_Cave	90000	15.02899	24.42314	8.110478	16.31266	1131.487	36.83742
Kudjal_Yolgah_Cave	91000	15.20909	24.87585	7.950784	16.92506	1154.33	35.5863
Kudjal_Yolgah_Cave	92000	15.20909	24.87585	7.950784	16.92506	1154.33	35.5863
Kudjal_Yolgah_Cave	93000	15.23665	24.96447	7.976819	16.98765	1180.171	34.53942
Kudjal_Yolgah_Cave	94000	15.23665	24.96447	7.976819	16.98765	1180.171	34.53942
Kudjal_Yolgah_Cave	95000	15.30713	24.87605	8.11492	16.76113	1187.608	45.38061
Kudjal_Yolgah_Cave	96000	15.30713	24.87605	8.11492	16.76113	1187.608	45.38061
Kudjal_Yolgah_Cave	97000	15.34107	24.51176	8.311613	16.20014	1209.637	48.02406
Kudjal_Yolgah_Cave	98000	15.34107	24.51176	8.311613	16.20014	1209.637	48.02406
Kudjal_Yolgah_Cave	99000	15.5101	24.21314	8.787323	15.42582	1128.883	48.83562
Kudjal_Yolgah_Cave	100000	15.5101	24.21314	8.787323	15.42582	1128.883	48.83562
Lake_Victoria	1000	16.89665	33.09528	3.923516	29.17177	244.9736	46.11444
Lake_Victoria	2000	16.98777	32.86621	4.3421	28.52411	259.1362	46.11444
Lake_Victoria	3000	16.97198	32.5434	4.38556	28.15784	241.8094	46.11444
Lake_Victoria	4000	16.64087	32.25428	4.669733	27.58455	276.5533	46.11444
Lake_Victoria	5000	16.7534	31.43967	4.650596	26.78908	278.162	46.11444
Lake_Victoria	6000	16.61939	30.91213	4.193692	26.71844	227.1883	46.11444
Lake_Victoria	7000	16.89002	30.46513	4.233139	26.23199	270.8002	46.11444
Lake_Victoria	8000	16.63654	29.75707	4.269114	25.48796	290.4411	46.11444
Lake_Victoria	9000	16.27757	29.66726	4.355062	25.31219	257.63	46.11444
Lake_Victoria	10000	16.19867	29.72402	4.429517	25.2945	312.2018	46.11444
Lake_Victoria	11000	15.99867	29.35762	3.9635923	25.39403	291.2763	46.11444
Lake_Victoria	12000	15.52577	29.701	3.4140728	26.28692	303.3076	46.11444
Lake_Victoria	13000	15.44466	29.56142	3.4842434	26.07718	253.66	46.11444
Lake_Victoria	14000	15.32917	30.12285	3.3658199	26.75703	263.2411	46.11444
Lake_Victoria	15000	14.76711	29.26985	2.4255011	26.84435	146.9112	46.11444
Lake_Victoria	16000	13.93821	28.82192	1.4761392	27.34578	186.3629	46.11444
Lake_Victoria	17000	14.04048	29.39757	1.1005224	28.29705	178.905	46.11444
Lake_Victoria	18000	14.01104	29.46093	1.0034418	28.45749	151.1447	46.11444
Lake_Victoria	19000	13.97515	29.98451	1.1292372	28.85527	175.5519	46.11444
Lake_Victoria	20000	13.79842	29.21431	0.7226192	28.49169	172.5344	46.11444
Lake_Victoria	21000	14.04945	29.6719	0.6966525	28.97525	171.2707	46.11444
Lake_Victoria	22000	14.02386	29.628	0.3426987	29.2853	147.7034	46.11444
Lake_Victoria	23000	13.78774	29.62494	1.0950491	28.52989	172.7129	46.11444
Lake_Victoria	24000	13.78774	29.62494	1.0950491	28.52989	172.7129	46.11444
Lake_Victoria	25000	13.6365	28.66268	1.4504354	27.21224	219.1103	46.11444
Lake_Victoria	26000	13.6365	28.66268	1.4504354	27.21224	219.1103	46.11444

Lake_Victoria	27000	14.06266	28.3282	2.2056613	26.12254	192.9445	46.11444
Lake_Victoria	28000	14.06266	28.3282	2.2056613	26.12254	192.9445	46.11444
Lake_Victoria	29000	14.12466	27.67783	2.6944907	24.98334	271.5123	46.11444
Lake_Victoria	30000	14.12466	27.67783	2.6944907	24.98334	271.5123	46.11444
Lake_Victoria	31000	14.41882	28.3895	2.940576	25.44892	257.9265	46.11444
Lake_Victoria	32000	14.41882	28.3895	2.940576	25.44892	257.9265	46.11444
Lake_Victoria	33000	14.14741	27.64265	2.360627	25.28202	226.153	46.11444
Lake_Victoria	34000	14.14741	27.64265	2.360627	25.28202	226.153	46.11444
Lake_Victoria	35000	14.3676	28.42981	2.444631	25.98518	211.5575	46.11444
Lake_Victoria	36000	14.3676	28.42981	2.444631	25.98518	211.5575	46.11444
Lake_Victoria	37000	14.41862	28.90191	2.419057	26.48285	193.7953	46.11444
Lake_Victoria	38000	14.41862	28.90191	2.419057	26.48285	193.7953	46.11444
Lake_Victoria	39000	14.50474	29.55428	1.826122	27.72816	205.8658	46.11444
Lake_Victoria	40000	14.50474	29.55428	1.826122	27.72816	205.8658	46.11444
Lake_Victoria	41000	14.62236	30.16463	1.719323	28.4453	182.2199	46.11444
Lake_Victoria	42000	14.62236	30.16463	1.719323	28.4453	182.2199	46.11444
Lake_Victoria	43000	15.06748	30.97699	1.938126	29.03886	187.4837	46.11444
Lake_Victoria	44000	15.06748	30.97699	1.938126	29.03886	187.4837	46.11444
Lake_Victoria	45000	15.15897	30.53298	2.190393	28.34259	199.4259	46.11444
Lake_Victoria	46000	15.15897	30.53298	2.190393	28.34259	199.4259	46.11444
Lake_Victoria	47000	15.13034	30.72299	1.934835	28.78816	185.5039	46.11444
Lake_Victoria	48000	15.13034	30.72299	1.934835	28.78816	185.5039	46.11444
Lake_Victoria	49000	15.61974	31.47966	2.377179	29.10248	135.0708	46.11444
Lake_Victoria	50000	15.61974	31.47966	2.377179	29.10248	135.0708	46.11444
Lake_Victoria	51000	15.57837	31.28752	2.29427	28.99325	190.2574	46.11444
Lake_Victoria	52000	15.57837	31.28752	2.29427	28.99325	190.2574	46.11444
Lake_Victoria	53000	15.05779	29.80676	2.812521	26.99423	216.7296	46.11444
Lake_Victoria	54000	15.05779	29.80676	2.812521	26.99423	216.7296	46.11444
Lake_Victoria	55000	15.43843	29.54881	3.241676	26.30714	160.4333	46.11444
Lake_Victoria	56000	15.43843	29.54881	3.241676	26.30714	160.4333	46.11444
Lake_Victoria	57000	15.56055	29.44345	3.407086	26.03637	196.1986	46.11444
Lake_Victoria	58000	15.56055	29.44345	3.407086	26.03637	196.1986	46.11444
Lake_Victoria	59000	14.87106	28.28455	3.164936	25.11961	237.7662	46.11444
Lake_Victoria	60000	14.87106	28.28455	3.164936	25.11961	237.7662	46.11444
Lake_Victoria	61000	14.27041	27.92753	2.825657	25.10187	228.1268	46.11444
Lake_Victoria	62000	14.27041	27.92753	2.825657	25.10187	228.1268	46.11444
Lake_Victoria	63000	14.0449	28.36634	2.334347	26.03199	252.5933	46.11444
Lake_Victoria	64000	14.0449	28.36634	2.334347	26.03199	252.5933	46.11444
Lake_Victoria	65000	13.94205	28.64012	2.006616	26.63351	260.1291	46.11444
Lake_Victoria	66000	13.94205	28.64012	2.006616	26.63351	260.1291	46.11444
Lake_Victoria	67000	14.50589	29.56809	2.374423	27.19367	235.5686	46.11444
Lake_Victoria	68000	14.50589	29.56809	2.374423	27.19367	235.5686	46.11444
Lake_Victoria	69000	15.06139	30.56685	2.438528	28.12832	158.8622	46.11444
Lake_Victoria	70000	15.06139	30.56685	2.438528	28.12832	158.8622	46.11444
Lake_Victoria	71000	16.1039	32.42101	3.188174	29.23284	158.9968	46.11444
Lake_Victoria	72000	16.1039	32.42101	3.188174	29.23284	158.9968	46.11444
Lake_Victoria	73000	16.16461	31.86002	3.788686	28.07133	193.9503	46.11444
Lake_Victoria	74000	16.16461	31.86002	3.788686	28.07133	193.9503	46.11444
Lake_Victoria	75000	15.78111	30.31833	3.309472	27.00886	216.3044	46.11444
Lake_Victoria	76000	15.78111	30.31833	3.309472	27.00886	216.3044	46.11444
Lake_Victoria	77000	15.75225	29.56184	3.841487	25.72036	240.6225	46.11444
Lake_Victoria	78000	15.75225	29.56184	3.841487	25.72036	240.6225	46.11444
Lake_Victoria	79000	16.27353	29.24307	4.712748	24.53032	178.7248	46.11444
Lake_Victoria	80000	16.27353	29.24307	4.712748	24.53032	178.7248	46.11444
Lake_Victoria	81000	15.87426	28.35599	4.112982	24.243	260.4442	46.11444
Lake_Victoria	82000	15.87426	28.35599	4.112982	24.243	260.4442	46.11444
Lake_Victoria	83000	15.82965	29.25931	4.447269	24.81204	298.6381	46.11444
Lake_Victoria	84000	15.82965	29.25931	4.447269	24.81204	298.6381	46.11444
Lake_Victoria	85000	15.91937	29.68081	4.453042	25.22777	230.1091	46.11444
Lake_Victoria	86000	15.91937	29.68081	4.453042	25.22777	230.1091	46.11444
Lake_Victoria	87000	15.62973	30.49073	3.39798	27.09275	236.9806	46.11444
Lake_Victoria	88000	15.62973	30.49073	3.39798	27.09275	236.9806	46.11444
Lake_Victoria	89000	15.97435	31.68447	3.077684	28.60678	191.2699	46.11444
Lake_Victoria	90000	15.97435	31.68447	3.077684	28.60678	191.2699	46.11444
Lake_Victoria	91000	16.33769	33.40562	2.688986	30.71663	196.5143	46.11444
Lake_Victoria	92000	16.33769	33.40562	2.688986	30.71663	196.5143	46.11444
Lake_Victoria	93000	16.46937	34.31762	2.827703	31.48992	141.0576	46.11444
Lake_Victoria	94000	16.46937	34.31762	2.827703	31.48992	141.0576	46.11444
Lake_Victoria	95000	16.66879	34.0577	3.01959	31.03811	137.5425	46.11444
Lake_Victoria	96000	16.66879	34.0577	3.01959	31.03811	137.5425	46.11444
Lake_Victoria	97000	16.55715	32.48557	3.156588	29.32898	153.1838	46.11444
Lake_Victoria	98000	16.55715	32.48557	3.156588	29.32898	153.1838	46.11444
Lake_Victoria	99000	16.62043	31.50745	4.105433	27.40202	181.6204	46.11444
Lake_Victoria	100000	16.62043	31.50745	4.105433	27.40202	181.6204	46.11444
Lancefield_Swamp	1000	12.80717	27.2369	2.728138	24.50876	659.0457	419.5555
Lancefield_Swamp	2000	12.88806	26.7976	3.155054	23.64255	670.334	419.5555
Lancefield_Swamp	3000	12.85598	26.38464	3.182087	23.20256	663.3759	419.5555
Lancefield_Swamp	4000	12.52195	26.23295	3.276281	22.95667	714.5303	419.5555
Lancefield_Swamp	5000	12.59244	25.71755	3.196199	22.52135	688.7265	419.5555
Lancefield_Swamp	6000	12.44385	24.63069	2.719782	21.91091	634.0899	419.5555
Lancefield_Swamp	7000	12.65203	24.42421	2.821175	21.60303	632.0751	419.5555
Lancefield_Swamp	8000	12.50698	23.91807	2.870481	21.04758	655.3866	419.5555
Lancefield_Swamp	9000	12.20686	23.62346	3.000368	20.62309	679.2435	419.5555
Lancefield_Swamp	10000	12.15174	24.36048	3.056706	21.30378	714.535	419.5555
Lancefield_Swamp	11000	12.103505	23.5084	2.8401105	20.66829	717.0023	419.5555
Lancefield_Swamp	12000	11.426274	23.01993	2.2978265	20.72211	729.5513	419.5555
Lancefield_Swamp	13000	11.28457	23.12061	2.0538492	21.06676	663.9965	419.5555
Lancefield_Swamp	14000	11.218648	23.74583	1.9000937	21.84574	673.8731	419.5555
Lancefield_Swamp	15000	10.513448	23.65083	0.9068757	22.74395	531.3697	419.5555
Lancefield_Swamp	16000	9.824018	22.91558	0.167229	22.74835	583.9252	419.5555
Lancefield_Swamp	17000	9.981318	23.67603	0.1052012	23.57083	543.062	419.5555
Lancefield_Swamp	18000	9.870649	23.65378	-0.1613608	23.81514	511.8918	419.5555
Lancefield_Swamp	19000	9.956605	24.08819	-0.1707521	24.25895	539.4593	419.5555
Lancefield_Swamp	20000	9.803102	23.73378	-0.3858377	24.11962	573.7583	419.5555
Lancefield_Swamp	21000	9.848255	23.65719	-0.5682935	24.22548	537.2466	419.5555
Lancefield_Swamp	22000	9.550757	23.29968	-0.9980093	24.29769	488.0825	419.5555
Lancefield_Swamp	23000	9.761573	23.84015	-0.2601712	24.10032	525.5287	419.5555
Lancefield_Swamp	24000	9.761573	23.84015	-0.2601712	24.10032	525.5287	419.5555
Lancefield_Swamp	25000	9.754302	23.07161	0.1186312	22.95298	598.8813	419.5555
Lancefield_Swamp	26000	9.754302	23.07161	0.1186312	22.95298	598.8813	419.5555
Lancefield_Swamp	27000	10.133603	22.73514	0.7160652	22.01908	593.3602	419.5555
Lancefield_Swamp	28000	10.133603	22.73514	0.7160652	22.01908	593.3602	419.5555
Lancefield_Swamp	29000	10.316652	22.22308	0.9593258	21.26375	649.6209	419.5555
Lancefield_Swamp	30000	10.316652	22.22308	0.9593258	21.26375	649.6209	419.5555
Lancefield_Swamp	31000	10.51313	22.58629	1.1255788	21.46071	646.4757	419.5555

Lancefield_Swamp	32000	10.51313	22.58629	1.1255788	21.46071	646.4757	419.5555
Lancefield_Swamp	33000	10.34523	22.27789	1.0531026	21.22478	609.3754	419.5555
Lancefield_Swamp	34000	10.34523	22.27789	1.0531026	21.22478	609.3754	419.5555
Lancefield_Swamp	35000	10.43306	22.90532	1.0757494	21.82957	579.0881	419.5555
Lancefield_Swamp	36000	10.43306	22.90532	1.0757494	21.82957	579.0881	419.5555
Lancefield_Swamp	37000	10.46487	23.29356	1.1181248	22.17544	569.5181	419.5555
Lancefield_Swamp	38000	10.46487	23.29356	1.1181248	22.17544	569.5181	419.5555
Lancefield_Swamp	39000	10.71793	24.05204	0.7323078	23.31973	591.3658	419.5555
Lancefield_Swamp	40000	10.71793	24.05204	0.7323078	23.31973	591.3658	419.5555
Lancefield_Swamp	41000	10.66998	24.30086	0.6612861	23.63957	580.3671	419.5555
Lancefield_Swamp	42000	10.66998	24.30086	0.6612861	23.63957	580.3671	419.5555
Lancefield_Swamp	43000	10.84079	24.8075	0.2070965	24.6004	591.6661	419.5555
Lancefield_Swamp	44000	10.84079	24.8075	0.2070965	24.6004	591.6661	419.5555
Lancefield_Swamp	45000	11.02457	24.74258	0.4208248	24.32175	581.701	419.5555
Lancefield_Swamp	46000	11.02457	24.74258	0.4208248	24.32175	581.701	419.5555
Lancefield_Swamp	47000	10.97773	24.74223	0.2647354	24.47749	557.9207	419.5555
Lancefield_Swamp	48000	10.97773	24.74223	0.2647354	24.47749	557.9207	419.5555
Lancefield_Swamp	49000	11.04924	25.11886	0.3703682	24.74849	520.8555	419.5555
Lancefield_Swamp	50000	11.04924	25.11886	0.3703682	24.74849	520.8555	419.5555
Lancefield_Swamp	51000	11.27369	25.22589	0.4486643	24.77723	561.7296	419.5555
Lancefield_Swamp	52000	11.27369	25.22589	0.4486643	24.77723	561.7296	419.5555
Lancefield_Swamp	53000	10.82112	24.08145	1.0334392	23.04801	625.9542	419.5555
Lancefield_Swamp	54000	10.82112	24.08145	1.0334392	23.04801	625.9542	419.5555
Lancefield_Swamp	55000	10.97472	23.46555	1.2034985	22.26205	550.4021	419.5555
Lancefield_Swamp	56000	10.97472	23.46555	1.2034985	22.26205	550.4021	419.5555
Lancefield_Swamp	57000	11.16138	23.56437	1.3074872	22.25688	581.2831	419.5555
Lancefield_Swamp	58000	11.16138	23.56437	1.3074872	22.25688	581.2831	419.5555
Lancefield_Swamp	59000	10.73137	22.83527	1.2809603	21.55431	655.5561	419.5555
Lancefield_Swamp	60000	10.73137	22.83527	1.2809603	21.55431	655.5561	419.5555
Lancefield_Swamp	61000	10.45375	22.60754	1.4388469	21.1687	608.6632	419.5555
Lancefield_Swamp	62000	10.45375	22.60754	1.4388469	21.1687	608.6632	419.5555
Lancefield_Swamp	63000	10.33046	22.80439	1.1397452	21.66464	643.0085	419.5555
Lancefield_Swamp	64000	10.33046	22.80439	1.1397452	21.66464	643.0085	419.5555
Lancefield_Swamp	65000	10.35407	23.39239	0.9440754	22.44832	662.7257	419.5555
Lancefield_Swamp	66000	10.35407	23.39239	0.9440754	22.44832	662.7257	419.5555
Lancefield_Swamp	67000	10.63725	24.05662	0.8379086	23.21871	634.2028	419.5555
Lancefield_Swamp	68000	10.63725	24.05662	0.8379086	23.21871	634.2028	419.5555
Lancefield_Swamp	69000	10.82592	24.59204	0.8567372	23.7353	559.6763	419.5555
Lancefield_Swamp	70000	10.82592	24.59204	0.8567372	23.7353	559.6763	419.5555
Lancefield_Swamp	71000	11.53801	26.2962	1.204091	25.09211	533.3102	419.5555
Lancefield_Swamp	72000	11.53801	26.2962	1.204091	25.09211	533.3102	419.5555
Lancefield_Swamp	73000	11.67724	25.6457	1.739191	23.90651	617.465	419.5555
Lancefield_Swamp	74000	11.67724	25.6457	1.739191	23.90651	617.465	419.5555
Lancefield_Swamp	75000	11.37753	24.51	1.358213	23.15179	637.4922	419.5555
Lancefield_Swamp	76000	11.37753	24.51	1.358213	23.15179	637.4922	419.5555
Lancefield_Swamp	77000	11.25888	23.53585	1.765734	21.77012	674.8501	419.5555
Lancefield_Swamp	78000	11.25888	23.53585	1.765734	21.77012	674.8501	419.5555
Lancefield_Swamp	79000	11.52907	23.19385	2.331035	20.86282	590.2495	419.5555
Lancefield_Swamp	80000	11.52907	23.19385	2.331035	20.86282	590.2495	419.5555
Lancefield_Swamp	81000	11.31507	22.29551	2.064006	20.23151	680.3613	419.5555
Lancefield_Swamp	82000	11.31507	22.29551	2.064006	20.23151	680.3613	419.5555
Lancefield_Swamp	83000	11.68803	23.01278	2.981488	20.03129	717.9921	419.5555
Lancefield_Swamp	84000	11.68803	23.01278	2.981488	20.03129	717.9921	419.5555
Lancefield_Swamp	85000	11.30699	23.22099	2.423576	20.79741	668.3351	419.5555
Lancefield_Swamp	86000	11.30699	23.22099	2.423576	20.79741	668.3351	419.5555
Lancefield_Swamp	87000	11.43767	24.13876	2.026989	22.11177	651.7602	419.5555
Lancefield_Swamp	88000	11.43767	24.13876	2.026989	22.11177	651.7602	419.5555
Lancefield_Swamp	89000	11.32421	25.16958	1.392519	23.77706	593.4099	419.5555
Lancefield_Swamp	90000	11.32421	25.16958	1.392519	23.77706	593.4099	419.5555
Lancefield_Swamp	91000	11.97662	27.07692	1.098091	25.97882	598.6833	419.5555
Lancefield_Swamp	92000	11.97662	27.07692	1.098091	25.97882	598.6833	419.5555
Lancefield_Swamp	93000	11.81242	27.55011	1.006559	26.54355	514.3035	419.5555
Lancefield_Swamp	94000	11.81242	27.55011	1.006559	26.54355	514.3035	419.5555
Lancefield_Swamp	95000	12.04735	27.36268	1.209167	26.15351	519.1979	419.5555
Lancefield_Swamp	96000	12.04735	27.36268	1.209167	26.15351	519.1979	419.5555
Lancefield_Swamp	97000	11.69983	25.99739	1.367709	24.62968	557.1922	419.5555
Lancefield_Swamp	98000	11.69983	25.99739	1.367709	24.62968	557.1922	419.5555
Lancefield_Swamp	99000	11.96026	25.11435	2.017767	23.09658	577.6588	419.5555
Lancefield_Swamp	100000	11.96026	25.11435	2.017767	23.09658	577.6588	419.5555
Mammoth_Cave	1000	15.65348	24.63853	8.659369	15.97916	1064.222	57.5757
Mammoth_Cave	2000	15.75634	24.6187	8.777328	15.84137	1108.338	56.95478
Mammoth_Cave	3000	15.70492	24.38464	8.907191	15.47744	1130.548	56.41308
Mammoth_Cave	4000	15.56582	24.05301	8.867358	15.18565	1141.138	56.13699
Mammoth_Cave	5000	15.5681	23.98129	8.980975	15.00031	1130.494	56.04103
Mammoth_Cave	6000	15.60578	24.14386	8.891938	15.25192	1145.354	55.75
Mammoth_Cave	7000	15.97051	24.47577	9.323369	15.1524	1148.571	54.45258
Mammoth_Cave	8000	15.80044	24.17812	9.235932	14.94218	1106.94	53.65189
Mammoth_Cave	9000	15.51369	23.81608	9.139382	14.6767	1116.531	51.2575
Mammoth_Cave	10000	15.46621	23.74612	9.067594	14.67853	1064.719	46.30499
Mammoth_Cave	11000	15.59734	23.87964	9.097976	14.78166	1100.4368	39.52273
Mammoth_Cave	12000	15.01161	23.43469	8.579977	14.85471	1080.9426	28.8314
Mammoth_Cave	13000	14.75694	23.29108	8.295524	14.99556	1076.5558	26.6086
Mammoth_Cave	14000	14.72459	23.24693	8.179913	15.06701	1074.8472	25.96517
Mammoth_Cave	15000	14.24139	22.82243	7.70208	15.12035	1076.7528	25.72646
Mammoth_Cave	16000	13.09779	22.84186	5.980461	16.8614	985.7774	25.20312
Mammoth_Cave	17000	12.62714	24.32124	4.42841	19.89283	895.6552	24.77642
Mammoth_Cave	18000	12.50812	24.42835	4.321391	20.10696	898.0898	24.77642
Mammoth_Cave	19000	12.62606	24.62997	4.277765	20.3522	902.7986	24.77642
Mammoth_Cave	20000	12.40785	24.42624	4.051768	20.37447	904.0475	24.77642
Mammoth_Cave	21000	12.54167	24.46865	3.734348	20.7343	875.6848	24.77642
Mammoth_Cave	22000	12.1779	23.93848	3.481334	20.45715	848.8455	24.61111
Mammoth_Cave	23000	12.32087	24.02088	3.936624	20.08425	897.7261	24.61111
Mammoth_Cave	24000	12.32087	24.02088	3.936624	20.08425	897.7261	24.61111
Mammoth_Cave	25000	12.47892	24.23127	4.037971	20.1933	884.2087	24.77642
Mammoth_Cave	26000	12.47892	24.23127	4.037971	20.1933	884.2087	24.77642
Mammoth_Cave	27000	12.78323	23.66027	4.793723	18.86655	920.1155	24.77642
Mammoth_Cave	28000	12.78323	23.66027	4.793723	18.86655	920.1155	24.77642
Mammoth_Cave	29000	13.19083	23.94425	5.438779	18.50547	931.2445	25.06132
Mammoth_Cave	30000	13.19083	23.94425	5.438779	18.50547	931.2445	25.06132
Mammoth_Cave	31000	13.57178	24.21385	5.76635	18.4475	940.1076	25.34078
Mammoth_Cave	32000	13.57178	24.21385	5.76635	18.4475	940.1076	25.34078
Mammoth_Cave	33000	13.45711	23.40599	6.070285	17.3357	949.5594	25.47427
Mammoth_Cave	34000	13.45711	23.40599	6.070285	17.3357	949.5594	25.47427
Mammoth_Cave	35000	13.76456	23.65914	6.468184	17.19095	997.8962	25.34078
Mammoth_Cave	36000	13.76456	23.65914	6.468184	17.19095	997.8962	25.34078

Mammoth_Cave	37000	13.86513	23.46653	6.786896	16.67964	1041.8899	25.47427
Mammoth_Cave	38000	13.86513	23.46653	6.786896	16.67964	1041.8899	25.47427
Mammoth_Cave	39000	13.48474	24.86034	5.266641	19.5937	933.6008	25.72646
Mammoth_Cave	40000	13.48474	24.86034	5.266641	19.5937	933.6008	25.72646
Mammoth_Cave	41000	13.51492	24.72781	5.598298	19.12951	998.8045	26.07874
Mammoth_Cave	42000	13.51492	24.72781	5.598298	19.12951	998.8045	26.07874
Mammoth_Cave	43000	14.19298	24.13736	6.801324	17.33604	1107.9573	26.19144
Mammoth_Cave	44000	14.19298	24.13736	6.801324	17.33604	1107.9573	26.19144
Mammoth_Cave	45000	14.00626	24.64497	6.305242	18.33973	1078.009	26.19144
Mammoth_Cave	46000	14.00626	24.64497	6.305242	18.33973	1078.009	26.19144
Mammoth_Cave	47000	13.84667	25.16858	5.692578	19.476	1021.5567	26.19144
Mammoth_Cave	48000	13.84667	25.16858	5.692578	19.476	1021.5567	26.19144
Mammoth_Cave	49000	14.68823	23.81492	7.709465	16.10545	1132.239	26.2965
Mammoth_Cave	50000	14.68823	23.81492	7.709465	16.10545	1132.239	26.2965
Mammoth_Cave	51000	14.31456	24.49894	6.736322	17.76261	1089.729	26.19144
Mammoth_Cave	52000	14.31456	24.49894	6.736322	17.76261	1089.729	26.19144
Mammoth_Cave	53000	14.52832	23.86983	7.467487	16.40234	1123.522	26.19144
Mammoth_Cave	54000	14.52832	23.86983	7.467487	16.40234	1123.522	26.19144
Mammoth_Cave	55000	14.69434	23.43745	7.899209	15.53824	1101.495	25.84848
Mammoth_Cave	56000	14.69434	23.43745	7.899209	15.53824	1101.495	25.84848
Mammoth_Cave	57000	14.82946	23.39647	8.267693	15.12878	1084.866	25.84848
Mammoth_Cave	58000	14.82946	23.39647	8.267693	15.12878	1084.866	25.84848
Mammoth_Cave	59000	14.32823	23.29991	7.553968	15.74594	1055.926	25.96517
Mammoth_Cave	60000	14.32823	23.29991	7.553968	15.74594	1055.926	25.96517
Mammoth_Cave	61000	13.45189	24.13161	5.752106	18.3795	932.424	25.84848
Mammoth_Cave	62000	13.45189	24.13161	5.752106	18.3795	932.424	25.84848
Mammoth_Cave	63000	13.18086	23.888	5.487252	18.40075	920.4357	25.96517
Mammoth_Cave	64000	13.18086	23.888	5.487252	18.40075	920.4357	25.96517
Mammoth_Cave	65000	12.83017	24.45842	4.750762	19.70766	893.0936	25.84848
Mammoth_Cave	66000	12.83017	24.45842	4.750762	19.70766	893.0936	25.84848
Mammoth_Cave	67000	13.04524	24.53791	4.948052	19.58986	930.5558	26.19144
Mammoth_Cave	68000	13.04524	24.53791	4.948052	19.58986	930.5558	26.19144
Mammoth_Cave	69000	14.07939	24.18978	6.507333	17.68244	1047.0292	26.6086
Mammoth_Cave	70000	14.07939	24.18978	6.507333	17.68244	1047.0292	26.6086
Mammoth_Cave	71000	14.91359	24.12391	8.01097	16.11294	1157.918	33.49136
Mammoth_Cave	72000	14.91359	24.12391	8.01097	16.11294	1157.918	33.49136
Mammoth_Cave	73000	14.96962	23.95574	8.015412	15.94033	1139.54	41.88414
Mammoth_Cave	74000	14.96962	23.95574	8.015412	15.94033	1139.54	41.88414
Mammoth_Cave	75000	14.87418	23.37486	8.151423	15.22344	1148.28	44.96978
Mammoth_Cave	76000	14.87418	23.37486	8.151423	15.22344	1148.28	44.96978
Mammoth_Cave	77000	14.89677	23.37708	8.398487	14.9786	1118.628	44.66046
Mammoth_Cave	78000	14.89677	23.37708	8.398487	14.9786	1118.628	44.66046
Mammoth_Cave	79000	15.31511	23.33389	8.935754	14.39814	1086.164	42.19529
Mammoth_Cave	80000	15.31511	23.33389	8.935754	14.39814	1086.164	42.19529
Mammoth_Cave	81000	15.25891	23.37262	8.978312	14.39431	1053.496	42.60863
Mammoth_Cave	82000	15.25891	23.37262	8.978312	14.39431	1053.496	42.60863
Mammoth_Cave	83000	15.21348	23.43463	8.972734	14.4619	1077.45	44.66046
Mammoth_Cave	84000	15.21348	23.43463	8.972734	14.4619	1077.45	44.66046
Mammoth_Cave	85000	15.34074	23.81984	8.877457	14.94238	1072.676	41.88414
Mammoth_Cave	86000	15.34074	23.81984	8.877457	14.94238	1072.676	41.88414
Mammoth_Cave	87000	14.60155	24.51504	7.298839	17.21621	1024.292	34.53942
Mammoth_Cave	88000	14.60155	24.51504	7.298839	17.21621	1024.292	34.53942
Mammoth_Cave	89000	15.02899	24.42314	8.110478	16.31266	1131.487	36.83742
Mammoth_Cave	90000	15.02899	24.42314	8.110478	16.31266	1131.487	36.83742
Mammoth_Cave	91000	15.20909	24.87585	7.950784	16.92506	1154.33	35.5863
Mammoth_Cave	92000	15.20909	24.87585	7.950784	16.92506	1154.33	35.5863
Mammoth_Cave	93000	15.23665	24.96447	7.976819	16.98765	1180.171	34.53942
Mammoth_Cave	94000	15.23665	24.96447	7.976819	16.98765	1180.171	34.53942
Mammoth_Cave	95000	15.30713	24.87605	8.11492	16.76113	1187.608	45.38061
Mammoth_Cave	96000	15.30713	24.87605	8.11492	16.76113	1187.608	45.38061
Mammoth_Cave	97000	15.34107	24.51176	8.311613	16.20014	1209.637	48.02406
Mammoth_Cave	98000	15.34107	24.51176	8.311613	16.20014	1209.637	48.02406
Mammoth_Cave	99000	15.5101	24.21314	8.787323	15.42582	1128.883	48.83562
Mammoth_Cave	100000	15.5101	24.21314	8.787323	15.42582	1128.883	48.83562
McEachern_Cave	1000	13.61749	25.37256	5.119259	20.2533	649.7623	89.28706
McEachern_Cave	2000	13.77704	25.27439	5.538159	19.73624	706.883	89.08868
McEachern_Cave	3000	13.80656	25.22587	5.56112	19.66475	674.8355	88.81369
McEachern_Cave	4000	13.62155	25.01243	5.597193	19.41524	717.2048	88.66716
McEachern_Cave	5000	13.59809	24.88922	5.577238	19.31198	733.5566	88.43919
McEachern_Cave	6000	13.38833	24.04423	5.23213	18.8121	692.4436	88.20072
McEachern_Cave	7000	13.58761	24.20773	5.457026	18.75071	642.5984	87.43223
McEachern_Cave	8000	13.44231	22.38543	6.308594	16.07683	711.1473	66.85782
McEachern_Cave	9000	13.18676	21.29799	6.42238	14.8756	772.0142	64.23569
McEachern_Cave	10000	13.39695	22.36945	6.108785	16.26067	722.8278	57.70105
McEachern_Cave	11000	13.15454	21.40272	6.258564	15.14416	761.8419	50.57447
McEachern_Cave	12000	12.90101	21.52797	5.779613	15.74836	685.6405	36.26885
McEachern_Cave	13000	12.51321	21.03545	5.525851	15.5096	672.2721	29.78049
McEachern_Cave	14000	12.54777	21.52523	5.529033	15.99619	659.8419	26.96
McEachern_Cave	15000	11.53465	20.17608	4.57937	15.59671	622.408	23.59254
McEachern_Cave	16000	10.95418	19.88241	3.739442	16.14297	662.5613	20.67832
McEachern_Cave	17000	11.40491	20.7293	4.177743	16.55155	616.029	18.45055
McEachern_Cave	18000	11.2229	20.09233	4.018737	16.07359	622.2464	16.86703
McEachern_Cave	19000	11.40843	20.64989	4.025977	16.62391	603.9984	15.28284
McEachern_Cave	20000	11.17756	20.40933	3.911872	16.49745	645.3867	15.28284
McEachern_Cave	21000	11.23347	20.42037	3.798826	16.62154	594.5869	14.926471
McEachern_Cave	22000	10.81177	19.79845	3.382217	16.41623	566.1849	11.182055
McEachern_Cave	23000	11.17371	20.6631	3.810152	16.85295	613.9684	9.758043
McEachern_Cave	24000	11.17371	20.6631	3.810152	16.85295	613.9684	9.758043
McEachern_Cave	25000	11.32834	20.42801	4.084359	16.34365	625.4268	14.926471
McEachern_Cave	26000	11.32834	20.42801	4.084359	16.34365	625.4268	14.926471
McEachern_Cave	27000	11.48122	19.98816	4.576126	15.41203	612.0605	17.220407
McEachern_Cave	28000	11.48122	19.98816	4.576126	15.41203	612.0605	17.220407
McEachern_Cave	29000	11.60924	19.52678	4.990034	14.53674	654.4417	20.17688
McEachern_Cave	30000	11.60924	19.52678	4.990034	14.53674	654.4417	20.17688
McEachern_Cave	31000	11.98128	19.97656	5.353029	14.62353	661.2812	21.01122
McEachern_Cave	32000	11.98128	19.97656	5.353029	14.62353	661.2812	21.01122
McEachern_Cave	33000	11.69974	19.73845	4.876129	14.86233	625.7769	21.66573
McEachern_Cave	34000	11.69974	19.73845	4.876129	14.86233	625.7769	21.66573
McEachern_Cave	35000	11.74412	20.42186	4.776682	15.64518	629.533	21.01122
McEachern_Cave	36000	11.74412	20.42186	4.776682	15.64518	629.533	21.01122
McEachern_Cave	37000	11.74183	20.38646	4.830925	15.55554	642.0444	22.47727
McEachern_Cave	38000	11.74183	20.38646	4.830925	15.55554	642.0444	22.47727
McEachern_Cave	39000	12.15165	21.15317	4.924697	16.22847	624.6606	24.21789
McEachern_Cave	40000	12.15165	21.15317	4.924697	16.22847	624.6606	24.21789
McEachern_Cave	41000	11.99827	21.30197	4.677167	16.62481	623.1663	27.263

McEachern_Cave	42000	11.99827	21.30197	4.677167	16.62481	623.1663	27.263
McEachern_Cave	43000	12.08051	21.58607	4.795044	16.79102	668.2124	27.86398
McEachern_Cave	44000	12.08051	21.58607	4.795044	16.79102	668.2124	27.86398
McEachern_Cave	45000	12.29905	21.67782	4.797311	16.88051	658.6199	28.31231
McEachern_Cave	46000	12.29905	21.67782	4.797311	16.88051	658.6199	28.31231
McEachern_Cave	47000	12.39388	21.77414	4.891486	16.88266	621.5445	27.86398
McEachern_Cave	48000	12.39388	21.77414	4.891486	16.88266	621.5445	27.86398
McEachern_Cave	49000	12.14472	21.67883	4.60187	17.07697	637.9935	29.49088
McEachern_Cave	50000	12.14472	21.67883	4.60187	17.07697	637.9935	29.49088
McEachern_Cave	51000	12.51007	22.00039	5.105624	16.89477	645.2091	29.05144
McEachern_Cave	52000	12.51007	22.00039	5.105624	16.89477	645.2091	29.05144
McEachern_Cave	53000	12.14996	21.20316	4.891365	16.3118	672.3555	28.16342
McEachern_Cave	54000	12.14996	21.20316	4.891365	16.3118	672.3555	28.16342
McEachern_Cave	55000	12.03588	20.64813	5.1852	15.46293	636.1911	25.59649
McEachern_Cave	56000	12.03588	20.64813	5.1852	15.46293	636.1911	25.59649
McEachern_Cave	57000	12.36837	20.94054	5.329547	15.61099	671.7037	24.68116
McEachern_Cave	58000	12.36837	20.94054	5.329547	15.61099	671.7037	24.68116
McEachern_Cave	59000	12.03992	20.20742	5.384083	14.82334	676.5349	25.74817
McEachern_Cave	60000	12.03992	20.20742	5.384083	14.82334	676.5349	25.74817
McEachern_Cave	61000	11.82618	20.01328	5.149373	14.8639	636.396	25.13974
McEachern_Cave	62000	11.82618	20.01328	5.149373	14.8639	636.396	25.13974
McEachern_Cave	63000	11.65306	20.14108	4.863451	15.27762	634.2393	25.74817
McEachern_Cave	64000	11.65306	20.14108	4.863451	15.27762	634.2393	25.74817
McEachern_Cave	65000	11.7203	20.46303	4.79786	15.66517	667.2502	24.83454
McEachern_Cave	66000	11.7203	20.46303	4.79786	15.66517	667.2502	24.83454
McEachern_Cave	67000	11.84154	20.83158	4.902401	15.92918	670.6616	29.05144
McEachern_Cave	68000	11.84154	20.83158	4.902401	15.92918	670.6616	29.05144
McEachern_Cave	69000	11.77985	21.08287	4.75433	16.32854	643.6029	31.36124
McEachern_Cave	70000	11.77985	21.08287	4.75433	16.32854	643.6029	31.36124
McEachern_Cave	71000	12.69038	22.50703	5.487121	17.01991	691.9689	42.82301
McEachern_Cave	72000	12.69038	22.50703	5.487121	17.01991	691.9689	42.82301
McEachern_Cave	73000	12.75312	22.30784	5.732277	16.57557	710.7904	52.43281
McEachern_Cave	74000	12.75312	22.30784	5.732277	16.57557	710.7904	52.43281
McEachern_Cave	75000	12.45455	21.60713	5.277383	16.32975	705.351	55.82099
McEachern_Cave	76000	12.45455	21.60713	5.277383	16.32975	705.351	55.82099
McEachern_Cave	77000	12.47913	20.9717	5.579798	15.3919	689.589	55.31289
McEachern_Cave	78000	12.47913	20.9717	5.579798	15.3919	689.589	55.31289
McEachern_Cave	79000	12.79652	20.90418	6.041666	14.86252	670.5649	52.94234
McEachern_Cave	80000	12.79652	20.90418	6.041666	14.86252	670.5649	52.94234
McEachern_Cave	81000	12.83298	20.72065	6.008212	14.71244	705.5792	53.28144
McEachern_Cave	82000	12.83298	20.72065	6.008212	14.71244	705.5792	53.28144
McEachern_Cave	83000	13.08241	21.37173	6.356866	15.01486	703.3217	55.31289
McEachern_Cave	84000	13.08241	21.37173	6.356866	15.01486	703.3217	55.31289
McEachern_Cave	85000	12.59266	20.86761	5.939028	14.92858	715.0342	52.43281
McEachern_Cave	86000	12.59266	20.86761	5.939028	14.92858	715.0342	52.43281
McEachern_Cave	87000	12.6555	21.60684	5.84272	15.76412	711.6633	46.44834
McEachern_Cave	88000	12.6555	21.60684	5.84272	15.76412	711.6633	46.44834
McEachern_Cave	89000	12.57786	22.2083	5.412322	16.79598	698.2507	48.40944
McEachern_Cave	90000	12.57786	22.2083	5.412322	16.79598	698.2507	48.40944
McEachern_Cave	91000	12.92066	23.22146	5.213381	18.00808	684.5845	48.08083
McEachern_Cave	92000	12.92066	23.22146	5.213381	18.00808	684.5845	48.08083
McEachern_Cave	93000	12.7991	23.57797	5.199418	18.37855	663.7682	46.44834
McEachern_Cave	94000	12.7991	23.57797	5.199418	18.37855	663.7682	46.44834
McEachern_Cave	95000	12.88058	23.42105	5.204692	18.21636	637.9754	57.0167
McEachern_Cave	96000	12.88058	23.42105	5.204692	18.21636	637.9754	57.0167
McEachern_Cave	97000	12.88124	23.04024	5.269401	17.77084	645.5457	59.75378
McEachern_Cave	98000	12.88124	23.04024	5.269401	17.77084	645.5457	59.75378
McEachern_Cave	99000	13.06003	22.2268	5.859188	16.36762	660.8441	61.12747
McEachern_Cave	100000	13.06003	22.2268	5.859188	16.36762	660.8441	61.12747
Morwell	1000	12.70471	24.85665	3.734256	21.12239	825.8261	203.2756
Morwell	2000	12.93579	24.83745	4.271803	20.56565	854.698	203.2756
Morwell	3000	12.95687	24.738	4.435215	20.30279	867.9802	203.2756
Morwell	4000	12.67373	24.56423	4.398533	20.1657	919.8005	203.2756
Morwell	5000	12.72747	24.43724	4.087028	20.35021	885.3069	203.2756
Morwell	6000	12.49924	23.43088	3.689182	19.7417	855.1328	203.2756
Morwell	7000	12.63913	23.12094	3.817823	19.30312	808.3172	203.2756
Morwell	8000	12.55169	22.86021	3.88692	18.97329	816.4379	203.2756
Morwell	9000	12.33648	22.59177	3.818131	18.77364	878.4991	203.2756
Morwell	10000	12.38501	23.45292	4.00334	19.44958	898.1456	203.2756
Morwell	11000	12.34358	22.54844	3.882373	18.66607	915.9813	203.2756
Morwell	12000	11.31418	21.71964	2.398089	19.32155	930.5481	203.2756
Morwell	13000	11.39371	21.83451	2.804179	19.03033	881.0754	203.2756
Morwell	14000	11.49812	22.46325	2.940326	19.52292	935.3857	203.2756
Morwell	15000	11.35289	23.37193	2.724873	20.64706	887.2296	203.2756
Morwell	16000	10.56474	22.55093	1.630298	20.92064	887.5314	203.2756
Morwell	17000	10.89802	23.25237	1.889069	21.3633	870.4555	203.2756
Morwell	18000	10.80294	23.45249	1.640794	21.8117	838.4587	203.2756
Morwell	19000	10.81396	23.75866	1.58729	22.17137	879.3627	203.2756
Morwell	20000	10.6861	23.42701	1.355364	22.07165	900.6935	203.2756
Morwell	21000	10.66555	23.18412	1.2061245	21.97799	863.712	203.2756
Morwell	22000	10.34615	22.75232	0.8474621	21.90486	806.4921	203.2756
Morwell	23000	10.55289	23.42645	1.343055	22.0834	848.2916	203.2756
Morwell	24000	10.55289	23.42645	1.343055	22.0834	848.2916	203.2756
Morwell	25000	10.55214	22.69163	1.7283901	20.96324	922.2391	203.2756
Morwell	26000	10.55214	22.69163	1.7283901	20.96324	922.2391	203.2756
Morwell	27000	10.88883	22.37731	2.22278	20.15453	916.8764	203.2756
Morwell	28000	10.88883	22.37731	2.22278	20.15453	916.8764	203.2756
Morwell	29000	11.39175	21.43269	3.718751	17.71394	997.6516	203.2756
Morwell	30000	11.39175	21.43269	3.718751	17.71394	997.6516	203.2756
Morwell	31000	11.69807	21.87964	3.975804	17.90384	1014.7307	203.2756
Morwell	32000	11.69807	21.87964	3.975804	17.90384	1014.7307	203.2756
Morwell	33000	11.03301	21.9715	2.419498	19.552	923.0913	203.2756
Morwell	34000	11.03301	21.9715	2.419498	19.552	923.0913	203.2756
Morwell	35000	11.10766	22.43885	2.346618	20.09223	883.4611	203.2756
Morwell	36000	11.10766	22.43885	2.346618	20.09223	883.4611	203.2756
Morwell	37000	11.12409	22.97933	2.343286	20.63604	876.3052	203.2756
Morwell	38000	11.12409	22.97933	2.343286	20.63604	876.3052	203.2756
Morwell	39000	11.56707	23.70974	2.347114	21.36263	920.251	203.2756
Morwell	40000	11.56707	23.70974	2.347114	21.36263	920.251	203.2756
Morwell	41000	11.42671	23.88975	2.15868	21.73107	897.0997	203.2756
Morwell	42000	11.42671	23.88975	2.15868	21.73107	897.0997	203.2756
Morwell	43000	11.81142	23.5742	3.009873	20.56433	957.3231	203.2756
Morwell	44000	11.81142	23.5742	3.009873	20.56433	957.3231	203.2756
Morwell	45000	11.9651	23.54216	3.297141	20.24502	936.6077	203.2756
Morwell	46000	11.9651	23.54216	3.297141	20.24502	936.6077	203.2756

Morwell	47000	11.98047	23.5786	3.239478	20.33912	928.8051	203.2756
Morwell	48000	11.98047	23.5786	3.239478	20.33912	928.8051	203.2756
Morwell	49000	12.01397	23.75258	3.476399	20.27619	913.0048	203.2756
Morwell	50000	12.01397	23.75258	3.476399	20.27619	913.0048	203.2756
Morwell	51000	12.19105	23.85918	3.246925	20.61226	932.1275	203.2756
Morwell	52000	12.19105	23.85918	3.246925	20.61226	932.1275	203.2756
Morwell	53000	11.85066	23.08725	3.858037	19.22922	1003.2644	203.2756
Morwell	54000	11.85066	23.08725	3.858037	19.22922	1003.2644	203.2756
Morwell	55000	11.92853	22.47591	4.063233	18.41268	933.5988	203.2756
Morwell	56000	11.92853	22.47591	4.063233	18.41268	933.5988	203.2756
Morwell	57000	12.21763	22.72181	4.345953	18.37585	975.2208	203.2756
Morwell	58000	12.21763	22.72181	4.345953	18.37585	975.2208	203.2756
Morwell	59000	11.79674	22.06368	4.044313	18.01937	1011.4393	203.2756
Morwell	60000	11.79674	22.06368	4.044313	18.01937	1011.4393	203.2756
Morwell	61000	11.20074	22.32653	2.802489	19.52404	910.963	203.2756
Morwell	62000	11.20074	22.32653	2.802489	19.52404	910.963	203.2756
Morwell	63000	11.10719	22.41018	2.621142	19.78903	959.0259	203.2756
Morwell	64000	11.10719	22.41018	2.621142	19.78903	959.0259	203.2756
Morwell	65000	11.23446	23.04115	2.674461	20.36669	980.4067	203.2756
Morwell	66000	11.23446	23.04115	2.674461	20.36669	980.4067	203.2756
Morwell	67000	11.67707	23.00973	3.707222	19.30251	996.0953	203.2756
Morwell	68000	11.67707	23.00973	3.707222	19.30251	996.0953	203.2756
Morwell	69000	11.59844	23.1585	3.474017	19.68449	911.2817	203.2756
Morwell	70000	11.59844	23.1585	3.474017	19.68449	911.2817	203.2756
Morwell	71000	12.57655	24.76032	4.416776	20.34355	953.6174	203.2756
Morwell	72000	12.57655	24.76032	4.416776	20.34355	953.6174	203.2756
Morwell	73000	12.47908	24.11996	4.373311	19.74664	994.906	203.2756
Morwell	74000	12.47908	24.11996	4.373311	19.74664	994.906	203.2756
Morwell	75000	12.38375	23.50583	4.448882	19.05695	1034.5284	203.2756
Morwell	76000	12.38375	23.50583	4.448882	19.05695	1034.5284	203.2756
Morwell	77000	12.22546	22.70324	4.532909	18.17033	1064.4318	203.2756
Morwell	78000	12.22546	22.70324	4.532909	18.17033	1064.4318	203.2756
Morwell	79000	12.53473	22.4101	5.26182	17.14828	997.5111	203.2756
Morwell	80000	12.53473	22.4101	5.26182	17.14828	997.5111	203.2756
Morwell	81000	12.18096	21.65652	4.503254	17.15327	1021.783	203.2756
Morwell	82000	12.18096	21.65652	4.503254	17.15327	1021.783	203.2756
Morwell	83000	11.91334	22.03054	3.657789	18.37276	949.4597	203.2756
Morwell	84000	11.91334	22.03054	3.657789	18.37276	949.4597	203.2756
Morwell	85000	12.48494	22.48119	5.479596	17.00159	1062.599	203.2756
Morwell	86000	12.48494	22.48119	5.479596	17.00159	1062.599	203.2756
Morwell	87000	12.2954	23.11265	4.532998	18.57965	987.8854	203.2756
Morwell	88000	12.2954	23.11265	4.532998	18.57965	987.8854	203.2756
Morwell	89000	12.36648	24.03484	4.427484	19.60736	977.6052	203.2756
Morwell	90000	12.36648	24.03484	4.427484	19.60736	977.6052	203.2756
Morwell	91000	12.72059	25.38376	3.961953	21.42181	979.175	203.2756
Morwell	92000	12.72059	25.38376	3.961953	21.42181	979.175	203.2756
Morwell	93000	12.46259	25.41091	3.634044	21.77686	876.0339	203.2756
Morwell	94000	12.46259	25.41091	3.634044	21.77686	876.0339	203.2756
Morwell	95000	12.56483	25.23269	3.664224	21.56847	890.6921	203.2756
Morwell	96000	12.56483	25.23269	3.664224	21.56847	890.6921	203.2756
Morwell	97000	12.29795	24.33929	3.735802	20.60349	918.6904	203.2756
Morwell	98000	12.29795	24.33929	3.735802	20.60349	918.6904	203.2756
Morwell	99000	12.52362	23.78308	4.207403	19.57568	921.77	203.2756
Morwell	100000	12.52362	23.78308	4.207403	19.57568	921.77	203.2756
Rockhampton	1000	22.13127	32.46991	9.785522	22.68438	973.6601	60.48322
Rockhampton	2000	21.90201	31.92963	9.558422	22.37121	940.6354	58.5
Rockhampton	3000	21.94837	31.89144	9.617606	22.27383	880.1387	53.6098
Rockhampton	4000	21.56664	31.51329	9.347594	22.1657	897.2151	49.73188
Rockhampton	5000	22.199	32.05088	10.256283	21.79459	714.3323	48.4321
Rockhampton	6000	21.83512	31.72696	9.81012	21.91684	784.1558	46.31926
Rockhampton	7000	21.49144	31.34548	9.383114	21.96237	1042.0793	30.49417
Rockhampton	8000	21.66955	31.13731	9.922604	21.21471	1022.4043	29.61775
Rockhampton	9000	21.8339	31.27356	10.527234	20.74632	807.1882	29.3948
Rockhampton	10000	21.95384	31.08385	10.724799	20.35905	709.5452	28.54445
Rockhampton	11000	22.04329	30.52349	11.746784	18.77671	818.1718	28.54445
Rockhampton	12000	21.31972	30.41368	10.15834	20.25534	737.9657	28.54445
Rockhampton	13000	21.16263	30.63257	9.333241	21.29933	724.1471	28.54445
Rockhampton	14000	20.83319	30.16298	9.337835	20.82514	810.3118	28.54445
Rockhampton	15000	20.49856	29.93214	8.506867	21.42527	800.4586	28.54445
Rockhampton	16000	19.21747	29.2859	6.76956	22.51634	822.4504	28.54445
Rockhampton	17000	18.54992	29.07035	5.599026	23.47132	830.3702	28.54445
Rockhampton	18000	18.49002	29.72894	4.145184	25.58375	724.4694	28.54445
Rockhampton	19000	18.07679	29.54267	3.66859	25.87407	759.9825	28.54445
Rockhampton	20000	18.16104	29.50674	3.517095	25.98965	737.9102	28.54445
Rockhampton	21000	18.05357	29.17042	3.524976	25.64544	748.0905	28.54445
Rockhampton	22000	17.73491	29.11341	3.065204	26.04821	714.3575	28.54445
Rockhampton	23000	18.06237	29.22633	3.68983	25.5365	820.0468	28.54445
Rockhampton	24000	18.06237	29.22633	3.68983	25.5365	820.0468	28.54445
Rockhampton	25000	17.83371	28.82375	4.338556	24.48519	875.8	28.54445
Rockhampton	26000	17.83371	28.82375	4.338556	24.48519	875.8	28.54445
Rockhampton	27000	18.80718	29.1128	5.087154	24.02565	848.9592	28.54445
Rockhampton	28000	18.80718	29.1128	5.087154	24.02565	848.9592	28.54445
Rockhampton	29000	19.26102	28.89511	6.696293	22.19882	861.9782	28.54445
Rockhampton	30000	19.26102	28.89511	6.696293	22.19882	861.9782	28.54445
Rockhampton	31000	19.32058	28.82563	6.931358	21.89427	921.6142	28.54445
Rockhampton	32000	19.32058	28.82563	6.931358	21.89427	921.6142	28.54445
Rockhampton	33000	19.22565	28.64152	7.266069	21.37545	940.7484	28.54445
Rockhampton	34000	19.22565	28.64152	7.266069	21.37545	940.7484	28.54445
Rockhampton	35000	19.6541	29.2552	7.944849	21.31035	852.0897	28.54445
Rockhampton	36000	19.6541	29.2552	7.944849	21.31035	852.0897	28.54445
Rockhampton	37000	19.7128	29.51674	7.908665	21.60807	892.1142	28.54445
Rockhampton	38000	19.7128	29.51674	7.908665	21.60807	892.1142	28.54445
Rockhampton	39000	19.14346	29.63407	6.01928	23.61479	893.0568	28.54445
Rockhampton	40000	19.14346	29.63407	6.01928	23.61479	893.0568	28.54445
Rockhampton	41000	19.2312	29.71537	5.799106	23.91627	873.0388	28.54445
Rockhampton	42000	19.2312	29.71537	5.799106	23.91627	873.0388	28.54445
Rockhampton	43000	19.74745	30.2021	6.293947	23.90815	888.9932	28.54445
Rockhampton	44000	19.74745	30.2021	6.293947	23.90815	888.9932	28.54445
Rockhampton	45000	19.75313	30.54836	6.047522	24.50083	800.3154	28.54445
Rockhampton	46000	19.75313	30.54836	6.047522	24.50083	800.3154	28.54445
Rockhampton	47000	19.1654	30.29677	4.820292	25.47648	903.7048	28.54445
Rockhampton	48000	19.1654	30.29677	4.820292	25.47648	903.7048	28.54445
Rockhampton	49000	20.64224	30.98188	6.536458	24.44542	735.0768	28.54445
Rockhampton	50000	20.64224	30.98188	6.536458	24.44542	735.0768	28.54445
Rockhampton	51000	20.17813	30.16462	6.424764	23.73985	756.8297	28.54445

Rockhampton	52000	20.17813	30.16462	6.424764	23.73985	756.8297	28.54445
Rockhampton	53000	20.06496	30.05814	7.110634	22.94751	852.1879	28.54445
Rockhampton	54000	20.06496	30.05814	7.110634	22.94751	852.1879	28.54445
Rockhampton	55000	20.67552	30.37704	8.001807	22.37523	788.9348	28.54445
Rockhampton	56000	20.67552	30.37704	8.001807	22.37523	788.9348	28.54445
Rockhampton	57000	21.04893	30.12157	8.765532	21.35604	758.2075	28.54445
Rockhampton	58000	21.04893	30.12157	8.765532	21.35604	758.2075	28.54445
Rockhampton	59000	20.18906	29.20307	8.210652	20.99242	847.5136	28.54445
Rockhampton	60000	20.18906	29.20307	8.210652	20.99242	847.5136	28.54445
Rockhampton	61000	19.27697	28.64778	7.191448	21.45633	893.051	28.54445
Rockhampton	62000	19.27697	28.64778	7.191448	21.45633	893.051	28.54445
Rockhampton	63000	19.3487	28.72095	7.874331	20.84662	944.0009	28.54445
Rockhampton	64000	19.3487	28.72095	7.874331	20.84662	944.0009	28.54445
Rockhampton	65000	18.90805	29.18183	6.185406	22.99643	919.2919	28.54445
Rockhampton	66000	18.90805	29.18183	6.185406	22.99643	919.2919	28.54445
Rockhampton	67000	19.54319	30.1683	6.320681	23.84762	787.2469	28.54445
Rockhampton	68000	19.54319	30.1683	6.320681	23.84762	787.2469	28.54445
Rockhampton	69000	20.18283	30.78926	7.150046	23.63921	817.2625	28.54445
Rockhampton	70000	20.18283	30.78926	7.150046	23.63921	817.2625	28.54445
Rockhampton	71000	20.87086	31.52645	7.432156	24.0943	895.6539	28.54445
Rockhampton	72000	20.87086	31.52645	7.432156	24.0943	895.6539	28.54445
Rockhampton	73000	21.34495	31.72348	8.239056	23.48442	821.0416	28.54445
Rockhampton	74000	21.34495	31.72348	8.239056	23.48442	821.0416	28.54445
Rockhampton	75000	21.16308	30.93783	8.138647	22.79918	754.7357	28.54445
Rockhampton	76000	21.16308	30.93783	8.138647	22.79918	754.7357	28.54445
Rockhampton	77000	21.09188	30.59744	8.048719	22.54872	764.4056	28.54445
Rockhampton	78000	21.09188	30.59744	8.048719	22.54872	764.4056	28.54445
Rockhampton	79000	21.61598	30.37242	9.611651	20.76077	743.6302	28.54445
Rockhampton	80000	21.61598	30.37242	9.611651	20.76077	743.6302	28.54445
Rockhampton	81000	21.47837	30.05336	10.046852	20.00651	792.3893	28.54445
Rockhampton	82000	21.47837	30.05336	10.046852	20.00651	792.3893	28.54445
Rockhampton	83000	21.6306	30.2903	11.471539	18.81876	796.6544	28.54445
Rockhampton	84000	21.6306	30.2903	11.471539	18.81876	796.6544	28.54445
Rockhampton	85000	21.73971	30.51779	11.013501	19.50429	848.2335	28.54445
Rockhampton	86000	21.73971	30.51779	11.013501	19.50429	848.2335	28.54445
Rockhampton	87000	20.65143	30.62028	9.302576	21.3177	971.3602	28.54445
Rockhampton	88000	20.65143	30.62028	9.302576	21.3177	971.3602	28.54445
Rockhampton	89000	20.8827	31.25001	7.880649	23.36936	906.1409	28.54445
Rockhampton	90000	20.8827	31.25001	7.880649	23.36936	906.1409	28.54445
Rockhampton	91000	21.41663	32.56275	7.284397	25.27835	824.3748	28.54445
Rockhampton	92000	21.41663	32.56275	7.284397	25.27835	824.3748	28.54445
Rockhampton	93000	21.12506	32.3618	7.03969	25.32211	885.7458	28.54445
Rockhampton	94000	21.12506	32.3618	7.03969	25.32211	885.7458	28.54445
Rockhampton	95000	21.46798	32.87597	6.869125	26.00685	820.92	28.54445
Rockhampton	96000	21.46798	32.87597	6.869125	26.00685	820.92	28.54445
Rockhampton	97000	21.13377	31.83447	6.939999	24.89447	769.9094	28.98991
Rockhampton	98000	21.13377	31.83447	6.939999	24.89447	769.9094	28.98991
Rockhampton	99000	21.8339	31.27356	10.527234	20.74632	807.1882	29.3948
Rockhampton	100000	21.83858	32.22695	8.235761	23.99119	702.8977	29.09663
South_Walker_Creek	1000	20.83133	32.02835	7.498617	24.52973	975.2863	296.9644
South_Walker_Creek	2000	20.65674	31.46409	7.38088	24.08321	962.0165	296.9644
South_Walker_Creek	3000	20.77273	31.5562	7.503648	24.05255	877.157	296.9644
South_Walker_Creek	4000	20.4403	31.2664	7.273206	23.99319	932.0151	296.9644
South_Walker_Creek	5000	21.17957	31.78243	8.260751	23.52168	854.8489	296.9644
South_Walker_Creek	6000	20.63662	31.66774	7.287242	24.3805	810.0821	296.9644
South_Walker_Creek	7000	20.45682	31.07804	7.391272	23.68677	1014.4091	296.9644
South_Walker_Creek	8000	20.64449	31.10098	8.014247	23.08673	1006.7997	296.9644
South_Walker_Creek	9000	20.6032	31.15001	8.055602	23.09441	863.8716	296.9644
South_Walker_Creek	10000	21.03036	30.83577	8.887691	21.94807	882.5091	296.9644
South_Walker_Creek	11000	21.14996	30.85793	8.872233	21.9857	839.1193	296.9644
South_Walker_Creek	12000	20.73767	30.71508	8.563468	22.15161	768.8173	296.9644
South_Walker_Creek	13000	20.4933	30.76166	7.615601	23.14606	760.7704	296.9644
South_Walker_Creek	14000	20.08008	30.33645	7.447004	22.88945	820.9799	296.9644
South_Walker_Creek	15000	19.42924	29.67207	6.642943	23.02913	797.4689	296.9644
South_Walker_Creek	16000	18.51022	29.07489	5.741467	23.33342	837.9603	296.9644
South_Walker_Creek	17000	18.29763	28.8274	5.860178	22.96722	937.2797	296.9644
South_Walker_Creek	18000	18.32854	29.55465	4.672053	24.8826	850.7343	296.9644
South_Walker_Creek	19000	17.90942	29.53494	4.217696	25.31725	892.0278	296.9644
South_Walker_Creek	20000	18.03056	29.40967	4.035728	25.37394	862.9201	296.9644
South_Walker_Creek	21000	17.85214	29.03058	3.70287	25.32771	849.8763	296.9644
South_Walker_Creek	22000	17.57593	28.97092	3.069409	25.90151	820.8049	296.9644
South_Walker_Creek	23000	17.85784	28.99237	3.799433	25.19294	909.9036	296.9644
South_Walker_Creek	24000	17.85784	28.99237	3.799433	25.19294	909.9036	296.9644
South_Walker_Creek	25000	17.54441	28.63125	4.455698	24.17555	950.6416	296.9644
South_Walker_Creek	26000	17.54441	28.63125	4.455698	24.17555	950.6416	296.9644
South_Walker_Creek	27000	18.53468	29.00625	4.870816	24.13543	895.8975	296.9644
South_Walker_Creek	28000	18.53468	29.00625	4.870816	24.13543	895.8975	296.9644
South_Walker_Creek	29000	18.87979	28.94412	6.310335	22.63379	951.4189	296.9644
South_Walker_Creek	30000	18.87979	28.94412	6.310335	22.63379	951.4189	296.9644
South_Walker_Creek	31000	19.09562	28.95412	6.681314	22.2728	945.6777	296.9644
South_Walker_Creek	32000	19.09562	28.95412	6.681314	22.2728	945.6777	296.9644
South_Walker_Creek	33000	18.72662	28.52799	6.75064	21.77735	974.1265	296.9644
South_Walker_Creek	34000	18.72662	28.52799	6.75064	21.77735	974.1265	296.9644
South_Walker_Creek	35000	18.96647	29.13762	6.842947	22.29468	882.3459	296.9644
South_Walker_Creek	36000	18.96647	29.13762	6.842947	22.29468	882.3459	296.9644
South_Walker_Creek	37000	18.8426	29.1167	6.57492	22.54178	920.8994	296.9644
South_Walker_Creek	38000	18.8426	29.1167	6.57492	22.54178	920.8994	296.9644
South_Walker_Creek	39000	18.74474	29.36113	5.909972	23.45116	979.8618	296.9644
South_Walker_Creek	40000	18.74474	29.36113	5.909972	23.45116	979.8618	296.9644
South_Walker_Creek	41000	18.73866	29.4843	5.244299	24.24	926.088	296.9644
South_Walker_Creek	42000	18.73866	29.4843	5.244299	24.24	926.088	296.9644
South_Walker_Creek	43000	18.85925	29.92314	4.930462	24.99267	921.839	296.9644
South_Walker_Creek	44000	18.85925	29.92314	4.930462	24.99267	921.839	296.9644
South_Walker_Creek	45000	19.13791	30.53325	4.932345	25.6009	870.278	296.9644
South_Walker_Creek	46000	19.13791	30.53325	4.932345	25.6009	870.278	296.9644
South_Walker_Creek	47000	18.60278	30.16643	4.124308	26.04212	951.5393	296.9644
South_Walker_Creek	48000	18.60278	30.16643	4.124308	26.04212	951.5393	296.9644
South_Walker_Creek	49000	19.58234	30.8633	4.556691	26.30661	751.6265	296.9644
South_Walker_Creek	50000	19.58234	30.8633	4.556691	26.30661	751.6265	296.9644
South_Walker_Creek	51000	19.47774	30.3001	4.779497	25.52061	825.694	296.9644
South_Walker_Creek	52000	19.47774	30.3001	4.779497	25.52061	825.694	296.9644
South_Walker_Creek	53000	19.19921	30.03986	5.285271	24.75459	886.6633	296.9644
South_Walker_Creek	54000	19.19921	30.03986	5.285271	24.75459	886.6633	296.9644
South_Walker_Creek	55000	19.68617	30.29469	6.112593	24.1821	812.2233	296.9644
South_Walker_Creek	56000	19.68617	30.29469	6.112593	24.1821	812.2233	296.9644

South_Walker_Creek	57000	20.12334	30.28686	6.866334	23.42052	774.6726	296.9644
South_Walker_Creek	58000	20.12334	30.28686	6.866334	23.42052	774.6726	296.9644
South_Walker_Creek	59000	19.39231	29.17503	6.681088	22.49394	863.7833	296.9644
South_Walker_Creek	60000	19.39231	29.17503	6.681088	22.49394	863.7833	296.9644
South_Walker_Creek	61000	18.89245	28.61608	6.888484	21.7276	940.7583	296.9644
South_Walker_Creek	62000	18.89245	28.61608	6.888484	21.7276	940.7583	296.9644
South_Walker_Creek	63000	18.85699	28.54431	7.674269	20.87004	1005.7493	296.9644
South_Walker_Creek	64000	18.85699	28.54431	7.674269	20.87004	1005.7493	296.9644
South_Walker_Creek	65000	18.62795	28.90681	6.512156	22.39465	990.4564	296.9644
South_Walker_Creek	66000	18.62795	28.90681	6.512156	22.39465	990.4564	296.9644
South_Walker_Creek	67000	19.24483	30.29089	6.115119	24.17577	886.4923	296.9644
South_Walker_Creek	68000	19.24483	30.29089	6.115119	24.17577	886.4923	296.9644
South_Walker_Creek	69000	19.34025	30.59727	5.579468	25.01781	877.8013	296.9644
South_Walker_Creek	70000	19.34025	30.59727	5.579468	25.01781	877.8013	296.9644
South_Walker_Creek	71000	19.6846	31.29514	5.237109	26.05803	912.8068	296.9644
South_Walker_Creek	72000	19.6846	31.29514	5.237109	26.05803	912.8068	296.9644
South_Walker_Creek	73000	20.26219	31.61567	6.218843	25.39682	860.8771	296.9644
South_Walker_Creek	74000	20.26219	31.61567	6.218843	25.39682	860.8771	296.9644
South_Walker_Creek	75000	20.12405	31.04305	5.936295	25.10676	777.0225	296.9644
South_Walker_Creek	76000	20.12405	31.04305	5.936295	25.10676	777.0225	296.9644
South_Walker_Creek	77000	20.07988	30.68929	5.96098	24.72831	807.2613	296.9644
South_Walker_Creek	78000	20.07988	30.68929	5.96098	24.72831	807.2613	296.9644
South_Walker_Creek	79000	20.68398	30.51635	7.744302	22.77205	751.0934	296.9644
South_Walker_Creek	80000	20.68398	30.51635	7.744302	22.77205	751.0934	296.9644
South_Walker_Creek	81000	20.62217	30.18731	8.187522	21.99978	802.6785	296.9644
South_Walker_Creek	82000	20.62217	30.18731	8.187522	21.99978	802.6785	296.9644
South_Walker_Creek	83000	21.01119	30.46036	9.935355	20.52501	801.5793	296.9644
South_Walker_Creek	84000	21.01119	30.46036	9.935355	20.52501	801.5793	296.9644
South_Walker_Creek	85000	20.7223	30.27255	9.507555	20.765	849.6055	296.9644
South_Walker_Creek	86000	20.7223	30.27255	9.507555	20.765	849.6055	296.9644
South_Walker_Creek	87000	19.78665	30.48964	8.042446	22.4472	1010.0717	296.9644
South_Walker_Creek	88000	19.78665	30.48964	8.042446	22.4472	1010.0717	296.9644
South_Walker_Creek	89000	19.76252	30.90638	6.062113	24.84426	934.0051	296.9644
South_Walker_Creek	90000	19.76252	30.90638	6.062113	24.84426	934.0051	296.9644
South_Walker_Creek	91000	20.21296	32.30421	5.077241	27.22697	878.4196	296.9644
South_Walker_Creek	92000	20.21296	32.30421	5.077241	27.22697	878.4196	296.9644
South_Walker_Creek	93000	19.9473	32.09183	4.658245	27.43359	924.5728	296.9644
South_Walker_Creek	94000	19.9473	32.09183	4.658245	27.43359	924.5728	296.9644
South_Walker_Creek	95000	20.373	32.79049	4.56075	28.22974	823.2569	296.9644
South_Walker_Creek	96000	20.373	32.79049	4.56075	28.22974	823.2569	296.9644
South_Walker_Creek	97000	20.21738	31.92322	4.829113	27.0941	794.7776	296.9644
South_Walker_Creek	98000	20.21738	31.92322	4.829113	27.0941	794.7776	296.9644
South_Walker_Creek	99000	20.95985	32.52004	6.107705	26.41234	743.9541	296.9644
South_Walker_Creek	100000	20.95985	32.52004	6.107705	26.41234	743.9541	296.9644
Spring_Creek	1000	13.83522	24.70001	5.496933	19.20308	658.6118	85.39286
Spring_Creek	2000	14.00059	24.54985	5.991376	18.55847	710.2686	84.06565
Spring_Creek	3000	14.06766	24.55121	6.064485	18.48672	677.9615	83.46515
Spring_Creek	4000	13.84719	24.27124	6.065528	18.20572	718.5605	82.01786
Spring_Creek	5000	13.81513	24.20316	6.011889	18.19127	740.614	81.41654
Spring_Creek	6000	13.61969	23.25791	5.685652	17.57226	691.105	80.32944
Spring_Creek	7000	13.79185	23.32023	5.774645	17.54559	666.723	78.76538
Spring_Creek	8000	13.62132	22.75445	5.608251	17.1462	683.734	76.85594
Spring_Creek	9000	13.38978	22.13425	6.074544	16.05971	713.6675	74.7326
Spring_Creek	10000	13.51276	23.27453	5.721611	17.55292	718.8608	68.85313
Spring_Creek	11000	13.32883	22.18297	5.811635	16.37133	724.0272	62.37112
Spring_Creek	12000	12.902	22.02027	5.175614	16.84466	710.3072	55.52731
Spring_Creek	13000	12.59224	21.76755	4.981358	16.78619	687.5956	55.28587
Spring_Creek	14000	12.62478	22.31702	4.980783	17.33624	677.8603	55.14778
Spring_Creek	15000	11.71467	21.53269	4.144393	17.38829	644.1693	55.14778
Spring_Creek	16000	10.98782	21.18833	3.027956	18.16037	683.8204	55.14778
Spring_Creek	17000	11.31841	22.49709	3.181907	19.31518	641.7701	55.14778
Spring_Creek	18000	11.14716	21.9343	3.050823	18.88348	645.0394	55.14778
Spring_Creek	19000	11.35031	22.48591	3.047086	19.43882	629.5984	55.14778
Spring_Creek	20000	11.10764	22.19035	2.911438	19.27891	674.8824	55.14778
Spring_Creek	21000	11.15533	21.80297	2.583679	19.21929	624.2827	55.14778
Spring_Creek	22000	10.73325	21.12457	2.154127	18.97044	592.975	55.14778
Spring_Creek	23000	11.1315	22.46183	2.877034	19.5848	637.9139	55.14778
Spring_Creek	24000	11.1315	22.46183	2.877034	19.5848	637.9139	55.14778
Spring_Creek	25000	11.28978	22.21675	3.199198	19.01755	664.3677	55.14778
Spring_Creek	26000	11.28978	22.21675	3.199198	19.01755	664.3677	55.14778
Spring_Creek	27000	11.49029	21.55093	3.75163	17.7993	650.4204	55.14778
Spring_Creek	28000	11.49029	21.55093	3.75163	17.7993	650.4204	55.14778
Spring_Creek	29000	11.59143	20.921	4.185618	16.73538	696.6213	55.14778
Spring_Creek	30000	11.59143	20.921	4.185618	16.73538	696.6213	55.14778
Spring_Creek	31000	11.95779	21.42884	4.511288	16.91756	699.5879	55.14778
Spring_Creek	32000	11.95779	21.42884	4.511288	16.91756	699.5879	55.14778
Spring_Creek	33000	11.71921	21.05048	4.090798	16.95968	659.2299	55.14778
Spring_Creek	34000	11.71921	21.05048	4.090798	16.95968	659.2299	55.14778
Spring_Creek	35000	11.77885	21.77571	4.063365	17.71235	659.4142	55.14778
Spring_Creek	36000	11.77885	21.77571	4.063365	17.71235	659.4142	55.14778
Spring_Creek	37000	11.81962	21.70503	4.210619	17.49441	664.6917	55.14778
Spring_Creek	38000	11.81962	21.70503	4.210619	17.49441	664.6917	55.14778
Spring_Creek	39000	12.10626	22.82026	3.924819	18.89544	657.9233	55.14778
Spring_Creek	40000	12.10626	22.82026	3.924819	18.89544	657.9233	55.14778
Spring_Creek	41000	11.97813	22.89193	3.75547	19.13646	648.3715	55.14778
Spring_Creek	42000	11.97813	22.89193	3.75547	19.13646	648.3715	55.14778
Spring_Creek	43000	12.1319	23.00267	4.041571	18.9611	687.9805	55.14778
Spring_Creek	44000	12.1319	23.00267	4.041571	18.9611	687.9805	55.14778
Spring_Creek	45000	12.32598	23.1332	3.947214	19.18599	679.4899	55.14778
Spring_Creek	46000	12.32598	23.1332	3.947214	19.18599	679.4899	55.14778
Spring_Creek	47000	12.35618	23.28261	3.909801	19.37281	643.6973	55.14778
Spring_Creek	48000	12.35618	23.28261	3.909801	19.37281	643.6973	55.14778
Spring_Creek	49000	12.28034	23.11562	4.006038	19.10958	655.2008	55.28587
Spring_Creek	50000	12.28034	23.11562	4.006038	19.10958	655.2008	55.28587
Spring_Creek	51000	12.58053	23.44289	4.313227	19.12966	664.8429	55.28587
Spring_Creek	52000	12.58053	23.44289	4.313227	19.12966	664.8429	55.28587
Spring_Creek	53000	12.18937	22.46234	4.310679	18.15166	697.3799	55.14778
Spring_Creek	54000	12.18937	22.46234	4.310679	18.15166	697.3799	55.14778
Spring_Creek	55000	12.21205	21.91606	4.779377	17.13668	661.6468	55.14778
Spring_Creek	56000	12.21205	21.91606	4.779377	17.13668	661.6468	55.14778
Spring_Creek	57000	12.53194	22.2121	4.861472	17.35062	698.8205	55.14778
Spring_Creek	58000	12.53194	22.2121	4.861472	17.35062	698.8205	55.14778
Spring_Creek	59000	12.09818	21.41636	4.749742	16.66662	710.2961	55.14778
Spring_Creek	60000	12.09818	21.41636	4.749742	16.66662	710.2961	55.14778
Spring_Creek	61000	11.81868	21.41614	4.373425	17.04272	671.8735	55.14778

Spring_Creek	62000	11.81868	21.41614	4.373425	17.04272	671.8735	55.14778
Spring_Creek	63000	11.6487	21.62049	4.061942	17.55854	670.8434	55.14778
Spring_Creek	64000	11.6487	21.62049	4.061942	17.55854	670.8434	55.14778
Spring_Creek	65000	11.67946	22.20291	3.912825	18.29008	713.4247	55.14778
Spring_Creek	66000	11.67946	22.20291	3.912825	18.29008	713.4247	55.14778
Spring_Creek	67000	11.84064	22.43863	4.065374	18.37325	705.4695	55.28587
Spring_Creek	68000	11.84064	22.43863	4.065374	18.37325	705.4695	55.28587
Spring_Creek	69000	11.89563	22.51186	4.155913	18.35594	664.0392	55.28587
Spring_Creek	70000	11.89563	22.51186	4.155913	18.35594	664.0392	55.28587
Spring_Creek	71000	12.84298	24.04432	4.989961	19.05436	698.5035	57.14609
Spring_Creek	72000	12.84298	24.04432	4.989961	19.05436	698.5035	57.14609
Spring_Creek	73000	12.96194	23.82569	5.299169	18.52652	731.184	64.02063
Spring_Creek	74000	12.96194	23.82569	5.299169	18.52652	731.184	64.02063
Spring_Creek	75000	12.67355	23.04649	4.895525	18.15097	740.4109	67.08897
Spring_Creek	76000	12.67355	23.04649	4.895525	18.15097	740.4109	67.08897
Spring_Creek	77000	12.64224	22.2064	5.180242	17.02616	728.1091	66.73658
Spring_Creek	78000	12.64224	22.2064	5.180242	17.02616	728.1091	66.73658
Spring_Creek	79000	13.00701	22.19623	5.72107	16.47516	694.8123	64.25669
Spring_Creek	80000	13.00701	22.19623	5.72107	16.47516	694.8123	64.25669
Spring_Creek	81000	12.8864	21.65093	5.409362	16.24157	727.0928	65.08344
Spring_Creek	82000	12.8864	21.65093	5.409362	16.24157	727.0928	65.08344
Spring_Creek	83000	13.14981	22.01861	5.873983	16.14463	723.9	66.73658
Spring_Creek	84000	13.14981	22.01861	5.873983	16.14463	723.9	66.73658
Spring_Creek	85000	12.76492	22.11376	5.642101	16.47166	752.8342	64.02063
Spring_Creek	86000	12.76492	22.11376	5.642101	16.47166	752.8342	64.02063
Spring_Creek	87000	12.78445	22.93325	5.285954	17.6473	734.6475	58.40367
Spring_Creek	88000	12.78445	22.93325	5.285954	17.6473	734.6475	58.40367
Spring_Creek	89000	12.73722	23.65689	4.953279	18.70361	720.4703	61.07891
Spring_Creek	90000	12.73722	23.65689	4.953279	18.70361	720.4703	61.07891
Spring_Creek	91000	13.14724	24.78445	4.728635	20.05581	704.5743	60.60961
Spring_Creek	92000	13.14724	24.78445	4.728635	20.05581	704.5743	60.60961
Spring_Creek	93000	13.00667	25.20908	4.699965	20.50912	669.8277	58.40367
Spring_Creek	94000	13.00667	25.20908	4.699965	20.50912	669.8277	58.40367
Spring_Creek	95000	13.09164	24.93422	4.768437	20.16578	649.7379	67.55794
Spring_Creek	96000	13.09164	24.93422	4.768437	20.16578	649.7379	67.55794
Spring_Creek	97000	13.0382	24.44084	4.763207	19.67763	654.8939	70.73924
Spring_Creek	98000	13.0382	24.44084	4.763207	19.67763	654.8939	70.73924
Spring_Creek	99000	13.25248	23.50955	5.442618	18.06693	678.4122	71.67984
Spring_Creek	100000	13.25248	23.50955	5.442618	18.06693	678.4122	71.67984
Strathdownie	1000	13.57373	25.88059	4.856124	21.02447	644.054	82.97334
Strathdownie	2000	13.72052	25.71977	5.318244	20.40153	697.2743	82.97334
Strathdownie	3000	13.74139	25.63533	5.3566	20.27873	662.5064	82.97334
Strathdownie	4000	13.55022	25.42	5.392956	20.02704	708.446	82.97334
Strathdownie	5000	13.50865	25.2268	5.365706	19.86109	735.0766	82.97334
Strathdownie	6000	13.31495	24.41212	5.002111	19.41001	685.7188	82.97334
Strathdownie	7000	13.53175	24.47691	5.206565	19.27035	639.639	82.97334
Strathdownie	8000	13.36843	23.93227	5.000268	18.932	663.7549	82.97334
Strathdownie	9000	13.04856	23.32633	5.336101	17.99022	703.4619	82.97334
Strathdownie	10000	13.14432	24.26255	4.971107	19.29145	703.2275	82.97334
Strathdownie	11000	12.98668	23.37666	5.085504	18.29116	707.394	82.97334
Strathdownie	12000	12.45719	22.98383	4.385919	18.59791	671.7231	82.97334
Strathdownie	13000	12.24738	22.87247	4.242015	18.63046	650.679	82.97334
Strathdownie	14000	12.29395	23.47401	4.267855	19.20616	639.4055	82.97334
Strathdownie	15000	11.6275	23.04187	3.601084	19.44078	598.7113	82.97334
Strathdownie	16000	10.84795	22.56817	2.427356	20.14081	642.6822	82.97334
Strathdownie	17000	11.27432	23.98406	2.622172	21.36189	595.3712	82.97334
Strathdownie	18000	11.09999	23.42402	2.548825	20.8752	594.9004	82.97334
Strathdownie	19000	11.30271	23.95982	2.501904	21.45791	581.1479	82.97334
Strathdownie	20000	11.07613	23.69127	2.393043	21.29822	625.0796	82.97334
Strathdownie	21000	11.17834	23.40199	2.068773	21.33321	581.5159	82.97334
Strathdownie	22000	10.77493	22.80029	1.656981	21.14331	552.0961	82.97334
Strathdownie	23000	11.11285	23.94716	2.344387	21.60277	594.189	82.97334
Strathdownie	24000	11.11285	23.94716	2.344387	21.60277	594.189	82.97334
Strathdownie	25000	11.24311	23.64173	2.634452	21.00727	612.1708	82.97334
Strathdownie	26000	11.24311	23.64173	2.634452	21.00727	612.1708	82.97334
Strathdownie	27000	11.42455	23.00634	3.170351	19.83599	594.7319	82.97334
Strathdownie	28000	11.42455	23.00634	3.170351	19.83599	594.7319	82.97334
Strathdownie	29000	11.60202	22.50043	3.685899	18.81453	648.867	82.97334
Strathdownie	30000	11.60202	22.50043	3.685899	18.81453	648.867	82.97334
Strathdownie	31000	11.92888	22.90013	4.022075	18.87805	651.6102	82.97334
Strathdownie	32000	11.92888	22.90013	4.022075	18.87805	651.6102	82.97334
Strathdownie	33000	11.61471	22.46067	3.546561	18.91411	608.587	82.97334
Strathdownie	34000	11.61471	22.46067	3.546561	18.91411	608.587	82.97334
Strathdownie	35000	11.65737	23.17163	3.4958	19.67583	609.0965	82.97334
Strathdownie	36000	11.65737	23.17163	3.4958	19.67583	609.0965	82.97334
Strathdownie	37000	11.67746	23.08206	3.612021	19.47004	617.6335	82.97334
Strathdownie	38000	11.67746	23.08206	3.612021	19.47004	617.6335	82.97334
Strathdownie	39000	12.05847	24.30994	3.42044	20.8895	602.2731	82.97334
Strathdownie	40000	12.05847	24.30994	3.42044	20.8895	602.2731	82.97334
Strathdownie	41000	11.92064	24.34282	3.218413	21.1244	597.8538	82.97334
Strathdownie	42000	11.92064	24.34282	3.218413	21.1244	597.8538	82.97334
Strathdownie	43000	12.0781	24.45391	3.575214	20.8787	643.6303	82.97334
Strathdownie	44000	12.0781	24.45391	3.575214	20.8787	643.6303	82.97334
Strathdownie	45000	12.30109	24.63574	3.474048	21.16169	633.8223	82.97334
Strathdownie	46000	12.30109	24.63574	3.474048	21.16169	633.8223	82.97334
Strathdownie	47000	12.38269	24.87035	3.449843	21.42051	599.2501	82.97334
Strathdownie	48000	12.38269	24.87035	3.449843	21.42051	599.2501	82.97334
Strathdownie	49000	12.24319	24.62679	3.527582	21.09921	610.7126	82.97334
Strathdownie	50000	12.24319	24.62679	3.527582	21.09921	610.7126	82.97334
Strathdownie	51000	12.53542	24.95855	3.880827	21.07772	619.2721	82.97334
Strathdownie	52000	12.53542	24.95855	3.880827	21.07772	619.2721	82.97334
Strathdownie	53000	12.1421	23.94759	3.763156	20.18443	651.2055	82.97334
Strathdownie	54000	12.1421	23.94759	3.763156	20.18443	651.2055	82.97334
Strathdownie	55000	12.16463	23.46272	4.263308	19.19942	617.9431	82.97334
Strathdownie	56000	12.16463	23.46272	4.263308	19.19942	617.9431	82.97334
Strathdownie	57000	12.46726	23.69561	4.371849	19.32376	656.5477	82.97334
Strathdownie	58000	12.46726	23.69561	4.371849	19.32376	656.5477	82.97334
Strathdownie	59000	12.02488	22.85604	4.290405	18.56564	662.3447	82.97334
Strathdownie	60000	12.02488	22.85604	4.290405	18.56564	662.3447	82.97334
Strathdownie	61000	11.74112	22.8755	3.780483	19.09502	621.9592	82.97334
Strathdownie	62000	11.74112	22.8755	3.780483	19.09502	621.9592	82.97334
Strathdownie	63000	11.56599	23.09877	3.489515	19.60925	620.554	82.97334
Strathdownie	64000	11.56599	23.09877	3.489515	19.60925	620.554	82.97334
Strathdownie	65000	11.65481	23.71753	3.370541	20.34699	653.7647	82.97334
Strathdownie	66000	11.65481	23.71753	3.370541	20.34699	653.7647	82.97334

Strathdownie	67000	11.86861	24.02135	3.581248	20.4401	655.2706	82.97334
Strathdownie	68000	11.86861	24.02135	3.581248	20.4401	655.2706	82.97334
Strathdownie	69000	11.87306	24.03187	3.661573	20.37029	622.6459	82.97334
Strathdownie	70000	11.87306	24.03187	3.661573	20.37029	622.6459	82.97334
Strathdownie	71000	12.88075	25.68559	4.601751	21.08384	665.1644	82.97334
Strathdownie	72000	12.88075	25.68559	4.601751	21.08384	665.1644	82.97334
Strathdownie	73000	12.90454	25.28665	4.826542	20.4601	687.6149	82.97334
Strathdownie	74000	12.90454	25.28665	4.826542	20.4601	687.6149	82.97334
Strathdownie	75000	12.63452	24.54039	4.43419	20.1062	689.272	82.97334
Strathdownie	76000	12.63452	24.54039	4.43419	20.1062	689.272	82.97334
Strathdownie	77000	12.57901	23.67538	4.678679	18.9967	674.4808	82.97334
Strathdownie	78000	12.57901	23.67538	4.678679	18.9967	674.4808	82.97334
Strathdownie	79000	12.96853	23.67518	5.231881	18.4433	655.1234	82.97334
Strathdownie	80000	12.96853	23.67518	5.231881	18.4433	655.1234	82.97334
Strathdownie	81000	12.77678	23.01181	4.938633	18.07318	689.3612	82.97334
Strathdownie	82000	12.77678	23.01181	4.938633	18.07318	689.3612	82.97334
Strathdownie	83000	12.76754	23.05844	5.134103	17.92434	687.0129	82.97334
Strathdownie	84000	12.76754	23.05844	5.134103	17.92434	687.0129	82.97334
Strathdownie	85000	12.68228	23.63175	5.080466	18.55128	699.9004	82.97334
Strathdownie	86000	12.68228	23.63175	5.080466	18.55128	699.9004	82.97334
Strathdownie	87000	12.67213	24.37875	4.732327	19.64642	687.5321	82.97334
Strathdownie	88000	12.67213	24.37875	4.732327	19.64642	687.5321	82.97334
Strathdownie	89000	12.68571	25.16886	4.461845	20.70702	675.2263	82.97334
Strathdownie	90000	12.68571	25.16886	4.461845	20.70702	675.2263	82.97334
Strathdownie	91000	13.04684	26.2286	4.202332	22.02627	654.4664	82.97334
Strathdownie	92000	13.04684	26.2286	4.202332	22.02627	654.4664	82.97334
Strathdownie	93000	12.90499	26.62184	4.174365	22.44748	626.9679	82.97334
Strathdownie	94000	12.90499	26.62184	4.174365	22.44748	626.9679	82.97334
Strathdownie	95000	13.01393	26.45225	4.205316	22.24694	601.2972	82.97334
Strathdownie	96000	13.01393	26.45225	4.205316	22.24694	601.2972	82.97334
Strathdownie	97000	12.93187	25.80782	4.214057	21.59376	612.7683	82.97334
Strathdownie	98000	12.93187	25.80782	4.214057	21.59376	612.7683	82.97334
Strathdownie	99000	13.13678	24.86822	4.879156	19.98906	634.4723	82.97334
Strathdownie	100000	13.13678	24.86822	4.879156	19.98906	634.4723	82.97334
Tight_Entrance_Cave	1000	15.65348	24.63853	8.659369	15.97916	1064.222	57.5757
Tight_Entrance_Cave	2000	15.75634	24.6187	8.777328	15.84137	1108.338	56.95478
Tight_Entrance_Cave	3000	15.70492	24.38464	8.907191	15.47744	1130.548	56.41308
Tight_Entrance_Cave	4000	15.56582	24.05301	8.867358	15.18565	1141.138	56.13699
Tight_Entrance_Cave	5000	15.5681	23.98129	8.980975	15.00031	1130.494	56.04103
Tight_Entrance_Cave	6000	15.60578	24.14386	8.891938	15.25192	1145.354	55.75
Tight_Entrance_Cave	7000	15.97051	24.47577	9.323369	15.1524	1148.571	54.45258
Tight_Entrance_Cave	8000	15.80044	24.17812	9.235932	14.94218	1106.94	53.65189
Tight_Entrance_Cave	9000	15.51369	23.81608	9.139382	14.6767	1116.531	51.2575
Tight_Entrance_Cave	10000	15.46621	23.74612	9.067594	14.67853	1064.719	46.30499
Tight_Entrance_Cave	11000	15.59734	23.87964	9.097976	14.78166	1100.4368	39.52273
Tight_Entrance_Cave	12000	15.01161	23.43469	8.579977	14.85471	1080.9426	28.8314
Tight_Entrance_Cave	13000	14.75694	23.29108	8.295524	14.99556	1076.5558	26.6086
Tight_Entrance_Cave	14000	14.72459	23.24693	8.179913	15.06701	1074.8472	25.96517
Tight_Entrance_Cave	15000	14.24139	22.82243	7.70208	15.12035	1076.7528	25.72646
Tight_Entrance_Cave	16000	13.09779	22.84186	5.980461	16.8614	985.7774	25.20312
Tight_Entrance_Cave	17000	12.62714	24.32124	4.42841	19.89283	895.6552	24.77642
Tight_Entrance_Cave	18000	12.50812	24.42835	4.321391	20.10696	898.0898	24.77642
Tight_Entrance_Cave	19000	12.62606	24.62997	4.277765	20.3522	902.7986	24.77642
Tight_Entrance_Cave	20000	12.40785	24.42624	4.051768	20.37447	904.0475	24.77642
Tight_Entrance_Cave	21000	12.54167	24.46865	3.734348	20.7343	875.6848	24.77642
Tight_Entrance_Cave	22000	12.1779	23.93848	3.481334	20.45715	848.8455	24.61111
Tight_Entrance_Cave	23000	12.32087	24.02088	3.936624	20.08425	897.7261	24.61111
Tight_Entrance_Cave	24000	12.32087	24.02088	3.936624	20.08425	897.7261	24.61111
Tight_Entrance_Cave	25000	12.47892	24.23127	4.037971	20.1933	884.2087	24.77642
Tight_Entrance_Cave	26000	12.47892	24.23127	4.037971	20.1933	884.2087	24.77642
Tight_Entrance_Cave	27000	12.78323	23.66027	4.793723	18.86655	920.1155	24.77642
Tight_Entrance_Cave	28000	12.78323	23.66027	4.793723	18.86655	920.1155	24.77642
Tight_Entrance_Cave	29000	13.19083	23.94425	5.438779	18.50547	931.2445	25.06132
Tight_Entrance_Cave	30000	13.19083	23.94425	5.438779	18.50547	931.2445	25.06132
Tight_Entrance_Cave	31000	13.57178	24.21385	5.76635	18.4475	940.1076	25.34078
Tight_Entrance_Cave	32000	13.57178	24.21385	5.76635	18.4475	940.1076	25.34078
Tight_Entrance_Cave	33000	13.45711	23.40599	6.070285	17.3357	949.5594	25.47427
Tight_Entrance_Cave	34000	13.45711	23.40599	6.070285	17.3357	949.5594	25.47427
Tight_Entrance_Cave	35000	13.76456	23.65914	6.468184	17.19095	997.8962	25.34078
Tight_Entrance_Cave	36000	13.76456	23.65914	6.468184	17.19095	997.8962	25.34078
Tight_Entrance_Cave	37000	13.86513	23.46653	6.786896	16.67964	1041.8899	25.47427
Tight_Entrance_Cave	38000	13.86513	23.46653	6.786896	16.67964	1041.8899	25.47427
Tight_Entrance_Cave	39000	13.48474	24.86034	5.266641	19.5937	933.6008	25.72646
Tight_Entrance_Cave	40000	13.48474	24.86034	5.266641	19.5937	933.6008	25.72646
Tight_Entrance_Cave	41000	13.51492	24.72781	5.598298	19.12951	998.8045	26.07874
Tight_Entrance_Cave	42000	13.51492	24.72781	5.598298	19.12951	998.8045	26.07874
Tight_Entrance_Cave	43000	14.19298	24.13736	6.801324	17.33604	1107.9573	26.19144
Tight_Entrance_Cave	44000	14.19298	24.13736	6.801324	17.33604	1107.9573	26.19144
Tight_Entrance_Cave	45000	14.00626	24.64497	6.305242	18.33973	1078.009	26.19144
Tight_Entrance_Cave	46000	14.00626	24.64497	6.305242	18.33973	1078.009	26.19144
Tight_Entrance_Cave	47000	13.84667	25.16858	5.692578	19.476	1021.5567	26.19144
Tight_Entrance_Cave	48000	13.84667	25.16858	5.692578	19.476	1021.5567	26.19144
Tight_Entrance_Cave	49000	14.68823	23.81492	7.709465	16.10545	1132.239	26.2965
Tight_Entrance_Cave	50000	14.68823	23.81492	7.709465	16.10545	1132.239	26.2965
Tight_Entrance_Cave	51000	14.31456	24.49894	6.736322	17.76261	1089.729	26.19144
Tight_Entrance_Cave	52000	14.31456	24.49894	6.736322	17.76261	1089.729	26.19144
Tight_Entrance_Cave	53000	14.52832	23.86983	7.467487	16.40234	1123.522	26.19144
Tight_Entrance_Cave	54000	14.52832	23.86983	7.467487	16.40234	1123.522	26.19144
Tight_Entrance_Cave	55000	14.69434	23.43745	7.899209	15.53824	1101.495	25.84848
Tight_Entrance_Cave	56000	14.69434	23.43745	7.899209	15.53824	1101.495	25.84848
Tight_Entrance_Cave	57000	14.82946	23.39647	8.267693	15.12878	1084.866	25.84848
Tight_Entrance_Cave	58000	14.82946	23.39647	8.267693	15.12878	1084.866	25.84848
Tight_Entrance_Cave	59000	14.32823	23.29991	7.553968	15.74594	1055.926	25.96517
Tight_Entrance_Cave	60000	14.32823	23.29991	7.553968	15.74594	1055.926	25.96517
Tight_Entrance_Cave	61000	13.45189	24.13161	5.752106	18.3795	932.424	25.84848
Tight_Entrance_Cave	62000	13.45189	24.13161	5.752106	18.3795	932.424	25.84848
Tight_Entrance_Cave	63000	13.18086	23.888	5.487252	18.40075	920.4357	25.96517
Tight_Entrance_Cave	64000	13.18086	23.888	5.487252	18.40075	920.4357	25.96517
Tight_Entrance_Cave	65000	12.83017	24.45842	4.750762	19.70766	893.0936	25.84848
Tight_Entrance_Cave	66000	12.83017	24.45842	4.750762	19.70766	893.0936	25.84848
Tight_Entrance_Cave	67000	13.04524	24.53791	4.948052	19.58986	930.5558	26.19144
Tight_Entrance_Cave	68000	13.04524	24.53791	4.948052	19.58986	930.5558	26.19144
Tight_Entrance_Cave	69000	14.07939	24.18978	6.507333	17.68244	1047.0292	26.6086
Tight_Entrance_Cave	70000	14.07939	24.18978	6.507333	17.68244	1047.0292	26.6086
Tight_Entrance_Cave	71000	14.91359	24.12391	8.01097	16.11294	1157.918	33.49136

Tight_Entrance_Cave	72000	14.91359	24.12391	8.01097	16.11294	1157.918	33.49136
Tight_Entrance_Cave	73000	14.96962	23.95574	8.015412	15.94033	1139.54	41.88414
Tight_Entrance_Cave	74000	14.96962	23.95574	8.015412	15.94033	1139.54	41.88414
Tight_Entrance_Cave	75000	14.87418	23.37486	8.151423	15.22344	1148.28	44.96978
Tight_Entrance_Cave	76000	14.87418	23.37486	8.151423	15.22344	1148.28	44.96978
Tight_Entrance_Cave	77000	14.89677	23.37708	8.398487	14.9786	1118.628	44.66046
Tight_Entrance_Cave	78000	14.89677	23.37708	8.398487	14.9786	1118.628	44.66046
Tight_Entrance_Cave	79000	15.31511	23.33389	8.935754	14.39814	1086.164	42.19529
Tight_Entrance_Cave	80000	15.31511	23.33389	8.935754	14.39814	1086.164	42.19529
Tight_Entrance_Cave	81000	15.25891	23.37262	8.978312	14.39431	1053.496	42.60863
Tight_Entrance_Cave	82000	15.25891	23.37262	8.978312	14.39431	1053.496	42.60863
Tight_Entrance_Cave	83000	15.21348	23.43463	8.972734	14.4619	1077.45	44.66046
Tight_Entrance_Cave	84000	15.21348	23.43463	8.972734	14.4619	1077.45	44.66046
Tight_Entrance_Cave	85000	15.34074	23.81984	8.877457	14.94238	1072.676	41.88414
Tight_Entrance_Cave	86000	15.34074	23.81984	8.877457	14.94238	1072.676	41.88414
Tight_Entrance_Cave	87000	14.60155	24.51504	7.298839	17.21621	1024.292	34.53942
Tight_Entrance_Cave	88000	14.60155	24.51504	7.298839	17.21621	1024.292	34.53942
Tight_Entrance_Cave	89000	15.02899	24.42314	8.110478	16.31266	1131.487	36.83742
Tight_Entrance_Cave	90000	15.02899	24.42314	8.110478	16.31266	1131.487	36.83742
Tight_Entrance_Cave	91000	15.20909	24.87585	7.950784	16.92506	1154.33	35.5863
Tight_Entrance_Cave	92000	15.20909	24.87585	7.950784	16.92506	1154.33	35.5863
Tight_Entrance_Cave	93000	15.23665	24.96447	7.976819	16.98765	1180.171	34.53942
Tight_Entrance_Cave	94000	15.23665	24.96447	7.976819	16.98765	1180.171	34.53942
Tight_Entrance_Cave	95000	15.30713	24.87605	8.11492	16.76113	1187.608	45.38061
Tight_Entrance_Cave	96000	15.30713	24.87605	8.11492	16.76113	1187.608	45.38061
Tight_Entrance_Cave	97000	15.34107	24.51176	8.311613	16.20014	1209.637	48.02406
Tight_Entrance_Cave	98000	15.34107	24.51176	8.311613	16.20014	1209.637	48.02406
Tight_Entrance_Cave	99000	15.5101	24.21314	8.787323	15.42582	1128.883	48.83562
Tight_Entrance_Cave	100000	15.5101	24.21314	8.787323	15.42582	1128.883	48.83562
Yellabidde_Cave	1000	17.9183	31.39362	7.085425	24.30819	523.3479	126.6547
Yellabidde_Cave	2000	17.77807	30.97933	6.769306	24.21003	556.5638	126.6547
Yellabidde_Cave	3000	17.71531	30.4255	6.829507	23.59599	541.3716	126.2433
Yellabidde_Cave	4000	17.4518	30.151	7.049009	23.10199	571.5708	125.4187
Yellabidde_Cave	5000	17.71276	30.35471	7.156028	23.19868	559.1113	125.1411
Yellabidde_Cave	6000	17.3505	29.40342	6.883939	22.51948	566.2082	125.1411
Yellabidde_Cave	7000	18.15498	29.91053	8.113416	21.79712	553.691	125.1411
Yellabidde_Cave	8000	17.87792	29.59979	7.831048	21.76874	542.5732	125.1411
Yellabidde_Cave	9000	17.04552	27.88621	7.258647	20.62757	592.2999	125.1411
Yellabidde_Cave	10000	17.52337	28.81375	7.375336	21.43841	560.6449	125.1411
Yellabidde_Cave	11000	17.09785	27.6847	7.548659	20.13604	594.2524	125.1411
Yellabidde_Cave	12000	16.85506	28.55559	6.735293	21.8203	540.2275	125.1411
Yellabidde_Cave	13000	16.89544	28.68021	6.816586	21.86362	508.9048	125.1411
Yellabidde_Cave	14000	16.49494	28.72045	6.590567	22.12988	533.7118	125.1411
Yellabidde_Cave	15000	16.00767	28.7145	6.177534	22.53697	481.7349	125.1411
Yellabidde_Cave	16000	15.4027	28.23939	5.518203	22.72118	507.5429	125.1411
Yellabidde_Cave	17000	15.70886	29.49761	5.158678	24.33893	535.7145	125.1411
Yellabidde_Cave	18000	15.66436	29.91298	5.285609	24.62737	536.3757	125.1411
Yellabidde_Cave	19000	15.63907	29.89477	5.157578	24.73719	540.5662	125.1411
Yellabidde_Cave	20000	15.54344	30.26303	5.035629	25.2274	547.7684	125.1411
Yellabidde_Cave	21000	15.71396	29.56998	4.953933	24.61605	534.233	125.1411
Yellabidde_Cave	22000	15.48267	29.14398	4.881521	24.26246	546.4691	125.1411
Yellabidde_Cave	23000	15.46548	29.64653	5.019113	24.62741	551.4481	125.1411
Yellabidde_Cave	24000	15.46548	29.64653	5.019113	24.62741	551.4481	125.1411
Yellabidde_Cave	25000	15.43229	29.55448	4.843525	24.71095	544.9963	125.1411
Yellabidde_Cave	26000	15.43229	29.55448	4.843525	24.71095	544.9963	125.1411
Yellabidde_Cave	27000	15.68233	28.59327	5.729183	22.86409	545.2278	125.1411
Yellabidde_Cave	28000	15.68233	28.59327	5.729183	22.86409	545.2278	125.1411
Yellabidde_Cave	29000	15.75694	28.02712	6.242967	21.78416	539.9641	125.1411
Yellabidde_Cave	30000	15.75694	28.02712	6.242967	21.78416	539.9641	125.1411
Yellabidde_Cave	31000	16.07475	27.97012	6.700684	21.26943	530.124	125.1411
Yellabidde_Cave	32000	16.07475	27.97012	6.700684	21.26943	530.124	125.1411
Yellabidde_Cave	33000	15.65892	27.7775	6.309991	21.46751	548.4128	125.1411
Yellabidde_Cave	34000	15.65892	27.7775	6.309991	21.46751	548.4128	125.1411
Yellabidde_Cave	35000	15.97362	28.52141	6.269985	22.25143	525.9309	125.1411
Yellabidde_Cave	36000	15.97362	28.52141	6.269985	22.25143	525.9309	125.1411
Yellabidde_Cave	37000	15.96085	29.10393	6.186048	22.91788	513.7402	125.1411
Yellabidde_Cave	38000	15.96085	29.10393	6.186048	22.91788	513.7402	125.1411
Yellabidde_Cave	39000	16.12194	29.36579	5.768165	23.59763	545.7834	125.1411
Yellabidde_Cave	40000	16.12194	29.36579	5.768165	23.59763	545.7834	125.1411
Yellabidde_Cave	41000	16.28821	30.71155	5.897272	24.81428	560.3321	125.1411
Yellabidde_Cave	42000	16.28821	30.71155	5.897272	24.81428	560.3321	125.1411
Yellabidde_Cave	43000	16.3133	30.13087	6.057977	24.07289	550.4371	125.1411
Yellabidde_Cave	44000	16.3133	30.13087	6.057977	24.07289	550.4371	125.1411
Yellabidde_Cave	45000	16.47893	30.67908	5.734216	24.94486	550.7206	125.1411
Yellabidde_Cave	46000	16.47893	30.67908	5.734216	24.94486	550.7206	125.1411
Yellabidde_Cave	47000	16.60607	30.69674	5.987971	24.70877	556.2358	125.1411
Yellabidde_Cave	48000	16.60607	30.69674	5.987971	24.70877	556.2358	125.1411
Yellabidde_Cave	49000	16.49374	30.21344	6.345987	23.86746	530.2392	125.1411
Yellabidde_Cave	50000	16.49374	30.21344	6.345987	23.86746	530.2392	125.1411
Yellabidde_Cave	51000	16.68066	30.18335	6.261744	23.9216	542.9287	125.1411
Yellabidde_Cave	52000	16.68066	30.18335	6.261744	23.9216	542.9287	125.1411
Yellabidde_Cave	53000	16.49306	29.26872	6.529035	22.73969	545.3087	125.1411
Yellabidde_Cave	54000	16.49306	29.26872	6.529035	22.73969	545.3087	125.1411
Yellabidde_Cave	55000	16.39546	29.22775	6.406292	22.82145	525.0292	125.1411
Yellabidde_Cave	56000	16.39546	29.22775	6.406292	22.82145	525.0292	125.1411
Yellabidde_Cave	57000	16.45219	29.13765	6.792164	22.34548	527.0099	125.1411
Yellabidde_Cave	58000	16.45219	29.13765	6.792164	22.34548	527.0099	125.1411
Yellabidde_Cave	59000	16.26003	28.21774	7.236068	20.98167	508.9199	125.1411
Yellabidde_Cave	60000	16.26003	28.21774	7.236068	20.98167	508.9199	125.1411
Yellabidde_Cave	61000	16.03462	28.06893	6.283495	21.78544	523.3369	125.1411
Yellabidde_Cave	62000	16.03462	28.06893	6.283495	21.78544	523.3369	125.1411
Yellabidde_Cave	63000	15.80865	28.29596	6.295928	22.00003	523.0744	125.1411
Yellabidde_Cave	64000	15.80865	28.29596	6.295928	22.00003	523.0744	125.1411
Yellabidde_Cave	65000	15.83046	29.68267	5.932959	23.74971	535.6098	125.1411
Yellabidde_Cave	66000	15.83046	29.68267	5.932959	23.74971	535.6098	125.1411
Yellabidde_Cave	67000	16.04303	30.09659	5.949261	24.14733	529.8279	125.1411
Yellabidde_Cave	68000	16.04303	30.09659	5.949261	24.14733	529.8279	125.1411
Yellabidde_Cave	69000	16.50681	30.60954	6.086445	24.5231	504.9846	125.1411
Yellabidde_Cave	70000	16.50681	30.60954	6.086445	24.5231	504.9846	125.1411
Yellabidde_Cave	71000	17.04021	31.52509	7.032604	24.49248	475.3963	125.1411
Yellabidde_Cave	72000	17.04021	31.52509	7.032604	24.49248	475.3963	125.1411
Yellabidde_Cave	73000	16.97134	30.8835	6.804657	24.07885	520.0945	125.1411
Yellabidde_Cave	74000	16.97134	30.8835	6.804657	24.07885	520.0945	125.1411
Yellabidde_Cave	75000	16.68287	29.51332	7.067413	22.44591	501.6167	125.1411
Yellabidde_Cave	76000	16.68287	29.51332	7.067413	22.44591	501.6167	125.1411

Yellabidde_Cave	77000	16.64664	28.59126	7.238503	21.35276	515.7154	125.1411
Yellabidde_Cave	78000	16.64664	28.59126	7.238503	21.35276	515.7154	125.1411
Yellabidde_Cave	79000	17.17832	28.95447	7.917497	21.03697	479.5969	125.1411
Yellabidde_Cave	80000	17.17832	28.95447	7.917497	21.03697	479.5969	125.1411
Yellabidde_Cave	81000	16.91224	28.02454	7.648047	20.37649	509.9204	125.1411
Yellabidde_Cave	82000	16.91224	28.02454	7.648047	20.37649	509.9204	125.1411
Yellabidde_Cave	83000	16.97345	28.03187	7.641379	20.39049	540.5462	125.1411
Yellabidde_Cave	84000	16.97345	28.03187	7.641379	20.39049	540.5462	125.1411
Yellabidde_Cave	85000	16.93594	29.00791	7.335938	21.67197	484.3967	125.1411
Yellabidde_Cave	86000	16.93594	29.00791	7.335938	21.67197	484.3967	125.1411
Yellabidde_Cave	87000	16.75314	29.79927	6.98319	22.81608	509.734	125.1411
Yellabidde_Cave	88000	16.75314	29.79927	6.98319	22.81608	509.734	125.1411
Yellabidde_Cave	89000	16.95896	31.23674	6.318189	24.91855	506.8622	125.1411
Yellabidde_Cave	90000	16.95896	31.23674	6.318189	24.91855	506.8622	125.1411
Yellabidde_Cave	91000	17.20714	32.22495	5.923442	26.30151	509.0899	125.1411
Yellabidde_Cave	92000	17.20714	32.22495	5.923442	26.30151	509.0899	125.1411
Yellabidde_Cave	93000	17.29269	32.56964	6.243344	26.3263	517.654	125.1411
Yellabidde_Cave	94000	17.29269	32.56964	6.243344	26.3263	517.654	125.1411
Yellabidde_Cave	95000	17.35804	32.47457	6.509459	25.96511	548.1843	125.1411
Yellabidde_Cave	96000	17.35804	32.47457	6.509459	25.96511	548.1843	125.1411
Yellabidde_Cave	97000	17.3151	31.45973	6.531035	24.92869	552.6522	125.1411
Yellabidde_Cave	98000	17.3151	31.45973	6.531035	24.92869	552.6522	125.1411
Yellabidde_Cave	99000	17.37629	30.08349	7.104666	22.97882	536.4062	125.1411
Yellabidde_Cave	100000	17.37629	30.08349	7.104666	22.97882	536.4062	125.1411

Dataset S5: Overview of bone weathering stages, FTIR results, ZooMS results, and deamidation estimates for individual samples.

Sample	Site	Weathering stage	ZooMS success	%Gln	FTIR (Am1/P)	FTIR (Am2/P)
CP999	Boodie Cave	3	NO	0	NA	NA
CP1000	Boodie Cave	3	NO	0	NA	NA
CP1001	Boodie Cave	3	NO	0	NA	NA
CP1002	Boodie Cave	3	NO	0	NA	NA
CP1003	Boodie Cave	4	NO	0	NA	NA
CP1004	Boodie Cave	4	NO	0	NA	NA
CP1005	Boodie Cave	3	NO	0	NA	NA
CP1006	Boodie Cave	3	NO	0	NA	NA
CP1007	Boodie Cave	3	NO	0	NA	NA
CP1008	Boodie Cave	4	NO	0	NA	NA
CP1009	Boodie Cave	3	NO	0	NA	NA
CP1010	Boodie Cave	4	NO	0	NA	NA
CP1011	Boodie Cave	4	NO	0	NA	NA
CP1012	Boodie Cave	3	NO	0	NA	NA
CP1013	Boodie Cave	4	NO	0	NA	NA
CP1014	Boodie Cave	3	NO	0	NA	NA
CP1015	Boodie Cave	4	NO	0	NA	NA
CP1016	Boodie Cave	4	NO	0	NA	NA
CP1017	Boodie Cave	3	NO	0	NA	NA
CP1018	Boodie Cave	3	NO	0	NA	NA
CP1019	Boodie Cave	3	NO	0	NA	NA
CP1020	Boodie Cave	4	NO	0	NA	NA
CP1021	Boodie Cave	4	NO	0	NA	NA
CP1022	Boodie Cave	4	NO	0	NA	NA
CP1023	Boodie Cave	4	NO	0	NA	NA
CP1024	Boodie Cave	4	NO	0	NA	NA
CP1025	Boodie Cave	4	NO	0	NA	NA
CP1026	Boodie Cave	4	NO	0	NA	NA
CP1027	Boodie Cave	4	NO	0	NA	NA
CP1028	Boodie Cave	4	NO	0	NA	NA
CP1029	Boodie Cave	4	NO	0	NA	NA
CP1030	Boodie Cave	3	NO	0	NA	NA
CP1031	Boodie Cave	3	NO	0	NA	NA
CP1032	Boodie Cave	3	NO	0	NA	NA
CP1033	Boodie Cave	3	NO	0	NA	NA
CP1034	Boodie Cave	3	NO	0	NA	NA
CP1035	Boodie Cave	4	NO	0	NA	NA
CP1036	Boodie Cave	4	NO	0	NA	NA
CP1037	Boodie Cave	4	NO	0	NA	NA
CP1038	Boodie Cave	4	NO	0	NA	NA
CP1039	Boodie Cave	3	NO	0	NA	NA
CP154	Broken River (Tripot Cave)	2	YES	0.252	0.18666667	0.33333333
CP155	Broken River (Tripot Cave)	2	NO	0	0.069869	0.15283843
CP156	Broken River (Tripot Cave)	2	YES	0.3285	0.09021113	0.09021113
CP157	Broken River (Tripot Cave)	2	YES	0.7695	0.08716707	0.08716707
CP158	Broken River (Tripot Cave)	2	YES	0.231	0.07042254	0.11971831
CP159	Broken River (Tripot Cave)	2	NO	0	0.0631068	0.17475728
CP160	Broken River (Tripot Cave)	2	YES	0.549	0.05555556	0.11111111
CP161	Broken River (Tripot Cave)	2	YES	0.316	0.06024096	0.19678715
CP162	Broken River (Tripot Cave)	2	YES	0.3185	0.08806818	0.08806818
CP163	Broken River (Tripot Cave)	2	YES	0.444	0.05921053	0.05921053
CP164	Broken River (Tripot Cave)	2	YES	0.268	0.06914894	0.0781418
CP165	Broken River (Tripot Cave)	2	YES	0.298	0.07514451	0.08381503
CP166	Broken River (Tripot Cave)	2	YES	0.5285	0.07100592	0.1183432
CP167	Broken River (Tripot Cave)	2	YES	0.274	0.07093426	0.07093426
CP168	Broken River (Tripot Cave)	2	NO	0	0.06285714	0.12
CP1118	Broken River (Millenium Cave)	4	YES	0.9195	0.0546875	0.05859375
CP1119	Broken River (Millenium Cave)	3	YES	0.988	0.17777778	0.17777778
CP1120	Broken River (Millenium Cave)	3	YES	0.931	0.18468468	0.18468468
CP1121	Broken River (Millenium Cave)	3	YES	0.9675	0.018604651	0.018604651
CP1122	Broken River (Millenium Cave)	4	YES	0.772	0.015625	0.015625
CP1123	Broken River (Millenium Cave)	3	YES	0.967	0.06785714	0.07142857
CP1124	Broken River (Millenium Cave)	3	YES	0.8735	0.15	0.15
CP1125	Broken River (Robert Broom Cave)	4	NO	0	0.02962963	0.03703704
CP1126	Broken River (Robert Broom Cave)	4	NO	0	0.03588517	0.04545455
CP1127	Broken River (Robert Broom Cave)	4	NO	0	0.04109589	0.05936073
CP1128	Broken River (Robert Broom Cave)	4	NO	0	0.03389831	0.03389831
CP1129	Broken River (Robert Broom Cave)	4	NO	0	0.02688172	0.02867384
CP1130	Broken River (Robert Broom Cave)	4	NO	0	0.03125	0.03125
CP1131	Broken River (Robert Broom Cave)	4	NO	0	0.03240741	0.08796296
CP1132	Broken River (Robert Broom Cave)	4	NO	0	0.03755869	0.03755869
CP1133	Broken River (Robert Broom Cave)	4	NO	0	0.02292994	0.02802548
CP1134	Broken River (Robert Broom Cave)	4	NO	0	0.05472637	0.05970149
CP1135	Broken River (Robert Broom Cave)	3	NO	0	0.02727273	0.02878788
CP1136	Broken River (Robert Broom Cave)	4	NO	0	0.02643172	0.03964758
CP1137	Broken River (Robert Broom Cave)	3	NO	0	0.02554745	0.02919708

CP1138	Broken River (Robert Broom Cave)	3	NO	0	0.01894737	0.02105263
CP1139	Broken River (Three Avenues)	3	NO	0	0.05327869	0.05737705
CP1140	Broken River (Three Avenues)	3	YES	0.6015	0.066313	0.066313
CP1141	Broken River (Three Avenues)	3	YES	0.5615	0.14173228	0.14173228
CP1142	Broken River (Tripot Cave)	3	NO	0	0.08635097	0.09749304
CP1154	Broken River (Beehive)	4	NO	0	0.032	0.03866667
CP1155	Broken River (Beehive)	4	NO	0	0.03594771	0.04248366
CP1156	Broken River (Beehive)	4	NO	0	0.03411131	0.04308797
CP1157	Broken River (Beehive)	4	NO	0	0.03475936	0.03743316
CP1158	Broken River (Beehive)	4	NO	0	0.05529954	0.10599078
CP1236	Broken River (Tripot Cave)	4	YES	1	0.12444444	0.12444444
CP1237	Broken River (Tripot Cave)	3	YES	0.8405	0.20869565	0.20869565
CP1238	Broken River (Tripot Cave)	3	YES	0.934	0.08186196	0.09630819
CP1239	Broken River (Tripot Cave)	4	YES	0.7845	0.08528428	0.08528428
CP1240	Broken River (Tripot Cave)	4	YES	0.9375	0.10185185	0.10185185
CP1241	Broken River (Tripot Cave)	4	NO	0	0.03921569	0.07254902
CP1242	Broken River (Tripot Cave)	4	NO	0	NA	NA
CP1243	Broken River (Tripot Cave)	4	YES	0.811	0.05315615	0.05315615
CP1244	Broken River (Tripot Cave)	4	NO	0	0.07112971	0.07112971
CP1245	Broken River (Millenium Cave)	3	YES	0.781	0.12578616	0.12578616
CP1246	Broken River (Millenium Cave)	3	YES	0.958	0.25833333	0.25833333
CP1247	Broken River (Millenium Cave)	4	YES	0.9795	0.17241379	0.17241379
CP1249	Broken River (Millenium Cave)	4	YES	0.319	0.05250597	0.05727924
CP242	Buchan Caves (Foul Air Cave)	4	NO	0	0.02697095	0.0373444
CP243	Buchan Caves (Foul Air Cave)	4	NO	0	0.02832244	0.04139434
CP244	Buchan Caves (Foul Air Cave)	4	NO	0	0.03252886	0.04407135
CP245	Buchan Caves (Foul Air Cave)	4	NO	0	0.0345679	0.04197531
CP246	Buchan Caves (Foul Air Cave)	4	NO	0	0.02702703	0.03840683
CP247	Buchan Caves (Foul Air Cave)	4	NO	0	0.02624672	0.03412073
CP248	Buchan Caves (Foul Air Cave)	4	NO	0	0.03886926	0.05300353
CP249	Buchan Caves (Foul Air Cave)	4	NO	0	0.03271028	0.04205607
CP250	Buchan Caves (Foul Air Cave)	4	NO	0	0.02706027	0.03567036
CP298	Buchan Caves (Pot Luck Cave)	4	NO	0	NA	NA
CP311	Buchan Caves (Pot Luck Cave)	3	NO	0	NA	NA
CP333	Buchan Caves (Foul Air Cave)	4	NO	0	0.03787879	0.07007576
CP334	Buchan Caves (Foul Air Cave)	4	NO	0	0.03131749	0.04319654
CP335	Buchan Caves (Foul Air Cave)	4	NO	0	0.02896082	0.04258944
CP336	Buchan Caves (Foul Air Cave)	4	NO	0	0.02956989	0.03629032
CP337	Buchan Caves (Foul Air Cave)	4	NO	0	0.03225806	0.04207574
CP338	Buchan Caves (Foul Air Cave)	4	YES	0.6045	0.03370787	0.03370787
CP339	Buchan Caves (Foul Air Cave)	4	NO	0	0.03225806	0.05049088
CP340	Buchan Caves (Foul Air Cave)	4	NO	0	0.04411765	0.05882353
CP341	Buchan Caves (Foul Air Cave)	4	NO	0	0.02884615	0.04447115
CP376	Buchan Caves (Foul Air Cave)	4	NO	0	0.05555556	0.06349206
CP377	Buchan Caves (Foul Air Cave)	4	NO	0	0.033241	0.04432133
CP001	Darling Downs	3	NO	0	NA	NA
CP002	Darling Downs	3	NO	0	NA	NA
CP003	Darling Downs	4	NO	0	NA	NA
CP004	Darling Downs	3	NO	0	NA	NA
CP005	Darling Downs	3	NO	0	NA	NA
CP006	Darling Downs	3	NO	0	NA	NA
CP007	Darling Downs	3	NO	0	NA	NA
CP080	Darling Downs	3	NO	0	0.0875	0.125
CP081	Darling Downs	3	NO	0	0.08080808	0.09090909
CP082	Darling Downs	3	NO	0	0.09565217	0.11304348
CP083	Darling Downs	3	NO	0	0.04251386	0.05545287
CP084	Darling Downs	3	NO	0	0.0523416	0.07162534
CP085	Darling Downs	3	NO	0	0.05769231	0.07211539
CP086	Darling Downs	3	NO	0	NA	NA
CP087	Darling Downs	4	NO	0	0.06040269	0.0704698
CP088	Darling Downs	3	NO	0	0.04751131	0.08597285
CP089	Darling Downs	3	NO	0	0.04016064	0.04819277
CP090	Darling Downs	3	NO	0	0.04895105	0.06993007
CP091	Darling Downs	3	NO	0	0.06382979	0.06737589
CP179	Darling Downs (Dalby)	3	NO	0	NA	NA
CP180	Darling Downs (Ned's Gully)	4	NO	0	NA	NA
CP1259	Darling Downs	4	NO	0	0.04975124	0.13432836
CP1264	Darling Downs	3	NO	0	0.05777778	0.08444444
CP767	Devil's Lair	4	NO	0	0.08888889	0.23888889
CP768	Devil's Lair	4	YES	0.6005	0.17567568	0.23648649
CP769	Devil's Lair	4	NO	0	0.08275862	0.11724138
CP770	Devil's Lair	4	YES	0.6755	0.13913043	0.15652174
CP771	Devil's Lair	4	YES	0.7665	0.08741259	0.11888112
CP772	Devil's Lair	3	YES	0.556	0.11538462	0.13846154
CP773	Devil's Lair	3	YES	0.7245	0.05341246	0.06379822
CP774	Devil's Lair	3	YES	0.831	0.07772021	0.15284974
CP775	Devil's Lair	3	YES	0.5855	0.072	0.256
CP776	Devil's Lair	3	YES	0.8175	0.07446809	0.15602837
CP777	Devil's Lair	3	YES	0.687	0.1980198	0.1980198
CP778	Devil's Lair	3	YES	0.515	0.16382253	0.16382253

CP779	Devil's Lair	4	NO	0	NA	NA	
CP780	Devil's Lair	3	NO	0	NA	NA	
CP781	Devil's Lair	4	YES	0.6495		0.05913978	0.07526882
CP782	Devil's Lair	3	YES	0.662		0.23039216	0.26470588
CP783	Devil's Lair	4	YES	0.5325		0.125	0.125
CP784	Devil's Lair	4	YES	0.815		0.07048458	0.10572687
CP785	Devil's Lair	4	NO	0		0.08917197	0.14012739
CP786	Devil's Lair	4	YES	0.7725		0.09375	0.15178571
CP787	Devil's Lair	4	YES	0.5815		0.10344828	0.12068966
CP788	Devil's Lair	4	YES	0.543		0.07553957	0.0971223
CP789	Devil's Lair	4	YES	0.6825		0.11397059	0.15073529
CP790	Devil's Lair	4	YES	0.4855		0.12224939	0.12224939
CP791	Devil's Lair	4	YES	0.569		0.07282913	0.10084034
CP792	Devil's Lair	4	YES	0.528		0.07279693	0.11111111
CP793	Devil's Lair	3	YES	0.5895		0.14054054	0.14054054
CP794	Devil's Lair	3	YES	0.552		0.11351351	0.15135135
CP795	Devil's Lair	4	YES	0.6055		0.05714286	0.1047619
CP796	Devil's Lair	3	YES	0.6395		0.05882353	0.06352941
CP797	Devil's Lair	4	NO	0		0.1547619	0.25595238
CP798	Devil's Lair	4	YES	0.5255		0.25	0.25
CP799	Devil's Lair	4	YES	0.673		0.08527132	0.10852713
CP800	Devil's Lair	3	YES	0.579		0.10200364	0.1129326
CP801	Devil's Lair	3	YES	0.4845		0.22772277	0.22772277
CP802	Devil's Lair	4	YES	0.5515		0.0472103	0.06008584
CP803	Devil's Lair	4	YES	0.4565		0.06403941	0.14778325
CP804	Devil's Lair	3	YES	0.6255		0.16981132	0.16981132
CP805	Devil's Lair	3	NO	0		0.10909091	0.13333333
CP806	Devil's Lair	3	YES	0.687		0.11231884	0.16304348
CP807	Devil's Lair	4	NO	0	NA	NA	
CP808	Devil's Lair	3	YES	0.5615		0.12820513	0.13675214
CP809	Devil's Lair	4	YES	0.6625		0.06422018	0.09480122
CP810	Devil's Lair	3	YES	0.5915		0.11278295	0.12781955
CP811	Devil's Lair	3	YES	0.808		0.18918919	0.22522523
CP812	Devil's Lair	3	YES	0.514	NA	NA	
CP813	Devil's Lair	4	YES	0.7115		0.17391304	0.1863354
CP814	Devil's Lair	4	NO	0	NA	NA	
CP815	Devil's Lair	3	YES	0.553		0.1048951	0.2027972
CP816	Devil's Lair	3	YES	0.4965		0.16193182	0.16193182
CP817	Devil's Lair	4	NO	0		0.06007067	0.09540636
CP818	Devil's Lair	4	NO	0		0.06015038	0.13909774
CP819	Devil's Lair	4	NO	0		0.0631068	0.18446602
CP820	Devil's Lair	4	NO	0		0.05022831	0.12328767
CP821	Devil's Lair	4	YES	0.5145		0.06593407	0.12637363
CP822	Devil's Lair	4	YES	0.76		0.07865169	0.16853933
CP823	Devil's Lair	4	YES	0.632	NA	NA	
CP824	Devil's Lair	4	YES	0.5925		0.07772021	0.21243523
CP825	Devil's Lair	3	YES	0.74		0.11864407	0.22033898
CP826	Devil's Lair	4	YES	0.471		0.195	0.195
CP827	Devil's Lair	4	YES	0.5175		0.10227273	0.32954545
CP828	Devil's Lair	3	YES	0.5125		0.09259259	0.21604938
CP829	Devil's Lair	4	YES	0.4645		0.15652174	0.3826087
CP830	Devil's Lair	4	YES	0.4945		0.15584416	0.19047619
CP831	Devil's Lair	3	YES	0.5075		0.1409396	0.1409396
CP832	Devil's Lair	3	YES	0.5465		0.08092486	0.13294798
CP833	Devil's Lair	3	YES	0.432		0.136	0.144
CP834	Devil's Lair	3	YES	0.578		0.1038961	0.16883117
CP835	Devil's Lair	3	YES	0.5675		0.13492063	0.23015873
CP836	Devil's Lair	3	YES	0		0.13461538	0.16025641
CP837	Devil's Lair	3	YES	0.578		0.08474576	0.10169492
CP838	Devil's Lair	4	YES	0.4865		0.09090909	0.1048951
CP839	Devil's Lair	3	YES	0.5455		0.10614525	0.12290503
CP840	Devil's Lair	3	YES	0.537		0.07751938	0.12403101
CP841	Devil's Lair	4	YES	0.412		0.08780488	0.12195122
CP842	Devil's Lair	4	YES	0.4635		0.11442786	0.18905473
CP843	Devil's Lair	3	YES	0.5		0.18571429	0.18571429
CP844	Devil's Lair	3	NO	0		0.07522124	0.08849558
CP845	Devil's Lair	4	YES	0.4365		0.112	0.152
CP846	Devil's Lair	4	YES	0.56		0.05472637	0.14925373
CP847	Devil's Lair	4	YES	0.6445		0.11724138	0.17241379
CP848	Devil's Lair	3	YES	0.4375		0.09234234	0.1036036
CP849	Devil's Lair	4	YES	0.645		0.11486486	0.25
CP850	Devil's Lair	4	YES	0.5705		0.10526316	0.24210526
CP851	Devil's Lair	3	YES	0.3775		0.08924949	0.13590264
CP852	Devil's Lair	4	YES	0.54		0.16551724	0.17931034
CP853	Devil's Lair	3	YES	0.65		0.15757576	0.15757576
CP854	Devil's Lair	4	YES	0.8245		0.09615385	0.12820513
CP855	Devil's Lair	4	YES	0.5475		0.09011628	0.15406977
CP856	Devil's Lair	3	YES	0.577		0.17848411	0.17848411
CP857	Devil's Lair	4	YES	0.537		0.06569343	0.08759124
CP858	Devil's Lair	4	YES	0.6		0.09467456	0.11538462

CP859	Devil's Lair	4	YES	0.519		0.13863636	0.13863636
CP860	Devil's Lair	4	YES	0.684		0.09342561	0.13148789
CP861	Devil's Lair	3	YES	0.499		0.16666667	0.16666667
CP862	Devil's Lair	3	YES	0.4455		0.14364641	0.18232044
CP863	Devil's Lair	3	YES	0.671		0.17985612	0.23021583
CP864	Devil's Lair	3	YES	0.397		0.08910891	0.13366337
CP865	Devil's Lair	4	YES	0.5765		0.07185629	0.12874251
CP866	Devil's Lair	4	YES	0.5125		0.07002188	0.08315098
CP413	Kudjal Yolgah Cave	4	NO	0		0.03472222	0.05092593
CP414	Kudjal Yolgah Cave	4	NO	0		0.04632153	0.04904632
CP415	Kudjal Yolgah Cave	4	NO	0		0.03669725	0.0412844
CP416	Kudjal Yolgah Cave	4	NO	0		0.0320781	0.0348675
CP417	Kudjal Yolgah Cave	4	NO	0		0.05250597	0.05250597
CP418	Kudjal Yolgah Cave	4	NO	0		0.02816901	0.03051643
CP419	Kudjal Yolgah Cave	4	NO	0		0.03485255	0.04021448
CP420	Kudjal Yolgah Cave	4	NO	0		0.03080082	0.0349076
CP421	Kudjal Yolgah Cave	4	NO	0		0.03673469	0.03877551
CP422	Kudjal Yolgah Cave	4	NO	0		0.03112033	0.03319502
CP423	Kudjal Yolgah Cave	4	YES	0.289		0.04294479	0.04907975
CP424	Kudjal Yolgah Cave	4	NO	0		0.0449827	0.05536332
CP425	Kudjal Yolgah Cave	4	NO	0		0.03612167	0.0418251
CP426	Kudjal Yolgah Cave	4	NO	0		0.04074074	0.04074074
CP427	Kudjal Yolgah Cave	4	NO	0	NA	NA	
CP428	Kudjal Yolgah Cave	4	NO	0		0.04057279	0.04534606
CP429	Kudjal Yolgah Cave	4	NO	0	NA	NA	
CP430	Kudjal Yolgah Cave	4	NO	0	NA	NA	
CP431	Kudjal Yolgah Cave	4	NO	0		0.04291845	0.05793991
CP432	Kudjal Yolgah Cave	4	NO	0		0.03727715	0.03889789
CP433	Kudjal Yolgah Cave	4	NO	0	NA	NA	
CP434	Kudjal Yolgah Cave	4	NO	0		0.04301075	0.0483871
CP435	Kudjal Yolgah Cave	4	NO	0		0.03501946	0.04085603
CP436	Kudjal Yolgah Cave	4	YES	0.528		0.04241071	0.05133929
CP437	Kudjal Yolgah Cave	4	NO	0		0.03418803	0.04558405
CP438	Kudjal Yolgah Cave	4	NO	0		0.04643963	0.05572755
CP439	Kudjal Yolgah Cave	4	NO	0		0.03097345	0.0420354
CP440	Kudjal Yolgah Cave	4	YES	0.5355		0.04276986	0.05702648
CP441	Kudjal Yolgah Cave	4	YES	0.304		0.03496503	0.04428904
CP442	Kudjal Yolgah Cave	4	YES	0.2385		0.03448276	0.04433498
CP443	Kudjal Yolgah Cave	4	YES	0.3545		0.02970297	0.03960396
CP444	Kudjal Yolgah Cave	4	YES	0.3105		0.02840909	0.03409091
CP445	Kudjal Yolgah Cave	4	YES	0.326		0.03968254	0.04761905
CP446	Kudjal Yolgah Cave	4	YES	0.319		0.03676471	0.04779412
CP447	Kudjal Yolgah Cave	4	YES	0.301		0.06965174	0.07960199
CP448	Kudjal Yolgah Cave	4	YES	0.3165		0.04504505	0.05855856
CP449	Kudjal Yolgah Cave	4	NO	0		0.03044496	0.03981265
CP450	Kudjal Yolgah Cave	4	YES	0.318		0.02927581	0.03697997
CP451	Kudjal Yolgah Cave	4	YES	0.39		0.064	0.072
CP452	Kudjal Yolgah Cave	4	NO	0	NA	NA	
CP453	Kudjal Yolgah Cave	4	YES	0.7195		0.05045872	0.06880734
CP454	Kudjal Yolgah Cave	4	YES	0.5285	NA	NA	
CP455	Kudjal Yolgah Cave	4	NO	0		0.04371585	0.04918033
CP456	Kudjal Yolgah Cave	4	NO	0		0.04025424	0.04449153
CP457	Kudjal Yolgah Cave	4	YES	0.587	NA	NA	
CP458	Kudjal Yolgah Cave	4	NO	0		0.04878049	0.05691057
CP459	Kudjal Yolgah Cave	4	YES	0.7515		0.04658385	0.05900621
CP460	Kudjal Yolgah Cave	4	NO	0		0.04656863	0.05392157
CP461	Kudjal Yolgah Cave	4	NO	0		0.04188482	0.05759162
CP462	Kudjal Yolgah Cave	4	YES	0.4705		0.03994294	0.04279601
CP463	Kudjal Yolgah Cave	4	YES	0.556		0.05022831	0.05479452
CP464	Kudjal Yolgah Cave	4	YES	0.5185		0.04761905	0.05952381
CP465	Kudjal Yolgah Cave	4	YES	0.665		0.06097561	0.07926829
CP466	Kudjal Yolgah Cave	4	YES	0.5185		0.05	0.07142857
CP467	Kudjal Yolgah Cave	4	NO	0		0.02915952	0.03945111
CP468	Kudjal Yolgah Cave	4	NO	0		0.0250298	0.02741359
CP469	Kudjal Yolgah Cave	4	YES	0.469		0.0776699	0.08737864
CP470	Kudjal Yolgah Cave	4	NO	0		0.03089888	0.03932584
CP471	Kudjal Yolgah Cave	4	NO	0		0.02681992	0.03065134
CP472	Kudjal Yolgah Cave	4	YES	0.346		0.03629032	0.04435484
CP473	Kudjal Yolgah Cave	4	NO	0		0.02382655	0.03291714
CP474	Kudjal Yolgah Cave	4	YES	0.315		0.04237288	0.05508475
CP475	Kudjal Yolgah Cave	4	YES	0.3005		0.03571429	0.04323308
CP476	Kudjal Yolgah Cave	4	NO	0		0.05641026	0.06153846
CP477	Kudjal Yolgah Cave	4	YES	0.493	NA	NA	
CP478	Kudjal Yolgah Cave	4	NO	0		0.0373444	0.04149378
CP479	Kudjal Yolgah Cave	4	YES	0.758		0.04597701	0.06436782
CP480	Kudjal Yolgah Cave	4	NO	0		0.06060606	0.07070707
CP481	Kudjal Yolgah Cave	4	NO	0		0.03571429	0.0467033
CP482	Kudjal Yolgah Cave	4	NO	0		0.02754491	0.02994012
CP483	Kudjal Yolgah Cave	4	NO	0		0.03491272	0.03740648
CP484	Kudjal Yolgah Cave	4	NO	0		0.03519062	0.04252199

CP485	Kudjal Yolgah Cave	4	YES	0.3675	0.05454545	0.07272727
CP486	Kudjal Yolgah Cave	4	NO	0	0.03160271	0.03837472
CP487	Kudjal Yolgah Cave	4	YES	0.451	0.07692308	0.08461538
CP488	Kudjal Yolgah Cave	4	YES	0.3375	0.04700855	0.05555556
CP1257	Kudjal Yolgah Cave	3	NO	0	0.03813559	0.04661017
CP1258	Kudjal Yolgah Cave	3	NO	0	0.03903904	0.03903904
CP284	Lake Victoria	3	NO	0	0.03191489	0.04468085
CP285	Lake Victoria	3	NO	0	0.04958678	0.05785124
CP286	Lake Victoria	3	NO	0	0.03422619	0.04613095
CP287	Lake Victoria	3	NO	0	0.03783784	0.04864865
CP288	Lake Victoria	3	NO	0	0.04145078	0.06217617
CP289	Lake Victoria	3	NO	0	0.03947368	0.05526316
CP290	Lake Victoria	3	NO	0	0.04782609	0.05652174
CP291	Lake Victoria	3	NO	0	0.03374233	0.0398773
CP292	Lake Victoria	3	NO	0	0.02093398	0.02898551
CP293	Lake Victoria	3	NO	0	0.05	0.0625
CP251	Lancefield Swamp	4	NO	0	0.03550296	0.03550296
CP252	Lancefield Swamp	3	NO	0	0.03144654	0.03459119
CP253	Lancefield Swamp	3	NO	0	0.0334728	0.0334728
CP254	Lancefield Swamp	4	NO	0	0.03448276	0.03448276
CP255	Lancefield Swamp	4	NO	0	0.03703704	0.04320988
CP256	Lancefield Swamp	4	NO	0	0.03753351	0.03753351
CP257	Lancefield Swamp	3	NO	0	0.03333333	0.04285714
CP258	Lancefield Swamp	4	NO	0	0.03163445	0.03163445
CP259	Lancefield Swamp	4	NO	0	0.0328084	0.0328084
CP260	Lancefield Swamp	4	NO	0	0.0450237	0.04739336
CP261	Lancefield Swamp	4	NO	0	0.06542056	0.06542056
CP262	Lancefield Swamp	4	NO	0	0.04201681	0.04201681
CP263	Lancefield Swamp	4	NO	0	0.05200946	0.05437352
CP264	Lancefield Swamp	4	NO	0	0.05448718	0.05448718
CP265	Lancefield Swamp	4	NO	0	0.05511811	0.05511811
CP266	Lancefield Swamp	4	NO	0	0.04255319	0.04432624
CP267	Lancefield Swamp	4	NO	0	0.03459459	0.03459459
CP268	Lancefield Swamp	4	NO	0	0.05555556	0.0625
CP269	Lancefield Swamp	4	NO	0	0.05092593	0.05555556
CP270	Lancefield Swamp	4	NO	0	0.05025971	0.05025971
CP271	Lancefield Swamp	4	NO	0	0.04651163	0.04651163
CP272	Lancefield Swamp	4	NO	0	0.05714286	0.06428571
CP273	Lancefield Swamp	4	NO	0	0.04472843	0.04472843
CP274	Lancefield Swamp	4	NO	0	0.0430622	0.0430622
CP275	Lancefield Swamp	4	NO	0	0.05565863	0.05751391
CP305	Lancefield Swamp	3	NO	0	0.05797101	0.06763285
CP306	Lancefield Swamp	3	NO	0	0.11968085	0.13297872
CP307	Lancefield Swamp	3	YES	0.669	0.0620915	0.06535948
CP308	Lancefield Swamp	3	NO	0	0.04411765	0.04411765
CP309	Lancefield Swamp	3	NO	0	0.04022989	0.04022989
CP403	Mammoth Cave	4	NO	0	0.05594406	0.06713287
CP404	Mammoth Cave	4	NO	0	0.06506849	0.09246575
CP405	Mammoth Cave	4	YES	0.891	0.09090909	0.24242424
CP406	Mammoth Cave	4	NO	0	0.09917355	0.17355372
CP407	Mammoth Cave	4	NO	0	0.06306306	0.10585586
CP408	Mammoth Cave	3	NO	0	0.03759398	0.06265664
CP409	Mammoth Cave	4	NO	0	0.09961686	0.11494253
CP410	Mammoth Cave	4	NO	0	0.08284024	0.1183432
CP411	Mammoth Cave	3	NO	0	0.07352941	0.09926471
CP412	Mammoth Cave	4	NO	0	0.0691358	0.1037037
CP1255	Mammoth Cave	3	NO	0	0.05531915	0.08368794
CP1256	Mammoth Cave	3	NO	0	0.0668693	0.09422492
CP217	McEachern Cave	4	NO	0	0.04545455	0.04679144
CP218	McEachern Cave	4	NO	0	0.04602511	0.05020921
CP219	McEachern Cave	4	NO	0	0.02921647	0.03187251
CP220	McEachern Cave	4	NO	0	0.0339233	0.03539823
CP221	McEachern Cave	4	NO	0	0.04191617	0.0499002
CP222	McEachern Cave	4	NO	0	0.05226481	0.06271777
CP223	McEachern Cave	4	NO	0	0.04712042	0.04973822
CP224	McEachern Cave	4	NO	0	0.04545455	0.04820937
CP225	McEachern Cave	4	NO	0	0.05185185	0.05555556
CP226	McEachern Cave	4	NO	0	0.05077263	0.05960265
CP310	McEachern Cave	3	YES	0.9455	0.08955224	0.08955224
CP312	McEachern Cave	4	NO	0	0.03969754	0.05671078
CP361	McEachern Cave	4	NO	0	0.05113636	0.0625
CP362	McEachern Cave	4	NO	0	0.05136986	0.06164384
CP363	McEachern Cave	4	NO	0	0.05909091	0.06818182
CP364	McEachern Cave	4	NO	0	0.03442879	0.04225352
CP365	McEachern Cave	4	NO	0	0.03623188	0.04202899
CP366	McEachern Cave	4	NO	0	0.05140187	0.06074766
CP367	McEachern Cave	4	NO	0	0.04166667	0.05
CP368	McEachern Cave	4	NO	0	0.06617647	0.08088235
CP369	McEachern Cave	4	NO	0	0.04622871	0.05352798
CP370	McEachern Cave	4	NO	0	0.04567308	0.04807692

CP371	McEachern Cave	4	NO	0		0.03818616	0.04534606
CP372	McEachern Cave	4	NO	0		0.03753027	0.05811138
CP373	McEachern Cave	4	NO	0		0.03035714	0.05
CP187	Morwell	4	NO	0		0.2818792	0.31879195
CP188	Morwell	4	NO	0		0.10465116	0.11627907
CP189	Morwell	4	NO	0		0.06830601	0.07923497
CP190	Morwell	3	NO	0		0.07303371	0.08426966
CP191	Morwell	3	NO	0		0.06161137	0.07582938
CP192	Morwell	3	NO	0		0.04496788	0.05567452
CP193	Morwell	3	NO	0		0.03767123	0.04452055
CP194	Morwell	3	NO	0		0.07826087	0.07826087
CP195	Morwell	3	NO	0		0.0625	0.06944444
CP196	Morwell	3	NO	0		0.04142012	0.0591716
CP197	Morwell	3	NO	0		0.04373178	0.04956268
CP354	Morwell	3	NO	0		0.09090909	0.09090909
CP355	Morwell	3	NO	0		0.06642066	0.099631
CP356	Morwell	3	NO	0		0.06514085	0.09683099
CP357	Morwell	3	NO	0		0.10526316	0.14912281
CP358	Morwell	3	NO	0		0.06379585	0.09250399
CP359	Morwell	3	NO	0		0.07518797	0.10526316
CP360	Morwell	3	NO	0		0.07089552	0.10447761
CP374	Morwell	3	NO	0		0.07988166	0.09467456
CP375	Morwell	3	NO	0		0.07246377	0.10869565
CP008	Rockhampton Region (Colosseum Chambe	NA	NO	0	NA	NA	
CP009	Rockhampton Region (Colosseum Chambe	NA	NO	0	NA	NA	
CP010	Rockhampton Region (Colosseum Chambe	NA	NO	0	NA	NA	
CP011	Rockhampton Region (Colosseum Chambe	NA	NO	0	NA	NA	
CP012	Rockhampton Region (Colosseum Chambe	NA	NO	0	NA	NA	
CP013	Rockhampton Region (Colosseum Chambe	NA	NO	0	NA	NA	
CP014	Rockhampton Region (Colosseum Chambe	NA	NO	0	NA	NA	
CP015	Rockhampton Region (Colosseum Chambe	NA	NO	0	NA	NA	
CP016	Rockhampton Region (Colosseum Chambe	NA	NO	0	NA	NA	
CP017	Rockhampton Region (Colosseum Chambe	NA	NO	0	NA	NA	
CP018	Rockhampton Region (Colosseum Chambe	NA	NO	0	NA	NA	
CP019	Rockhampton Region (Colosseum Chambe	NA	NO	0	NA	NA	
CP020	Rockhampton Region (Colosseum Chambe	NA	NO	0	NA	NA	
CP021	Rockhampton Region (Colosseum Chambe	NA	NO	0	NA	NA	
CP022	Rockhampton Region (Colosseum Chambe	NA	NO	0	NA	NA	
CP023	Rockhampton Region (Colosseum Chambe	NA	NO	0	NA	NA	
CP024	Rockhampton Region (Colosseum Chambe	NA	NO	0	NA	NA	
CP025	Rockhampton Region (Colosseum Chambe	NA	NO	0	NA	NA	
CP026	Rockhampton Region (Colosseum Chambe	NA	NO	0	NA	NA	
CP027	Rockhampton Region (Colosseum Chambe	NA	NO	0	NA	NA	
CP028	Rockhampton Region (Colosseum Chambe	NA	NO	0	NA	NA	
CP029	Rockhampton Region (Colosseum Chambe	NA	NO	0	NA	NA	
CP030	Rockhampton Region (Colosseum Chambe	NA	NO	0	NA	NA	
CP031	Rockhampton Region (Colosseum Chambe	NA	NO	0	NA	NA	
CP032	Rockhampton Region (Colosseum Chambe	NA	NO	0	NA	NA	
CP033	Rockhampton Region (Colosseum Chambe	NA	NO	0	NA	NA	
CP034	Rockhampton Region (Colosseum Chambe	NA	NO	0	NA	NA	
CP035	Rockhampton Region (Colosseum Chambe	NA	NO	0	NA	NA	
CP036	Rockhampton Region (Colosseum Chambe	NA	NO	0	NA	NA	
CP037	Rockhampton Region (Colosseum Chambe	NA	NO	0	NA	NA	
CP038	Rockhampton Region (Colosseum Chambe	NA	NO	0	NA	NA	
CP039	Rockhampton Region (Colosseum Chambe	NA	NO	0	NA	NA	
CP040	Rockhampton Region (Colosseum Chambe	NA	NO	0	NA	NA	
CP041	Rockhampton Region (Colosseum Chambe	NA	NO	0	NA	NA	
CP042	Rockhampton Region (Colosseum Chambe	NA	NO	0	NA	NA	
CP043	Rockhampton Region (Colosseum Chambe	NA	NO	0	NA	NA	
CP044	Rockhampton Region (Colosseum Chambe	NA	NO	0	NA	NA	
CP045	Rockhampton Region (Colosseum Chambe	NA	NO	0	NA	NA	
CP046	Rockhampton Region (Colosseum Chambe	NA	NO	0	NA	NA	
CP094	Rockhampton Region (Colosseum Chambe	NA	NO	0		0.03835616	0.05616438
CP095	Rockhampton Region (Colosseum Chambe	NA	NO	0		0.07194245	0.07194245
CP096	Rockhampton Region (Colosseum Chambe	NA	NO	0		0.04617834	0.06687898
CP097	Rockhampton Region (Colosseum Chambe	NA	NO	0		0.04697987	0.06040268
CP098	Rockhampton Region (Colosseum Chambe	NA	NO	0		0.05327869	0.06147541
CP099	Rockhampton Region (Colosseum Chambe	NA	NO	0		0.05292479	0.05571031
CP100	Rockhampton Region (Colosseum Chambe	NA	NO	0		0.04555809	0.05922551
CP101	Rockhampton Region (Colosseum Chambe	NA	NO	0		0.03542207	0.04133858
CP102	Rockhampton Region (Colosseum Chambe	NA	NO	0		0.0458221	0.05929919
CP103	Rockhampton Region (Colosseum Chambe	NA	NO	0		0.05232558	0.06976744
CP104	Rockhampton Region (Colosseum Chambe	NA	NO	0		0.04094828	0.0625
CP105	Rockhampton Region (Colosseum Chambe	NA	NO	0		0.04040404	0.04713805
CP106	Rockhampton Region (Colosseum Chambe	NA	NO	0		0.03605016	0.04545455
CP107	Rockhampton Region (Colosseum Chambe	NA	NO	0		0.04932735	0.05829596
CP108	Rockhampton Region (Colosseum Chambe	NA	NO	0		0.03910615	0.04655493
CP109	Rockhampton Region (Colosseum Chambe	NA	NO	0		0.03971963	0.05140187
CP110	Rockhampton Region (Colosseum Chambe	NA	NO	0		0.05389222	0.06586826
CP111	Rockhampton Region (Colosseum Chambe	NA	NO	0		0.07207207	0.07207207

CP112	Rockhampton Region (Colosseum Chambe	NA	NO	0	0.03624161	0.0442953
CP113	Rockhampton Region (Colosseum Chambe	NA	NO	0	0.03956835	0.05035971
CP114	Rockhampton Region (Colosseum Chambe	NA	NO	0	0.03676471	0.06176471
CP115	Rockhampton Region (Colosseum Chambe	NA	NO	0	0.05263158	0.10526316
CP116	Rockhampton Region (Colosseum Chambe	NA	NO	0	0.035	0.05166667
CP117	Rockhampton Region (Colosseum Chambe	NA	NO	0	0.03773585	0.05424528
CP118	Rockhampton Region (Colosseum Chambe	NA	NO	0	0.05263158	0.0877193
CP119	Rockhampton Region (Colosseum Chambe	NA	NO	0	0.04316547	0.07913669
CP120	Rockhampton Region (Colosseum Chambe	NA	NO	0	0.04193548	0.06129032
CP121	Rockhampton Region (Colosseum Chambe	NA	NO	0	0.04792332	0.0798722
CP122	Rockhampton Region (Colosseum Chambe	NA	NO	0	0.03717472	0.06319703
CP123	Rockhampton Region (Colosseum Chambe	NA	NO	0	0.03597122	0.06714628
CP124	Rockhampton Region (Colosseum Chambe	NA	NO	0	0.0430622	0.05741627
CP125	Rockhampton Region (Colosseum Chambe	NA	NO	0	0.05590062	0.06832298
CP126	Rockhampton Region (Colosseum Chambe	NA	NO	0	0.03636364	0.04090909
CP127	Rockhampton Region (Colosseum Chambe	NA	NO	0	0.02857143	0.03809524
CP128	Rockhampton Region (Colosseum Chambe	NA	NO	0	0.03475936	0.05347594
CP129	Rockhampton Region (Colosseum Chambe	NA	NO	0	0.04166667	0.08333333
CP130	Rockhampton Region (Colosseum Chambe	NA	NO	0	0.0375	0.04375
CP131	Rockhampton Region (Colosseum Chambe	NA	NO	0	0.04784689	0.05741627
CP132	Rockhampton Region (Colosseum Chambe	NA	NO	0	0.03112314	0.03247632
CP133	Rockhampton Region (Colosseum Chambe	NA	NO	0	0.03333333	0.04545455
CP134	Rockhampton Region (Colosseum Chambe	NA	NO	0	0.04411765	0.05672269
CP135	Rockhampton Region (Colosseum Chambe	NA	NO	0	0.03862661	0.05579399
CP136	Rockhampton Region (Colosseum Chambe	NA	NO	0	0.03797468	0.06962025
CP137	Rockhampton Region (Colosseum Chambe	NA	NO	0	0.03255814	0.04418605
CP138	Rockhampton Region (Colosseum Chambe	NA	NO	0	0.04444444	0.05714286
CP139	Rockhampton Region (Colosseum Chambe	NA	NO	0	0.04230769	0.07692308
CP140	Rockhampton Region (Colosseum Chambe	NA	NO	0	0.03532609	0.05706522
CP141	Rockhampton Region (Colosseum Chambe	NA	NO	0	0.03598972	0.05141388
CP142	Rockhampton Region (Colosseum Chambe	NA	NO	0	0.04109589	0.04109589
CP143	Rockhampton Region (Colosseum Chambe	NA	NO	0	0.03468208	0.06936416
CP144	Rockhampton Region (Colosseum Chambe	NA	NO	0	0.03597122	0.03597122
CP145	Rockhampton Region (Colosseum Chambe	NA	NO	0	0.05050505	0.08080808
CP146	Rockhampton Region (Colosseum Chambe	NA	NO	0	0.0443038	0.08227848
CP147	Rockhampton Region (Colosseum Chambe	NA	NO	0	0.036	0.068
CP148	Rockhampton Region (Colosseum Chambe	NA	NO	0	0.05405405	0.05405405
CP149	Rockhampton Region (Colosseum Chambe	NA	NO	0	0.04511278	0.07518797
CP150	Rockhampton Region (Colosseum Chambe	NA	NO	0	0.03915663	0.05722892
CP151	Rockhampton Region (Colosseum Chambe	NA	NO	0	0.0440678	0.09830508
CP152	Rockhampton Region (Colosseum Chambe	NA	NO	0	0.03861789	0.05691057
CP153	Rockhampton Region (Colosseum Chambe	NA	NO	0	0.05649718	0.06779661
CP749	Rockhampton Region (Honeymoon Suite)	4	NO	0	0.02614379	0.04901961
CP750	Rockhampton Region (Honeymoon Suite)	4	NO	0	0.01981506	0.03038309
CP751	Rockhampton Region (Honeymoon Suite)	4	NO	0	0.02190722	0.02963918
CP752	Rockhampton Region (Honeymoon Suite)	4	NO	0	0.04891304	0.08152174
CP753	Rockhampton Region (Honeymoon Suite)	4	NO	0	0.04093567	0.07602339
CP754	Rockhampton Region (Honeymoon Suite)	4	NO	0	0.0418251	0.09505703
CP755	Rockhampton Region (Honeymoon Suite)	4	NO	0	0.05454545	0.10454545
CP756	Rockhampton Region (Honeymoon Suite)	4	NO	0	0.04504505	0.05630631
CP757	Rockhampton Region (Honeymoon Suite)	4	NO	0	0.03130148	0.05271829
CP758	Rockhampton Region (Honeymoon Suite)	4	NO	0	0.056	0.072
CP759	Rockhampton Region (Honeymoon Suite)	4	YES	0.659	0.04407713	0.04683196
CP760	Rockhampton Region (Honeymoon Suite)	4	NO	0	0.04659498	0.09677419
CP761	Rockhampton Region (Honeymoon Suite)	4	NO	0	0.07185629	0.08383234
CP762	Rockhampton Region (Honeymoon Suite)	4	NO	0	0.05602241	0.07282913
CP763	Rockhampton Region (Honeymoon Suite)	4	NO	0	0.04160888	0.0443828
CP764	Rockhampton Region (Honeymoon Suite)	4	NO	0	0.05501618	0.09798738
CP765	Rockhampton Region (Honeymoon Suite)	4	YES	0.6305	0.04201681	0.04201681
CP766	Rockhampton Region (Honeymoon Suite)	4	NO	0	0.0443038	0.04746835
CP1143	Rockhampton Region (Colosseum Chambe	4	NO	0	0.04	0.05333333
CP1144	Rockhampton Region (Colosseum Chambe	4	NO	0	0.06024096	0.10240964
CP1145	Rockhampton Region (Colosseum Chambe	4	NO	0	0.03614458	0.04417671
CP1146	Rockhampton Region (Colosseum Chambe	4	NO	0	0.03896104	0.05844156
CP1147	Rockhampton Region (Colosseum Chambe	4	NO	0	0.04330709	0.06692913
CP1148	Rockhampton Region (Colosseum Chambe	4	NO	0	0.04460967	0.06319703
CP1219	Rockhampton Region (Colosseum Chambe	4	NO	0	0.04081633	0.04719388
CP1220	Rockhampton Region (Colosseum Chambe	4	NO	0	0.0515873	0.07936508
CP1221	Rockhampton Region (Colosseum Chambe	3	NO	0	0.04979253	0.06639004
CP1222	Rockhampton Region (Colosseum Chambe	3	NO	0	NA	NA
CP1223	Rockhampton Region (Colosseum Chambe	4	NO	0	0.03166667	0.03666667
CP1224	Rockhampton Region (Colosseum Chambe	4	NO	0	0.03594771	0.06535948
CP1225	Rockhampton Region (Colosseum Chambe	4	NO	0	0.03853955	0.05273834
CP1226	Rockhampton Region (Colosseum Chambe	4	NO	0	0.05691057	0.07317073
CP1227	Rockhampton Region (Colosseum Chambe	3	NO	0	0.04024145	0.04627767
CP1228	Rockhampton Region (Colosseum Chambe	4	NO	0	0.06711409	0.06711409
CP1229	Rockhampton Region (Colosseum Chambe	4	NO	0	0.03830645	0.04233871
CP1230	Rockhampton Region (Colosseum Chambe	3	NO	0	0.04854369	0.05501618
CP1231	Rockhampton Region (Colosseum Chambe	4	NO	0	0.05490196	0.05490196
CP1232	Rockhampton Region (Colosseum Chambe	3	NO	0	0.05394191	0.06224066

CP1233	Rockhampton Region (Colosseum Chambe NA		NO		0	0.0474934	0.05013193
CP1234	Rockhampton Region (Colosseum Chambe	3	NO		0	0.03370787	0.03595506
CP1235	Rockhampton Region (Colosseum Chambe	3	NO		0	0.04910714	0.05803571
CP579	South Walker Creek (SW9)	4	NO		0	0.05506608	0.05506608
CP580	South Walker Creek (SW9)	4	NO		0	0.03636364	0.03636364
CP581	South Walker Creek (SW9)	4	NO		0	0.05665025	0.05665025
CP582	South Walker Creek (SW9)	4	NO		0	0.05223881	0.05223881
CP583	South Walker Creek (SW9)	4	NO		0	0.06620209	0.06620209
CP584	South Walker Creek (SW9)	4	NO		0	0.04043127	0.04043127
CP585	South Walker Creek (SW9)	4	NO		0	0.04065041	0.04065041
CP586	South Walker Creek (SW9)	4	NO		0	0.03037383	0.03154206
CP587	South Walker Creek (SW9)	4	NO		0	0.03867403	0.04051565
CP588	South Walker Creek (SW9)	4	NO		0	0.03021583	0.03165468
CP589	South Walker Creek (SW9)	4	NO		0	0.02927581	0.02927581
CP590	South Walker Creek (SW9)	4	NO		0	0.05246914	0.05246914
CP591	South Walker Creek (SW9)	4	NO		0	0.0330033	0.0330033
CP592	South Walker Creek (SW9)	4	NO		0	0.03791469	0.03791469
CP593	South Walker Creek (SW9)	4	NO		0	0.06038647	0.06038647
CP594	South Walker Creek (SW9)	4	NO		0	0.04878049	0.04878049
CP595	South Walker Creek (SW9)	4	NO		0	0.03762376	0.03762376
CP596	South Walker Creek (SW9)	4	NO		0	0.04301075	0.0483871
CP597	South Walker Creek (SW9)	4	NO		0	0.04615385	0.04615385
CP598	South Walker Creek (SW9)	4	NO		0	0.02941177	0.03267974
CP599	South Walker Creek (SW9)	4	NO		0	0.03359684	0.03359684
CP600	South Walker Creek (SW9)	4	NO		0	0.03432494	0.03661327
CP601	South Walker Creek (SW9)	4	NO		0	0.03975535	0.03975535
CP602	South Walker Creek (SW9)	4	NO		0	0.028125	0.03125
CP603	South Walker Creek (SW9)	4	NO		0	0.03321033	0.03321033
CP604	South Walker Creek (SW9)	4	NO		0	0.04	0.04
CP605	South Walker Creek (SW9)	4	NO		0	0.03470032	0.03470032
CP606	South Walker Creek (SW9)	4	NO		0	0.02540107	0.02540107
CP607	South Walker Creek (SW9)	4	NO		0	0.03153153	0.03153153
CP608	South Walker Creek (SW9)	4	NO		0	0.0304	0.0304
CP609	South Walker Creek (SW9)	4	NO		0	0.05285412	0.05285412
CP610	South Walker Creek (SW9)	4	NO		0	0.03939963	0.03939963
CP611	South Walker Creek (SW9)	4	NO		0	0.04745763	0.04745763
CP612	South Walker Creek (SW9)	4	NO		0	0.03714286	0.04
CP613	South Walker Creek (SW9)	4	NO		0	0.03185596	0.03185596
CP614	South Walker Creek (SW9)	4	NO		0	0.03703704	0.03703704
CP615	South Walker Creek (SW9)	4	NO		0	0.04666667	0.04666667
CP616	South Walker Creek (SW9)	4	NO		0	0.05077263	0.05077263
CP617	South Walker Creek (SW9)	4	NO		0	0.03571429	0.04285714
CP618	South Walker Creek (SW9)	4	NO		0	0.05699482	0.05699482
CP619	South Walker Creek (SW9)	4	NO		0	0.04035874	0.04484305
CP276	Spring Creek	3	NO		0	0.03878583	0.04384486
CP277	Spring Creek	4	NO		0	0.04651163	0.04883721
CP278	Spring Creek	4	NO		0	0.04198473	0.04198473
CP279	Spring Creek	3	NO		0	0.03921569	0.04139434
CP280	Spring Creek	4	NO		0	0.04656319	0.04656319
CP281	Spring Creek	4	NO		0	0.0460251	0.05439331
CP282	Spring Creek	3	NO		0	0.06008584	0.06652361
CP283	Spring Creek	4	NO		0	0.03739837	0.04227642
CP343	Spring Creek	4	NO		0	0.05421687	0.06325301
CP344	Spring Creek	3	YES		0.1735	0.06545455	0.07636364
CP345	Spring Creek	3	NO		0	0.05737705	0.06557377
CP346	Spring Creek	4	NO		0	0.06626506	0.07228916
CP347	Spring Creek	3	YES		0.1595	0.0483871	0.05241935
CP348	Spring Creek	4	NO		0	0.05940594	0.05940594
CP349	Spring Creek	3	NO		0	0.05629139	0.05629139
CP227	Strathdownie	3	NO		0	0.0385289	0.0525394
CP228	Strathdownie	4	NO		0	0.04888889	0.07555556
CP229	Strathdownie	4	NO		0	0.06508876	0.06508876
CP230	Strathdownie	3	NO		0	0.03107345	0.0480226
CP231	Strathdownie	3	NO		0	0.03726708	0.04968944
CP232	Strathdownie	4	NO		0	0.03448276	0.06034483
CP233	Strathdownie	3	NO		0	0.04025424	0.07627119
CP234	Strathdownie	4	NO		0	0.02978723	0.04539007
CP235	Strathdownie	4	NO		0	0.03418803	0.04558405
CP236	Strathdownie	3	NO		0	0.03438395	0.0487106
CP237	Strathdownie	4	NO		0	0.04651163	0.05943152
CP238	Strathdownie	4	NO		0	0.02216749	0.02955665
CP239	Strathdownie	3	NO		0	0.03631285	0.05865922
CP240	Strathdownie	3	NO		0	0.02777778	0.04385965
CP241	Strathdownie	3	NO		0	0.03143418	0.04715128
CP489	Tight Entrance Cave	4	NO		0	NA	NA
CP490	Tight Entrance Cave	4	NO		0	NA	NA
CP491	Tight Entrance Cave	4	NO		0	0.04195804	0.06993007
CP492	Tight Entrance Cave	4	NO		0	0.10666667	0.18666667
CP493	Tight Entrance Cave	4	NO		0	0.02625298	0.0548926
CP494	Tight Entrance Cave	4	NO		0	0.0362117	0.06128134

CP495	Tight Entrance Cave	4	NO	0		0.04935622	0.07081545
CP496	Tight Entrance Cave	4	NO	0		0.03542234	0.06811989
CP497	Tight Entrance Cave	4	NO	0		0.02920723	0.05006954
CP498	Tight Entrance Cave	4	NO	0		0.02749141	0.04639175
CP499	Tight Entrance Cave	4	NO	0		0.02088452	0.03439803
CP500	Tight Entrance Cave	4	NO	0		0.04104478	0.06343284
CP501	Tight Entrance Cave	4	NO	0		0.05369128	0.11409396
CP502	Tight Entrance Cave	4	NO	0		0.04666667	0.06666667
CP503	Tight Entrance Cave	4	NO	0		0.03738318	0.04672897
CP504	Tight Entrance Cave	4	NO	0		0.02122642	0.03773585
CP505	Tight Entrance Cave	4	NO	0	NA	NA	
CP506	Tight Entrance Cave	4	NO	0	NA	NA	
CP507	Tight Entrance Cave	4	NO	0		0.03010033	0.04013378
CP508	Tight Entrance Cave	4	NO	0		0.04926108	0.07881773
CP509	Tight Entrance Cave	4	NO	0		0.03125	0.05698529
CP510	Tight Entrance Cave	4	NO	0		0.04405286	0.05286344
CP511	Tight Entrance Cave	4	NO	0		0.04424779	0.05752212
CP512	Tight Entrance Cave	4	NO	0		0.04255319	0.06382979
CP513	Tight Entrance Cave	4	NO	0		0.02814259	0.04502814
CP514	Tight Entrance Cave	4	NO	0		0.04115226	0.05761317
CP515	Tight Entrance Cave	4	NO	0		0.07246377	0.21256039
CP516	Tight Entrance Cave	4	NO	0		0.02739726	0.05136986
CP517	Tight Entrance Cave	4	NO	0		0.0467033	0.05494505
CP518	Tight Entrance Cave	4	NO	0		0.04694836	0.08920188
CP519	Tight Entrance Cave	4	NO	0		0.04713805	0.06734007
CP520	Tight Entrance Cave	4	NO	0	NA	NA	
CP521	Tight Entrance Cave	4	NO	0		0.2777778	0.03240741
CP522	Tight Entrance Cave	4	NO	0	NA	NA	
CP523	Tight Entrance Cave	4	NO	0		0.03927492	0.09667674
CP524	Tight Entrance Cave	4	NO	0		0.06896552	0.17241379
CP525	Tight Entrance Cave	4	NO	0		0.03131991	0.04697987
CP526	Tight Entrance Cave	4	NO	0		0.02272727	0.03598485
CP527	Tight Entrance Cave	4	NO	0		0.02118003	0.03177005
CP528	Tight Entrance Cave	4	NO	0		0.03992016	0.06986028
CP529	Tight Entrance Cave	4	NO	0		0.04424779	0.07964602
CP530	Tight Entrance Cave	4	NO	0		0.02846975	0.04626335
CP531	Tight Entrance Cave	4	NO	0		0.05555556	0.08730159
CP532	Tight Entrance Cave	4	NO	0		0.01405152	0.03629977
CP533	Tight Entrance Cave	4	NO	0		0.02201258	0.03144654
CP534	Tight Entrance Cave	4	NO	0		0.03345725	0.08178439
CP535	Tight Entrance Cave	4	NO	0		0.02420857	0.04096834
CP536	Tight Entrance Cave	4	NO	0		0.02310924	0.03781513
CP537	Tight Entrance Cave	4	NO	0		0.06521739	0.2826087
CP538	Tight Entrance Cave	4	NO	0		0.03183024	0.04774536
CP539	Tight Entrance Cave	4	NO	0		0.02475248	0.03712871
CP540	Tight Entrance Cave	4	YES	0.6145		0.02884615	0.03461538
CP541	Tight Entrance Cave	4	NO	0		0.06	0.08
CP542	Tight Entrance Cave	4	NO	0	NA	NA	
CP543	Tight Entrance Cave	4	NO	0		0.04179104	0.06268657
CP544	Tight Entrance Cave	4	NO	0		0.03317536	0.04739336
CP545	Tight Entrance Cave	4	NO	0	NA	NA	
CP546	Tight Entrance Cave	4	NO	0		0.03349282	0.0861244
CP547	Tight Entrance Cave	4	NO	0		0.05128205	0.09401709
CP548	Tight Entrance Cave	4	NO	0		0.03578154	0.06026365
CP549	Tight Entrance Cave	4	NO	0		0.03804348	0.08152174
CP550	Tight Entrance Cave	4	NO	0		0.03654485	0.04651163
CP551	Tight Entrance Cave	4	NO	0		0.04741379	0.07327586
CP552	Tight Entrance Cave	4	NO	0		0.03521127	0.05985915
CP553	Tight Entrance Cave	4	NO	0		0.0306834	0.0446304
CP554	Tight Entrance Cave	4	NO	0		0.03351955	0.05586592
CP555	Tight Entrance Cave	4	NO	0		0.03616134	0.054242
CP556	Tight Entrance Cave	4	NO	0		0.02727273	0.04545455
CP557	Tight Entrance Cave	4	NO	0		0.02711324	0.05263158
CP558	Tight Entrance Cave	4	NO	0		0.02702703	0.04176904
CP559	Tight Entrance Cave	4	NO	0		0.04054054	0.05675676
CP560	Tight Entrance Cave	4	NO	0	NA	NA	
CP561	Tight Entrance Cave	4	NO	0		0.03076923	0.04307692
CP562	Tight Entrance Cave	4	NO	0		0.0280112	0.05042017
CP563	Tight Entrance Cave	4	NO	0		0.02639296	0.05571848
CP1159	Yellabidde Cave	3	YES	0.634		0.08264463	0.10330579
CP1160	Yellabidde Cave	3	YES	0.574		0.07417582	0.08241758
CP1161	Yellabidde Cave	3	NO	0		0.08465608	0.16931217
CP1162	Yellabidde Cave	3	NO	0		0.07758621	0.18534483
CP1163	Yellabidde Cave	3	YES	0.6525		0.08203125	0.12890625
CP1164	Yellabidde Cave	3	NO	0		0.08870968	0.10483871
CP1165	Yellabidde Cave	3	YES	0.7885		0.07279693	0.10344828
CP1166	Yellabidde Cave	3	NO	0		0.07692308	0.0989011
CP1167	Yellabidde Cave	3	NO	0		0.09322034	0.16949153
CP1168	Yellabidde Cave	3	YES	0.629		0.06185567	0.07474227
CP1169	Yellabidde Cave	3	YES	0.5775		0.05750799	0.0798722

CP1170	Yellabidde Cave	3	NO	0	0.09677419	0.11827957
CP1171	Yellabidde Cave	3	NO	0	0.09411765	0.11764706
CP1172	Yellabidde Cave	3	NO	0	0.07664234	0.08759124
CP1173	Yellabidde Cave	3	YES	0.6215	0.09205021	0.09623431
CP1174	Yellabidde Cave	3	NO	0	0.09230769	0.11794872
CP1175	Yellabidde Cave	3	YES	0.6355	0.0625	0.0875
CP1176	Yellabidde Cave	3	YES	0.6555	0.04957265	0.05982906
CP1177	Yellabidde Cave	3	YES	0.6835	0.08219178	0.0913242
CP1178	Yellabidde Cave	3	NO	0	0.08071749	0.11659193
CP1179	Yellabidde Cave	3	NO	0	0.04659498	0.07168459
CP1180	Yellabidde Cave	3	NO	0	0.04805492	0.0778032
CP1181	Yellabidde Cave	3	NO	0	0.04444444	0.08444444
CP1182	Yellabidde Cave	3	NO	0	0.04982206	0.10676157
CP1183	Yellabidde Cave	3	NO	0	0.04491726	0.08037825
CP1184	Yellabidde Cave	3	NO	0	0.04910714	0.08482143
CP1185	Yellabidde Cave	3	NO	0	0.04326923	0.08173077
CP1186	Yellabidde Cave	3	NO	0	0.06956522	0.17391304
CP1187	Yellabidde Cave	3	NO	0	0.05454545	0.11515152
CP1188	Yellabidde Cave	3	NO	0	0.07386364	0.09659091
CP1189	Yellabidde Cave	3	NO	0	0.03797468	0.06582278
CP1190	Yellabidde Cave	3	NO	0	0.05263158	0.06882591
CP1191	Yellabidde Cave	3	NO	0	0.06818182	0.11363636
CP1192	Yellabidde Cave	3	NO	0	0.05263158	0.07017544
CP1193	Yellabidde Cave	3	NO	0	0.06306306	0.09009009
CP1194	Yellabidde Cave	3	NO	0	0.04404145	0.06994819
CP1195	Yellabidde Cave	3	NO	0	0.05154639	0.0652921
CP1196	Yellabidde Cave	3	NO	0	0.06870229	0.09923664
CP1197	Yellabidde Cave	3	NO	0	0.05855856	0.13063063
CP1198	Yellabidde Cave	3	NO	0	0.04519774	0.06779661
CP1199	Yellabidde Cave	3	NO	0	0.05755396	0.15107914
CP1200	Yellabidde Cave	3	NO	0	0.06542056	0.11214953
CP1201	Yellabidde Cave	3	NO	0	0.06220096	0.0861244
CP1202	Yellabidde Cave	3	NO	0	0.05325444	0.07692308
CP1203	Yellabidde Cave	3	NO	0	0.06481481	0.10185185
CP1204	Yellabidde Cave	3	NO	0	0.05586592	0.09497207
CP1205	Yellabidde Cave	3	NO	0	0.05851064	0.07446809
CP1206	Yellabidde Cave	3	NO	0	0.08602151	0.11827957
CP1207	Yellabidde Cave	3	NO	0	0.06730769	0.09615385
CP1208	Yellabidde Cave	3	NO	0	0.06432749	0.10526316
CP1209	Yellabidde Cave	3	NO	0	0.05	0.06
CP1210	Yellabidde Cave	3	NO	0	0.05454545	0.08181818
CP1211	Yellabidde Cave	3	NO	0	0.05396825	0.13333333
CP1212	Yellabidde Cave	3	NO	0	0.05555556	0.07638889
CP1213	Yellabidde Cave	3	NO	0	0.05106383	0.06382979
CP1214	Yellabidde Cave	3	NO	0	0.07857143	0.12857143
CP1215	Yellabidde Cave	3	NO	0	0.04950495	0.06270627
CP1216	Yellabidde Cave	3	NO	0	0.05833333	0.1
CP1217	Yellabidde Cave	3	NO	0	0.05217391	0.06086857
CP1218	Yellabidde Cave	3	NO	0	0.04905063	0.07120253

8. Manuscript C

ZooMS and zooarchaeology, a match made in heaven? Integrating ZooMS into existing faunal records at Devil's Lair, SW Australia

Carli Peters[1,*], Noel Amano[1], Armita Ghassemifar[2], Helen Ryan[3], Mikael Siversson[3], Wayne Webb[4], Joe Dortch[2], Nicole Boivin[1,5,6,7,*]

1. Department of Archaeology, Max Planck Institute for Geoanthropology, Jena, Germany
2. School of Social Sciences, University of Western Australia, Perth, WA 6009, Australia
3. Western Australian Museum, Collections and Research, 49 Kew Street, Welshpool, WA 6106, Australia
4. Dowark Foundation, Walpole, WA 6398, Australia
5. School of Social Science, The University of Queensland, Brisbane, Qld 4071, Australia
6. Department of Anthropology, National Museum of Natural History, Smithsonian Institution, Washington DC, USA
7. Department of Anthropology and Archaeology, University of Calgary, Calgary, Canada

*Corresponding authors: Carli Peters and Nicole Boivin

Key words: Collagen fingerprinting; Zooarchaeology; Late Pleistocene; Southwest Australia

Abstract
Devil's Lair (Ngarlum Mia) currently provides the oldest evidence for human occupation of Southwest Australia at ca. 50 thousand years ago. However, in many cases, morphological identification of faunal remains at the site is challenging due to large-scale fragmentation of the osseous remains. To combat this issue, this study makes use of Zooarchaeology by Mass Spectrometry (ZooMS) to identify fragmented faunal remains from Devil's Lair. ZooMS results are incorporated with zooarchaeological and bulk bone DNA metabarcoding data to get a deeper understanding of the faunal assemblage at Devil's Lair. We show that an inflated number of macropods (kangaroos and wallabies) is present in the ZooMS-identified assemblage, which indicates a high degree of macropod carcass processing by humans and/or carnivores. Furthermore, this study shows that ZooMS can be successfully employed to study Late Pleistocene Australian faunal assemblages, which highlights the potential of future palaeoproteomics studies targeting Late Pleistocene material from Australia.

1. Introduction
The study of faunal diversity and exploitation in the past can provide important insights into human-animal and human-environment relationships and interactions in the past. However, for many sites in Australia our understanding of past subsistence strategies is dampened by low levels of organic preservation, rendering analysis of osseous remains impossible (Langley et al., 2011, Monks, 2021). At sites where organic remains are preserved, mostly limestone caves (Langley et al., 2011), bones are often highly fragmented, which makes it difficult to taxonomically identify of the osseous material, or to disentangle the taphonomic history of the assemblage (Cosgrove et al., 1990, Price and Webb, 2006, Manne and Veth, 2015). Devil's Lair (Ngarlum Mia) currently provides the earliest evidence for human occupation in Southwest Australia dating back to around 50 thousand years ago (kyr) (Turney et al., 2001). The site thus has the potential to provide us with critical information to better understand early human exploitation of local endemic fauna in this region of the world.

The faunal assemblage of Devil's Lair is characterized by a high degree of bone fragmentation. Faunal remains at the site were extensively processed as part of human exploitation strategies. Tasmanian

devils, whose presence at the site is evident from fossil material and coprolites, further fragmented the faunal remains by chewing and/or ingesting the bones. This resulted in a faunal assemblage that is mainly represented by small bone fragments lacking diagnostic features, while also lacking clear taphonomic indicators of human processing (Dortch and Wright, 2010). While an exact measure of fragmentation degrees is not available for Devil's Lair, the nearby site of Tunnel Cave has similar levels of fragmentation. At this site, only 4% of bone fragments was taxonomically identified (Dortch, 2004). Combined with osteomorphological similarities between closely related taxa, which further complicates the identification of the bone fragments, this reduced the number of bones that were taxonomically identified, thus limiting our understanding of faunal diversity and subsistence strategies at Devil's Lair in the past (Dortch and Wright, 2010). Zooarchaeology by Mass Spectrometry (ZooMS) has the potential to help overcome these issues and increase the resolution of the zooarchaeological record.

ZooMS, or collagen fingerprinting, is a high-throughput approach that can be used to identify faunal remains based on differences in collagen type I (COL1), the most abundant protein in bone, skin, antler, and dentine, between taxonomic groups (Buckley et al., 2009). Collagen fingerprinting is a faster and cheaper alternative to ancient DNA (aDNA)-based approaches (Buckley et al., 2009, Richter et al., 2020). At the same time, proteins generally preserve better over longer time periods, and are more resistant to degradation in harsh environments, such as hot, humid, or tropical contexts (Rybczynski et al., 2013, Demarchi et al., 2016, Cappellini et al., 2019). As a result, ZooMS is increasingly used to identify large numbers of bone fragments that are unidentifiable with morphological approaches (e.g. Welker et al., 2015, Sinet-Mathiot et al., 2019, Brown et al., 2021b). ZooMS can thus be used to increase the number of taxonomically identified remains at Devil's Lair to increase our understanding of the faunal diversity at the site. Furthermore, data on the taxonomic composition of the fragmented material can be beneficial to our understanding of the taphonomic history of the faunal assemblage.

ZooMS thus offers a complementary approach to the study of the zooarchaeological record and some initial efforts have already been made to bridge the gap between ZooMS and zooarchaeology. Many of these initial efforts have focused exclusively on expanding the number of identified bone fragments (e.g., Welker et al., 2015, Sinet-Mathiot et al., 2019, Brown et al., 2021b), while other studies combined the two methods to come to more specific taxonomic identifications with ZooMS. For example, van den Hurk et al. (2021) increased the resolution of ZooMS identifications based on morphological information about the size and dimensions of the specimens. Similarly, Silvestrini et al. (2022) utilized the size and thickness of the bone fragments for more specific taxonomic identifications with ZooMS. These initial studies already show the value in combining ZooMS and zooarchaeology. However, zooarchaeological methods are geared towards deciphering human behaviour, such as subsistence and hunting strategies, in the past, and do not solely focus on the taxonomic identification of faunal remains. Hence, the importance of quantification units like MNI (minimum number of individuals, MNE (minimum number of elements), and MAU (minimum number of animal units), in zooarchaeological research.

In this study, we further explore the broader question of how to best incorporate ZooMS results into existing faunal records and units of quantification, by focusing on the faunal assemblage of Devil's Lair. ZooMS analyses were performed to complement previous zooarchaeological analysis (Balme et al., 1978, Dortch and Wright, 2010) and bulk bone DNA metabarcoding analysis of the faunal assemblage (Murray et al., 2013). The results of these three approaches are compared and then pulled together to get a deeper understanding of the faunal assemblage at Devil's Lair. We explore in-depth what can be learned from each of the methods, what their strengths and weaknesses are, and most importantly, how they can be best combined for maximum effect.

2. Devil's Lair (Ngarlum Mia)

Devil's Lair is located in the Leeuwin Naturaliste National Park, Southwest Australia (Figure 1). A Pleistocene-aged limestone ridge, the Tamala Limestone, runs throughout this National Park, and is home to a large concentration of Late Pleistocene/Early Holocene cave sites, including Devil's Lair, other archaeological sites, such as Tunnel Cave and Witchcliffe Rock Shelter, and Rainbow Cave (Dortch and Wright, 2010), and palaeontological sites with fossil remains of extinct megafauna such as

Kudjal Yolgah Cave (Jankowski et al., 2016), Mammoth Cave (Archer et al., 1980), and Tight Entrance Cave (Prideaux et al., 2000, Prideaux et al., 2010).

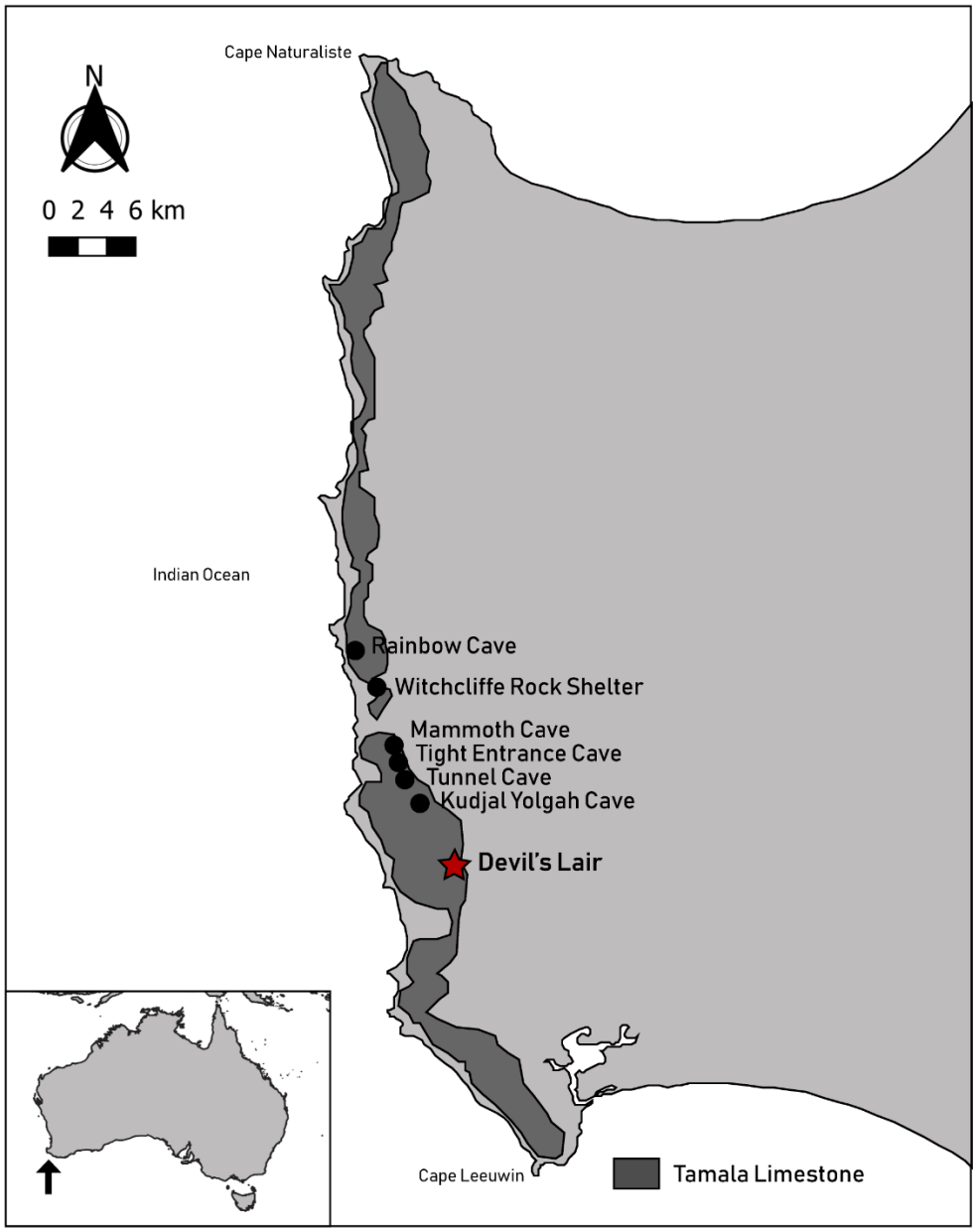

Figure 1: The location of Devil's Lair and other archaeological and palaeontological sites mentioned in the text.

Initial excavations at Devil's Lair were carried out in the 1970s and revealed extensive evidence for human occupation of the site during the Late Pleistocene (Balme et al., 1978, Dortch, 1979). The stratigraphic sequence has a maximum depth of 660 cm and consists of sandy sediments with flowstones and carbonate-cemented sediment bands running throughout (Dortch, 1979). The base of the stratigraphic sequence has been dated to >55 kyr ago using a combination of radiocarbon dating, optically stimulated luminescence (OSL), electron spin resonance (ESR), and U-series dating (Turney et al., 2001). A small number of stone tools has been recovered from layers 32-38, providing limited evidence for initial human occupation of the site 47-48 kyr ago. The earliest robust evidence for human occupation comes from layer 30 with the presence of a larger number of stone tools and animal bones dating to ca. 45 kyr ago (Dortch, 1979, Turney et al., 2001).

A broad range of fauna was identified in the zooarchaeological assemblage of the oldest stratigraphic layers (Periods I and II), including skinks, *Isoodon* (short-nosed bandicoot), *Perameles* (long-nosed bandicoot), *Pseudocheirus* (ringtail possum), *Trichosurus* (brushtail possum), *Potorous* (potoroo), *Bettongia penicillate* (bettong), *Setonix* (quokka), *Petrogale* (rock wallaby), *Notamacropus eugenii* (tammar wallaby), *Notamacropus irma* (brush wallaby), and *Macropus fuliginosus* (western grey kangaroo) (Balme et al., 1978, Dortch, 2004, Dortch and Wright, 2010). Additionally, a handful of megafauna bones were recovered from the deposits pre-dating human occupation, although their distinct taphonomic signature – the megafauna remains are carbonate encrusted - suggests they were washed in (Dortch, 1979). Faunal diversity at Devil's Lair was further examined using ancient DNA bulk bone metabarcoding (Murray et al., 2013). These results mostly supported zooarchaeological work; many of the same genera were detected as were identified morphologically. However, bulk bone metabarcoding did increase the number of small mammals, bird and reptile species identified at the site. Furthermore, *Tarsipes rostratus* (honey possum), previously absent from morphological analyses, was identified (Murray et al., 2013).

3. Methods

3.1. Material

In total, 94 bone fragments were sampled from layers 18-39, trenches 7d, 8, and 9 (Figure 2). Samples from these horizons were targeted since they represent the earliest occupation phases of the site (Periods I and II following Dortch (2004)). Horizon 39 is the stratigraphic layer below the first occupation layer and was dated with OSL-dating to 51.1 ± 2.6 kyr (Turney et al., 2001). Horizon 18 was radiocarbon dated to 31.4 ± 1.5 kyr (Dortch, 2004). All material is currently stored in the Archaeology and Palaeontology collections of the Western Australian Museum in Perth, Australia.

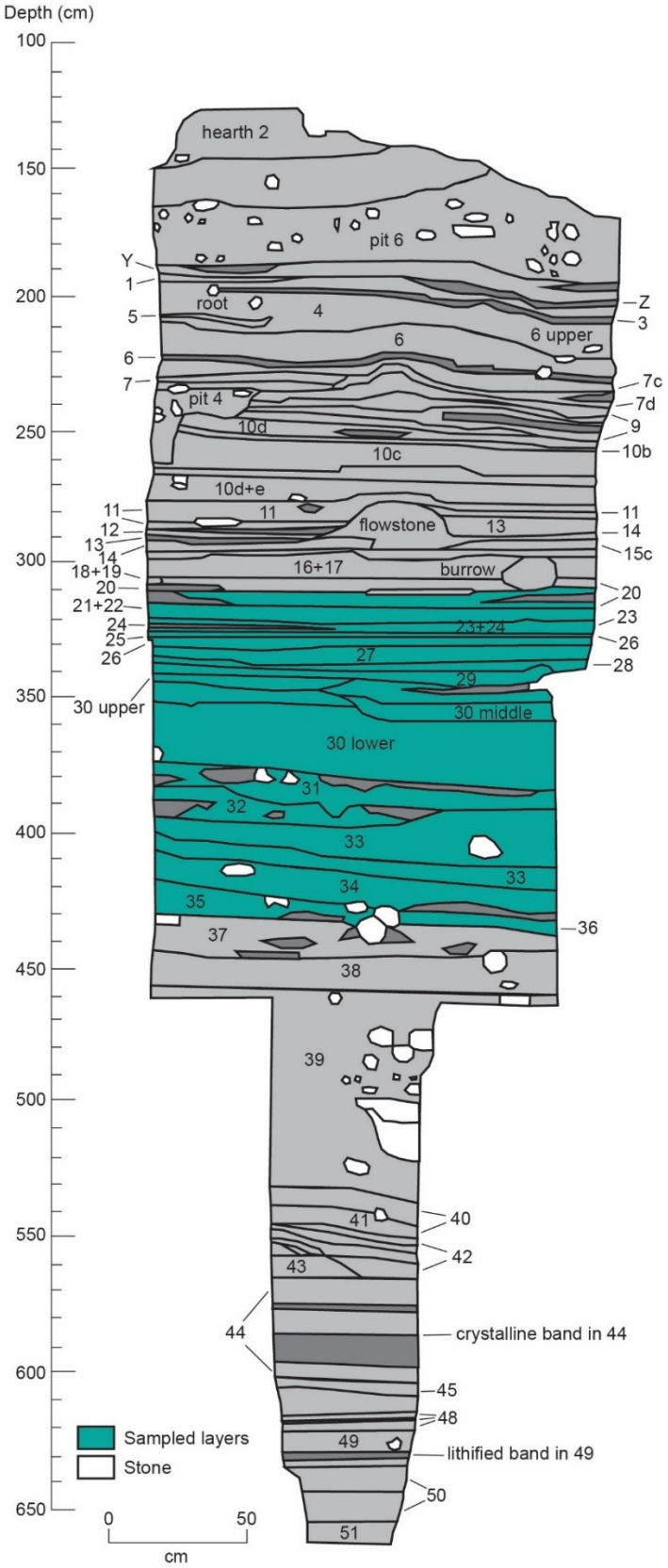

Figure 2: Stratigraphic sequence of Devil's Lair, east section of trench 9 (after Dortch, 1979, Turney et al., 2001). Layers that were sampled from for ZooMS analysis are highlighted.

Bone fragments of both larger and smaller than 2 cm in length were targeted, with an equal proportion of each size class targeted for each horizon, with the aim to represent small-, medium- and large-sized animals in the faunal assemblage. For each bone fragment, information about the length of the fragment

(<2 cm, 2-4 cm, >4 cm), body size class (small, medium-small, medium, medium-large, large), and the skeletal element (if identifiable) was also recorded to further aid comparison to and integration with zooarchaeological data following ZooMS analysis.

3.2. Zooarchaeology by Mass Spectrometry (ZooMS)

Collagen was extracted from the bone samples following a destructive, acid-soluble approach adapted from previously published methods (Buckley et al., 2009, Van der Sluis et al., 2014). Extraction blanks were run with alongside each set of extractions. Between 50-70 mg of bone powder was demineralized in 400 µl of 0.6 M hydrochloric acid (HCl) for 5 days. The samples were heated for 30 min at 65ºC, after which the supernatant was transferred to a 10 kDa ultrafilter (Microcon, Merck Millipore®) and centrifuged until completely passed through the filter. The samples were washed twice by adding 300 µl of 50 mM ammonium bicarbonate (AmBic) to the ultrafilter and centrifuging until completely passed through the filter. The fraction that did not pass through the filter was resuspended in 100 µl of 50 mM AmBic and digested on the filter with 1 µl of 0.4 µg/µl trypsin solution (Pierce™ Trypsin Protease, Thermo Scientific) for 18 h at 37ºC. Subsequent to enzymatic digestion, the samples were centrifuged a final time until completely passed through the filter. Peptides were then purified and concentrated using C18 ZipTips (Pierce™ C18 Tips, Thermo Scientific).

The resulting collagen extracts were spotted in duplicate onto an MTP Groundsteel 384-target plate, together with matrix solution (α-cyano-4-hydroxycinnamic acid of 10 mg/ml in 50% acetonitrile (ACN)/0.1% trifluoracetic acid (TFA)). Samples were analysed using an Autoflex Speed LRF matrix-assisted laser desorption/ionization time of flight mass spectrometer (MALDI-TOF-MS, Bruker Daltonics) with a smartbeam-II laser. A SNAP averaging algorithm was used to obtain monoisotopic masses (C: 4.9384, N: 1.3577, O: 1.4773, S: 0.00417, H: 7.7583). Resulting MALDI spectra were visually inspected using FlexAnalysis v. 3.4 (Bruker Daltonics) and taxonomically identified using a database of existing marsupial peptide markers (Buckley et al., 2017, Peters et al., 2021). The resulting taxonomic identifications were reported as ZooMS taxa (Table S1).

4. Results

ZooMS analysis from the Devil's Lair faunal assemblage yielded a high success rate. Of the 94 bone fragments included in the analysis, 83 (88,3%) had sufficient collagen preservation to yield collagen peptides visible in MALDI-ToF-MS spectra. No significant difference in ZooMS success rates has been observed between Period I (95,5%) and Period II (82%). An overview of the taxa identified with ZooMS is presented in Table 1, and a detailed overview of the results can be found in Supplementary Dataset 1.

Table 1: ZooMS NISP (number of identified specimens) counts for Devil's Lair, Periods I and II.

	Period I	**Period II**
ZooMS taxa		
Dasyuridae	1	
Sarcophilus		1
Dasyuromorphia total	**1**	**1**
Peramelidae	4	
Peramelemorphia total	**4**	**0**
Phascolarctos/Lasiorhinus	1	
Pseudocheiridae	4	
Lagostrophus	11	
Osphranter/Notamacropus/Lagorchestes	2	3
Macropus	4	14
Notamacropus/Wallabia		1
Notamacropus irma	1	8
Macropodidae	4	3
Macropodidae/Phalangeridae	1	1
Diprotodontia total	**28**	**30**
Marsupialia		1
Unknown	9	9
Total	**42**	**41**

Overall, the ZooMS results are in line with the taxa that were previously reported at Devil's Lair through morphological identification of the faunal assemblage. Macropods represent the largest component of the ZooMS-identified assemblage for both Period I (n=22) and Period II (n=29). Next to macropods, other taxa present in the ZooMS-identified assemblage of Period I are Dasyuridae (n=1), Peramelidae (n=4), *Phascolarctos/Lasiorhinus* (n=1), and Pseudocheiridae (n=4). For Period II, only *Sarcophilus* (n=1) was identified in addition to the large number of macropods.

Eleven specimens were identified as the ZooMS taxon *Lagostrophus* (Table S1). *Lagostrophus* was not identified morphologically at Devil's Lair, although it is known to have occurred in Southwest Australia in the past; the animal was extirpated from mainland Australia at the beginning of the twentieth century (Short and Turner, 1992). Its identification in the ZooMS-identified assemblage would thus represent the first record of this taxon at Devil's Lair, and would add to our understanding of the geographic distribution of this now extirpated animal. Alternatively, *Simosthenurus occidentalis* has a similar marker profile as *Lagostrophus* (Buckley et al., 2017, Peters et al., 2021), and has been identified morphologically in the lowermost layers of the site (Period I) along with remains of other sthenurine kangaroos (Balme et al., 1978, Dortch, 2004). However, the taphonomic history of these specimens suggests that they were washed into the sequence, thus questioning their association with other remains in the same layers (Dortch, 1979). The possible identification of *Simosthenurus* remains in the ZooMS-identified assemblage would thus serve as further evidence towards the presence of this extinct animal in the faunal assemblage of Devil's Lair.

In addition to the 71 specimens that could be taxonomically identified, there were 18 specimens with good quality MALDI spectra, but which could not be identified as any taxa currently available in the ZooMS reference database. These unidentifiable specimens can be arranged into 6 groups with similar peptide marker sets. Five of these groups have COL1α1 508-519 (P1) at *m/z* 1162, and COL1α2 484-498 (B) at *m/z* 1453, which is typical for marsupials (Peters et al., 2021). These specimens are thus most likely to represent other marsupial taxa that are not currently represented in the ZooMS reference database, although it has to be noted that peptide marker COL1α1 508-519 (P1) at *m/z* 1162 has also been reported as a peptide marker for reptiles (Harvey et al., 2019) and birds (Codlin et al., 2022). The sixth group, represented by only a single specimen, has a marker profile that is not typical for marsupials, but also does not match to any other taxa currently in the ZooMS reference database.

5. Discussion

5.1. Taphonomic insights

In addition to the taxonomic identification of fragmented fauna, the results of the ZooMS analysis can also give us insight into the taphonomic processes involved in the formation of the faunal assemblage. Firstly, when comparing the ZooMS results for Devil's Lair with zooarchaeological data, macropods seem to play a more significant role in the faunal assemblage than previously assumed (Figure 3). Particularly striking is that the majority of long bone fragments included in the ZooMS analyses were identified as macropod, while ZooMS-identified vertebrae showed a strikingly different taxonomic signature that includes more small- to medium-sized animals (Figure S1). Postcranial remains of macropods are notoriously difficult to identify morphologically because of osteological similarities between species (Mein and Manne, 2021), and is further complicated by the high fragmentation rate that characterizes the faunal assemblage of Devil's Lair. This could explain why such a large percentage of macropods is reflected in the ZooMS-identified long bone fragments. Alternatively, the large percentage of macropods in the ZooMS-identified assemblage could represent a bias of the used sampling strategy.

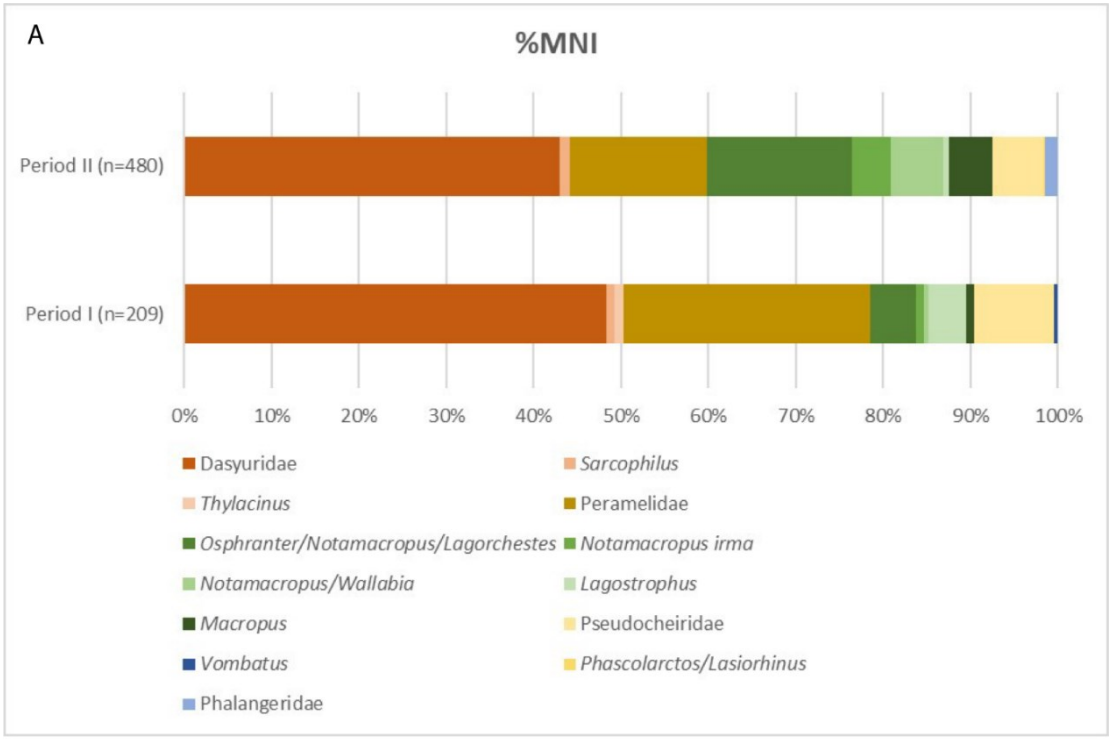

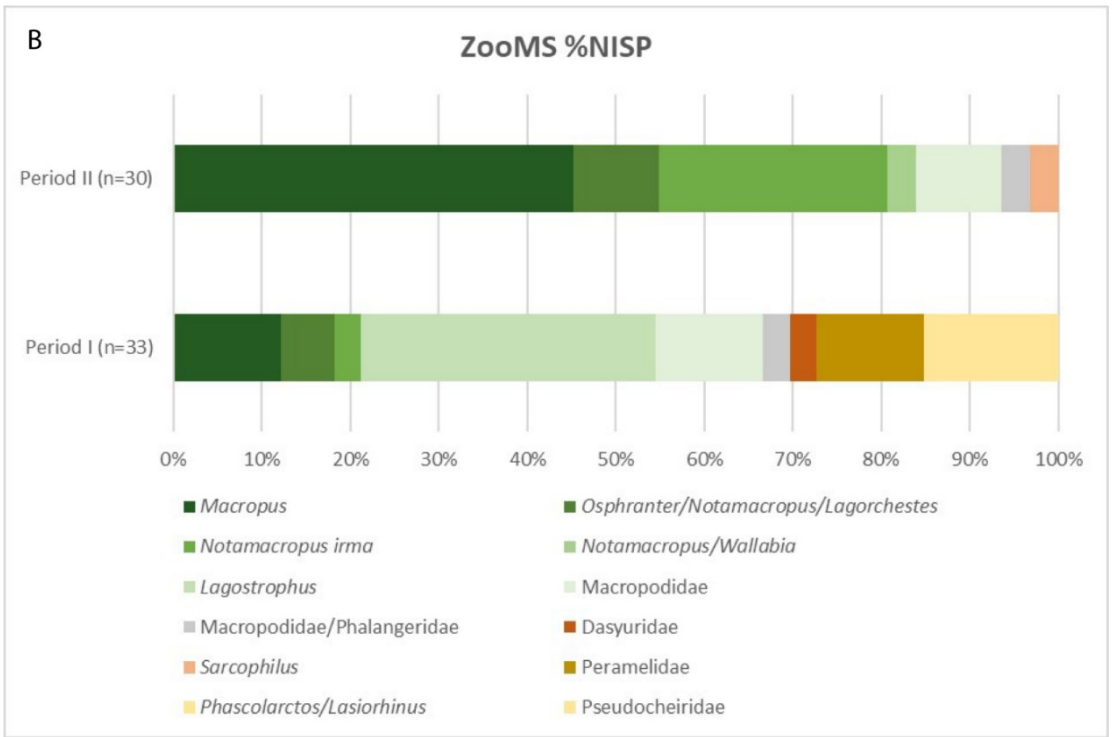

Figure 3: Panel A: Stacked bar graph of %MNI (minimum number of individuals) of zooarchaeological investigations (Balme et al., 1978, Dortch, 2004) converted to ZooMS taxa. Rodents and bats were excluded from %MNI calculations. NISP counts are not available for Devil's Lair (Dortch and Wright, 2010), therefore MNI was used. Panel B: Stacked bar graph with ZooMS %NISP per stratigraphic layer. Failed samples and samples that could not be taxonomically identified were excluded from %NISP calculations.

The inflated NISP counts of macropods observed with ZooMS could possibly indicate a higher frequency of macropod carcass processing by humans than previously thought, leading to highly fragmented postcranial material that is difficult to identify morphologically. Similar observations have been made with respect to the taxa identified at Fumane Cave, a Late Pleistocene site in Italy. Here, a significant increase in *Bos/Bison* remains was observed when the fragmented assemblage was analysed with ZooMS. The high fragmentation rate observed at this site was therefore attributed to human processing of *Bos/Bison* carcasses as part of human subsistence strategies (Sinet-Mathiot et al., 2019).

Alternatively, the high fragmentation rate of macropod remains at Devil's Lair could be a taphonomic signature of an intense period of scavenging by Tasmanian devils at the site. At Denisova Cave, ZooMS analysis of the fragmented fauna also revealed an inflated number of large animal taxa, resulting from human and carnivore fragmentation of the bone assemblage (Brown et al., 2021b). However, it is important to keep in mind that %MNI and %NISP counts cannot be compared to each other one-on-on due to differences in interpretative power (Lyman, 2018). To illustrate, larger animals also leave a larger number of bone fragments when fragmented, which could have also led to the inflated NISP counts for macropods observed in the ZooMS-identified assemblage of Devil's Lair.

When comparing the %NISP of the ZooMS-identified assemblage with the body class sizes of the specimens, it also becomes evident that bone fragments assigned to large-sized animals were best-represented in the set of analysed specimens (Figure 4a). This might further explain the difference in macropod representation between the morphologically and ZooMS-identified datasets. Interestingly, fragment length did not seem to have a great impact on the taxa identified in the ZooMS analysis. The majority of identified specimens had a fragment length of <2 cm and 2-4 cm (Figure 4b). The largest taxa identified in the ZooMS assemblage, macropods, also reflect this distribution in fragment length in the %NISP count, while fragments >4 cm were not preferentially identified as these larger taxa (Supplementary Figure 2).

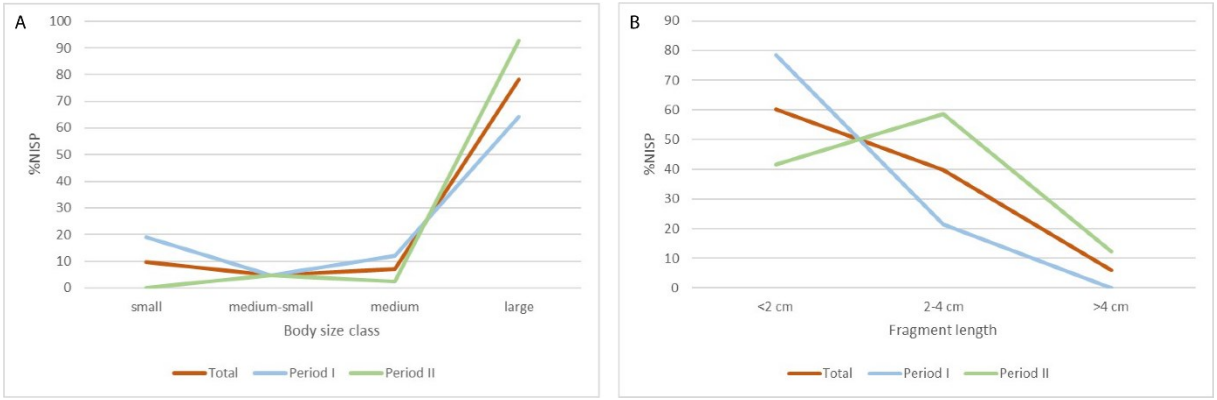

Figure 4: ZooMS %NISP by a) body size class, and b) fragment length.

5.2. Faunal diversity at Devil's Lair

The results from the ZooMS analysis also provide insight into faunal diversity at Devil's Lair in the past. Overall, the ZooMS-identified assemblage of Period I seems to display a higher level of faunal diversity than the assemblage of Period II, in which macropods represent the majority of identified specimens (Figure 3b). The suite of taxa identified in the ZooMS-assemblage have a wide range of environmental preferences (Table S1). Ringtail possum, phascogale, tammar wallaby, and Tasmanian devil mainly prefer more closed, forested environments, while the brush wallaby and banded-hare wallaby prefer woodlands or shrublands. Western grey kangaroo, short-nosed bandicoot, and other macropods in the region can be characterized as generalists preferring more mixed environments with both forests and open patches (Dortch, 2004, Dortch and Wright, 2010). The decrease in the number of taxa with a preference towards forested environments between Periods I and II, indicates a trend towards more open environments, while more closed forested environments also persisted on a smaller scale despite a decrease in levels of rainfall. We would thus expect there to be a vegetation mosaic (Figure 5). This is in line with our current knowledge of plant communities represented in the Leeuwin-Naturaliste National Park, which features a wide variety of environments, from closed-forest canopies to open scrublands (Dortch, 2004, Dortch and Wright, 2010).

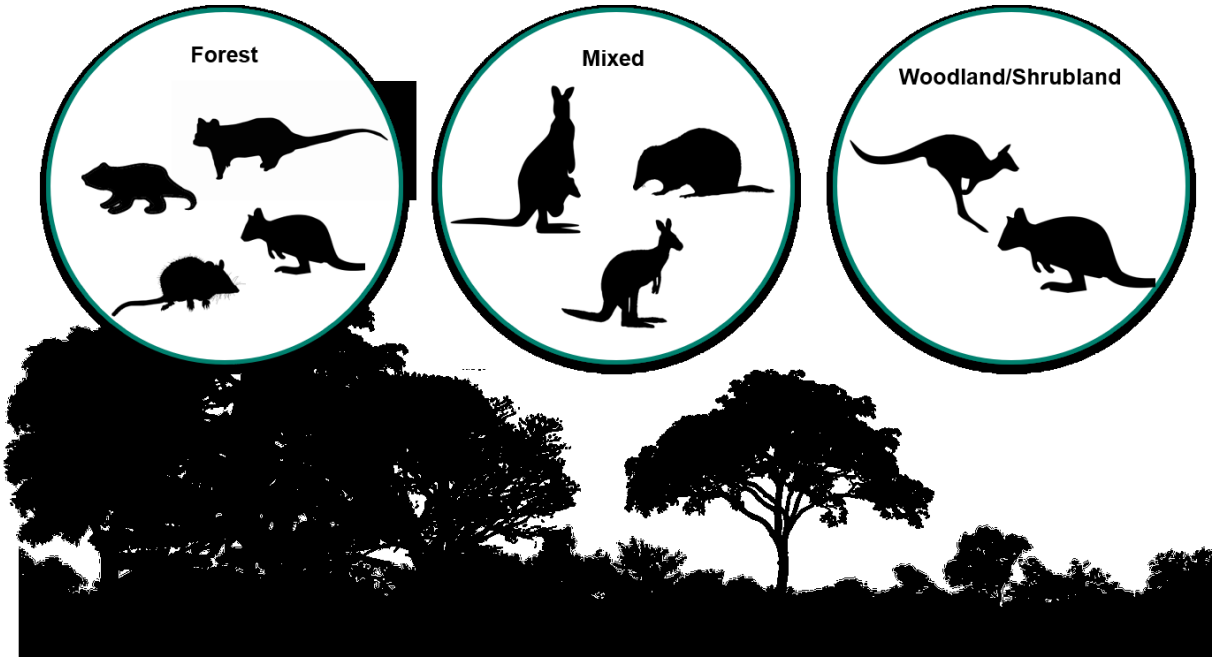

Figure 5: Impression of the mixed vegetation preferences of fauna identified at Devil's Lair with ZooMS.

The ZooMS-identified assemblage also revealed the presence of the ZooMS taxon *Lagostrophus* at Devil's Lair. This either represents the first record of *Lagostrophus* at the site, or provides further evidence for the presence of extinct sthenurine kangaroos during Period I. However, more in-depth palaeoproteomics or aDNA analysis is required to further disentangle the taxonomic origin of these specimens. Next to the taxa that were identified in the ZooMS analysis, 6 marker sets were identified that could not be matched to any taxa currently available in the ZooMS reference database. Although the number of taxa for which ZooMS markers are readily available has been steadily increasing over the years (Brown et al., 2021a), the reference database is far from comprehensive. This is also key for ZooMS studies in Australia, as reference markers are only available for less than 25 taxa (Peters et al., 2021). More efforts are thus required to develop peptide markers for an increased number of taxa. In the future, this could lead to the identification of the samples that were marked as unidentifiable in this study, and thus a further understanding of faunal diversity at Devil's Lair.

5.3. Integrating zooarchaeology, ZooMS and bulk bone DNA metabarcoding

Zooarchaeology, ZooMS, and bulk bone DNA metabarcoding all have the potential to contribute to the study of past fauna in their own unique ways. When combined, these methods have the potential to significantly amplify our understanding of past faunal exploitation and diversity. At Devil's Lair, the number and assortment of taxa identified varies between methods (Figure 6), and these methods thus give different insights into faunal diversity in the past. The largest number of uniquely identified taxa were identified morphologically. Pademelon (*Thylogale*) was identified exclusively with bulk bone DNA metabarcoding, while most noteworthy in the ZooMS-identified assemblage is the identification of the ZooMS taxon *Lagostrophus*, the identification of which is questionable zooarchaeologically due to issues of site disturbance.

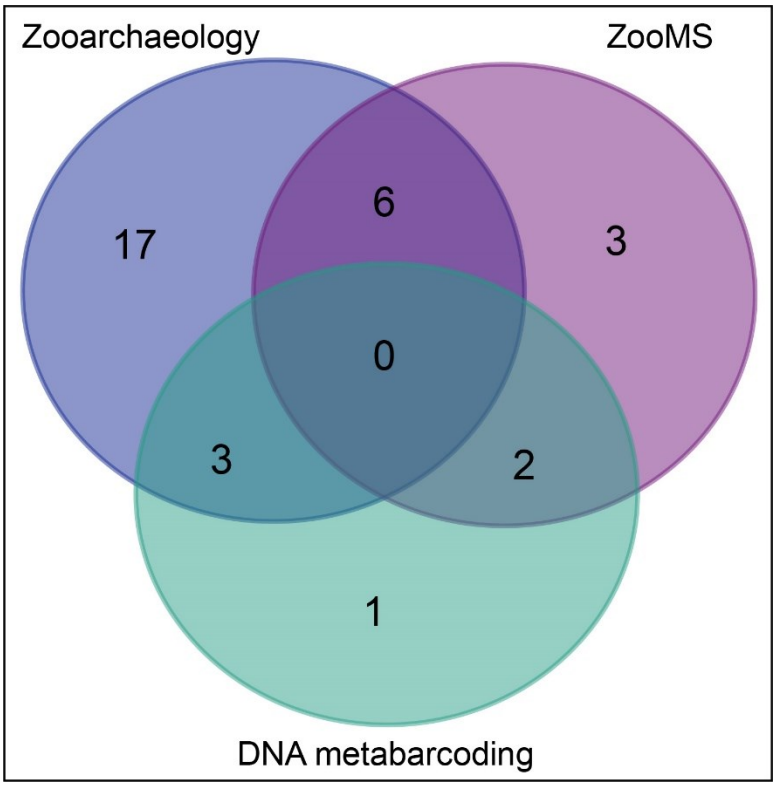

Figure 6: Venn diagram comparing the number of medium- to large-sized taxa identified at Devil's Lair (Periods I and II) with zooarchaeology (Dortch, 2004), bulk bone DNA metabarcoding (Murray et al., 2013), and ZooMS. Venn diagram was created with an online tool, accessible at http://bioinformatics.psb.ugent.be/webtools/Venn/.

The most straightforward explanations for the disparity in the number of taxa identified morphologically versus with biomolecular methods is sampling bias, and the lack of available genetic and proteomic reference data for many Australian taxa. An alternative explanation by Murray et al. (2013) is that the main reason for the limited interpretative power of bulk bone DNA metabarcoding at Devil's Lair could be DNA damage, rather than the absence of genetic data. For ZooMS however, the limited size of the reference database does seem to play a major role in the number of taxa identified in the Devil's Lair assemblage. The addition of the six currently unidentifiable peptide marker sets would already significantly increase the taxonomic diversity recovered with ZooMS at the site.

In addition to differences in taxonomic diversity recovered, it is also important to consider the unique strengths and weaknesses of each method, and how they can be combined for maximum effect. Zooarchaeology, most importantly, is a non-destructive approach to the identification of faunal remains that can be effectively employed to taxonomically identify cranial and dental remains, while the identification of highly fragmented postcranial often remains problematic (Mein and Manne, 2021). Even though zooarchaeology is somewhat limited for the morphological identification of highly fragmented remains, it remains the only method that can be used to quantify other aspects of the faunal assemblage, such as differential element preservation, and in that way can provide information about hunting and subsistence strategies in the past. Highly fragmented remains can be successfully targeted with ZooMS, although a limited taxonomic specificity, often family- or genus-level (Peters et al., 2021), can be reached with this method. Bulk bone DNA metabarcoding allows for the identification of fragmented remains, at higher taxonomic specificity, but the main trade-off is that it is not possible to get any quantitative metrics from this type of data, nor would it possible to identify which fossil in the bulk-bone sample is responsible for particularly intriguing finds; something that is possible with ZooMS.

When considering how to combine these three methods for maximum effect, it thus becomes evident that there are still many challenges that need to be overcome, specifically with regards to methods of quantification. More efforts are required to integrate ZooMS results into existing zooarchaeological metrics such as MNI, MNE, and MAU calculations. The main issue in linking these different methods

is combining different data types to get a holistic overview of the faunal assemblage. At Devil's Lair, this issue is illustrated by the absence of available NISP counts for the zooarchaeological assemblage (Dortch and Wright, 2010). This prohibits direct comparisons with, and integration of ZooMS results with existing zooarchaeological data. Furthermore, it is important to emphasize that the inflation of NISP counts with ZooMS, does not necessarily signify any changes to MNI, MNE, and MAU counts, which are generally most informative when interpreting zooarchaeological data. This does not mean there is no way forward, however. Especially promising targets for integrating ZooMS with zooarchaeological metrics are microfauna remains, which are often difficult to identify morphologically, except for when cranial remains are present (Andrews, 1990). Microfauna have already been shown to be an outstanding target for ZooMS analysis (Buckley et al., 2016, Prendergast et al., 2017, Buckley and Herman, 2019, Buckley and Cheylan, 2020). The calculation of MNI, MNE, and MAU estimates of faunal remains from archaeological deposits can be greatly benefit from a true integration of ZooMS and zooarchaeology.

6. Conclusion

In this study, we have successfully targeted fragmented fauna from Devil's Lair, a Late Pleistocene site in southwest Australia, for analysis with ZooMS. This study thus shows that it is possible to successfully extract ancient bone proteins from mainland Australia for taxonomic identification. This highlights the potential of future studies to successfully target Australian faunal material for palaeoproteomic analysis either with ZooMS to analyze bone tools or characterize fragmented faunal assemblages, or with shotgun palaeoproteomics to get a proteome-deep understanding of past Australian fauna dating back to the Late Pleistocene. For example, the overall lack of megafauna remains currently is one of the biggest challenges in estimating geographic ranges and extinction chronologies for many megafauna species (Price et al., 2018, Swift et al., 2019, Johnson et al., 2021). ZooMS has significant potential to increase the number of identified megafauna specimens to forward our understanding of the extinction of these animals.

At Devil's Lair, ZooMS data was integrated with existing zooarchaeological and bulk bone DNA metabarcoding records to highlight the promise of these methods when they are combined for maximum potential. However, critical challenges concerning the lack of data compatibility between the three methods, as well as limitations of reference databases for bulk bone DNA metabarcoding and ZooMS, still need to be addressed in the future to improve the potential of both methods to study Australian fauna. The integration of ZooMS into zooarchaeological datasets remains a critical challenge moving forward. More practical solutions will come only from the development of sampling strategies that are specifically geared towards this purpose.

ZooMS has the ability to give a voice to the fragmented unidentifiable bones from faunal assemblages, which are often uninformative in morphological analysis. In this way ZooMS can support zooarchaeological studies of the fossil record and give insight into faunal diversity and subsistence strategies in the past. At Devil's Lair, the inflated number of macropods identified in the fragmented ZooMS-identified assemblage indicates that macropods at the site were more heavily processed by humans or carnivores than assumed previously. ZooMS analysis of fragmented faunal remains thus has the potential to give insight into the taphonomic history of zooarchaeological assemblages, in particular with regards to the fragmentation of faunal remains as part of past human subsistence strategies, or carnivore scavenging.

Acknowledgements

We are grateful to the Pibulmun Wadandi Yunungjarli people, and specifically the Webb family as the Traditional Custodians, for granting us access to the material and supporting this study. We would also like to thank Alex Baynes for useful discussions about the paper, and Sandra Hebestreit for technical assistance with ZooMS extractions. This study was supported by the Max Planck Society.

References

Andrews, P. (1990). Owls, caves and fossils: Predation, preservation and accumulation of small mammal bones in caves, with an analysis of the Pleistocene cave faunas from Westbury-Sub-Mendip, Somerset, UK (University of Chicago Press).

Archer, M., Crawford, I. M. & Merrilees, D. (1980). Incisions, breakages and charring, some probably man-made, in fossil bones from Mammoth Cave, Western Australia. Alcheringa: An Australasian Journal of Palaeontology *4*, 115-131. doi.org/10.1080/03115518008619643.

Balme, J., Merrilees, D. & Porter, J. K. (1978). Late Quaternary mammal remains, spanning about 30 000 years, from excavations in Devil's Lair, Western Australia. Journal of the Royal Society of Western Australia *61*, 33-65.

Brown, S., Douka, K., Collins, M. J. & Richter, K. K. (2021a). On the standardization of ZooMS nomenclature. Journal of Proteomics *235*, 104041. doi.org/10.1016/j.jprot.2020.104041.

Brown, S., Wang, N., Oertle, A., Kozlikin, M. B., Shunkov, M. V., Derevianko, A. P., Comeskey, D., Jope-Street, B., Harvey, V. L., Chowdhury, M. P., et al. (2021b). Zooarchaeology through the lens of collagen fingerprinting at Denisova Cave. Scientific Reports *11*, 15457. doi.org/10.1038/s41598-021-94731-2.

Buckley, M., Collins, M., Thomas-Oates, J. & Wilson, J. C. (2009). Species identification by analysis of bone collagen using matrix-assisted laser desorption/ionisation time-of-flight mass spectrometry. Rapid Communications in Mass Spectrometry *23*, 3843-3854. doi.org/10.1002/rcm.4316.

Buckley, M., Gu, M., Shameer, S., Patel, S. & Chamberlain, A. T. (2016). High-throughput collagen fingerprinting of intact microfaunal remains; a low-cost method for distinguishing between murine rodent bones. Rapid Communications in Mass Spectrometry *30*, 805-812. doi.org/10.1002/rcm.7483.

Buckley, M., Cosgrove, R., Garvey, J. & Prideaux, G. J. (2017). Identifying remains of extinct kangaroos in Late Pleistocene deposits using collagen fingerprinting. Journal of Quaternary Science *32*, 653-660. doi.org/10.1002/jqs.2964.

Buckley, M. & Herman, J. (2019). Species identification of Late Pleistocene bat bones using collagen fingerprinting. International Journal of Osteoarchaeology *29*, 1051-1059. doi.org/10.1002/oa.2818.

Buckley, M. & Cheylan, M. (2020). Collagen fingerprinting for the species identification of archaeological amphibian remains. Boreas *49*, 709-717. doi.org/10.1111/bor.12443.

Cappellini, E., Welker, F., Pandolfi, L., Ramos-Madrigal, J., Samodova, D., Rüther, P. L., Fotakis, A. K., Lyon, D., Moreno-Mayar, J. V., Bukhsianidze, M., et al. (2019). Early Pleistocene enamel proteome from Dmanisi resolves *Stephanorhinus* phylogeny. Nature *574*, 103-107. doi.org/10.1038/s41586-019-1555-y.

Codlin, M. C., Douka, K. & Richter, K. K. (2022). An application of ZooMS to identify archaeological avian fauna from Teotihuacan, Mexico. Journal of Archaeological Science *148*, 105692. doi.org/10.1016/j.jas.2022.105692.

Cosgrove, R., Allen, J. & Marshall, B. (1990). Palaeo-ecology and Pleistocene human occupation in South Central Tasmania. Antiquity *64*, 59-78. doi.org/10.1017/S0003598X00077309.

Demarchi, B., Hall, S., Roncal-Herrero, T., Freeman, C. L., Woolley, J., Crisp, M. K., Wilson, J. C., Fotakis, A. K., Fischer, R., Kessler, B., et al. (2016). Protein sequences bound to mineral surfaces persist into deep time. eLife *5*, e17092. doi.org/10.7554/eLife.17092.

Dortch, C. (1979). Devil's Lair, an example of prolonged cave use in Western Australia. World Archaeology *10*, 258-279. doi.org/10.1080/00438243.1979.9979736.

Dortch, J. (2004). Palaeo-environmental change and the persistence of human occupation in South-Western Australian forests (Archaeopress).

Dortch, J. & Wright, H. (2010). Identifying palaeo-environments and changes in Aboriginal subsistence from dual-patterned faunal assemblages, South-Western Australia. Journal of Archaeological Science *37*, 1053-1064. doi.org/10.1016/j.jas.2009.12.006.

Harvey, V. L., Egerton, V. M., Chamberlain, A. T., Manning, P. L., Sellers, W. I. & Buckley, M. (2019). Interpreting the historical terrestrial vertebrate biodiversity of Cayman Brac (Greater Antilles, Caribbean) through collagen fingerprinting. The Holocene *29*, 531-542. doi.org/10.1177/0959683618824793.

Jankowski, N. R., Gully, G. A., Jacobs, Z., Roberts, R. G. & Prideaux, G. J. (2016). A late Quaternary vertebrate deposit in Kudjal Yolgah Cave, South-Western Australia: Refining regional Late Pleistocene extinctions. Journal of Quaternary Science *31*, 538-550. doi.org/10.1002/jqs.2877.

Johnson, C. N., Dortch, J. & Worthy, T. H. (2021). Interactions with megafauna. In The Oxford handbook of the archaeology of Indigenous Australia and New Guinea. McNiven, I. J. & David, B. eds. (Oxford University Press). doi.org/10.1093/oxfordhb/9780190095611.013.10.

Langley, M., Clarkson, C. & Ulm, S. (2011). From small holes to grand narratives: The impact of taphonomy and sample size on the modernity debate in Australia and New Guinea. Journal of Human Evolution *61*, 197-208. doi.org/10.1016/j.jhevol.2011.03.002.

Lyman, R. L. (2018). Observations on the history of zooarchaeological quantitative units: Why NISP, then MNI, then NISP again? Journal of Archaeological Science: Reports *18*, 43-50. doi.org/10.1016/j.jasrep.2017.12.051.

Manne, T. & Veth, P. (2015). Late Pleistocene and early Holocene exploitation of estuarine communities in Northwestern Australia. Quaternary International *385*, 112-123. doi.org/10.1016/j.quaint.2014.12.049.

Mein, E. & Manne, T. (2021). Identifying marsupials from Australian archaeological sites: current methodological challenges and opportunities in zooarchaeological practice. Archaeology in Oceania *56*, 133-141. doi.org/doi.org/10.1002/arco.5234.

Monks, C. (2021). The role of terrestrial, estuarine, and marine foods in dynamic Holocene environments and adaptive coastal economies in Southwestern Australia. Quaternary International *597*, 5-23. doi.org/10.1016/j.quaint.2020.07.020.

Murray, D., Haile, J., Dortch, J., White, N. E., Haouchar, D., Bellgard, M. I., Allcock, R. J., Prideaux, G. J. & Bunce, M. (2013). Scrapheap challenge: A novel bulk-bone metabarcoding method to investigate ancient DNA in faunal assemblages. Scientific Reports *3*, 3371. doi.org/10.1038/srep03371.

Peters, C., Richter, K. K., Manne, T., Dortch, J., Paterson, A., Travouillon, K., Louys, J., Price, G. J., Petraglia, M., Crowther, A., et al. (2021). Species identification of Australian marsupials using collagen fingerprinting. Royal Society Open Science *8*, 211229. doi.org/10.1098/rsos.211229.

Prendergast, M. E., Buckley, M., Crowther, A., Frantz, L., Eager, H., Lebrasseur, O., Hutterer, R., Hulme-Beaman, A., Van Neer, W., Douka, K., et al. (2017). Reconstructing Asian faunal introductions to eastern Africa from multi-proxy biomolecular and archaeological datasets. PLoS ONE *12*, e0182565. doi.org/10.1371/journal.pone.0182565.

Price, G. J. & Webb, G. E. (2006). Late Pleistocene sedimentology, taphonomy and megafauna extinction on the Darling Downs, Southeastern Queensland. Australian Journal of Earth Sciences *53*, 947-970. doi.org/10.1080/08120090600880842.

Price, G. J., Louys, J., Tyler Faith, J., Lorenzen, E. D. & Westaway, M. C. (2018). Big data little help in megafauna mysteries. Nature *558*, 23-25. doi.org/10.1038/d41586-018-05330-7.

Prideaux, G. J., Gully, G. A., Ayliffe, L. K., Bird, M. I. & Roberts, R. G. (2000). Tight Entrance Cave, southwestern Australia: A late Pleistocene vertebrate deposit spanning more than 180 ka. Journal of Vertebrate Paleontology *20*, 62A-63A.

Prideaux, G. J., Gully, G. A., Couzens, A. M. C., Ayliffe, L. K., Jankowski, N. R., Jacobs, Z., Roberts, R. G., Hellstrom, J. C., Gagan, M. K. & Hatcher, L. M. (2010). Timing and dynamics of Late Pleistocene mammal extinctions in Southwestern Australia. Proceedings of the National Academy of Sciences of the United States of America *107*, 22157-22162. doi.org/10.1073/pnas.1011073107.

Richter, K. K., McGrath, K., Masson-MacLean, E., Hickinbotham, S., Tedder, A., Britton, K., Bottomley, Z., Dobney, K., Hulme-Beaman, A., Zona, M., et al. (2020). What's the catch? Archaeological application of rapid collagen-based species identification. Journal of Archaeological Science *116*, 105116. doi.org/10.1016/j.jas.2020.105116.

Rybczynski, N., Gosse, J. C., Harington, C. R., Wogelius, R. A., Hidy, A. J. & Buckley, M. (2013). Mid-Pliocene warm-period deposits in the High Arctic yield insight into camel evolution. Nature Communications *4*, 1-9. doi.org/10.1038/ncomms2516.

Short, J. & Turner, B. (1992). The distribution and abundance of the banded and rufous hare-wallabies, *Lagostrophus fasciatus* and *Lagorchestes hirsutus*. Biological Conservation *60*, 157-166. doi.org/10.1016/0006-3207(92)91249-R.

Silvestrini, S., Lugli, F., Romandini, M., Real, C., Sommella, E., Salviati, E., Arrighi, S., Bortolini, E., Figus, C., Higgins, O. A., et al. (2022). Integrating ZooMS and zooarchaeology: New data from

the Uluzzian levels of Uluzzo C Rock Shelter, Roccia San Sebastiano cave and Riparo del Broion. PLoS ONE *17*, e0275614. doi.org/10.1371/journal.pone.0275614.

Sinet-Mathiot, V., Smith, G. M., Romandini, M., Wilcke, A., Peresani, M., Hublin, J.-J. & Welker, F. (2019). Combining ZooMS and zooarchaeology to study Late Pleistocene hominin behaviour at Fumane (Italy). Scientific Reports *9*, 12350. doi.org/10.1038/s41598-019-48706-z.

Swift, J. A., Bunce, M., Dortch, J., Douglass, K., Tyler Faith, J., Fellows Yates, J. A., Field, J., Haberle, S. G., Jacob, E., Johnson, C. N., et al. (2019). Micro methods for megafauna: Novel approaches to Late Quaternary extinctions and their contributions to faunal conservation in the Anthropocene. BioScience *69*, 877-887. doi.org/10.1093/biosci/biz105.

Turney, C. S. M., Bird, M. I., Fifield, L. K., Roberts, R. G., Smith, M., Dortch, C. E., Grün, R., Lawson, E., Ayliffe, L. K., Miller, G. H., et al. (2001). Early human occupation at Devil's Lair, Southwestern Australia 50,000 years ago. Quaternary Research *55*, 3-13. doi.org/10.1006/qres.2000.2195.

van den Hurk, Y., Rielly, K. & Buckley, M. (2021). Cetacean exploitation in Roman and medieval London: Reconstructing whaling activities by applying zooarchaeological, historical, and biomolecular analysis. Journal of Archaeological Science: Reports *36*, 102795. doi.org/10.1016/j.jasrep.2021.102795.

Van der Sluis, L. G., Hollund, H. I., Buckley, M., De Louw, P. G. B., Rijsdijk, K. F. & Kars, H. (2014). Combining histology, stable isotope analysis and ZooMS collagen fingerprinting to investigate the taphonomic history and dietary behaviour of extinct giant tortoises from the Mare aux Songes deposit on Mauritius. Palaeogeography, Palaeoclimatology, Palaeoecology *416*, 80-91. doi.org/10.1016/j.palaeo.2014.06.003.

Welker, F., Soressi, M., Rendu, W., Hublin, J.-J. & Collins, M. (2015). Using ZooMS to identify fragmentary bone from the Late Middle/Early Upper Palaeolithic sequence of Les Cottés, France. Journal of Archaeological Science *54*, 279-286. doi.org/10.1016/j.jas.2014.12.010.

Supplementary Information

ZooMS and zooarchaeology, a match made in heaven? Integrating ZooMS into existing faunal records at Devil's Lair, SW Australia

Carli Peters[1,*], Noel Amano[1], Armita Ghassemifar[2], Helen Ryan[3], Mikael Siversson[3], Wayne Webb[4], Joe Dortch[2], Nicole Boivin[1,5,6,7,*]

1. Department of Archaeology, Max Planck Institute for Geoanthropology, Jena, Germany
2. School of Social Sciences, University of Western Australia, Perth, WA 6009, Australia
3. Western Australian Museum, Collections and Research, 49 Kew Street, Welshpool, WA 6106, Australia
4. Dowark Foundation, Walpole, WA 6398, Australia
5. School of Social Science, The University of Queensland, Brisbane, Qld 4071, Australia
6. Department of Anthropology, National Museum of Natural History, Smithsonian Institution, Washington DC, USA
7. Department of Anthropology and Archaeology, University of Calgary, Calgary, Canada

*Corresponding authors: Carli Peters and Nicole Boivin

Supplementary Figures

Supplementary Figure 1: Stacked bar graph of ZooMS %NISP per skeletal element.

Supplementary Figure 2: %NISP per taxa compared to fragment length.

Supplementary Tables

Supplementary Table 1: ZooMS taxa. Extant, locally extirpated and extinct medium- to large-sized mammals known from the Leeuwin-Naturaliste Region, grouped together as ZooMS taxa. Habitat preferences and current conservation status of each species are indicated. Data from Balme et al. (1978), Dortch (2004), Dortch and Wright (2010), and Murray et al. (2013).

Other Supplementary Materials for this Manuscript

Supplementary Dataset 1: ZooMS results for individual samples.

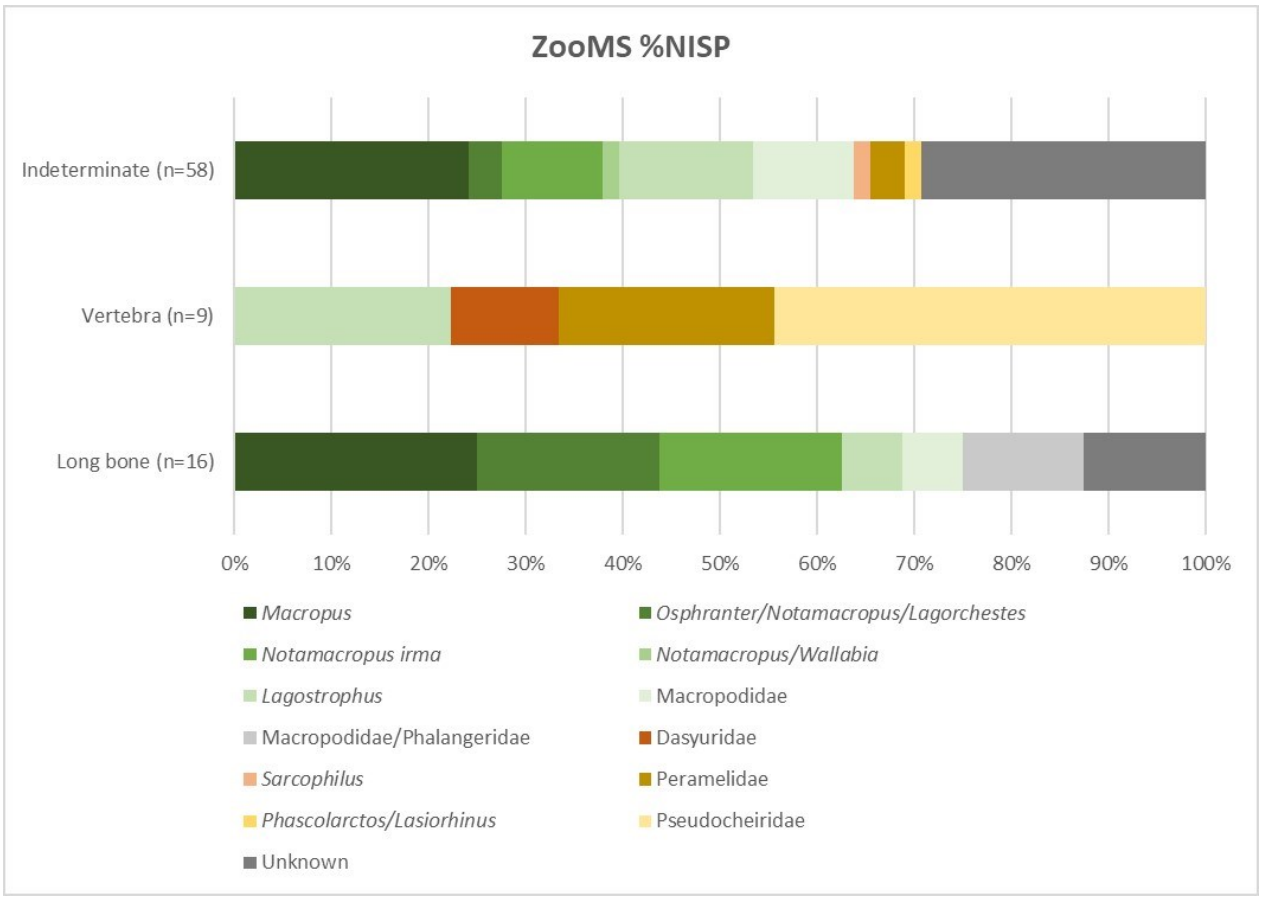

Fig. S1. Stacked bar graph of ZooMS %NISP per skeletal element.

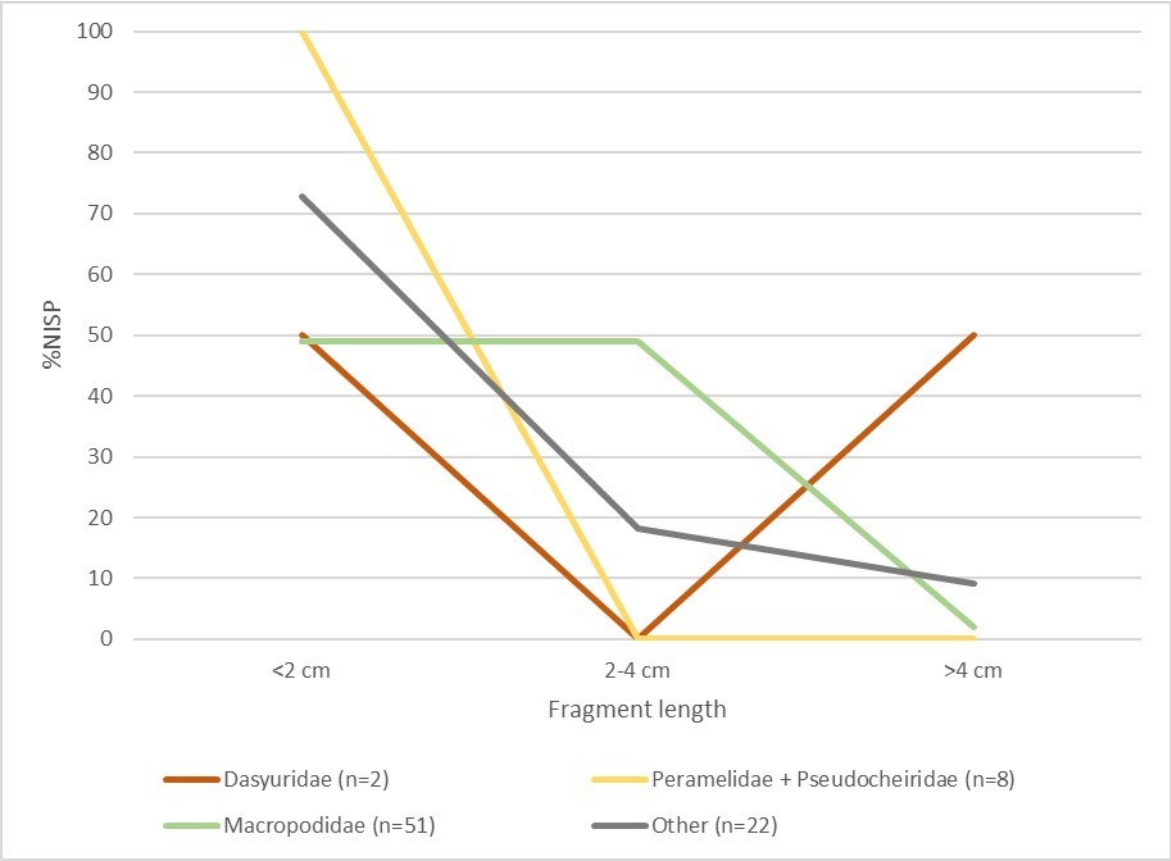

Fig. S2. %NISP per taxa compared to fragment length.

Table S1. ZooMS taxa. Extant, locally extirpated and extinct medium- to large-sized mammals known from the Leeuwin-Naturaliste Region, grouped together as ZooMS taxa. Habitat preferences and current conservation status of each species are indicated. Data from Balme et al. (1978), Dortch (2004), Dortch and Wright (2010), and Murray et al. (2013).

ZooMS taxon	Family	Genus	Species	Common (Nyoongar) names	Identified morphologically at Devil's Lair	Habitat preference	Conservation status
Tachyglossidae	Tachyglossidae	*Tachyglossus*	*aculeatus*	Short-beaked echidna			Locally extirpated?
		Zaglossus	*hacketti*	Giant echidna			Extinct
Thylacinus	Thylacinidae	*Thylacinus*	*cynocephalus*	Thylacine	x		Extinct
Dasyuridae	Dasyuridae	*Dasyurus*	*geoffroi*	Native cat (Chuditch)	x		Extant
		Antechinus	*flavipes*	Yellow-footed antechinus (Mardo)	x		Extant
		Phascogale	*tapoatafa*	Brush-tailed phascogale (Tuan)	x		Extant
		Sminthopsis	*griseoventer*	Grey-bellied dunnart	x		Extant
Sarcophilus	Dasyuridae	*Sarcophilus*	*harissii*	Tasmanian devil	x		Locally extirpated
Peramelidae	Peramelidae	*Isoodon*	*obesulus*	Southern brown bandicoot (Quenda)	x	Temperate forest/woodland/ shrubland	Extant
		Perameles	*bougainville*	Western barred bandicoot	x	Temperate woodland/shrubland	Locally extirpated
Vombatus	Vombatidae	*Vombatus*	*hacketii*		x		Extinct
Phascolarctos/Lasiorhinus	Phascolarctidae	*Phascolarctos*	*cinereus*	Koala	x		Locally extirpated
Phalangeridae	Phalangeridae	*Trichosurus*	*vulpecula vulpecula*	Common brush-tailed possum (Gnuraren)	x	Tropical/temperate forest/woodland	Extant
Pseudocheiridae	Pseudocheiridae	*Pseudocheirus*	*peregrinus occidentalis*	Western ring-tailed possum (Nworra)	x	Tropical/temperate forest/woodland	Extant
Lagostrophus[1]	Macropodidae	*Lagostrophus*	*fasciatus*	Banded hare-wallaby			Locally extirpated
		Protemnodon	*brehus*	Sthenurine kangaroo	x		Extinct
		Simosthenurus	*browneorum*	Sthenurine kangaroo	x		Extinct

Osphranter/Notamacropus/ Lagorchestes[1]	Macropodidae	*Setonix*	*brachyurus*	Quokka (Kwaker)	x	Temperate forest/woodland	Extant
		Lagorchestes	*hirsutus*	Rufous hare-wallaby	x		Locally extirpated
		Onynchogalea	*lunata*	Crescent nail-tail wallaby			Extinct
		Petrogale	*lateralis*	Black-footed rock-wallaby	x	Tropical/temperate shrubland	Locally extirpated
Macropus[1]	Macropodidae	*Macropus*	*fuliginosus*	Western grey kangaroo (Yongar)	x	Temperate forest/woodland/ shrubland	Extant
Notamacropus/Wallabia[1]	Macropodidae	*Notamacropus*	*eugenii*	Tammar wallaby (Tammar)	x	Temperate forest/woodland/ shrubland	Extant
Notamacropus irma[1]	Macropodidae	*Notamacropus*	*irma*	Brush wallaby (Gurhra)	x	Temperate forest/woodland	Extant
Canidae	Canidae	*Canis*	*familiaris dingo*	Dingo			Extant
Unknown	Diprotodontidae	*Zygomaturus*	*trilobus*		x		Extinct
	Thylacoleonidae	*Thylacoleo*	*carnifex*	Marsupial lion			Extinct
	Burramyidae	*Cercatetus*	*concinnus*	Western pygmy possum	x		Extant
	Tarsipedidae	*Tarsipes*	*rostratus*	Honey possum	x		Extant
	Potoroidae	*Bettongia*	*penicillata*	Brush-tailed bettong (Woylie)	x	Tropical/temperate forest/woodland/ shrubland	Extant
			lessueur	Burrowing bettong (Burdi)	x	Temperate woodland/shrubland	Locally extirpated
		Potorous	*tridactylus*	Long-nosed potoroo (Garlgyte)	x	Temperate forest	Extant

[1]The ZooMS taxon ‘Macropodidae’ is used when characteristic peptide markers to distinguish between the various macropod groups, are missing.

Dataset S1. ZooMS results for individual samples.

SI References

Balme, J. Merrilees, D. & Porter, J.K. (1978). Late Quaternary mammal remains spanning about 30 000 years, from excavations in Devil's Lair, Western Australia. Journal of the Royal Society of Western Australia *61*, 33-65.

Dortch, J. (2004). Palaeo-environmental change and the persistence of human occupation in South-Western Australian forests (Archaeopress).

Dortch, J. & Wright, H. (2010). Identifying palaeo-environments and changes in Aboriginal subsistence from dual-patterned faunal assemblages, south-western Australia. Journal of Archaeological Science *37*, 1053-1064. doi.org/10.1016/j.jas.2009.12.006.

Murray, D., Haile, J., Dortch, J., White, N.E., Haouchar, D., Bellgard, M.I., Allcock, R.J., Prideaux, G.J. & Bunce, M. (2013). Scrapheap challenge: A novel bulk-bone metabarcoding method to investigate ancient DNA in faunal assemblage. Scientific Reports *3*, 3371. doi.org/10.1038/srep03371.

Dataset S1: ZooMS results for individual samples.

Extraction Number	WAM Reference Number	Trench	Sedimentary layer	Period (following Dortch 2004)	Fragment length	Body size class	Skeletal element	ZooMS taxon
CP767	76.8.765	7d	mixed 27-29	II	2-4 cm	large	indeterminate	x
CP768	76.8.765	7d	mixed 27-29	II	<2 cm	large	indeterminate	*Osphranter/Notamacropus/Lagorchestes*
CP769	76.8.765	7d	mixed 27-29	II	<2 cm	large	indeterminate	x
CP770	76.8.765	7d	mixed 27-29	II	<2 cm	large	indeterminate	unknown
CP771	77.6.511	9 (south end)	mixtures of 29, 30-upper, 30-lower	II	>4 cm	large	long bone	unknown
CP772	77.6.511	9 (south end)	mixtures of 29, 30-upper, 30-lower	II	2-4 cm	large	indeterminate	*Macropus*
CP773	77.6.511	9 (south end)	mixtures of 29, 30-upper, 30-lower	II	<2 cm	large	indeterminate	unknown
CP774	77.6.511	9 (south end)	mixtures of 29, 30-upper, 30-lower	II	<2 cm	large	indeterminate	unknown
CP775	77.6.511	9 (south end)	mixtures of 29, 30-upper, 30-lower	II	<2 cm	medium-small	long bone	*Osphranter/Notamacropus/Lagorchestes*
CP776	77.6.511	9 (south end)	mixtures of 29, 30-upper, 30-lower	II	<2 cm	medium-small	femur	unknown
CP783	77.4.875	8	25	II	>4 cm	large	indeterminate	*Sarcophilus*
CP784	77.4.875	8	25	II	2-4 cm	large	indeterminate	unknown
CP785	77.4.875	8	25	II	2-4 cm	large	long bone	x
CP786	77.4.875	8	25	II	2-4 cm	large	indeterminate	unknown
CP787	77.4.875	8	25	II	2-4 cm	large	indeterminate	*Macropus*
CP788	76.7.410	9 (north)	31	I	<2 cm	large	indeterminate	*Lagostrophus*
CP789	76.7.410	9 (north)	31	I	2-4 cm	large	indeterminate	unknown
CP790	76.7.410	9 (north)	31	I	2-4 cm	large	indeterminate	Macropodidae
CP791	76.7.410	9 (north)	31	I	<2 cm	medium-small	indeterminate	*Lagostrophus*
CP792	76.7.410	9 (north)	31	I	<2 cm	medium-small	indeterminate	unknown
CP793	76.6.626	9 (north)	33	I	2-4 cm	large	indeterminate	*Macropus*
CP794	76.6.626	9 (north)	33	I	<2 cm	large	indeterminate	*Notamacropus irma*
CP795	76.6.626	9 (north)	33	I	<2 cm	large	indeterminate	unknown
CP796	76.6.626	9 (north)	33	I	<2 cm	large	indeterminate	unknown
CP797	76.7.993-5	9 (south)	30 (lower part)	I	<2 cm	large	indeterminate	x
CP798	76.7.993-5	9 (south)	30 (lower part)	I	2-4 cm	large	costa	Macropodidae
CP799	76.7.993-5	9 (south)	30 (lower part)	I	<2 cm	large	indeterminate	unknown
CP800	76.7.993-5	9 (south)	30 (lower part)	I	<2 cm	large	phalanx	Macropodidae/Phalangeridae
CP801	76.7.993-5	9 (south)	30 (lower part)	I	<2 cm	large	indeterminate	unknown
CP802	76.6.442-3	9 (north)	34	I	<2 cm	large	indeterminate	unknown
CP803	76.6.442-3	9 (north)	34	I	<2 cm	large	indeterminate	*Phascolarctos /Lasiorhinus*
CP804	76.6.442-3	9 (north)	34	I	<2 cm	large	vertebra	Dasyuridae
CP805	76.6.442-3	9 (north)	34	I	<2 cm	large	vertebra	*Lagostrophus*
CP806	76.6.442-3	9 (north)	34	I	<2 cm	large	indeterminate	unknown
CP807	77.4.822-4	8	23	II	>4 cm	large	indeterminate	x
CP808	77.4.822-4	8	23	II	<2 cm	large	long bone	*Macropus*
CP809	77.4.822-4	8	23	II	>4 cm	large	indeterminate	*Notamacropus irma*
CP810	77.4.822-4	8	23	II	2-4 cm	large	indeterminate	*Macropus*
CP811	77.4.822-4	8	23	II	2-4 cm	large	long bone	*Macropus*
CP812	76.9.242	8	27	II	<2 cm	large	indeterminate	marsupial
CP813	76.9.242	8	27	II	2-4 cm	large	indeterminate	unknown
CP814	76.9.242	8	27	II	<2 cm	large	indeterminate	x
CP815	76.9.242	8	27	II	<2 cm	large	indeterminate	*Macropus*
CP816	76.9.242	8	27	II	2-4 cm	large	indeterminate	*Notamacropus irma*
CP817	76.8.580	7d	29	II	2-4 cm	large	costa	x
CP818	76.8.580	7d	29	II	2-4 cm	large	costa	x
CP819	76.8.580	7d	29	II	<2 cm	large	indeterminate	x
CP820	76.8.580	7d	29	II	<2 cm	large	indeterminate	x
CP821	76.8.580	7d	29	II	<2 cm	large	indeterminate	*Macropus*
CP822	77.4.755	9	20	II	2-4 cm	large	long bone	*Notamacropus irma*

CP823	77.4.755	9	20	II	2-4 cm	large	indeterminate	*Macropus*
CP824	77.4.755	9	20	II	2-4 cm	large	indeterminate	*Macropus*
CP825	77.4.755	9	20	II	2-4 cm	large	indeterminate	*Macropus*
CP826	77.4.755	9	20	II	<2 cm	large	indeterminate	*Macropus*
CP827	76.6.350	9 (north)	35	I	2-4 cm	large	indeterminate	Macropodidae
CP828	76.6.350	9 (north)	35	I	<2 cm	small	indeterminate	*Macropus*
CP829	76.6.350	9 (north)	35	I	<2 cm	large	indeterminate	Macropodidae
CP830	76.6.350	9 (north)	35	I	<2 cm	large	indeterminate	*Macropus*
CP831	76.6.350	9 (north)	35	I	<2 cm	small	indeterminate	*Lagostrophus*
CP832	76.7.136	9 (north)	32	I	<2 cm	small	vertebra	Peramelidae
CP833	76.7.136	9 (north)	32	I	<2 cm	small	caudal vertebra	Pseudocheiridae
CP834	76.7.136	9 (north)	32	I	<2 cm	small	vertebra	Peramelidae
CP835	76.7.136	9 (north)	32	I	<2 cm	small	indeterminate	Peramelidae
CP836	76.7.136	9 (north)	32	I	<2 cm	small	tibia	*Lagostrophus*
CP837	76.6.863-4	8	32 (lower part)	I	<2 cm	large	indeterminate	*Lagostrophus*
CP838	76.6.863-4	8	32 (lower part)	I	<2 cm	large	indeterminate	*Lagostrophus*
CP839	76.6.863-4	8	32 (lower part)	I	<2 cm	small	indeterminate	Peramelidae
CP840	76.6.863-4	8	32 (lower part)	I	<2 cm	large	indeterminate	*Lagostrophus*
CP841	76.6.863-4	8	32 (lower part)	I	<2 cm	large	indeterminate	*Lagostrophus*
CP842	76.7.572	8	30-31 (mixed)	I	<2 cm	medium	vertebra	Pseudocheiridae
CP843	76.7.572	8	30-31 (mixed)	I	<2 cm	medium	long bone	*Osphranter/Notamacropus/Lagorchestes*
CP844	76.7.572	8	30-31 (mixed)	I	<2 cm	medium	ulna (proximal)	x
CP845	76.7.572	8	30-31 (mixed)	I	2-4 cm	large	long bone	*Osphranter/Notamacropus/Lagorchestes*
CP846	76.7.572	8	30-31 (mixed)	I	2-4 cm	large	cranium	*Macropus*
CP847	77.4.806	8	22	II	2-4 cm	large	indeterminate	*Notamacropus irma*
CP848	77.4.806	8	22	II	2-4 cm	large	long bone	*Notamacropus irma*
CP849	77.4.806	8	22	II	2-4 cm	large	indeterminate	*Macropus*
CP850	77.4.806	8	22	II	<2 cm	large	indeterminate	*Notamacropus irma*
CP851	77.4.806	8	22	II	<2 cm	large	indeterminate	Macropodidae
CP852	76.9.113-4	8	26	II	2-4 cm	large	long bone	Macropodidae
CP853	76.9.113-4	8	26	II	<2 cm	large	indeterminate	*Notamacropus irma*
CP854	76.9.113-4	8	26	II	2-4 cm	large	carpal	*Notamacropus irma*
CP855	76.9.113-4	8	26	II	<2 cm	medium	indeterminate	*Notamacropus/Wallabia*
CP856	76.9.113-4	8	26	II	>4 cm	large	long bone	Macropodidae/Phalangeridae
CP857	77.4.862	9	24	II	<2 cm	large	indeterminate	Macropodidae
CP858	77.4.862	9	24	II	<2 cm	large	indeterminate	unknown
CP859	77.4.862	9	24	II	2-4 cm	large	long bone	*Macropus*
CP860	77.4.862	9	24	II	2-4 cm	large	long bone	*Macropus*
CP861	77.4.862	9	24	II	2-4 cm	large	indeterminate	*Osphranter/Notamacropus/Lagorchestes*
CP862	76.8.220	9 (north)	30 (lower part)	I	<2 cm	medium	caudal vertebra	Pseudocheiridae
CP863	76.8.220	9 (north)	30 (lower part)	I	<2 cm	medium	indeterminate	unknown
CP864	76.8.220	9 (north)	30 (lower part)	I	<2 cm	medium	vertebra	Pseudocheiridae
CP865	76.8.220	9 (north)	30 (lower part)	I	2-4 cm	large	vertebra	*Lagostrophus*
CP866	76.8.220	9 (north)	30 (lower part)	I	2-4 cm	large	indeterminate	*Lagostrophus*

9. Manuscript D

Leveraging palaeoproteomics to address conservation and restoration agendas

Carli Peters[1,*], Kristine K. Richter[2], Jens-Christian Svenning[3], Nicole Boivin[1,4,5,6,*]

1. Department of Archaeology, Max Planck Institute for the Science of Human History, Jena, Germany
2. Department of Anthropology, Harvard University, Cambridge, MA, USA
3. Center for Biodiversity Dynamics in a Changing World (BIOCHANGE), Department of Biology, Aarhus University, Aarhus, Denmark
4. School of Social Science, The University of Queensland, Brisbane, Qld 4071, Australia
5. Department of Anthropology, National Museum of Natural History, Smithsonian Institution, Washington DC, USA
6. Department of Anthropology and Archaeology, University of Calgary, Calgary, Canada

*Corresponding authors: Carli Peters and Nicole Boivin

iScience

CellPress
OPEN ACCESS

Review

Leveraging palaeoproteomics to address conservation and restoration agendas

Carli Peters,[1,*] Kristine K. Richter,[2] Jens-Christian Svenning,[3] and Nicole Boivin[1,4,5,6,*]

SUMMARY

Archaeological and paleontological records offer tremendous yet often untapped potential for examining long-term biodiversity trends and the impact of climate change and human activity on ecosystems. Yet, zooarchaeological and fossil remains suffer various limitations, including that they are often highly fragmented and morphologically unidentifiable, preventing them from being optimally leveraged for addressing fundamental research questions in archaeology, paleontology, and conservation paleobiology. Here, we explore the potential of palaeoproteomics—the study of ancient proteins—to serve as a critical tool for creating richer, more informative datasets about biodiversity change that can be leveraged to generate more realistic, constructive, and effective conservation and restoration strategies into the future.

WHAT IS THE SCOPE FOR CONSERVATION PALAEOPROTEOMICS?

Earth's animal species are currently disappearing at such a rapid rate that scholars have suggested our planet is witnessing what may become its sixth mass extinction event (Barnosky et al., 2011; Davis et al., 2018). Since the year 1500, over 300 vertebrate species have gone extinct (Davis et al., 2018) and one-fifth of all extant vertebrates are currently threatened with extinction (Hoffmann et al., 2010). The global loss of biodiversity—the culmination of processes of extinction, extirpation, and population decline—is the result of many millennia of intensifying human-mediated ecosystem transformation through overexploitation, habitat degradation and conversion, invasive species introductions, and other pressures (Butchart et al., 2010; Dirzo et al., 2014; Boivin et al., 2016). Human-induced global warming, together with expected growth in both global human population and per capita consumption (Dirzo et al., 2014; Barnosky et al., 2017), will likely put an even bigger strain on already vulnerable ecosystems in the future. Therefore, it is crucial to develop optimal and scientifically informed conservation, restoration, and rewilding strategies that will mediate the future loss of biodiversity and functioning of the ecosystem.

A long-term perspective on ecosystem change is critical to adapting conservation strategies to combat current climatic and environmental challenges (Willis and Birks, 2006; Scharf, 2014; Barnosky et al., 2017). Fields such as paleontology, paleobiology, archaeobiology, zooarchaeology, paleoecology, and historical ecology provide indispensable long-term data about changes to biotic communities and the role of humans in their transformation (Dietl and Flessa, 2011; Dietl et al., 2015; Fordham et al., 2020). Early ecosystem transformations include massive species losses and range declines, notably among megafauna (Sandom et al., 2014; Smith et al., 2018) and island endemics (Kouvari and van der Geer, 2018), in addition to shifts in the distribution, composition, abundance, and diversity of plant and animal communities (Boivin et al., 2016; Roberts et al., 2017). The necessity of taking such long-term data into account when assessing baselines, establishing conservation targets, and managing and restoring ecosystems is increasingly recognized (e.g., Willis et al., 2010; Dietl et al., 2015; Barak et al., 2016; Fordham et al., 2020; Boivin and Crowther, 2021).

Although these historical fields have a crucial role to play in developing informed and effective conservation approaches, their utility is hindered by important limitations, with taphonomic processes in particular yielding biased and incomplete datasets that are suboptimal for establishing baselines or evaluating climatic or anthropogenic impacts. With respect to faunal remains, the focus of our discussion, these limitations can be severe. Although preservation can sometimes be excellent, zooarchaeological and paleontological remains are more often heavily fragmented and even morphologically unidentifiable, limiting their potential to reveal long-term changes to biodiversity, understand and model processes of species

[1]Department of Archaeology, Max Planck Institute for the Science of Human History, Jena, Germany

[2]Department of Anthropology, Harvard University, Cambridge, MA, USA

[3]Center for Biodiversity Dynamics in a Changing World (BIOCHANGE), Department of Biology, Aarhus University, Aarhus, Denmark

[4]School of Social Science, The University of Queensland, Brisbane, QLD 4071, Australia

[5]Department of Anthropology, National Museum of Natural History, Smithsonian Institution, Washington, DC, USA

[6]Department of Anthropology and Archaeology, University of Calgary, Calgary, Canada

*Correspondence: peters@shh.mpg.de (C.P.), boivin@shh.mpg.de (N.B.)

https://doi.org/10.1016/j.isci.2022.104195

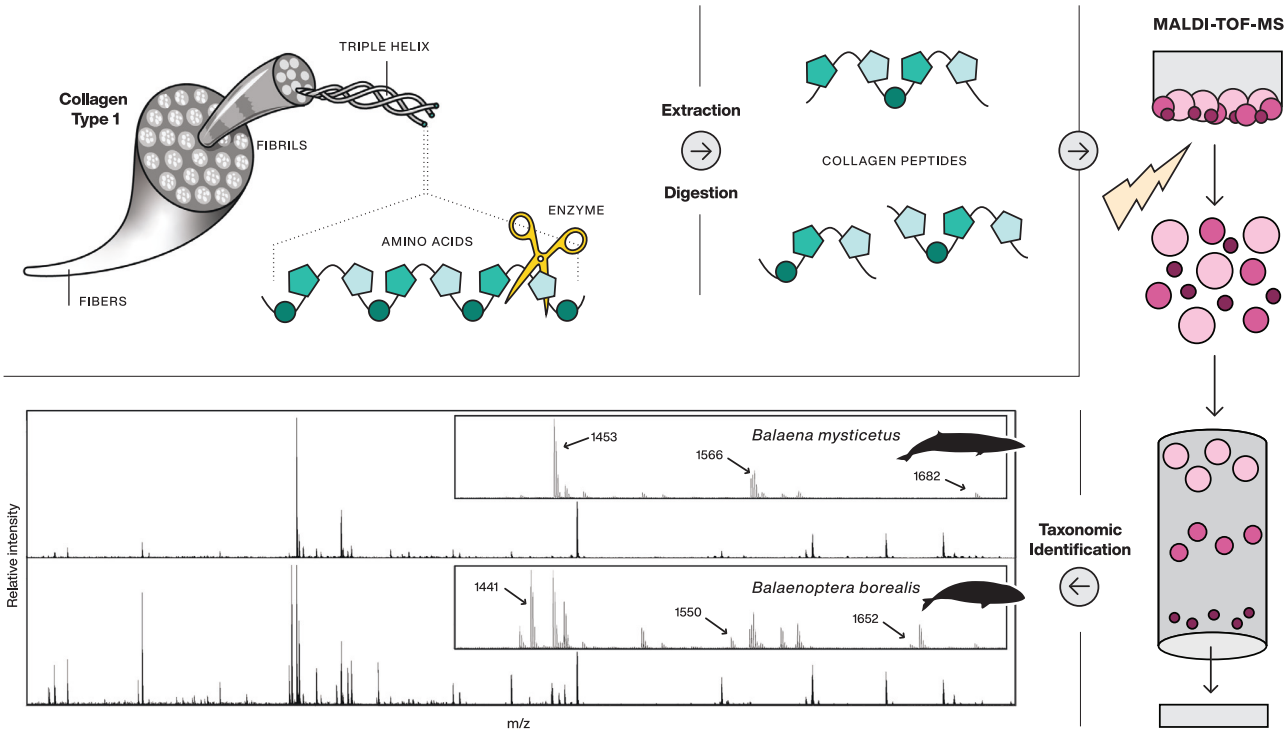

Figure 1. Schematic overview of ZooMS workflow (adapted from Brown et al., 2021a).

invasion, extinction and extirpation, and accurately and consistently measure anthropogenic alterations to ecosystems. In regions with high erosion and/or wind deflation or where cultural traditions favor mobility, zooarchaeological assemblages can even be lacking altogether.

In recent decades, biomolecular methods have significantly transformed the study of ancient faunal remains, enabling improvements in the analysis of ancient animals and assemblages. In particular, ancient DNA (aDNA) has been applied to better understand phylogenetic patterns, extinction mechanisms, and domestication processes across a wide range of faunal species (e.g., Haile et al., 2009; MacHugh et al., 2017). Ancient DNA methods have also been used to address conservation agendas (e.g., Leonard, 2008; Hofman et al., 2015; Waters and Grosser, 2016). However, challenges of aDNA preservation mean that this biomolecular approach has limited applicability, with often minimal potential in hot, humid, and tropical environments, as well as in the study of older assemblages. To address this challenge, new approaches that examine ancient proteins rather than aDNA have been adopted in the recent years. Proteins are an attractive target for conservation studies because they can be preserved over longer time periods in a wider array of contexts than aDNA and are also more resistant to degradation in warm environments (Buckley et al., 2009; Rybczynski et al., 2013; Demarchi et al., 2016; Hendy et al., 2018; Welker et al., 2019).

Two key approaches currently exist for examining ancient proteins – peptide mass fingerprinting and shotgun palaeoproteomics. Both are mass spectrometry-based approaches, which involve the detection of ionized peptides, thereby enabling the identification of peptide sequences and the characterization of proteins in a sample (Cappellini et al., 2014; Hendy, 2021). Zooarchaeology by Mass Spectrometry (ZooMS; Figure 1) is a peptide mass fingerprinting technique focused on collagen type I (COL1), a well-characterized and generally robust protein that also plays a key role in both radiometric dating and stable isotopic reconstructions of ancient diet (Pestle and Colvard, 2012). Applications of ZooMS draw on the fact that the amino acid sequence of COL1—the most abundant protein in bone, skin, antler, and dentine—varies across different taxonomic groups (Buckley et al., 2009).

ZooMS involves extraction of peptides from the targeted material, which are then analyzed using matrix-assisted laser desorption/ionization mass spectrometry (MALDI-ToF-MS), generating a spectrum with the

mass-to-charge ratios of the individual peptides in the sample. The spectra are compared to a reference database of spectra from known taxa to taxonomically identify collagen-bearing materials. This approach is increasingly used in the field of archaeology to taxonomically identify highly fragmented and/or morphologically unidentifiable faunal remains (Buckley et al., 2017b; Sinet-Mathiot et al., 2019; Brown et al., 2021b). ZooMS is a relatively cheap and fast method (Buckley et al., 2009; Welker et al., 2015b; Richter et al., 2020), making it applicable to larger-scale assemblages than many other biomolecular methods.

In contrast to peptide mass fingerprinting in which only the predominant peptides in a sample are visualized, shotgun palaeoproteomics targets a much larger percentage of a sample's peptides by using liquid chromatography tandem mass spectrometry (LC-MS/MS) to provide a much higher resolution. The peptides in a sample are identified following two fragmentation steps. First, the mass of each peptide is detected in the first mass analyzer. The most frequently occurring peptides are further fragmented and measured again in a second mass analyzer. The amino acid sequences of the peptides in the sample can then be identified through comparison to large reference databases (Hendy, 2021). Shotgun proteomics provides the opportunity to examine phylogenetic relationships in materials that are too old or poorly preserved to yield aDNA (Rybczynski et al., 2013; Welker et al., 2015a). It can also be used to identify the sex of prehistoric individuals (Stewart et al., 2017), the presence of particular fauna, and to explore human-animal relationships from indirect sources such as dental calculus (e.g., Wilkin et al., 2021). With shotgun proteomics, it is also possible, as it is not with ZooMS, to detect posttranslational modifications of individual amino acids, allowing insight into the degradation patterns and authenticity of ancient proteins (Van Doorn et al., 2012; Cleland et al., 2015, 2021). The wealth of information that can be derived from a single sample makes shotgun proteomics more informative and versatile than peptide mass fingerprinting. However, the trade-off for this information is increased cost and time input per sample. Although studies using peptide mass fingerprinting can easily analyze hundreds or even thousands of samples (Richter et al., 2011; Brown et al., 2016, 2021b), most shotgun palaeoproteomic studies analyze only a fraction of this amount.

Protein-based methods are not new in archaeology (Abelsen, 1954; Hare and Abelsen, 1968; Newman and Julig, 1989; Johnson and Miller, 1997; Ostrom et al., 2000; Kooyman et al., 2001; Buckley et al., 2009, 2011; Cappellini et al., 2014); however, methodological improvements over the past decade (Van Doorn et al., 2011; Van der Sluis et al., 2014; McGrath et al., 2019) have seen their increasing application to a wide range of archaeological, human evolutionary, and art historical questions (for a more in-depth review about the historical perspective of ancient protein-based methods and their applications, please see Buckley (2018); Welker (2018); Villanova and Porcar (2019); Hendy (2021), and references therein). Critically, a broad array of materials are suitable for palaeoproteomic analysis, including bone (Buckley et al., 2009; Cappellini et al., 2012; Cleland et al., 2015, 2016; Welker et al., 2015b), antler (Von Holstein et al., 2014; Ashby et al., 2015), mollusc shell (Sakalauskaite et al., 2020), eggshell (Demarchi et al., 2019), ivory (Coutu et al., 2016), dentine and enamel (Cappellini et al., 2019; Welker et al., 2019), dental calculus (Warinner et al., 2014; Bleasdale et al., 2021; Wilkin et al., 2021), leather (Brandt et al., 2014), parchment (Fiddyment et al., 2015), hair (Solazzo et al., 2013), textiles (Gong et al., 2016), ceramic residues (Solazzo et al., 2008), and preserved food remains (Yang et al., 2014).

We argue that given their extraordinary advantages, ancient protein-based studies hold significant potential not only to understand the archaeological record and changes to human diets and economies through time but also to address biodiversity and conservation agendas. To date, this potential has been only minimally explored. Nonetheless, some insights have been acquired, and we review recent developments here to demonstrate the future potential of conservation palaeoproteomics. Drawing upon examples from a range of regions and time periods, we outline seven key ecological conservation issues that ancient proteins can help to address (Figure 2).

ASSESSING SPECIES RICHNESS

The global loss of biodiversity is one of the most significant threats faced by ecosystems today (Hoffmann et al., 2010; Barnosky et al., 2011; Davis et al., 2018). Estimates of species diversity and composition are crucial for making accurate inferences concerning the magnitude and rate of biodiversity loss, information that is crucial to contemporary conservation efforts (Butchart et al., 2010) as well as for informing restoration strategies (Monsarrat and Svenning, 2021). However, these estimates are often based solely on the organisms represented in modern ecosystems, not accounting for ecosystem transformations in the past.

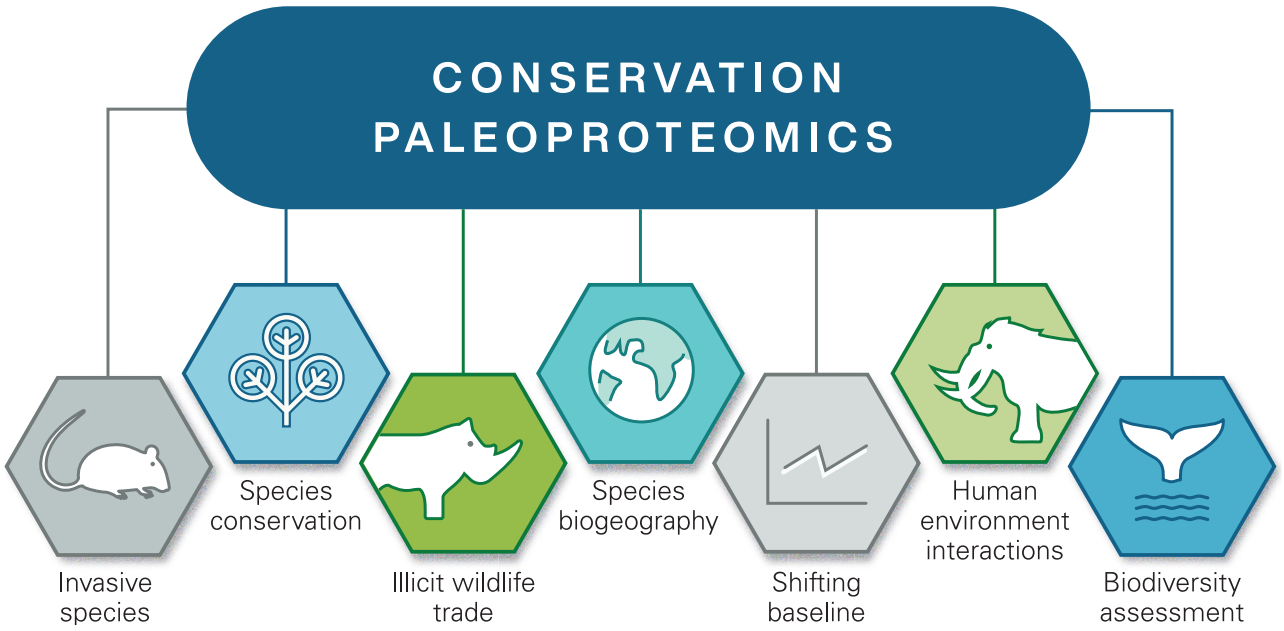

Figure 2. Seven key issues that conservation palaeoproteomics can target to help deliver more informed and effective conservation strategies.

Paleontological data have thus been recognized as a useful proxy to help better understand and contextualize biotic community structure and the dynamics of species richness over time (Dietl et al., 2015; Kidwell, 2015).

The application of palaeoproteomic techniques such as peptide mass fingerprinting has significant potential to help quantify and improve understanding of biodiversity in the past, complementing morphological analyses and increasing both the accuracy of faunal identifications as well as the number of taxonomically identified fossil remains at archaeological and paleontological sites. Among their advantages is that palaeoproteomic approaches allow the analysis of a broader diversity of materials for examining past species composition. Although the primary focus of analysis is often on a subset of morphologically identifiable specimens, palaeoproteomics offers the ability to study other faunal materials, including unidentifiable postcranial elements, bone tools, objects and their production waste (Ashby et al., 2015; McGrath et al., 2019; Jensen et al., 2020), taphonomically degraded material from owl pellets (Buckley et al., 2016; Buckley and Herman, 2019), and flowstone-encased faunal material (Harvey et al., 2019a), for example.

Perhaps its most significant advantage, however, is that ZooMS allows for the identification of fragmented faunal material. As noted, fragmented bone often makes up a significant proportion of archaeological and paleontological assemblages (Welker et al., 2015b; Brown et al., 2016; Sinet-Mathiot et al., 2019). Examples from the UK, Italy, and France show that ZooMS analyses of Late Pleistocene assemblages have significantly increased the number of identified faunal specimens, revealing a greater degree of taxonomic richness than previously understood (Welker et al., 2015b; Buckley et al., 2017b; Sinet-Mathiot et al., 2019). Proteomic analyses of fragmented remains from Final Mousterian and Uluzzian contexts at Fumane, Italy, for example, expanded biodiversity records at the site by providing evidence for two previously unidentified taxonomic groups of ecological and cultural importance, namely elephants (Elephantidae) and rhinoceroses (Rhinocerotidae) (Sinet-Mathiot et al., 2019). The analysis also increased the proportion of *Bos/Bison* specimens in the assemblage, suggesting that percussion-based carcass fragmentation of large *Bos/Bison* bone diaphyses severely fragmented the remains of this taxonomic group, making it difficult to identify the species morphologically, and biasing taxonomic assessments (Sinet-Mathiot et al., 2019). Meanwhile, peptide mass fingerprinting from the Châtelperronian contexts at Les Cottés, France, increased the number of identified faunal specimens by 30%. This was linked to a concomitant increase in taxonomic richness, with ZooMS yielding almost double the number of taxa identified through morphological analyses (Welker et al., 2015b).

Late Pleistocene contexts have so far provided the most well-developed examples of how palaeoproteomic methods can help to more accurately assess past species richness, in some cases taking researchers back to a point in time at which human impacts were more minimal. Holocene contexts also merit further investigation in this regard. Species identifications in these assemblages are often focused on large-sized animals that were exploited by humans (Crees et al., 2019), leaving taxonomic richness at the other end of the size spectrum poorly understood. Meanwhile, the study of marine diversity holds particular promise as a target of peptide mass fingerprinting because of the high variability of collagen sequences in fish species (Richter et al., 2011, 2020; Harvey et al., 2018). The ability to study morphologically uninformative marine remains with ZooMS provides great potential to significantly improve our understanding of biodiversity trends and baselines in marine ecosystems (see below).

ESTABLISHING ECOLOGICAL BASELINES

Ecological baselines often refer to ecosystem conditions perceived to predate human-mediated ecosystem transformation. These baselines are used in conservation biology to inform management strategies for species conservation and ecosystem restoration (Willis et al., 2010; Hofman et al., 2015). Ecological baselines are often based on local conditions before European colonization or widespread industrialization, drawing on the assumption that these were close to natural, prehuman baselines (Froyd and Willis, 2008). However, preindustrial as well as pre-European human impacts were frequently far more substantial than has been appreciated (Boivin et al., 2016; Ellis et al., 2016, 2021), meaning that we must look earlier in time, in some cases back to the Late Pleistocene to identify pre-anthropogenic baselines to inform conservation targets (Rodrigues et al., 2019).

Beyond this, climate change complicates the relationship between looking back to a 'natural' state and looking forward to a 'healthy' future ecosystem (Keulartz, 2016). Once again, past conditions provide critical information, for example, by providing insight into faunal functional diversity across varying climatic conditions (Svenning, 2020) and typical levels of community change (Williams et al., 2021). The documentation of ecological baselines offers insight into the climatic potential for biodiversity and mechanisms of long-term biodiversity maintenance (Svenning, 2020) as well as ecosystem responses to climatic stresses (Barnosky et al., 2017) and can thus help guide future restoration efforts under diverse climate change scenarios.

The utility of ZooMS for establishing baselines is highlighted by a number of recent studies focused on marine fauna (Biard et al., 2017; Harvey et al., 2018, 2019b; Rodrigues et al., 2018; Richter et al., 2020). Gray whale baselines, for example, have been clarified using collagen fingerprinting. A coastal whale species with extant populations in the Pacific Ocean, gray whales were also previously present in the North Atlantic, though the paucity of historical records for the species suggested they were naturally rare there (Clapham and Link, 2007). Collagen fingerprinting, together with molecular genetics and radiocarbon dating, has now clarified that the species began to decline in the Western Atlantic Basin in the Late Pleistocene (Garrison et al., 2019). Meanwhile ZooMS studies in the Western Mediterranean not only extend the known distribution of the gray whale but also reveal that the species was likely relatively common there as recently as the Roman period (Rodrigues et al., 2018). Such studies help to reveal the complex climatic and anthropogenic factors that have shaped cetacean population dynamics through time, including the role of forgotten whaling industries (Rodrigues et al., 2019). Such information can be drawn upon to more accurately evaluate population changes, supporting existing IUCN and Living Planet Index frameworks that aim to understand the impact of human activities on present-day ecosystems (Rodrigues et al., 2019).

Meanwhile, ZooMS has also provided crucial information on human exploitation of marine turtles in several regions (Harvey et al., 2019b; Peters et al., 2021; Winter et al., 2021). Species identification of sea turtles among faunal assemblages is often challenging because of the lack of robust osteomorphological reference material as well as the fragmentary nature of many turtle remains (Winter et al., 2021). ZooMS data has been combined with other molecular methods to begin to help clarify pre-commercial fisheries baselines in the Mediterranean, where the paucity of historically-informed baselines has made it challenging to gauge human impacts and the ecological potential of turtle taxa when setting conservation targets (Winter et al., 2021). The utility of ZooMS in providing historical baseline data for marine turtles has also been highlighted in the Caribbean, where the method enabled identification of less morphologically diagnostic

young turtles and highly fragmented remains from collections that had been stored for almost one hundred years in less-than-optimal microclimatic conditions (Harvey et al., 2019b).

DETECTING SHIFTS IN SPECIES ABUNDANCE AND GEOGRAPHIC RANGE

Global warming and human activities are significantly impacting the species abundance and geographic range of many faunal species. Knowing which species are likely to migrate and to where in response to climate change and other anthropogenic impacts is crucial to the development of appropriate conservation and mediation strategies. Accordingly, improving our understanding of species abundance and geographic ranges and predicting shifts in these parameters are important goals of ecological research (Willis and Birks, 2006; McGuire and Davis, 2014; Dietl et al., 2015). Meta-analyses of archaeofaunal and paleoclimatic data can provide insights into species abundance and geographic ranges during past climatic conditions, helping to improve prediction of future shifts in biogeography and guiding management strategies for the future (Lyman, 2012; McGuire and Davis, 2014; Hofman et al., 2015).

ZooMS offers useful potential for helping track species abundance and range shifts. Some of this potential is revealed in studies of cave contexts because caves are important in the life histories of many species, serving as dens for predators, hibernation locations for bats, and roosting sites for birds, for example. Caves also offer important reservoirs of paleontological specimens, trapping bones in depositional settings, which may be conducive to long-term preservation depending on geological, hydrological, and other conditions. Faunal assemblages from cave deposits are accordingly a useful resource for assessing and reconstructing past geographical species ranges (Frick et al., 2020). ZooMS analyses of Late Pleistocene microfauna remains from Pin Hole Cave, England, revealed the geographical presence of several now extirpated species, including horseshoe bat (Buckley and Herman, 2019) and moor frog (Buckley and Cheylan, 2020). Palaeoproteomic identification of eggshell remains from El Miron Cave, Spain, revealed that it once lay within the geographical range of the bearded vulture (Demarchi et al., 2019).

ZooMS has also been used to suggest shifts in species abundance. An intriguing ZooMS study of bone and antler combs from archaeological sites in Denmark shows increasing sourcing of antler from reindeer, located far to the north in the circumpolar subarctic and boreal zone. This may reflect growing pressure on local populations of red deer and a concomitant decrease in their abundance (Ashby et al., 2015). This study highlights the utility of crafted artifacts as well as production waste in reconstructing past biodiversity shifts. But caution in the interpretation of such patterns is also warranted. Another ZooMS study of Mesolithic bone points from southern Scandinavia, for example, showed that raw material selection reflected not just biodiversity changes but also cultural choices (Jensen et al., 2020).

DISENTANGLING HUMAN-ENVIRONMENT INTERACTIONS

Human activities are having a major impact on ecosystems all around the globe, but teasing human impacts apart from natural processes is not always a straightforward task. Investigation of the archaeological record can provide new insight into human-environmental relationships in the past, helping to disentangle human impacts and natural processes (Dietl and Flessa, 2011; Hofman et al., 2015; Barak et al., 2016) and supporting efforts to conserve present-day ecosystems that are threatened by human-induced climatic and environmental changes.

Studies of megafaunal extinctions are one area where ancient protein studies are poised to make an important contribution. The extinction of many megafauna species at the end of the late Quaternary led to a significant global loss of biodiversity and ecosystem function (Sandom et al., 2014; Malhi et al., 2016; Galetti et al., 2018). The exact dynamics, relative importance, and interactions of human and climatic drivers as potential drivers of these megafauna losses remain debated. Providing better data on past megafauna distributions across space and time will be important for strengthening analyses of extinction dynamics and their drivers. Yet, the underrepresentation of dated megafaunal fossils in the archaeological and paleontological records currently problematizes precise estimates of extinction chronologies and geographical ranges for many megafauna taxa (Price et al., 2018b; Swift et al., 2019). As part of combined, multidisciplinary investigations, ZooMS studies have the potential to contribute significantly to our understanding of both, especially now that peptide markers for megafauna species are becoming increasingly widely available (Buckley et al., 2011, 2017a; Van der Sluis et al., 2014; Welker et al., 2015b; Mychajliw et al., 2020). The ability of ZooMS to identify ancient hominin remains (e.g., Brown et al., 2016; Welker et al., 2016) can also contribute to

refining dispersal chronologies and clarifying the chronological overlap between human arrival and megafauna extinctions.

Parallel to efforts to understand the cause of megafaunal extinctions, there is also interest in their effects. Today there is increasing appreciation for the ecological importance of megafauna (Bakker et al., 2016; Malhi et al., 2022) and the changes to vegetation cover, ecosystem structure, biogeochemical cycling and land surface albedo that resulted from megafaunal loss (Doughty et al., 2013). Efforts to restore these lost ecosystem functions have resulted in trophic rewilding projects in which locally extirpated or novel keystone species are being reintroduced (Lorimer et al., 2015; Cortlett, 2016; Svenning et al., 2016). By contributing to a better understanding of past species ranges and the effects of megafaunal extinctions on broader ecosystems, ancient protein studies have significant potential to inform and strengthen rewilding science and practice (Dietl et al., 2015; Svenning et al., 2016). Notably, improved understanding of past megafauna distributions and ecologies is crucial for informing on megafauna recovery potential and its ecological importance (Monsarrat and Svenning, 2021), for example, in relation to large-herbivore assemblage structure (Schowanek et al., 2021) and associated effects on plant migration rates (Fricke et al., 2022). In addition, improving assessments of megafauna recovery potential is important for informing restoration efforts to enhance climate mitigation and adaptation (Malhi et al., 2022).

TRACKING THE INTRODUCTION OF NON-NATIVE SPECIES

The introduction of non-native species can have a severe impact on local biodiversity as well as ecosystem structure and function and can ultimately lead to extirpation, trophic cascades, and even extinction of native species (Gurevitch and Padilla, 2004; Hofman et al., 2015; Boivin et al., 2016; Barnosky et al., 2017). Improvements in the identification and tracking of introduced species are thus of critical concern for generating appropriate conservation strategies (Dietl and Flessa, 2011; Prendergast et al., 2017; Hofman and Rick, 2018). However, some issues are not always clear, such as knowing whether a species is introduced or endemic and the effect it had on the local ecosystems (Barak et al., 2016; Barnosky et al., 2017). Further complicating the situation are instances in which non-native species have functionally replaced exterminated native species (Lundgren et al., 2020). Data on the past is increasingly central to efforts to understand and address issues concerning introduced species and their impacts (Gurevitch and Padilla, 2004; Willis and Birks, 2006).

Palaeoproteomic methods are increasingly being employed to help track the introduction of non-native species, clarifying the status of potentially invasive species, and allowing more effective examination of their subsequent impact on ecosystems. Several studies, for example, have used peptide mass fingerprinting to track the introduction to island ecosystems of murid rodents, which negatively impacted endemic island fauna through habitat degradation and resource competition (Shiels et al., 2014). The Iron Age introduction of the black rat, a native of Asia, to the eastern African coast has been tracked using a combination of peptide mass fingerprinting, aDNA, and dental morphology. This study showed that the black rat was introduced to eastern Africa by the mid-first millennium CE (Prendergast et al., 2017). ZooMS has also been used to trace the arrival of murid rodents to the Cayman Islands following human colonization and to shed further light on their impact on endemic fauna (Harvey et al., 2019a).

Peptide mass fingerprinting is also increasingly being used to directly track the spread of a broad range of domesticated species, including in eastern Africa (Culley et al., 2021; Janzen et al., 2021), southern Africa (Le Meillour et al., 2020; Coutu et al., 2021) and central and eastern Asia (Taylor et al., 2018, 2020). Species-specific palaeoproteomic identification of milk proteins in human dental calculus (Wilkin et al., 2020, 2021; Bleasdale et al., 2021) has further contributed to this effort and is particularly useful in regions where zooarchaeological evidence is lacking for taphonomic or cultural reasons. Studying the introduction of domesticated species is critical to conservation efforts as many have played a significant role in transforming local ecosystems (Boivin et al., 2016; Hofman and Rick, 2018). The introduction of herd animals, for example, has shaped the formation of open landscapes (Ventresca Miller et al., 2020) as well as soil enriched hotspots (Marshall et al., 2018), and in many of the world's islands, domesticated and commensal species introduced by early colonizing populations have had a significant impact on endemic plant and animal populations (Boivin et al., 2016). Proteomic and other biochemical analyses of coprolites from a Neolithic settlement on the Orkney Islands have provided further evidence of such trends, revealing the consumption of local micromammals by domestic dogs (Romaniuk et al., 2020).

IDENTIFYING ILLICITLY TRADED MATERIAL

The international trade in wildlife and wildlife-derived products includes a considerable number of illicitly traded materials originating from endangered species (Galimberti et al., 2015). Many specimens that are illicitly traded are heavily processed or consist only of fragmentary remains (Jacobs and Baker, 2018) and are thus difficult to identify based on morphology alone. DNA-based methods are already being used to identify wildlife products (Eaton et al., 2010; Galimberti et al., 2015; Jacobs and Baker, 2018). However, proteomic approaches offer a quicker and cheaper means to identify these specimens and thus have the potential to aid the identification of illegally traded materials in resource and funding-limited contexts.

The application of ZooMS on collagen-based materials such as bone and ivory (Coutu et al., 2016; Coutu and Damgaard, 2019) has the potential to provide taxonomic identification of illicitly traded material. There is also emerging interest in using peptide mass fingerprinting of keratinous materials (Solazzo et al., 2011, 2013), such as hair, horn, and baleen, to identify illicit trade, such as of rhinoceros horn powder (Price et al., 2018a) or contraband fiber (Azémard et al., 2021). In South America, for example, wild camelids are endangered by poaching and black-market sale of their fibers, and proteomic analysis can be used to help identify the origin of confiscated animal fibers particularly when DNA is degraded because of taphonomic and diagenetic processes (Azémard et al., 2021). At the same time, peptide markers still require validation, diagnostic peptides are infrequently detected, and issues of hybridization challenge proteomic identification of domestic camelid species in particular. Yet, diagnostic peptides, when present, appear to enable absolute identification of vicuña fiber. As producers of the finest camelid fiber, vicuña was poached almost to extinction before receiving protection; however, they still suffer from illegal hunting and sale, making them a species of significant conservation interest.

PRIORITIZING SPECIES FOR CONSERVATION

Palaeoproteomic techniques also hold significant potential to help resolve phylogenetic relationships between extant and extinct species and are particularly beneficial when aDNA is not preserved. Analysis of 1.77-million-year-old protein sequences has been used to assess phylogenetic relationships between extant and extinct rhinoceroses, for example, revealing a close relationship between the extinct *Coelodonta* and *Stephanorhinus* and extant *Dicerorhinus* (Welker et al., 2017; Cappellini et al., 2019). Similarly, the phylogeny of recently extinct endemic South American ungulates has been resolved using palaeoproteomics (Welker et al., 2015a). Palaeoproteomic analyses of ancient collagen have also been used to generate phylogenetic reconstructions of several species of extinct West Indies island-shrews. This research revealed the presence of a number of distinct clades and species in this biodiversity hotspot, with interpopulation variability perhaps attributable to sexual dimorphism, providing new insights into the evolution and biogeography of these extinct species (Buckley et al., 2020). By improving our understanding of the origin, evolution, and distribution of this extinct shrew lineage, proteomic sequencing helps improve estimates of past species richness, which has been obscured by the magnitude of recent extinctions in the Caribbean (Buckley et al., 2020). Such data help improve understanding of faunal community structure in the West Indies today, broadly contributing to regional conservation management strategies.

Although the application of palaeoproteomics for phylogenetic reconstruction is a nascent area of research, its potential application in conservation assessments deserves further attention moving forward especially in biogeographic regions where aDNA is poorly preserved. Estimates of phylogenetic diversity are often used to prioritize species for conservation, with preservation of species diversity, genetic variation, and unique evolutionary histories as the ultimate goal (Rolland et al., 2012; Pellens and Grandcolas, 2016; Upham et al., 2019). Phylogenetic reconstructions of modern and extinct taxa can also help resolve past dispersal and extinction events that have shaped biotic communities today (Lamsdell et al., 2017), estimate biogeographical ranges of past lineages (Lawing and Matzke, 2014), and identify possible replacements for extinct species in rewilding projects (Svenning et al., 2016).

THE FUTURE OF CONSERVATION PALAEOPROTEOMICS

The modern biodiversity crisis is one of the most pressing challenges of the Anthropocene. As researchers increasingly recognize the importance of information about the past to studying, understanding, and conserving biodiversity today, a novel suite of methods is being brought to bear on resolving long-standing as well as emerging questions in biodiversity research. We demonstrate that the key among the newest

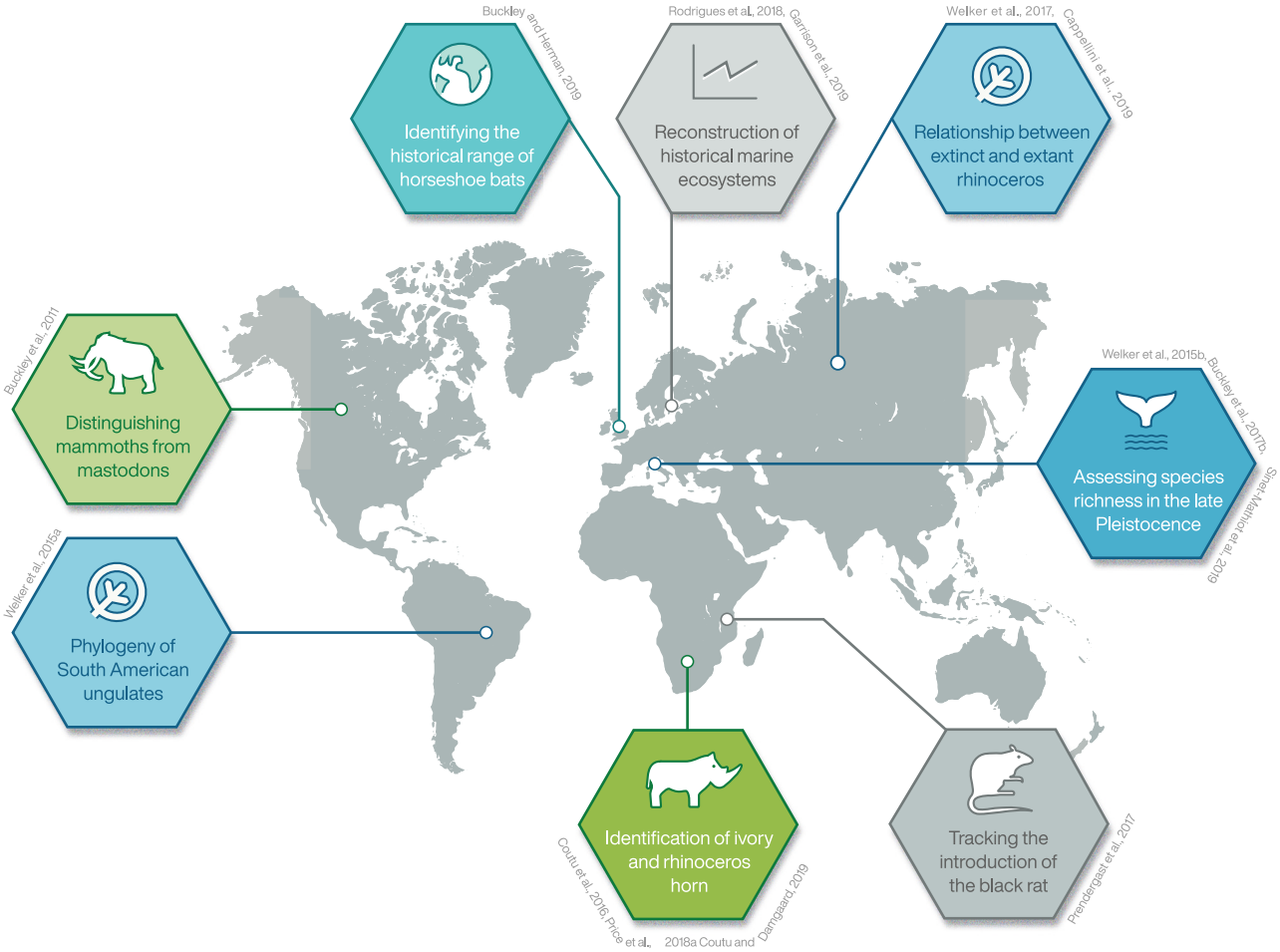

Figure 3. Case studies highlighting the potential of palaeoproteomics techniques to address key conservation requirements.

and most cutting-edge tools is palaeoproteomics, a method that draws on the long-term preservation of certain proteins and the taxonomic information contained within them. Our review demonstrates that although there are still challenges that need to be addressed, palaeoproteomics has the potential to contribute to improved recovery of a range of different types of data useful to conservation efforts (Figure 3). Although palaeoproteomics has only been minimally instrumentalized in biodiversity, conservation, restoration, and rewilding research to date, numerous studies already point to its significant potential to address issues ranging from establishing baselines and assessing range shifts to tracking the spread of introduced species.

At the same time, the application of palaeoproteomics for conservation purposes does not come without caveats. Protein-based methods are still at an early stage of development, and more work is needed to address the challenges of contamination and ancient protein authentication, particularly in shotgun proteomics studies (Hendy et al., 2018; Cleland et al., 2021). Further work is also needed to gain a better understanding of the degradation pathways of ancient proteins and the circumstances in which they preserve in the archaeological record (Van Doorn et al., 2012; Demarchi et al., 2016; Cleland et al., 2021). This research will provide important clarification as to how applicable palaeoproteomics will be in different regions of the world and for different time periods.

Beyond this, limitations to current reference libraries are also significant. The incompleteness of reference collections significantly shapes the taxonomic diversity recovered in paaleoproteomics studies. The majority of reference markers developed for ZooMS to date belongs to medium- to large-sized Eurasian mammals. Although recent years have seen the expansion of the reference library to include a larger variety of

ecologically interesting taxa such as micromammals (Buckley and Herman, 2019; Harvey et al., 2019a; Buckley et al., 2020), fish (Richter et al., 2011, 2020; Harvey et al., 2018), amphibians (Buckley and Cheylan, 2020), and reptiles (Harvey et al., 2019b), significant development of databases is still required. The lack of reference sequences at genomic or transcriptomic level for many species of interest further contributes to the paucity of available reference datasets (Sakalauskaite et al., 2020). To maximize the potential of palaeoproteomics for conservation research, more investment will be needed in developing the peptide markers and protein sequence data that are critical references for ancient protein studies.

On the other hand, the increasing number of reference data for taxa that are difficult to identify morphologically, such as micromammals, fish, birds, reptiles, and amphibians also represents critical progress. These taxa are important environmental indicators, and their more accurate and widespread identification offers significant potential to enable improved reconstruction of past ecosystems and associated assessments of recovery potential. Further growth of these reference datasets will no doubt pay significant dividends. Even with an expanded database, however, ancient protein studies will still be limited by the variability of protein sequences between taxa. This is specifically problematic for ZooMS studies, because COL1 is a functionally constrained protein with a slow rate of evolutionary change. In practice, this means that taxonomic resolution with ZooMS is often limited to family-level or genus-level resolution.

At a broader level, another key challenge is that it will take time and effort to integrate palaeoproteomics into existing conservation and restoration frameworks. Although zooarchaeology and paleontology have had decades to develop methods and metrics suitable to addressing conservation agendas, palaeoproteomics is only beginning to consider how its methods are suitable for this purpose. Accordingly, one of the major investments required in the near future will be the development of approaches that will enable incorporation of ZooMS data into the already well-established framework for faunal metrics that exists in zooarchaeology. Quantitative measures such as number of identified specimens (NISP), minimum number of elements (MNE), and minimum number of individuals (MNI) have been developed to address the issue of multiple bone fragments from the same individual, providing information critical to reconstructions of biodiversity changes through time. As ZooMS moves away from screening hundreds to thousands of fragmentary bones to a more holistic approach that is well-incorporated within existing zooarchaeological frameworks, such quantitative measures will need to be redefined.

Despite these initial caveats, the last decade has seen many exciting developments that will improve the applicability of ZooMS and other proteomics-based methods to a wider range of ecological and conservation questions in the future. Researchers have recently established a more standardized nomenclature system for ZooMS peptide markers (Brown et al., 2021a), for example. Development of open-source software for the automated examination of ZooMS spectral data, which would significantly decrease the time required for manual data analysis while simultaneously providing a way for researchers with only limited training to analyze ZooMS data is also underway (Gu and Buckley, 2018; Hickinbotham et al., 2020). In addition, new initiatives are in motion to develop minimally destructive screening methods, such as Fourier transform infrared spectroscopy (FTIR) and amino acid racemization, to assess the degree of molecular degradation of fossil material before paleoproteomic analysis (Pothier Bouchard et al., 2019; Kontopoulos et al., 2020; Presslee et al., 2021). The rapid identification of well-preserved specimens allows for the development of more suitable and sustainable sampling strategies that promote sustainable study of a fossil record that is not unlimited (Pálsdóttir et al., 2019). Finally, at a more practical level, the growing investment in new laboratories and palaeoproteomics facilities and the steadily rising number of trained ZooMS and palaeoproteomics researchers reflect the tremendous potential of ancient protein research and will increasingly allow a broader range of palaeoproteomics applications as the method becomes established in archaeology and paleontology.

Of course, the addition of biomolecular techniques to study the fossil record does not resolve its inherently biased nature as a result of site-specific formation histories and preservation conditions (Wolverton and Lyman, 2012), and palaeoproteomics is not a panacea for modern conservation efforts. Instead, it is the application of biomolecular approaches like palaeoproteomics in concert with more established methods like paleobiology, zooarchaeology, and palaeontology that provides a powerful new conservation tool, with the potential to significantly expand our knowledge and understanding of ecosystems in the past as well as the ecology of both extinct and extant species (Evans et al., 2016; Faurby and Araújo, 2018; Mychajliw et al., 2020). As numerous examples cited here demonstrate, interdisciplinary studies that combine

palaeoproteomics with additional biomolecular methods such as stable isotope or aDNA analysis also offer significant potential. Combined palaeoproteomic and stable isotope methods have, for example, been used to investigate the dietary behavior of extinct giant tortoises on Mauritius (Van der Sluis et al., 2014) and the historical ivory trade in eastern Africa (Coutu et al., 2016), whereas other approaches have combined palaeoproteomics and aDNA (Biard et al., 2017; Prendergast et al., 2017; Taylor et al., 2018). We accordingly highlight the need for an interdisciplinary approach, involving close collaboration and communication between all relevant fields from the start of a project onward.

As archaeology increasingly reorients from a strict focus on the past to a wider remit that includes addressing the major challenges in the Anthropocene (Boivin and Crowther, 2021), palaeoproteomics is poised to become a critical tool in the discipline's toolbox. We emphasize the wide suite of questions this method is suited to address and the increasing contribution it can make as part of interdisciplinary investigations. Palaeoproteomics is not just a research tool but also offers a cheaper and in some cases more accessible approach to addressing certain practical conservation challenges, including the identification of illicitly traded wildlife material. We suggest that with sufficient investment and development, palaeoproteomics will become an important tool in historically-informed conservation research and practice in the coming decade, clarifying long-term trends and helping support a new phase of close collaboration between archaeological and biodiversity research initiatives.

LIMITATIONS OF THE STUDY

This review argues that palaeoproteomics has significant potential to inform conservation, restoration, and rewilding strategies. Studies that directly support this argument are not yet abundant. The purpose of this review is to raise awareness concerning how the analysis of ancient proteins can be leveraged to examine biodiversity and environmental changes, to encourage further research in this area.

ACKNOWLEDGMENTS

We would like to thank M. O'Reilly for help with figure designs. We are also grateful to the three anonymous reviewers, whose comments and suggestions helped to improve the paper. This work was supported by the Max Planck Society. J.C.S. considers this work a contribution to his VILLUM Investigator project "Biodiversity Dynamics in a Changing World" funded by Villum Fonden (grant 16549).

AUTHOR CONTRIBUTIONS

Conceptualization, C.P. and N.B.; Writing – Original Draft: C.P. and N.B.; Writing – Review & Editing, C.P., K.K.R., J.C.S., and N.B.; Supervision: N.B.

DECLARATION OF INTERESTS

The authors declare no competing interests.

REFERENCES

Abelsen, P.H. (1954). Amino acids in fossils. Science *119*, 576.

Ashby, S.P., Coutu, A.N., and Sindbæk, S.M. (2015). Urban networks and Arctic outlands: crafts specialists and reindeer antler in Viking towns. Eur. J. Archaeol. *18*, 679–704. https://doi.org/10.1179/1461957115Y.0000000003.

Azémard, C., Dufour, E., Zazzo, A., Wheeler, J.C., Goepfert, N., Marie, A., and Zirah, S. (2021). Untangling the fibre ball: proteomic characterization of South American camelid hair fibres by untargeted multivariate analysis and molecular networking. J. Prot. *231*, 104040. https://doi.org/10.1016/j.jprot.2020.104040.

Bakker, E.S., Gill, J.L., Johnson, C.N., Vera, F.W.M., Sandom, C.J., Asner, G.P., and Svenning, J.-C. (2016). Combining paleo-data and modern exclosure experiments to assess the impact of megafauna extinctions on woody vegetation. Proc. Natl. Acad. Sci. U S A *113*, 847–855. https://doi.org/10.1073/pnas.1502545112.

Barak, R.S., Hipp, A.L., Cavendar-Bares, J., Pearse, W.D., Hotchkiss, S.C., Lynch, E.A., Callaway, J.C., Calcote, R., and Larkin, D.J. (2016). Taking the long view: integrating recorded, archeological, paleoecological, and evolutionary data into ecological restoration. Int. J. Plant Sci. *177*, 90–102. https://doi.org/10.1086/683394.

Barnosky, A.D., Hadly, E.A., Gonzalez, P., Head, J., Polly, P.D., Lawing, A.M., Eronen, J.T., Ackerly, D.D., Alex, K., Biber, E., et al. (2017). Merging paleobiology with conservation biology to guide the future of terrestrial ecosystems. Science *355*, eaah4787. https://doi.org/10.1126/science.aah4787.

Barnosky, A.D., Matzke, N., Tomiya, S., Wogan, G.O.U., Swartz, B., Quental, T.B., Marshall, C.R., McGuire, J.L., Lindsey, E.L., Maguire, K.C., et al. (2011). Has the Earth's sixth mass extinction already arrived? Nature *471*, 51–57. https://doi.org/10.1038/nature09678.

Biard, V., Gol'din, P., Gladilina, E., Vishnyakova, K., McGrath, K., Vieira, F.G., Wales, N., Fontaine, M.C., Speller, C., and Olsen, M.T. (2017). Genomic and proteomic identification of late holocene remains: setting baselines for black sea odontocetes. J. Archaeol. Sci. Rep. *15*, 262–271. https://doi.org/10.1016/j.jasrep.2017.07.008.

Bleasdale, M., Richter, K.K., Janzen, A., Brown, S., Scott, A., Zech, J., Wilkin, S., Wang, K., Schiffels, S., Desideri, J., et al. (2021). Ancient proteins provide evidence of dairy consumption in eastern Africa. Nat. Commun. *12*, 1–11. https://doi.org/10.1038/s41467-020-20682-3.

Boivin, N., and Crowther, A. (2021). Mobilizing the past to shape a better Anthropocene. Nat. Ecol.

Evol. *5*, 273–284. https://doi.org/10.1038/s41559-020-01361-4.

Boivin, N.L., Zeder, M.A., Fuller, D.Q., Crowther, A., Larson, G., Erlandson, J.M., Denham, T., and Petraglia, M.D. (2016). Ecological consequences of human niche construction: examining long-term anthropogenic shaping of global species distributions. Proc. Natl. Acad. Sci. U S A *113*, 6388–6396. https://doi.org/10.1073/pnas.1525200113.

Brandt, L.Ø., Schmidt, A.L., Mannering, U., Sarret, M., Kelstrup, C.D., Olsen, J.V., and Cappellini, E. (2014). Species identification of archaeological skin objects from Danish bogs: comparison between mass spectrometry-based peptide sequencing and microscopy-based methods. PLoS One *9*, e106875. https://doi.org/10.1371/journal.pone.0106875.

Brown, S., Douka, K., Collins, M.J., and Richter, K.K. (2021a). On the standardization of ZooMS nomenclature. J. Prot. *235*, 104041. https://doi.org/10.1016/j.jprot.2020.104041.

Brown, S., Higham, T., Slon, V., Pääbo, S., Meyer, M., Douka, K., Brock, F., Comeskey, D., Procopio, N., Shunkov, M., et al. (2016). Identification of a new hominin bone from Denisova Cave, Siberia using collagen fingerprinting and mitochondrial DNA analysis. Sci. Rep. *6*, 23559. https://doi.org/10.1038/srep23559.

Brown, S., Wang, N., Oertle, A., Kozlikin, M.B., Shunkov, M.V., Derevianko, A.P., Comeskey, D., Jope-Street, B., Harvey, V.L., Chowdhury, M.P., et al. (2021b). Zooarchaeology through the lens of collagen fingerprinting at Denisova Cave. Sci. Rep. *11*, 15457. https://doi.org/10.1038/s41598-021-94731-2.

Buckley, M., and Cheylan, M. (2020). Collagen fingerprinting for the species identification of archaeological amphibian remains. Boreas *49*, 709–717. https://doi.org/10.1111/bor.12443.

Buckley, M., and Herman, J. (2019). Species identification of Late Pleistocene bat bones using collagen fingerprinting. Int. J. Osteoarchaeol. *29*, 1051–1059. https://doi.org/10.1002/oa.2818.

Buckley, M. (2018). Zooarchaeology by Mass Spectrometry (ZooMS). Collagen fingerprinting for the species identification of archaeological bone fragments. In Zooarchaeology in practice, C.M. Giovas and M.J. Lefebre, eds. (Springer), pp. 227–247. https://doi.org/10.1007/978-3-319-64763-0.

Buckley, M., Collins, M., Thomas-Oates, J., and Wilson, J.C. (2009). Species identification by analysis of bone collagen using matrix-assisted laser desorption/ionisation time-of-flight mass spectrometry. Rapid Commun. Mass Spectrom. *23*, 3843–3854. https://doi.org/10.1002/rcm.4316.

Buckley, M., Cosgrove, R., Garvey, J., and Prideaux, G.J. (2017a). Identifying remains of extinct kangaroos in Late Pleistocene deposits using collagen fingerprinting. J. Quarter. Sci. *32*, 653–660.

Buckley, M., Gu, M., Shameer, S., Patel, S., and Chamberlain, A.T. (2016). High-throughput collagen fingerprinting of intact microfaunal remains; A low-cost method for distinguishing between murine rodent bones. Rapid Commun. Mass Spectrom. *30*, 805–812. https://doi.org/10.1002/rcm.7483.

Buckley, M., Harvey, V.L., and Chamberlain, A.T. (2017b). Species identification and decay assessment of Late Pleistocene fragmentary vertebrate remains from Pin Hole Cave (Creswell Crags, UK) using collagen fingerprinting. Boreas *46*, 402–411. https://doi.org/10.1111/bor.12225.

Buckley, M., Harvey, V.L., Orihuela, J., Mychajliw, A.M., Keating, J.N., Milan, J., Almonte, N., Lawless, C., Chamberlain, A.T., Egerton, V.M., and Manning, P.L. (2020). Collagen sequence analysis reveals evolutionary history of extinct West Indies *Nesophontes* (island-shrews). Mol. Biol. Evol. *37*, 2931–2943. https://doi.org/10.1093/molbev/msaa137.

Buckley, M., Larkin, D.J., and Collins, M. (2011). Mammoth and mastodon collagen sequences: survival and utility. Geochim. Cosmochim. Acta *75*, 2007–2016. https://doi.org/10.1016/j.gca.2011.01.022.

Butchart, S., Walpole, M., Collen, B., Van Strien, A., Scharlemann, J.P.W., Almond, R.E.A., Baillie, J.E.M., Bomhard, B., Brown, C., et al. (2010). Global biodiversity: indicators of recent declines. Science *328*, 1164–1168. https://doi.org/10.1126/science.1187512.

Cappellini, E., Collins, M., and Gilbert, M.T.P. (2014). Unlocking ancient protein palimpsests. Science *343*, 1320–1322. https://doi.org/10.1126/science.1249274.

Cappellini, E., Jensen, L.J., Szklarczyk, D., Ginolhac, A., da Fonseca, R.A.R., Stafford, T.W., Holen, S.R., Collins, M.J., Orlando, L., Willerslev, E., et al. (2012). Proteomic analysis of a Pleistocene mammoth femur reveals more than one hundred ancient bone proteins. J. Proteome Res. *11*, 917–926. https://doi.org/10.1021/pr200721u.

Cappellini, E., Welker, F., Pandolfi, L., Ramos-Madrigal, J., Samodova, D., Rüther, P.L., Fotakis, A.K., Lyon, D., Moreno-Mayar, J.V., Bukhsianidze, M., et al. (2019). Early Pleistocene enamel proteome from Dmanisi resolves *Stephanorhinus* phylogeny. Nature *574*, 103–107. https://doi.org/10.1038/s41586-019-1555-y.

Clapham, P., and Link, J.S. (2007). Whales, whaling and ecosystems in the north atlantic ocean. In Whales, whaling, and ocean ecosystems, J.A. Estes, D.P. Demaster, D.F. Doak, T.M. Williams, and R.L. Brownell, eds. (University of California Press), pp. 314–323. https://doi.org/10.1525/9780520933200-028.

Cleland, T.P., Schroeter, E.R., and Colleary, C. (2021). Diagenetiforms: a new term to explain protein changes as a result of diagenesis in paleoproteomics. J. Prot. *230*, 103992. https://doi.org/10.1016/j.jprot.2020.103992.

Cleland, T.P., Schroeter, E.R., and Schweitzer, M.H. (2015). Biologically and diagenetically derived peptide modifications in moa collagens. Proc. R. Soc. B *282*, 20150015. https://doi.org/10.1098/rspb.2015.0015.

Cleland, T.P., Schroeter, E.R., Feranec, R.S., and Vashishth, D. (2016). Peptide sequences from the first *Castoroides ohioensis* skull and the utility of old museum collections for palaeoproteomics. Proc. R. Soc. B *283*, 20160593. https://doi.org/10.1098/rspb.2016.0593.

Cortlett, R.T. (2016). Restoration, reintroductions, and rewilding in a changing world. Trends Ecol. Evol. *31*, 453–462. https://doi.org/10.1016/j.tree.2016.02.017.

Coutu, A.N., and Damgaard, K. (2019). From tusk to town: ivory trade and craftmanship along the Red Sea. Stud. Late Antiq. *3*, 508–546. https://doi.org/10.1525/sla.2019.3.4.508.

Coutu, A.N., Taurozzi, A.J., Mackie, M., Jensen, T.Z.T., Collins, M.J., and Sealy, J. (2021). Palaeoproteomics confirm earliest domesticated sheep in southern Africa ca. 2000 BP. Sci. Rep. *11*, 6631. https://doi.org/10.1038/s41598-021-85756-8.

Coutu, A.N., Whitelaw, G., Le Roux, P., and Sealy, J. (2016). Earliest evidence for the ivory trade in southern Africa: isotopic and ZooMS analysis of seventh-tenth century AD ivory from KwaZulu-natal. Afr. Archaeol. Rev. *33*, 411–435. https://doi.org/10.1007/s10437-016-9232-0.

Crees, J.J., Collen, B., and Turvey, S.T. (2019). Bias, incompleteness and the 'known unknowns' in the Holocene faunal record. Philos. Trans. R. Soc. B *473*, 20190216. https://doi.org/10.1098/rstb.2019.0216.

Culley, C., Janzen, A., Brown, S., Prendergast, M.E., Shipton, C., Ndiema, E., Petraglia, M.D., Boivin, N., and Crowther, A. (2021). Iron age hunting and herding in coastal eastern Africa: ZooMS identification of domesticates and wild bovids at Panga ya Saidi, Kenya. J. Archaeol. Sci. *130*, 105368. https://doi.org/10.1016/j.jas.2021.105368.

Davis, M., Faurby, S., and Svenning, J.-C. (2018). Mammal diversity will take millions of years to recover from the current biodiversity crisis. Proc. Natl. Acad. Sci. U S A *115*, 11262–11267. https://doi.org/10.1073/pnas.1804906115.

Demarchi, B., Hall, S., Roncal-Herrero, T., Freeman, C.L., Woolley, J., Crisp, M.K., Wilson, J.C., Fotakis, A.K., Fischer, R., Kessler, B., et al. (2016). Protein sequences bound to mineral surfaces persist into deep time. eLife *5*, e17092. https://doi.org/10.7554/eLife.17092.

Demarchi, B., Presslee, S., Gutiérrez-Zugasti, I., González-Morales, M., Marín-Arroyo, A.B., Straus, L.G., and Fischer, R. (2019). Birds of prey and humans in prehistoric europe: a view from El mirón cave, cantabria (Spain). J. Archaeol. Sci. Rep. *24*, 244–252. https://doi.org/10.1016/j.jasrep.2019.01.010.

Dietl, G.P., and Flessa, K.W. (2011). Conservation paleobiology: putting the dead to work. Trends Ecol. Evol. *26*, 30–37. https://doi.org/10.1016/j.tree.2010.09.010.

Dietl, G.P., Kidwell, S.M., Brenner, M., Burney, D.A., Flessa, K.W., Jackson, S.T., and Koch, P.L. (2015). Conservation paleobiology: leveraging knowledge of the past to inform conservation and restoration. Annu. Rev. Earth Planet. Sci. *43*, 79–103. https://doi.org/10.1146/annurev-earth-040610-133349.

Dirzo, R., Young, H.S., Galetti, M., Ceballos, G., Isaac, N.J.B., and Collen, B. (2014). Defaunation in

the Anthropocene. Science *345*, 401–406. https://doi.org/10.1126/science.1251817.

Doughty, C.E., Wolf, A., and Malhi, Y. (2013). The legacy of the Pleistocene megafauna extinctions on nutrient availability in Amazonia. Nat. Geosci. *6*, 761–764. https://doi.org/10.1038/ngeo1895.

Eaton, M.J., Meyers, G.L., Kolokotronis, S.-O., Leslie, M.S., Martin, A.P., and Amato, A. (2010). Barcoding bushmeat: molecular identification of central african and South American harvested vertebrates. Conserv. Genet. *11*, 1389–1404. https://doi.org/10.1007/s10592-009-9967-0.

Ellis, E.C., Gauthier, N., Klein Goldewijk, K., Bliege Bird, R., Boivin, N., Díaz, S., Fuller, D.Q., Gill, J.L., Kaplan, J.O., Kingston, N., et al. (2021). People have shaped most of terrestrial nature for at least 12,000 years. Proc. Natl. Acad. Sci. U S A *118*. e2023483118. https://doi.org/10.1073/pnas.2023483118.

Ellis, E., Maslin, M., Boivin, N.L., and Bauer, A. (2016). Involve social scientists in defining the Anthropocene. Nature *540*, 192–193. https://doi.org/10.1038/540192a.

Evans, S., Briz i Godino, I., Álvarez, M., Roswsell, K., Collier, P., Prosser de Goodall, R.N., Mulvulle, J., Lacrouts, A., Collins, M., and Speller, C. (2016). Using combined biomolecular methods to explore whale exploitation and social aggregation in hunter-gatherer-Fisher society in Tierra del Fuego. J. Archaeol. Sci. Rep. *6*, 757–767. https://doi.org/10.1016/j.jasrep.2015.10.025.

Faurby, S., and Araújo, M.B. (2018). Anthropogenic range contractions bias species climate change forecasts. Nat. Clim. Chang. *8*, 252–256. https://doi.org/10.10138/s41558-018-0089-x.

Fiddyment, S., Holsinger, B., Ruzzier, C., Devine, A., Binois, A., Albarella, U., Fischer, R., Nichols, E., Curtis, A., Cheese, E., et al. (2015). Animal origin of 13th-century uterine vellum revealed using noninvasive peptide fingerprinting. Proc. Natl. Acad. Sci. U S A *112*, 15066–15071. https://doi.org/10.1073/pnas.1512264112.

Fordham, D.A., Jackson, S.T., Brown, S.C., Huntley, B., Brook, B.W., Dahl-Jensen, D., Gilbert, M.T.P., Otto-Bliesner, B.L., Svensson, A., Theodoridis, S., et al. (2020). Using paleo-archives to safeguard biodiversity under climate change. Science *369*, eabc5654. https://doi.org/10.1126/science.abc5654.

Frick, W.F., Kingston, T., and Flanders, J. (2020). A review of the major threats and challenges to global bat conservation. Ann. N.Y. Acad. Sci. *1469*, 15–25. https://doi.org/10.1111/nyas.14045.

Fricke, E.C., Ordonez, A., Rogers, H.S., and Svenning, J.-C. (2022). The effects of defaunation on plants capacity to track climate change. Science *375*, 210–214. https://doi.org/10.1126/science.abk3510.

Froyd, C.A., and Willis, K.J. (2008). Emerging issues in biodiversity & conservation management: the need for a palaeoecological perspective. Quat. Sci. Rev. *27*, 1723–1732. https://doi.org/10.1016/j.quascirev.2008.06.006.

Galetti, M., Moleón, M., Jordano, P., Pires, M.M., Guimarães, P.R., Jr., Pape, T., Nichols, E., Hansen, D.M., Olesen, J.M., Munk, M., et al. (2018). Ecological and evolutionary legacy of megafauna extinctions. Biol. Rev. *93*, 845–862. https://doi.org/10.1111/brv.12374.

Galimberti, A., Sandionigi, A., Bruno, A., Bellati, A., and Casiraghi, M. (2015). DNA barcoding in mammals: what's new and where next? Hystrix *26*, 13–24. https://doi.org/10.4404/hystric-26.1-11347.

Garrison, E.G., Morgan, G.S., McGrath, K., Speller, C., and Cherkinsky, A. (2019). Recent dating of extinct Atlantic gray whale fossils, (*Eschrichtius robustus*), Georgia Bight and Florida, western Atlantic Ocean. PeerJ. *7*, e6381. https://doi.org/10.7717/peerj.6381.

Gong, Y., Li, L., Gong, D., Yin, H., and Zhang, J. (2016). Biomolecular evidence of silk from 8,500 Years ago. PLoS One *11*, e0168042. https://doi.org/10.1371/journal.pone.0168042.

Gu, M., and Buckley, M. (2018). Semi-supervised machine learning for automated species identification by collagen peptide mass fingerprinting. BMC Bioinformatics *19*, 241. https://doi.org/10.1186/s12859-018-2221-3.

Gurevitch, J., and Padilla, D.K. (2004). Are invasive species a major cause of extinctions? Trends Ecol. Evol. *19*, 470–474. https://doi.org/10.1016/j.tree.2004.07.005.

Haile, J., Froese, D.G., MacPhee, R.D.E., Roberts, R.G., Arnold, L.J., Reyes, A.V., Rasmussen, M., Nielsen, R., Brook, B.W., Robinson, S., et al. (2009). Ancient DNA reveals late survival of mammoth and horse in interior Alaska. Proc. Natl. Acad. Sci. U S A *106*, 22352–22357. https://doi.org/10.1073/pnas.0912510106.

Hare, P.E., and Abelsen, P.H. (1968). Racemization of amino acids in fossil shells. Carnegie Inst. Wash. Yearb. *66*, 526–528.

Harvey, V.L., Daugnora, L., and Buckley, M. (2018). Species identification of ancient Lithuanian fish remains using collagen fingerprinting. J. Archaeol. Sci. *98*, 102–111. https://doi.org/10.1016/j.jas.2018.07.006.

Harvey, V.L., Egerton, V.M., Chamberlain, A.T., Manning, P.L., Sellers, W.I., and Buckley, M. (2019a). Interpreting the historical terrestrial vertebrate biodiversity of Cayman Brac (Greater Antilles, Caribbean) through collagen fingerprinting. Holocene *29*, 531–542. https://doi.org/10.1177/0959683618824793.

Harvey, V.L., LeFebvre, M.J., deFrance, S.D., Toftgaard, C., Drosou, K., Kitchener, A.C., and Buckley, M. (2019b). Preserved collagen reveals species identity in archaeological marine turtle bones from Caribbean and Florida sites. R. Soc. Open Sci. *6*, 191137. https://doi.org/10.1098/rsos.191137.

Hendy, J. (2021). Ancient protein analysis in archaeology. Sci. Adv. *7*, eabb9314. https://doi.org/10.1126/sciadv.abb9314.

Hendy, J., Welker, F., Demarchi, B., Speller, C., Warinner, C., and Collins, M. (2018). A guide to ancient protein studies. Nat. Ecol. Evol. *2*, 791–799. https://doi.org/10.1038/s41559-018-0510-x.

Hickinbotham, S., Fiddyment, S., Stinson, T.L., and Collins, M. (2020). How to get your goat: automated identification of species from MALDI-ToF spectra. Bioinformatics *36*, 3719–3725. https://doi.org/10.1093/bioinformatics/btaa181.

Hoffmann, M., Hilton-Taylor, C., Angulo, A., Böhm, M., Brooks, T.M., Butchart, S., Carpenter, K.E., Chanson, J., Collen, B., Cox, N.A., et al. (2010). The impact of conservation on the status of the world's vertebrates. Science *330*, 1503–1509. https://doi.org/10.1126/science.1194442.

Hofman, C.A., and Rick, T. (2018). Ancient biological invasions and island ecosystems: tracking translocations of wild plants and animals. J. Archaeol. Res. *26*, 65–115. https://doi.org/10.1007/s.10814-017-9105-3.

Hofman, C.A., Rick, T., Fleischer, R.C., and Maldonado, J.E. (2015). Conservation archaeogenomics: ancient DNA and biodiversity in the Anthropocene. Trends Ecol. Evol. *30*, 540–549. https://doi.org/10.1016/j.tree.2015.06.008.

Jacobs, R.L., and Baker, B.W. (2018). The species dilemma and its potential impact on enforcing wildlife trade laws. Evol. Anthropol. *27*, 261–266. https://doi.org/10.1002/evan.21751.

Janzen, A., Richter, K.K., Mwebi, O., Brown, S., Onduso, V., Gatwiri, F., Ndiema, E., Katongo, M., Goldstein, S.T., Douka, K., et al. (2021). Distinguishing african bovids using zooarchaeology by mass spectrometry (ZooMS): new peptide markers and insights into iron Age economies in Zambia. PLoS One *16*, e0251061. https://doi.org/10.1371/journal.pone.0251061.

Jensen, T.Z.T., Sjöström, A., Fischer, A., Rosengren, E., Lanigan, L.T., Bennike, O., Richter, K.K., Gron, K.J., Mackie, M., Mortensen, M.F., et al. (2020). An integrated analysis of Maglemose bone points reframes the Early Mesolithic of Southern Scandinavia. Sci. Rep. *10*, 17244. https://doi.org/10.1038/s41598-020-74258-8.

Johnson, B.J., and Miller, G.H. (1997). Archaeological applications of amino acid racemization. Archaeometry *39*, 265–287. https://doi.org/10.1111/j.1475-4754.1997.tb00806.x.

Keulartz, J. (2016). Future directions for conservation. Environ. Values *25*, 385–407. https://doi.org/10.3197/096327116X14661540759115.

Kidwell, S.M. (2015). Biology in the Anthropocene: challenges and insights from young fossil records. Proc. Natl. Acad. Sci. U S A *112*, 4922–4929. https://doi.org/10.1073/pnas.1403660112.

Kontopoulos, I., Penkman, K., Mullin, V., Winkelbach, L., Unterländer, M., Scheu, A., Kreutzer, S., Hansen, H.B., Margaryan, A., Teasdale, M.D., et al. (2020). Screening archaeological bone for palaeogenetic and palaeoproteomic studies. PLoS One *15*, e0235146. https://doi.org/10.1371/journal.one.0235146.

Kooyman, B., Newman, M.E., Cluney, C., Lobb, M., Tolman, S., McNeil, P., and Hills, L.V. (2001). Identification of horse exploitation by Clovis hunters based on protein analysis. Am. Antiq. *66*, 686–691. https://doi.org/10.2307/2694181.

Kouvari, M., and van der Geer, A.A.E. (2018). Biogeography of extinction: the demise of insular mammals from the Late Pleistocene till today. Palaeogeogr. Palaeoclimatol. Palaeoecol. *505*, 295–304. https://doi.org/10.1016/j.palaeo.2018.06.008.

Lamsdell, J.C., Congreve, C.R., Hopkins, M.J., Krug, A.Z., and Patzkowsky, M.E. (2017). Phylogenetic paleoecology: tree-thinking and ecology in deep time. Trends Ecol. Evol. *32*, 452–463. https://doi.org/10.1016/j.tree.2017.03.002.

Lawing, A.M., and Matzke, N. (2014). Conservation paleobiology needs phylogenetic methods. Ecography *37*, 1109–1122. https://doi.org/10.1111/ecog.00783.

Le Meillour, L., Zirah, S., Zazzo, A., Cersoy, S., Détroit, F., Imalwa, E., Lebon, M., Nankela, A., Tombret, O., Pleurdeau, D., et al. (2020). Palaeoproteomics gives new insight into early southern African pastoralism. Sci. Rep. *10*, 14427. https://doi.org/10.1038/s41598-020-71374-3.

Leonard, J.A. (2008). Ancient DNA applications for wildlife conservation. Mol. Ecol. *17*, 4186–4196. https://doi.org/10.1111/j.1365-294X.2008.03891.x.

Lorimer, J., Sandom, C., Jepson, P., Doughty, C., Barua, M., and Kirby, K.J. (2015). Rewilding: science, practice, and politics. Annu. Rev. Env. Resour. *40*, 39–62. https://doi.org/10.1146/annurev-environ-102014-021406.

Lundgren, E.J., Ramp, D., Rowan, J., Middleton, O., Schowanek, S.D., Sanisidro, O., Carroll, S.P., Davis, M., Sandom, C., Svenning, J.-C., et al. (2020). Introduced herbivores restore Late Pleistocene ecological functions. Proc. Natl. Acad. Sci. U S A *117*, 7871–7878. https://doi.org/10.1073/pnas.1915769117.

Lyman, R.L. (2012). A warrant for applied palaeozoology. Biol. Rev. *87*, 513–535. https://doi.org/10.1111/j.1469-185X.2011.00207.x.

MacHugh, D.E., Larson, G., and Orlando, L. (2017). Taming the past: ancient DNA and the study of animal domestication. Annu. Rev. Anim. Biosci. *5*, 329–351. https://doi.org/10.1146/annurev-animal-022516-022747.

Malhi, Y., Doughty, C.E., Galetti, M., Smith, F.A., Svenning, J.-C., and Terborgh, J.W. (2016). Megafauna and ecosystem function from the Pleistocene to the Anthropocene. Proc. Natl. Acad. Sci. U S A *113*, 838–846. https://doi.org/10.1073/pnas.1502540113.

Malhi, Y., Lander, T., le Roux, E., Stevens, N., Macias-Fauria, M., Wedding, L., Girardin, C., Kristensen, J.Å., Sandom, C.J., Evans, T.D., et al. (2022). The role of large wild animals in climate change mitigation and adaptation. Curr. Biol. *32*, R181–R196. https://doi.org/10.1016/j.cub.2022.01.041.

Marshall, F., Reid, R.E.B., Goldstein, S., Storozum, M., Wreschnig, A., Hu, L., Kiura, P., Shahack-Gross, R., and Ambrose, S.H. (2018). Ancient herders enriched and restructured African grasslands. Nature *561*, 387–390. https://doi.org/10.1038/s42586-018-0456-9.

McGrath, K., Rowsell, K., St-Pierre, C.G., Tedder, A., Foody, G., Roberts, C., Speller, C., and Collins, M. (2019). Identifying archaeological bone via non-destructive ZooMS and the materiality of symbolic expression: examples from Iroquoian bone points. Sci. Rep. *9*, 1–10. https://doi.org/10.1038/s41598-019-47299-x.

McGuire, J.L., and Davis, E. (2014). Conservation paleobiogeography: the past, present and future of species distributions. Ecography *37*, 1092–1094. https://doi.org/10.1111/ecog.01337.

Monsarrat, S., and Svenning, J.-C. (2021). Using recent baselines as benchmarks for megafauna restoration places an unfair burden on the Global South. Ecography. https://doi.org/10.1111/ecog.05795.

Mychajliw, A.M., Rick, T., Dagtas, N.D., Erlandson, J.M., Culleton, B.J., Kennett, D.J., Buckley, M., and Hofman, C.A. (2020). Biogeographic problem-solving reveals the Late Pleistocene translocation of a short-faced bear to the California Channel Islands. Sci. Rep. *10*, 15172. https://doi.org/10.1038/s41598-020-71572-z.

Newman, M., and Julig, P. (1989). The identification of protein residues on lithic artifacts from a stratified boreal forest site. Can. J. Archaeol. *13*, 119–132.

Ostrom, P.H., Schall, M., Gandhi, H., Shen, T.-L., Hauschka, P.V., Strahler, J.R., and Gage, D.A. (2000). New strategies for characterizing ancient proteins using matrix-assisted laser desorption ionization mass spectrometry. Geochim. Cosmochim. Acta *64*, 1043–1050. https://doi.org/10.1016/S0016-7037(99)00381-6.

Pálsdóttir, A.H., Bläuer, A., Rannamäe, E., Boessenkool, S., and Hallsson, J.H. (2019). Not a limitless resource: ethics and guidelines for destructive sampling of archaeofaunal remains. R. Soc. Open Sci. *6*, 191059. https://doi.org/10.1098/rsos.191059.

Pellens, R., and Grandcolas, P. (2016). Biodiversity Conservation and Phylogenetic Systematics. Preserving Our Evolutionary Heritage in an Extinction Crisis (SpringerNature), p. 390. https://doi.org/10.1007/978-3-319-22461-9.

Pestle, W.J., and Colvard, M. (2012). Bone collagen preservation in the tropics: a case study from ancient Puerto Rico. J. Archaeol. Sci. *39*, 2079–2090. https://doi.org/10.1016/j.jas.2012.03.008.

Peters, C., Richter, K.K., Manne, T., Dortch, J., Paterson, A., Travouillon, K., Louys, J., Price, G.J., Petraglia, M., Crowther, A., et al. (2021). Species identification of Australian marsupials using collagen fingerprinting. R. Soc. Open Sci. *8*, 211229. https://doi.org/10.1098/rsos.211229.

Pothier Bouchard, G., Mentzer, S.M., Riel-Salvatore, J., Hodgkins, J., Miller, C.E., Negrino, F., Wogelius, R.A., and Buckley, M. (2019). Portable FTIR for on-site screening of archaeological bone intended for ZooMS collagen fingerprint analysis. J. Archaeol. Sci. Rep. *26*, 101862. https://doi.org/10.1016/j.jasrep.2019.05.027.

Prendergast, M.E., Buckley, M., Crowther, A., Frantz, L., Eager, H., Lebrasseur, O., Hutterer, R., Hulme-Beaman, A., Van Neer, W., Douka, K., et al. (2017). Reconstructing Asian faunal introductions to eastern Africa from multi-proxy biomolecular and archaeological datasets. PLoS One *12*, e0182565. https://doi.org/10.1371/journal.pone.0182565.

Presslee, S., Penkman, K., Fischer, R., Richards-Slidel, E., Southon, J., Hospitaleche, C.A., Collins, M., and MacPhee, R.D.E. (2021). Assessment of different screening methods for selecting palaeontological bone samples for peptide screening. J. Prot. *230*, 103986. https://doi.org/10.1016/j.jprot.2929.103986.

Price, E.R., McClure, P.J., Jacobs, R.L., and Espinoza, E.O. (2018a). Identification of rhinoceros keratin using direct analysis time time-of-flight mass spectrometry and multivariate statistical analysis. Rapid Commun. Mass Spectrom. *32*, 2106–2112. https://doi.org/10.1002/rcm.8285.

Price, G.J., Louys, J., Tyler Faith, J., Lorenzen, E.D., and Westaway, M.C. (2018b). Big data little help in megafauna mysteries. Nature *558*, 23–25. https://doi.org/10.1038/d41586-018-05330-7.

Richter, K.K., McGrath, K., Masson-MacLean, E., Hickinbotham, S., Tedder, A., Britton, K., Bottomley, Z., Dobney, K., Hulme-Beaman, A., Zona, M., et al. (2020). What's the catch? Archaeological application of rapid collagen-based species identification. J. Archaeol. Sci. *116*, 105116. https://doi.org/10.1016/j.jas.2020.105116.

Richter, K.K., Wilson, J.C., Jones, A.K.G., Buckley, M., Van Doorn, N.L., and Collins, M. (2011). Fish 'n chips: ZooMS peptide mass fingerprinting in a 96 well plate format to identify fish bone fragments. J. Archaeol. Sci. *38*, 1502–1510. https://doi.org/10.1016/j.jas.2011.02.014.

Roberts, P., Hunt, C., Arroyo-Kalin, M., Evans, D., and Boivin, N. (2017). The deep human prehistory of global tropical forests and its relevance for modern conservation. Nat. Plants *3*, 17093. https://doi.org/10.1038/nplants.2017.93.

Rodrigues, A.S.L., Charpentier, A., Bernal-Casasola, D., Gardeisen, A., Nores, C., Millán, J.A.P., McGrath, K., and Speller, C. (2018). Forgotten Mediterranean calving grounds of grey and North Atlantic right whales: evidence from Roman archaeological records. Proc. R. Soc. B *285*, 20180961. https://doi.org/10.1098/rspb.2018.0961.

Rodrigues, A.S.L., Monsarrat, S., Charpentier, A., Brooks, T.M., Hoffmann, M., Reeves, R., Palomares, M.L.D., and Turvey, S.T. (2019). Unshifting the baseline: a framework for documenting historical population changes and assessing long-term anthropogenic impacts. Philos. Trans. R. Soc. B *374*, 20190220. https://doi.org/10.1098/rstb.2019.0220.

Rolland, J., Cadotte, M.W., Davies, J., Devictor, V., Lavergne, S., Mouquet, N., Pavoine, S., Rodrigues, A.S.L., Thuiller, W., Turcati, L., et al. (2012). Using phylogenies in conservation: new perspectives. Biol. Lett. *8*, 692–694. https://doi.org/10.1098/rsbl.2011.1024.

Romaniuk, A.A., Panciroli, E., Buckley, M., Chowdhury, M.P., Willars, C., Herman, J.S., Troalen, L.G., Shepherd, A.N., Clarke, D.V., Sheridan, A., et al. (2020). Combined visual and biochemical analyses confirm depositor and diet for Neolithic coprolites from Skara Brae.

Archaeol. Anthropol. Sci. *12*, 1–15. https://doi.org/10.1007/s12520-020-01225-9.

Rybczynski, N., Gosse, J.C., Harington, C.R., Wogelius, R.A., Hidy, A.J., and Buckley, M. (2013). Mid-Pliocene warm-period deposits in the high arctic yield insight into camel evolution. Nat. Commun. *4*, 1–9. https://doi.org/10.1038/ncomms2516.

Sakalauskaite, J., Marin, F., Pergolizzi, B., and Demarchi, B. (2020). Shell palaeoproteomics: first application of peptide mass fingerprinting for the rapid identification of mollusc shells in archaeology. J. Prot. *227*, 103920. https://doi.org/10.1016/j.jprot.2020.103920.

Sandom, C., Faurby, S., Sandel, B., and Svenning, J.-C. (2014). Global late Quaternary megafauna extinctions linked to humans, not climate change. Proc. R. Soc. B Biol. Sci. *281*, 20133254. https://doi.org/10.1098/rspb.2013.3254.

Scharf, E.A. (2014). Deep time: the emerging role of archaeology in landscape ecology. Lands. Ecol. *29*, 563–569. https://doi.org/10.1007/s10980-014-9997-y.

Schowanek, S.D., Davis, M., Lundgren, E.J., Middleton, O., Rowan, J., Pedersen, R.Ø., Ramp, D., Sandom, C.J., and Svenning, J.-C. (2021). Reintroducing extirpated herbivores could partially reverse the late Quaternary decline of large and grazing species. Glob. Ecol. Biogeogr. *30*, 896–908. https://doi.org/10.1111/geb.13264.

Shiels, A.B., Pitt, W.C., Sugihara, R.T., and Witmer, G.W. (2014). Biology and impacts of Pacific island invasive species. 11. *Rattus rattus*, the black rat (Rodentia: muridae). Pac. Sci. *68*, 145–184. https://doi.org/10.2984/68.2.1.

Sinet-Mathiot, V., Smith, G.M., Romandini, M., Wilcke, A., Peresani, M., Hublin, J.-J., and Welker, F. (2019). Combining ZooMS and zooarchaeology to study late Pleistocene hominin behaviour at Fumane (Italy). Sci. Rep. *9*, 12350. https://doi.org/10.1038/s41598-019-48706-z.

Smith, F.A., Elliott Smith, R.E., Lyons, S.K., and Payne, J.L. (2018). Body size downgrading of mammals over the late Quaternary. Science *360*, 310–313. https://doi.org/10.1126/science.aao5987.

Solazzo, C., Fitzhugh, W.W., Rolando, C., and Tokarski, C. (2008). Identification of protein remains in archaeological potsherds by proteomics. Anal. Chem. *80*, 4590–4597. https://doi.org/10.1021/ac800515v.

Solazzo, C., Heald, S., Ballard, M.W., Ashford, D.A., DePriest, P.T., Koestler, R.J., and Collins, M. (2011). Proteomics and Coast Salish blankets: a tale of shaggy dogs? Antiquity *85*, 1418–1432. https://doi.org/10.1017/S0003598X00062141.

Solazzo, C., Wadsley, M., Dyer, J.M., Clerens, S., Collins, M., and Plowman, J. (2013). Characterisation of novel α-keratin peptide markers for species identification in keratinous tissues using mass spectrometry. Rapid Commun. Mass Spectrom. *27*, 2685–2698. https://doi.org/10.1002/rcm.6730.

Stewart, N.A., Gerlach, R.F., Gowland, R.L., Gron, K.J., and Montgomery, J. (2017). Sex determination of human remains from peptides in tooth enamel. Proc. Natl. Acad. Sci. U S A *114*, 13649–13654. https://doi.org/10.1073/pnas.1714926115.

Svenning, J.-C. (2020). Rewilding should be central to global restoration efforts. O. Earth *3*, 657–660. https://doi.org/10.1016/j.oneear.2020.11.014.

Svenning, J.-C., Pedersen, P.B.M., Donlan, C.J., Ejrnæs, R., Faurby, S., Galetti, M., Hansen, D.M., Brandel, B., Sandom, C., Terborgh, J.W., et al. (2016). Science for a wilder Anthropocene: synthesis and future directions for trophic rewilding research. Proc. Natl. Acad. Sci. U S A *113*, 898–906. https://doi.org/10.1073/pnas.1502556112.

Swift, J.A., Bunce, M., Dortch, J., Douglass, K., Tyler Faith, J., Fellows Yates, J.A., Field, J., Haberle, S.G., Jacob, E., Johnson, C.N., et al. (2019). Micro methods for megafauna: novel approaches to late quaternary extinctions and their contributions to faunal conservation in the Anthropocene. BioScience *69*, 877–887. https://doi.org/10.1093/biosci/biz105.

Taylor, W.T.T., Clark, J., Bayarsaikhan, J., Tusvshinjargal, T., Jobe, T.J., Fitzhugh, W.W., Kortum, R., Spengler, R.N., Shnaider, S., Frederik, V.S., Isaac, H., et al. (2020). Early pastoral economies and herding transitions in eastern eurasia. Sci. Rep. *10*, 1–15. https://doi.org/10.1038/s41598-020-57735-y.

Taylor, W.T.T., Shnaider, S., Abdykanova, A., Fages, A., Welker, F., Irmer, F., Seguin-Orlando, A., Khan, N., Douka, K., Kolobova, K., et al. (2018). Early pastoral economies along the ancient silk road: biomolecular evidence from the alay valley, Kyrgyzstan. PLoS One *13*. e0205646. https://doi.org/10.1371/journal.pone.0205646.

Upham, N.S., Esselstyn, J.A., and Jetz, W. (2019). Inferring the mammal tree: species-level sets of phylogenies for questions in ecology, evolution, and conservation. PLoS Biol. *17*. e3000494. https://doi.org/10.1371/journal.pbio.3000494.

Van der Sluis, L.G., Hollund, H.I., Buckley, M., De Louw, P.G.B., Rijsdijk, K.F., and Kars, H. (2014). Combining histology, stable isotope analysis and ZooMS collagen fingerprinting to investigate the taphonomic history and dietary behaviour of extinct giant tortoises from the Mare aux Songes deposit on Mauritius. Palaeogeogr. Palaeoclimatol. Palaeoecol. *416*, 80–91. https://doi.org/10.1016/j.palaeo.2014.06.003.

Van Doorn, N.L., Hollund, H.I., and Collins, M. (2011). A novel and non-destructive approach for ZooMS analysis: ammonium bicarbonate buffer extraction. Archaeol. Anthropol. Sci. *3*, 281–289. https://doi.org/10.1007/s12520-011-0067-y.

Van Doorn, N.L., Wilson, J.C., Hollund, H.I., Soressi, M., and Collins, M. (2012). Site-specific deamidation of glutamine: a new marker of bone collagen deterioration. Rapid Commun. Mass Spectrom. *26*, 2319–2327. https://doi.org/10.1002/rcm.6351.

Ventresca Miller, A., Spengler, R.N., Haruda, A., Miller, B.K., Wilkin, S., Robinson, S., Roberts, P., and Boivin, N.L. (2020). Ecosystem engineering among ancient ppstoralists in northern central Asia. Front. Earth Sci. *8*, 168. https://doi.org/10.3389/feart.2020.00168.

Villanova, C., and Porcar, M. (2019). Art-omics: multi-omics meet archaeology and art conservation. Microb. Biotechnol. *13*, 435–441. https://doi.org/10.1111/1751-7951.13480.

Von Holstein, I.C.C., Ashby, S.P., Van Doorn, N.L., Sachs, S.M., Buckley, M., Meiri, M., Barnes, I., Brundle, A., and Collins, M. (2014). Searching for scandinavians in pre-viking scotland: molecular fingerprinting of early medieval combs. J. Archaeol. Sci. *41*, 1–6. https://doi.org/10.1016/j.jas.2013.07.026.

Warinner, C., Hendy, J., Speller, C., Cappellini, E., Fischer, R., Trachsel, C., Arneborg, J., Lynnerup, N., Craig, O.E., Swallow, D.M., et al. (2014). Direct evidence of milk consumption from ancient human dental calculus. Sci. Rep. *4*, 1–6. https://doi.org/10.1038/srep07104.

Waters, J.M., and Grosser, S. (2016). Managing shifting species: ancient DNA reveals conservation conundrums in a dynamic world. Bioessays *38*, 1177–1184. https://doi.org/10.1002/bies.201600044.

Welker, F. (2018). Palaeoproteomics for human evolution studies. Quat. Sci. Rev. *190*, 137–147. https://doi.org/10.1016/j.quascirev.2018.04.033.

Welker, F., Collins, M., Thomas, J.A., Wadsley, M., Brace, S., Cappellini, E., Turvey, S.T., Reguero, M., Gelfo, J.N., Kramarz, A., et al. (2015a). Ancient proteins resolve the evolutionary history of Darwin's South American ungulates. Nature *522*, 81–84. https://doi.org/10.1038/nature14249.

Welker, F., Hajdinjak, M., Talamo, S., Jaouen, K., Dannemann, M., David, F., Julien, M., Meyer, M., Kelso, J., Barnes, I., et al. (2016). Palaeoproteomic evidence identifies archaic hominins associated with the Châtelperronian at the Grotte du Renne. Proc. Natl. Acad. Sci. U S A *113*, 11162–11167. https://doi.org/10.1073/pnas.1605834113.

Welker, F., Ramos-Madrigal, J., Kuhlwilm, M., Liao, W., Gutenbrunner, P., de Manuel, M., Samodova, D., Mackie, M., Allentoft, M.E., Bacon, A.-M., et al. (2019). Enamel proteome shows that *Gigantopithecus* was an early diverging pongine. Nature *576*, 262–265. https://doi.org/10.1038/s41586-019-1728-8.

Welker, F., Smith, G.M., Hutson, J.M., Kindler, L., Garcia-Moreno, A., Villaluenga, A., Turner, E., and Gaudzinski-Windheuser. (2017). Middle Pleistocene protein sequences from the rhinoceros genus *Stephanorhinus* and the phylogeny of extant and extinct Middle/Late Pleistocene Rhinocerotidae. PeerJ *5*, e3033. https://doi.org/10.7717/peerj.3033.

Welker, F., Soressi, M., Rendu, W., Hublin, J.-J., and Collins, M. (2015b). Using ZooMS to identify fragmentary bone from the late middle/early upper palaeolithic sequence of Les Cottés, France. J. Archaeol. Sci. *54*, 279–286. https://doi.org/10.1016/j.jas.2014.12.010.

Wilkin, S., Ventresca Miller, A., Fernandes, R., Spengler, R., Taylor, W.T.T., Brown, D.R., Reich, D., Kennett, D.J., Culleton, B.J., Kunz, L., et al. (2021). Dairying enabled early bronze age yamnaya steppe expansions. Nature *598*, 629–633. https://doi.org/10.1038/s41586-021-03798-4.

Wilkin, S., Ventresca Miller, A., Taylor, W.T.T., Miller, B.K., Hagan, R., Bleasdale, M., Scott, A.,

Gankhuyg, S., Ramsøe, A., Uliziibayar, S., et al. (2020). Dairy pastoralism sustained eastern Eurasian steppe populations for 5,000 years. Nat. Ecol. Evol. *4*, 346–355. https://doi.org/10.1038/s41559-020-1120-y.

Williams, J.W., Ordonez, A., and Svenning, J.-C. (2021). A unifying framework for studying and managing climate-driven rates of ecological change. Nat. Ecol. Evol. *5*, 17–26. https://doi.org/10.1038/s41559-020-01344-5.

Willis, K.J., and Birks, H.J.B. (2006). What is natural? The need for a long-Term perspective in biodiversity conservation. Science *314*, 1261–1265. https://doi.org/10.1126/science.1122667.

Willis, K.J., Bailey, R.M., Bhagwat, S.A., and Birks, H.J.B. (2010). Biodiversity baselines, thresholds and resilience: testing predictions and assumptions using palaeoecological data. Trends Ecol. Evol. *25*, 583–591. https://doi.org/10.1016/j.tree.2010.07.006.

Winter, R.M., de Kock, W., Palsbøll, P.J., and Çakirlar, C. (2021). Potential applications of biomolecular archaeology to the ecohistory of sea turtles and groupers in Levant coastal antiquity. J. Archaeol. Sci. Rep. *36*, 102872. https://doi.org/10.1016/j.jasrep.2021.102872.

Wolverton, S., and Lyman, R.L. (2012). Conservation Biology and Applied Zooarchaeology (The University of Arizona Press).

Yang, Y., Shevchenko, A., Knaust, A., Abuduresule, I., Li, W., Hu, X., Wang, C., and Shevchenko, A. (2014). Proteomics evidence for kefir dairy in early bronze age China. J. Arch. Sci. *45*, 178–186. https://doi.org/10.1016/j.jas.2014.02.005.

10. Discussion

As noted in Chapters 1 and 4, the main objective of this thesis was to explore the potential of ZooMS in Australian contexts. In Chapter 1, two major challenges were identified that restricted the application of ZooMS in Australia, namely:

- the absence of reference markers for a large number of Australian animals and;
- a limited understanding of collagen preservation in Australia.

In this thesis, these two major issues were addressed. In Manuscript A, ZooMS peptide markers were developed for an extended number of Australian marsupials and monotremes, while Manuscript B systematically explored the patterns and mechanisms of collagen preservation in Australian fossil assemblages.

With the two major challenges confounding ZooMS studies in Australia addressed, Manuscript C utilized the newly developed ZooMS markers to taxonomically identify fragmented faunal remains from Devil's Lair, a Late Pleistocene site in southwest Australia. The results from these analyses were compared to the available zooarchaeological records at the site to further explore how ZooMS and zooarchaeology can complement and enhance each other in order to maximise the potential information gained from faunal assemblages. In so doing, Manuscript C met the third major objective of this thesis:

- to undertake an Australian case study integrating ZooMS and zooarchaeology in order to assess their potential as complementary approaches for the study of past faunal assemblages

In what follows, I seek to highlight the major contribution this thesis has made in making major inroads into addressing the two identified major challenges that need to be overcome to effectively apply ZooMS in Australian contexts and that can help to guide its application within well-informed zooarchaeological contexts. I then summarise some of the key remaining challenges facing ZooMS and proteomics applications in Australian archaeology and palaeontology before highlighting other potential applications. Here, I also focus on the contributions of Manuscript D which explored the way in which ZooMS and shotgun palaeoproteomics can be used to inform conservation, restoration and rewilding strategies.

10.1. Building a ZooMS reference database

In Manuscript A, ZooMS reference markers were developed for 23 medium- to large-sized Australian marsupial taxa, and one monotreme (Peters et al., 2021), thus significantly expanding the ZooMS reference database available for the country's fauna, compared to the nine incomplete marker profiles that were available previously (Buckley et al., 2017). In total, there are now 26 medium- to large-sized Australian marsupials represented in the ZooMS reference database and one monotreme, adding, at last, an Australian dimension to the existing global ZooMS reference database. The inclusion of a larger number of marsupials and monotremes is particularly important from ecological, archaeological, and palaeontological perspectives, since these animals inhabit a wide range of ecosystems, and they were often targeted as part of subsistence strategies in the past (Dortch and Wright, 2010, Cosgrove and Garvey, 2017).

The development of reference markers for an increased number of marsupial taxa has also shown that, overall, genus-level specificity can be reached for this mammalian Infraclass when making taxonomic identifications with ZooMS, although for some taxa, such as *Notamacropus irma*, species-level identifications are possible. This is particularly important since fragmented remains of Australian macropod taxa are notoriously difficult to identify due to morphological similarities between species (Fillios and Blake, 2015, Mein and Manne, 2021). The ability to differentiate between these taxa with

ZooMS thus has the potential to provide us with more detailed information about macropod diversity and exploitation in the past. The ZooMS reference markers that were developed as part of this thesis are now available for all researchers wanting to use ZooMS to identify collagen-bearing materials from Australia, opening up a wide range of future applications that will be discussed in more detail in section 10.5.

10.2. Collagen preservation in Australia

Manuscript B further explored the patterns and mechanisms of collagen preservation in Australia. In this study, it was shown that, although challenging, it is possible to successfully apply ZooMS to zooarchaeological materials from Australian contexts with extremely harsh preservation conditions, as well as to those dating back to the Late Pleistocene. The successful extraction of ancient proteins from Tripot Cave (northeast Australia, with a chronometric age between 300-70 ka) is particularly significant, since it exceeds chemical predictions of collagen preservation for a site of this age situated in this region of the world (Manuscript B). The results of this study thus push back the limit of collagen preservation in such contexts, which has major implications for the potential application of ZooMS as a new methodology to study early faunal processes in Australia, such as the Late Quaternary extinction of megafauna, for example.

The mechanisms responsible for this exceptional preservation at Tripot Cave were further explored in Manuscript B. Collagen is protected from degradation as a result of its strong association with bone bioapatite. Once this bioapatite starts to degrade, collagen will start to degrade shortly after (Covington et al., 2006). It is hypothesized that, at Tripot Cave, the persistent introduction of other mineral components resulted in the remineralization of the bone and prevented the collapse of the mineral phase of the bone, thus protecting the collagen from degradation. Unfortunately, the exact mechanisms leading to this phenomenon could not be disentangled in the present study due to the absence of detailed information about the geochemistry of the cave, which awaits future analysis. The exceptional collagen preservation observed at Tripot Cave nonetheless already has some significance for our understanding of the potential mechanisms involved in the deep-time survival of collagen in the archaeological and palaeontological record.

In addition to the exceptional preservation of collagen observed at Tripot Cave, fragmented faunal remains from a nineteenth-century open-air site on Barrow Island, with summer temperatures of up to 50 °C, were also successfully analyzed with ZooMS (Manuscript A, Peters et al., 2021), as were faunal remains from Late Pleistocene deposits from Devil's Lair in southwest Australia, with a chronometric age of up to 50 ka (Manuscript C). An earlier study also successfully targeted Late Pleistocene material originating from the generally more favorable preservation conditions of Tasmania dating to around 50 ka (Buckley et al., 2017). Overall, the work that was conducted as part of this thesis (Manuscripts A, B and C) has demonstrated that collagen preservation in Australia is good enough for successful ZooMS studies in different regions of the country, and for sites of different ages.

10.3. ZooMS and zooarchaeology – Stronger together

One of the major developments that is needed to strengthen the position of ZooMS in the next decade is the integration of the method into established zooarchaeological analytical approaches. The application of biomolecular methods to study the archaeological record has increased significantly over the past decades. It is, however, important to bear in mind that the fundamentals of archaeological research, namely, that the context, integrity of the stratigraphic sequence, and confident dating of a site are crucial to developing research questions that can be tested to make meaningful conclusions. In Manuscript C, the question of how to best combine ZooMS and zooarchaeology was explored through the analysis of the faunal assemblage of Devil's Lair, a well-dated Late Pleistocene site in southwest Australia with a stratigraphic sequence of over 6 m in depth.

10.3.1. Sampling

The development of a suitable sampling strategy that considers site-specific knowledge about stratigraphy, taphonomy, chronology, and zooarchaeology, amongst others, is the first key step to developing an appropriate sampling strategy for ZooMS. In order to integrate ZooMS with zooarchaeological datasets, it should, for example, be considered as to whether sampling bone fragments of different fragment lengths (e.g. smaller or larger than 2 cm), or fragments with different levels of cortical thickness, will provide a better representation of the entire faunal diversity at a given site (as was trialed in Manuscript C), or whether samples should specifically target specific skeletal elements that are difficult to taxonomically identify based on morphological characteristics alone. Instead of sampling thousands of fragmented bones trying to find human remains (Brown et al., 2016, Welker et al., 2016, Brown et al., 2022), or purely to inflate NISP (number of individual specimen) counts (Sinet-Mathiot et al., 2019, Brown et al., 2021c, Silvestrini et al., 2022), more thought could be given to how a more limited application of ZooMS can help to address specific zooarchaeological questions. A sampling strategy should then be developed accordingly, also considering the stratigraphy and chronology of a given site.

10.3.2. Integration into zooarchaeological metrics

Crucial to improving the integration of ZooMS and zooarchaeology, is the development of metrics for ZooMS data that can be tied into zooarchaeological metrics of quantification such as MNI (minimum number of individuals) and MNE (minimum number of elements). For example, by focusing on skeletal elements that could not be identified morphologically, ZooMS results can subsequently compared to and ideally tied back into zooarchaeological MNE and MNI metrics. In Manuscript C, an inflated number of macropods was identified in the ZooMS assemblage of the Late Pleistocene site Devil's Lair. When grouped by the different skeletal elements the samples were taken from, it was shown that the majority of long-bone fragments included in the ZooMS-analysis originated from macropods, while vertebrae showed a much wider faunal diversity. This indicated that the frequency and/or intensity of macropod carcass processing by humans or carnivores was much higher than thought on the basis of the zooarchaeological assemblage alone.

Similarly, in zooarchaeology, the ageing of skeletal elements can be used to generate kill-off patterns for a given species. This can feed into our understanding of herding strategies or human subsistence in the past (Ruscillo, 2014). However, not all skeletal elements that can be aged can also be confidently assigned to a given taxon. ZooMS identifications of these elements can directly tie into the analysis of kill-off patterns. For example, the morphologically difficult to distinguish sheep and goat can be separated using ZooMS (Buckley et al., 2010). Such information can then be used to investigate kill-off patterns for sheep and goat separately, allowing assessments of differences in kill-off patterns, and thus herding and subsistence strategies between the two species. Similarly, ZooMS identifications of unidentifiable bones with taphonomic indicators of carcass processing, such as cut-marks, percussion damage or evidence of scraping can give further insight into past subsistence and exploitation strategies. To illustrate, at Fumane Cave, a Late Pleistocene site in Italy, a high frequency of percussion marks was identified on *Bos/Bison* long bone fragments in the ZooMS-identified assemblage, while such marks were absent in the morphologically identified assemblage. This was interpreted as evidence of high levels of carcass processing of this taxa by the humans frequenting site (Sinet-Mathiot et al., 2019), something that was missed in zooarchaeological analysis.

Microfauna remains are a particularly promising target for ZooMS studies with regard to the integration into zooarchaeological metrics. Small microfauna bones are often difficult to identify taxonomically, especially in the absence of cranial or dental remains, but can be successfully targeted with ZooMS (Buckley et al., 2016, Prendergast et al., 2017, Buckley and Herman, 2019, Buckley and Cheylan, 2020).

The identification of complete postcranial elements of microfauna can directly feed into the calculation of zooarchaeological metrics for these taxa.

10.3.3. Narrowing down ZooMS identifications

Zooarchaeological data can also work in tandem with ZooMS data by helping to narrow down ZooMS identifications on the basis of osteological characteristics of the bone fragment being analysed. For example, van den Hurk et al. (2021) and van den Hurk and McGrath (2021) used ZooMS to identify cetacean remains from Roman to medieval London, and Iron age to post-medieval Scotland, respectively. To increase taxonomic specificity following ZooMS analysis, specimens with genus-level identifications were reanalyzed morphologically to narrow down ZooMS identifications to species-level identifications based on the dimensions of the vertebrae and the size of the specimens (van den Hurk and McGrath, 2021, van den Hurk et al., 2021). Similarly, Silvestrini et al. (2022) narrowed down ZooMS identifications of fragmented remains based on the size of the bone fragment and the thickness of the cortical bone (Silvestrini et al., 2022). Here, the size and thickness of the bone fragment were shown to be further indicators that could be used to help determine the animal size-class of the sampled specimen, information which could subsequently be used to narrow down ZooMS identifications.

For all these methods of integrating ZooMS and zooarchaeology, it is crucial that zooarchaeological data, such as skeletal element, animal size-class, and fragment size, as well as taphonomic signatures on the bone are recorded and can be matched back to the ZooMS sample of interest. This also highlights the importance of working together closely with zooarchaeologists, who often are highly knowledgeable about the fauna at a given site, as well as the site's environment. ZooMS will reach its maximal potential only as an integrative approach when combined with zooarchaeology and other biomolecular methods.

10.4. Methodological challenges and future work

While the papers of this thesis have supported major advances in the application of ZooMS to archaeological and palaeontological contexts in Australia, there remain a number of methodological challenges that need to be resolved before ZooMS can truly become a staple method in Australian zooarchaeology and palaeontology. For one, a large number of Australian taxa are still absent from the ZooMS reference database. Even when ZooMS reference markers are available, however, taxonomic resolution often limits the inferences that can be made from ZooMS data. Furthermore, collagen preservation is anything but ideal in the harsh conditions imposed by the Australian climate. More work is also needed to integrate ZooMS into existing zooarchaeological analytical approaches. While there have been some initial efforts to bridge the gap between ZooMS and zooarchaeology, a systematic effort to combine the two approaches, starting with study design and sample selection and extending all the way through to data interpretation, is still lacking. Finally, at the time of writing this thesis, there are still no dedicated ZooMS facilities in Australia. Yet, the availability of dedicated ZooMS facilities and trained ZooMS researchers is critical to the successful implementation of ZooMS as part of Australian zooarchaeology and palaeontology. In this section, these challenges will be discussed in more detail.

10.4.1. Reference database and taxonomic resolution

One major issue with respect to the application of ZooMS in Australia remains the limited taxonomic coverage of the ZooMS reference database. The reference database, although significantly expanded for Australian taxa by the research in this thesis (Manuscript A, Peters et al., 2021), is still heavily biased towards medium- to large-sized European mammals, while only a fraction of the total faunal diversity on the Australian continent, past and present, is represented. However, to make taxonomic identifications with ZooMS, the availability of ZooMS peptide markers for the taxa of interest is key. Particularly noteworthy is the complete absence of Australia's smaller mammals, birds, reptiles, and

amphibians from the ZooMS reference database, which significantly limits the interpretative power of ZooMS in the country. Since the availability of taxa in the ZooMS reference database has a direct impact on the faunal diversity identified, it will be critical to further expand the reference database to enhance the potential of ZooMS in Australian contexts. As part of ongoing research, I am involved in further expanding the ZooMS reference database to include more Australian fauna, including extinct megafaunal species, and a number of Australian rodents, such as the giant rat *Conilurus*. This work will further the number of Australian taxa for which ZooMS reference markers are available, and thus further increases the faunal diversity that can be recovered through ZooMS studies in Australia.

An associated issue is the lack of data sharing in the ZooMS community (Richter et al., 2022). With the continuous expansion of the global reference database, it is crucial to compare newly developed peptide marker sets to previously published marker profiles to achieve the highest level of taxonomic specificity possible. This is particularly important when novel peptide markers are discovered and reported. The absence of publicly accessible reference data prevents the incorporation of novel markers for taxa already in the reference database. This issue was also encountered when developing ZooMS peptide markers for Manuscript A (Peters et al., 2021). The new set of markers could not be verified against the previously published marker profiles, nor was it possible to assign two newly identified peptide markers to the taxa previously published. This further highlights the importance of making raw ZooMS data publicly available. Accordingly, the raw data associated with Manuscript A was made publicly available alongside its scientific publication.

Next to challenges associated with the reference database, another factor challenging the practical implementation of ZooMS in Australian contexts is the limited taxonomic resolution that can be reached for some taxa. Genus-level specificity can be achieved for most Australian taxa, but macropods specifically have limited taxonomic resolution with ZooMS (Manuscript A, Peters et al., 2021), thus compromising the interpretative power of ZooMS. To some extent, challenges of taxonomic specificity can be overcome by incorporating ZooMS results with data on species biogeography and available zooarchaeological records, although this can only improve taxonomic identifications to a limited extent. Alternatively, a higher resolution can be reached with the incorporation of other biomolecular techniques, such as shotgun palaeoproteomics or ancient DNA. However, the tradeoff for this increased resolution is increased costs and time for data analysis, which limits the number of samples that can be analysed.

10.4.2. Collagen preservation in Australia

Another major challenge faced by people aiming to incorporate ZooMS into the study of Australian faunal assemblages is the overall low preservation of collagen at many archaeological and palaeontological sites as a result of the country's often harsh environmental conditions (Manuscript B). The preservation of collagen generally becomes an even bigger issue when dealing with older material. The work that was part of this thesis has shown that it is possible to successfully extract ancient proteins from Late Pleistocene Australian deposits, with an age of 70 ka having been reached in ZooMS analysis of fauna from Tripot Cave. However, more research is needed in the future to identify the exact geochemical conditions that have led to the exceptional preservation of collagen at this site. In addition to climatic conditions, such as temperature and humidity, collagen preservation seems to also depend heavily on site-specific burial and micro-environmental conditions (Manuscript B). This highlights the need for the use of rapid, minimally-destructive pre-screening techniques, such as FTIR, or small-scale pilot studies on fossil assemblages, prior to destructively analyzing highly valuable fossil material, especially when the degree of biomolecular preservation is questionable or unknown. Fossil material is a finite resource that is forever lost when destructively analysed as part of biomolecular studies, and it should thus also be treated as such (Austin et al., 2019, Pálsdóttir et al., 2019). This is particularly important when dealing with rare remains, such as extinct megafauna fossils.

The successful analysis of ancient proteins from Pleistocene Australian deposits also has broader implications regarding the preservation of biomolecules in other harsh environments, such as the tropics. The demonstration of the feasibility of analyzing ancient proteins from Australia thus uncovers an entirely new suite of Pleistocene sites that could be suitable for analysis with palaeoproteomics, opening up possibilities for targeting novel human evolutionary questions in these areas. However, even though collagen was successfully extracted from a number of sites included in the research that was conducted as part of this thesis, preservation will remain one of the major challenges in larger-scale applications of ZooMS and other palaeoproteomics analyses in Australia. This is also reflected in the large number of samples analysed for this thesis that did not yield successful results (Manuscript B). An interesting target for future palaeoproteomics studies will be archaeological materials that originate from central Australian contexts. Samples from this region were not included in the research undertaken for this thesis, but highly arid conditions are known to enhance the preservation potential of ancient proteins (Shevchenko et al., 2014).

Methodological advances in sample preparation, mass spectrometry, and data analysis also have the potential to push back the temporal limit of ZooMS studies in Australian contexts even further. Methodological advances in aDNA and shotgun palaeoproteomics have extended the limits of these methods numerous times (e.g. Dabney et al., 2013, Orlando et al., 2013, Cappellini et al., 2019). For example, it has recently been shown that it is possible to extract peptide sequences from eggshell from the Tibetan Plateau, China, dating back to the late Miocene (>6.5 Myr); the first evidence of ancient protein survival into the Miocene (Demarchi et al., 2022a). Similar methodological advances for ZooMS, should help to increase the spatial coverage and time-depth the method can reach in Australia.

10.5. Potential areas of application of ZooMS and palaeoproteomics in Australia

Regardless of the challenges outlined in section 10.4 and the developments needed to better integrate ZooMS into zooarchaeological records as discussed in section 10.3, this thesis has shown that the large-scale application of peptide mass fingerprinting already has significant potential to contribute to the study of faunal remains from Australian contexts (Figure 10.1). In Chapter 2, key regions that would be most suitable to target with palaeoproteomics approaches were identified. These exciting new research avenues - investigating past subsistence strategies, reconstructing faunal diversity, tracking species introductions, and forwarding our understanding of extinctions and extirpations - are addressed in more detail below. Then, it is further explored how palaeoproteomics approaches can be used to inform conservation and restoration strategies in Australia specifically.

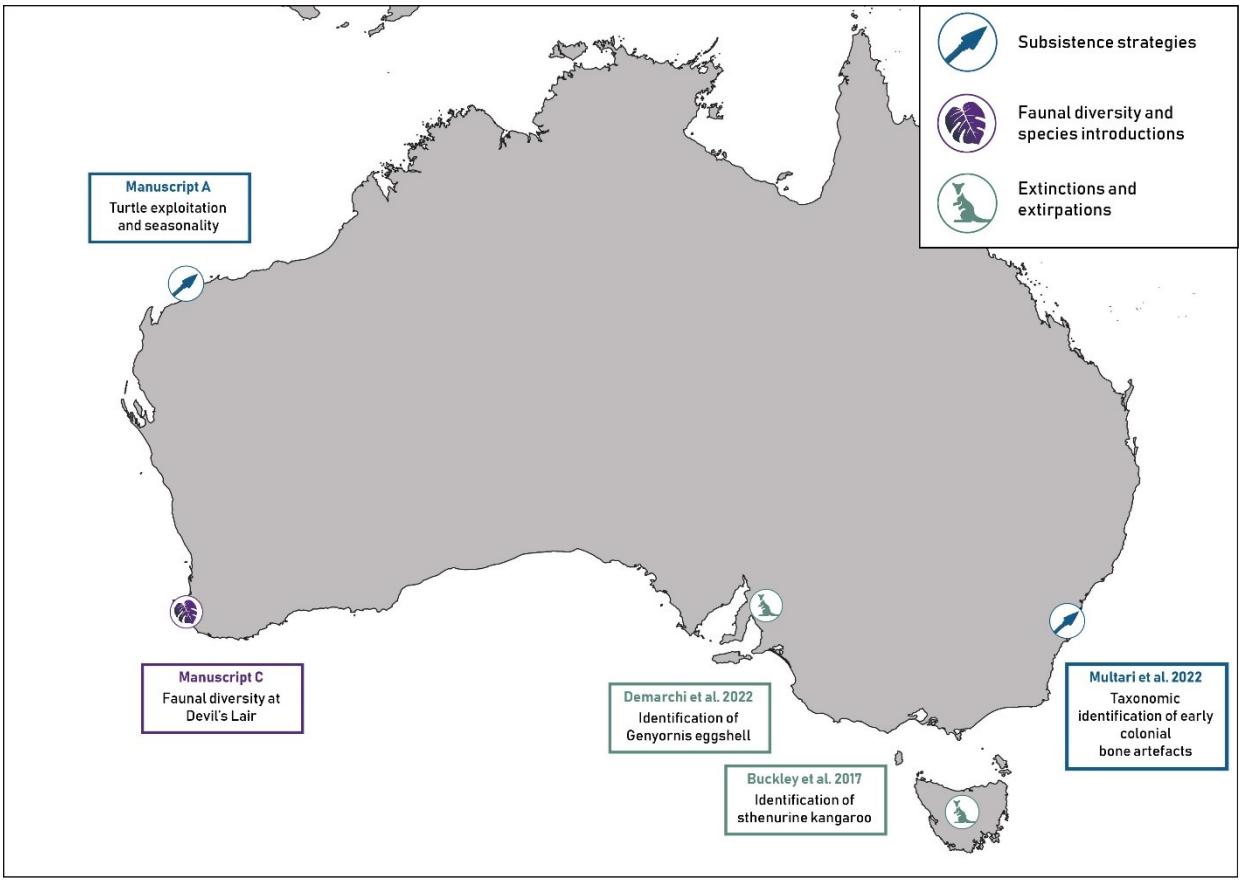

Figure 10.1: Overview of the research avenues targeted by ZooMS and palaeoproteomics studies in Australia to date.

10.5.1. Subsistence strategies

The analysis of highly fragmented bone assemblages with ZooMS has the potential to provide more detailed information on past subsistence strategies, especially when combined with available zooarchaeological records. For example, ZooMS analysis of a Late Pleistocene bone assemblage from Fumane, Italy, has shown that long bone shafts of *Bos/*Bison make up a significant proportion of the fragmented bone material. It has been suggested that anthropogenic carcass processing resulted in the high fragmentation of the faunal assemblage at the site (Sinet-Mathiot et al., 2019). Similarly, at Denisova Cave, Russia, ZooMS analysis revealed an increased proportion of cervids and bovids compared to zooarchaeological analyses. The high fragmentation rate of prey animals, which is in line with the level of fragmentation found in hominin bones at the site, indicates that although hominins may have been responsible for the accumulation of fauna, carnivores further processed and fragmented the bones at the site (Brown et al., 2021c).

For the research that was part of this thesis, ZooMS revealed the presence of domesticated bovid bones in the colonial settlement of Bandicoot Bay. Barreled meats were often imported to pearling stations, although the presence of domesticated animals at the site had not been identified during zooarchaeological analysis. Green sea turtle represents another taxon that was identified with ZooMS, but not through morphological studies. The presence of green sea turtle, drawing upon knowledge of their nesting habits, has been interpreted as evidence that the site was occupied during the summer season. These turtles may have been targeted as part of the subsistence strategy of the Aboriginal laborers at the site (Manuscript A, Peters et al., 2021). At Devil's Lair, a combined approach utilizing ZooMS and zooarchaeology resulted in a deeper understanding of the faunal assemblage and human subsistence strategies at the site. The inflated NISP count of macropods in the fragmented assemblage

identified with ZooMS indicates a higher degree of processing of macropod bones at the site than previously assumed. This could be either the result of human subsistence strategies, or could indicate a high degree of bone fragmentation by Tasmanian devils at the site (Manuscript C).

Another way in which ZooMS could help shed light on past human behavior and subsistence is through the study of bone tools. The production of bone tools often leads to the loss of morphological characteristics that can be used to taxonomically identify the species of origin. ZooMS offers a solution to provenance these bone tools and provide insight into their origin (Desmond et al., 2018, Bradfield et al., 2019, Jensen et al., 2020b). Bone tools were also a common item in the toolkit of Aboriginal communities (Allen et al., 2016, Langley et al., 2016). In Australia, the only study to date that utilizes ZooMS for this purpose involved the analysis of six bone artefacts from early nineteenth century Sydney. All bone artefacts included in this study were identified as cattle, despite the fact that sheep farming was more intensive in the region than cattle farming as evidenced by the historical record and previous zooarchaeological investigations. The identification of these artefacts as cattle has thus been interpreted as reflecting the socio-economic status of the inhabitants of the area (Multari et al., 2022). In addition to informing us about human lifeways and social inequities during the early colonial period, the further identification of bone artefacts with ZooMS also has the potential to significantly advance our understanding of raw material selection prior to the colonial settlement of Australia.

10.5.2. Biodiversity trends and species introductions

ZooMS also has the potential to shed light on biodiversity trends and faunal turnovers in the past (Manuscript D, Peters et al., 2022). For example, ZooMS has been used to identify geographic range shifts of the horseshoe bat (Buckley and Herman, 2019) and the moor frog (Buckley and Cheylan, 2020) from Late Pleistocene cave deposits in England. At Devil's Lair, the ZooMS-identified assemblage also revealed some information regarding faunal diversity at the site in the past (Manuscript C). Although the limited sample size confines the interpretative power of ZooMS in this instance, some insights have been acquired nevertheless. The 10 taxa that were identified at the site have a wide range of environmental preferences, ranging from closed forests to open woodlands or scrublands. This accordingly demonstrates that even with a small sample size, a wide range of fauna can already be identified through ZooMS alone. At larger sample sizes, ZooMS thus has significant potential to address questions of faunal turnovers in Australia in the past and their relationship to human economic and social contexts or climate changes (addressed in more detail in Chapter 2), for example by tracking the introduction the dingo, domesticated animals, or other non-native species.

In terms of examining biodiversity trends and tracking the introduction of non-native species to Australia, small mammals, such as bandicoots, rodents, and dasyurids are a particularly promising target for potential future ZooMS studies in Australia. These animals are often overlooked in zooarchaeological and palaeontological records because they are difficult to distinguish morphologically (Moro, 1991, Wayne et al., 2017), but they are valuable environmental indicators (Manuscript D, Peters et al., 2022). Work in eastern Africa and the Cayman Islands, has demonstrated the ability of ZooMS to identify small mammals, and in these case studies specifically to track the introduction of murid rodents (Prendergast et al., 2017, Harvey et al., 2019a). Once ZooMS reference markers are available for Australian micromammals, ZooMS will have the potential to significantly enhance our understanding of biodiversity shifts in these smaller mammals. I am currently involved in a study that aims to develop ZooMS peptide markers for a number of Australian rodents, including species in the genera *Conilurus*, *Rattus*, *Pseudomys, Zyzomys, Notomys*, *Uromys*, and *Leggadina*. The availability of reference markers for these taxa will significantly increase the potential of ZooMS to inform studies of micromammal diversity and turnovers in the past, which in turn can contribute to the reconstruction of palaeoenvironmental conditions and variations therein. At the same time, the identification of murid rodents in microfaunal assemblages can help shed light on the spread of these pest animals across Australia.

10.5.3. Extinctions and extirpations

Finally, ZooMS has significant potential to contribute to future studies of past extinctions and extirpations (Manuscript D, Peters et al., 2022). For megafaunal studies specifically, ZooMS used in tandem with chronometric dating techniques can contribute to our understanding of extinction chronologies and possible overlap of megafauna species with early human arrival and climatic changes, as well as the reconstruction of the geographic ranges of extinct taxa. One of the main issues in understanding Late Quaternary megafauna extinctions in Australia is the significant knowledge gaps existing for many species and regions. Furthermore, the distribution of megafauna fossil sites in Australia is heavily biased, with the majority of fossil sites located in the southern half of the continent (Field et al., 2008, Johnson et al., 2021). Data on species biochronology and palaeobiogeography is mostly patchy and high-quality data is often missing (Black et al., 2012, Wroe et al., 2013, Price et al., 2018, Saltré et al., 2019, Swift et al., 2019, Johnson et al., 2021, Price et al., 2021). For many species, specimens have only been reported at a handful of sites (Price et al., 2018, Hocknull et al., 2020, Johnson et al., 2021), and even fewer specimens have been reliably dated (Webb, 2013, Price et al., 2021). The underrepresentation of (dated) megafaunal remains leads to a high level of uncertainty in estimates of extinction chronologies and geographical ranges for many extinct taxa (Wroe et al., 2013, Bartlett et al., 2016, Price et al., 2018, Swift et al., 2019). This makes it difficult to test extinction hypotheses, both on a regional and on a continental scale. ZooMS offers a way to increase the number of identified megafauna specimens on the Australian continent, thus providing new data that can be used to test extinction hypotheses.

Another way in which ZooMS can contribute to the study of extinct megafauna is through a coupled approach using both ZooMS and stable isotope analysis. Additional megafauna specimens identified with ZooMS can subsequently be analysed with stable isotope analysis to forward our understanding of megafauna feeding ecology and dietary habits (Price et al., 2017, Swift et al., 2019). Although ZooMS reference markers for megafauna have not been established as part of the research of this thesis, I am currently involved in further research that aims to establish ZooMS reference markers for megafauna species. At the moment, preliminary peptide markers have been identified for five taxa: *Macropus titan*, *Protemnodon anak*, *Zygomaturus trilobus*, *Palorchestes azael*, and *Vombatus mitchelli*. This new set of markers has also been used to reassess the faunal assemblage of Devil's Lair (Manuscript C). Megafauna bones have previously been identified in this assemblage, but their distinct taphonomic profile indicates that these were washed into the sequence (Dortch, 1979). As it stands now, the new peptide markers confirm the absence of megafauna remains in Devil's Lair primary deposits. It is important to note however, that even with the discovery of additional megafaunal remains or possibly early human remains, the Signor-Lipps effect needs to be considered. The Signor-Lipps effect states that last appearance dates are not equivalent to extinction dates, and first appearance dates are not equivalent to first arrival dates (Signor et al., 1982). This thus needs to be considered when modelling first and last appearance dates of late surviving megafauna and early humans in Australia.

Beyond ZooMS, the application of shotgun palaeoproteomics also has the potential to resolve phylogenetic relationships between extinct megafauna and extant marsupials. Little is known about the phylogenetic placement of many of Australia's extinct megafauna, mostly because of a lack of aDNA preservation. The only species from which aDNA has successfully been extracted are *Simosthenurus occidentalis* and *Protemnodon anak*. Both these specimens originated from high-altitude cave sites in Tasmania with relatively favourable climatic conditions. This allowed investigations into their phylogenetic relationships to extant macropods, revealing three distinct macropod lineages: Macropodinae (wallabies and kangaroos, and to which *Protemnodon* is most closely related), Lagostrophinae (the banded hare-wallaby *Lagostrophus fasciatus*), and Sthenurinae (extinct short-faced kangaroos, including *Simosthenurus*) which are most closely related to Lagostrophinae (Llamas et al., 2014, Cascini et al., 2019). However, in the absence of aDNA, investigations into the phylogenetic relationships of other megafaunal species have so far remained impossible.

Palaeoproteomics has already proven to be a promising method for reconstructing phylogenetic relationships in the absence of aDNA. For example, palaeoproteomics has been used to reconstruct the phylogeny of recently extinct South American ungulates (Welker et al., 2015a), and similarly the phylogenetic relationships between extant and extinct rhinoceroses (Welker et al., 2017, Cappellini et al., 2019). Perhaps of most significance is the phylogenetic placement of early hominins with palaeoproteomics, which was previously unresolved due to the limited temporal reach of aDNA (Chen et al., 2019, Welker et al., 2020). Palaeoprotomic analysis of these early hominins revealed that *Homo antecessor* is a sister lineage to later species in the hominin lineage (Welker et al., 2020).

I am currently further exploring whether the collagen extracted to develop ZooMS reference markers for extinct megafauna can be used to reconstruct COL1 sequences of these extinct taxa with *de novo* sequencing, with the aim of using these sequences for subsequent phylogenetic reconstructions. Alternatively, in the future, the reconstruction of the phylogenetic relationships of extinct megafauna can be further investigated with dental enamel samples. Proteins generally preserve better into deep-time when bound to dental enamel than to bone. Furthermore, dental enamel also has a bigger proteome, meaning that a higher resolution can be reached when used for phylogenetic studies (Cappellini et al., 2019, Welker et al., 2020).

10.5.4. Conservation palaeoproteomics in Australia

Manuscript D (Peters et al., 2022) explored how ZooMS and palaeoproteomics can be used to inform conservation, restoration, and rewilding strategies. Although this thesis represents the first major study applying ZooMS to identify fauna from Australian fossil assemblages, ZooMS and other palaeoproteomics approaches also hold significant potential for supporting the development of conservation and restoration strategies in Australia in the future. Even the limited number of materials that currently has been analyzed with ZooMS in Australia already provide some insights into biodiversity, species distributions, and the introduction of non-native species to Australia; data that could be used to aid the development of conservation and restoration strategies in Australia in the future.

One area for which ZooMS holds particular promise is tracking the introduction of non-native species, specifically the introduction of domesticates and murid rodents following European colonization. As part of the research that was conducted for this thesis, domesticated bovid, most likely introduced to the site as barreled meat for food provisioning, was identified in the ZooMS assemblage of the early colonial pearlshell fishery at Bandicoot Bay (Manuscript A, Peters et al., 2021). ZooMS can also be used to inform the reconstruction of the past geographic distribution of animal species, and thereby providing important information for the development of ecological baselines. For example, the geographic distribution of the gray whale in the past has been clarified with ZooMS (as discussed in Manuscript D, Peters et al., 2022). Originally, gray whales were thought to occur only in the Pacific Ocean, but the species has been identified with ZooMS as far as the Western Atlantic Basin (Garrison et al., 2019) and the Western Mediterranean (Rodrigues et al., 2018). For Australia, ZooMS can be particularly useful for the reconstruction of ecological baselines for marine fauna, since peptide markers are available for almost all species of whales, dolphins (Buckley et al., 2014), and marine turtles (Harvey et al., 2019b). The usefulness of ZooMS to identify marine taxa in Australia was partly demonstrated in the study of the fragmented Bandicoot Bay assemblage (Manuscript A, Peters et al., 2021). The presence of sea turtles at the site was known from zooarchaeological investigations, although it was unclear which species were represented. ZooMS analysis identified two specimens as green sea turtle. Similarly, at Devil's Lair the identification of 11 specimens as *Lagostrophus*, an animal extirpated from southwest Australia in the present-day, also sheds light on its past geographic distribution and the subsequent changes this has undergone (Manuscript C).

Further insights can be acquired, and an increasingly larger number of conservation and restoration questions explored, when the application of ZooMS becomes a more prevalent method used to study

Australian faunal assemblages. For example, more wide-scale application of ZooMS could aid our understanding of species for which their conservation status, or timing of extinction, is unclear. I am currently involved in a study aiming to shed light on the possible recent extinction of the Capricorn rabbit rat (*Conilurus capricornensis*). This species is only known from dental remains recovered from Pleistocene until very recent Holocene deposits from eastern Queensland. Although often assumed to be extinct, it has been hypothesized that this animal is still extant in eastern Queensland today (Cramb and Hocknull, 2010). Little is known about the full extent of the biogeographic range of *C. capricornensis*, as well as the other two species in the *Conilurus* genus, *Conilurus penicillatus* (extant, although population sizes suffered from severe range contractions) and *Conilurus albipes* (extinct following European colonization) (Cramb and Hocknull, 2010, Firth et al., 2010). Better knowledge about their past distribution may help us better understand the reasons for their decline following European colonization, unravel whether *C. capricornensis* is truly extinct, and inform conservation efforts focused on the extant *C. penicillatus*.

Finally, ZooMS has the potential to inform the development of restoration and rewilding projects. In the case of Australia, there have been discussions recently about efforts to resurrect the thylacine, for example. While efforts to re-introduce extinct species do not address the key challenges faced by conservation in the current global biodiversity decline (Sandler, 2017), there are other ways in which the loss of ecosystem function following the extinction of keystone species, such as the thylacine, can be restored. Rewilding projects, in which novel keystone species are introduced (Lorimer et al., 2015, Svenning et al., 2016), are the most apparent choice in this regard. In order to find fitting rewilding replacements for extinct species, knowledge about their past distributions and ecologies is key (Monsarrat and Svenning, 2022). ZooMS has significant potential to contribute to research in this regard. The inclusion of ZooMS can increase our understanding of the past geographic distribution of the thylacine by uncovering a larger number of fragmented thylacine bones. This can inform rewilding projects that aim to restore ecosystem function following the loss of the thylacine by identifying areas in which such functional loss has taken place. Similarly, efforts to reintroduce the Tasmanian Devil to mainland Australia, following its extirpation in the mid-Holocene, can significantly benefit from more detailed knowledge about their past geographic distribution to identify habitats that are suitable to the reintroduction of this animal (Hunter et al., 2015, Westaway et al., 2019).

10.6. Conclusion

The research that was conducted for this thesis represents the largest application of ZooMS to the study of Australian fauna to date. This thesis has shown the great potential of ZooMS to increase our understanding of faunal assemblages in Australia, and the reference markers that were developed as part of this thesis are now available for other research groups to use. At the same time, this thesis highlighted the ongoing challenges associated with collagen preservation in Australia, the availability of reference data, and taxonomic specificity of ZooMS peptide markers. Importantly, this research also has significant implications for other regions of the world where collagen preservation was long thought to be unamenable to long-term preservation because of harsh environmental conditions. The successful application of ZooMS at Australian Late Pleistocene sites beyond chemical predictions of preservation potential raises the possibility of successful palaeoproteomics research in many of these regions that until now have remained devoid of such analyses. ZooMS has enormous potential for the study of Australian faunal assemblages, and can help address research questions that have until now remained unattainable in its absence, including but not limited to the study of past subsistence strategies, the reconstruction of past faunal diversity and tracking the introduction of non-native species, and obtaining a better understanding of extinctions and extirpations in the past. It will be interesting to see how the work represented in this thesis will be used to address these questions in the future.

Future advances in collagen extraction methods and subsequent data analysis have great potential to further improve the resolution of the information we can retrieve from ZooMS studies. Recently, it was

shown that it is possible to differentiate between horse and donkey with ZooMS, something not possible previously, when digesting collagen with the enzyme chymotrypsin instead of trypsin during collagen extraction (Paladugu et al., 2023). This study accordingly shows the great strides that can still be made with regards to method development, and that making relatively small changes to the extraction methods used for ZooMS can already make a big impact. When considering Australian contexts specifically, the use of another enzyme during collagen extraction might similarly enable us to, in the future, differentiate between closely related taxa, such as macropods, that are currently difficult to distinguish with ZooMS. Additionally, the development of software for the automated detection of ZooMS spectra would significantly decrease the time needed for data analysis for the large number of samples often run in ZooMS studies. This would further increase the ease at which the method can be incorporated into standard zooarchaeological investigations. The first steps have already been made in this regard (Gu and Buckley, 2018, Hickinbotham et al., 2020), but further efforts are required to develop a user-friendly, open-access software specifically for this purpose.

More efforts are also required to expand the ZooMS reference database to include a larger number of taxa, including not only marsupials, but also reptiles, amphibians, birds and fish inhabiting Australia in the past and/or present. At the same time, it will be important to establish new ZooMS facilities in Australia to maximize the reach of the method. The development of a small number of dedicated ZooMS laboratories across Australia, to which researchers from other local universities and institutes could send their samples, would already make great strides to the applicability of the method in the country. These advances are important, not just for Australia, but on a global scale. There are many other regions that have played key roles in the evolution and development of our species, but for which ZooMS studies are not yet possible due to the paucity of taxa available in the ZooMS reference database and the absence of ZooMS facilities outside of Europe and North America. A critical aspect in this regard is the sharing of raw data upon publication, which should become the standard in all ZooMS studies, and the development of a curated, open-access database bringing together all existing ZooMS markers to enable new ZooMS researchers an easy entry into the field.

11. References

Abelson, P. H. (1954). Amino acids in fossils. Science *119*, 576.

Akerman, K. & Willing, T. (2009). An ancient rock painting of a marsupial lion, *Thylacoleo carnifex*, from the Kimberley, Western Australia. Antiquity *83*, 1-4.

Allen, H., Langley, M. C. & Taçon, P. S. C. (2016). Bone projectile points in prehistoric Australia: Evidence from archaeologically recovered implements, ethnography and rock art. In Osseous projectile weaponry. Langley, M. ed. (Springer). doi.org/10.1007/978-94-012-0899-7_14.

Alves, J. M., Carneiro, M., Day, J. P., Welch, J. J., Duckworth, J. A., Cox, T. E., Letnic, M., Strive, T., Ferrand, N. & Jiggins, F. M. (2022). A single introduction of wild rabbits triggered the biological invasion of Australia. Proceedings of the National Academy of Sciences *119*, e2122734119. doi.org/10.1073/pnas.2122734119.

Antonosyan, M., Seersholm, F. V., Grealy, A. C., Barham, M., Werndly, D., Margaryan, A., Cieślik, A., Stafford, T. W., Allentoft, M. E., Bunce, M., et al. (2019). Ancient DNA shows high faunal diversity in the Lesser Caucasus during the Late Pleistocene. Quaternary Science Reviews *219*, 102-111. doi.org/10.1016/j.quascirev.2019.07.012.

Ashby, S. P., Coutu, A. N. & Sindbæk, S. M. (2015). Urban networks and arctic outlands: Craft specialists and reindeer antler in Viking towns. European Journal of Archaeology *18*, 679-704. doi.org/10.1179/1461957115Y.0000000003.

Austin, R. M., Sholts, S. B., Williams, L., Kistler, L. & Hofman, C. A. (2019). To curate the molecular past, museums need a carefully considered set of best practices. Proceedings of the National Academy of Sciences *116*, 1471-1474. doi.org/10.1073/pnas.1822038116.

Baird, R. (1991). The dingo as a possible factor in the disappearance of *Gallinula mortierii* from the Australian mainland. Emu *91*, 121-122. doi.org/10.1071/MU9910121.

Balme, J. & Morse, K. (2006). Shell beads and social behaviour in Pleistocene Australia. Antiquity *80*, 799-811. doi.org/10.1017/S0003598X00094436.

Balme, J. & O'Connor, S. (2016). Dingoes and Aboriginal social organization in Holocene Australia. Journal of Archaeological Science: Reports *7*, 775-781. doi.org/10.1016/j.jasrep.2015.08.015.

Balme, J., O'Connor, S. & Fallon, S. (2018). New dates on dingo bones from Madura Cave provide oldest firm evidence for arrival of the species in Australia. Scientific Reports *8*, 9933. doi.org/10.1038/s41598-018-28324-x.

Barbieri, R., Mekni, R., Levasseur, A., Chabrière, E., Signoli, M., Tzortzis, S., Aboudharam, G. & Drancourt, M. (2017). Paleoproteomics of the dental pulp: The plague paradigm. PLoS ONE *12*, e0180552. doi.org/10.1371/journal.pone.0180552.

Barnosky, A. D. (2008). Megafauna biomass tradeoff as a driver of Quaternary and future extinctions. Proceedings of the National Academy of Sciences *105*, 11543-11548. doi.org/10.1073/pnas.0801918105.

Barnosky, A. D., Hadly, E. A., Gonzalez, P., Head, J., Polly, P. D., Lawing, A. M., Eronen, J. T., Ackerly, D. D., Alex, K., Biber, E., et al. (2017). Merging paleobiology with conservation biology to guide the future of terrestrial ecosystems. Science *355*, eaah4787. doi.org/10.1126/science.aah4787.

Barrows, T. T., Fitzsimmons, K. E., Mills, S. C., Tumney, J., Pappin, D. & Stern, N. (2020). Late Pleistocene lake level history of Lake Mungo, Australia. Quaternary Science Reviews *238*, 106338. doi.org/10.1016/j.quascirev.2020.106338.

Bartlett, L. J., Williams, D. R., Prescott, G. W., Balmford, A., Green, R. E., Eriksson, A., Valdes, P. J., Singarayer, J. S. & Manica, A. (2016). Robustness despite uncertainty: Regional climate data reveal the dominant role of humans in explaining global extinctions of Late Quaternary megafauna. Ecography *39*, 152-161. doi.org/10.1111/ecog.01566.

Beasley, M. M., Bartelink, E. J., Taylor, L. & Miller, R. M. (2014). Comparison of transmission FTIR, ATR, and DRIFT spectra: Implications for assessment of bone bioapatite diagenesis. Journal of Archaeological Science *46*, 16-22. doi.org/10.1016/j.jas.2014.03.008.

Bellwood, P. & Hiscock, P. (2013). Australia and the Pacific Basin during the Holocene. In The human past. Third edition. Scarre, C. ed. (Thames & Hudson Ltd).

Bird, M. I., Hutley, L. B., Lawes, M. J., Lloyd, J., Luly, J. G., Ridd, P. V., Roberts, R. G., Ulm, S. & Wurster, C. M. (2013). Humans, megafauna and environmental change in tropical Australia. Journal of Quaternary Science *28*, 439-452. doi.org/10.1002/jqs.2639.

Bird, M. I., O'Grady, D. & Ulm, S. (2016). Humans, water, and the colonization of Australia. Proceedings of the National Academy of Sciences *113*, 11477-11482. doi.org/10.1073/pnas.1608470113.

Black, K. H., Archer, M., Hand, S. J. & Godthelp, H. (2012). The rise of Australian marsupials: A synopsis of biostratigraphic, phylogenetic, palaeoecological and palaeobiogeographic understanding. In Earth and life. Talent, J. A. ed. (Springer Science+Business Media B.V.). doi.org/10.1007/978-90-481-3428-1_35.

Boivin, N. L., Zeder, M. A., Fuller, D. Q., Crowther, A., Larson, G., Erlandson, J. M., Denham, T. & Petraglia, M. D. (2016). Ecological consequences of human niche construction: Examining long-term anthropogenic shaping of global species distributions. Proceedings of the National Academy of Sciences *113*, 6388-6396. doi.org/10.1073/pnas.1525200113.

Bowman, D. M. J. S. & Prior, L. D. (2004). Impact of Aboriginal landscape burning on woody vegetation in *Eucalyptus tetrodonta* savanna in Arnhem Land, northern Australia. Journal of Biogeography *31*, 807-817. doi.org/10.1111/j.1365-2699.2004.01077.x.

Bradfield, J., Forssman, T., Spindler, L. & Antonites, A. R. (2019). Identifying the animal species used to manufacture bone arrowheads in South Africa. Archaeological and Anthropological Sciences *11*, 2419-2434. doi.org/10.1007/s12520-018-0688-5.

Brandt, L. Ø., Schmidt, A. L., Mannering, U., Sarret, M., Kelstrup, C. D., Olsen, J. V. & Cappellini, E. (2014). Species identification of archaeological skin objects from Danish bogs: Comparison between mass spectrometry-based peptide sequencing and microscopy-based methods. PLoS ONE *9*, e106875. doi.org/10.1371/journal.pone.0106875.

Brandt, L. Ø., Ebsen, J. A. & Haase, K. (2020). Leather shoes in early Danish cities: Choices of animal resources and specialization of crafts in Viking and Medieval Denmark. European Journal of Archaeology *23*, 428-450. doi.org/10.1017/eaa.2020.2.

Brook, B. W. & Johnson, C. N. (2006). Selective hunting of juveniles as a cause of the imperceptible overkill of the Australian Pleistocene megafauna. Alcheringa: An Australasian Journal of Palaeontology *30*, 39-48. doi.org/10.1080/03115510609506854.

Brown, O. J. F. (2006). Tasmanian devil (*Sarcophilus harrisii*) extinction on the Australian mainland in the mid-Holocene: Multicausality and ENSO intensification. Alcheringa: An Australasian Journal of Palaeontology *30*, 49-57. doi.org/10.1080/03115510609506855.

Brown, S., Higham, T., Slon, V., Pääbo, S., Meyer, M., Douka, K., Brock, F., Comeskey, D., Procopio, N., Shunkov, M., et al. (2016). Identification of a new hominin bone from Denisova Cave, Siberia using collagen fingerprinting and mitochondrial DNA analysis. Scientific Reports *6*, 23559. doi.org/10.1038/srep23559.

Brown, S., Douka, K., Collins, M. J. & Richter, K. K. (2021a). On the standardization of ZooMS nomenclature. Journal of Proteomics *235*, 104041. doi.org/10.1016/j.jprot.2020.104041.

Brown, S., Kozlikin, M., Shunkov, M., Derevianko, A., Higham, T., Douka, K. & Richter, K. K. (2021b). Examining collagen preservation through glutamine deamidation at Denisova Cave. Journal of Archaeological Science *133*, 105454. doi.org/10.1016/j.jas.2021.105454.

Brown, S., Wang, N., Oertle, A., Kozlikin, M. B., Shunkov, M. V., Derevianko, A. P., Comeskey, D., Jope-Street, B., Harvey, V. L., Chowdhury, M. P., et al. (2021c). Zooarchaeology through the lens of collagen fingerprinting at Denisova Cave. Scientific Reports *11*, 15457. doi.org/10.1038/s41598-021-94731-2.

Brown, S., Massilani, D., Kozlikin, M. B., Shunkov, M. V., Derevianko, A. P., Stoessel, A., Jope-Street, B., Meyer, M., Kelso, J., Pääbo, S., et al. (2022). The earliest Denisovans and their cultural adaptation. Nature Ecology & Evolution *6*, 28-35. doi.org/10.1038/s41559-021-01581-2.

Brüniche-Olsen, A., Jones, M. E., Austin, J. J., Burridge, C. P. & Holland, B. R. (2014). Extensive population decline in the Tasmanian devil predates European settlement and devil facial tumour disease. Biology Letters *10*, 20140619. doi.org/10.1098/rsbl.2014.0619.

Brüniche–Olsen, A., Jones, M. E., Burridge, C. P., Murchison, E. P., Holland, B. R. & Austin, J. J. (2018). Ancient DNA tracks the mainland extinction and island survival of the Tasmanian devil. Journal of Biogeography *45*, 963-976. doi.org/10.1111/jbi.13214.

Buckley, M., Walker, A., Ho, S. Y. W., Yang, Y., Smith, C., Ashton, P., Thomas Oates, J., Cappellini, E., Koon, H., Penkman, K., et al. (2008). Comment on "Protein sequences from mastodon and *Tyrannosaurus rex* revealed by mass spectrometry". Science *319*, 33. doi.org/10.1126/science.1147046.

Buckley, M., Collins, M., Thomas-Oates, J. & Wilson, J. C. (2009). Species identification by analysis of bone collagen using matrix-assisted laser desorption/ionisation time-of-flight mass spectrometry. Rapid Communications in Mass Spectrometry *23*, 3843-3854. doi.org/10.1002/rcm.4316.

Buckley, M., Whitcher Kansa, S., Howard, S., Campbell, S., Thomas-Oates, J. & Collins, M. (2010). Distinguishing between archaeological sheep and goat bones using a single collagen peptide. Journal of Archaeological Science *37*, 13-20. doi.org/10.1016/j.jas.2009.08.020.

Buckley, M., Larkin, D. J. & Collins, M. (2011). Mammoth and mastodon collagen sequences: Survival and utility. Geochimica et Cosmochimica Acta *75*, 2007-2016. doi.org/10.1016/j.gca.2011.01.022.

Buckley, M., Fraser, S., Herman, J., Melton, N. D., Mulville, J. & Pálsdóttir, A. H. (2014). Species identification of archaeological marine mammals using collagen fingerprinting. Journal of Archaeological Science *41*, 631-641. doi.org/10.1016/j.jas.2013.08.021.

Buckley, M., Gu, M., Shameer, S., Patel, S. & Chamberlain, A. T. (2016). High-throughput collagen fingerprinting of intact microfaunal remains; a low-cost method for distinguishing between murine rodent bones. Rapid Communications in Mass Spectrometry *30*, 805-812. doi.org/10.1002/rcm.7483.

Buckley, M., Cosgrove, R., Garvey, J. & Prideaux, G. J. (2017). Identifying remains of extinct kangaroos in Late Pleistocene deposits using collagen fingerprinting. Journal of Quaternary Science *32*, 653-660. doi.org/10.1002/jqs.2964.

Buckley, M. (2018). Zooarchaeology by Mass Spectrometry (ZooMS) Collagen fingerprinting for the species identification of archaeological bone fragments. In Zooarchaeology in practice. Giovas, C. M. & LeFebvre, M. J. eds. (Springer). doi.org/10.1007/978-3-319-64763-0.

Buckley, M. & Herman, J. (2019). Species identification of Late Pleistocene bat bones using collagen fingerprinting. International Journal of Osteoarchaeology *29*, 1051-1059. doi.org/10.1002/oa.2818.

Buckley, M., Recabarren, O. P., Lawless, C., García, N. & Pino, M. (2019). A molecular phylogeny of the extinct South American gomphothere through collagen sequence analysis. Quaternary Science Reviews *224*, 105882. doi.org/10.1016/j.quascirev.2019.105882.

Buckley, M. & Cheylan, M. (2020). Collagen fingerprinting for the species identification of archaeological amphibian remains. Boreas *49*, 709-717. doi.org/10.1111/bor.12443.

Buckley, M., Harvey, V. L., Orihuela, J., Mychajliw, A. M., Keating, J. N., Milan, J. N. A., Lawless, C., Chamberlain, A. T., Egerton, V. M. & Manning, P. L. (2020). Collagen sequence analysis reveals evolutionary history of extinct West Indies *Nesophontes* (island-shrews). Molecular Biology and Evolution *37*, 2931-2943. doi.org/10.1093/molbev/msaa137.

Burbidge, A. A. & Manly, B. F. J. (2002). Mammal extinctions on Australian islands: Causes and conservation implications. Journal of Biogeography *29*, 465-473. doi.org/10.1046/j.1365-2699.2002.00699.x.

Butchart, S., H.M., Walpole, M., Collen, B., Van Strien, A., Scharlemann, J. P. W., Almond, R. E. A., Baillie, J. E. M., Bomhard, B., Brown, C., Bruno, J., et al. (2010). Global biodiversity: Indicators of recent declines. Science *328*, 1164-1168. doi.org/10.1126/science.1187512.

Cappellini, E., Jensen, L. J., Szklarczyk, D., Ginolhac, A., da Fonseca, R. A. R., Stafford, T. W., Holen, S. R., Collins, M. J., Orlando, L., Willerslev, E., et al. (2012). Proteomic analysis of a Pleistocene mammoth femur reveals more than one hundred ancient bone proteins. Journal of Proteome Research *11*, 917-926. doi.org/10.1021/pr200721u.

Cappellini, E., Collins, M. & Gilbert, M. T. P. (2014). Unlocking ancient protein palimpsests. Science *343*, 1320-1322. doi.org/10.1126/science.1249274.

Cappellini, E., Welker, F., Pandolfi, L., Ramos-Madrigal, J., Samodova, D., Rüther, P. L., Fotakis, A. K., Lyon, D., Moreno-Mayar, J. V., Bukhsianidze, M., et al. (2019). Early Pleistocene enamel proteome from Dmanisi resolves *Stephanorhinus* phylogeny. Nature *574*, 103-107. doi.org/10.1038/s41586-019-1555-y.

Cardillo, M., Mace, G. M., Jones, K. E., Bielby, J., Bininda-Emonds, O. R. P., Sechrest, W., Orme, C. D. L. & Purvis, A. (2005). Multiple causes of high extinction risk in large mammal species. Science *309*, 1239-1241. doi.org/10.1126/science.1116030.

Cascini, M., Mitchell, K. J., Cooper, A. & Phillips, M. J. (2019). Reconstructing the evolution of giant extinct kangaroos: Comparing the utility of DNA, morphology, and total evidence. Systematic Biology *68*, 520-537. doi.org/10.1093/sysbio/syy080.

Chen, F., Welker, F., Shen, C.-C., Bailey, S. E., Bergmann, I., Davis, S., Xia, H., Wang, H., Fischer, R., Freidline, S. E., et al. (2019). A late Middle Pleistocene Denisovan mandible from the Tibetan Plateau. Nature *569*, 409-412. doi.org/10.1038/s41586-019-1139-x.

Child, A. M. (1995). Towards and understanding of the microbial decomposition of archaeological bone in the burial environment. Journal of Archaeological Science *22*, 165-174. doi.org/10.1006/jasc.1995.0018.

Cienkosz-Stepańczak, B., Szostek, K. & Lisowska-Gaczorek, A. (2021). Optimizing FTIR method for characterizing diagenetic alteration of skeletal material. Journal of Archaeological Science: Reports *38*, 103059. doi.org/10.1016/j.jasrep.2021.103059.

Clarkson, C., Jacobs, Z., Marwick, B., Fullagar, R., Wallis, L., Smith, M., Roberts, R. G., Hayes, E., Lowe, K., Carah, X., et al. (2017). Human occupation of northern Australia by 65,000 years ago. Nature *547*, 306-310. doi.org/10.1038/nature22968.

Cobden, R., Clarkson, C., Price, G. J., David, B., Geneste, J.-M., Delannoy, J.-J., Barker, B., Lamb, L. & Gunn, R. G. (2017). The identification of extinct megafauna in rock art using geometric morphometrics: A *Genyornis newtoni* painting in Arnhem Land, northern Australia? Journal of Archaeological Science *87*, 95-107. doi.org/10.1016/j.jas.2017.09.013.

Codlin, M. C., Douka, K. & Richter, K. K. (2022). An application of ZooMS to identify archaeological avian fauna from Teotihuacan, Mexico. Journal of Archaeological Science *148*, 105692. doi.org/10.1016/j.jas.2022.105692.

Colleary, C., Lamadrid, H. M., O'Reilly, S. S., Dolocan, A. & Nesbitt, S. J. (2021). Molecular preservation in mammoth bone and variation based on burial environment. Scientific Reports *11*, 2662. doi.org/10.1038/s41598-021-81849-6.

Collins, M., Nielsen-Marsh, C. M., Hiller, J., Smith, C. I., Roberts, J. P., Prigodich, R. V., Wess, T. J., Scapo, J., Millard, A. R. & Turner-Walker, G. (2002). The survival of organic matter in bone: A review. Archaeometry *44*, 383-394. doi.org/10.1111/1475-4754.t01-1-00071.

Cosgrove, R., Field, J., Garvey, J., Brenner-Coltrain, J., Goede, A., Charles, B., Wroe, S., Pike-Tay, A., Grün, R., Aubert, M., et al. (2010). Overdone overkill – The archaeological perspective on Tasmanian megafaunal extinctions. Journal of Archaeological Science *37*, 2486-2503. doi.org/10.1016/j.jas.2010.05.009.

Cosgrove, R. & Garvey, J. (2017). Behavioural inferences from Late Pleistocene Aboriginal Australia: Seasonality, butchery, and nutrition in southwest Tasmania. In The Oxford handbook of zooarchaeology. Albarella, U., Rizzetto, M., Russ, H., Vickers, K. & Viner-Daniels, S. eds. (Oxford University Press). doi.org/10.1093/oxfordhb/9780199686476.013.49.

Coutu, A. N., Whitelaw, G., Le Roux, P. & Sealy, J. (2016). Earliest evidence for the ivory trade in Southern Africa: Isotopic and ZooMS analysis of seventh-tenth century AD ivory from KwaZulu-Natal. African Archaeological Review *33*, 411-435. doi.org/10.1007/s10437-016-9232-0.

Coutu, A. N. & Damgaard, K. (2019). From tusk to town: Ivory trade and craftmanship along the Red Sea. Studies in Late Antiquity *3*, 508-546. doi.org/10.1525/sla.2019.3.4.508.

Coutu, A. N., Taurozzi, A. J., Mackie, M., Jensen, T. Z. T., Collins, M. J. & Sealy, J. (2021). Palaeoproteomics confirm earliest domesticated sheep in southern Africa ca. 2000 BP. Scientific Reports *11*, 6631. doi.org/10.1038/s41598-021-85756-8.

Covington, A. D., Song, L., Suparno, O., Collins, M. J. & Koon, H. E. C. (2006). Link-Lock: The mechanism of stabilising collagen by chemical reactions. Journal of the Society of Leather Technologists and Chemists *92*, 1-7.

Cramb, J. & Hocknull, S. A. (2010). New Quaternary records of *Conilurus* (Rodentia: Muridae) from eastern and northern Australia with the description of a new species. Zootaxa *2634*, 41-56. doi.org/10.11646/zootaxa.2634.1.3.

Culley, C., Janzen, A., Brown, S., Prendergast, M. E., Shipton, C., Ndiema, E., Petraglia, M. D., Boivin, N. & Crowther, A. (2021). Iron Age hunting and herding in coastal eastern Africa: ZooMS identification of domesticates and wild bovids at Panga ya Saidi, Kenya. Journal of Archaeological Science *130*, 105368. doi.org/10.1016/j.jas.2021.105368.

Dabney, J., Knapp, M., Glocke, I., Gansauge, M.-T., Weihmann, A., Nickel, B., Valdiosera, C., García, N., Pääbo, S., Arsuaga, J.-L., et al. (2013). Complete mitochondrial genome sequence of a Middle Pleistocene cave bear reconstructed from ultrashort DNA fragments. Proceedings of the National Academy of Sciences *110*, 15758-15763. doi.org/10.1073/pnas.1314445110.

David, B., Delannoy, J.-J., Mialanes, J., Clarkson, C., Petchey, F., Geneste, J.-M., Manne, T., Bird, M. I., Barker, B., Richards, T., et al. (2019). 45,610–52,160 years of site and landscape occupation at Nawarla Gabarnmang, Arnhem Land plateau (northern Australia). Quaternary Science Reviews *215*, 64-85. doi.org/10.1016/j.quascirev.2019.04.027.

David, B., Arnold, L. J., Delannoy, J.-J., Fresløv, J., Urwin, C., Petchey, F., McDowell, M. C., Mullett, R., Mialanes, J., Wood, R., et al. (2021). Late survival of megafauna refuted for Cloggs Cave, SE Australia: Implications for the Australian Late Pleistocene megafauna extinction debate. Quaternary Science Reviews *253*, 106781. doi.org/10.1016/j.quascirev.2020.106781.

Davidson, I. (2013). Peopling the last new worlds: The first colonisation of Sahul and the Americas. Quaternary International *285*, 1-29. doi.org/10.1016/j.quaint.2012.09.023.

Davis, M., Faurby, S. & Svenning, J.-C. (2018). Mammal diversity will take millions of years to recover from the current biodiversity crisis. Proceedings of the National Academy of Sciences *115*, 11262-11267. doi.org/10.1073/pnas.1804906115.

Demarchi, B., Hall, S., Roncal-Herrero, T., Freeman, C. L., Woolley, J., Crisp, M. K., Wilson, J. C., Fotakis, A. K., Fischer, R., Kessler, B., et al. (2016). Protein sequences bound to mineral surfaces persist into deep time. eLife *5*, e17092. doi.org/10.7554/eLife.17092.

Demarchi, B., Mackie, M., Li, Z., Deng, T., Collins, M. J. & Clarke, J. (2022a). Survival of mineral-bound peptides into the Miocene. bioRxiv, 2022.08.19.502663. doi.org/10.1101/2022.08.19.502663.

Demarchi, B., Stiller, J., Grealy, A., Mackie, M., Deng, Y., Gilbert, T., Clarke, J., Legendre, L. J., Boano, R., Sicheritz-Pontén, T., et al. (2022b). Ancient proteins resolve controversy over the identity of *Genyornis* eggshell. Proceedings of the National Academy of Sciences, e2109326119. doi.org/10.1073/pnas.2109326119.

DeSantis, L. R. G., Field, J. H., Wroe, S. & Dodson, J. R. (2017). Dietary responses of Sahul (Pleistocene Australia–New Guinea) megafauna to climate and environmental change. Paleobiology *43*, 181-195. doi.org/10.1017/pab.2016.50.

Desmond, A., Barton, N., Bouzouggar, A., Douka, K., Fernandez, P., Humphrey, L., Morales, J., Turner, E. & Buckley, M. (2018). ZooMS identification of bone tools from the North African Later Stone Age. Journal of Archaeological Science *98*, 149-157. doi.org/10.1016/j.jas.2018.08.012.

Dietl, G. P. & Flessa, K. W. (2011). Conservation paleobiology: Putting the dead to work. Trends in Ecology and Evolution *26*, 30-37. doi.org/10.1016/j.tree.2010.09.010.

Dietl, G. P., Kidwell, S. M., Brenner, M., Burney, D. A., Flessa, K. W., Jackson, S. T. & Koch, P. L. (2015). Conservation paleobiology: Leveraging knowledge of the past to inform conservation and restoration. Annual Reviews of Earth and Planetary Sciences *43*, 79-103. doi.org/10.1146/annurev-earth-040610-133349.

Dirzo, R., Young, H. S., Galetti, M., Ceballos, G., Isaac, N. J. B. & Collen, B. (2014). Defaunation in the Anthropocene. Science *345*, 401-406. doi.org/10.1126/science.1251817.

Dortch, C. (1979). Devil's Lair, an example of prolonged cave use in Western Australia. World Archaeology *10*, 258-279. doi.org/10.1080/00438243.1979.9979736.

Dortch, J. (2004). Palaeo-environmental change and the persistence of human occupation in South-Western Australian forests (Archaeopress).

Dortch, J. & Wright, H. (2010). Identifying palaeo-environments and changes in Aboriginal subsistence from dual-patterned faunal assemblages, south-western Australia. Journal of Archaeological Science *37*, 1053-1064. doi.org/10.1016/j.jas.2009.12.006.

Doughty, C. E., Wolf, A. & Malhi, Y. (2013). The legacy of the Pleistocene megafauna extinctions on nutrient availability in Amazonia. Nature Geoscience *6*, 761-764. doi.org/10.1038/ngeo1895.

Doughty, C. E., Roman, J., Faurby, S., Wolf, A., Haque, A., Bakker, E. S., Malhi, Y., Dunning, J. B. & Svenning, J.-C. (2016). Global nutrient transport in a world of giants. Proceedings of the National Academy of Sciences *113*, 868-873. doi.org/10.1073/pnas.1502549112.

Doughty, C. E., Prys-Jones, T. O., Faurby, S., Abraham, A. J., Hepp, C., Leshyk, V., Fofanov, V. Y., Nieto, N. C., Svenning, J.-C. & Galetti, M. (2020). Megafauna decline have reduced pathogen dispersal which may have increased emergent infectious diseases. Ecography *43*, 1107-1117. doi.org/10.1111/ecog.05209.

Ebsen, J. A., Haase, K., Larsen, R., Sommer, D. V. P. & Brandt, L. Ø. (2019). Identifying archaeological leather – Discussing the potential of grain pattern analysis and zooarchaeology by mass spectrometry (ZooMS) through a case study involving medieval shoe parts from Denmark. Journal of Cultural Heritage *39*, 21-31. doi.org/10.1016/j.culher.2019.04.008.

Eda, M., Morimoto, M., Mizuta, T. & Inoué, T. (2020). ZooMS for birds: Discrimination of Japanese archaeological chickens and indigenous pheasants using collagen peptide fingerprinting. Journal of Archaeological Science: Reports *34*, 102635. doi.org/10.1016/j.jasrep.2020.102635.

Faillace, K. E., Foody, M. G. B. & Madgwick, R. (2020). Exploring the potential of TEM analysis for understanding cooking at prehistoric feasting sites. Scientific Reports *10*, 13635. doi.org/10.1038/s41598-020-70628-4.

Fenner, F. (2010). Deliberate introduction of the European rabbit, *Oryctolagus cuniculus,* into Australia. Rev Sci Tech *29*, 103-11. doi.org/10.20506/rst.29.1.1964.

Fiddyment, S., Holsinger, B., Ruzzier, C., Devine, A., Binois, A., Albarella, U., Fischer, R., Nichols, E., Curtis, A., Cheese, E., et al. (2015). Animal origin of 13th-century uterine vellum revealed using noninvasive peptide fingerprinting. Proceedings of the National Academy of Sciences *112*, 15066-15071. doi.org/10.1073/pnas.1512264112.

Field, J., Fullagar, R. & Lord, G. (2001). A large area archaeological excavation at Cuddie Springs. Antiquity *75*, 696-702. doi.org/10.1017/S0003598X00089195.

Field, J., Fillios, M. & Wroe, S. (2008). Chronological overlap between humans and megafauna in Sahul (Pleistocene Australia–New Guinea): A review of the evidence. Earth-Science Reviews *89*, 97-115. doi.org/10.1016/j.earscirev.2008.04.006.

Field, J., Wroe, S., Trueman, C. N., Garvey, J. & Wyatt-Spratt, S. (2013). Looking for the archaeological signature in Australian Megafaunal extinctions. Quaternary International *285*, 76-88. doi.org/10.1016/j.quaint.2011.04.013.

Fillios, M. & Blake, N. (2015). Animal bones in Australian archaeology (Sydney University Press).

Firth, R. S. C., Brook, B. W., Woinarski, J. C. Z. & Fordham, D. A. (2010). Decline and likely extinction of a northern Australian native rodent, the Brush-tailed Rabbit-rat *Conilurus penicillatus*. Biological Conservation *143*, 1193-1201. doi.org/10.1016/j.biocon.2010.02.027.

Flannery, T. F. (1990). Pleistocene faunal loss: Implications of the aftershock for Australia's past and future. Archaeology in Oceania *25*, 45-55. doi.org/10.1002/j.1834-4453.1990.tb00232.x.

Flannery, T. F. (1994). The future eaters (Melbourne).

Fletcher, M.-S., Hall, T. & Alexandra, A. N. (2021). The loss of an indigenous constructed landscape following British invasion of Australia: An insight into the deep human imprint on the Australian landscape. Ambio *50*, 138-149. doi.org/10.1007/s13280-020-01339-3.

Fotakis, A. K., Denham, S. D., Mackie, M., Orbegozo, M. I., Mylopotamitaki, D., Gopalakrishnan, S., Sicheritz-Pontén, T., Olsen, J. V., Cappellini, E., Zhang, G., et al. (2020). Multi-omic detection of *Mycobacterium leprae* in archaeological human dental calculus. Philosophical Transactions of the Royal Society B: Biological Sciences *375*, 20190584. doi.org/10.1098/rstb.2019.0584.

Galetti, M., Moleón, M., Jordano, P., Pires, M. M., Guimarães Jr., P. R., Pape, T., Nichols, E., Hansen, D., Olesen, J. M., Munk, M., et al. (2018). Ecological and evolutionary legacy of megafauna extinctions. Biological Reviews *93*, 845-862. doi.org/10.1111/brv.12374.

Garrison, E. G., Morgan, G. S., McGrath, K., Speller, C. & Cherkinsky, A. (2019). Recent dating of extinct Atlantic gray whale fossils, (*Eschrichtius robustus*), Georgia Bight and Florida, western Atlantic Ocean. PeerJ *7*, e6381. doi.org/10.7717/peerj.6381.

Geber, J., Tromp, M., Scott, A., Bouwman, A., Nanni, P., Grossmann, J., Hendy, J. & Warinner, C. (2019). Relief food subsistence revealed by microparticle and proteomic analyses of dental calculus from victims of the Great Irish Famine. Proceedings of the National Academy of Sciences *116*, 19380-19385. doi.org/10.1073/pnas.1908839116.

Gillespie, R., Brook, B. W. & Baynes, A. (2006). Short overlap of humans and megafauna in Pleistocene Australia. Alcheringa: An Australasian Journal of Palaeontology *30*, 163-186. doi.org/10.1080/03115510609506861.

Gillespie, R. (2008). Updating Martin's global extinction model. Quaternary Science Reviews *27*, 2522-2529. doi.org/10.1016/j.quascirev.2008.09.007.

Gong, Y., Li, L., Gong, D., Yin, H. & Zhang, J. (2016). Biomolecular evidence of silk from 8,500 Years ago. PLoS ONE *11*, e0168042. doi.org/10.1371/journal.pone.0168042.

Gott, B. (2005). Aboriginal fire management in south-eastern Australia: Aims and frequency. Journal of Biogeography *32*, 1203-1208. doi.org/10.1111/j.1365-2699.2004.01233.x.

Gourion-Arsiquaud, S., West, P. A. & Boskey, A. L. (2008). Fourier Transform-Infrared Microspectroscopy and microscopic imaging. In Osteoporosis: Methods and protocols. Westendorf, J. J. ed. (Humana Press). doi.org/10.1007/978-1-59745-104-8_20.

Gu, M. & Buckley, M. (2018). Semi-supervised machine learning for automated species identification by collagen peptide mass fingerprinting. BMC Bioinformatics *19*, 241. doi.org/10.1186/s12859-018-2221-3.

Gunn, R. G., Douglas, L. C. & Whear, R. L. (2011). What bird is that? Identifying a probable painting of *Genyornis newtoni* in Western Arnhem Land. Australian Archaeology *73*, 12-12. doi.org/10.1080/03122417.2011.11961918.

Hacker, R. B. & McDonald, S. E. (2021). Prospects for sustainable use of the pastoral areas of Australia's southern rangelands: A synthesis. The Rangeland Journal *43*, 185-209. doi.org/10.1071/RJ21036.

Hallam, S. J. (2014). Fire and hearth: A study of Aboriginal usage and European usurpation in south-western Australia (UWA Publishing).

Hamm, G., Mitchell, P., Arnold, L. J., Prideaux, G. J., Questiaux, D., Spooner, N. A., Levchenko, V. A., Foley, E. C., Worthy, T. H., Stephenson, B., et al. (2016). Cultural innovation and megafauna interaction in the early settlement of arid Australia. Nature *539*, 280-283. doi.org/10.1038/nature20125.

Hanna, E. & Cardillo, M. (2014). Island mammal extinctions are determined by interactive effects of life history, island biogeography and mesopredator suppression. Global Ecology and Biogeography *23*, 395-404. doi.org/10.1111/geb.12103.

Hare, P. E. & Abelsen, P. H. (1968). Racemization of amino acids in fossil shells. Carnegie Inst. Washington Yearb. *66*, 526-528.

Harvey, V. L., Daugnora, L. & Buckley, M. (2018). Species identification of ancient Lithuanian fish remains using collagen fingerprinting. Journal of Archaeological Science *98*, 102-111. doi.org/10.1016/j.jas.2018.07.006.

Harvey, V. L., Egerton, V. M., Chamberlain, A. T., Manning, P. L., Sellers, W. I. & Buckley, M. (2019a). Interpreting the historical terrestrial vertebrate biodiversity of Cayman Brac (Greater Antilles, Caribbean) through collagen fingerprinting. The Holocene *29*, 531-542. doi.org/10.1177/0959683618824793.

Harvey, V. L., LeFebvre, M. J., deFrance, S. D., Toftgaard, C., Drosou, K., Kitchener, A. C. & Buckley, M. (2019b). Preserved collagen reveals species identity in archaeological marine turtle bones from Caribbean and Florida sites. Royal Society Open Science *6*, 191137. doi.org/10.1098/rsos.191137.

Hedges, R. E. M. (2002). Bone diagenesis: An overview of processes. Archaeometry *44*, 319-328. doi.org/10.1111/1475-4754.00064.

Hendy, J., Colonese, A. C., Franz, I., Fernandes, R., Fischer, R., Orton, D., Lucquin, A., Spindler, L., Anvari, J., Stroud, E., et al. (2018a). Ancient proteins from ceramic vessels at Çatalhöyük West reveal the hidden cuisine of early farmers. Nature Communications *9*, 4064. doi.org/10.1038/s41467-018-06335-6.

Hendy, J., Warriner, C., Bouwman, A., Collins, M., Fiddyment, S., Fischer, R., Hagan, R., Hofman, C. A., Holst, M., Chaves, E., et al. (2018b). Proteomic evidence of dietary sources in ancient dental calculus. Proceedings of the Royal Society B *285*, 20180977. doi.org/10.1098/rspb.2018.0977.

Hendy, J., Welker, F., Demarchi, B., Speller, C., Warinner, C. & Collins, M. (2018c). A guide to ancient protein studies. Nature Ecology and Evolution *2*, 791-799. doi.org/10.1038/s41559-018-0510-x.

Hendy, J. (2021). Ancient protein analysis in archaeology. Science Advances *7*, eabb9314. doi.org/10.1126/sciadv.abb9314.
Henriksen, K. & Karsdal, M. A. (2019). Chapter 1 - Type I collagen. In Biochemistry of collagens, laminins and elastin (Second Edition). Karsdal, M. A. ed. (Academic Press). doi.org/10.1016/B978-0-12-817068-7.00001-X.
Hickinbotham, S., Fiddyment, S., Stinson, T.L. & Collins, M. (2020). How to get your goat: automated identification of species from MALDI-ToD spectra. Bioinformatics *36*, 3719-3725. doi.org/10.1093/bioinformatics/btaa181.
Hocknull, S. A., Lewis, R., Arnold, L. J., Pietsch, T., Joannes-Boyau, R., Price, G. J., Moss, P., Wood, R., Dosseto, A., Louys, J., et al. (2020). Extinction of eastern Sahul megafauna coincides with sustained environmental deterioration. Nature Communications *11*, 2250. doi.org/10.1038/s41467-020-15785-w.
Hunter, D. O., Britz, T., Jones, M. & Letnic, M. (2015). Reintroduction of Tasmanian devils to mainland Australia can restore top-down control in ecosystems where dingoes have been extirpated. Biological Conservation *191*, 428-435. doi.org/10.1016/j.biocon.2015.07.030.
Jans, M. M. E., Nielsen-Marsh, C. M., Smith, C. I., Collins, M. J. & Kars, H. (2004). Characterisation of microbial attack on archaeological bone. Journal of Archaeological Science *31*, 87-95. doi.org/10.1016/j.jas.2003.07.007.
Janzen, A., Richter, K. K., Mwebi, O., Brown, S., Onduso, V., Gatwiri, F., Ndiema, E., Katongo, M., Goldstein, S. T., Douka, K., et al. (2021). Distinguishing African bovids using Zooarchaeology by Mass Spectrometry (ZooMS): New peptide markers and insights into Iron Age economies in Zambia. PLoS ONE *16*, e0251061. doi.org/10.1371/journal.pone.0251061.
Jensen, T. Z. T., Mackie, M., Taurozzi, A. J., Lanigan, L. T., Gundelach, C., Olsen, J. V., Sørensen, S. A., Collins, M., Sørensen, M. & Schroeder, H. (2020a). The biomolecular characterization of a finger ring contextually dated to the emergence of the Early Neolithic from Syltholm, Denmark. Royal Society Open Science *7*, 191172. doi.org/10.1098/rsos.191172.
Jensen, T. Z. T., Sjöström, A., Fischer, A., Rosengren, E., Lanigan, L. T., Bennike, O., Richter, K. K., Gron, K. J., Mackie, M., Mortensen, M. F., et al. (2020b). An integrated analysis of Maglemose bone points reframes the Early Mesolithic of Southern Scandinavia. Scientific Reports *10*, 17244. doi.org/10.1038/s41598-020-74258-8.
Jersie-Christensen, R. R., Lanigan, L. T., Lyon, D., Mackie, M., Belstrøm, D., Kelstrup, C. D., Fotakis, A. K., Willerslev, E., Lynnerup, N., Jensen, L. J., et al. (2018). Quantitative metaproteomics of medieval dental calculus reveals individual oral health status. Nature Communications *9*, 4744. doi.org/10.1038/s41467-018-07148-3.
Johnson, C. N. & Wroe, S. (2003). Causes of extinction of vertebrates during the Holocene of mainland Australia: Arrival of the dingo, or human impact? The Holocene *13*, 941-948. doi.org/10.1191/0959683603hl682fa.
Johnson, C. N. (2006). Australia's Mammal Extinctions: A 50000 Year History (Cambridge University Press).
Johnson, C. N. (2009). Ecological consequences of Late Quaternary extinctions of megafauna. Proceedings of the Royal Society B: Biological Sciences *276*, 2509-2519. doi.org/10.1098/rspb.2008.1921.
Johnson, C. N. & Brook, B. W. (2011). Reconstructing the dynamics of ancient human populations from radiocarbon dates: 10 000 years of population growth in Australia. Proceedings of the Royal Society B: Biological Sciences *278*, 3748-3754. doi.org/10.1098/rspb.2011.0343.
Johnson, C. N., Alroy, J., Beeton, N. J., Bird, M., Brook, B. W., Cooper, A., Gillespie, R., Herrando-Pérez, S., Jacobs, Z., Miller, G. H., et al. (2016). What caused extinction of the Pleistocene megafauna of Sahul? Proceedings of the Royal Society B *283*. doi.org/10.1098/rspb.2015.2399.
Johnson, C. N., Dortch, J. & Worthy, T. H. (2021). Interactions with megafauna. In The Oxford handbook of the archaeology of Indigenous Australia and New Guinea. McNiven, I. J. & David, B. eds. (Oxford University Press). doi.org/10.1093/oxfordhb/9780190095611.013.10.
Kendall, C., Eriksen, A. M. H., Kontopoulos, I., Collins, M. J. & Turner-Walker, G. (2018). Diagenesis of archaeological bone and tooth. Palaeogeography, Palaeoclimatology, Palaeoecology *491*, 21-37. doi.org/10.1016/j.palaeo.2017.11.041.

Koch, P. L. & Barnosky, A. D. (2006). Late Quaternary extinctions: State of the debate. Annual Review of Ecology, Evolution, and Systematics *37*, 215-250. doi.org/10.1146/annurev.ecolsys.34.011802.132415.

Kontopoulos, I., Penkman, K., Mullin, V. E., Winkelbach, L., Unterländer, M., Scheu, A., Kreutzer, S., Hansen, H. B., Margaryan, A., Teasdale, M. D., et al. (2020). Screening archaeological bone for palaeogenetic and palaeoproteomic studies. PLoS ONE *15*, e0235146. doi.org/10.1371/journal.pone.0235146.

Kooyman, B., Newman, M. E., Cluney, C., Lobb, M., Tolman, S., McNeil, P. & Hills, L. V. (2001). Identification of horse exploitation by Clovis hunters based on protein analysis. American Antiquity *66*, 686-691. doi.org/10.2307/2694181.

Kos, A. M. (2003). Characterisation of post-depositional taphonomic processes in the accumulation of mammals in a pitfall cave deposit from southeastern Australia. Journal of Archaeological Science *30*, 781-796. doi.org/10.1016/S0305-4403(02)00252-2.

Langley, M., Clarkson, C. & Ulm, S. (2011). From small holes to grand narratives: The impact of taphonomy and sample size on the modernity debate in Australia and New Guinea. Journal of Human Evolution *61*, 197-208. doi.org/10.1016/j.jhevol.2011.03.002.

Langley, M., O'Connor, S. & Aplin, K. (2016). A >46,000-year-old kangaroo bone implement from Carpenter's Gap 1 (Kimberley, northwest Australia). Quaternary Science Reviews *154*, 199-213. doi.org/10.1016/j.quascirev.2016.11.006.

Langley, M., Clarkson, C. & Ulm, S. (2019). Symbolic expression in Pleistocene Sahul, Sunda and Wallacea. Quaternary Science Reviews *221*, 105883. doi.org/10.1016/j.quascirev.2019.105883.

Le Meillour, L., Zirah, S., Zazzo, A., Cersoy, S., Détroit, F., Imalwa, E., Lebon, M., Nankela, A., Tombret, O., Pleurdeau, D., et al. (2020). Palaeoproteomics gives new insight into early southern African pastoralism. Scientific Reports *10*, 14427. doi.org/10.1038/s41598-020-71374-3.

Lebon, M., Reiche, I., Gallet, X., Bellot-Gurlet, L. & Zazzo, A. (2016). Rapid quantification of bone collagen content by ATR-FTIR spectroscopy. Radiocarbon *58*, 131-145. doi.org/10.1017/RDC.2015.11.

Letnic, M. (2007). The impacts of pastoralism on the fauna of arid Australia. In Animals of arid Australia: Out on their own? Dickman, C., Lunney, D. & Burgin, S. eds. (Royal Zoological Society of New South Wales). doi.org/10.7882/fs.2007.041.

Letnic, M., Fillios, M. & Crowther, M. S. (2012). Could direct killing by larger dingoes have caused the extinction of the thylacine from mainland Australia? PLoS ONE *7*, e34877. doi.org/10.1371/journal.pone.0034877.

Letnic, M., Fillios, M. & Crowther, M. (2014). The arrival and impacts of the dingo. In Carnivores of Australia: Past, present and future. Glen, A. & Dickman, C. eds. (CSIRO Publishing).

Li, L., Gong, Y., Yin, H. & Gong, D. (2015). Different types of peptide detected by mass spectrometry among fresh silk and archaeological silk remains for distinguishing modern contamination. PLoS ONE *10*, e0132827. doi.org/10.1371/journal.pone.0132827.

Li, X., Lin, C. & O'Connor, P. B. (2010). Glutamine deamidation: Differentiation of glutamic acid and γ-glutamic acid in peptides by Electron Capture Dissociation. Analytical Chemistry *82*, 3606-3615. doi.org/10.1021/ac9028467.

Lima-Ribeiro, M. S. & Diniz-Filho, J. A. F. (2014). Obstinate overkill in Tasmania? The closest gaps do not probabilistically support human involvement in megafaunal extinctions. Earth-Science Reviews *135*, 59-64. doi.org/10.1016/j.earscirev.2014.04.005.

Lindahl, T. & Nyberg, B. (1972). Rate of depurination of native deoxyribonucleic acid. Biochemistry *11*, 3610-3618. doi.org/10.1021/bi00769a018.

Llamas, B., Brotherton, P., Mitchell, K. J., Templeton, J. E. L., Thomson, V. A., Metcalf, J. L., Armstrong, K. N., Kasper, M., Richards, S. M., Camens, A. B., et al. (2014). Late Pleistocene Australian marsupial DNA clarifies the affinities of extinct megafaunal kangaroos and wallabies. Molecular Biology and Evolution *32*, 574-584. doi.org/10.1093/molbev/msu338.

Llewelyn, J., Strona, G., McDowell, M. C., Johnson, C. N., Peters, K. J., Stouffer, D. B., de Visser, S. N., Saltré, F. & Bradshaw, C. J. A. (2022). Sahul's megafauna were vulnerable to plant-community changes due to their position in the trophic network. Ecography. doi.org/10.1111/ecog.06089.

Lorimer, J., Sandom, C., Jepson, P., Doughty, C., Barua, M. & Kirby, K. J. (2015). Rewilding: Science, practice, and politics. Annual Review of Environment and Resources *40*, 39-62. doi.org/10.1146/annurev-environ-102014-021406.

Lourandos, H. (1997). Continent of hunter-gatherers: New perspectives in Australian prehistory (Cambridge University Press).

Loy, T. H. & Wood, A. R. (1989). Blood residue analysis at Çayönü Tepesi, Turkey. Journal of Field Archaeology *16*, 451-460. doi.org/10.1179/jfa.1989.16.4.451.

Lugli, F., Di Rocco, G., Vazzana, A., Genovese, F., Pinetti, D., Cilli, E., Carile, M. C., Silvestrini, S., Gabanini, G., Arrighi, S., et al. (2019). Enamel peptides reveal the sex of the Late Antique 'Lovers of Modena'. Scientific Reports *9*, 13130. doi.org/10.1038/s41598-019-49562-7.

Mackie, M., Hendy, J., Lowe, A., D., Sperduti, A., Holst, M., Collins, M. & Speller, C. (2017). Preservation of the metaproteome: Variability of protein preservation in ancient dental calculus. STAR: Science & Technology of Archaeological Research *3*, 74-86. doi.org/10.1080/20548923.2017.1361629.

Maixner, F., Sarhan, M. S., Huang, K. D., Tett, A., Schoenafinger, A., Zingale, S., Blanco-Míguez, A., Manghi, P., Cemper-Kiesslich, J., Rosendahl, W., et al. (2021). Hallstatt miners consumed blue cheese and beer during the Iron Age and retained a non-Westernized gut microbiome until the Baroque period. Current Biology *31*, 5149-5162. doi.org/10.1016/j.cub.2021.09.031.

Malhi, Y., Doughty, C. E., Galetti, M., Smith, F. A., Svenning, J.-C. & Terborgh, J. W. (2016). Megafauna and ecosystem function from the Pleistocene to the Anthropocene. Proceedings of the National Academy of Sciences *113*, 838-846. doi.org/10.1073/pnas.1502540113.

Manne, T. & Veth, P. (2015). Late Pleistocene and early Holocene exploitation of estuarine communities in northwestern Australia. Quaternary International *385*, 112-123. doi.org/10.1016/j.quaint.2014.12.049.

Mariani, M., Connor, S. E., Theuerkauf, M., Herbert, A., Kuneš, P., Bowman, D., Fletcher, M.-S., Head, L., Kershaw, A. P., Haberle, S. G., et al. (2022). Disruption of cultural burning promotes shrub encroachment and unprecedented wildfires. Frontiers in Ecology and the Environment *20*, 292-300. doi.org/10.1002/fee.2395.

Marshall, B. & Cosgrove, R. (1990). Tasmanian Devil (*Sarcophilus harrisii*) scat-bone: Signature criteria and archaeological implications. Archaeology in Oceania *25*, 102-113. doi.org/10.1002/j.1834-4453.1990.tb00240.x.

Martin, P. S. (1967). Prehistoric overkill. In Pleistocene extinctions. Martin, P. S. & Wright, H. E. eds. (Yale University Press).

Martin, P. S. & Klein, R. G. (1984). Quaternary extinctions: A prehistoric revolution (University of Arizona Press).

Martisius, N. L., Welker, F., Dogandžić, T., Grote, M. N., Rendu, W., Sinet-Mathiot, V., Wilcke, A., McPherron, S. J. P., Soressi, M. & Steele, T. E. (2020). Non-destructive ZooMS identification reveals strategic bone tool raw material selection by Neandertals. Scientific Reports *10*, 1-12. doi.org/10.1038/s41598-020-64358-w.

Matthiesen, H., Høier Eriksen, A. M., Hollesen, J. & Collins, M. (2021). Bone degradation at five Arctic archaeological sites: Quantifying the importance of burial environment and bone characteristics. Journal of Archaeological Science *125*, 105296. doi.org/10.1016/j.jas.2020.105296.

McGrath, K., Rowsell, K., St-Pierre, C. G., Tedder, A., Foody, G., Roberts, C., Speller, C. & Collins, M. (2019). Identifying archaeological bone via non-destructive ZooMS and the materiality of symbolic expression: Examples from Iroquoian bone points. Scientific Reports *9*, 1-10. doi.org/10.1038/s41598-019-47299-x.

Mein, E. & Manne, T. (2021). Identifying marsupials from Australian archaeological sites: Current methodological challenges and opportunities in zooarchaeological practice. Archaeology in Oceania *56*, 133-141. doi.org/doi.org/10.1002/arco.5234.

Menzies, B. R., Renfree, M. B., Heider, T., Mayer, F., Hildebrandt, T. B. & Pask, A. J. (2012). Limited genetic diversity preceded extinction of the Tasmanian tiger. PLoS ONE *7*, e35433. doi.org/10.1371/journal.pone.0035433.

Miller, G., Fogel, M., Magee, J., Gagan, M. K., Clarke, S. J. & Johnson, B. J. (2005). Ecosystem collapse in Pleistocene Australia and a human role in megafaunal extinction. Science *309*, 287-290. doi.org/10.1126/science.1111288.

Miller, G., Magee, J., Smith, M., Spooner, N., Baynes, A., Lehman, S., Fogel, M., Johnston, H., Williams, D., Clark, P., et al. (2016). Human predation contributed to the extinction of the Australian megafaunal bird *Genyornis newtoni* ~ 47 ka. Nature Communications *7*. doi.org/10.1038/ncomms10496.

Miscamble, T. & Manne, T. (2016). A taphonomic signature for quolls in the Australian archaeological record. Journal of Archaeological Science: Reports *7*, 689-699. doi.org/10.1016/j.jasrep.2016.01.011.

Monsarrat, S. & Svenning, J.-C. (2022). Using recent baselines as benchmarks for megafauna restoration places an unfair burden on the Global South. Ecography. doi.org/10.1111/ecog.05795.

Moro, D. (1991). The distribution of small mammal species in relation to heath vegetation near Cape Otway, Victoria. Wildlife Research *18*, 605-617. doi.org/10.1071/WR9910605.

Morris, S. D., Kearney, M. R., Johnson, C. N. & Brook, B. W. (2022). Too hot for the devil? Did climate change cause the mid-Holocene extinction of the Tasmanian devil *Sacrophilus harrisii* from mainland Australia? Ecography *2022*. doi.org/10.1111/ecog.05799.

Multari, D. H., Sullivan, G. J., Hartley, M., Power, R. K. & Haynes, P. A. (2022). Species identification of early colonial bone artefacts excavated from Pyrmont, Australia, by mass spectrometric identification of collagen peptides. bioRxiv, 2022.05.13.491741. doi.org/10.1101/2022.05.13.491741.

Murphy, B. P., Williamson, G. J. & Bowman, D. M. J. S. (2012). Did central Australian megafaunal extinction coincide with abrupt ecosystem collapse or gradual climate change? Global Ecology and Biogeography *21*, 142-151. doi.org/10.1111/j.1466-8238.2011.00668.x.

Murray, D., Haile, J., Dortch, J., White, N. E., Haouchar, D., Bellgard, M. I., Allcock, R. J., Prideaux, G. J. & Bunce, M. (2013). Scrapheap Challenge: A novel bulk-bone metabarcoding method to investigate ancient DNA in faunal assemblages. Scientific Reports *3*, 3371. doi.org/10.1038/srep03371.

Mychajliw, A. M., Rick, T. C., Dagtas, N. D., Erlandson, J. M., Culleton, B. J., Kennett, D. J., Buckley, M. & Hofman, C. A. (2020). Biogeographic problem-solving reveals the Late Pleistocene translocation of a short-faced bear to the California Channel Islands. Scientific Reports *10*, 15172. doi.org/10.1038/s41598-020-71572-z.

Newman, M. & Julig, P. (1989). The identification of protein residues on lithic artifacts from a Stratified boreal forest site. Canadian Journal of Archaeology / Journal Canadien d'Archéologie *13*, 119-132.

Nielsen-Marsh, C. M. & Hedges, R. E. M. (2000). Patterns of diagenesis in bone I: The effects of site environments. Journal of Archaeological Science *27*, 1139-1150. doi.org/10.1006/jasc.1999.0537.

Orlando, L., Ginolhac, A., Zhang, G., Froese, D., Albrechtsen, A., Stiller, M., Schubert, M., Cappellini, E., Petersen, B., Moltke, I., et al. (2013). Recalibrating *Equus* evolution using the genome sequence of an early Middle Pleistocene horse. Nature *499*, 74-78. doi.org/10.1038/nature12323.

Ostrom, P. H., Schall, M., Gandhi, H., Shen, T.-L., Hauschka, P. V., Strahler, J. R. & Gage, D. A. (2000). New strategies for characterizing ancient proteins using matrix-assisted laser desorption ionization mass spectrometry. Geochimica et Cosmochimica Acta *64*, 1043-1050. doi.org/10.1016/S0016-7037(99)00381-6.

Paladugu, R., Richter, K.K., Valente, M.J., Gabriel, S., Detry, C., Warinner, C. & Barrocas Dias, C. (2023). Your horse is a donkey! Identifying domesticated equids from Western Iberia using collagen fingerprinting. Journal of Archaeological Science *149*, 105696. doi.org/10.1016/j.jas.2022.105696.

Pal Chowdhury, M., Wogelius, R., Manning, P. L., Metz, L., Slimak, L. & Buckley, M. (2019). Collagen deamidation in archaeological bone as an assessment for relative decay rates. Archaeometry *61*, 1382-1398. doi.org/10.1111/arcm.12492.

Pal Chowdhury, M., Choudhury, K. D., Bouchard, G. P., Riel-Salvatore, J., Negrino, F., Benazzi, S., Slimak, L., Frasier, B., Szabo, V., Harrison, R., et al. (2021). Machine learning ATR-FTIR spectroscopy data for the screening of collagen for ZooMS analysis and mtDNA in archaeological bone. Journal of Archaeological Science *126*, 105311. doi.org/10.1016/j.jas.2020.105311.

Pálsdóttir, A. H., Bläuer, A., Rannamäe, E., Boessenkool, S. & Hallsson, J. H. (2019). Not a limitless resource: Ethics and guidelines for destructive sampling of archaeofaunal remains. Royal Society Open Science *6*, 191059. doi.org/10.1098/rsos.191059.

Parker, G. J., Yip, J. M., Eerkens, J. W., Salemi, M., Durbin-Johnson, B., Kiesow, C., Haas, R., Buikstra, J. E., Klaus, H., Regan, L. A., et al. (2019). Sex estimation using sexually dimorphic amelogenin protein fragments in human enamel. Journal of Archaeological Science *101*, 169-180. doi.org/10.1016/j.jas.2018.08.011.

Peacock, D. & Abbott, I. (2014). When the 'native cat' would 'plague': Historical hyperabundance in the quoll (Marsupialia: Dasyuridae) and an assessment of the role of disease, cats and foxes in its curtailment. Australian Journal of Zoology *62*, 294-344. doi.org/10.1071/ZO14029.

Peters, C., Richter, K. K., Manne, T., Dortch, J., Paterson, A., Travouillon, K., Louys, J., Price, G. J., Petraglia, M., Crowther, A., et al. (2021). Species identification of Australian marsupials using collagen fingerprinting. Royal Society Open Science *8*, 211229. doi.org/10.1098/rsos.211229.

Peters, C., Richter, K. K., Svenning, J.-C. & Boivin, N. (2022). Leveraging palaeoproteomics to address conservation and restoration agendas. iScience *25*, 104195. doi.org/10.1016/j.isci.2022.104195.

Petherick, L., Bostock, H., Cohen, T. J., Fitzsimmons, K., Tibby, J., Fletcher, M. S., Moss, P., Reeves, J., Mooney, S., Barrows, T., et al. (2013). Climatic records over the past 30 ka from temperate Australia – A synthesis from the Oz-INTIMATE workgroup. Quaternary Science Reviews *74*, 58-77. doi.org/10.1016/j.quascirev.2012.12.012.

Pettitt, P. (2013). The rise of modern humans. In The human past. Third Edition. Scarre, C. ed. (Thames & Hudson Ltd).

Pothier Bouchard, G., Mentzer, S. M., Riel-Salvatore, J., Hodgkins, J., Miller, C. E., Negrino, F., Wogelius, R. & Buckley, M. (2019). Portable FTIR for on-site screening of archaeological bone intended for ZooMS collagen fingerprint analysis. Journal of Archaeological Science: Reports *26*, 101862. doi.org/10.1016/j.jasrep.2019.05.027.

Prendergast, M. E., Buckley, M., Crowther, A., Frantz, L., Eager, H., Lebrasseur, O., Hutterer, R., Hulme-Beaman, A., Van Neer, W., Douka, K., et al. (2017). Reconstructing Asian faunal introductions to eastern Africa from multi-proxy biomolecular and archaeological datasets. PLoS ONE *12*, e0182565. doi.org/10.1371/journal.pone.0182565.

Prendergast, M. E., Janzen, A., Buckley, M. & Grillo, K. M. (2019). Sorting the sheep from the goats in the Pastoral Neolithic: Morphological and biomolecular approaches at Luxmanda, Tanzania. Archaeological and Anthropological Sciences *11*, 3047-3062. doi.org/10.1007/s12520-018-0737-0.

Presslee, S., Penkman, K., Fischer, R., Richards-Slidel, E., Southon, J., Hospitaleche, C. A., Collins, M. & MacPhee, R. (2021). Assessment of different screening methods for selecting palaeontological bone samples for peptide sequencing. Journal of Proteomics *230*, 103986. doi.org/10.1016/j.jprot.2020.103986.

Price, G. J., Webb, G. E., Zhao, J.-x., Feng, Y.-x., Murray, A. S., Cooke, B. N., Hocknull, S. A. & Sobbe, I. H. (2011). Dating megafaunal extinction on the Pleistocene Darling Downs, eastern Australia: The promise and pitfalls of dating as a test of extinction hypotheses. Quaternary Science Reviews *30*, 899-914. doi.org/10.1016/j.quascirev.2011.01.011.

Price, G. J., Ferguson, K. J., Webb, G. E., Feng, Y.-x., Higgins, P., Nguyen, A. D., Zhao, J.-x., Joannes-Boyau, R. & Louys, J. (2017). Seasonal migration of marsupial megafauna in Pleistocene Sahul (Australia&-New Guinea). Proceedings of the Royal Society B: Biological Sciences *284*, 20170785. doi.org/10.1098/rspb.2017.0785.

Price, G. J., Louys, J., Tyler Faith, J., Lorenzen, E. D. & Westaway, M. C. (2018). Big data little help in megafauna mysteries. Nature *558*, 23-25. doi.org/10.1038/d41586-018-05330-7.

Price, G. J., Fitzsimmons, K. E., Nguyen, A. D., Zhao, J.-x., Feng, Y.-x., Sobbe, I. H., Godthelp, H., Archer, M. & Hand, S. J. (2021). New ages of the world's largest-ever marsupial: *Diprotodon optatum* from Pleistocene Australia. Quaternary International *603*, 64-73. doi.org/10.1016/j.quaint.2021.06.013.

Prideaux, G. J. (2004). Systematics and evolution of the sthenurine kangaroos (University of California Press).

Procopio, N. & Buckley, M. (2017). Minimizing laboratory-induced decay in bone proteomics. Journal of Proteome Research *16*, 447-458. doi.org/10.1021/acs.jproteome.6b00564.

Prowse, T. A. A., Johnson, C. N., Bradshaw, C. J. A. & Brook, B. W. (2014). An ecological regime shift resulting from disrupted predator-prey interactions in Holocene Australia. Ecology *95*, 693-702. doi.org/10.1890/13-0746.1.

Ramsøe, A., Van Heekeren, V., Ponce, P., Fischer, R., Barnes, I., Speller, C. & Collins, M. (2020). DeamiDATE 1.0: Site-specific deamidation as a tool to assess authenticity of members of ancient proteomes. Journal of Archaeological Science *115*, 105080. doi.org/10.1016/j.jas.2020.105080.

Reeves, J. M., Bostock, H. C., Ayliffe, L. K., Barrows, T. T., De Deckker, P., Devriendt, L. S., Dunbar, G. B., Drysdale, R. N., Fitzsimmons, K. E., Gagan, M. K., et al. (2013). Palaeoenvironmental change in tropical Australasia over the last 30,000 years – A synthesis by the OZ-INTIMATE group. Quaternary Science Reviews *74*, 97-114. doi.org/10.1016/j.quascirev.2012.11.027.

Ricard-Blum, S. (2011). The collagen family. Cold Spring Harbor perspectives in biology *3*, a004978-a004978. doi.org/10.1101/cshperspect.a004978.

Richards, H. L., Wells, R. T., Evans, A. R., Fitzgerald, E. M. G. & Adams, J. W. (2019). The extraordinary osteology and functional morphology of the limbs in Palorchestidae, a family of strange extinct marsupial giants. PLoS ONE *14*, e0221824. doi.org/10.1371/journal.pone.0221824.

Richter, K. K., Wilson, J. C., Jones, A. K. G., Buckley, M., Van Doorn, N. L. & Collins, M. (2011). Fish 'n chips: ZooMS peptide mass fingerprinting in a 96 well plate format to identify fish bone fragments. Journal of Archaeological Science *38*, 1502-1510. doi.org/10.1016/j.jas.2011.02.014.

Richter, K. K., McGrath, K., Masson-MacLean, E., Hickinbotham, S., Tedder, A., Britton, K., Bottomley, Z., Dobney, K., Hulme-Beaman, A., Zona, M., et al. (2020). What's the catch? Archaeological application of rapid collagen-based species identification. Journal of Archaeological Science *116*, 105116. doi.org/10.1016/j.jas.2020.105116.

Richter, K. K., Codlin, M. C., Seabrook, M. & Warinner, C. (2022). A primer for ZooMS applications in archaeology. Proceedings of the National Academy of Sciences *119*, e2109323119. doi.org/10.1073/pnas.2109323119.

Rick, T., Harvey, V. L. & Buckley, M. (2019). Collagen fingerprinting and the Chumash billfish fishery, Santa Barbara Channel, California, USA. Archaeological and Anthropological Sciences *11*, 6639-6648. doi.org/10.1007/s12520-019-00930-4.

Roberts, P., Buhrich, A., Caetano-Andrade, V., Cosgrove, R., Fairbairn, A., Florin, S. A., Vanwezer, N., Boivin, N., Hunter, B., Mosquito, D., et al. (2021). Reimagining the relationship between Gondwanan forests and Aboriginal land management in Australia's "Wet Tropics". iScience *24*, 102190. doi.org/10.1016/j.isci.2021.102190.

Roberts, R. G., Flannery, T. F., Ayliffe, L. K., Yoshida, H., Olley, J. M., Prideaux, G. J., Laslett, G. M., Baynes, A., Smith, M. A., Jones, R., et al. (2001). New ages for the last Australian megafauna: Continent-wide extinction about 46,000 years ago. Science *292*, 1888-1892. doi.org/10.1126/science.1060264.

Roberts, S. J., Smith, C. I., Millard, A. & Collins, M. J. (2002). The taphonomy of cooked bone: characterizing boiling and its physico–chemical effects. Archaeometry *44*, 485-494. doi.org/10.1111/1475-4754.t01-1-00080.

Rodrigues, A. S. L., Charpentier, A., Bernal-Casasola, D., Gardeisen, A., Nores, C., Millán, J. A. P., McGrath, K. & Speller, C. (2018). Forgotten Mediterranean calving grounds of grey and North Atlantic right whales: evidence from Roman archaeological records. Proceedings of the Royal Society B *285*, 20180961. doi.org/10.1098/rspb.2018.0961.

Rodrigues, A. S. L., Monsarrat, S., Charpentier, A., Brooks, T. M., Hoffmann, M., Reeves, R., Palomares, M. L. D. & Turvey, S. T. (2019). Unshifting the baseline: A framework for documenting historical population changes and assessing long-term anthropogenic impacts. Philosophical Transactions Royal Society B *374*. doi.org/10.1098/rstb.2019.0220.

Ruffini-Ronzani, N., Nieus, J.-F., Soncin, S., Hickinbotham, S., Dieu, M., Bouhy, J., Charles, C., Ruzzier, C., Falmagne, T., Hermand, X., et al. (2021). A biocodicological analysis of the medieval library and archive from Orval Abbey, Belgium. Royal Society Open Science *8*, 210210. doi.org/10.1098/rsos.210210.

Rule, S., Brook, B. W., Haberle, S. G., Turney, C. S. M., Kershaw, A. P. & Johnson, C. N. (2012). The aftermath of megafaunal extinction: Ecosystem transformation in Pleistocene Australia. Science *335*, 1483-1486. doi.org/10.1126/science.1214261.

Runge, A. K. W., Hendy, J., Richter, K. K., Masson-MacLean, E., Britton, K., Mackie, M., McGrath, K., Collins, M., Cappellini, E. & Speller, C. (2021). Palaeoproteomic analyses of dog palaeofaeces reveal a preserved dietary and host digestive proteome. Proceedings of the Royal Society B: Biological Sciences *288*, 20210020. doi.org/doi:10.1098/rspb.2021.0020.

Ruscillo, D. (2014). Zooarchaeology: Methods of collecting age and sex data. In Encyclopedia of global archaeology. Smith, C. ed. (Springer New York). doi.org/10.1007/978-1-4419-0465-2_2163.

Rybczynski, N., Gosse, J. C., Harington, C. R., Wogelius, R. A., Hidy, A. J. & Buckley, M. (2013). Mid-Pliocene warm-period deposits in the High Arctic yield insight into camel evolution. Nature Communications *4*, 1-9. doi.org/10.1038/ncomms2516.

Saltré, F., Rodríguez-Rey, M., Brook, B. W., Johnson, C. N., Turney, C. S. M., Alroy, J., Cooper, A., Beeton, N. J., Bird, M., Fordham, D. A., et al. (2016). Climate change not to blame for late Quaternary megafauna extinctions in Australia. Nature Communications *7*. doi.org/10.1038/ncomms10511.

Saltré, F., Chadoeuf, J., Peters, K. J., McDowell, M. C., Friedrich, T., Timmermann, A., Ulm, S. & Bradshaw, C. J. A. (2019). Climate-human interaction associated with southeast Australian megafauna extinction patterns. Nature Communications *10*, 5311. doi.org/10.1038/s41467-019-13277-0.

Sandler, R. (2017). De-extinction and conservation genetics in the Anthropocene. Hastings Center Report *47*, S43-S47. doi.org/10.1002/hast.751.

Scharf, E. A. (2014). Deep time: The emerging role of archaeology in landscape ecology. Landscape Ecology *29*, 563-569. doi.org/10.1007/s10980-014-9997-y.

Schroeder, R. A. & Bada, J. L. (1976). A review of the geochemical applications of the amino acid racemization reaction. Earth Science Reviews *12*, 347. doi.org/10.1016/0012-8252(76)90011-8.

Schroeter, E. R. & Cleland, T. P. (2016). Glutamine deamidation: an indicator of antiquity, or preservational quality? Rapid Communications in Mass Spectrometry *30*, 251-255. doi.org/10.1002/rcm.7445.

Schuster, R., Germain, R. R., Bennett, J. R., Reo, N. J. & Arcese, P. (2019). Vertebrate biodiversity on indigenous-managed lands in Australia, Brazil, and Canada equals that in protected areas. Environmental Science & Policy *101*, 1-6. doi.org/10.1016/j.envsci.2019.07.002.

Scott, A., Power, R. C., Altmann-Wendling, V., Artzy, M., Martin, A. P., Eisenmann, S., Hagan, R., Salazar-García, D. C., Salmon, Y., Yegorov, D., et al. (2021). Exotic foods reveal contact between South Asia and the Near East during the second millennium BCE. Proceedings of the National Academy of Sciences *118*, e2014956117. doi.org/10.1073/pnas.2014956117.

Seersholm, F. V., Werndly, D. J., Grealy, A., Johnson, T., Keenan Early, E. M., Lundelius, E. L., Winsborough, B., Farr, G. E., Toomey, R., Hansen, A. J., et al. (2020). Rapid range shifts and megafaunal extinctions associated with late Pleistocene climate change. Nature Communications *11*, 2770. doi.org/10.1038/s41467-020-16502-3.

Seersholm, F. V., Grealy, A., McDowell, M. C., Cole, T. L., Arnold, L. J., Prideaux, G. J. & Bunce, M. (2021). Ancient DNA from bulk bone reveals past genetic diversity of vertebrate fauna on Kangaroo Island, Australia. Quaternary Science Reviews *262*, 106962. doi.org/10.1016/j.quascirev.2021.106962.

Sheppard, A. & Glanznig, A. 2021. Fighting plagues and predators. Australia's path towards pest and weed-free future. Canberra: CSIRO.

Shevchenko, A., Yang, Y., Knaust, A., Thomas, H., Jiang, H., Lu, E., Wang, C. & Shevchenko, A. (2014). Proteomics identifies the composition and manufacturing recipe of the 2500-year old sourdough bread from Subeixi cemetery in China. Journal of Proteomics *105*, 363-371. doi.org/10.1016/j.jprot.2013.11.016.

Shevchenko, A., Schuhmann, A., Thomas, H. & Wetzel, G. (2018). Fine Endmesolithic fish caviar meal discovered by proteomics in foodcrusts from archaeological site Friesack 4 (Brandenburg, Germany). PLoS ONE *13*, e0206483. doi.org/10.1371/journal.pone.0206483.

Shoulders, M. D. & Raines, R. T. (2009). Collagen structure and stability. Annual review of biochemistry *78*, 929-958. doi.org/10.1146/annurev.biochem.77.032207.120833.

Signor, P. W., III, Lipps, J. H., Silver, L. T. & Schultz, P. H. (1982). Sampling bias, gradual extinction patterns and catastrophes in the fossil record. In Geological implications of impacts of large asteroids and comets on the Earth. (Geological Society of America). doi.org/10.1130/SPE190-p291.

Silvestrini, S., Lugli, F., Romandini, M., Real, C., Sommella, E., Salviati, E., Arrighi, S., Bortolini, E., Figus, C., Higgins, O. A., et al. (2022). Integrating ZooMS and zooarchaeology: New data from the Uluzzian levels of Uluzzo C Rock Shelter, Roccia San Sebastiano cave and Riparo del Broion. PLoS ONE *17*, e0275614. doi.org/10.1371/journal.pone.0275614.

Simpson, J. P., Penkman, K. E. H., Demarchi, B., Koon, H., Collins, M. J., Thomas-Oates, J., Shapiro, B., Stark, M. & Wilson, J. (2016). The effects of demineralisation and sampling point variability on the measurement of glutamine deamidation in type I collagen extracted from bone. Journal of Archaeological Science *69*, 29-38. doi.org/10.1016/j.jas.2016.02.002.

Sinet-Mathiot, V., Smith, G. M., Romandini, M., Wilcke, A., Peresani, M., Hublin, J.-J. & Welker, F. (2019). Combining ZooMS and zooarchaeology to study Late Pleistocene hominin behaviour at Fumane (Italy). Scientific Reports *9*, 12350. doi.org/10.1038/s41598-019-48706-z.

Sinet-Mathiot, V., Martisius, N. L., Schulz-Kornas, E., van Casteren, A., Tsanova, T. R., Sirakov, N., Spasov, R., Welker, F., Smith, G. M. & Hublin, J.-J. (2021). The effect of eraser sampling for proteomic analysis on Palaeolithic bone surface microtopography. Scientific Reports *11*, 23611. doi.org/10.1038/s41598-021-02823-w.

Smith, C. I., Chamberlain, A. T., Riley, M. S., Stringer, C. & Collins, M. J. (2003). The thermal history of human fossils and the likelihood of successful DNA amplification. Journal of Human Evolution *45*, 203-217. doi.org/10.1016/S0047-2484(03)00106-4.

Smith, F. A., Elliott Smith, R. E., Lyons, S. K., Payne, J. L. & Villaseñor, A. (2019). The accelerating influence of humans on mammalian macroecological patterns over the late Quaternary. Quaternary Science Reviews *211*, 1-16. doi.org/10.1016/j.quascirev.2019.02.031.

Solazzo, C., Fitzhugh, W. W., Rolando, C. & Tokarski, C. (2008). Identification of protein remains in archaeological potsherds by proteomics. Analytical Chemistry *80*, 4590-4597. doi.org/10.1021/ac800515v.

Solazzo, C. (2019). Characterizing historical textiles and clothing with proteomics. Conservar Património *31*, 97-114. doi.org/10.14568/cp2018031.

Spengler, R. N., Petraglia, M., Roberts, P., Ashastina, K., Kistler, L., Mueller, N. G. & Boivin, N. (2021). Exaptation traits for megafaunal mutualisms as a factor in plant domestication. Frontiers in Plant Science *12*, 649394. doi.org/10.3389/fpls.2021.649394.

Sponheimer, M., Ryder, C. M., Fewlass, H., Smith, E. K., Pestle, W. J. & Talamo, S. (2019). Saving old bones: A non-destructive method for bone collagen prescreening. Scientific Reports *9*, 13928. doi.org/10.1038/s41598-019-50443-2.

Stewart, N. A., Gerlach, R. F., Gowland, R. L., Gron, K. J. & Montgomery, J. (2017). Sex determination of human remains from peptides in tooth enamel. Proceedings of the National Academy of Sciences *114*, 13649-13654. doi.org/10.1073/pnas.1714926115.

Stover, D. A. & Verrelli, B. C. (2010). Comparative vertebrate evolutionary analyses of type I collagen: Potential of COL1a1 gene structure and intron variation for common bone-related diseases. Molecular Biology and Evolution *28*, 533-542. doi.org/10.1093/molbev/msq221.

Surovell, T. A. (2008). Extinctions of big game. Encyclopedia of archaeology *2*, 1365-1374.

Svenning, J.-C., Pedersen, P. B. M., Donlan, C. J., Ejrnæs, R., Faurby, S., Galetti, M., Hansen, D. M., Sandel, B., Sandom, C. J., Terborgh, J. W., et al. (2016). Science for a wilder Anthropocene: Synthesis and future directions for trophic rewilding research. Proceedings of the National Academy of Sciences *113*, 898-906. doi.org/10.1073/pnas.1502556112.

Swift, J. A., Bunce, M., Dortch, J., Douglass, K., Tyler Faith, J., Fellows Yates, J. A., Field, J., Haberle, S. G., Jacob, E., Johnson, C. N., et al. (2019). Micro methods for megafauna: Novel approaches to Late Quaternary extinctions and their contributions to faunal conservation in the Anthropocene. BioScience *69*, 877-887. doi.org/10.1093/biosci/biz105.

Talamo, S., Urbanowski, M., Picin, A., Nowaczewska, W., Vazzana, A., Binkowski, M., Cercatillo, S., Diakowski, M., Fewlass, H., Marciszak, A., et al. (2021). A 41,500 year-old decorated ivory

pendant from Stajnia Cave (Poland). Scientific Reports *11*, 22078. doi.org/10.1038/s41598-021-01221-6.

Taylor, W. T. T., Shnaider, S., Abdykanova, A., Fages, A., Welker, F., Irmer, F., Seguin-Orlando, A., Khan, N., Douka, K., Kolobova, K., et al. (2018). Early pastoral economies along the Ancient Silk Road: Biomolecular evidence from the Alay Valley, Kyrgyzstan. PLoS ONE *13*, e0205646. doi.org/10.1371/journal.pone.0205646.

Taylor, W. T. T., Clark, J., Bayarsaikhan, J., Tusvshinjargal, T., Jobe, Thompson, J., Fitzhugh, W. W., Kortum, R., Spengler, R. N., Shnaider, S., et al. (2020). Early pastoral economies and herding transitions in Eastern Eurasia. Scientific Reports *10*, 1001. doi.org/10.1038/s41598-020-57735-y.

Taylor, W. T. T., Pruvost, M., Posth, C., Rendu, W., Krajcarz, M. T., Abdykanova, A., Brancaleoni, G., Spengler, R. N., Hermes, T., Schiavinato, S., et al. (2021). Evidence for the early dispersal of domestic sheep into Central Asia. Nature Human Behaviour. doi.org/10.1038/s41562-021-01083-y.

Teasdale, M. D., Fiddyment, S., Vnouček, J., Mattiangeli, V., Speller, C., Binois, A., Carver, M., Dand, C., Newfield, T. P., Webb, C. C., et al. (2017). The York Gospels: A 1000-year biological palimpsest. Royal Society Open Science *4*, 170988. doi.org/10.1098/rsos.170988.

Trueman, C. N. G., Behrensmeyer, A. K., Tuross, N. & Weiner, S. (2004). Mineralogical and compositional changes in bones exposed on soil surfaces in Amboseli National Park, Kenya: Diagenetic mechanisms and the role of sediment pore fluids. Journal of Archaeological Science *31*, 721-739. doi.org/10.1016/j.jas.2003.11.003.

Trueman, C. N. G., Field, J., Dortch, J., Charles, B. & Wroe, S. (2005). Prolonged coexistence of humans and megafauna in Pleistocene Australia. Proceedings of the National Academy of Sciences *102*, 8381-8385. doi.org/10.1073/pnas.0408975102.

Turney, C. S. M., Bird, M. I., Fifield, L. K., Roberts, R. G., Smith, M., Dortch, C. E., Grün, R., Lawson, E., Ayliffe, L. K., Miller, G. H., et al. (2001). Early human occupation at Devil's Lair, Southwestern Australia 50,000 years ago. Quaternary Research *55*, 3-13. doi.org/10.1006/qres.2000.2195.

Turney, C. S. M., Flannery, T. F., Roberts, R. G., Reid, C., Fifield, L. K., Higham, T., Jacobs, Z., Kemp, N., Colhoun, E. A., Kalin, R. M., et al. (2008). Late-surviving megafauna in Tasmania, Australia, implicate human involvement in their extinction. Proceedings of the National Academy of Sciences *105*, 12150-12153. doi.org/10.1073/pnas.0801360105.

Tyler Faith, J. & O'Connell, J. F. (2011). Revisiting the late Pleistocene mammal extinction record at Tight Entrance Cave, southwestern Australia. Quaternary Research *76*, 397-400. doi.org/10.1016/j.yqres.2011.08.001.

Tyler Faith, J., Dortch, J., Jones, C., Shulmeister, J. & Travouillon, K. J. (2017). Large mammal species richness and late Quaternary precipitation change in south-western Australia. Journal of Quaternary Science *32*, 760-769. doi.org/10.1002/jqs.2888.

van den Hurk, Y. & McGrath, K. (2021). Whaling in Iron Age to post-medieval Scotland. Proceedings of the Society of Antiquaries of Scotland *150*, 451-474. doi.org/10.9750/PSAS.150.13.24.

van den Hurk, Y., Rielly, K. & Buckley, M. (2021). Cetacean exploitation in Roman and medieval London: Reconstructing whaling activities by applying zooarchaeological, historical, and biomolecular analysis. Journal of Archaeological Science: Reports *36*, 102795. doi.org/10.1016/j.jasrep.2021.102795.

Van der Kaars, S., Miller, G., Turney, C. S. M., Cook, E. J., Nürnberg, D., Schönfeld, J., Peter Kershaw, A. & Lehman, S. (2017). Humans rather than climate the primary cause of Pleistocene megafaunal extinction in Australia. Nature Communications *8*. doi.org/10.1039/ncomms14142.

Van der Sluis, L. G., Hollund, H. I., Buckley, M., De Louw, P. G. B., Rijsdijk, K. F. & Kars, H. (2014). Combining histology, stable isotope analysis and ZooMS collagen fingerprinting to investigate the taphonomic history and dietary behaviour of extinct giant tortoises from the Mare aux Songes deposit on Mauritius. Palaeogeography, Palaeoclimatology, Palaeoecology *416*, 80-91. doi.org/10.1016/j.palaeo.2014.06.003.

Van Doorn, N. L., Hollund, H. I. & Collins, M. (2011). A novel and non-destructive approach for ZooMS analysis: Ammonium bicarbonate buffer extraction. Archaeological and Anthropological Sciences *3*, 281-289. doi.org/10.1007/s12520-011-0067-y.

Van Doorn, N. L., Wilson, J. C., Hollund, H. I., Soressi, M. & Collins, M. (2012). Site-specific deamidation of glutamine: A new marker of bone collagen deterioration. Rapid Communications in Mass Spectrometry *26*, 2319-2327. doi.org/10.1002/rcm.6351.

Veth, P., Ward, I., Manne, T., Ulm, S., Ditchfield, K., Dortch, J., Hook, F., Petchey, F., Hogg, A., Questiaux, D., et al. (2017). Early human occupation of a maritime desert, Barrow Island, North-West Australia. Quaternary Science Reviews *168*, 19-29. doi.org/10.1016/j.quascirev.2017.05.002.

Veth, P., Ditchfield, K., Bateman, M., Ouzman, S., Benoit, M., Motta, A. P., Lewis, D. & Harper, S. (2019). Minjiwarra: Archaeological evidence of human occupation of Australia's northern Kimberley by 50,000 BP. Australian Archaeology *85*, 115-125. doi.org/10.1080/03122417.2019.1650479.

Von Holstein, I. C. C., Ashby, S. P., Van Doorn, N. L., Sachs, S. M., Buckley, M., Meiri, M., Barnes, I., Brundle, A. & Collins, M. (2014). Searching for Scandinavians in pre-Viking Scotland: Molecular fingerprinting of Early Medieval combs. Journal of Archaeological Science *41*, 1-6. doi.org/10.1016/j.jas.2013.07.026.

Wang, N., Brown, S., Richter, K. K., Ditchfield, P., Hebestreit, S., Kozilikin, M., Luu, S., Wedage, O., Grimaldi, S., Chazen, M., et al. (2021). Testing the efficacy and comparability of ZooMS protocols on archaeological bone. Journal of Proteomics *233*, 104078. doi.org/10.1016.j.jprot.2020.104078.

Warinner, C., Hendy, J., Speller, C., Cappellini, E., Fischer, R., Trachsel, C., Arneborg, J., Lynnerup, N., Craig, O. E., Swallow, D. M., et al. (2014a). Direct evidence of milk consumption from ancient human dental calculus. Scientific Reports *4*, 1-6. doi.org/10.1038/srep07104.

Warinner, C., Rodrigues, J. F. M., Vyas, R., Trachsel, C., Shved, N., Grossmann, J., Radini, A., Hancock, Y., Tito, R. Y., Fiddyment, S., et al. (2014b). Pathogens and host immunity in the ancient human oral cavity. Nature Genetics *46*, 336-344. doi.org/10.1038/ng.2906.

Wayne, A. F., Wilson, B. A. & Woinarski, J. C. Z. (2017). Falling apart? Insights and lessons from three recent studies documenting rapid and severe decline in terrestrial mammal assemblages of northern, south-eastern and south-western Australia. Wildlife Research *44*, 114-126. doi.org/10.1071/WR16178.

Webb, S. (2013). Corridors to extinction and the Australian megafauna (Elsevier).

Welker, F., Collins, M., Thomas, J. A., Wadsley, M., Brace, S., Cappellini, E., Turvey, S. T., Reguero, M., Gelfo, J. N., Kramarz, A., et al. (2015a). Ancient proteins resolve the evolutionary history of Darwin's South American ungulates. Nature *522*, 81-84. doi.org/10.1038/nature14249.

Welker, F., Soressi, M., Rendu, W., Hublin, J.-J. & Collins, M. (2015b). Using ZooMS to identify fragmentary bone from the Late Middle/Early Upper Palaeolithic sequence of Les Cottés, France. Journal of Archaeological Science *54*, 279-286. doi.org/10.1016/j.jas.2014.12.010.

Welker, F., Hajdinjak, M., Talamo, S., Jaouen, K., Dannemann, M., David, F., Julien, M., Meyer, M., Kelso, J., Barnes, I., et al. (2016). Palaeoproteomic evidence identifies archaic hominins associated with the Châtelperronian at the Grotte du Renne. Proceedings of the National Academy of Sciences *113*, 11162-11167. doi.org/10.1073/pnas.1605834113.

Welker, F., Smith, G. M., Hutson, J. M., Kindler, L., Garcia-Moreno, A., Villaluenga, A., Turner, E. & Gaudzinski-Windheuser (2017). Middle Pleistocene protein sequences from the rhinoceros genus *Stephanorhinus* and the phylogeny of extant and extinct Middle/Late Pleistocene Rhinocerotidae. PeerJ *5*, e3033. doi.org/10.7717/peerj.3033.

Welker, F., Ramos-Madrigal, J., Kuhlwilm, M., Liao, W., Gutenbrunner, P., de Manuel, M., Samodova, D., Mackie, M., Allentoft, M. E., Bacon, A.-M., et al. (2019). Enamel proteome shows that *Gigantopithecus* was an early diverging pongine. Nature *576*, 262-265. doi.org/10.1038/s41586-019-1728-8.

Welker, F., Ramos-Madrigal, J., Gutenbrunner, P., Mackie, M., Tiwary, S., Rakownikow Jersie-Christensen, R., Chiva, C., Dickinson, M. R., Kuhlwilm, M., de Manuel, M., et al. (2020). The dental proteome of *Homo antecessor*. Nature *580*, 235-238. doi.org/10.1038/s41586-020-2153-8.

Westaway, M. C., Price, G., Miscamble, T., McDonald, J., Cramb, J., Ringma, J., Grün, R., Jones, D. & Collard, M. (2019). A palaeontological perspective on the proposal to reintroduce Tasmanian

devils to mainland Australia to suppress invasive predators. Biological Conservation *232*, 187-193. doi.org/10.1016/j.biocon.2019.02.002.
White, L. & Booth, T. J. (2014). The origin of bacteria responsible for bioerosion to the internal bone microstructure: Results from experimentally-deposited pig carcasses. Forensic Science International *239*, 92-102. doi.org/10.1016/j.forsciint.2014.03.024.
White, L. C., Mitchell, K. J. & Austin, J. J. (2018a). Ancient mitochondrial genomes reveal the demographic history and phylogeography of the extinct, enigmatic thylacine (*Thylacinus cynocephalus*). Journal of Biogeography *45*, 1-13. doi.org/10.1111/jbi.13101.
White, L. C., Saltré, F., Bradshaw, C. J. A. & Austin, J. J. (2018b). High-quality fossil dates support a synchronous, Late Holocene extinction of devils and thylacines in mainland Australia. Biology Letters *14*, 20170642. doi.org/10.1098/rsbl.2017.0642.
Wilkin, S., Ventresca Miller, A., Fernandes, R., Spengler, R., Taylor, W. T. T., Brown, D. R., Reich, D., Kennett, D. J., Culleton, B. J., Kunz, L., et al. (2021). Dairying enabled Early Bronze Age Yamnaya steppe expansions. Nature *598*, 629-633. doi.org/10.1038/s41586-021-03798-4.
Willis, K. J. & Birks, H. J. B. (2006). What is natural? The need for a long-term perspective in biodiversity conservation. Science *314*, 1261-1265. doi.org/10.1126/science.1122667.
Wilson, J. C., Van Doorn, N. L. & Collins, M. (2012). Assessing the extent of bone degradation using glutamine deamidation in collagen. Analytical Chemistry *84*, 9041-9048. doi.org/10.1021/ac301333t.
Woinarski, J. C. Z., Burbidge, A. A. & Harrison, P. L. (2015). Ongoing unraveling of a continental fauna: Decline and extinction of Australian mammals since European settlement. Proceedings of the National Academy of Sciences *112*, 4531-4540. doi.org/10.1073/pnas.1417301112.
Woinarski, J. C. Z., Braby, M. F., Burbidge, A. A., Coates, D., Garnett, S. T., Fensham, R. J., Legge, S. M., McKenzie, N. L., Silcock, J. L. & Murphy, B. P. (2019). Reading the black book: The number, timing, distribution and causes of listed extinctions in Australia. Biological Conservation *239*, 108261. doi.org/10.1016/j.biocon.2019.108261.
Wroe, S. & Field, J. (2006). A review of the evidence for a human role in the extinction of Australian megafauna and an alternative interpretation. Quaternary Science Reviews *25*, 2692-2703. doi.org/10.1016/j.quascirev.2006.03.005.
Wroe, S., Clausen, P., McHenry, C., Moreno, K. & Cunningham, E. (2007). Computer simulation of feeding behaviour in the thylacine and dingo as a novel test for convergence and niche overlap. Proceedings of the Royal Society B: Biological Sciences *274*, 2819-2828. doi.org/10.1098/rspb.2007.0906.
Wroe, S., Field, J. H., Archer, M., Grayson, D. K., Price, G. J., Louys, J., Faith, J. T., Webb, G. E., Davidson, I. & Mooney, S. D. (2013). Climate change frames debate over the extinction of megafauna in Sahul (Pleistocene Australia-New Guinea). Proceedings of the National Academy of Sciences *110*, 8777-8781. doi.org/10.1073/pnas.1302698110.
Yokoyama, Y., Lambeck, K., De Deckker, P., Johnston, P. & Fifield, L. K. (2000). Timing of the Last Glacial Maximum from observed sea-level minima. Nature *406*, 713-716. doi.org/10.1038/35021035.

12. Summary

In recent years, the development and adoption of a new palaeoproteomics method, Zooarchaeology by Mass Spectrometry (ZooMS, or peptide mass fingerprinting), has revolutionized the study of fragmented faunal remains from archaeological deposits. ZooMS has the ability to taxonomically identify faunal remains that are unidentifiable on the basis of their morphological features. In this way, ZooMS can be used to address research questions regarding faunal diversity and human-animal relationships in the past, and uncover the provenance of bone tools and objects. The majority of ZooMS studies to date have focused on medium- to large-sized mammals from Eurasian contexts, although the focus of ZooMS studies is slowly shifting to include other regions and taxa.

The main purpose of this thesis is to explore the potential of peptide mass fingerprinting for the study of Australian faunal assemblages. In the first part of this thesis, existing challenges for the application of ZooMS in Australian contexts, namely, a lack of available references, are addressed. First, collagen peptide markers are developed for 24 endemic Australian animals. These newly developed markers are then used to identify 134 fragmented bones from a colonial-era pearl shell fishery at Bandicoot Bay, Barrow Island. It is shown that ZooMS can effectively be used to identify fragmented marsupial remains.

This thesis then further explores challenges associated with biomolecular preservation in Australia due to the unfavorable climatic conditions across the country. In total, 765 bone fragments from 17 localities were analyzed with Fourier Transform Infrared Spectroscopy (FTIR) and ZooMS to get a better understanding of the nature of collagen preservation in Australia across time and space and in different depositional contexts. Deamidation rates were calculated to get further insight into the preservation of collagen at these sites. It is shown that collagen preservation is best in limestone caves. The results were also compared to chemical predictions of preservation potential showing that at some sites the survival of collagen exceeds this theoretical limit. The results of this analysis show that the preservation of collagen in Australia is highly variable, and that its survival cannot be predicted using solely climatic variables but instead also depends on micro-environmental conditions. The preservation of collagen at Late Pleistocene Australian sites has significant implications for collagen preservation in other regions of the world where preservation was previously deemed challenging, such as the tropics.

With the two major challenges confounding the use of ZooMS to study Australian assemblages resolved, the next part of this thesis then discusses the application of ZooMS for the identification of a total of 94 fragmented faunal remains from the Late Pleistocene site Devil's Lair, Southwest Australia. The results of the ZooMS analysis are brought together with existing zooarchaeological and bulk bone DNA metabarcoding data to get a more in-depth understanding of the faunal assemblage at the site. This combined approach shows that ZooMS can provide valuable information regarding the taphonomic history of a faunal assemblage, in addition to increasing the number of identified fragments.

The study of past biodiversity can also provide important long-term data about ecosystem transformations in the past. Such data is critical to consider when establishing conservation targets. In the final part of this thesis, it is explored how the study of ancient proteins with ZooMS and shotgun palaeoproteomics can be used to inform conservation and restoration agendas. Seven key areas are identified in which the study of ancient proteins can contribute: assessing species richness, establishing ecological baselines, detecting shifts in species abundance and geographic range, disentangling human-environment interactions, tracking the introduction of non-native species, identifying illicitly traded material, and prioritizing species for conservation.

In sum, this thesis represents the largest application of ZooMS to Australian contexts to date and paves the way for future ZooMS studies in Australia. The novel marsupial and monotreme peptide markers developed as part of this thesis are now available for researchers globally, while the better understanding of the spatial and temporal limit of collagen preservation in Australia acquired as part of this thesis can

be used to guide future studies to determine the preservation potential of a given site. Overall, this thesis highlights the immense potential of ZooMS to inform us about faunal diversity and turnovers in Australia in the past.

13. Zusammenfassung

Die Entwicklung und Einführung der neuen Paläoproteomik-Methode *Zooarchaeology by Mass Spectrometry* (ZooMS, oder *peptide mass fingerprinting*) hat die Untersuchung fragmentierter Faunareste aus archäologischen Ablagerungen revolutioniert. ZooMS ist in der Lage, kleinste, nicht morphologisch bestimmbare Tierknochenfragmente taxonomisch zu identifizieren. Dadurch kann ZooMS beitragen, Forschungsfragen zur Faunavielfalt und Mensch-Tier-Beziehungen in der Vergangenheit zu beantworten, und die Herkunft von Knochenwerkzeugen und -objekten aufzudecken. Die Mehrheit der bisherigen ZooMS-Studien konzentrierte sich vor allem auf mittelgroße und große Säugetiere aus eurasischen Kontexten, doch in den letzten Jahren verlagerte sich der Fokus der ZooMS-Studien langsam auf andere Regionen und Tierarten.

Das Hauptziel der vorliegenden Dissertation ist es, das Potenzial des *peptide mass fingerprinting* für das Studium australischer Faunaresten zu untersuchen. Der erste Teil der Dissertation befasst sich mit bestehenden Herausforderungen der Anwendung von ZooMS in australischen Kontexten, problematisiert das derzeit noch unzureichend verfügbare Referenzmaterial. Zu diesem Zwecke wurden zunächst Kollagenpeptidemarker für 24 endemische australische Tierarten entwickelt. Durch diese neu entwickelten Marker konnten 134 fragmentierte Knochen aus einer Perlenfischerei aus der Kolonialzeit in Bandicoot Bay, Barrow Island identifiziert werden. Diese Resultate bestätigen deutlich die Eignung der ZooMS-Methode zur Identifizierung fragmentierte Beuteltierreste.

Des Weiteren untersucht die Dissertation den biomolekularen Erhaltungszustand von Knochenmaterial in Australien aufgrund der ungünstigen klimatischen Bedingungen im ganzen Land. Insgesamt wurden 765 Knochenfragmente von 17 Orten mit *Fourier Transform Infrared Spectroscopy* (FTIR) und ZooMS analysiert, um ein besseres Verständnis der Art der Kollagenerhaltung in Australien zu erhalten. Dafür wurden Proben aus unterschiedlichen Regionen, Perioden und Ablagerungskontexte untersucht und Deamidierungsraten ermittelt, Es hat sich gezeigt, dass die Kollagenkonservierung in Kalksteinhöhlen am besten ist. Die Ergebnisse wurden zusätzlich mit chemischen Prognosen hinsichtlich des Konservierungspotentials verglichen, die zeigten, dass das Vorhandensein von Kollagen an einigen Stellen diese theoretische Grenze überschreitet. Die Resultate dieser Analyse zeigen, dass die Erhaltung von Kollagen in Australien sehr variabel ist und sein Vorhandensein nicht nur anhand klimatischer Variablen vorhergesagt werden kann, sondern auch von Mikroumgebungsbedingungen abhängt. Die Erhaltung von Kollagen an spätpleistozänen Fundorten in Australien hat erhebliche Auswirkungen auf die Kollagenerhaltung in andere Regionen der Welt, in denen die Erhaltung als schwierig galt, wie zum Beispiel in den Tropen.

Nachdem die beiden großen Herausforderungen der Verwendung von ZooMS zur Untersuchung australischer Ansammlungen gelöst wurden, diskutiert der nächste Teil dieser Dissertation die Anwendung von ZooMS zur Identifizierung von insgesamt 94 fragmentierten Faunaresten des spätpleistozänen Fundort Devil's Lair in Südwestaustralien. Die Ergebnisse der ZooMS-Analyse werden mit bestehenden zooarchäologischen und *bulk bone DNA metabarcoding* Daten zusammengeführt, um ein tieferes Verständnis der Fauna dieser Fundstelle zu erhalten. Dieser kombinierte Ansatz zeigt, dass ZooMS wertvolle Informationen über die taphonomische Geschichte einer Faunasammlung liefern kann, vor allem in Bezug auf die Anzahl identifizierter Fragmente.

Die Untersuchung vergangener Biodiversität kann auch wichtige langfristige Daten über Ökosystemveränderungen in der Vergangenheit liefern. Solche Daten müssen bei der Festlegung von Erhaltungszielen unbedingt berücksichtigt werden. Im letzten Teil der Dissertation wird untersucht, wie die Analyse Paläoproteine mit ZooMS und *shotgun palaeoproteomics* genutzt werden kann um über mögliche Erhaltungs- und Restaurierung-Maßnahmen zu informieren. Es werden sieben Schlüsselbereiche identifiziert, in denen die Untersuchung alter Proteine einen Beitrag leisten kann: Bewertung des Artenreichtums, Festlegung ökologischer Basislinien, Erkennung von Verschiebungen

in der Artenhäufigkeit und der geografischen Reichweite, Entwirrung der Wechselwirkungen zwischen Mensch und Umwelt, Verfolgung der Einführung nicht heimischer Arten, Identifizierung illegal gehandelter Materialien, und Priorisierung von Arten für die Erhaltung.

Zusammenfassend stellt diese Dissertation die bisher größte Anwendung von ZooMS in australischen Kontexten dar und ebnet den Weg für zukünftige ZooMS-Studien in Australien. Die im Rahmen dieser Dissertation entwickelten neuartigen Beuteltier- und Monotreme-Peptidmarker stehen nun Forschern weltweit zur Verfügung. Zusätzlich trägt das im Rahmen dieser Dissertation erworbene Wissen der räumlichen und zeitlichen Grenzen der Kollagenkonservierung in Australien zum besseren Verständnis über den Erhaltungszustand von Kollagen in Knochen und legt damit einen wichtigen Grundstein für zukünftige Studien. Insgesamt hebt diese Dissertation das immense Potenzial von ZooMS hervor, dass uns über die Faunavielfalt und -fluktuationen in Australien in der Vergangenheit zu informieren.

14. Declaration of Honour (Eigenständigkeitserklärung)

Ich erkläre,

dass mir die geltende Promotionsordnung der Fakultät bekannt ist;

dass ich die Dissertation selbst angefertigt, keine Textabschnitte eines Dritten oder eigener Prüfungsarbeiten ohne Kennzeichnung übergenommen und alle von mir benutzten Hilfsmittel, persönlichen Mitteilungen und Quellen in meiner Arbeit angegeben habe;

dass mich ausschließlich die folgenden Personen bei der Auswahl und Auswertung des Materials sowie bei der Herstellung des Manuskripts unterstützt haben;

dass die Hilfe einer kommerziellen Promotionsvermittlung nicht in Anspruch genommen wurde und dass Dritte weder unmittelbar noch mittelbar geldwerte Leistungen von mir für die Arbeiten enthalten haben, die in Zusammenhang mit dem Inhalt der vorgelegten Dissertation stehen;

dass ich die Dissertation noch nicht als Prüfungsarbeit für eine staatliche oder andere wissenschaftliche Prüfung eingereicht habe;

dass ich nicht die gleiche, eine in wesentlichen Teilen ähnliche oder eine andere Abhandlung bei einer anderen Hochschule als Dissertation eingereicht habe.

Jena, 28.11.2022

Carli Antoinette Elisabeth Peters

15. Declaration of Originality (Selbstständigkeitserklärung)

Ich erkläre, dass ich die vorliegende Arbeit selbständig und unter Verwendung der angegebenen Hilfsmittel, persönlichen Mitteilungen und Quellen angefertigt habe.

Jena, 28.11.2022

Carli Antoinette Elisabeth Peters

16. Acknowledgements

I would not have been able to realize this thesis without the help and support of so many people over the last couple of years, including everyone in the Department of Archaeology at the Max Planck Institute of Geoanthropology in Jena. I am especially grateful to my supervisor, Nicole Boivin, for her support during my PhD. These last three years have without a doubt been stressful and chaotic, but you always tried your best to guide me through it. You have taught me so much about academia in general, but also about what it takes to be a strong woman in a leadership position. Thank you.

Thanks to my Australian colleagues and collaborators Gilbert Price, Julien Louys, Joe Dortch, Tiina Manne, and Alison Crowther for trusting me to take on this project. Wayne Webb, thank you for supporting our study of the Devil's Lair faunal assemblage. None of this would have been possible without any of you.

I would also like to thank Patrick Roberts, Noel Amano, and Kristine Korzow Richter for their guidance and support throughout this journey. I am also grateful to everyone in my PhD cohort, specifically to Barbara Huber and Ayushi Nayak for helping me take my mind off work and relax, and to my wonderful office mates Phoebe Heddell-Stevens and Basira Mir-Makhamad for our daily chats and coffee breaks when working at the office.

Finally, I would like to thank my parents, Hans Peters and Anne-Marie Peters-Wagenaars, for always supporting me in everything I wanted to pursue ever since I was a little girl. I want to dedicate this thesis to Sef Peters, who was so excited for me to start this journey, but cannot see me finish it. I know he would have been incredibly proud.